ISSN 1007-9327 (print)
ISSN 2219-2840 (online)

World Journal of *Gastroenterology*

World J Gastroenterol 2022 July 21; 28(27): 3282-3534

Published by Baishideng Publishing Group Inc

World Journal of Gastroenterology

Contents

Weekly Volume 28 Number 27 July 21, 2022

REVIEW

MINIREVIEWS

ORIGINAL ARTICLE

Basic Study

World Journal of Gastroenterology

Weekly Volume 28 Number 27 July 21, 2022

Contents

Contents

ABOUT COVER

AIMS AND SCOPE

The primary aim of *World Journal of Gastroenterology* (*WJG*, *World J Gastroenterol*) is to provide scholars and readers from various fields of gastroenterology and hepatology with a platform to publish high-quality basic and clinical research articles and communicate their research findings online. *WJG* mainly publishes articles reporting research results and findings obtained in the field of gastroenterology and hepatology and covering a wide range of topics including gastroenterology, hepatology, gastrointestinal endoscopy, gastrointestinal surgery, gastrointestinal oncology, and pediatric gastroenterology.

INDEXING/ABSTRACTING

The *WJG* is now abstracted and indexed in Science Citation Index Expanded (SCIE, also known as SciSearch®), Current Contents/Clinical Medicine, Journal Citation Reports, Index Medicus, MEDLINE, PubMed, PubMed Central, Scopus, Reference Citation Analysis, China National Knowledge Infrastructure, China Science and Technology Journal Database, and Superstar Journals Database. The 2022 edition of Journal Citation Reports® cites the 2021 impact factor (IF) for *WJG* as 5.374; IF without journal self cites: 5.187; 5-year IF: 5.715; Journal Citation Indicator: 0.84; Ranking: 31 among 93 journals in gastroenterology and hepatology; and Quartile category: Q2. The *WJG*'s CiteScore for 2021 is 8.1 and Scopus CiteScore rank 2021: Gastroenterology is 18/149.

RESPONSIBLE EDITORS FOR THIS ISSUE

NAME OF JOURNAL
World Journal of Gastroenterology

ISSN
ISSN 1007-9327 (print) ISSN 2219-2840 (online)

LAUNCH DATE
October 1, 1995

FREQUENCY
Weekly

EDITORS-IN-CHIEF
Andrzej S Tarnawski

EDITORIAL BOARD MEMBERS
http://www.wjgnet.com/1007-9327/editorialboard.htm

PUBLICATION DATE
July 21, 2022

INSTRUCTIONS TO AUTHORS
https://www.wjgnet.com/bpg/gerinfo/204

GUIDELINES FOR ETHICS DOCUMENTS
https://www.wjgnet.com/bpg/GerInfo/287

GUIDELINES FOR NON-NATIVE SPEAKERS OF ENGLISH
https://www.wjgnet.com/bpg/gerinfo/240

PUBLICATION ETHICS
https://www.wjgnet.com/bpg/GerInfo/288

PUBLICATION MISCONDUCT
https://www.wjgnet.com/bpg/gerinfo/208

ARTICLE PROCESSING CHARGE
https://www.wjgnet.com/bpg/gerinfo/242

STEPS FOR SUBMITTING MANUSCRIPTS
https://www.wjgnet.com/bpg/GerInfo/239

ONLINE SUBMISSION
https://www.f6publishing.com

World Journal of Gastroenterology

Submit a Manuscript: https://www.f6publishing.com

World J Gastroenterol 2022 July 21; 28(27): 3282-3296

DOI: 10.3748/wjg.v28.i27.3282

ISSN 1007-9327 (print) ISSN 2219-2840 (online)

REVIEW

Hepatitis B and circadian rhythm of the liver

Ivana Skrlec, Jasminka Talapko

Specialty type: Gastroenterology and hepatology

Provenance and peer review: Invited article; Externally peer reviewed.

Peer-review model: Single blind

Peer-review report's scientific quality classification

Grade A (Excellent): A, A
Grade B (Very good): B
Grade C (Good): C
Grade D (Fair): 0
Grade E (Poor): 0

P-Reviewer: Jiang W, China; Miyoshi E, Japan; Shkodina A, Ukraine
A-Editor: de Melo FF, Brazil

Received: January 11, 2022
Peer-review started: January 11, 2022
First decision: March 8, 2022
Revised: March 15, 2022
Accepted: June 13, 2022
Article in press: June 13, 2022
Published online: July 21, 2022

Ivana Skrlec, Department of Biophysics, Biology, and Chemistry, Faculty of Dental Medicine and Health, J. J. Strossmayer University of Osijek, Osijek 31000, Croatia

Jasminka Talapko, Department of Anatomy Histology, Embryology, Pathology Anatomy and Pathology Histology, Faculty of Dental Medicine and Health, Osijek 31000, Croatia

Corresponding author: Ivana Skrlec, MSc, PhD, Assistant Professor, Department of Biophysics, Biology, and Chemistry, Faculty of Dental Medicine and Health, J. J. Strossmayer University of Osijek, 21 Crkvena, Osijek 31000, Croatia. iskrlec@fdmz.hr

Abstract

The circadian rhythm in humans is determined by the central clock located in the hypothalamus's suprachiasmatic nucleus, and it synchronizes the peripheral clocks in other tissues. Circadian clock genes and clock-controlled genes exist in almost all cell types. They have an essential role in many physiological processes, including lipid metabolism in the liver, regulation of the immune system, and the severity of infections. In addition, circadian rhythm genes can stimulate the immune response of host cells to virus infection. Hepatitis B virus (HBV) infection is the leading cause of liver disease and liver cancer globally. HBV infection depends on the host cell, and hepatocyte circadian rhythm genes are associated with HBV replication, survival, and spread. The core circadian rhythm proteins, REV-ERB and brain and muscle ARNTL-like protein 1, have a crucial role in HBV replication in hepatocytes. In addition to influencing the virus's life cycle, the circadian rhythm also affects the pharmacokinetics and efficacy of antiviral vaccines. Therefore, it is vital to apply antiviral therapy at the appropriate time of day to reduce toxicity and improve the effectiveness of antiviral treatment. For these reasons, understanding the role of the circadian rhythm in the regulation of HBV infection and host responses to the virus provides us with a new perspective of the interplay of the circadian rhythm and anti-HBV therapy. Therefore, this review emphasizes the importance of the circadian rhythm in HBV infection and the optimization of antiviral treatment based on the circadian rhythm-dependent immune response.

Key Words: Circadian rhythm; Clock genes; Hepatitis B virus; Immune system; Liver

Core Tip: Some studies in the literature contribute to the association of the circadian rhythm and liver pathophysiology associated with hepatitis B virus (HBV) infection. However, this is the first review to report the latest molecular mechanisms of HBV infection, including cellular circadian rhythm disorders, circadian clock-related immune response, therapeutic strategies in improving health outcomes, and the significance of personalized medicine and chronotherapy in treating chronic HBV infections.

Citation: Skrlec I, Talapko J. Hepatitis B and circadian rhythm of the liver. *World J Gastroenterol* 2022; 28(27): 3282-3296
URL: https://www.wjgnet.com/1007-9327/full/v28/i27/3282.htm
DOI: https://dx.doi.org/10.3748/wjg.v28.i27.3282

INTRODUCTION

The circadian rhythm in humans is determined by the central clock found in the hypothalamus's suprachiasmatic nucleus (SCN) which receives light signals from the retina[1]. Endogenous functional circadian rhythms are active in peripheral tissues. For example, the circadian clock in humans, expressed in almost every cell, consists of a whole range of transcription-translation feedback loops[2]. Furthermore, all peripheral clocks in every tissue are synchronized by the central clock in the SCN[3]. Therefore, circadian clock genes and clock-controlled genes (CCG) exist in almost all cell types. Approximately 10%-40% of the genome is encoded in a circadian manner[4]. Furthermore, most physiological processes, such as lipid metabolism, immune system regulation, and infection severity, are under circadian control, and therefore circadian rhythm disorders can result in pathophysiological changes downstream[4,5].

The liver has a vital role in maintaining energy homeostasis within the body. The primary biochemical reactions within the liver are involved in the breakdown and generation of glucose, which is associated with fatty acid metabolism[6]. In addition, the metabolic functions of the liver show rhythmic fluctuations with a periodicity of 24 h[6]. Hepatitis-causing viruses depend closely on hepatocytes for replication, survival, and spread[6]. In addition, viral infection can disrupt the hepatocytes' circadian rhythm[5]. Circadian rhythm transcription factors alter liver metabolism and are linked with various conditions, including viral infection, fatty liver disease, diabetes, and hepatocellular carcinoma (HCC)[1].

What makes the hepatitis B virus (HBV) significantly different from other hepatotropic viruses is its global impact on human health[7], namely, infections caused by this virus result in liver disease, which is a growing global problem[8]. According to the World Health Organization (WHO), it is estimated that 296 million people lived with chronic hepatitis B in 2019, and that 1.5 million new infections are detected each year[9]. Furthermore, due to HBV infection in 2019, mainly from cirrhosis and HCC, about 820000 people died[10]. Hepatitis B can develop in an acute or chronic form[11]. Most infected people do not have any symptoms, which does not mean that there is no disease. Symptoms of acute infection usually occur 2 mo to 3 mo after infection and are nonspecific[12,13].

The HBV begins to multiply within the first 3 d of infection[14]. Whether and to what extent liver damage occurs depends on the infected person's immune system, the infectious dose, and the site of virus entry. Tissue compatibility antigens and interferon promote the viral antigens' [hepatitis B surface antigen (HBsAg), hepatitis B envelope antigen (HbeAg), and hepatitis B core antigen (HBcAg)] exposure to cytotoxic T lymphocytes[15]. If there is no adequate response by these cells, milder signs of the disease occur, which may progress to the development of chronic hepatitis[16]. About 10% of acute HBV infections progress to a chronic form[17]. Chronic HBV can be clinically manifested as mild conditions to severe chronic hepatitis[18], which, in untreated cases, results in 8%-20% of cases with cirrhosis and HCC[19]. Persistent hepatitis is a mild disease that occurs in 8%-10% of patients, occasionally causing elevated aminotransferases, but generally does not progress toward cirrhosis and has a favorable prognosis[20]. HBV plays a significant role in the development of HCC, which can occur many years after chronic infection[21]. Still, typically the HBV is not a cytopathogen, and cell damage is thought to be mediated by a persistently unproductive immune response[17].

Therefore, this mini-review highlights the significance of the circadian rhythm in HBV infection, and the effectiveness of therapy in relation to the circadian rhythm-dependent immune response.

HBV

The epidemiological model of the spread of HBV and human immunodeficiency virus (HIV) is the same, but HBV is 50-100 times more infectious than HIV[22]. The source of infection is people with HBV infection[23]. However, the geographical prevalence of HBV infection varies[24]. In addition, it depends

on several factors, such as different modes of transmission in the population and the age at which the infection originated, which relates to the likelihood of progression to chronic infection[25].

HBV is mainly transmitted by percutaneous or mucosal exposure to infected blood or body fluids [26]. Perinatal transmission is the primary route of infection in endemic regions[27], while the most direct route in the low-endemic regions is sexual transmission[28]. Globally, the epidemiology of HBV infection is changing, influenced by infant vaccination programs and migration between low- and high-prevalence populations[29]. On the basis of the available data, it is estimated that the prevalence of new chronic HBV cases is 70% in developing countries[30].

On the basis of the prevalence of the HBsAg, the epidemiology of HBV in certain areas of the world can be classified into one of three categories (Table 1)[31]: Low prevalence areas (< 2%), medium prevalence areas (2%-7%), and high prevalence areas (> 8% HBsAg prevalence)[32]. These categories are important for understanding the transmission and outcome of infection, and the consequences of chronic hepatitis B[25].

Biology and life cycle of HBV

HBV is a DNA virus with ten known genotypes, labeled A-J. HBV belongs to the group of hepatotropic viruses from the family Hepadnaviridae, genus Orthohepadnavirus[33]. It is a small round virus of a very complex structure, 42 nm in diameter, with a double shell (Dane particle) (Table 2)[33]. Genotypes are divided into subgenotypes due to the significant variability of the nucleotide sequences[34]. They are based on a more than 4% difference along the entire genome. In addition, HBV genotypes and subgenotypes are related by geographical distribution, and also related to the pathogenesis and outcome of HBV infection (Table 3)[35].

The HBV genome has 3.2 kb long, relaxed circular, partially double-stranded DNA (rcDNA)[36]. The minus strand is complete, while the plus strand is regularly incomplete with a stable 5′ end, but an inconsistent 3′ end. The 5′ end of the plus strand is covalently linked to the RNA with a 5′ cap formation. In addition, the viral polymerase (reverse transcriptase) is covalently bound to the 5′ end of the minus strand[36,37].

Linear DNA is the direct precursor of viral DNA that is randomly incorporated into the hepatocytes' DNA throughout infection. Incorporated DNA has no role in virus replication[37,38]. The HBV genome is highly compact, with four open reading frames (ORFs) overlapping multiple times and encoding seven proteins[39]. All ORFs are identical orientations and encoded by the negative strand of DNA[40]. Thanks to the ORFs, the coding capacity increases, and DNA is transcribed one and a half to two times because there is no stop codon[41]. In addition to ORF, there are six start codons, four promoters, and two transcription enhancers[42].

ORF C encodes the nuclear core antigen HBc and envelope E antigen (HBe)[39]. The precore protein in serum indicates active virus replication[43]. The presence of HBeAg in serum suggests prevented or decreased virus replication. HBeAg can repress the cellular immune response to HBsAg, thereby reducing perinatal transmission and promoting chronic infection[37,44]. The longest ORF is the P gene, encoding most of the virus genome (80%) and viral polymerase (reverse transcriptase)[45]. The ORF X encoding hepatitis B protein X (HBx) activates viral RNA transcription[37,38]. HBx causes the progression of the cell cycle and is essential for activating the transcription of covalently closed circular DNA (cccDNA) and pregenomic RNA (pgRNA) after infection[37]. ORF S codes three different sizes of the surface S antigen (S-small, M-medium, and L-large HBs)[46]. The M- and L-HBs have additional PreS2 and PreS1 domains[39]. The PreS1 region, present in L-HBsAg, possesses a binding domain for the sodium taurocholate co-transporting polypeptide (NTCP) receptors, essential for viral internalization[37,47]. HBsAg are embedded in the outer lipid envelope, and the inner nucleocapsid structure contains the DNA genome, HBcAg, and viral polymerase (reverse transcriptase)[48]. In addition, HbeAg is between the nucleus and the outer shell[49].

HBV replicates in hepatocytes *via* pgRNA (Figure 1)[35]. The entry of the virus into the hepatocyte is the first step in its life cycle[50]. After the virus enters the liver, S-HBsAg recognizes heparan sulfate proteoglycans (HSPG) on the hepatocytes, and binds them with low affinity[51]. A high-affinity interaction between the PreS1 region of the L-HBs protein and NTCP follows[52]. Later, the virus envelope and the hepatocytes' membrane merge, releasing the nucleocapsid into the cytoplasm[53]. After the capsid shell is removed, the viral genome is transferred to the nucleus. As a result, viral DNA enters the nucleus of the hepatocytes. The relaxed circular (rc) genome is restored, resulting in cccDNA [54]. Viral DNA can be integrated into the hepatocytes' DNA, and is a constant HBsAg source[55]. The cccDNA is a template for pgRNA production and the transcription of all viral mRNAs[37]. On this basis, cccDNA in the hepatocytes can stimulate virus replication[56]. The cccDNA is associated with cellular histones and forms a minichromosome. Each viral protein has a promoter and mRNA, except for reverse transcriptase, translated from the same pgRNA as the virus core protein[37,44]. The onset of infection is indicated by the expression of core proteins and polymerase from pgRNA. HBc is a phosphoprotein and a subunit of the viral nucleocapsid. The core proteins are constructed into nucleocapsids, icosahedral shells of 120 dimers[57]. They merge with RNA and are assembled into core particles. Viral DNA synthesis takes place in the core particles, followed by packaging of pgRNA and polymerase[37,47]. Upon completing viral DNA synthesis by reverse transcription, viral particles can exit the hepatocytes in two ways. First, while envelope protein levels are low, core particles recycle and

Table 1 Prevalence of hepatitis B surface antigen

	Low prevalence area (< 2%)	Area of medium prevalence (2%-7%)	Area of high prevalence (> 8%)
Geographical areas	United states, Canada, and Western European countries	Parts of Russia, border Eurasian, and Asian-African areas	Asia, sub-Saharan Africa, South, and Central America
% of the world population	12%	43%	45%

Table 2 Classification of hepatitis B virus

Genus	Orthohepadnavirus
Family	Hepadnaviridae
Species	HBV
Genotypes	A-J
Virion	42 nm, spherical
Envelope	Yes (HBs)
Genome	Circular ds/ssDNA
Genome size	3.2 kb
Sensitivity	Acid-sensitive
Virus antigens	HBsAg, HBcAg, HBeAg, polymerase

HBV: Hepatitis B virus; HBs: Hepatitis B surface protein; ds/ssDNA: Double-stranded/single-stranded DNA; HBsAg: Hepatitis B surface antigen; HBcAg: Hepatitis B nuclear core antigen; HBeAg: Hepatitis B envelope E antigen.

Table 3 Prevalence of hepatitis B virus genotypes and subgenotypes

Genotype	Subgenotype	Prevalence
A	A1 -A6	Africa, India, Northern Europe, USA
B	B1-B8	Asia, USA
C	C1-C14	Asia, USA
D	D1-D9	India, Middle East, Southern Europe, USA
E	F1-F4	West and South Africa
F		Central and South America
G		Europe, USA
H		Central and South America, California (USA)
I	I1-12	Vietnam
J		Japan

USA: United States.

enter the nucleus, resulting in the replenishment of cccDNA[37,39]. Later, the core particles gather with the envelope proteins in the endoplasmic reticulum, enter the secretory pathway, and are discharged from hepatocytes into the blood[58]. In addition to infectious virions (Dane particles), incomplete subviral particles are secreted by secretory pathways (such as spheres and filaments lacking nucleocapsid proteins and naked nucleocapsids)[59]. The virus emerges on the surface of the hepatocytes by budding, and can thus infect another cell[52]. Once created in the cell nucleus, the cccDNA minichromosome is very difficult to eliminate from infected cells, where it can survive until the death of the host cell[56].

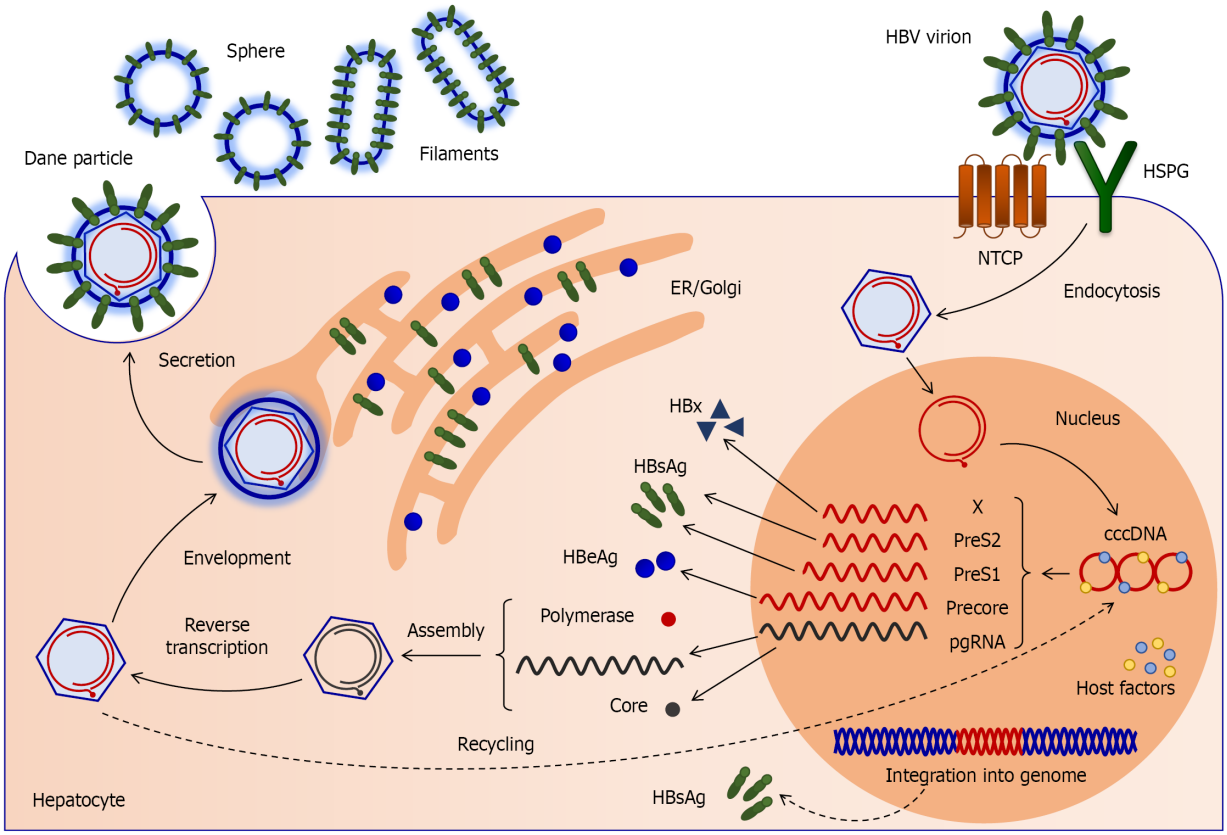

DOI: 10.3748/wjg.v28.i27.3282

Figure 1 Hepatitis B virus life cycle. Hepatitis B virus (HBV) enters hepatocytes *via* interaction with the heparan sulfate proteoglycan (HSPG), followed by the sodium taurocholate co-transporting polypeptide (NTCP) receptor. The virus envelope and the hepatocytes' membrane merge, releasing the nucleocapsid into the cytoplasm. The viral genome is transferred to the nucleus after the capsid is removed. The relaxed circular genome is restored in the nucleus, resulting in covalently closed circular DNA (cccDNA), and viral DNA could be integrated into the host DNA. Integrated viral DNA is a constant source of hepatitis B surface antigen (dashed line). The cccDNA is a template for pregenomic RNA (pgRNA) production and the transcription of all viral mRNAs. In addition, the cccDNA is associated with host factors and cellular histones, and forms a minichromosome. The core proteins are constructed into nucleocapsids together with pgRNA. Viral polymerase converts the pgRNA to relax circular DNA, resulting in a mature nucleocapsid. The core particles can recycle and replenish cccDNA (dashed line), or gather with the envelope proteins in the endoplasmic reticulum and Golgi, and enter the secretory pathway. Through the secretory process, virions gain surface antigens and are secreted as infectious virions-Dane particles. Also, incomplete subviral particles are secreted, such as spheres and filaments lacking nucleocapsid proteins. HSP: Heparan sulfate proteoglycan; NTCP: Sodium taurocholate co-transporting polypeptide receptor; cccDNA: Covalently closed circular DNA; pgRNA: Pregenomic RNA; HBx: Hepatitis B protein X; HBsAg: Hepatitis B surface antigen; HBe: E antigen; ER: Endoplasmatic reticulum.

CIRCADIAN RHYTHM

The molecular basis of the circadian rhythm includes transcriptional and translocation feedback loops. In addition, the circadian rhythm is driven by the circadian locomotor output cycles kaput (CLOCK), and brain and muscle ARNTL-like protein 1 (BMAL1 or ARNTL) transcription factors. In contrast, transcription repressors are period (PER) and cryptochrome (CRY) transcription factors. The central transcription factors that make up the activation and positive part of the molecular clock are BMAL1 and CLOCK. The heterodimer CLOCK-BMAL1 enters the nucleus, where it initiates transcription by binding to a specific sequence, the E-box, in promoters of the target genes. CLOCK's main downstream goals include *BMAL1* and its repressors, cryptochrome (*CRY1*, *CRY2*), and period (*PER1*, *PER2*, and *PER3*) and multiple CCG[60]. CRYs and PERs accumulate during the positive loop in the cytoplasm. They are controlled by F-box/LRR-repeat protein 3 (FBXL3) and casein kinase 1 (CK1) ε and CK1δ[4,61]. CK1ε and CK1δ phosphorylate PERs for degradation, while FBXL3 stimulates CRYs degradation. If CK1ε phosphorylates heterodimer PER-CRY, it enters the nucleus and suppresses the CLOCK-BMAL1 heterodimer. By suppressing their activator, CRYs and PERs suppress their own expression[62]. Posttranslational phosphorylation of CRYs and PERs promotes their degradation, which triggers a new circadian cycle, with increased binding of the CLOCK-BMAL1 heterodimer to the E-box of CCG[2,63].

The second regulatory loop includes the retinoic acid receptor-related orphan receptor (*ROR*) α and *RORγ*, and the *REV-ERBα* and *REV-ERBβ* genes. The CLOCK-BMAL1 heterodimer initiates their transcription by binding to the E-box elements of their promoters. RORs and REV-ERBs receptors bind to the ROR element (RORE). REV-ERBα and β inhibit transcription, while RORα and γ stimulate expression of target genes. RORs and REV-ERBs together create cyclic fluctuations in the expression of

many CCG, including the regulation of *BMAL1* transcription[6,64]. REV-ERBα accumulates rapidly and prevents *BMAL1* transcription, while RORα accumulates more slowly and promotes *BMAL1* transcription. In this way, the stability and robustness of the rhythmicity of the internal clock system are enhanced[2,63].

An additional independent feedback loop includes the helix-loop-helix e40 family (DEC1 or BHLHE40) and DEC2 (BHLHE41) that prevent CLOCK-BMAL1 activity[65]. The CLOCK-BMAL1 heterodimer stimulates the expression of *DEC1* and *DEC2* by binding to the E-box of their promoters. Conversely, DECs suppress transcription of genes with E-box elements in the promoter, including transcription of itself and CRYs and PERs, due to its binding to the E-box[66]. In addition, the CLOCK-BMAL1 heterodimer affects the expression of other CCG by stimulating D-box binding protein (DBP) transcription, by binding to E-box elements on the promoter[67]. DBP rhythmically triggers genes with D-box elements in the promoter[2,4].

The transcriptional and translational feedback loop creates rhythms in the expression and levels of downstream CCG[4]. All of these connected feedback loops create a circadian rhythm. For example, CCGs containing RORE elements in promoters are transcribed during the active phase. In contrast, the genes' promoters containing E-box and D-box elements are transcribed during the resting phase[63].

The circadian rhythm is controlled at the transcriptional and posttranslational levels, including cellular pathways, transcription factors, epigenetic changes, and posttranslational modifications[68]. Many posttranslational modifications of clock elements include acetylation, phosphorylation, ubiquitylation, and sumoylation[4,63]. Epigenetic modifications, such as DNA methylation, histone modifications, and non-coding RNAs, interfere with the target genes' transcription and post-transcriptional expression, including clock genes[69]. Different patterns of histone modifications, such as histone deacetylase sirtuin 1 (SIRT1), or microRNA, can be direct and indirect modulators in maintaining different aspects of circadian rhythm function[53,70].

Liver physiology and circadian rhythm

With a lack of environmental signs, such as the alternation of light and dark, food intake affects the circadian rhythm of the liver[6]. Circadian rhythms largely control different genes, levels of proteins, and the enzymes in the liver[2]. The circadian rhythm and liver metabolism are connected through the peroxisome proliferator-activated receptors (PPARs) α and γ[6,71]. PPARα controls the transcription of genes participating in lipid and glucose metabolism, while PPARγ is involved in lipogenic processes because it binds eicosanoids from omega-3 or omega-6 fatty acids[4,72]. Both genes are rhythmically expressed, and their expression is controlled by PER2, which directly regulates *BMAL1* transcription (Figure 2). The binding of PPARα to PPAR response elements (PPRE) in the *BMAL1* promoter leads to its transcription. Also, PPARα interacts with PER2 in the liver to impact the expression of target genes [73]. In the positive feedback loop in the liver, BMAL1 and CLOCK control the circadian oscillations of *PPARα*[4], and thus the expression of enzymes participating in glucose and lipid homeostasis, and the biosynthesis of bile acids and apolipoproteins[6]. REV-ERBα is implicated in the control of bile acid synthesis[74]. Adiponectin, triggered by BMAL1 and CLOCK *via* the transcription of *PPARγ* and its coactivator 1α (PGC-1α), is involved in glucose and lipid metabolism[75].

In addition, gluconeogenesis is controlled in a circadian manner in the liver *via* CRY1 and CRY2, which prevent signaling *via* the secondary messenger cyclic adenosine monophosphate (cAMP)[76]. Moreover, AMP-activated protein kinase (AMPK) can influence circadian cycle length by phosphorylating CRYs and directing it to degradation[4]. Activation of RORα in the liver may impact lipid metabolism and control hepatic steatosis by triggering AMPK[77]. Furthermore, CLOCK controls glycogenesis in the liver by acting on glycogen synthase 2 expression[78]. Disorders of the *CLOCK* and *BMAL1* genes lead to impaired glucose homeostasis[6]. Histone deacetylase SIRT1 prevents hepatic steatosis by controlling lipid homeostasis by positive binding of PPARα and PGC1α coactivators, or by direct action on BMAL1[70].

Circadian rhythm and HBV

There is a functional association between virus replication and circadian dysfunction in the pathogenesis of liver disease[79]. HBV has been revealed to impact the liver clock genes and disrupt the internal molecular clock in order to make better use of hepatocytes for self-replication[80]. HBV is randomly incorporated into the human genome, yet there are sites where it is incorporated more frequently, such as circadian rhythm-related elements, *CLOCK*, and *BMAL1*. Those elements are one way that the circadian rhythm is associated with diseases caused by HBV infection[81]. HBV replicates in the liver where around 20% of genes exhibit a rhythmic expression pattern, implying that the virus has successfully evolved to persist in the liver[5,50]. Integrated copies of HBV, which have regulatory elements similar to circadian rhythm genes, present additional circadian rhythm motifs in the infected cell, resulting in undesirable oscillations of specific genes, or disrupted circadian rhythms of the hepatocytes, and are a risk factor for cancer[50].

The circadian rhythm impacts gene expression in the liver and thus HBV replication[50]. In patients with HBV infection, a reduction in *BMAL1* and an increase in *REV-ERBα* and *REV-ERBβ* transcription have been observed compared to healthy subjects, which indicates that circadian rhythm gene transcription is impaired in HBV infection[50]. In hepatocytes, decreased expression or deletion of *REV-*

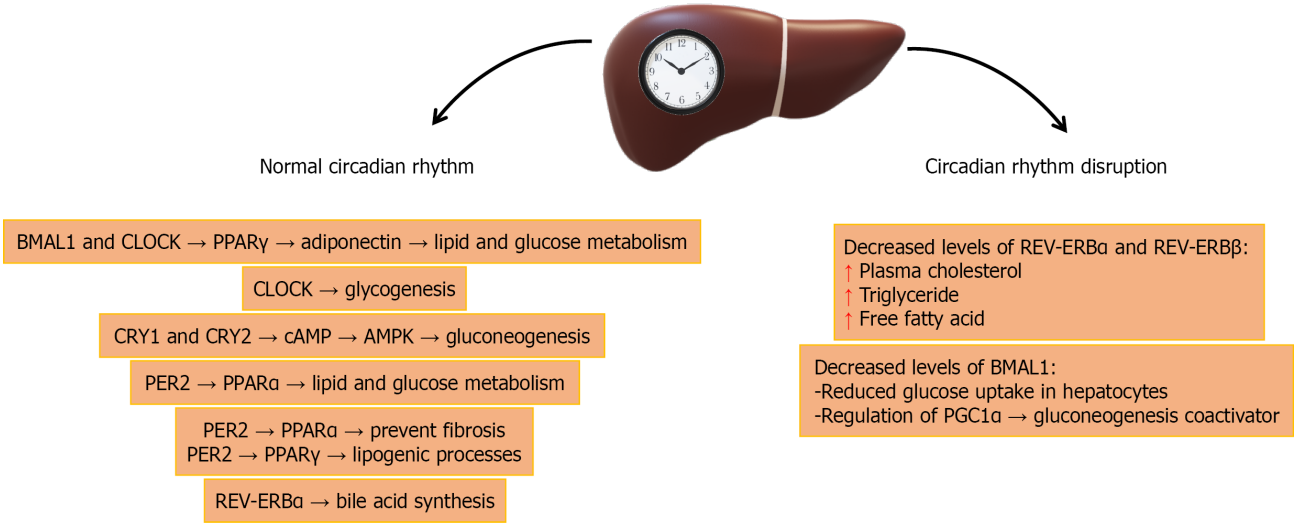

DOI: 10.3748/wjg.v28.i27.3282

Figure 2 Role of circadian rhythm genes in liver metabolism. BMAL1: Brain and muscle ARNTL-like protein 1; CLOCK: Circadian locomotor output cycles kaput; PPAR: Peroxisome proliferator-activated receptors; CRY: Cryptochrome; PER: Period; ROR: Retinoic acid receptor-related orphan receptor; cAMP: Cyclic adenosine monophosphate; AMPK: AMP-activated protein kinase; PGC1α: PPAR coactivator 1α.

ERBα and *REV-ERBβ* in hepatocytes increases plasma cholesterol, triglycerides, and free fatty acid levels [63]. In addition, REV-ERB binds and controls NTCP expression, and stimulation of *REV-ERB* prevents HBV from entering the hepatocytes[50]. The NTCP receptor has a circadian pattern in hepatocytes[82]. Decreased expression of *BMAL1* in hepatocytes leads to reduced glucose uptake. In addition, BMAL1 regulates the transcription of the *PGC1α* gene, a coactivator of gluconeogenesis[63]. Thus, PPARα can prevent the development of fibrosis[63], and it is known that HBV dysregulates PPARα and PPARγ[6]. Also, BMAL1 binds HBV DNA, and controls viral genome expression and new viral particle formation [50].

The impaired circadian rhythm in HCC may favor the selective survival of cancer cells and facilitate carcinogenesis[83]. An increased risk of developing HCC is linked with chronic HBV infection. The HBx protein is linked with HCC due to the disturbance of cell proliferation[19]. It is a possible cause of significantly reduced transcription levels of the *BMAL1*, *PER3*, *CRY1*, *CRY2*, and *CK1ε* genes in HCC [84]. At the same time, elevated HBx expression in HCC results in increased *CLOCK*, *PER1*, and *PER2* expression[1,85]. In addition, abnormal expression of *REV-ERBα* was observed in a cell line that stably expressed HBV[86]. The circadian rhythm acts *via* REV-ERBα in the liver on hepatocyte nuclear factor 4 alpha (HNF4α), and thus directs the action of glucocorticoid receptors on energy metabolism (Figure 3). Consequently, the interactions between CRY and glucocorticoid receptors affect carbohydrate metabolism, hence transacting *PER2*[87]. HNF4α increases the transcription of pgRNA in hepatoma cells and thus affects HBV biosynthesis[88]. In addition, P2-HNF4α inhibits the expression of *BMAL1*, leading to the localization of P1-HNF4α from the nucleus to the cytoplasm. *BMAL1* is expressed in healthy hepatocytes, but tumor growth is prevented if *BMAL1* expression is induced in HNF4α-positive tumor cells[89]. The possible reason for the inhibition of tumor growth is that BMAL1 mediates the transcription of *P53* pathway genes, a well-known tumor-suppressor gene[90]. DNA viruses rely more on host transcription for gene expression; however, *BMAL1* deficiency increases virus replication. REV-ERBα has a protective effect because it reduces the inflammatory response, thus decreasing the severity of the disease. Thus, REV-ERBα agonists inhibit HBV replication, while BMAL1 promotes virus replication. Nevertheless, as BMAL1 stimulates oscillations in genes that metabolize drugs and sensitivity to toxicity, it also promotes HBV infection in hepatocytes[91].

HBV infection leads to overexpression of *RORα* and *RORγ*[92]. *RORγ* overexpression is associated with promoter methylation and HBx protein. Furthermore, HBx-induced *RORγ* may facilitate the proliferation and migration of hepatoma cells[93], and RORα may be a possible diagnostic and prognostic biomarker for disease severity[94]. Overexpression of *RORα*, *CRY2*, and *PER1* is associated with a better survival of HCC patients, and regulating the circadian rhythm gene may help in the chronotherapy of such patients[94]. HBV infection leads to disruptions of the *CLOCK* gene and its downstream circadian genes and other CCGs[2]. All the above indicates that circadian rhythm disorders caused by a virus may contribute to the pathogenesis of cancer.

Immunopathogenesis of chronic HBV infection and circadian rhythm

Clinical manifestations of chronic hepatitis B result from a cellular and humoral immune response to the recognized target antigenic viral epitopes, HBcAg and HBsAg[21]. Integration of HBV into the

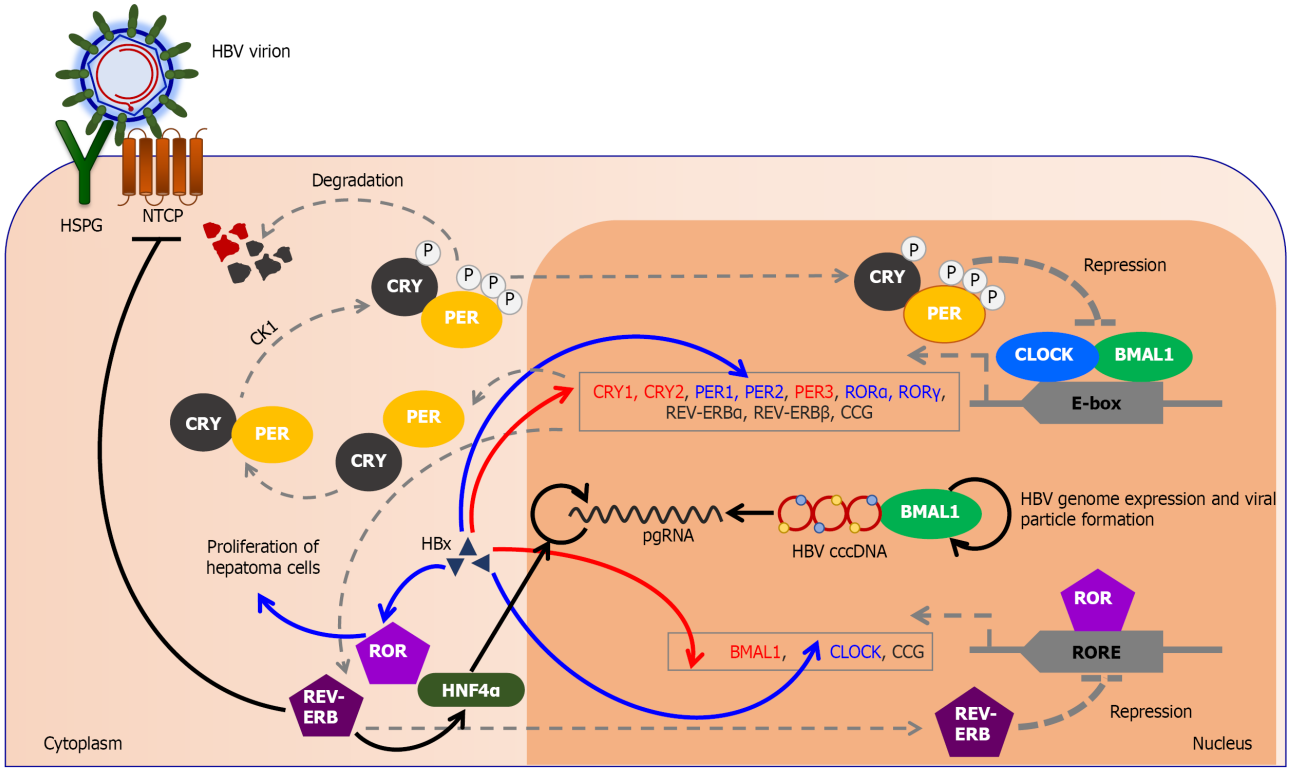

DOI: 10.3748/wjg.v28.i27.3282

Figure 3 Relationship between circadian rhythm genes and hepatitis B virus replication. Gray dashed lines indicate normal circadian rhythm in hepatocytes. Black arrows show the association between core clock proteins and hepatitis B virus (HBV) entry into hepatocytes and its replication. Increased levels of REV-ERB protein prevent the entry of HBV into hepatocytes by impaired action on the sodium taurocholate co-transporting polypeptide (NTCP) receptor. Brain and muscle ARNTL-like protein 1 (BMAL1) protein binds HBV DNA and thus controls viral genome expression and the formation of new viral particles. In infected hepatocytes, REV-ERB through HNF4α mediator increases pregenomic RNA (pgRNA) transcription, while HNF4α inhibits BMAL1 expression, promoting HBV replication. Red arrows indicate circadian rhythm genes inhibited by hepatitis B protein X (HBx) protein (BMAL1, CRY1, CRY2, and PER3). Conversely, HBx increases *CLOCK*, *PER1*, *PER2*, and *RORγ* gene expression (indicated by blue arrows). Increased expression of *RORγ* leads to the proliferation of hepatoma cells. BMAL1: Brain and muscle ARNTL-like protein 1; cccDNA: Covalently closed circular DNA; CCG: Clock-controlled genes; CLOCK: Circadian locomotor output cycles kaput; CK1: Casein kinase 1; CRY: Cryptochrome; HBx: Hepatitis B protein X; HNF4α: Hepatocyte nuclear factor 4 alpha; HSP: Heparan sulfate proteoglycan; NTCP: Sodium taurocholate co-transporting polypeptide receptor; PER: Period; pgRNA: Pregenomic RNA; ROR: Retinoic acid receptor-related orphan receptor; RORE: ROR element.

hepatocytes' genome serves as a constant source of HBsAg during chronic infection. It may induce dysfunctional T-cell responses, and favor harmful immunopathology and disease progression to fibrosis and cirrhosis[95]. Hepatocytes expressing HBcAg are recognized and attacked by cytotoxic $CD8^+$ lymphocytes (CTL)[96]. The increase in alanine aminotransferase is the result of hepatocyte lysis[97]. HBcAg has strong immunogenicity and can cause the antigen-specific T-cell responses necessary for controlling HBV infection. HBcAg stimulates the production of interleukin 6 (IL)-6, IL-10, IL-17A, IL-22, IL-23, and transforming growth factor β (TGFβ) by peripheral blood mononuclear cells[98]. In addition, the immunosuppressive cytokine IL-10 negatively controls the expansion of Th17 cells, which plays a part in the existence and promotion of HBV infection[46]. Persistent HBV infection is marked by a poor immune response due to the poor response of $CD4^+$ lymphocytes in the early phases of infection. This results in qualitatively and quantitatively weaker $CD8^+$ T cell responses[21].

In addition to other viral proteins, HBeAg is also important for the persistence of infection, as it suppresses the humoral and cellular immune response to HbcAg, weakens the action of CTL on HBcAg, and allows the maintenance of the infection[99]. The predominance of Th-1 over the Th-2 cytokine response, with the production of IL-2, interferon-alpha (IFN-α), and lymphotoxin-β receptor (LT-βR), is responsible for virus elimination during acute and chronic HBV infections[100]. Conversely, the predominance of Th-2 cytokine response is responsible for maintaining chronic infection, with IL-4, IL-5, and IL-10, which enhance the humoral immune response[98].

Many innate and adaptive immune system elements are under circadian regulation[1], and the adaptive immune response mediates virus removal and liver disease[95]. Cellular immune rhythms are synchronized with the central clock in the SCN[6]. Innate and adaptive immune system cells have a molecular clock that controls their rhythmic activity over 24 h[101]. Certain functions of the innate immune system rely on the hepatocytes' circadian rhythm[5,65]. Increased amounts of pro-inflammatory hormones such as growth hormone, prolactin, and melatonin and cytokines such as IL-1 and TNF-α are present during the rest period. In addition, immune rhythms are affected by hormonal

rhythms, so cortisol regulates the number of naive T cells. Epinephrine influences the number of CTL cells over 24 h[102].

Furthermore, the transcription factor CRY2 links the circadian rhythm and the innate immune system [103]. Moreover, CLOCK and BMAL1 control transcription of the pattern recognition receptor, which is involved in nucleic acid detection during viral infections[104]. RORγ regulates the differentiation of Th17 cells, which secrete IL-17, an essential regulator of pro-inflammatory signaling[93]. REV-ERBα has a protective effect in various inflammatory processes[105]. Additionally, the suppression of REV-ERB receptors elevates virus-associated mortality by promoting the inflammatory response[106]. The circadian hormone melatonin has protective and antiviral actions and a role in the inflammatory response[105]. Melatonin increased IFN-γ levels during viral infection, decreased Venezuelan equine encephalomyelitis virus (VEE) levels, and reduced mortality rates in mice infected with VEE. The protective impact of melatonin is associated with increased IL-1β production because it acts as a cytokine modulator and antioxidant[107]. This shows the positive role of the circadian rhythm in regulating antiviral immunity[91].

ANTIVIRAL THERAPY

There are two main drugs for HBV infection therapy: Nucleoside/nucleotide analogs (NAs), which interfere with viral DNA synthesis during reverse transcription, and IFN-α[108,109]. NAs effectively inhibit virus replication and may suppress the generation of new cccDNA[109]. Existing drugs can suppress virus replication, slow fibrosis progression, and decrease infectivity, but rarely remove the cccDNA responsible for HBV persistence[108]. Therefore, the development of therapy aims to achieve a "functional healing" state, *i.e.*, the removal of cccDNA from hepatocytes[110,111]. However, in the treatment of HBV infection, NAs rarely eliminate the virus, that is, they do not eradicate HBV from the liver[95]. This is because each HBV surface protein (S, M, and L) has an HBsAg determinant. Therefore, HBsAg circulates in the bloodstream of HBV patients, mainly in non-infectious subviral spheres and filaments[95].

Alternative therapeutic strategies are based on silencing viral genes using RNA interference (RNAi) [108] and antisense oligonucleotide (ASO) technology[110]. Both approaches are based on the effective suppression of HBV replication in patients with chronic HBV infection[108,110]. RNAi is a mechanism for silencing genes after transcription, and can be used in mammalian cells against viral infections[108]. ASO technology prevents HBV antigen production by targeting all HBV genome transcripts in infected hepatocytes[10,110]. It is based on NAs that act on viral polymerase but do not influence the cccDNA transcription[110]. ASO and other nucleic acid-based therapies may potentially decrease the tolerogenic outcome of the high HBsAg levels characteristic of chronic infection[63,110].

Role of circadian rhythm in antiviral therapy

One of the principles of personalized medicine is to optimize the time of day for administration of drugs whose action is affected by the circadian rhythm[5,112]. Circadian oscillations can affect vaccine responses to viral pathogens[91]. The direct impact of the circadian rhythm on the cellular and humoral immune reaction is mediated by melatonin and cortisol. Research on the severe acute respiratory syndrome coronavirus 2 (SARS-CoV-2) has shown that melatonin can affect circadian clocks and modulate the immune response during viral infections and thus impact virus replication[113]. Therefore, vaccination in the morning or evening may impact the immune response to the vaccine[114]. Thus, it was observed that patients vaccinated against the SARS-CoV-2 in the morning had significantly lower C-reactive protein levels compared to patients vaccinated in the evening[115]. Making a simple effort to determine the appropriate time for administration of drugs or vaccine can improve the drug's effectiveness and reduce side effects[5]. However, studying the interaction of the circadian rhythm and virus replication may lead to a better knowledge of viral infections and the associated immune response, discovery of new antiviral targets, improvement of existing treatments, and therapy for chronic infections[5]. Chronic infection is linked with a weakened immune response, and poor T-cell responses that fail to control HBV replication[50]. The effectiveness of current antiviral therapies could be enhanced by modulating the timing of vaccine administration. For example, the engineered T cell receptor activity showed a circadian pattern upon antigen activation. However, this daily effect was attenuated in *CLOCK* mutant mice, emphasizing the importance of timing T cell therapy to maximize antiviral immunity[1].

Many studies show that the efficacy or toxicity of treatment depends on the dosing time in many diseases. Also, inter-individual variations in the circadian rhythm resulting from lifestyle differences should be considered[116]. The efficiency of the DNA virus vaccine can be enhanced by specifying the time of day for vaccination. For example, some studies have found that patients immunized in the morning produce a more significant antibody response to hepatitis A and influenza vaccines[1,117]. In addition, morning vaccination is considered to significantly increase responses to viral-specific antibodies, compared to afternoon vaccination[1]. As viruses are intracellular pathogens that replicate within host cells, given the high association of circadian rhythm transcription factors with cell

transcription, the circadian rhythm plays a vital role in determining host susceptibility to viral infections and the immune response[1].

Circadian clock-modulating small molecules may help inhibit or activate circadian rhythm proteins and enzymes in viral infections. Thus, the small molecule SRT2183 modulates the circadian clock that inhibits SARS-CoV-2 replication[118] because it modulates physiological and circadian rhythm gene expression[119]. Inhibiting *BMAL1* expression and overexpression of *REV-ERB via* circadian rhythm-modulating small molecules may prevent dengue virus, hepatitis C virus, Zika virus, and HIV1 virus replication. In addition, clock genes have antiviral abilities that can be applied to HBV[120]. One of the effective circadian clock-modulating small molecules in treating HBV infections is GSK4112, a synthetic ligand for REV-ERB, but it is not suitable for *in vivo* use due to its poor pharmacokinetic properties. In contrast, ARN5187 is a REV-ERBβ agonist with dual function, an inhibitor of REV-ERB and autophagy [121]. SR9009 is a REV-ERBα agonist based on the chemical structure of GSK4112. It has better pharmacokinetic properties than GSK4112 and affects many oncogenes. In addition, REV-ERBα is known to regulate cancer development by inhibiting proliferation[121], and hence SR9009 inhibits *BMAL1* and prevents the entry and replication of HBV into hepatocytes[50].

Challenges associated with antiviral drug development, including circadian clock-modulating small molecules, may be adverse effects or suboptimal pharmacokinetics. Therefore, for an antiviral agent to succeed, the target drug should be distributed locally to avoid unfavorable consequences on other tissues.

CONCLUSION

Interaction exists between viruses and the circadian rhythm of hepatocytes. Infection susceptibility depends on the infectivity of the inoculum, the mode of transmission, the length of exposure to the virus, and the time of the day infection occurs[1]. Understanding how HBV interacts with the circadian rhythm of hepatocytes may influence the treatment of infections[1]. Viruses are among the most critical human carcinogens[6], and pharmacotherapy and chronotherapy should be united to treat or prevent viral infections[1]. Research on the impact of viral infections on the circadian rhythm may help detect new antiviral targets and optimize the timing of immune-based therapies[1]. The main challenge in treating HBV infection is eradicating or silencing the cccDNA[50]. By acting on specific components of the circadian rhythm, such as REV-ERB and BMAL1, HBV can be prevented from entering hepatocytes and producing new virions. In addition to lifestyle changes, circadian rhythm-focused approaches may provide new therapeutic options in treating HBV infections[63].

FOOTNOTES

Author contributions: Škrlec I did the majority of the writing and prepared the figures; Talapko J did some writing and prepared the tables; all authors have read and approved the final manuscript.

Conflict-of-interest statement: There are no conflicts of interest to report.

Country/Territory of origin: Croatia

ORCID number: Ivana Skrlec 0000-0003-1842-930X; Jasminka Talapko 0000-0001-5957-0807.

S-Editor: Chen YL
L-Editor: Wang TQ
P-Editor: Chen YL

REFERENCES

1 **Zhuang X**, Rambhatla SB, Lai AG, McKeating JA. Interplay between circadian clock and viral infection. *J Mol Med (Berl)* 2017; **95**: 1283-1289 [PMID: 28963570 DOI: 10.1007/s00109-017-1592-7]

2 **Zhou D**, Wang Y, Chen L, Jia L, Yuan J, Sun M, Zhang W, Wang P, Zuo J, Xu Z, Luan J. Evolving roles of circadian rhythms in liver homeostasis and pathology. *Oncotarget* 2016; **7**: 8625-8639 [PMID: 26843619 DOI: 10.18632/oncotarget.7065]

3 **Škrlec I**, Milic J, Heffer M, Peterlin B, Wagner J. Genetic variations in circadian rhythm genes and susceptibility for myocardial infarction. *Genet Mol Biol* 2018; **41**: 403-409 [PMID: 29767668 DOI: 10.1590/1678-4685-GMB-2017-0147]

4 **Saran AR**, Dave S, Zarrinpar A. Circadian Rhythms in the Pathogenesis and Treatment of Fatty Liver Disease. *Gastroenterology* 2020; **158**: 1948-1966.e1 [PMID: 32061597 DOI: 10.1053/j.gastro.2020.01.050]

5 **Borrmann H**, McKeating JA, Zhuang X. The Circadian Clock and Viral Infections. *J Biol Rhythms* 2021; **36**: 9-22 [PMID: 33161818 DOI: 10.1177/0748730420967768]

6 **Vinciguerra M**, Mazzoccoli G, Piccoli C, Tataranni T, Andriulli A, Pazienza V. Exploitation of host clock gene machinery by hepatitis viruses B and C. *World J Gastroenterol* 2013; **19**: 8902-8909 [PMID: 24379614 DOI: 10.3748/wjg.v19.i47.8902]

7 **Cheng Z**, Lin P, Cheng N. HBV/HIV Coinfection: Impact on the Development and Clinical Treatment of Liver Diseases. *Front Med (Lausanne)* 2021; **8**: 713981 [PMID: 34676223 DOI: 10.3389/fmed.2021.713981]

8 **Al-Sadeq DW**, Taleb SA, Zaied RE, Fahad SM, Smatti MK, Rizeq BR, Al Thani AA, Yassine HM, Nasrallah GK. Hepatitis B Virus Molecular Epidemiology, Host-Virus Interaction, Coinfection, and Laboratory Diagnosis in the MENA Region: An Update. *Pathogens* 2019; **8** [PMID: 31083509 DOI: 10.3390/PATHOGENS8020063]

9 **Liang Y**, Bai X, Liu X, Zhang Z, Pang X, Nie L, Qiu W, Zhao W, Hu G. Hepatitis B Vaccination Coverage Rates and Associated Factors: A Community-Based, Cross-Sectional Study Conducted in Beijing, 2019-2020. *Vaccines (Basel)* 2021; **9** [PMID: 34696178 DOI: 10.3390/VACCINES9101070]

10 **Yuen MF**, Heo J, Jang JW, Yoon JH, Kweon YO, Park SJ, Tami Y, You S, Yates P, Tao Y, Cremer J, Campbell F, Elston R, Theodore D, Paff M, Bennett CF, Kwoh TJ. Safety, tolerability and antiviral activity of the antisense oligonucleotide bepirovirsen in patients with chronic hepatitis B: a phase 2 randomized controlled trial. *Nat Med* 2021; **27**: 1725-1734 [PMID: 34642494 DOI: 10.1038/s41591-021-01513-4]

11 **Splawn LM**, Bailey CA, Medina JP, Cho JC. Heplisav-B vaccination for the prevention of hepatitis B virus infection in adults in the United States. *Drugs Today (Barc)* 2018; **54**: 399-405 [PMID: 30090877 DOI: 10.1358/dot.2018.54.7.2833984]

12 **Kappus MR**, Sterling RK. Extrahepatic manifestations of acute hepatitis B virus infection. *Gastroenterol Hepatol (N Y)* 2013; **9**: 123-126 [PMID: 23983659 DOI: 10.1016/s0976-0016(11)60191-9]

13 **Chen L**, Bao D, Gu L, Gu Y, Zhou L, Gao Z, Huang Y. Co-infection with hepatitis B virus among tuberculosis patients is associated with poor outcomes during anti-tuberculosis treatment. *BMC Infect Dis* 2018; **18**: 295 [PMID: 29970037 DOI: 10.1186/s12879-018-3192-8]

14 **Yue L**, Li C, Xu M, Wu M, Ding J, Liu J, Zhang X, Yuan Z. Probing the spatiotemporal patterns of HBV multiplication reveals novel features of its subcellular processes. *PLoS Pathog* 2021; **17**: e1009838 [PMID: 34370796 DOI: 10.1371/journal.ppat.1009838]

15 **Le Bert N**, Gill US, Hong M, Kunasegaran K, Tan DZM, Ahmad R, Cheng Y, Dutertre CA, Heinecke A, Rivino L, Tan A, Hansi NK, Zhang M, Xi S, Chong Y, Pflanz S, Newell EW, Kennedy PTF, Bertoletti A. Effects of Hepatitis B Surface Antigen on Virus-Specific and Global T Cells in Patients With Chronic Hepatitis B Virus infection. *Gastroenterology* 2020; **159**: 652-664 [PMID: 32302614 DOI: 10.1053/j.gastro.2020.04.019]

16 **Terrault NA**, Lok ASF, McMahon BJ, Chang KM, Hwang JP, Jonas MM, Brown RS Jr, Bzowej NH, Wong JB. Update on prevention, diagnosis, and treatment of chronic hepatitis B: AASLD 2018 hepatitis B guidance. *Hepatology* 2018; **67**: 1560-1599 [PMID: 29405329 DOI: 10.1002/hep.29800]

17 **Lim HK**, Jeffrey GP, Ramm GA, Soekmadji C. Pathogenesis of Viral Hepatitis-Induced Chronic Liver Disease: Role of Extracellular Vesicles. *Front Cell Infect Microbiol* 2020; **10**: 587628 [PMID: 33240824 DOI: 10.3389/fcimb.2020.587628]

18 **Peng L**, Gao ZL, Wang YM, He DM, Zhao JM, Bai XF, Wang XJ, Peng L. Clinical Manifestations and Laboratory Tests of AECHB and Severe Hepatitis (Liver Failure). In: Ning Q. Acute Exacerbation of Chronic Hepatitis B. Dordrecht: Springer, 2019:1-89

19 **Alqahtani SA**, Colombo M. Viral hepatitis as a risk factor for the development of hepatocellular carcinoma. *Hepatoma Res* 2020; **6**: 58 [DOI: 10.20517/2394-5079.2020.49]

20 **Wu J**, Han M, Li J, Yang X, Yang D. Immunopathogenesis of HBV Infection. *Adv Exp Med Biol* 2020; **1179**: 71-107 [PMID: 31741334 DOI: 10.1007/978-981-13-9151-4_4]

21 **Cai Y**, Yin W. The Multiple Functions of B Cells in Chronic HBV Infection. *Front Immunol* 2020; **11**: 582292 [PMID: 33381113 DOI: 10.3389/fimmu.2020.582292]

22 **Kafeero HM**, Ndagire D, Ocama P, Kudamba A, Walusansa A, Sendagire H. Prevalence and predictors of hepatitis B virus (HBV) infection in east Africa: evidence from a systematic review and meta-analysis of epidemiological studies published from 2005 to 2020. *Arch Public Health* 2021; **79**: 167 [PMID: 34537079 DOI: 10.1186/s13690-021-00686-1]

23 **Nelson NP**, Easterbrook PJ, McMahon BJ. Epidemiology of Hepatitis B Virus Infection and Impact of Vaccination on Disease. *Clin Liver Dis* 2016; **20**: 607-628 [PMID: 27742003 DOI: 10.1016/j.cld.2016.06.006]

24 **MacLachlan JH**, Cowie BC. Hepatitis B virus epidemiology. *Cold Spring Harb Perspect Med* 2015; **5**: a021410 [PMID: 25934461 DOI: 10.1101/cshperspect.a021410]

25 **Nguyen MH**, Wong G, Gane E, Kao JH, Dusheiko G. Hepatitis B Virus: Advances in Prevention, Diagnosis, and Therapy. *Clin Microbiol Rev* 2020; **33** [PMID: 32102898 DOI: 10.1128/CMR.00046-19]

26 **Schillie S**, Vellozzi C, Reingold A, Harris A, Haber P, Ward JW, Nelson NP. Prevention of Hepatitis B Virus Infection in the United States: Recommendations of the Advisory Committee on Immunization Practices. *MMWR Recomm Rep* 2018; **67**: 1-31 [PMID: 29939980 DOI: 10.15585/mmwr.rr6701a1]

27 **Drazilova S**, Kristian P, Janicko M, Halanova M, Safcak D, Dorcakova PD, Marekova M, Pella D, Madarasova-Geckova A, Jarcuska P, HepaMeta Team. What is the Role of the Horizontal Transmission of Hepatitis B Virus Infection in Young Adult and Middle-Aged Roma Population Living in the Settlements in East Slovakia? *Int J Environ Res Public Health* 2020; **17** [PMID: 32397342 DOI: 10.3390/IJERPH17093293]

28 **Weis-Torres SMDS**, Fitts SMF, Cardoso WM, Higa Junior MG, Lima LA, Bandeira LM, Castro VOL, Carneiro FA, Iglecias LMM, Cesar GA, Tanaka TSO, Puga MAM, Rezende GR, Croda J, Lago BV, Motta-Castro ARC. High level of

exposure to hepatitis B virus infection in a vulnerable population of a low endemic area: A challenge for vaccination coverage. *Int J Infect Dis* 2020; **90**: 46-52 [PMID: 31589921 DOI: 10.1016/j.ijid.2019.09.029]

29 **de Villiers MJ**, Nayagam S, Hallett TB. The impact of the timely birth dose vaccine on the global elimination of hepatitis B. *Nat Commun* 2021; **12**: 6223 [PMID: 34711822 DOI: 10.1038/s41467-021-26475-6]

30 **Guimarães LCDC**, Brunini S, Guimarães RA, Galdino-Júnior H, Minamisava R, da Cunha VE, Santos JRS, Silveira-Lacerda EP, Souza CM, de Oliveira VLB, Albernaz GC, de Menezes TG, Rezza G. Epidemiology of hepatitis B virus infection in people living in poverty in the central-west region of Brazil. *BMC Public Health* 2019; **19**: 443 [PMID: 31035990 DOI: 10.1186/s12889-019-6828-8]

31 **Makuza JD**, Rwema JOT, Ntihabose CK, Dushimiyimana D, Umutesi J, Nisingizwe MP, Serumondo J, Semakula M, Riedel DJ, Nsanzimana S. Prevalence of hepatitis B surface antigen (HBsAg) positivity and its associated factors in Rwanda. *BMC Infect Dis* 2019; **19**: 381 [PMID: 31053097 DOI: 10.1186/s12879-019-4013-4]

32 **Fattahi MR**, Mehrabani D, Mehvarz S, Jaliani NZ, Alipour A, Davarpanah MA. The Seroprevalence of Hepatitis B in Akbar Abad Village, Kavar, Southern Iran. *Int J Prev Med* 2014; **5**: S223-S230 [PMID: 26622994]

33 **McNaughton AL**, D'Arienzo V, Ansari MA, Lumley SF, Littlejohn M, Revill P, McKeating JA, Matthews PC. Insights From Deep Sequencing of the HBV Genome-Unique, Tiny, and Misunderstood. *Gastroenterology* 2019; **156**: 384-399 [PMID: 30268787 DOI: 10.1053/j.gastro.2018.07.058]

34 **Locarnini SA**, Littlejohn M, Yuen LKW. Origins and Evolution of the Primate Hepatitis B Virus. *Front Microbiol* 2021; **12**: 653684 [PMID: 34108947 DOI: 10.3389/fmicb.2021.653684]

35 **Zhang ZH**, Wu CC, Chen XW, Li X, Li J, Lu MJ. Genetic variation of hepatitis B virus and its significance for pathogenesis. *World J Gastroenterol* 2016; **22**: 126-144 [PMID: 26755865 DOI: 10.3748/wjg.v22.i1.126]

36 **Tsukuda S**, Watashi K. Hepatitis B virus biology and life cycle. *Antiviral Res* 2020; **182**: 104925 [PMID: 32866519 DOI: 10.1016/j.antiviral.2020.104925]

37 **Seeger C**, Mason WS, Lai MMC. Molecular Biology of Hepatitis Viruses. In: Arias IM, Alter HJ, Boyer JL, Cohen DE, Shafritz DA, Thorgeirsson SS, Wolkoff AW. The Liver: Biology and Pathobiology. Oxford, UK: John Wiley & Sons, Ltd, 2020: 793-820

38 **Mohebbi A**, Lorestani N, Tahamtan A, Kargar NL, Tabarraei A. An Overview of Hepatitis B Virus Surface Antigen Secretion Inhibitors. *Front Microbiol* 2018; **9**: 662 [PMID: 29675010 DOI: 10.3389/fmicb.2018.00662]

39 **Seeger C**, Mason WS. Molecular biology of hepatitis B virus infection. *Virology* 2015; **479-480**: 672-686 [PMID: 25759099 DOI: 10.1016/j.virol.2015.02.031]

40 **Patel N**, White SJ, Thompson RF, Bingham R, Weiß EU, Maskell DP, Zlotnick A, Dykeman E, Tuma R, Twarock R, Ranson NA, Stockley PG. HBV RNA pre-genome encodes specific motifs that mediate interactions with the viral core protein that promote nucleocapsid assembly. *Nat Microbiol* 2017; **2**: 17098 [PMID: 28628133 DOI: 10.1038/nmicrobiol.2017.98]

41 **Ko C**, Su J, Festag J, Bester R, Kosinska AD, Protzer U. Intramolecular recombination enables the formation of hepatitis B virus (HBV) cccDNA in mice after HBV genome transfer using recombinant AAV vectors. *Antiviral Res* 2021; **194**: 105140 [PMID: 34284057 DOI: 10.1016/j.antiviral.2021.105140]

42 **Altinel K**, Hashimoto K, Wei Y, Neuveut C, Gupta I, Suzuki AM, Dos Santos A, Moreau P, Xia T, Kojima S, Kato S, Takikawa Y, Hidaka I, Shimizu M, Matsuura T, Tsubota A, Ikeda H, Nagoshi S, Suzuki H, Michel ML, Samuel D, Buendia MA, Faivre J, Carninci P. Single-Nucleotide Resolution Mapping of Hepatitis B Virus Promoters in Infected Human Livers and Hepatocellular Carcinoma. *J Virol* 2016; **90**: 10811-10822 [PMID: 27681123 DOI: 10.1128/JVI.01625-16]

43 **Watanabe T**, Inoue T, Tanaka Y. Hepatitis B Core-Related Antigen and New Therapies for Hepatitis B. *Microorganisms* 2021; **9** [PMID: 34683404 DOI: 10.3390/MICROORGANISMS9102083]

44 **Philips CA**, Ahamed R, Abduljaleel JK, Rajesh S, Augustine P. Critical Updates on Chronic Hepatitis B Virus Infection in 2021. *Cureus* 2021; **13**: e19152 [PMID: 34733599 DOI: 10.7759/cureus.19152]

45 **Pavesi A**. Origin, Evolution and Stability of Overlapping Genes in Viruses: A Systematic Review. *Genes (Basel)* 2021; **12** [PMID: 34073395 DOI: 10.3390/genes12060809]

46 **Zhao F**, Xie X, Tan X, Yu H, Tian M, Lv H, Qin C, Qi J, Zhu Q. The Functions of Hepatitis B Virus Encoding Proteins: Viral Persistence and Liver Pathogenesis. *Front Immunol* 2021; **12**: 691766 [PMID: 34456908 DOI: 10.3389/fimmu.2021.691766]

47 **Pazienza V**, Niro GA, Fontana R, Vinciguerra M, Andriulli A. Advance in molecular diagnostic tools for hepatitis B virus detection. *Clin Chem Lab Med* 2013; **51**: 1707-1717 [PMID: 23612658 DOI: 10.1515/cclm-2013-0136]

48 **Hu J**, Liu K. Complete and Incomplete Hepatitis B Virus Particles: Formation, Function, and Application. *Viruses* 2017; **9** [PMID: 28335554 DOI: 10.3390/V9030056]

49 **Pastor F**, Herrscher C, Patient R, Eymieux S, Moreau A, Burlaud-Gaillard J, Seigneuret F, de Rocquigny H, Roingeard P, Hourioux C. Direct interaction between the hepatitis B virus core and envelope proteins analyzed in a cellular context. *Sci Rep* 2019; **9**: 16178 [PMID: 31700077 DOI: 10.1038/s41598-019-52824-z]

50 **Zhuang X**, Forde D, Tsukuda S, D'Arienzo V, Mailly L, Harris JM, Wing PAC, Borrmann H, Schilling M, Magri A, Rubio CO, Maidstone RJ, Iqbal M, Garzon M, Minisini R, Pirisi M, Butterworth S, Balfe P, Ray DW, Watashi K, Baumert TF, McKeating JA. Circadian control of hepatitis B virus replication. *Nat Commun* 2021; **12**: 1658 [PMID: 33712578 DOI: 10.1038/s41467-021-21821-0]

51 **Watashi K**, Wakita T. Hepatitis B Virus and Hepatitis D Virus Entry, Species Specificity, and Tissue Tropism. *Cold Spring Harb Perspect Med* 2015; **5**: a021378 [PMID: 26238794 DOI: 10.1101/cshperspect.a021378]

52 **Zeyen L**, Prange R. Host Cell Rab GTPases in Hepatitis B Virus Infection. *Front Cell Dev Biol* 2018; **6**: 154 [PMID: 30510928 DOI: 10.3389/fcell.2018.00154]

53 **Lamontagne RJ**, Bagga S, Bouchard MJ. Hepatitis B virus molecular biology and pathogenesis. *Hepatoma Res* 2016; **2**: 163-186 [PMID: 28042609 DOI: 10.20517/2394-5079.2016.05]

54 **Marchetti AL**, Guo H. New Insights on Molecular Mechanism of Hepatitis B Virus Covalently Closed Circular DNA Formation. *Cells* 2020; **9** [PMID: 33172220 DOI: 10.3390/CELLS9112430]

55 **Tu T**, Zhang H, Urban S. Hepatitis B Virus DNA Integration: In Vitro Models for Investigating Viral Pathogenesis and Persistence. *Viruses* 2021; **13** [PMID: 33530322 DOI: 10.3390/V13020180]

56 **Wang G**, Guan J, Khan NU, Li G, Shao J, Zhou Q, Xu L, Huang C, Deng J, Zhu H, Chen Z. Potential capacity of interferon-α to eliminate covalently closed circular DNA (cccDNA) in hepatocytes infected with hepatitis B virus. *Gut Pathog* 2021; **13**: 22 [PMID: 33845868 DOI: 10.1186/s13099-021-00421-9]

57 **Karayiannis P**. Hepatitis B virus: virology, molecular biology, life cycle and intrahepatic spread. *Hepatol Int* 2017; **11**: 500-508 [PMID: 29098564 DOI: 10.1007/s12072-017-9829-7]

58 **Jiang B**, Hildt E. Intracellular Trafficking of HBV Particles. *Cells* 2020; **9** [PMID: 32887393 DOI: 10.3390/CELLS9092023]

59 **Inan N**, Tabak F. Hepatitis B Virus: Biology and Life Cycle. *Viral Hepat J* 2015; **21**: 1-7 [DOI: 10.4274/vhd.36036]

60 **Škrlec I**, Milić J, Cilenšek I, Petrovič D, Wagner J, Peterlin B. Circadian clock genes and myocardial infarction in patients with type 2 diabetes mellitus. *Gene* 2019; **701**: 98-103 [PMID: 30905809 DOI: 10.1016/j.gene.2019.03.038]

61 **Zhao M**, Xing H, Chen M, Dong D, Wu B. Circadian clock-controlled drug metabolism and transport. *Xenobiotica* 2020; **50**: 495-505 [PMID: 31544568 DOI: 10.1080/00498254.2019.1672120]

62 **Škrlec I**, Milić J, Steiner R. The Impact of the Circadian Genes *CLOCK* and *ARNTL* on Myocardial Infarction. *J Clin Med* 2020; **9** [PMID: 32050674 DOI: 10.3390/JCM9020484]

63 **Mukherji A**, Bailey SM, Staels B, Baumert TF. The circadian clock and liver function in health and disease. *J Hepatol* 2019; **71**: 200-211 [PMID: 30930223 DOI: 10.1016/j.jhep.2019.03.020]

64 **Škrlec I**. Circadian rhythm and myocardial infarction. *Med Flum* 2019; **55**: 32-42 [DOI: 10.21860/medflum2019_216321]

65 **Haspel JA**, Anafi R, Brown MK, Cermakian N, Depner C, Desplats P, Gelman AE, Haack M, Jelic S, Kim BS, Laposky AD, Lee YC, Mongodin E, Prather AA, Prendergast BJ, Reardon C, Shaw AC, Sengupta S, Szentirmai É, Thakkar M, Walker WE, Solt LA. Perfect timing: circadian rhythms, sleep, and immunity - an NIH workshop summary. *JCI Insight* 2020; **5** [PMID: 31941836 DOI: 10.1172/JCI.INSIGHT.131487]

66 **Shi D**, Chen J, Wang J, Yao J, Huang Y, Zhang G, Bao Z. Circadian Clock Genes in the Metabolism of Non-alcoholic Fatty Liver Disease. *Front Physiol* 2019; **10**: 423 [PMID: 31139087 DOI: 10.3389/fphys.2019.00423]

67 **Mukherji A**, Dachraoui M, Baumert TF. Perturbation of the circadian clock and pathogenesis of NAFLD. *Metabolism* 2020; **111S**: 154337 [PMID: 32795560 DOI: 10.1016/j.metabol.2020.154337]

68 **Kim YH**, Lazar MA. Transcriptional Control of Circadian Rhythms and Metabolism: A Matter of Time and Space. *Endocr Rev* 2020; **41** [PMID: 32392281 DOI: 10.1210/ENDREV/BNAA014]

69 **Dandri M**. Epigenetic modulation in chronic hepatitis B virus infection. *Semin Immunopathol* 2020; **42**: 173-185 [PMID: 32185454 DOI: 10.1007/s00281-020-00780-6]

70 **Kong F**, Li Q, Zhang F, Li X, You H, Pan X, Zheng K, Tang R. Sirtuins as Potential Therapeutic Targets for Hepatitis B Virus Infection. *Front Med (Lausanne)* 2021; **8**: 751516 [PMID: 34708060 DOI: 10.3389/fmed.2021.751516]

71 **Du L**, Ma Y, Liu M, Yan L, Tang H. Peroxisome Proliferators Activated Receptor (PPAR) agonists activate hepatitis B virus replication in vivo. *Virol J* 2017; **14**: 96 [PMID: 28545573 DOI: 10.1186/s12985-017-0765-x]

72 **Dubuquoy L**, Louvet A, Hollebecque A, Mathurin P, Dharancy S. Peroxisome proliferator-activated receptors in HBV-related infection. *PPAR Res* 2009; **2009**: 145124 [PMID: 19365584 DOI: 10.1155/2009/145124]

73 **Charoensuksai P**, Xu W. PPARs in Rhythmic Metabolic Regulation and Implications in Health and Disease. *PPAR Res* 2010; **2010** [PMID: 20871864 DOI: 10.1155/2010/243643]

74 **Le Martelot G**, Claudel T, Gatfield D, Schaad O, Kornmann B, Lo Sasso G, Moschetta A, Schibler U. REV-ERBalpha participates in circadian SREBP signaling and bile acid homeostasis. *PLoS Biol* 2009; **7**: e1000181 [PMID: 19721697 DOI: 10.1371/journal.pbio.1000181]

75 **Kawai M**, Rosen CJ. PPARγ: a circadian transcription factor in adipogenesis and osteogenesis. *Nat Rev Endocrinol* 2010; **6**: 629-636 [PMID: 20820194 DOI: 10.1038/nrendo.2010.155]

76 **Zhang EE**, Liu Y, Dentin R, Pongsawakul PY, Liu AC, Hirota T, Nusinow DA, Sun X, Landais S, Kodama Y, Brenner DA, Montminy M, Kay SA. Cryptochrome mediates circadian regulation of cAMP signaling and hepatic gluconeogenesis. *Nat Med* 2010; **16**: 1152-1156 [PMID: 20852621 DOI: 10.1038/nm.2214]

77 **Kim EJ**, Yoon YS, Hong S, Son HY, Na TY, Lee MH, Kang HJ, Park J, Cho WJ, Kim SG, Koo SH, Park HG, Lee MO. Retinoic acid receptor-related orphan receptor α-induced activation of adenosine monophosphate-activated protein kinase results in attenuation of hepatic steatosis. *Hepatology* 2012; **55**: 1379-1388 [PMID: 22183856 DOI: 10.1002/hep.25529]

78 **Kalsbeek A**, la Fleur S, Fliers E. Circadian control of glucose metabolism. *Mol Metab* 2014; **3**: 372-383 [PMID: 24944897 DOI: 10.1016/j.molmet.2014.03.002]

79 **Diallo AB**, Coiffard B, Leone M, Mezouar S, Mege JL. For Whom the Clock Ticks: Clinical Chronobiology for Infectious Diseases. *Front Immunol* 2020; **11**: 1457 [PMID: 32733482 DOI: 10.3389/fimmu.2020.01457]

80 **Mazzoccoli G**, Vinciguerra M, Carbone A, Relógio A. The Circadian Clock, the Immune System, and Viral Infections: The Intricate Relationship Between Biological Time and Host-Virus Interaction. *Pathogens* 2020; **9** [PMID: 32012758 DOI: 10.3390/PATHOGENS9020083]

81 **Wu C**, Guo X, Li M, Shen J, Fu X, Xie Q, Hou Z, Zhai M, Qiu X, Cui Z, Xie H, Qin P, Weng X, Hu Z, Liang J. DeepHBV: a deep learning model to predict hepatitis B virus (HBV) integration sites. *BMC Ecol Evol* 2021; **21**: 138 [PMID: 34233610 DOI: 10.1186/s12862-021-01869-8]

82 **Zhuang X**, Edgar RS, McKeating JA. The role of circadian clock pathways in viral replication. *Semin Immunopathol* 2022; **44**: 175-182 [PMID: 35192001 DOI: 10.1007/s00281-021-00908-2]

83 **Sulli G**, Lam MTY, Panda S. Interplay between Circadian Clock and Cancer: New Frontiers for Cancer Treatment. *Trends Cancer* 2019; **5**: 475-494 [PMID: 31421905 DOI: 10.1016/j.trecan.2019.07.002]

84 **Jiang Y**, Shen X, Fasae MB, Zhi F, Chai L, Ou Y, Feng H, Liu S, Liu Y, Yang S. The Expression and Function of Circadian Rhythm Genes in Hepatocellular Carcinoma. *Oxid Med Cell Longev* 2021; **2021**: 4044606 [PMID: 34697563 DOI: 10.1155/2021/4044606]

85 **Yang SL**, Yu C, Jiang JX, Liu LP, Fang X, Wu C. Hepatitis B virus X protein disrupts the balance of the expression of circadian rhythm genes in hepatocellular carcinoma. *Oncol Lett* 2014; **8**: 2715-2720 [PMID: 25360177 DOI: 10.3892/OL.2014.2570]

86 **Li H**, Lu YF, Chen H, Liu J. Dysregulation of metallothionein and circadian genes in human hepatocellular carcinoma. *Chronobiol Int* 2017; **34**: 192-202 [PMID: 27997226 DOI: 10.1080/07420528.2016.1256300]

87 **Caratti G**, Iqbal M, Hunter L, Kim D, Wang P, Vonslow RM, Begley N, Tetley AJ, Woodburn JL, Pariollaud M, Maidstone R, Donaldson IJ, Zhang Z, Ince LM, Kitchen G, Baxter M, Poolman TM, Daniels DA, Stirling DR, Brocker C, Gonzalez F, Loudon AS, Bechtold DA, Rattray M, Matthews LC, Ray DW. REVERBa couples the circadian clock to hepatic glucocorticoid action. *J Clin Invest* 2018; **128**: 4454-4471 [PMID: 30179226 DOI: 10.1172/JCI96138]

88 **Li M**, Wang Y, Xia X, Mo P, Xu J, Yu C, Li W. Steroid receptor coactivator 3 inhibits hepatitis B virus gene expression through activating Akt signaling to prevent HNF4α nuclear translocation. *Cell Biosci* 2019; **9**: 64 [PMID: 31417670 DOI: 10.1186/s13578-019-0328-5]

89 **Fekry B**, Ribas-Latre A, Baumgartner C, Deans JR, Kwok C, Patel P, Fu L, Berdeaux R, Sun K, Kolonin MG, Wang SH, Yoo SH, Sladek FM, Eckel-Mahan K. Incompatibility of the circadian protein BMAL1 and HNF4α in hepatocellular carcinoma. *Nat Commun* 2018; **9**: 4349 [PMID: 30341289 DOI: 10.1038/s41467-018-06648-6]

90 **Shkodina AD**, Tan SC, Hasan MM, Abdelgawad M, Chopra H, Bilal M, Boiko DI, Tarianyk KA, Alexiou A. Roles of clock genes in the pathogenesis of Parkinson's disease. *Ageing Res Rev* 2022; **74**: 101554 [DOI: 10.1016/J.ARR.2021.101554]

91 **Pearson JA**, Voisey AC, Boest-Bjerg K, Wong FS, Wen L. Circadian Rhythm Modulation of Microbes During Health and Infection. *Front Microbiol* 2021; **12**: 721004 [PMID: 34512600 DOI: 10.3389/fmicb.2021.721004]

92 **Qi ZX**, Wang LY, Fan YC, Zhang JJ, Li T, Wang K. Increased peripheral RORα and RORγt mRNA expression is associated with acute-on-chronic hepatitis B liver failure. *J Viral Hepat* 2012; **19**: 811-822 [PMID: 23043388 DOI: 10.1111/j.1365-2893.2012.01603.x]

93 **Huang Y**, Liang H, He C, Peng F. Hepatitis B Virus X Protein-Induced RORγ Expression to Promote the Migration and Proliferation of Hepatocellular Carcinoma. *Biomed Res Int* 2019; **2019**: 5407126 [PMID: 31781621 DOI: 10.1155/2019/5407126]

94 **Liang Y**, Wang S, Huang X, Chai R, Tang Q, Yang R, Wang X, Zheng K. Dysregulation of Circadian Clock Genes as Significant Clinic Factor in the Tumorigenesis of Hepatocellular Carcinoma. *Comput Math Methods Med* 2021; **2021**: 8238833 [PMID: 34745328 DOI: 10.1155/2021/8238833]

95 **Iannacone M**, Guidotti LG. Immunobiology and pathogenesis of hepatitis B virus infection. *Nat Rev Immunol* 2022; **22**: 19-32 [PMID: 34002067 DOI: 10.1038/s41577-021-00549-4]

96 **Tan A**, Koh S, Bertoletti A. Immune Response in Hepatitis B Virus Infection. *Cold Spring Harb Perspect Med* 2015; **5**: a021428 [PMID: 26134480 DOI: 10.1101/cshperspect.a021428]

97 **Ghosh A**, Onsager C, Mason A, Arriola L, Lee W, Mubayi A. The role of oxygen intake and liver enzyme on the dynamics of damaged hepatocytes: Implications to ischaemic liver injury *via* a mathematical model. *PLoS One* 2021; **16**: e0230833 [PMID: 33886563 DOI: 10.1371/journal.pone.0230833]

98 **Gu Y**, Lian Y, Gu L, Chen L, Li X, Zhou L, Huang Y, Wang J. Correlations between cytokines produced by T cells and clinical-virological characteristics in untreated chronic hepatitis B patients. *BMC Infect Dis* 2019; **19**: 216 [PMID: 30832595 DOI: 10.1186/s12879-019-3853-2]

99 **Matsumura S**, Yamamoto K, Shimada N, Okano N, Okamoto R, Suzuki T, Hakoda T, Mizuno M, Higashi T, Tsuji T. High frequency of circulating HBcAg-specific CD8 T cells in hepatitis B infection: a flow cytometric analysis. *Clin Exp Immunol* 2001; **124**: 435-444 [PMID: 11472405 DOI: 10.1046/J.1365-2249.2001.01561.X]

100 **Meier MA**, Suslov A, Ketterer S, Heim MH, Wieland SF. Hepatitis B virus covalently closed circular DNA homeostasis is independent of the lymphotoxin pathway during chronic HBV infection. *J Viral Hepat* 2017; **24**: 662-671 [PMID: 28182305 DOI: 10.1111/jvh.12689]

101 **Pick R**, He W, Chen CS, Scheiermann C. Time-of-Day-Dependent Trafficking and Function of Leukocyte Subsets. *Trends Immunol* 2019; **40**: 524-537 [PMID: 31109762 DOI: 10.1016/j.it.2019.03.010]

102 **Dimitrov S**, Benedict C, Heutling D, Westermann J, Born J, Lange T. Cortisol and epinephrine control opposing circadian rhythms in T cell subsets. *Blood* 2009; **113**: 5134-5143 [PMID: 19293427 DOI: 10.1182/blood-2008-11-190769]

103 **Narasimamurthy R**, Hatori M, Nayak SK, Liu F, Panda S, Verma IM. Circadian clock protein cryptochrome regulates the expression of proinflammatory cytokines. *Proc Natl Acad Sci U S A* 2012; **109**: 12662-12667 [PMID: 22778400 DOI: 10.1073/pnas.1209965109]

104 **Silver AC**, Arjona A, Walker WE, Fikrig E. The circadian clock controls toll-like receptor 9-mediated innate and adaptive immunity. *Immunity* 2012; **36**: 251-261 [PMID: 22342842 DOI: 10.1016/j.immuni.2011.12.017]

105 **Crespo I**, Fernández-Palanca P, San-Miguel B, Álvarez M, González-Gallego J, Tuñón MJ. Melatonin modulates mitophagy, innate immunity and circadian clocks in a model of viral-induced fulminant hepatic failure. *J Cell Mol Med* 2020; **24**: 7625-7636 [PMID: 32468679 DOI: 10.1111/jcmm.15398]

106 **Griffett K**, Bedia-Diaz G, Elgendy B, Burris TP. REV-ERB agonism improves liver pathology in a mouse model of NASH. *PLoS One* 2020; **15**: e0236000 [PMID: 33002003 DOI: 10.1371/journal.pone.0236000]

107 **Srinivasan V**, Mohamed M, Kato H. Melatonin in bacterial and viral infections with focus on sepsis: a review. *Recent Pat Endocr Metab Immune Drug Discov* 2012; **6**: 30-39 [PMID: 22264213 DOI: 10.2174/187221412799015317]

108 **van den Berg F**, Limani SW, Mnyandu N, Maepa MB, Ely A, Arbuthnot P. Advances with RNAi-Based Therapy for Hepatitis B Virus Infection. *Viruses* 2020; **12** [PMID: 32759756 DOI: 10.3390/V12080851]

109 **Pierra Rouviere C**, Dousson CB, Tavis JE. HBV replication inhibitors. *Antiviral Res* 2020; **179**: 104815 [PMID: 32380149 DOI: 10.1016/j.antiviral.2020.104815]

110 **Liang TJ**. Hepatitis B: a new weapon against an old enemy. *Nat Med* 2021; **27**: 1672-1673 [PMID: 34642493 DOI: 10.1038/s41591-021-01512-5]

111 **Raimondo G**, Locarnini S, Pollicino T, Levrero M, Zoulim F, Lok AS; Taormina Workshop on Occult HBV Infection Faculty Members. Update of the statements on biology and clinical impact of occult hepatitis B virus infection. *J Hepatol*

2019; **71**: 397-408 [PMID: 31004683 DOI: 10.1016/j.jhep.2019.03.034]

112 **Greco CM**, Sassone-Corsi P. Personalized medicine and circadian rhythms: Opportunities for modern society. *J Exp Med* 2020; **217** [PMID: 32433754 DOI: 10.1084/JEM.20200702]

113 **Maiese K**. Circadian Clock Genes: Targeting Innate Immunity for Antiviral Strategies Against COVID-19. *Curr Neurovasc Res* 2020; **17**: 531-533 [PMID: 33272180 DOI: 10.2174/1567202617666201203110008]

114 **Karabay O**, Temel A, Koker AG, Tokel M, Ceyhan M, Kocoglu E. Influence of circadian rhythm on the efficacy of the hepatitis B vaccination. *Vaccine* 2008; **26**: 1143-1144 [PMID: 18255201 DOI: 10.1016/j.vaccine.2007.12.046]

115 **De Giorgi A**, Fabbian F, Di Simone E, Greco S, De Giorgio R, Zuliani G, Passaro A, Caselli E, Manfredini R; OUTCOME-INTMED-COV19 Study Collaborators. Morning vs. evening administration of antiviral therapy in COVID-19 patients. A preliminary retrospective study in Ferrara, Italy. *Eur Rev Med Pharmacol Sci* 2020; **24**: 8219-8225 [PMID: 32767353 DOI: 10.26355/eurrev_202008_22511]

116 **Ruben MD**, Smith DF, FitzGerald GA, Hogenesch JB. Dosing time matters. *Science* 2019; **365**: 547-549 [PMID: 31395773 DOI: 10.1126/science.aax7621]

117 **Kurupati RK**, Kossenkoff A, Kannan S, Haut LH, Doyle S, Yin X, Schmader KE, Liu Q, Showe L, Ertl HCJ. The effect of timing of influenza vaccination and sample collection on antibody titers and responses in the aged. *Vaccine* 2017; **35**: 3700-3708 [PMID: 28583307 DOI: 10.1016/j.vaccine.2017.05.074]

118 **Sultan A**, Ali R, Sultan T, Ali S, Khan NJ, Parganiha A. Circadian clock modulating small molecules repurposing as inhibitors of SARS-CoV-2 M^{pro} for pharmacological interventions in COVID-19 pandemic. *Chronobiol Int* 2021; **38**: 971-985 [PMID: 33820462 DOI: 10.1080/07420528.2021.1903027]

119 **Sultan A**. Identification and development of clock-modulating small molecules-an emerging approach to fine-tune the disrupted circadian clocks. *Biol Rhythm Res* 2018; **50**: 769-786 [DOI: 10.1080/09291016.2018.1498197]

120 **Borrmann H**, Davies R, Dickinson M, Pedroza-Pacheco I, Schilling M, Vaughan-Jackson A, Magri A, James W, Balfe P, Borrow P, McKeating JA, Zhuang X. Pharmacological activation of the circadian component REV-ERB inhibits HIV-1 replication. *Sci Rep* 2020; **10**: 13271 [PMID: 32764708 DOI: 10.1038/s41598-020-70170-3]

121 **Wang S**, Li F, Lin Y, Wu B. Targeting REV-ERBα for therapeutic purposes: promises and challenges. *Theranostics* 2020; **10**: 4168-4182 [PMID: 32226546 DOI: 10.7150/thno.43834]

World Journal of Gastroenterology

Submit a Manuscript: https://www.f6publishing.com

World J Gastroenterol 2022 July 21; 28(27): 3297-3313

DOI: 10.3748/wjg.v28.i27.3297

ISSN 1007-9327 (print) ISSN 2219-2840 (online)

REVIEW

Tumor microenvironment in pancreatic ductal adenocarcinoma: Implications in immunotherapy

Caitlyn Smith, Wei Zheng, Jixin Dong, Yaohong Wang, Jinping Lai, Xiuli Liu, Feng Yin

Specialty type: Gastroenterology and hepatology

Provenance and peer review: Invited article; Externally peer reviewed.

Peer-review model: Single blind

Peer-review report's scientific quality classification

Grade A (Excellent): 0
Grade B (Very good): B
Grade C (Good): C, C
Grade D (Fair): 0
Grade E (Poor): 0

P-Reviewer: Plougmann JI, Denmark; Tantau AI, Romania; Zhao CF, China

Received: January 16, 2022
Peer-review started: January 16, 2022
First decision: April 11, 2022
Revised: April 22, 2022
Accepted: June 19, 2022
Article in press: June 19, 2022
Published online: July 21, 2022

Caitlyn Smith, Department of Pathology and Anatomical Sciences, University of Missouri School of Medicine, Columbia, MO 65212, United States

Wei Zheng, Department of Pathology, Emory University School of Medicine, Atlanta, GA 30322, United States

Jixin Dong, Eppley Institute for Research in Cancer and Allied Diseases, Fred and Pamela Buffett Cancer Center, University of Nebraska Medical Center, Omaha, NE 68198, United States

Yaohong Wang, Department of Pathology, Microbiology and Immunology, Vanderbilt University Medical Center, Nashville, TN 37232, United States

Jinping Lai, Department of Pathology and Laboratory Medicine, Kaiser Permanente Sacramento Medical Center, Sacramento, CA 95825, United States

Xiuli Liu, Department of Pathology and Immunology, Washington University, St. Louis, MO 63110, United States

Feng Yin, Department of Pathology and Anatomical Sciences, University of Missouri, Columbia, MO 65212, United States

Corresponding author: Feng Yin, MD, PhD, Assistant Professor, Department of Pathology and Anatomical Sciences, University of Missouri, One Hospital Drive, MSB M263, Columbia, MO 65212, United States. fengyin@health.missouri.edu

Abstract

Pancreatic ductal adenocarcinoma is one of the most aggressive and lethal cancers. Surgical resection is the only curable treatment option, but it is available for only a small fraction of patients at the time of diagnosis. With current therapeutic regimens, the average 5-year survival rate is less than 10% in pancreatic cancer patients. Immunotherapy has emerged as one of the most promising treatment options for multiple solid tumors of advanced stage. However, its clinical efficacy is suboptimal in most clinical trials on pancreatic cancer. Current studies have suggested that the tumor microenvironment is likely the underlying barrier affecting immunotherapy drug efficacy in pancreatic cancer. In this review, we discuss the role of the tumor microenvironment in pancreatic cancer and the latest advances in immunotherapy on pancreatic cancer.

Key Words: Pancreatic ductal adenocarcinoma; Tumor microenvironment; Immunotherapy; Clinical trial; Chemotherapy; Treatment

Core Tip: Despite advances in basic and translational research, pancreatic cancer remains one of the most lethal cancers. Recent breakthroughs in immunotherapy have revolutionized cancer therapy and have shown great potential to transform pancreatic cancer treatment. However, due to the barrier related to the tumor microenvironment, pancreatic cancer has shown inferior treatment outcomes toward various immunotherapy regimens. Further efforts, such as combinatory immunotherapy or molecular tumor subtyping, are warranted to overcome immunotherapy resistance in pancreatic cancer.

Citation: Smith C, Zheng W, Dong J, Wang Y, Lai J, Liu X, Yin F. Tumor microenvironment in pancreatic ductal adenocarcinoma: Implications in immunotherapy. *World J Gastroenterol* 2022; 28(27): 3297-3313
URL: https://www.wjgnet.com/1007-9327/full/v28/i27/3297.htm
DOI: https://dx.doi.org/10.3748/wjg.v28.i27.3297

INTRODUCTION

Pancreatic ductal adenocarcinoma (PDAC) develops in the exocrine compartment of the pancreas and accounts for approximately 90% of pancreatic malignancies, making it the most common pancreatic neoplasm. Due to the lack of early diagnosis and limited treatment response, PDAC remains a highly aggressive and lethal malignancy and is the fourth leading cause of cancer-related death worldwide[1]. Although there has been notable progress in understanding tumor biology and the development of novel therapeutic regimens, the average 5-year survival rate is still less than 5%-10% in PDAC patients [1,2]. The clinical manifestations of pancreatic cancers are generally nonspecific, including weight loss, abdominal pain, thromboembolic disease, and type 2 diabetes[3,4]. In approximately 60%-70% of PDAC cases, the tumor arises from the head of the pancreas and could present as pancreatitis and obstructive jaundice[5]. Tumors of the pancreatic body and tail frequently have a poor prognosis due to their late presentation and associated advanced tumor stage[6].

The standard of care for resectable PDAC is surgical resection followed by adjuvant chemotherapy. Surgical resection remains the only curative therapy, but it is available for merely 10%-20% of patients at the time of diagnosis. Moreover, even with curative surgical resection, local recurrence and distal metastasis of PDAC are still quite common[7]. Advanced-stage PDAC is routinely treated with neoadjuvant chemotherapy, and the current first-line therapy regimens include gemcitabine, gemcitabine plus nab-paclitaxel, and FOLFIRINOX (the combination of oxaliplatin, leucovorin, fluorouracil, and irinotecan) [8]. Recently, the poly(adenosine diphosphate-ribose) polymerase inhibitor (PARPi) olaparib (Lynparza) has been approved for patients with germline BRCA-mutated metastatic pancreatic cancer[9]. The development of these neoadjuvant chemotherapy regimens has greatly improved patient survival and quality of life. However, a significant portion of PDAC eventually relapses despite surgical resection and/or neoadjuvant chemotherapy and leads to patient death[10,11].

The difficulties in treating pancreatic cancer lie at the cellular and genetic levels[12]. Mutational changes in pancreatic tumors lead to gene instability, tumor growth, and resistance to treatments[13]. In addition to the characteristic molecular landmarks, including oncogenic *KRAS* mutation and inactivation of the tumor suppressor genes *CDKN2A/P16*, *TP53,* and *SMAD4*, PDAC also frequently harbors mutations involving diverse cell signaling pathways[14]. The molecular heterogeneity likely accounts for its drug resistance in chemotherapy[15]. In addition, pancreatic cancer stem cells, accounting for approximately 1% of all pancreatic cancer cells, have the capacity for self-renewal and exhibit chemoresistance properties[16].

Immunotherapy has emerged as one of the most promising treatment options for advanced solid tumors, including lung, kidney, bladder, liver, and colorectal cancers[17]. Unfortunately, PDAC is notoriously resistant to immunotherapy, and thus far, most phase I/II clinical trials on PDAC have failed to demonstrate the desirable clinical efficacy of immunotherapy[18]. Of note, microsatellite instability (MSI), one of the predictive biomarkers for immune checkpoint blockade therapy, is only detected in a rare small portion of PDAC patients (less than 1%)[19,20]. On the other hand, emerging evidence has pinpointed the tumor microenvironment (TME) in PDAC as a critical component of treatment resistance toward immunotherapy[21,22].

In this review, we discuss the role of the tumor microenvironment and the latest advances in immunotherapy on pancreatic cancer through the search of peer-reviewed clinical and basic research articles related to this topic on PubMed, as well as the publicly accessible information on relevant

clinical trials through ClinicalTrials.gov.

TUMOR MICROENVIRONMENT IN PANCREATIC CANCER

PDAC is a type of stromal-rich cancer that frequently presents with a prominent desmoplastic reaction and is characterized by fibrogenic connective stromal tissue surrounding invasive carcinoma[23] (Figure 1). Desmoplastic reaction, or desmoplasia, is considered as the morphological basis of the TME. In general, the TME in PDAC demonstrates extensive desmoplasia, decreased stromal vascularization, and altered immune cell infiltration that lead to reduced drug activity and advancement of tumor progression. This process is characterized by an increase in the deposition of noncellular components, such as extracellular matrix (ECM), as well as an increase in the proliferation of cellular components, such as cancer-associated fibroblasts (CAFs) and immune cells[24,25]. Various cytokines, including interferons, interleukins, tumor necrosis factor (TNF), and transforming growth factor β (TGF-β), also play essential roles linking the TME cellular and noncellular components to regulate tumor growth, metastases, and drug resistance. Of note, the overall stroma is responsible for most of the tumor mass, but the stromal cellular components make up a relatively small fraction, approximately 10%-30%, of the tumor mass[26].

Noncellular components of the tumor microenvironment

The ECM is a significant factor in the initiation and progression of PDAC, and its deposition is associated with tumor migration, invasion, and poor prognosis[27]. The ECM is predominantly produced by cancer-associated pancreatic stellate cells (PSCs), a subtype of CAFs[28]. In PDAC, the ECM comprises most of the tumor mass and various matrix proteins, including collagen, fibronectin, proteoglycans, hyaluronan, proteolytic matrix metalloproteinases (MMPs), and tissue inhibitors of MMP [29]. Among ECM components of particular interest are hyaluronan and MMPs in tumor progression and prognosis in PDAC.

In general, ECM provides a rigid barrier leading to increased tumor pressure, decreased vascularization, and reduced drug delivery. A significant cause of drug resistance is the inability of conventional chemotherapeutic drugs such as gemcitabine to penetrate the thick stromal layer[30]. Therefore, it is rational to propose a combinatory therapeutic strategy for PDAC by targeting the tumor ECM. Hyaluronan, or hyaluronic acid (HA), is a glycosaminoglycan polymer and a major component of the ECM. Increased deposition of HA is associated with tumor metastases, drug resistance, and poor prognosis in PDAC[27,31]. Since stromal HA levels are dynamically regulated by synthases (to produce HA) and hyaluronidases (to degrade HA), hyaluronidase-based drug development has been a promising field in targeted therapy against the TME. The enzymatic depletion of hyaluronan through recombinant hyaluronidase (PEGPH20) has led to significantly increased overall survival when combined with neoadjuvant chemotherapy[32]. This is attributed mainly to improved delivery of systemic therapy through degradation of HA and remodeling of the TME. However, a recent phase IB/II randomized study (NCT01959139) of FOLFIRINOX plus pegylated recombinant PEGPH20 showed increased toxicity with this combination therapy and decreased overall survival (OS) (7.7 mo *vs* 14.4 mo) compared with FOLFIRINOX monotherapy[33]. Moreover, despite promising results of PEGPH20 in phase I-II studies, in a recent phase III randomized study (HALO 109-301), the addition of PEGPH20 to nab-paclitaxel/gemcitabine did not improve OS and progression-free survival (PFS) in patients with hyaluronan-high metastatic PDAC, and additional development of PEHPH20 in metastatic PDAC was halted[34].

MMPs are calcium-dependent metalloproteinases responsible for ECM protein degradation and are implicated in cancer initiation, growth, and metastasis. Clinical trial results with broad-spectrum MMP inhibitors were discouraging due to lack of specificity, associated toxicity, and insufficient clinical benefit[35], warranting further basic and translational studies to classify the role of individual MMPs in PDAC. Among MMP family members, the expression levels of MMP-2, MMP-7, MMP-9, and MMP-11 were significantly elevated in PDAC tumor tissues compared with normal pancreas samples[36,37]. Increased MMP-2 expression in PDAC leads to tumor invasion and progression[38-40]. MMP-7 expression is also associated with PDAC initiation and progression[41] and has been shown to be an independent prognostic factor for PDAC in a multivariate analysis. MMP-9 is significantly associated with pancreatic cancer progression and poor prognosis[37] and has emerged as a prognostic biomarker and potential therapeutic target. Highly selective and potent MMP-9 inhibitory antibodies have been developed for ulcerative colitis and colorectal cancer[42]. However, in a preclinical study, systemic ablation of MMP-9 facilitated pancreatic cancer growth and metastasis by creating a tumor-promoting TME[43]. This study has suggested a controversial role for MMP-9 in pancreatic cancer progression.

Additional studies have also demonstrated conflicting results in drugs targeting the tumor stroma. Olive *et al*[44] demonstrated that depletion of ECM in PDAC, through inhibition of the Sonic Hedgehog signaling pathway, promoted gemcitabine efficacy and improved survival. However, the involvement of the Sonic Hedgehog-dependent tumor stroma in PDAC has been controversial, as evidence shows that some components of the tumor stroma could actually act to restrain, rather than support, tumor

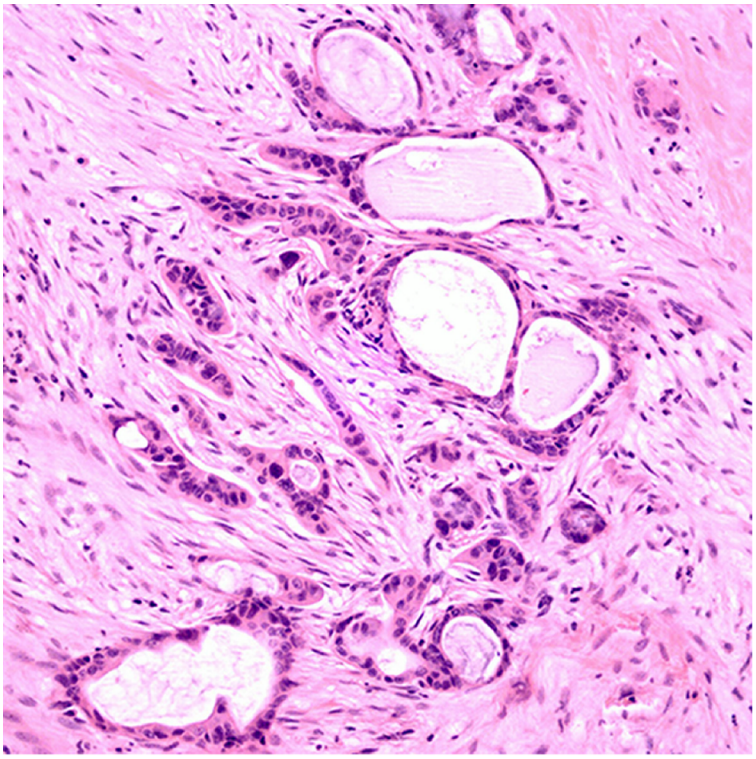

DOI: 10.3748/wjg.v28.i27.3297

Figure 1 Pancreatic ductal adenocarcinoma with an associated tumor microenvironment. Please note the desmoplastic stromal reaction surrounding the tumor glands, decreased stromal vascularization, and scattered infiltrating inflammatory cells (HE stain, 200 x).

growth[45]. All these failures indicate that targeting desmoplasia alone is insufficient for treating advanced PDAC. The tumor stroma has both tumor-promoting and tumor-suppressing functions, which are probably context dependent. The stromal heterogeneity should be considered for the development of targeted therapy.

Cellular components of the tumor microenvironment

PDAC displays unique immunologic hallmarks. The TME in PDAC consists of diverse cellular components, including CAFs, regulatory and cytotoxic lymphocytes, macrophages, and endothelial cells [46]. CAFs are the major TME cellular component responsible for the production and deposition of ECM proteins. The involvement of CAFs in the progression of PDAC has been a hot and controversial topic. Similar to the observations made with tumor stroma, CAFs also play dual functions in regulating PDAC progression. On the one hand, CAFs promote cancer progression and drug resistance through the deposition of dense ECM, the release of exosomes (extracellular vesicles), and metabolic support[47-49]. On the other hand, depletion of CAFs leads to accelerated PDAC progression and reduced survival in multiple preclinical studies[50,51]. These discrepancies are likely associated with the heterogeneity of CAFs[52,53], a concept supported by recent studies demonstrating the existence of multiple distinct and mutually exclusive CAF subtypes in pancreatic cancer[54,55]. CAF subtypes with diverse biomarkers, including α-smooth muscle actin (αSMA), fibroblast activation protein (FAP), S100A4, and platelet-derived growth factor receptor-β (PDGFRβ), have been identified[56]. Specifically, FAP-positive active CAFs have been linked to tumor-promoting functions by maintaining an immunosuppressive TME[57]. FAP is a type-II transmembrane serine protease, and its expression has been detected in both the tumor stroma and cancer cells in PDAC, with the highest expression in the tumor stroma at the tumor front [58]. FAP-positive CAFs potently shape the immune landscape in the TME by secreting TGF-β, VEGF, and multiple matrix processing enzymes[59,60], recruiting circulating myeloid-derived suppressor cells (MDSCs) into the tumor stroma[57], and inhibiting natural killer cell (NK) cytotoxicity and cytokine production[61]. FAP has been suggested as an ideal target for the TME, and its specific therapeutic reagents are in development[62].

In addition to CAFs, the TME also consists of multiple types of immunosuppressive cells, including regulatory T cells (Tregs), MDSCs, and tumor-associated macrophages (TAMs)[63]. These cells correlate to provide an immunosuppressive TME and have been under extensive preclinical and clinical investigation.

Tregs, defined as CD4+/CD25+/FOXP3+ T cells, are a subtype of repressive T cells that play an essential role in maintaining immune tolerance and preventing autoimmune disorders. Tregs can be found in PDAC and premalignant lesion intraductal papillary mucinous neoplasms (IPMNs). The

prevalence of Tregs in CD4+ T lymphocytes correlates significantly with the progression and invasion of IPMNs and is associated with poor prognosis in PDAC. The immunosuppressive function of Tregs has been attributed to the secretion of suppressive cytokines, including IL-10 and TGF-β1, and the induction of CD4+ T-cell death[64,65]. Preoperative chemoradiation therapy has been shown to decrease Tregs in PDAC[66]. However, in a recent study, depletion of Tregs in a mouse model caused accelerated tumor progression due to unexpected crosstalk between Tregs and CAFs in PDAC[67]. This study has challenged the current view and posed uncertainties in developing Treg-based targeted therapy.

MDSCs and TAMs have also been suggested as potential therapeutic targets against the TME. Even though these two cell types are considered as separate entities, they have no demarcated boundaries and share many common characteristics[68]. MDSCs are a group of heterogeneous immature myeloid cells and can potently suppress T-cell function in tumors[69]. The levels of MDSCs correlate with the progression of PDAC and have been proposed as a predictive biomarker of chemotherapy failure[70,71]. TAMs are circulating monocyte-derived macrophages in the tumor stroma and represent a significant population of immune cells within the TME. TAMs can be further subclassified into the M1 and M2 subtypes, with M1 being proinflammatory (antitumorigenic) and M2 being anti-inflammatory (protumorigenic)[72]. M2-polarized TAMs are associated with an unfavorable prognosis in PDAC[73]. Liu *et al*[74] revealed progressive accumulations of MDSCs and M2-polarized TAMs accompanied by dynamic reductions in cytotoxic T cells (CTLs) and helper T cells (Ths) in PDAC progression. Gemcitabine affects the TME by inhibiting the expansion of MDSCs and the induction of Th2 cells while promoting M2-polarized TAMs[74]. M2-polarized TAMs can also be induced by other chemotherapeutic agents, such as carboplatin and cisplatin, leading to increased secretion of interleukin-6 (IL-6), IL-10, and prostaglandin E2[75]. In addition, interferon-γ upregulates the expression of programmed death-ligand 1 (PD-L1) in MDSCs, resulting in an immunosuppressive environment[76]. Further investigations and clinical trials are needed to test the efficacy of targeting MDSCs and TAMs in pancreatic cancer.

IMMUNOTHERAPY IN PANCREATIC CANCER

Current treatment options for PDAC have limited effects on patient survival. The recent development of immunotherapy has improved clinical outcomes for various types of solid tumors[17] and can revolutionize cancer treatment in PDAC. Activating the patient's T cells is the principal basis for cancer immunotherapy. This is accomplished through multiple mechanisms, such as decreased tumor-specific antigen presentation, T-cell activation, T-cell infiltration into the pancreatic tumor, and elimination of cancer cells by T cells[77]. Multiple cancer immunotherapies have been introduced, including immune checkpoint inhibitors, cancer vaccines, and adoptive cell transfer.

Immune checkpoint inhibitors

Immune checkpoint molecules are a group of surface receptors expressed on various immune cells that transduce inhibitory signals to T cells upon ligand binding. These molecules play an important role in preventing an autoimmune attack against self-antigens. Due to strong immune selective pressure, cancer cells frequently adopt the power of immune checkpoint molecules to avoid immune destruction. Initially approved for the treatment of metastatic melanoma, immune checkpoint inhibitors (ICIs) have been cleared to treat various solid tumors, including advanced or metastatic urothelial carcinoma, non-small-cell lung cancer, colorectal cancer, triple-negative breast cancer, and head and neck squamous cell carcinoma[78,79]. Currently, FDA-approved immune checkpoint inhibitors (ICIs) include anti-CTLA-4 agents (ipilimumab), anti-PD-1 agents (nivolumab, pembrolizumab, cemiplimab) and anti-PD-L1 agents (atezolizumab, avelumab, durvalumab)[79].

ICIs have emerged as a new therapeutic option for pancreatic cancer. Unfortunately, most phase I and II clinical trials on ICI treatment have failed to show the desired beneficial effect in PDAC. Two independent phase II clinical trials have demonstrated unsatisfactory clinical outcomes on monotherapy with anti-CTLA-4 mAb (Table 1). Single-agent ipilimumab, an anti-CTLA-4 mAb, was ineffective for the treatment of advanced PDAC (NCT00112580) (https://clinicaltrials.gov/ct2/show/NCT00112580)[80,81]. Monotherapy with tremelimumab, another anti-CTLA-4 mAb, also yielded poor clinical outcomes in PDAC, with 18 out of 20 patients demonstrating progressive disease and a poor median OS of 4 mo (95%CI: 2.83-5.42 mo) (NCT02527434) (https://clinicaltrials.gov/ct2/show/NCT02527434).

Combination therapy with ipilimumab and gemcitabine, on the other hand, has demonstrated promising results due to the increased immune response by enhancing naïve T-cell activation[82]. In a phase 1b clinical trial (NCT01473940) (https://clinicaltrials.gov/ct2/show/NCT01473940), initial results on combination therapy with ipilimumab and gemcitabine showed that the treatment was tolerable, with a median PFS of 2.5 mo (95%CI: 0.8-4.8 mo) and a median OS of 8.5 mo (95%CI: 2.2-10.3 mo). In this study, five out of the 11 patients had stable disease, while two had a partial response. An ongoing clinical trial (NCT01928394) (https://clinicaltrials.gov/ct2/show/NCT01928394) is comparing nivolumab (anti-PD-1 mAb) monotherapy and combination therapy with nivolumab plus ipilimumab in patients with advanced or metastatic PDAC, and the results will be released in 2023.

Table 1 Complete immune checkpoint inhibitor-based clinical trials in pancreatic ductal adenocarcinoma

Strategy	Treatment	Phase	Number	Cancer stage	Outcomes
Immune checkpoint inhibitor (target) monotherapy	Tremelimumab (CTLA-4)	II	NCT02527434	Advanced/metastatic PDAC	Tremelimumab monotherapy is ineffective for metastatic PDAC.
	Ipilimumab (CTLA-4)	II	NCT00112580	Advanced PDAC	Ipilimumab monotherapy is ineffective for advanced PDAC.
	Atezolizumab (PD-L1)	I/II	NCT03829501	Advanced PDAC	No results reported yet
Immune checkpoint inhibitor (target) + immune checkpoint inhibitor(target)	Tremelimumab (CTLA-4) + Durvalumab (PD-L1)	II	NCT02558894	Metastatic PDAC	ORR 3.1% for combination therapy. (ORR 0% for monotherapy).
	Nivolumab (PD-1) + Ipilimumab (CTLA-4)	I/II	NCT01928394	Advanced/metastatic PDAC	No results reported yet
Immune checkpoint inhibitor (target) + chemotherapy	Tremelimumab (CTLA-4) + Gemcitabine	I	NCT00556023	Advanced PDAC	Median OS 7.4 mo (95%CI: 5.8-9.4 mo)
	Ipilimumab(CTLA-4) + Gemcitabine	Ib	NCT01473940	Advanced/metastatic PDAC	Median OS 6.90 mo (95%CI: 2.63–9.57 mo)
	Pembrolizumab (PD-1) + Gemcitabine and Nab-paclitaxel	Ib/II	NCT02331251	Advanced/metastatic PDAC	Median OS 15.0 mo (95%CI: 6.8–22.6 mo)
Immune Checkpoint Inhibitor (Target) + Target therapy	Durvalumab (PD-L1) + Galunisertib	I	NCT02734160	Metastatic PDAC	Median PFS 1.9 mo (95%CI: 1.5-2.2 mo); median OS was NR (95%CI: 3.6 mo, NR)
	Durvalumab (PD-L1) + Pexidartinib	I	NCT02777710	Advanced/metastatic PDAC	No results reported yet
Immune Checkpoint Inhibitor (Target) + Radiation Therapy	Tremelimumab (CTLA-4) + Durvalumab (PD-1) + SBRT	I/II	NCT02311361	Advanced/metastatic PDAC	ORR of 9.6% including 2 patients who achieved a durable partial response lasting over 12 mo

https://clinicaltrials.gov/. PDAC: Pancreatic ductal adenocarcinoma; CTLA-4: Cytotoxic T lymphocyte-associated antigen-4; PD-1: Programmed cell death protein 1; PD-L1: Programmed cell death ligand 1; OS: Overall survival; PFS: Progression-free survival; ORR: Overall response rate; NR: Not reached.

Notably, in a phase I clinical trial (NCT00556023) (https://clinicaltrials.gov/ct2/show/NCT00556023), a tolerable and safe profile was demonstrated by combination therapy with tremelimumab plus gemcitabine, warranting further study in patients with metastatic PDAC. Thirty-four patients were enrolled in the study, and the median OS was 7.4 mo (95%CI: 5.8-9.4 mo). Two patients achieved a partial response at the end of treatment[83]. A phase Ib/II study (NCT02331251) (https://clinicaltrials.gov/ct2/show/NCT02331251) was performed to evaluate the safety and efficacy of pembrolizumab, an anti-PD-1 mAb, in combination with gemcitabine plus nab-paclitaxel chemotherapy. The median PFS and OS were 9.1 and 15.0 mo for chemotherapy naïve-treated patients, respectively, and changes in tumor cell-free DNA copy number instability were considered to be a potential prognostic factor for OS[84].

A phase I study on atezolizumab, an engineered IgG1 mAb targeting PD-L1, showed tolerability at doses up to 20 mg/kg every three weeks in a Japanese cohort[85]. In a phase II randomized clinical trial (NCT02558894) (https://clinicaltrials.gov/ct2/show/NCT02558894), evaluation of durvalumab, an anti-PD-L1 agent, with or without tremelimumab in patients with metastatic PDAC was evaluated following the failure of 5-FU and gemcitabine-based chemotherapy[86]. No patients in the study responded to durvalumab monotherapy, and the efficacy analysis demonstrated an objective response rate (ORR) of 3.1% (95%CI: 0.08-16.22) with the combination therapy of durvalumab plus tremelimumab [86].

A high tumor mutational burden (TMB) in cancer cells tends to produce more immunogenic neoantigens and may predict immunotherapy response[87]. A phase II clinical trial (NCT05093231) (https://clinicaltrials.gov/ct2/show/NCT05093231) investigating the efficacy of pembrolizumab plus olaparib in metastatic pancreatic adenocarcinoma patients exhibiting high tumor mutation burden is ongoing, and the results will be released in 2026.

Based on the results from current clinical trials, further studies need to focus on the combined approaches using ICIs with different therapeutic approaches, including chemotherapy, radiotherapy, or additional innovative platforms of immunotherapy, such as cancer vaccine and adoptive cell transfer.

Therapeutic cancer vaccines

Therapeutic cancer vaccines include whole-cell vaccines, dendritic cells, DNA, and peptide vaccines that activate cancer antigen-specific cytotoxic T lymphocytes (CTLs), eliciting immunogenic antigen presentation and leading to an anticancer response[88]. One such pancreatic cancer vaccine is GVAX,

which is generated from irradiated pancreatic cancer cells expressing granulocyte-macrophage colony-stimulating factor (GM-CSF)[89] (Table 2). Upon vaccination, GVAX secretes GM-CSF, induces subsequent activation of antigen-presenting cell and T-cell priming, and stimulates the patient's immune system against pancreatic cancer cells[90]. GVAX was tolerable even at high doses, and the vaccination-induced increased delayed-type hypersensitivity response to autologous tumor cells[91]. In a phase II clinical trial on GVAX (NCT00084383) (https://clinicaltrials.gov/ct2/show/NCT00084383), sixty patients received GVAX 8-10 wk after surgical intervention, followed by adjuvant 5-FU-based chemoradiotherapy. The median PFS was 17.3 mo (95%CI: 14.6-22.8 mo), with a median OS of 24.8 mo (95%CI: 21.2-31.6 mo), which compares favorably with published data for resected PDAC[92]. Combinatory immunotherapy has aimed to induce a much more sustained antitumor T-cell response [93]. In a phase Ib trial for locally advanced, unresectable or metastatic PDAC (NCT00836407) (https://clinicaltrials.gov/ct2/show/NCT00836407), thirty patients received either ipilimumab monotherapy or ipilimumab plus GVAX cancer vaccine, and the median OS was 3.6 mo for the ipilimumab monotherapy group, compared to 5.7 mo in the group with combination therapy[94]. Although combinatory immunotherapy has shown its potential for advanced PDAC, more studies are needed to fully explore this novel therapeutic strategy's capability.

Few human leukocyte antigen (HLA)-A(*)2402-restricted tumor-associated antigens, including the KIF20A-10-66 peptide, have been identified in PDAC[95]. A phase I/II clinical trial in Japan showed a better prognosis in patients with metastatic PDAC and HLA-A*2402-positive status who received KIF20A-10-66 peptide vaccination as second-line treatment after failure of gemcitabine chemotherapy [96]. In two separate phase II clinical trials, KIF20A-derived peptide was evaluated in combination with two antiangiogenic cancer vaccines targeting vascular endothelial growth factor receptor 1 (VEGFR1) and VEGFR2. In the HLA-A*2402-matched group, patients with peptide-specific CTL induction had improved prognosis and increased OS[97,98]. Another HLA-A24-restricted antigenic peptide, SVN-2B, also functions as an immunogenic molecule. A vaccination protocol of SVN-2B in combination with interferon-α has demonstrated effective clinical and immunological responses for advanced PDAC[99].

Algenpantucel-L is a whole-cell pancreatic cancer vaccine with two irradiated allogenic human pancreatic cell lines (HAPa-1 and HAPa-2) expressing the murine enzyme (1,3)-galactosyltransferase (α GT)[100]. Of note, the αGT enzyme is the critical barrier to xenotransplantation due to hyperacute rejection[101]. As a result, Algenpantucel-L will induce a hyperacute rejection of the allograft cells through rapid activation of antibody-dependent cell-mediated cytotoxicity (ADCC), leading to a response against the patient's pancreatic cancer cells through epitope spreading[102]. A phase II, open-label trial (NCT00569387) (https://clinicaltrials.gov/ct2/show/NCT00569387) evaluated the use of the Algenpantucel-L tumor vaccine in combination with gemcitabine plus 5-FU chemoradiotherapy in patients with resected PDAC. Seventy patients were recruited in the study, and the 12-mo disease-free survival (DFS) and OS were 63% and 86%, respectively, suggesting that the Algenpantucel-L tumor vaccine could be administered with standard chemotherapy following surgical resection of pancreatic cancer[101]. Unfortunately, in a recent phase 3, open-label, randomized clinical trial (NCT01836432) (https://clinicaltrials.gov/ct2/show/NCT01836432), Algenpantucel-L failed to improve survival on borderline resectable or locally advanced PDAC receiving neoadjuvant chemoradiation therapy[103].

Overexpression of Mucin 1 (MUC-1), a type I transmembrane protein with O-linked glycosylation, plays a crucial role in oncogenic signaling to promote metastasis, angiogenesis, and invasion[104]. MUC-1 has served as a target for cancer vaccine immunotherapy[105]. Following surgical resection, a phase I/II study of a MUC1 peptide-loaded dendritic cell vaccine was conducted in 12 pancreaticobiliary cancer patients. Four out of twelve (33.3%) patients who received this MUC-1-based tumor vaccine were alive after four years without evidence of recurrence[106]. An optimized construct with MUC-1-variable number tandem repeats has been designed with much more potent immunogenicity [107].

Dendritic cell vaccines have been introduced to enhance the antitumor immune response through the stimulation of naïve T cells[108]. In a study evaluating the effectiveness of a dendritic cell vaccine in patients with advanced PDAC (NCT01410968) (https://clinicaltrials.gov/ct2/show/NCT01410968), autologous dendritic cells were isolated in HLA-A2-positive patients, loaded with three A-2 restricted peptides, and readministered as a cellular vaccine. The results were promising with the generation of antigen-specific T cells in three patients, as well as tolerable adverse effects[109]. In a phase I study in Japan, a Wilms' tumor 1 (WT1)-pulsed dendritic cell vaccine combined with chemotherapy showed safety and potential acquisition of immunity in resected PDAC[110]. Multiple associated studies have further supported the clinical benefits of dendritic cell-based vaccines in PDAC[111-113].

Approximately 95% of PDAC patients have mutations in the *KRAS* oncogene. Despite an early study suggesting an unproven efficacy by targeting mutated KRAS in PDAC[114], multiple subsequent clinical studies have demonstrated the clinical potential for such a therapeutic approach. A phase I/II clinical trial (NCT02261714) (https://clinicaltrials.gov/ct2/show/NCT02261714) evaluated the efficacy of a synthetic mutant RAS peptide vaccine with GM-CSF in PDAC. TG01, a mixture of 7 synthetic RAS peptides representing the most common *KRAS* mutations, combined with GM-CSF and gemcitabine was well tolerated with a robust immune response and improved clinical outcome[115]. One study demonstrated a long-term immune response and improved survival in patients with resected PDAC after KRAS vaccination[116]. An alternative KRAS-based tumor vaccine is GI-4000, a recombinant heat-

Table 2 Complete vaccine immunotherapy-based clinical trials in pancreatic ductal adenocarcinoma

Treatment	Phase	Number	Cancer stage	Outcomes
GVAX, 5-FU, chemoradiation	II	NCT00084383	Resected stage I/II PDAC	Median OS 24.8 mo (95%CI: 21.2-31.6 mo)
GVAX, cyclophosphamide, CRS-207	II	NCT01417000	Metastatic PDAC	Cy/GVAX and CRS-207 extended OS for PDAC patients, with minimal toxicity
GVAX, cyclophosphamide, CRS-207	II	NCT02004262	Metastatic PDAC	Cy/GVAX and CRS-207 did not show survival benefit over chemotherapy in patients with previously treated metastatic PDAC
GVAX, Ipilimumab, FOLFIRINOX	II	NCT01896869	Metastatic PDAC	Ipilimumab + GVAX group did not show survival benefit over chemotherapy [median OS 9.38 mo (95% CI, 5.0-12.2 mo) *vs* 14.7 mo (95%CI: 11.6-20.0 mo)]
Algenpantucel-L	II	NCT00569387	Surgically resected PDAC	The addition of algenpantucel-L to standard adjuvant therapy for resected pancreatic cancer may improve survival (12-mo DFS 62%, 12-mo OS 86%)
Gemcitabine, 5FU Chemoradiation, Algenpantucel-L	III	NCT01072981	Surgically Resected PDAC	No results reported yet
Dendritic cells pulsed with MUC-1/WT-1	I/II	NCT03114631	PDAC	Dendritic cells immunotherapy provided a favorable outcome in PDAC patents (12-mo OS 78.2% *vs* 33.8%)
GI-4000 (KRAS), Gemcitabine	II	NCT00300950	Non-metastatic, Post-resection PDAC	Overall, GI-4000 group showed a similar pattern of recurrence-free survival and OS compared with the placebo group. For stratified R1 resection subgroup, there was a trend in 1 year OS (72% *vs* 56%), an improvement in OS (523.5 *vs* 443.5 d (hazard ratio: 1.06; 95%CI: 0.53–2.13, P = 0.872), and increased frequency of immune responders (40% *vs* 8%; P = 0.062) for GI-4000 *vs* placebo.
Ras-peptide vaccine, IL-2, GM-CSF	II	NCT00019331	Metastatic PDAC	No results reported yet
GV1001 (telomerase peptide vaccine), Gemcitabine, Capecitabine	III	NCT00425360	Locally Advanced or Metastatic PDAC	Adding GV1001 vaccination to chemotherapy did not improve OS.

https://clinicaltrials.gov/. PDAC: Pancreatic ductal adenocarcinoma; Cy: cyclophosphamide; DFS: Disease-free survival; OS: Overall survival.

inactivated Saccharomyces cerevisiae yeast-derived vaccine expressing mutated KRAS proteins. A phase I trial revealed a favorable safety profile and immunogenicity of the GI-4000 cancer vaccine[117]. A subsequent phase II trial (NCT00300950) (https://clinicaltrials.gov/ct2/show/NCT00300950) compared GI-4000 plus gemcitabine with placebo plus gemcitabine alone in patients with resected PDAC carrying *KRAS* mutation. GI-4000 was well tolerated. It led to a similar median OS compared with placebo. However, compared with the placebo group, the GI-4000 group had a trend of improved OS (523.5 *vs* 443.5 d) and an increased frequency of immune responders (40% *vs* 8%) in the stratified R1 resection subgroup[118].

The GV1001 tumor vaccine consists of a fragment (16 amino acids) of human telomerase reverse transcriptase (hTERT) found in a high proportion in PDAC cancer cells and has been introduced as a novel therapeutic regimen[119]. In a phase I/II clinical trial evaluating the clinical outcomes in patients with unresectable PDAC, GV1001 plus GM-CSF elicited an immune response in 63% of patients, resulting in a median OS of 7.2 mo for immune responders compared to 2.9 mo for nonimmune responders[120]. However, in a randomized phase III study of patients with locally advanced and metastatic PDAC, combination therapy consisting of GV1001, gemcitabine, and capecitabine chemotherapy showed no improvement in OS compared to chemotherapy alone [6.9 mo (95%CI: 6.4–7.6 mo) *vs* 7.9 mo (95%CI: 7.1–8.8 mo)] (NCT00425360) (https://clinicaltrials.gov/ct2/show/NCT00425360) [121]. Another GV1001-based phase III clinical trial (NCT00358566) (https://clinicaltrials.gov/ct2/show/NCT00358566) was terminated early because of a lack of survival advantage.

Adoptive cell transfer

Adoptive cell transfer, also known as cellular immunotherapy, includes chimeric antigen receptor T-cell (CAR T cell) therapy and tumor-infiltrating lymphocyte (TIL) therapy[122,123]. CAR T-cell therapy is the most common type of adoptive cell transfer. Generally, it involves harvesting the patient's T cells, genetic modification to express surface chimeric antigen receptor, *ex vivo* expansion, and then transferring the cells back to enhance tumor immunity. In forty-three patients with PDAC who underwent radical pancreatectomy, gemcitabine plus adoptive cell transfer with T cells stimulated by the MUC1-expressing human pancreatic cancer cell line demonstrated a median OS of 14.7 mo[124]. Mesothelin is a tumor antigen highly expressed in PDAC[125]. In a preclinical study, CAR T-cell therapy targeting mesothelin demonstrated promising tumor-suppressive effects[126]. Amatuximab

Table 3 Complete adoptive cell transfer-based clinical trials in pancreatic ductal adenocarcinoma

Treatment	Phase	Number	Cancer stage	Outcomes
MORAb-009, Gemcitabine	II	NCT00570713	Advanced PDAC	MORAb-009 did not show survival benefit over placebo group [median OS 6.5 mo, 95%CI: 4.5–8.10 mo *vs* 6.9 mo 95%CI: 5.4–8.8 mo]
MORAb-009	I	NCT00325494	PDAC	No results reported yet
Radiolabeled Amatuximab (MORAb-009)	I	NCT01521325	PDAC	No results reported yet
Autologous Redirected RNA Mesothelin CAR T cells	I	NCT01897415	PDAC	No results reported yet
CART-133 T cells	I/II	NCT02541370	Relapsed and/or Chemotherapy Refractory Advanced PDAC	No results reported yet

https://clinicaltrials.gov/. PDAC: Pancreatic ductal adenocarcinoma; OS: Overall survival.

(MORab-009), a chimeric mAb targeting mesothelin, also led to reduced growth of mesothelin-expressing tumors, including PDAC[127]. In a phase I trial, the efficacy of MORAb-009 was tested in seven PDAC patients, and one patient had disease control for greater than six months[128]. However, in a phase II randomized placebo-controlled clinical trial (NCT00570713) (https://clinicaltrials.gov/show/NCT00570713) evaluating the efficacy of MORAb-009 plus gemcitabine, no significantly improved clinical outcome was observed [median OS: 6.5 mo (95%CI: 4.5–8.10 mo) *vs* 6.9 mo (95%CI: 5.4–8.8 mo)]. Compared with the development of ICIs and cancer vaccines, adoptive cell transfer therapy is still in the early development phase against pancreatic cancer (Table 3); more preclinical and clinical studies are needed to further explore its full clinical potential.

IMMUNOTHERAPY AND THE TUMOR MICROENVIRONMENT

Immunotherapy has thus far failed to fulfill its promise in PDAC. The underlying mechanisms appear to be complex and multifactorial primarily due to their unique genetic signatures, metabolic features, and immunosuppressive TME. Pancreatic cancers carry unique molecular genetic backgrounds. MSI in pancreatic cancer is extremely rare (approximately 1%). Oncogenic *KRAS* mutations, the most common mutation in PDAC, have also contributed to PDAC initiation and maintenance by producing an immunosuppressive TME[129].

Furthermore, altered metabolism of glucose, amino acids, and lipids and their crosstalk with the TME play essential roles in PDAC tumor progression[130]. Multiple lines of evidence have pinpointed the TME as one of the significant barriers to developing effective immunotherapy for PDAC. It is of great clinical interest to sensitize PDAC to immunotherapy through modification of the TME.

One such effort has been focused on CAFs in the TME. As an immunosuppressive component of the TME, FAP-positive CAFs potentially account for the ineffectiveness of immunotherapy in PDAC[131]. Another subtype of CAFs, characterized by the expression of the leucine-rich repeat-containing 15 (LRRC15) protein, could only be detected in pancreatic cancer tissue and is associated with poor response to anti-PD-L1 therapy[132]. Notably, FAP-positive CAFs are the only CAF subtype that expresses CXC motif chemokine ligand 12 (CXCL12). Ablation of FAP-positive CAFs or inhibition of CXCL12 uncovers the antitumor activity of CTLA-4 and PD-L1-based immunotherapy[133]. A phase I/II clinical trial (NCT03168139) (https://clinicaltrials.gov/ct2/show/NCT03168139) was conducted to evaluate the treatment effect of pembrolizumab in patients receiving docetaxel (NOX-A12), an agent targeting CXCL12 and TME in metastatic PDAC. No results have been reported yet.

Cellular components in the TME, including MDSCs and TAMs, are also promising targets in the combinatory strategy for immunotherapy. MDSCs and TAMs induce an immunosuppressive TME, partially through colony-stimulating factor 1 receptor (CSF1R) and focal adhesion kinase (FAK)[134]. Small molecular inhibitors of CSF1R or FAK can reprogram the TME and improve T lymphocyte-mediated pancreatic cancer destruction[135,136]. Multiple clinical trials with CSF1R or FAK inhibitors combined with immunotherapy are currently ongoing (Table 4).

CONCLUSION

Despite advances in translational research, PDAC remains a highly lethal malignancy. Recent breakthroughs in immunotherapy have revolutionized cancer therapy and have shown great potential to transform future PDAC treatment. However, PDAC has shown inferior treatment outcomes toward

Table 4 Ongoing clinical trials with immunotherapy plus agents targeting the tumor microenvironment in pancreatic ductal adenocarcinoma

Strategy	Treatment	Phase	Number	Cancer stage
Immune checkpoint inhibitor (target) + CAFs/CXCL12 targeted agents	Pembrolizumab(PD-1) + Olaptesed pegol	I/II	NCT03168139	Metastatic PDAC
Immune checkpoint inhibitor (target)+ CSF1R targeted agent	Durvalumab (PD-L1) + Pexidartinib	I	NCT02777710	Metastatic/Advanced PDAC
	Nivolumab (PD-1) + Cabiralizumab	I	NCT02526017	Advanced PDAC
	Nivolumab (PD-1) + Cabiralizumab + Gemcitabine	II	NCT03697564	Advanced PDAC (Stage IV)
Immune checkpoint inhibitor (target) + FAK targeted agent	Pembrolizumab(PD-1) + Defactinib	I/IIa	NCT02758587	Advanced PDAC
	Pembrolizumab(PD-1) + Defactinib + Gemcitabine	I	NCT02546531	Advanced PDAC
	Pembrolizumab (PD-1) + Defactinib	II	NCT03727880	Resectable PDAC

https://clinicaltrials.gov/. PDAC: Pancreatic ductal adenocarcinoma; CTLA-4: Cytotoxic T lymphocyte-associated antigen-4; PD-1: Programmed cell death protein 1; PD-L1: Programmed cell death ligand 1; CAFs: Cancer-associated fibroblasts; CXCL12: CXC motif chemokine ligand 12; CSF1R: Colony-stimulating factor 1 receptor; FAK: Focal adhesion kinase.

various immunotherapy regimens compared to other cancer types. The TME has been considered as the fundamental underlying barrier to therapy resistance. To overcome this therapeutic resistance, further investigations with innovative treatment strategies will be needed.

FOOTNOTES

Author contributions: Smith C and Yin F collected and analyzed the data, made the tables and figure, wrote and finalized the manuscript; Zheng W, Dong J, Wang Y, Lai J and Liu X critically reviewed the manuscript; and All authors have approved the final manuscript.

Conflict-of-interest statement: The authors declare no competing interests in this study.

Country/Territory of origin: United States

ORCID number: Caitlyn Smith 0000-0001-8944-0480; Wei Zheng 0000-0003-3193-2655; Jixin Dong 0000-0002-2757-4464; Yaohong Wang 0000-0001-5964-0465; Jinping Lai 0000-0001-5365-2481; Xiuli Liu 0000-0001-5791-2017; Feng Yin 0000-0002-8444-1123.

S-Editor: Ma YJ
L-Editor: A
P-Editor: Ma YJ

REFERENCES

1 **Siegel RL**, Miller KD, Fuchs HE, Jemal A. Cancer Statistics, 2021. *CA Cancer J Clin* 2021; **71**: 7-33 [PMID: 33433946 DOI: 10.3322/caac.21654]
2 **Miller KD**, Siegel RL, Lin CC, Mariotto AB, Kramer JL, Rowland JH, Stein KD, Alteri R, Jemal A. Cancer treatment and survivorship statistics, 2016. *CA Cancer J Clin* 2016; **66**: 271-289 [PMID: 27253694 DOI: 10.3322/caac.21349]
3 **Porta M**, Fabregat X, Malats N, Guarner L, Carrato A, de Miguel A, Ruiz L, Jariod M, Costafreda S, Coll S, Alguacil J, Corominas JM, Solà R, Salas A, Real FX. Exocrine pancreatic cancer: symptoms at presentation and their relation to tumour site and stage. *Clin Transl Oncol* 2005; **7**: 189-197 [PMID: 15960930 DOI: 10.1007/BF02712816]
4 **De Souza A**, Khawaja KI, Masud F, Saif MW. Metformin and pancreatic cancer: Is there a role? *Cancer Chemother Pharmacol* 2016; **77**: 235-242 [PMID: 26740120 DOI: 10.1007/s00280-015-2948-8]
5 **Corbo V**, Tortora G, Scarpa A. Molecular pathology of pancreatic cancer: from bench-to-bedside translation. *Curr Drug*

Targets 2012; **13**: 744-752 [PMID: 22458520 DOI: 10.2174/138945012800564103]
6 **Sperti C**, Pasquali C, Pedrazzoli S. Ductal adenocarcinoma of the body and tail of the pancreas. *J Am Coll Surg* 1997; **185**: 255-259 [PMID: 9291403 DOI: 10.1016/s1072-7515(97)00056-2]
7 **Griffin JF**, Smalley SR, Jewell W, Paradelo JC, Reymond RD, Hassanein RE, Evans RG. Patterns of failure after curative resection of pancreatic carcinoma. *Cancer* 1990; **66**: 56-61 [PMID: 2354408 DOI: 10.1002/1097-0142(19900701)66:1<56::aid-cncr2820660112>3.0.co;2-6]
8 **Mizrahi JD**, Surana R, Valle JW, Shroff RT. Pancreatic cancer. *Lancet* 2020; **395**: 2008-2020 [PMID: 32593337 DOI: 10.1016/S0140-6736(20)30974-0]
9 **Ettrich TJ**, Seufferlein T. Systemic Therapy for Metastatic Pancreatic Cancer. *Curr Treat Options Oncol* 2021; **22**: 106 [PMID: 34665339 DOI: 10.1007/s11864-021-00895-4]
10 **Oberstein PE**, Olive KP. Pancreatic cancer: why is it so hard to treat? *Therap Adv Gastroenterol* 2013; **6**: 321-337 [PMID: 23814611 DOI: 10.1177/1756283X13478680]
11 **Conroy T**, Desseigne F, Ychou M, Bouché O, Guimbaud R, Bécouarn Y, Adenis A, Raoul JL, Gourgou-Bourgade S, de la Fouchardière C, Bennouna J, Bachet JB, Khemissa-Akouz F, Péré-Vergé D, Delbaldo C, Assenat E, Chauffert B, Michel P, Montoto-Grillot C, Ducreux M; Groupe Tumeurs Digestives of Unicancer; PRODIGE Intergroup. FOLFIRINOX versus gemcitabine for metastatic pancreatic cancer. *N Engl J Med* 2011; **364**: 1817-1825 [PMID: 21561347 DOI: 10.1056/NEJMoa1011923]
12 **Sarantis P**, Koustas E, Papadimitropoulou A, Papavassiliou AG, Karamouzis MV. Pancreatic ductal adenocarcinoma: Treatment hurdles, tumor microenvironment and immunotherapy. *World J Gastrointest Oncol* 2020; **12**: 173-181 [PMID: 32104548 DOI: 10.4251/wjgo.v12.i2.173]
13 **Storz P**, Crawford HC. Carcinogenesis of Pancreatic Ductal Adenocarcinoma. *Gastroenterology* 2020; **158**: 2072-2081 [PMID: 32199881 DOI: 10.1053/j.gastro.2020.02.059]
14 **Grant TJ**, Hua K, Singh A. Molecular Pathogenesis of Pancreatic Cancer. *Prog Mol Biol Transl Sci* 2016; **144**: 241-275 [PMID: 27865459 DOI: 10.1016/bs.pmbts.2016.09.008]
15 **Samuel N**, Hudson TJ. The molecular and cellular heterogeneity of pancreatic ductal adenocarcinoma. *Nat Rev Gastroenterol Hepatol* 2011; **9**: 77-87 [PMID: 22183185 DOI: 10.1038/nrgastro.2011.215]
16 **Lee CJ**, Li C, Simeone DM. Human pancreatic cancer stem cells: implications for how we treat pancreatic cancer. *Transl Oncol* 2008; **1**: 14-18 [PMID: 18607507 DOI: 10.1593/tlo.08013]
17 **Pham T**, Roth S, Kong J, Guerra G, Narasimhan V, Pereira L, Desai J, Heriot A, Ramsay R. An Update on Immunotherapy for Solid Tumors: A Review. *Ann Surg Oncol* 2018; **25**: 3404-3412 [PMID: 30039324 DOI: 10.1245/s10434-018-6658-4]
18 **Katayama ES**, Hue JJ, Bajor DL, Ocuin LM, Ammori JB, Hardacre JM, Winter JM. A comprehensive analysis of clinical trials in pancreatic cancer: what is coming down the pike? *Oncotarget* 2020; **11**: 3489-3501 [PMID: 33014285 DOI: 10.18632/oncotarget.27727]
19 **Goggins M**, Offerhaus GJ, Hilgers W, Griffin CA, Shekher M, Tang D, Sohn TA, Yeo CJ, Kern SE, Hruban RH. Pancreatic adenocarcinomas with DNA replication errors (RER+) are associated with wild-type K-ras and characteristic histopathology. Poor differentiation, a syncytial growth pattern, and pushing borders suggest RER+. *Am J Pathol* 1998; **152**: 1501-1507 [PMID: 9626054]
20 **Wilentz RE**, Goggins M, Redston M, Marcus VA, Adsay NV, Sohn TA, Kadkol SS, Yeo CJ, Choti M, Zahurak M, Johnson K, Tascilar M, Offerhaus GJ, Hruban RH, Kern SE. Genetic, immunohistochemical, and clinical features of medullary carcinoma of the pancreas: A newly described and characterized entity. *Am J Pathol* 2000; **156**: 1641-1651 [PMID: 10793075 DOI: 10.1016/S0002-9440(10)65035-3]
21 **Foucher ED**, Ghigo C, Chouaib S, Galon J, Iovanna J, Olive D. Pancreatic Ductal Adenocarcinoma: A Strong Imbalance of Good and Bad Immunological Cops in the Tumor Microenvironment. *Front Immunol* 2018; **9**: 1044 [PMID: 29868007 DOI: 10.3389/fimmu.2018.01044]
22 **Ren B**, Cui M, Yang G, Wang H, Feng M, You L, Zhao Y. Tumor microenvironment participates in metastasis of pancreatic cancer. *Mol Cancer* 2018; **17**: 108 [PMID: 30060755 DOI: 10.1186/s12943-018-0858-1]
23 **Waghray M**, Yalamanchili M, di Magliano MP, Simeone DM. Deciphering the role of stroma in pancreatic cancer. *Curr Opin Gastroenterol* 2013; **29**: 537-543 [PMID: 23892539 DOI: 10.1097/MOG.0b013e328363affe]
24 **Ho WJ**, Jaffee EM, Zheng L. The tumour microenvironment in pancreatic cancer - clinical challenges and opportunities. *Nat Rev Clin Oncol* 2020; **17**: 527-540 [PMID: 32398706 DOI: 10.1038/s41571-020-0363-5]
25 **Hessmann E**, Buchholz SM, Demir IE, Singh SK, Gress TM, Ellenrieder V, Neesse A. Microenvironmental Determinants of Pancreatic Cancer. *Physiol Rev* 2020; **100**: 1707-1751 [PMID: 32297835 DOI: 10.1152/physrev.00042.2019]
26 **Erkan M**, Hausmann S, Michalski CW, Fingerle AA, Dobritz M, Kleeff J, Friess H. The role of stroma in pancreatic cancer: diagnostic and therapeutic implications. *Nat Rev Gastroenterol Hepatol* 2012; **9**: 454-467 [PMID: 22710569 DOI: 10.1038/nrgastro.2012.115]
27 **Whatcott CJ**, Diep CH, Jiang P, Watanabe A, LoBello J, Sima C, Hostetter G, Shepard HM, Von Hoff DD, Han H. Desmoplasia in Primary Tumors and Metastatic Lesions of Pancreatic Cancer. *Clin Cancer Res* 2015; **21**: 3561-3568 [PMID: 25695692 DOI: 10.1158/1078-0432.CCR-14-1051]
28 **Karagiannis GS**, Poutahidis T, Erdman SE, Kirsch R, Riddell RH, Diamandis EP. Cancer-associated fibroblasts drive the progression of metastasis through both paracrine and mechanical pressure on cancer tissue. *Mol Cancer Res* 2012; **10**: 1403-1418 [PMID: 23024188 DOI: 10.1158/1541-7786.MCR-12-0307]
29 **Ferrara B**, Pignatelli C, Cossutta M, Citro A, Courty J, Piemonti L. The Extracellular Matrix in Pancreatic Cancer: Description of a Complex Network and Promising Therapeutic Options. *Cancers (Basel)* 2021; **13** [PMID: 34503252 DOI: 10.3390/cancers13174442]
30 **Binenbaum Y**, Na'ara S, Gil Z. Gemcitabine resistance in pancreatic ductal adenocarcinoma. *Drug Resist Updat* 2015; **23**: 55-68 [PMID: 26690340 DOI: 10.1016/j.drup.2015.10.002]
31 **Kultti A**, Zhao C, Singha NC, Zimmerman S, Osgood RJ, Symons R, Jiang P, Li X, Thompson CB, Infante JR, Jacobetz MA, Tuveson DA, Frost GI, Shepard HM, Huang Z. Accumulation of extracellular hyaluronan by hyaluronan synthase 3

promotes tumor growth and modulates the pancreatic cancer microenvironment. *Biomed Res Int* 2014; **2014**: 817613 [PMID: 25147816 DOI: 10.1155/2014/817613]

32 **Provenzano PP**, Cuevas C, Chang AE, Goel VK, Von Hoff DD, Hingorani SR. Enzymatic targeting of the stroma ablates physical barriers to treatment of pancreatic ductal adenocarcinoma. *Cancer Cell* 2012; **21**: 418-429 [PMID: 22439937 DOI: 10.1016/j.ccr.2012.01.007]

33 **Gulley JL**, Borre M, Vogelzang NJ, Ng S, Agarwal N, Parker CC, Pook DW, Rathenborg P, Flaig TW, Carles J, Saad F, Shore ND, Chen L, Heery CR, Gerritsen WR, Priou F, Langkilde NC, Novikov A, Kantoff PW. Phase III Trial of PROSTVAC in Asymptomatic or Minimally Symptomatic Metastatic Castration-Resistant Prostate Cancer. *J Clin Oncol* 2019; **37**: 1051-1061 [PMID: 30817251 DOI: 10.1200/JCO.18.02031]

34 **Van Cutsem E**, Tempero MA, Sigal D, Oh DY, Fazio N, Macarulla T, Hitre E, Hammel P, Hendifar AE, Bates SE, Li CP, Hingorani SR, de la Fouchardiere C, Kasi A, Heinemann V, Maraveyas A, Bahary N, Layos L, Sahai V, Zheng L, Lacy J, Park JO, Portales F, Oberstein P, Wu W, Chondros D, Bullock AJ; HALO 109-301 Investigators. Randomized Phase III Trial of Pegvorhyaluronidase Alfa With Nab-Paclitaxel Plus Gemcitabine for Patients With Hyaluronan-High Metastatic Pancreatic Adenocarcinoma. *J Clin Oncol* 2020; **38**: 3185-3194 [PMID: 32706635 DOI: 10.1200/JCO.20.00590]

35 **Coussens LM**, Fingleton B, Matrisian LM. Matrix metalloproteinase inhibitors and cancer: trials and tribulations. *Science* 2002; **295**: 2387-2392 [PMID: 11923519 DOI: 10.1126/science.1067100]

36 **Bramhall SR**, Neoptolemos JP, Stamp GW, Lemoine NR. Imbalance of expression of matrix metalloproteinases (MMPs) and tissue inhibitors of the matrix metalloproteinases (TIMPs) in human pancreatic carcinoma. *J Pathol* 1997; **182**: 347-355 [PMID: 9349239 DOI: 10.1002/(SICI)1096-9896(199707)182:3<347::AID-PATH848>3.0.CO;2-J]

37 **Xu Y**, Li Z, Jiang P, Wu G, Chen K, Zhang X, Li X. The co-expression of MMP-9 and Tenascin-C is significantly associated with the progression and prognosis of pancreatic cancer. *Diagn Pathol* 2015; **10**: 211 [PMID: 26652622 DOI: 10.1186/s13000-015-0445-3]

38 **Okada Y**, Eibl G, Guha S, Duffy JP, Reber HA, Hines OJ. Nerve growth factor stimulates MMP-2 expression and activity and increases invasion by human pancreatic cancer cells. *Clin Exp Metastasis* 2004; **21**: 285-292 [PMID: 15554384 DOI: 10.1023/b:clin.0000046131.24625.54]

39 **Schneiderhan W**, Diaz F, Fundel M, Zhou S, Siech M, Hasel C, Möller P, Gschwend JE, Seufferlein T, Gress T, Adler G, Bachem MG. Pancreatic stellate cells are an important source of MMP-2 in human pancreatic cancer and accelerate tumor progression in a murine xenograft model and CAM assay. *J Cell Sci* 2007; **120**: 512-519 [PMID: 17227797 DOI: 10.1242/jcs.03347]

40 **Ellenrieder V**, Alber B, Lacher U, Hendler SF, Menke A, Boeck W, Wagner M, Wilda M, Friess H, Büchler M, Adler G, Gress TM. Role of MT-MMPs and MMP-2 in pancreatic cancer progression. *Int J Cancer* 2000; **85**: 14-20 [PMID: 10585576 DOI: 10.1002/(sici)1097-0215(20000101)85:1<14::aid-ijc3>3.0.co;2-o]

41 **Crawford HC**, Scoggins CR, Washington MK, Matrisian LM, Leach SD. Matrix metalloproteinase-7 is expressed by pancreatic cancer precursors and regulates acinar-to-ductal metaplasia in exocrine pancreas. *J Clin Invest* 2002; **109**: 1437-1444 [PMID: 12045257 DOI: 10.1172/JCI15051]

42 **Marshall DC**, Lyman SK, McCauley S, Kovalenko M, Spangler R, Liu C, Lee M, O'Sullivan C, Barry-Hamilton V, Ghermazien H, Mikels-Vigdal A, Garcia CA, Jorgensen B, Velayo AC, Wang R, Adamkewicz JI, Smith V. Selective Allosteric Inhibition of MMP9 Is Efficacious in Preclinical Models of Ulcerative Colitis and Colorectal Cancer. *PLoS One* 2015; **10**: e0127063 [PMID: 25961845 DOI: 10.1371/journal.pone.0127063]

43 **Grünwald B**, Vandooren J, Gerg M, Ahomaa K, Hunger A, Berchtold S, Akbareian S, Schaten S, Knolle P, Edwards DR, Opdenakker G, Krüger A. Systemic Ablation of MMP-9 Triggers Invasive Growth and Metastasis of Pancreatic Cancer *via* Deregulation of IL6 Expression in the Bone Marrow. *Mol Cancer Res* 2016; **14**: 1147-1158 [PMID: 27489361 DOI: 10.1158/1541-7786.MCR-16-0180]

44 **Olive KP**, Jacobetz MA, Davidson CJ, Gopinathan A, McIntyre D, Honess D, Madhu B, Goldgraben MA, Caldwell ME, Allard D, Frese KK, Denicola G, Feig C, Combs C, Winter SP, Ireland-Zecchini H, Reichelt S, Howat WJ, Chang A, Dhara M, Wang L, Rückert F, Grützmann R, Pilarsky C, Izeradjene K, Hingorani SR, Huang P, Davies SE, Plunkett W, Egorin M, Hruban RH, Whitebread N, McGovern K, Adams J, Iacobuzio-Donahue C, Griffiths J, Tuveson DA. Inhibition of Hedgehog signaling enhances delivery of chemotherapy in a mouse model of pancreatic cancer. *Science* 2009; **324**: 1457-1461 [PMID: 19460966 DOI: 10.1126/science.1171362]

45 **Cheng X**, Kim JY, Ghafoory S, Duvaci T, Rafiee R, Theobald J, Alborzinia H, Holenya P, Fredebohm J, Merz KH, Mehrabi A, Hafezi M, Saffari A, Eisenbrand G, Hoheisel JD, Wölfl S. Methylisoindigo preferentially kills cancer stem cells by interfering cell metabolism *via* inhibition of LKB1 and activation of AMPK in PDACs. *Mol Oncol* 2016; **10**: 806-824 [PMID: 26887594 DOI: 10.1016/j.molonc.2016.01.008]

46 **Truong LH**, Pauklin S. Pancreatic Cancer Microenvironment and Cellular Composition: Current Understandings and Therapeutic Approaches. *Cancers (Basel)* 2021; **13** [PMID: 34638513 DOI: 10.3390/cancers13195028]

47 **Richards KE**, Zeleniak AE, Fishel ML, Wu J, Littlepage LE, Hill R. Cancer-associated fibroblast exosomes regulate survival and proliferation of pancreatic cancer cells. *Oncogene* 2017; **36**: 1770-1778 [PMID: 27669441 DOI: 10.1038/onc.2016.353]

48 **Olivares O**, Mayers JR, Gouirand V, Torrence ME, Gicquel T, Borge L, Lac S, Roques J, Lavaut MN, Berthezène P, Rubis M, Secq V, Garcia S, Moutardier V, Lombardo D, Iovanna JL, Tomasini R, Guillaumond F, Vander Heiden MG, Vasseur S. Collagen-derived proline promotes pancreatic ductal adenocarcinoma cell survival under nutrient limited conditions. *Nat Commun* 2017; **8**: 16031 [PMID: 28685754 DOI: 10.1038/ncomms16031]

49 **Sousa CM**, Biancur DE, Wang X, Halbrook CJ, Sherman MH, Zhang L, Kremer D, Hwang RF, Witkiewicz AK, Ying H, Asara JM, Evans RM, Cantley LC, Lyssiotis CA, Kimmelman AC. Pancreatic stellate cells support tumour metabolism through autophagic alanine secretion. *Nature* 2016; **536**: 479-483 [PMID: 27509858 DOI: 10.1038/nature19084]

50 **Özdemir BC**, Pentcheva-Hoang T, Carstens JL, Zheng X, Wu CC, Simpson TR, Laklai H, Sugimoto H, Kahlert C, Novitskiy SV, De Jesus-Acosta A, Sharma P, Heidari P, Mahmood U, Chin L, Moses HL, Weaver VM, Maitra A, Allison JP, LeBleu VS, Kalluri R. Depletion of carcinoma-associated fibroblasts and fibrosis induces immunosuppression and

accelerates pancreas cancer with reduced survival. *Cancer Cell* 2014; **25**: 719-734 [PMID: 24856586 DOI: 10.1016/j.ccr.2014.04.005]

51 **Lee JJ**, Perera RM, Wang H, Wu DC, Liu XS, Han S, Fitamant J, Jones PD, Ghanta KS, Kawano S, Nagle JM, Deshpande V, Boucher Y, Kato T, Chen JK, Willmann JK, Bardeesy N, Beachy PA. Stromal response to Hedgehog signaling restrains pancreatic cancer progression. *Proc Natl Acad Sci U S A* 2014; **111**: E3091-E3100 [PMID: 25024225 DOI: 10.1073/pnas.1411679111]

52 **Biffi G**, Tuveson DA. Diversity and Biology of Cancer-Associated Fibroblasts. *Physiol Rev* 2021; **101**: 147-176 [PMID: 32466724 DOI: 10.1152/physrev.00048.2019]

53 **Helms E**, Onate MK, Sherman MH. Fibroblast Heterogeneity in the Pancreatic Tumor Microenvironment. *Cancer Discov* 2020; **10**: 648-656 [PMID: 32014869 DOI: 10.1158/2159-8290.CD-19-1353]

54 **Öhlund D**, Handly-Santana A, Biffi G, Elyada E, Almeida AS, Ponz-Sarvise M, Corbo V, Oni TE, Hearn SA, Lee EJ, Chio II, Hwang CI, Tiriac H, Baker LA, Engle DD, Feig C, Kultti A, Egeblad M, Fearon DT, Crawford JM, Clevers H, Park Y, Tuveson DA. Distinct populations of inflammatory fibroblasts and myofibroblasts in pancreatic cancer. *J Exp Med* 2017; **214**: 579-596 [PMID: 28232471 DOI: 10.1084/jem.20162024]

55 **Sahai E**, Astsaturov I, Cukierman E, DeNardo DG, Egeblad M, Evans RM, Fearon D, Greten FR, Hingorani SR, Hunter T, Hynes RO, Jain RK, Janowitz T, Jorgensen C, Kimmelman AC, Kolonin MG, Maki RG, Powers RS, Puré E, Ramirez DC, Scherz-Shouval R, Sherman MH, Stewart S, Tlsty TD, Tuveson DA, Watt FM, Weaver V, Weeraratna AT, Werb Z. A framework for advancing our understanding of cancer-associated fibroblasts. *Nat Rev Cancer* 2020; **20**: 174-186 [PMID: 31980749 DOI: 10.1038/s41568-019-0238-1]

56 **Kalluri R**. The biology and function of fibroblasts in cancer. *Nat Rev Cancer* 2016; **16**: 582-598 [PMID: 27550820 DOI: 10.1038/nrc.2016.73]

57 **Yang X**, Lin Y, Shi Y, Li B, Liu W, Yin W, Dang Y, Chu Y, Fan J, He R. FAP Promotes Immunosuppression by Cancer-Associated Fibroblasts in the Tumor Microenvironment *via* STAT3-CCL2 Signaling. *Cancer Res* 2016; **76**: 4124-4135 [PMID: 27216177 DOI: 10.1158/0008-5472.CAN-15-2973]

58 **Shi M**, Yu DH, Chen Y, Zhao CY, Zhang J, Liu QH, Ni CR, Zhu MH. Expression of fibroblast activation protein in human pancreatic adenocarcinoma and its clinicopathological significance. *World J Gastroenterol* 2012; **18**: 840-846 [PMID: 22371645 DOI: 10.3748/wjg.v18.i8.840]

59 **Ziani L**, Chouaib S, Thiery J. Alteration of the Antitumor Immune Response by Cancer-Associated Fibroblasts. *Front Immunol* 2018; **9**: 414 [PMID: 29545811 DOI: 10.3389/fimmu.2018.00414]

60 **Kobayashi H**, Enomoto A, Woods SL, Burt AD, Takahashi M, Worthley DL. Cancer-associated fibroblasts in gastrointestinal cancer. *Nat Rev Gastroenterol Hepatol* 2019; **16**: 282-295 [PMID: 30778141 DOI: 10.1038/s41575-019-0115-0]

61 **Li T**, Yi S, Liu W, Jia C, Wang G, Hua X, Tai Y, Zhang Q, Chen G. Colorectal carcinoma-derived fibroblasts modulate natural killer cell phenotype and antitumor cytotoxicity. *Med Oncol* 2013; **30**: 663 [PMID: 23873014 DOI: 10.1007/s12032-013-0663-z]

62 **Fitzgerald AA**, Weiner LM. The role of fibroblast activation protein in health and malignancy. *Cancer Metastasis Rev* 2020; **39**: 783-803 [PMID: 32601975 DOI: 10.1007/s10555-020-09909-3]

63 **Aliru ML**, Schoenhals JE, Venkatesulu BP, Anderson CC, Barsoumian HB, Younes AI, K Mahadevan LS, Soeung M, Aziz KE, Welsh JW, Krishnan S. Radiation therapy and immunotherapy: what is the optimal timing or sequencing? *Immunotherapy* 2018; **10**: 299-316 [PMID: 29421979 DOI: 10.2217/imt-2017-0082]

64 **Ren X**, Ye F, Jiang Z, Chu Y, Xiong S, Wang Y. Involvement of cellular death in TRAIL/DR5-dependent suppression induced by CD4(+)CD25(+) regulatory T cells. *Cell Death Differ* 2007; **14**: 2076-2084 [PMID: 17762882 DOI: 10.1038/sj.cdd.4402220]

65 **Gondek DC**, Lu LF, Quezada SA, Sakaguchi S, Noelle RJ. Cutting edge: contact-mediated suppression by CD4+CD25+ regulatory cells involves a granzyme B-dependent, perforin-independent mechanism. *J Immunol* 2005; **174**: 1783-1786 [PMID: 15699103 DOI: 10.4049/jimmunol.174.4.1783]

66 **Tsuchikawa T**, Hirano S, Tanaka E, Matsumoto J, Kato K, Nakamura T, Ebihara Y, Shichinohe T. Novel aspects of preoperative chemoradiation therapy improving anti-tumor immunity in pancreatic cancer. *Cancer Sci* 2013; **104**: 531-535 [PMID: 23363422 DOI: 10.1111/cas.12119]

67 **Zhang Y**, Lazarus J, Steele NG, Yan W, Lee HJ, Nwosu ZC, Halbrook CJ, Menjivar RE, Kemp SB, Sirihorachai VR, Velez-Delgado A, Donahue K, Carpenter ES, Brown KL, Irizarry-Negron V, Nevison AC, Vinta A, Anderson MA, Crawford HC, Lyssiotis CA, Frankel TL, Bednar F, Pasca di Magliano M. Regulatory T-cell Depletion Alters the Tumor Microenvironment and Accelerates Pancreatic Carcinogenesis. *Cancer Discov* 2020; **10**: 422-439 [PMID: 31911451 DOI: 10.1158/2159-8290.CD-19-0958]

68 **Ugel S**, De Sanctis F, Mandruzzato S, Bronte V. Tumor-induced myeloid deviation: when myeloid-derived suppressor cells meet tumor-associated macrophages. *J Clin Invest* 2015; **125**: 3365-3376 [PMID: 26325033 DOI: 10.1172/JCI80006]

69 **De Cicco P**, Ercolano G, Ianaro A. The New Era of Cancer Immunotherapy: Targeting Myeloid-Derived Suppressor Cells to Overcome Immune Evasion. *Front Immunol* 2020; **11**: 1680 [PMID: 32849585 DOI: 10.3389/fimmu.2020.01680]

70 **Markowitz J**, Brooks TR, Duggan MC, Paul BK, Pan X, Wei L, Abrams Z, Luedke E, Lesinski GB, Mundy-Bosse B, Bekaii-Saab T, Carson WE 3rd. Patients with pancreatic adenocarcinoma exhibit elevated levels of myeloid-derived suppressor cells upon progression of disease. *Cancer Immunol Immunother* 2015; **64**: 149-159 [PMID: 25305035 DOI: 10.1007/s00262-014-1618-8]

71 **Di Caro G**, Cortese N, Castino GF, Grizzi F, Gavazzi F, Ridolfi C, Capretti G, Mineri R, Todoric J, Zerbi A, Allavena P, Mantovani A, Marchesi F. Dual prognostic significance of tumour-associated macrophages in human pancreatic adenocarcinoma treated or untreated with chemotherapy. *Gut* 2016; **65**: 1710-1720 [PMID: 26156960 DOI: 10.1136/gutjnl-2015-309193]

72 **Lankadasari MB**, Mukhopadhyay P, Mohammed S, Harikumar KB. TAMing pancreatic cancer: combat with a double edged sword. *Mol Cancer* 2019; **18**: 48 [PMID: 30925924 DOI: 10.1186/s12943-019-0966-6]

73 **Hu H**, Hang JJ, Han T, Zhuo M, Jiao F, Wang LW. The M2 phenotype of tumor-associated macrophages in the stroma confers a poor prognosis in pancreatic cancer. *Tumour Biol* 2016; **37**: 8657-8664 [PMID: 26738860 DOI: 10.1007/s13277-015-4741-z]

74 **Liu Q**, Li Y, Niu Z, Zong Y, Wang M, Yao L, Lu Z, Liao Q, Zhao Y. Atorvastatin (Lipitor) attenuates the effects of aspirin on pancreatic cancerogenesis and the chemotherapeutic efficacy of gemcitabine on pancreatic cancer by promoting M2 polarized tumor associated macrophages. *J Exp Clin Cancer Res* 2016; **35**: 33 [PMID: 26879926 DOI: 10.1186/s13046-016-0304-4]

75 **Dijkgraaf EM**, Heusinkveld M, Tummers B, Vogelpoel LT, Goedemans R, Jha V, Nortier JW, Welters MJ, Kroep JR, van der Burg SH. Chemotherapy alters monocyte differentiation to favor generation of cancer-supporting M2 macrophages in the tumor microenvironment. *Cancer Res* 2013; **73**: 2480-2492 [PMID: 23436796 DOI: 10.1158/0008-5472.CAN-12-3542]

76 **Young K**, Hughes DJ, Cunningham D, Starling N. Immunotherapy and pancreatic cancer: unique challenges and potential opportunities. *Ther Adv Med Oncol* 2018; **10**: 1758835918816281 [PMID: 30574212 DOI: 10.1177/1758835918816281]

77 **Zhang J**, Wolfgang CL, Zheng L. Precision Immuno-Oncology: Prospects of Individualized Immunotherapy for Pancreatic Cancer. *Cancers (Basel)* 2018; **10** [PMID: 29385739 DOI: 10.3390/cancers10020039]

78 **Iwai Y**, Ishida M, Tanaka Y, Okazaki T, Honjo T, Minato N. Involvement of PD-L1 on tumor cells in the escape from host immune system and tumor immunotherapy by PD-L1 blockade. *Proc Natl Acad Sci U S A* 2002; **99**: 12293-12297 [PMID: 12218188 DOI: 10.1073/pnas.192461099]

79 **Twomey JD**, Zhang B. Cancer Immunotherapy Update: FDA-Approved Checkpoint Inhibitors and Companion Diagnostics. *AAPS J* 2021; **23**: 39 [PMID: 33677681 DOI: 10.1208/s12248-021-00574-0]

80 **Royal RE**, Levy C, Turner K, Mathur A, Hughes M, Kammula US, Sherry RM, Topalian SL, Yang JC, Lowy I, Rosenberg SA. Phase 2 trial of single agent Ipilimumab (anti-CTLA-4) for locally advanced or metastatic pancreatic adenocarcinoma. *J Immunother* 2010; **33**: 828-833 [PMID: 20842054 DOI: 10.1097/CJI.0b013e3181eec14c]

81 **Torphy RJ**, Zhu Y, Schulick RD. Immunotherapy for pancreatic cancer: Barriers and breakthroughs. *Ann Gastroenterol Surg* 2018; **2**: 274-281 [PMID: 30003190 DOI: 10.1002/ags3.12176]

82 **Plate JM**, Plate AE, Shott S, Bograd S, Harris JE. Effect of gemcitabine on immune cells in subjects with adenocarcinoma of the pancreas. *Cancer Immunol Immunother* 2005; **54**: 915-925 [PMID: 15782312 DOI: 10.1007/s00262-004-0638-1]

83 **Aglietta M**, Barone C, Sawyer MB, Moore MJ, Miller WH Jr, Bagalà C, Colombi F, Cagnazzo C, Gioeni L, Wang E, Huang B, Fly KD, Leone F. A phase I dose escalation trial of tremelimumab (CP-675,206) in combination with gemcitabine in chemotherapy-naive patients with metastatic pancreatic cancer. *Ann Oncol* 2014; **25**: 1750-1755 [PMID: 24907635 DOI: 10.1093/annonc/mdu205]

84 **Weiss GJ**, Blaydorn L, Beck J, Bornemann-Kolatzki K, Urnovitz H, Schütz E, Khemka V. Phase Ib/II study of gemcitabine, nab-paclitaxel, and pembrolizumab in metastatic pancreatic adenocarcinoma. *Invest New Drugs* 2018; **36**: 96-102 [PMID: 29119276 DOI: 10.1007/s10637-017-0525-1]

85 **Mizugaki H**, Yamamoto N, Murakami H, Kenmotsu H, Fujiwara Y, Ishida Y, Kawakami T, Takahashi T. Phase I dose-finding study of monotherapy with atezolizumab, an engineered immunoglobulin monoclonal antibody targeting PD-L1, in Japanese patients with advanced solid tumors. *Invest New Drugs* 2016; **34**: 596-603 [PMID: 27363843 DOI: 10.1007/s10637-016-0371-6]

86 **O'Reilly EM**, Oh DY, Dhani N, Renouf DJ, Lee MA, Sun W, Fisher G, Hezel A, Chang SC, Vlahovic G, Takahashi O, Yang Y, Fitts D, Philip PA. Durvalumab With or Without Tremelimumab for Patients With Metastatic Pancreatic Ductal Adenocarcinoma: A Phase 2 Randomized Clinical Trial. *JAMA Oncol* 2019; **5**: 1431-1438 [PMID: 31318392 DOI: 10.1001/jamaoncol.2019.1588]

87 **Jardim DL**, Goodman A, de Melo Gagliato D, Kurzrock R. The Challenges of Tumor Mutational Burden as an Immunotherapy Biomarker. *Cancer Cell* 2021; **39**: 154-173 [PMID: 33125859 DOI: 10.1016/j.ccell.2020.10.001]

88 **Salman B**, Zhou D, Jaffee EM, Edil BH, Zheng L. Vaccine therapy for pancreatic cancer. *Oncoimmunology* 2013; **2**: e26662 [PMID: 24498551 DOI: 10.4161/onci.26662]

89 **Rosenberg A**, Mahalingam D. Immunotherapy in pancreatic adenocarcinoma-overcoming barriers to response. *J Gastrointest Oncol* 2018; **9**: 143-159 [PMID: 29564181 DOI: 10.21037/jgo.2018.01.13]

90 **Laheru D**, Biedrzycki B, Jaffee EM. Development of a cytokine-modified allogeneic whole cell pancreatic cancer vaccine. *Methods Mol Biol* 2013; **980**: 175-203 [PMID: 23359154 DOI: 10.1007/978-1-62703-287-2_9]

91 **Jaffee EM**, Hruban RH, Biedrzycki B, Laheru D, Schepers K, Sauter PR, Goemann M, Coleman J, Grochow L, Donehower RC, Lillemoe KD, O'Reilly S, Abrams RA, Pardoll DM, Cameron JL, Yeo CJ. Novel allogeneic granulocyte-macrophage colony-stimulating factor-secreting tumor vaccine for pancreatic cancer: a phase I trial of safety and immune activation. *J Clin Oncol* 2001; **19**: 145-156 [PMID: 11134207 DOI: 10.1200/JCO.2001.19.1.145]

92 **Lutz E**, Yeo CJ, Lillemoe KD, Biedrzycki B, Kobrin B, Herman J, Sugar E, Piantadosi S, Cameron JL, Solt S, Onners B, Tartakovsky I, Choi M, Sharma R, Illei PB, Hruban RH, Abrams RA, Le D, Jaffee E, Laheru D. A lethally irradiated allogeneic granulocyte-macrophage colony stimulating factor-secreting tumor vaccine for pancreatic adenocarcinoma. A Phase II trial of safety, efficacy, and immune activation. *Ann Surg* 2011; **253**: 328-335 [PMID: 21217520 DOI: 10.1097/SLA.0b013e3181fd271c]

93 **Chung V**, Kos FJ, Hardwick N, Yuan Y, Chao J, Li D, Waisman J, Li M, Zurcher K, Frankel P, Diamond DJ. Evaluation of safety and efficacy of p53MVA vaccine combined with pembrolizumab in patients with advanced solid cancers. *Clin Transl Oncol* 2019; **21**: 363-372 [PMID: 30094792 DOI: 10.1007/s12094-018-1932-2]

94 **Le DT**, Lutz E, Uram JN, Sugar EA, Onners B, Solt S, Zheng L, Diaz LA Jr, Donehower RC, Jaffee EM, Laheru DA. Evaluation of ipilimumab in combination with allogeneic pancreatic tumor cells transfected with a GM-CSF gene in previously treated pancreatic cancer. *J Immunother* 2013; **36**: 382-389 [PMID: 23924790 DOI: 10.1097/CJI.0b013e31829fb7a2]

95 **Osawa R**, Tsunoda T, Yoshimura S, Watanabe T, Miyazawa M, Tani M, Takeda K, Nakagawa H, Nakamura Y, Yamaue H. Identification of HLA-A24-restricted novel T Cell epitope peptides derived from P-cadherin and kinesin family member 20A. *J Biomed Biotechnol* 2012; **2012**: 848042 [PMID: 22778556 DOI: 10.1155/2012/848042]

96 **Asahara S**, Takeda K, Yamao K, Maguchi H, Yamaue H. Phase I/II clinical trial using HLA-A24-restricted peptide vaccine derived from KIF20A for patients with advanced pancreatic cancer. *J Transl Med* 2013; **11**: 291 [PMID: 24237633 DOI: 10.1186/1479-5876-11-291]

97 **Suzuki N**, Hazama S, Iguchi H, Uesugi K, Tanaka H, Hirakawa K, Aruga A, Hatori T, Ishizaki H, Umeda Y, Fujiwara T, Ikemoto T, Shimada M, Yoshimatsu K, Shimizu R, Hayashi H, Sakata K, Takenouchi H, Matsui H, Shindo Y, Iida M, Koki Y, Arima H, Furukawa H, Ueno T, Yoshino S, Nakamura Y, Oka M, Nagano H. Phase II clinical trial of peptide cocktail therapy for patients with advanced pancreatic cancer: VENUS-PC study. *Cancer Sci* 2017; **108**: 73-80 [PMID: 27783849 DOI: 10.1111/cas.13113]

98 **Miyazawa M**, Katsuda M, Maguchi H, Katanuma A, Ishii H, Ozaka M, Yamao K, Imaoka H, Kawai M, Hirono S, Okada KI, Yamaue H. Phase II clinical trial using novel peptide cocktail vaccine as a postoperative adjuvant treatment for surgically resected pancreatic cancer patients. *Int J Cancer* 2017; **140**: 973-982 [PMID: 27861852 DOI: 10.1002/ijc.30510]

99 **Kameshima H**, Tsuruma T, Kutomi G, Shima H, Iwayama Y, Kimura Y, Imamura M, Torigoe T, Takahashi A, Hirohashi Y, Tamura Y, Tsukahara T, Kanaseki T, Sato N, Hirata K. Immunotherapeutic benefit of α-interferon (IFNα) in survivin2B-derived peptide vaccination for advanced pancreatic cancer patients. *Cancer Sci* 2013; **104**: 124-129 [PMID: 23078230 DOI: 10.1111/cas.12046]

100 **Coveler AL**, Rossi GR, Vahanian NN, Link C, Chiorean EG. Algenpantucel-L immunotherapy in pancreatic adenocarcinoma. *Immunotherapy* 2016; **8**: 117-125 [PMID: 26787078 DOI: 10.2217/imt.15.113]

101 **Hardacre JM**, Mulcahy M, Small W, Talamonti M, Obel J, Krishnamurthi S, Rocha-Lima CS, Safran H, Lenz HJ, Chiorean EG. Addition of algenpantucel-L immunotherapy to standard adjuvant therapy for pancreatic cancer: a phase 2 study. *J Gastrointest Surg* 2013; **17**: 94-100; discussion p. 100 [PMID: 23229886 DOI: 10.1007/s11605-012-2064-6]

102 **McCormick KA**, Coveler AL, Rossi GR, Vahanian NN, Link C, Chiorean EG. Pancreatic cancer: Update on immunotherapies and algenpantucel-L. *Hum Vaccin Immunother* 2016; **12**: 563-575 [PMID: 26619245 DOI: 10.1080/21645515.2015.1093264]

103 **Hewitt DB**, Nissen N, Hatoum H, Musher B, Seng J, Coveler AL, Al-Rajabi R, Yeo CJ, Leiby B, Banks J, Balducci L, Vaccaro G, LoConte N, George TJ, Brenner W, Elquza E, Vahanian N, Rossi G, Kennedy E, Link C, Lavu H. A Phase 3 Randomized Clinical Trial of Chemotherapy With or Without Algenpantucel-L (HyperAcute-Pancreas) Immunotherapy in Subjects With Borderline Resectable or Locally Advanced Unresectable Pancreatic Cancer. *Ann Surg* 2022; **275**: 45-53 [PMID: 33630475 DOI: 10.1097/SLA.0000000000004669]

104 **Nath S**, Mukherjee P. MUC1: a multifaceted oncoprotein with a key role in cancer progression. *Trends Mol Med* 2014; **20**: 332-342 [PMID: 24667139 DOI: 10.1016/j.molmed.2014.02.007]

105 **Behrens ME**, Grandgenett PM, Bailey JM, Singh PK, Yi CH, Yu F, Hollingsworth MA. The reactive tumor microenvironment: MUC1 signaling directly reprograms transcription of CTGF. *Oncogene* 2010; **29**: 5667-5677 [PMID: 20697347 DOI: 10.1038/onc.2010.327]

106 **Lepisto AJ**, Moser AJ, Zeh H, Lee K, Bartlett D, McKolanis JR, Geller BA, Schmotzer A, Potter DP, Whiteside T, Finn OJ, Ramanathan RK. A phase I/II study of a MUC1 peptide pulsed autologous dendritic cell vaccine as adjuvant therapy in patients with resected pancreatic and biliary tumors. *Cancer Ther* 2008; **6**: 955-964 [PMID: 19129927]

107 **Gong YF**, Zhou QB, Liao YD, Mai C, Chen TJ, Tang YQ, Chen RF. Optimized construction of MUC1-VNTR$_n$ DNA vaccine and its anti-pancreatic cancer efficacy. *Oncol Lett* 2017; **13**: 2198-2206 [PMID: 28454381 DOI: 10.3892/ol.2017.5717]

108 **Palucka K**, Ueno H, Fay J, Banchereau J. Dendritic cells and immunity against cancer. *J Intern Med* 2011; **269**: 64-73 [PMID: 21158979 DOI: 10.1111/j.1365-2796.2010.02317.x]

109 **Mehrotra S**, Britten CD, Chin S, Garrett-Mayer E, Cloud CA, Li M, Scurti G, Salem ML, Nelson MH, Thomas MB, Paulos CM, Salazar AM, Nishimura MI, Rubinstein MP, Li Z, Cole DJ. Vaccination with poly(IC:LC) and peptide-pulsed autologous dendritic cells in patients with pancreatic cancer. *J Hematol Oncol* 2017; **10**: 82 [PMID: 28388966 DOI: 10.1186/s13045-017-0459-2]

110 **Yanagisawa R**, Koizumi T, Koya T, Sano K, Koido S, Nagai K, Kobayashi M, Okamoto M, Sugiyama H, Shimodaira S. WT1-pulsed Dendritic Cell Vaccine Combined with Chemotherapy for Resected Pancreatic Cancer in a Phase I Study. *Anticancer Res* 2018; **38**: 2217-2225 [PMID: 29599342 DOI: 10.21873/anticanres.12464]

111 **Kimura Y**, Tsukada J, Tomoda T, Takahashi H, Imai K, Shimamura K, Sunamura M, Yonemitsu Y, Shimodaira S, Koido S, Homma S, Okamoto M. Clinical and immunologic evaluation of dendritic cell-based immunotherapy in combination with gemcitabine and/or S-1 in patients with advanced pancreatic carcinoma. *Pancreas* 2012; **41**: 195-205 [PMID: 21792083 DOI: 10.1097/MPA.0b013e31822398c6]

112 **Kobayashi M**, Shimodaira S, Nagai K, Ogasawara M, Takahashi H, Abe H, Tanii M, Okamoto M, Tsujitani S, Yusa S, Ishidao T, Kishimoto J, Shibamoto Y, Nagaya M, Yonemitsu Y; DC Vaccine Study Group at the Japan Society of Innovative Cell Therapy (J-SICT). Prognostic factors related to add-on dendritic cell vaccines on patients with inoperable pancreatic cancer receiving chemotherapy: a multicenter analysis. *Cancer Immunol Immunother* 2014; **63**: 797-806 [PMID: 24777613 DOI: 10.1007/s00262-014-1554-7]

113 **Takakura K**, Koido S, Kan S, Yoshida K, Mori M, Hirano Y, Ito Z, Kobayashi H, Takami S, Matsumoto Y, Kajihara M, Misawa T, Okamoto M, Sugiyama H, Homma S, Ohkusa T, Tajiri H. Prognostic markers for patient outcome following vaccination with multiple MHC Class I/II-restricted WT1 peptide-pulsed dendritic cells plus chemotherapy for pancreatic cancer. *Anticancer Res* 2015; **35**: 555-562 [PMID: 25550602]

114 **Abou-Alfa GK**, Chapman PB, Feilchenfeldt J, Brennan MF, Capanu M, Gansukh B, Jacobs G, Levin A, Neville D, Kelsen DP, O'Reilly EM. Targeting mutated K-ras in pancreatic adenocarcinoma using an adjuvant vaccine. *Am J Clin Oncol* 2011; **34**: 321-325 [PMID: 20686403 DOI: 10.1097/COC.0b013e3181e84b1f]

115 **Palmer DH**, Valle JW, Ma YT, Faluyi O, Neoptolemos JP, Jensen Gjertsen T, Iversen B, Amund Eriksen J, Møller AS, Aksnes AK, Miller R, Dueland S. TG01/GM-CSF and adjuvant gemcitabine in patients with resected RAS-mutant adenocarcinoma of the pancreas (CT TG01-01): a single-arm, phase 1/2 trial. *Br J Cancer* 2020; **122**: 971-977 [PMID: 32063605 DOI: 10.1038/s41416-020-0752-7]

116 **Wedén S**, Klemp M, Gladhaug IP, Møller M, Eriksen JA, Gaudernack G, Buanes T. Long-term follow-up of patients with resected pancreatic cancer following vaccination against mutant K-ras. *Int J Cancer* 2011; **128**: 1120-1128 [PMID: 20473937 DOI: 10.1002/ijc.25449]

117 **Cohn A**, Morse MA, O'Neil B, Whiting S, Coeshott C, Ferraro J, Bellgrau D, Apelian D, Rodell TC. Whole Recombinant Saccharomyces cerevisiae Yeast Expressing Ras Mutations as Treatment for Patients With Solid Tumors Bearing Ras Mutations: Results From a Phase 1 Trial. *J Immunother* 2018; **41**: 141-150 [PMID: 29528991 DOI: 10.1097/CJI.0000000000000219]

118 **Muscarella P**, Bekaii-Saab T, McIntyre K, Rosemurgy A, Ross SB, Richards DA, Fisher WE, Flynn PJ, Mattson A, Coeshott C, Roder H, Roder J, Harrell FE, Cohn A, Rodell TC, Apelian D. A Phase 2 Randomized Placebo-Controlled Adjuvant Trial of GI-4000, a Recombinant Yeast Expressing Mutated RAS Proteins in Patients with Resected Pancreas Cancer. *J Pancreat Cancer* 2021; **7**: 8-19 [PMID: 33786412 DOI: 10.1089/pancan.2020.0021]

119 **Suehara N**, Mizumoto K, Muta T, Tominaga Y, Shimura H, Kitajima S, Hamasaki N, Tsuneyoshi M, Tanaka M. Telomerase elevation in pancreatic ductal carcinoma compared to nonmalignant pathological states. *Clin Cancer Res* 1997; **3**: 993-998 [PMID: 9815776]

120 **Bernhardt SL**, Gjertsen MK, Trachsel S, Møller M, Eriksen JA, Meo M, Buanes T, Gaudernack G. Telomerase peptide vaccination of patients with non-resectable pancreatic cancer: A dose escalating phase I/II study. *Br J Cancer* 2006; **95**: 1474-1482 [PMID: 17060934 DOI: 10.1038/sj.bjc.6603437]

121 **Middleton G**, Silcocks P, Cox T, Valle J, Wadsley J, Propper D, Coxon F, Ross P, Madhusudan S, Roques T, Cunningham D, Falk S, Wadd N, Harrison M, Corrie P, Iveson T, Robinson A, McAdam K, Eatock M, Evans J, Archer C, Hickish T, Garcia-Alonso A, Nicolson M, Steward W, Anthoney A, Greenhalf W, Shaw V, Costello E, Naisbitt D, Rawcliffe C, Nanson G, Neoptolemos J. Gemcitabine and capecitabine with or without telomerase peptide vaccine GV1001 in patients with locally advanced or metastatic pancreatic cancer (TeloVac): an open-label, randomised, phase 3 trial. *Lancet Oncol* 2014; **15**: 829-840 [PMID: 24954781 DOI: 10.1016/S1470-2045(14)70236-0]

122 **Morotti M**, Albukhari A, Alsaadi A, Artibani M, Brenton JD, Curbishley SM, Dong T, Dustin ML, Hu Z, McGranahan N, Miller ML, Santana-Gonzalez L, Seymour LW, Shi T, Van Loo P, Yau C, White H, Wietek N, Church DN, Wedge DC, Ahmed AA. Promises and challenges of adoptive T-cell therapies for solid tumours. *Br J Cancer* 2021; **124**: 1759-1776 [PMID: 33782566 DOI: 10.1038/s41416-021-01353-6]

123 **Rohaan MW**, Wilgenhof S, Haanen JBAG. Adoptive cellular therapies: the current landscape. *Virchows Arch* 2019; **474**: 449-461 [PMID: 30470934 DOI: 10.1007/s00428-018-2484-0]

124 **Matsui H**, Hazama S, Sakamoto K, Shindo Y, Kanekiyo S, Nakashima M, Matsukuma S, Tokuhisa Y, Iida M, Suzuki N, Yoshimura K, Takeda S, Ueno T, Yoshino S, Oka M, Nagano H. Postoperative Adjuvant Therapy for Resectable Pancreatic Cancer With Gemcitabine and Adoptive Immunotherapy. *Pancreas* 2017; **46**: 994-1002 [PMID: 28697053 DOI: 10.1097/MPA.0000000000000880]

125 **Chen Y**, Ayaru L, Mathew S, Morris E, Pereira SP, Behboudi S. Expansion of anti-mesothelin specific CD4+ and CD8+ T cell responses in patients with pancreatic carcinoma. *PLoS One* 2014; **9**: e88133 [PMID: 24520352 DOI: 10.1371/journal.pone.0088133]

126 **Watanabe K**, Luo Y, Da T, Guedan S, Ruella M, Scholler J, Keith B, Young RM, Engels B, Sorsa S, Siurala M, Havunen R, Tähtinen S, Hemminki A, June CH. Pancreatic cancer therapy with combined mesothelin-redirected chimeric antigen receptor T cells and cytokine-armed oncolytic adenoviruses. *JCI Insight* 2018; **3** [PMID: 29618658 DOI: 10.1172/jci.insight.99573]

127 **Hassan R**, Ebel W, Routhier EL, Patel R, Kline JB, Zhang J, Chao Q, Jacob S, Turchin H, Gibbs L, Phillips MD, Mudali S, Iacobuzio-Donahue C, Jaffee EM, Moreno M, Pastan I, Sass PM, Nicolaides NC, Grasso L. Preclinical evaluation of MORAb-009, a chimeric antibody targeting tumor-associated mesothelin. *Cancer Immun* 2007; **7**: 20 [PMID: 18088084]

128 **Hassan R**, Cohen SJ, Phillips M, Pastan I, Sharon E, Kelly RJ, Schweizer C, Weil S, Laheru D. Phase I clinical trial of the chimeric anti-mesothelin monoclonal antibody MORAb-009 in patients with mesothelin-expressing cancers. *Clin Cancer Res* 2010; **16**: 6132-6138 [PMID: 21037025 DOI: 10.1158/1078-0432.CCR-10-2275]

129 **Collins MA**, Bednar F, Zhang Y, Brisset JC, Galbán S, Galbán CJ, Rakshit S, Flannagan KS, Adsay NV, Pasca di Magliano M. Oncogenic Kras is required for both the initiation and maintenance of pancreatic cancer in mice. *J Clin Invest* 2012; **122**: 639-653 [PMID: 22232209 DOI: 10.1172/JCI59227]

130 **Qin C**, Yang G, Yang J, Ren B, Wang H, Chen G, Zhao F, You L, Wang W, Zhao Y. Metabolism of pancreatic cancer: paving the way to better anticancer strategies. *Mol Cancer* 2020; **19**: 50 [PMID: 32122374 DOI: 10.1186/s12943-020-01169-7]

131 **Kraman M**, Bambrough PJ, Arnold JN, Roberts EW, Magiera L, Jones JO, Gopinathan A, Tuveson DA, Fearon DT. Suppression of antitumor immunity by stromal cells expressing fibroblast activation protein-alpha. *Science* 2010; **330**: 827-830 [PMID: 21051638 DOI: 10.1126/science.1195300]

132 **Dominguez CX**, Müller S, Keerthivasan S, Koeppen H, Hung J, Gierke S, Breart B, Foreman O, Bainbridge TW, Castiglioni A, Senbabaoglu Y, Modrusan Z, Liang Y, Junttila MR, Klijn C, Bourgon R, Turley SJ. Single-Cell RNA Sequencing Reveals Stromal Evolution into LRRC15^{+} Myofibroblasts as a Determinant of Patient Response to Cancer Immunotherapy. *Cancer Discov* 2020; **10**: 232-253 [PMID: 31699795 DOI: 10.1158/2159-8290.CD-19-0644]

133 **Feig C**, Jones JO, Kraman M, Wells RJ, Deonarine A, Chan DS, Connell CM, Roberts EW, Zhao Q, Caballero OL, Teichmann SA, Janowitz T, Jodrell DI, Tuveson DA, Fearon DT. Targeting CXCL12 from FAP-expressing carcinoma-associated fibroblasts synergizes with anti-PD-L1 immunotherapy in pancreatic cancer. *Proc Natl Acad Sci U S A* 2013; **110**: 20212-20217 [PMID: 24277834 DOI: 10.1073/pnas.1320318110]

134 **Osipov A**, Saung MT, Zheng L, Murphy AG. Small molecule immunomodulation: the tumor microenvironment and overcoming immune escape. *J Immunother Cancer* 2019; **7**: 224 [PMID: 31439034 DOI: 10.1186/s40425-019-0667-0]

135 **Li M**, Li M, Yang Y, Liu Y, Xie H, Yu Q, Tian L, Tang X, Ren K, Li J, Zhang Z, He Q. Remodeling tumor immune microenvironment *via* targeted blockade of PI3K-γ and CSF-1/CSF-1R pathways in tumor associated macrophages for pancreatic cancer therapy. *J Control Release* 2020; **321**: 23-35 [PMID: 32035193 DOI: 10.1016/j.jconrel.2020.02.011]

136 **Jiang H**, Hegde S, Knolhoff BL, Zhu Y, Herndon JM, Meyer MA, Nywening TM, Hawkins WG, Shapiro IM, Weaver

DT, Pachter JA, Wang-Gillam A, DeNardo DG. Targeting focal adhesion kinase renders pancreatic cancers responsive to checkpoint immunotherapy. *Nat Med* 2016; **22**: 851-860 [PMID: 27376576 DOI: 10.1038/nm.4123]

World Journal of Gastroenterology

Submit a Manuscript: https://www.f6publishing.com

World J Gastroenterol 2022 July 21; 28(27): 3314-3333

DOI: 10.3748/wjg.v28.i27.3314

ISSN 1007-9327 (print) ISSN 2219-2840 (online)

REVIEW

Crosstalk between dietary patterns, obesity and nonalcoholic fatty liver disease

Danijela Ristic-Medic, Joanna Bajerska, Vesna Vucic

Specialty type: Gastroenterology and hepatology

Provenance and peer review: Invited article; Externally peer reviewed.

Peer-review model: Single blind

Peer-review report's scientific quality classification

Grade A (Excellent): A
Grade B (Very good): 0
Grade C (Good): C
Grade D (Fair): 0
Grade E (Poor): 0

P-Reviewer: Tziomalos K, Greece; Xing HC, China

Received: January 17, 2022
Peer-review started: January 17, 2022
First decision: April 11, 2022
Revised: May 3, 2022
Accepted: June 18, 2022
Article in press: June 18, 2022
Published online: July 21, 2022

Danijela Ristic-Medic, Vesna Vucic, Group for Nutritional Biochemistry and Dietology, Centre of Research Excellence in Nutrition and Metabolism, Institute for Medical Research, National Institute of Republic Serbia, Belgrade PO Box 102, Serbia

Joanna Bajerska, Department of Human Nutrition and Dietetics, Poznań University of Life Sciences, Poznań 60-624, Poland

Corresponding author: Danijela Ristic-Medic, Doctor, MD, PhD, Professor, Senior Researcher, Group for Nutritional Biochemistry and Dietology, Centre of Research Excellence in Nutrition and Metabolism, Institute for Medical Research, National Institute of Republic Serbia, Tadeusa Koscuska 1, Belgrade PO Box 102, Serbia. dristicmedic@gmail.com

Abstract

The prevalence of nonalcoholic fatty liver disease (NAFLD) is rising worldwide, paralleling the epidemic of obesity. The liver is a key organ for the metabolism of proteins, fats and carbohydrates. Various types of fats and carbohydrates in isocaloric diets differently influence fat accumulation in the liver parenchyma. Therefore, nutrition can manage hepatic and cardiometabolic complications of NAFLD. Even moderately reduced caloric intake, which leads to a weight loss of 5%-10% of initial body weight, is effective in improving liver steatosis and surrogate markers of liver disease status. Among dietary patterns, the Mediterranean diet mostly prevents the onset of NAFLD. Furthermore, this diet is also the most recommended for the treatment of NAFLD patients. However, clinical trials based on the dietary interventions in NAFLD patients are sparse. Since there are only a few studies examining dietary interventions in clinically advanced stages of NAFLD, such as active and fibrotic steatohepatitis, the optimal diet for patients in these stages of the disease must still be determined. In this narrative review, we aimed to critically summarize the associations between different dietary patterns, obesity and prevention/risk for NAFLD, to describe specific dietary interventions' impacts on liver steatosis in adults with NAFLD and to provide an updated overview of dietary recommendations that clinicians potentially need to apply in their daily practice.

Key Words: Nonalcoholic fatty liver disease; Dietary patterns; Obesity; Diet; Mediterranean diet; Nutrition; Treatment; Clinical guidance

Core Tip: In this review, we emphasize that based on the current evidence, there is no consensus on the ideal macronutrient composition of the diet for nonalcoholic fatty liver disease (NAFLD) patients. We have shown that dietary habits are the most important factor in NAFLD prevention. The Mediterranean and healthy dietary pattern, characterized by high consumption of vegetables, fruits, nuts, olive oil, low-fat dairy products and fish, were linked with a reduced NAFLD risk. The Dietary Approach to Stop Hypertension diet, intermittent fasting and ketogenic diet are other dietary regimes that have growing interest among specialists who advise patients with NAFLD. Nevertheless, new studies designed to assess the effects of these diets on liver-related outcomes and liver histology are needed. We also noted that dietary advice should be personalized in NAFLD patients.

Citation: Ristic-Medic D, Bajerska J, Vucic V. Crosstalk between dietary patterns, obesity and nonalcoholic fatty liver disease. *World J Gastroenterol* 2022; 28(27): 3314-3333
URL: https://www.wjgnet.com/1007-9327/full/v28/i27/3314.htm
DOI: https://dx.doi.org/10.3748/wjg.v28.i27.3314

INTRODUCTION

Nonalcoholic fatty liver disease (NAFLD) is the accumulation of excess fat (more than 5%) in the liver parenchyma in people with no significant alcohol consumption or secondary causes of hepatic steatosis [1]. The prevalence of NAFLD is rising in many countries, paralleling the epidemic of obesity worldwide. The highest rates of NAFLD have been observed in North Africa (31%), the Middle East (32%) and Asia (27%)[2].

NAFLD represents a clinicopathological spectrum, ranging from benign hepatic steatosis to nonalcoholic steatohepatitis (NASH) and characterized by hepatocellular injury and inflammation, which leads to hepatic fibrosis[3,4]. Up to 20% of patients with fibrotic NASH progress to cirrhosis and associated complications[5,6]. Fibrotic NASH can lead to hepatocellular carcinoma, even at the pre-cirrhotic stage (Figure 1). Approximately 90% of the obese population, 60% of patients with diabetes type 2 and 50% of patients with dyslipidemia have NAFLD[6-8]. Moreover, NAFLD is a risk factor for severe coronavirus disease 2019, and thus nutritional prevention of coronavirus disease 2019 complications has been highlighted in a recent review[8].

Nevertheless, obesity, overnutrition, dietary components and a sedentary lifestyle are modifiable risk factors for NAFLD. Central obesity is probably the most significant modifiable risk factor for this disorder, which arises from energy imbalance[9]. The relationship between excessive caloric intake and the NAFLD development has been shown in interventional studies. Weight loss as a primary therapeutic approach produced clinically meaningful outcomes in patients with NAFLD[10,11]. However, the success of such weight loss interventions depends on the intensity of diet counseling and the frequency of visits to dietitians. Two dietary patterns that seem to promote the improvement of NAFLD with incorporated recommendations are the Mediterranean and the Dietary Approach to Stop Hypertension (DASH) diets[12].

This review critically summarizes the associations between dietary patterns, obesity and prevention/risk for NAFLD as well as the impact of specific dietary interventions on hepatic steatosis in adults with NAFLD. It also provides an updated overview of dietary recommendations that clinicians potentially need to apply in their daily practice.

LITERATURE SEARCH

This narrative review was based on PubMed electronic database search for relevant publications using the following terms ("fatty liver" OR "NAFLD" OR "non-alcoholic fatty liver disease" OR "steatosis of liver" OR "steatohepatitis" OR "steatosis") AND "obesity" AND ("diet" OR "dietary pattern" OR "dietary interventions" OR "nutrition") to identify the studies on the association between dietary patterns and NAFLD and specific clinical dietary intervention studies in adult patients with NAFLD. Also, we focused on systematic reviews with meta-analyses. Studies relevant to the topic, conducted in humans, published in English and preferably published in the last 10 years were included. All studies are checked in Reference Citation Analysis database (https://www.referencecitationanalysis.com/). The list of references was reduced because priority had been given to studies that are relevant to clinical practice. The final list of references was approved with the consent of the authors.

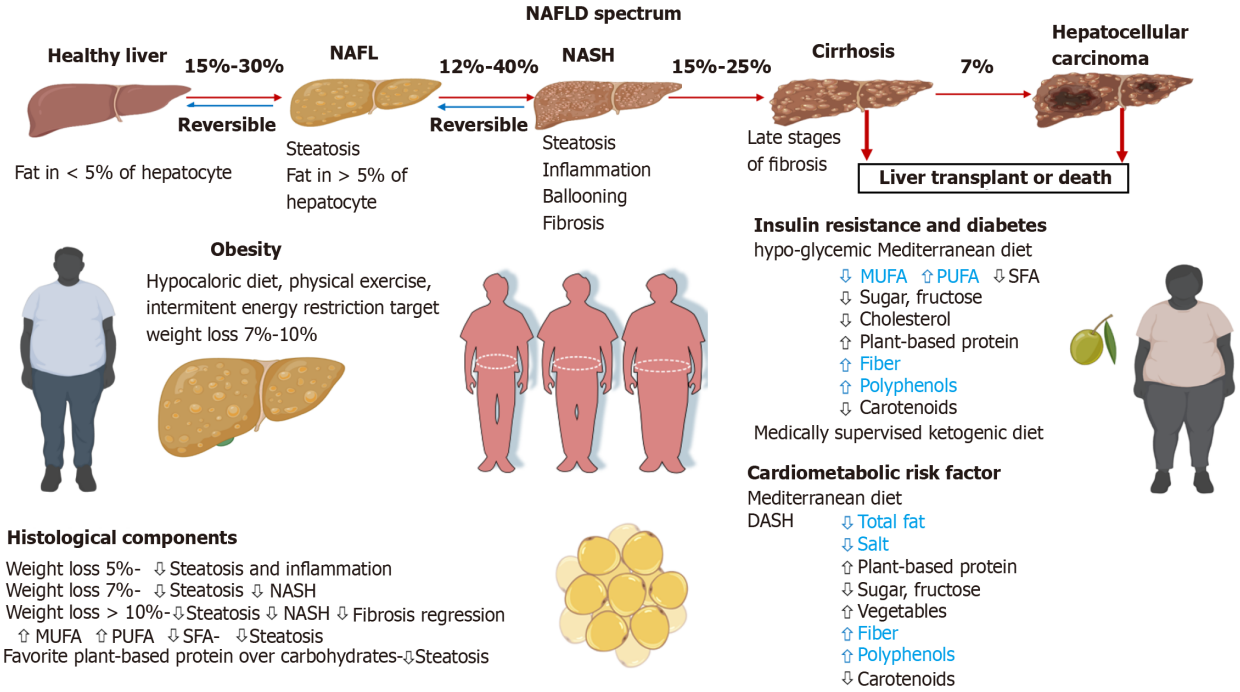

DOI: 10.3748/wjg.v28.i27.3314

Figure 1 Progression of nonalcoholic fatty liver to cirrhosis and/or liver cancer and suggested dietary intervention in nonalcoholic fatty liver disease patients according to risk factors. DASH: Dietary Approach to Stop Hypertension; MUFA: Monounsaturated fatty acid; NAFL: Nonalcoholic fatty liver; NAFLD: Nonalcoholic fatty liver disease; NASH: Nonalcoholic steatohepatitis; PUFA: Polyunsaturated fatty acid; SFA: Saturated fatty acid. Blue fonts indicate evidence-based proven effect of the dietary component. Created in Biorender.com.

MECHANISMS OF LIVER INJURY IN PATIENTS WITH OBESITY

The pathophysiology of NAFLD involves multiple genetic and environmental factors. Genetic factors include specific polymorphisms and epigenetic modifications. As the most common genetic determinant of NAFLD, the I148M variant of patatin-like phospholipase domain-containing protein 3 gene has been recognized[13]. Environmental factors are related to diet and lifestyle, hormonal disturbances, insulin resistance (IR), obesity, oxidative stress, lipotoxicity, unfavorable gut microbiota and many others[9]. Despite well-established risk factors for NAFLD, the pathways leading to the disease are not elucidated, but the role of the diet is undeniable.

It is known that the liver utilizes fatty acids and sugars as primary metabolic substrates, but the overload of these substances results in the accumulation of toxic lipid products[14]. These products increase oxidative stress by overproduction of reactive oxygen species and inflammation in hepatocytes that leads to liver injury. Moreover, a higher intake of saturated fatty acids (SFAs) promotes hepatic liver accumulation and the development and progression of NAFLD[15]. On the contrary, intake of unsaturated fats has a protective role[16].

Recent studies revealed the underlying mechanism of this process, highlighting mitochondrial dysfunction as a key player (reviewed by Meex and Blank[17]). Hepatocytes are very rich in mitochondria, and intake of SFAs induces changes in their structure and function. The process starts with liver steatosis due to reduced oxidation and enhanced lipolysis of adipose tissues. Steatosis affects the efficacy of the respiratory transport chain[18]. Consequently, overproduction of reactive oxygen species and lipid peroxidation arise, eventually resulting in inflammation, apoptosis and damage of the liver. In addition, SFAs from food enter the mitochondrial membrane and alter its permeability and fluidity, contributing further to NAFLD progression[19].

Besides the diet itself, obesity is also associated with NAFLD pathophysiology. In obesity, the capacity of an expanded adipose tissue to store lipids is limited, and the excess of lipids is stored in hepatocytes. The main form of lipids stored in the liver are triglycerides (TGs). Namely, high levels of free fatty acids in circulation, derived from enhanced lipolysis or diminished absorption by subcutaneous adipose tissue, bring ectopic fat accumulation, mostly in the liver. The sources of free fatty acids that form in the liver TG are not only from the diet (around 15%) but from increased lipolysis of TGs in adipose tissue (approximately 60%) and *de novo* lipogenesis (DNL) in the liver (25%) from dietary sugars, glucose and fructose[20]. This is supported by a study using stable isotopes, which has shown that accumulated lipids in the liver of NAFLD patients are mainly attributable to DNL. This stage of fat accumulation in the liver is the beginning of NAFLD, and managing obesity at this stage is of crucial importance. The lack of successful obesity treatment leads to intrahepatic inflammation and infiltration

of immune cells, such as lymphocytes, monocytes and neutrophils, which release cytokines in the liver [21]. This process not only intensifies inflammation but also promotes intrahepatic fibrogenesis, leading to progression of NAFLD to NASH.

Another relationship between obesity and NAFLD has been established through adipokines[22]. Adipokines are hormones derived from adipose tissue, and they are commonly represented by leptin and adiponectin. While their synthesis is balanced in people with normal weight, in obesity the dysregulation of pro- and anti-inflammatory adipokines is present. The enlarged, hypertrophic adipocytes produce proinflammatory adipokines and cytokines and promote IR. Adiponectin suppresses the secretion of proinflammatory cytokines (interleukin 6, tumor necrosis factor α), promotes the release of anti-inflammatory interleukin 10 and negatively correlates with visceral adipose tissue mass[23]. On the contrary, leptin is a product of white adipose tissue, and its level in circulation depends on the fat tissue mass and adipocyte size[24]. This is a satiety hormone with pleiotropic effects, and its concentration is a marker of obesity-related complications: Neuropathy and atherosclerosis[25,26]. Hyperleptinemia is considered crucial for NAFLD progression, although the exact mechanisms are still unclear. However, new findings pinpointed that leptin mediates pyroptotic-like cell death of macrophages and hepatocytes through infiltrated CD8+ T lymphocytes[27]. These results can provide a new strategy for future treatment of NAFLD.

Among the other risk factors, metabolic syndrome (MetS) has demonstrated the strongest association with NAFLD and its advanced stage, NASH. Since MetS is characterized by several features, including waist circumference, hypertension, hyperglycemia and dyslipidemia (low high-density lipoprotein cholesterol and/or high TG level), the clearest biological link with NAFLD development and progression was found for glucose level[28]. In line with this, 75% of patients with diabetes mellitus have NAFLD as well. This relation is bidirectional: Patients with NAFLD have a higher risk of developing diabetes[29]. Although IR is involved in NAFLD pathogenesis, improving IR is often insufficient to prevent further progression of NAFLD[30].

Furthermore, increased central adiposity, an important component of MetS, is considered a more significant marker of NAFLD than total body fat. This is expected, considering the role of visceral fats in the biosynthesis of adipokines. According to a recent study, there is a cross-talk between IR, adipose tissue inflammation and NAFLD, with dipeptidyl peptidase 4 as the key factor. This enzyme, secreted by the hepatocytes, has been shown to promote IR and inflammation of visceral adipose tissue[31]. In support of that, Barchetta *et al*[32] reported that levels and activity of dipeptidyl peptidase 4 in circulation are independently associated with NAFLD presence and severity in patients with or without other metabolic diseases and with various grades of obesity. The authors proposed dipeptidyl peptidase 4 as a novel marker for NAFLD/NASH risk stratification and follow-up of NAFLD patients.

ASSOCIATIONS BETWEEN DIETARY PATTERNS AND RISK OF NAFLD

Since people do not consume nutrients in isolation, the best option to describe the relationship between nutrition and health outcomes is the analysis of dietary patterns. Dietary patterns are a combination of a variety of foods habitually consumed by an individual, which together create synergistic effects on our health[33]. Two main dietary patterns, such as a "Western dietary pattern" and "Mediterranean dietary pattern" have been significantly associated (although in the opposite direction) with NAFLD, independently of potential confounders[34]. However, there are more dietary patterns (*e.g.*, healthy, traditional) identified for these associations.

Mediterranean dietary pattern and NAFLD

Mediterranean diet (MD) is a plant-based diet containing significant amounts of fiber, antioxidants, vegetable proteins, monounsaturated fat and polyunsaturated fatty acids (PUFAs), and with an appropriate n-6/n-3 PUFA ratio. This diet is known as a high-fat diet, with a fat intake of up to 45% of total daily calories[35]. The basic source of dietary fat in this diet is olive oil[33,36], where oleic acid, a monounsaturated fatty acid (MUFA), is a major component[37]. The MD is also characterized by high amounts of PUFAs. Dietary sources of the PUFAs, especially long-chain n-3 fatty acids, which include eicosapentaenoic acid and docosahexaenoic acid, in the MD are fish and nuts[38]. The MD is therefore rich in macronutrients that have been shown to have a beneficial effect on glucose and lipidic metabolism, and consequently on NAFLD[39]. The observational studies on the association between MD and NAFLD are summarized in Table 1. A reverse association between high adherence to MD and NAFLD odds, even after adjusting for some confounders such as age, sex, diabetes, physical activity, energy intake, smoking status and supplements use was seen in two case-control studies[40,41] and one cross-sectional study[42]. It should be highlighted that higher consumption of nuts, fruits and vegetables, legumes and fish as well as lower intake of meat were reported to be protective against NAFLD[43].

However, Entezari *et al*[40] observed that the reverse relationship between adherence to MD and odds of NAFLD disappeared after controlling for the anthropometric variables (body mass index and waist-to-hip ratio), which means that the MD may improve fatty liver by body weight modification,

Table 1 Association between the Mediterranean dietary patterns and nonalcoholic fatty liver disease

Ref.	Country/Region	Assess adherence to the MD	Food groups associated with lower risk NAFLD	Study design	Number of patients and age range	Main results	Associations
Entezari *et al* [40]	Iran	MDS	↑ Intake nuts and fruits, vegetables, legumes, high MUFA/PUFA ratio, cereals and fish. ↓ EI, low-fat dairy and meats	C-C	247 (43.7% male); 18–55 yr	↑ Adherence to MD was associated with ↓ risk of NAFLD after controlling for age (OR: 0.40, 95%CI: 0.17–0.95) and sex, diabetes, PA and supplement intake (OR: 0.36, 95%CI: 0.15–0.89). This association disappeared after adjusting for BMI, WHR (OR: 0.70, 95%CI: 0.25–1.97)	↓, After controlling for anthropometrical variables ↔
Giraldi *et al* [41]	Italy	MDS	↑ Legumes consumption ↓ risk of NAFLD (OR: 0.62; 95%CI: 0.38-0.99) and ↑ fish intake ↓ risk of NAFLD (OR: 0.38; 95%CI: 0.17-0.85)	C-C	815 (371 with NAFLD); 59 ± 16 yr; 444 controls; 45 ± 14 yr	↑ Adherence to the MD was associated with ↓ risk of NAFLD (OR: 0.83; 95%CI: 0.71-0.98) after controlling for age, sex, EI, diabetes status, smoking status, BMI and PA	↓
Baratta *et al* [42]	Italy	MD questionnaire	↓ Meat intake	C-S	584 patients (61.8% males) with cardiometabolic risk factors screened for the presence of liver steatosis; 56.2 ± 12.4 yr	↑ Adherence to MD was associated with ↓ risk of NAFLD (intermediate *vs* low tertile OR: 0.12; $P < 0.05$; high *vs* low tertile OR: 0.09; $P < 0.05$)	↓
Aller[45]	Spain	14-item MD assessment tool	-	C-S	82 NAFLD patients (42.7% low and 57.3% high steatosis grade, 68.3% steatohepatitis and 51.2% liver fibrosis mean age 44 + 11 yr	↑ Adherence to MD was associated with ↓ likelihood of having steatohepatitis OR: 0.43; 95%CI: 0.29-0.64 and steatosis OR: 0.42; 95%CI: 0.26- 0.70	↓
Park *et al*[46]	United States; 5 targeted racial/ethnic groups: African American, Native Hawaiian, Japanese American, Latino and White	Alternate MDS	-	Nested C-C	2959 with NAFLD (509 with cirrhosis; 2450 without cirrhosis) and 29292 controls; mean age 44.2 + 11.3 yr	↑ Adherence to MD was not associated with lower NAFLD risk	↔
Chan *et al* [47]	Hong Kong of China	MDS	↑ Vegetables and legumes, fruits and dried fruits, vitamin C	C-S	797 (41.7% males) 27.6% had a fatty liver aged ≥ 18 yr	MDS was not associated with the prevalence of NAFLD	↔
Kontogianni *et al*[44]	Greece	MDS	-	C-S	73 overweight/obese patients with NAFLD (69% males) *vs* 58 age-sex- and BMI matched controls; mean age 45 yr	No difference in the MDS was observed between patients and controls. One unit increase in the MDS was associated with ↓ likelihood of having NASH (OR: 0.64; 95%CI: 0.45-0.92), after controlling for sex and abdominal fat	↓

BMI: Body mass index; C-C: Case-control; C-S: Cross-sectional; CI: Confidence interval; EI: Energy intake; MD: Mediterranean diet; MDS: Mediterranean Diet Score; MUFA/PUFA: Monounsaturated fatty acids/Polyunsaturated fatty acids; NAFLD: Non-alcoholic fatty liver disease; OR: Odds ratio; WHR: Waist to hip ratio; PA: Physical activity.

modulation of lipid profile and inflammatory markers. Although Kontogianni *et al*[44] did not find a significant difference between NAFLD patients and controls in terms of adherence to the MD, higher adherence to this diet was inversely associated with alcoholic steatohepatitis. Similar results were seen

in the study by Aller *et al*[45].

On the other hand, in a nested and matched case-control study[46] as well as a cross-sectional study [47] it was found that adherence to the MD in any models (crude or adjusted to some confounders) was not associated with the risk of NAFLD. It should be highlighted that the dietary indices that measure adherence to the MD vary among the included studies. Hence, the specific dietary components and/or food items included within each of these indices and the methods used to evaluate compliance should be taken into consideration when interpreting obtained results. Nevertheless, a recent meta-analysis has proven that MD reduced the risk of NAFLD by 23%[43]. Also, the European Association for the Study of the Liver, and the European Association for the Study of Diabetes-European Association for the Study of Obesity Clinical Practice Guidelines have encouraged the MD as a lifestyle choice for treating the disease[48].

Various mechanisms may be associated with the beneficial effects of the MD on metabolic health and NAFLD, but the most important for this association is an appropriate fatty acid composition due to high MUFA content and an appropriate n-6/n-3 PUFA ratio[49]. It has been proven that MUFA may prevent the development of NAFLD by improving blood lipid concentrations, lowering body fat contents and decreasing postprandial adiponectin expression[50]. MUFAs (oleic acid) from olive oil have numerous beneficial effects on NAFLD, including decreased oxidized low-density lipoprotein, low-density lipoprotein cholesterol (LDL-C) and TG concentration, without the concomitant decrease in high-density lipoprotein cholesterol (HDL-C)[51], as well as lowering blood pressure and improving insulin sensitivity[37]. Additional effects of the MD relate to its polyphenol content. For example, polyphenols present in olive oil, such as oleuropein, hydroxytyrosol and tyrosol, have important antioxidant and anti-inflammatory effects[51]. The high content of dietary fiber both in soluble and insoluble forms in the MD is associated with a decrease in serum TGs and blood glucose[40]. The beneficial effect of the MD on NAFLD progression is also linked with an absence of added sugars and fructose in this diet.

Healthy dietary patterns and risk/prevalence of NAFLD

A healthy dietary pattern is defined as an appropriate intake of fruits & vegetables, nuts, olive oil, low-fat dairy products and fish. MD is one example of a healthy dietary pattern, but there are also other specific healthy diets. In Table 2, associations between healthy dietary patterns and the risk/prevalence of NAFLD are summarized.

In nine out of ten collected studies–in two prospective studies[52,53], four case-control studies[33,54-56], and three cross-sectional studies[57-59], a healthy dietary pattern was associated with a decreased risk of NAFLD independent of several confounders added to the models. Moreover, in a study by Chung *et al*[60] "simple meal pattern" characterized by a high intake of root and yellow vegetables, fruits, dairy products, eggs and nuts also exhibited an inverse correlation with NAFLD. Kalafati *et al*[55] found that individuals in the second quartile of the unsaturated fatty acids pattern, a dietary pattern with strong antioxidant properties, had 55.7% reduced odds of developing NAFLD than those in the first quartile, after adjusting for several confounders. However, higher consumption of unsaturated fatty acids was not associated with further protection from NAFLD, which may be explained by the fact that a greater intake of this diet leads to higher energy intake. Moreover, the mentioned authors found that the score for the prudent pattern (recognized also as a healthy dietary pattern) based on oil-based cooked vegetables, legumes, potatoes, fruits, vegetables and fatty fish was negatively associated with TG and uric acid levels, mediators of the associations between obesity and the incidence of NAFLD[61]. Only one study, presented by Alferink *et al*[62], found that adherence to vegetable and fish patterns (a kind of healthy pattern) was not associated with the risk of NAFLD.

The protective effect of healthy diets on the risk of the NAFLD could be a consequence of high consumption of vegetables and moderate intake of fruits, which are sources of antioxidant vitamins, such as vitamins A, E and C (protective against oxidative stress)[43]. Moreover, fruits and vegetables are good sources of dietary fiber, which has an inverse association with IR and the risk of NAFLD progression. Fish are sources of long-chain n-3 PUFAs, which are capable of reducing TGs and have a protective role against NAFLD[38].

Western and traditional dietary patterns and risk/prevalence of NAFLD

Although definitions of Western dietary patterns vary, this diet is often characterized by high consumption of soft drinks, red and processed meat and refined cereals, with concurrently low intake of fish, fruit and vegetables as well as whole grains[63]. Therefore, this diet is characterized by a high intake of animal and trans fats, sugar and fructose and a low intake of fiber and phytochemicals[52]. It was observed that when a western diet is provided in excess, even for a short period of 1 wk, it leads to increased hepatic steatosis[33]. In Table 2, associations between Western and traditional and healthy dietary patterns and the risk/prevalence of NAFLD are summarized.

Oddy *et al*[52], in their prospective cohort study, found that a higher score of the Western dietary pattern at 14 years of age was associated with a greater risk of NAFLD at 17 years. Similar results were obtained in other observational studies[34,56]. On the other hand, some studies report significant associations of this diet with the risk of NAFLD[58,60]. In the literature, the following dietary patterns familiar to the western patterns are also present: Fast food[54,55]; animal food/high protein[53,54]; red meat and alcohol[62]; high-salt[57]; high-fat dairy and refined grains[62]; high-carbohydrate/sweet/sugar/high

Table 2 Characteristics of the observational studies on the association between different dietary patterns and nonalcoholic fatty liver disease

Ref.	Country/Region	Dietary pattern	Food items in dietary patterns	Type of study	N, age	Main results	Associations
Oddy *et al*[52]	Australia	Western	Takeaway foods, confectionery, red meat, refined grains, processed meats, chips, sauces, full-fat dairy products and soft drinks	P	995. FFQ completed at 14 yr and liver ultrasound at 17 yr	Higher western pattern score at 14 yr was associated with ↑ risk of NAFLD at 17 yr (OR: 1.59; 95%CI: 1.17–2.14; $P < 0.05$) before adjustment to BMI	↑
		Healthy	Whole grains, fruit, vegetables, legumes, fish			A healthy diet at 14 yr appeared protective against NAFLD at 17 yr in centrally obese adolescents (OR: 0.63; 95%CI 0.41-0.96; $P < 0.05$)	↓
Salehi-Sahlabadi *et al* [34]	Iran	Western	Fast foods, soft drinks, processed meat, high-fat dairy products, hydrogenated fats, mayonnaise, salty snacks, sugar sweetened desserts, organ meats and refined grains	C-C	675 (450 with NAFLD) NAFLD: 38.6 ± 8.7 yr; Controls: 37.9 ± 8.9 yr	The western pattern was associated with ↑ risk for NAFLD after adjustment for age, sex, BMI, PA, SES and EI	↑
		Healthy	Fish, skinless poultry, low-fat dairy, fresh fruits, natural juices, canned fruits, dried fruits, vegetables, nuts, olive and garlic			A healthy pattern was associated with ↓ risk for NAFLD, after controlling for mentioned variables	↓
		Traditional	Red meat, organ meats, skinless poultry, eggs, yogurt drink, tea, legumes, tomato sauce, sugar sweetened-desserts, potato, condiments, salt, pickles and broth			Lack of association between traditional pattern and risk of NAFLD adjusted for mentioned variables	↔
Chung *et al*[60]	Korea	Western and high-carbohydrate	Processed meats, bread, soft drinks, pork, noodles, beef, cakes, snacks, beef soup, sugar, coffee, chicken, processed fish and refined grains	C-S	1190 (331 with NAFLD) NAFLD: 53 ± 9 yr; Controls: 51 ± 10 yr	Lack of association between Western/high-carbohydrate pattern and risk of NAFLD after adjustment for age, sex, WC, smoking status, EI, diabetes and hypertension	↔
		Traditional	Vegetables; fermented vegetables such as kimchi and jjangajji; fish and seafood; mush-rooms; fermented, processed, natural soybeans			↑ Adherence to the traditional pattern was associated with ↑ risk of NAFLD (OR: 1.85; 95%CI: 1.11-3.08; $P < 0.05$) after controlling for mentioned variables	↑
		Simple meal	Fruits, root and yellow vegetables, eggs, dairy products and nuts			↑ Adherence to the simple meal pattern was associated with ↓ risk of NAFLD (OR: 0.59; 95%CI: 0.34-1.00; $P < 0.05$), after controlling for mentioned variables	↓
Dehghanseresht *et al*[54]	Iran	Ordinary	Sweets, oils, fruits, white meats, refined grains, tea and coffee, salt, biscuits, snacks as well as red and organ meats	C-C	244 (122 with NAFLD) aged 19–70 yr	↑ Adherence to the ordinary pattern was associated with ↑ risk of NAFLD; $P < 0.001$	↑
		Traditional	Red and organ meats, dairy products, condiments, salt, tea and coffee and low			↑ Adherence to the traditional pattern was associated with ↑ risk of	↑

			intake of fruits			NAFLD $P < 0.001$	
		Vegetables and dairy (healthy pattern)	Vegetables, whole grains, legumes and nuts and dairy products			↑ Adherence to the vegetables and dairy pattern was ↓ association with NAFLD risk (OR: 0.23; 95%CI: 0.09–0.58; $P < 0.05$)	↓
		Fast food	Sauces, pickles, fast foods, soft drinks, snacks and biscuits			No association between Fast food patterns and the risk of NAFLD	↔
Yang *et al*[57]	China	Traditional Chinese	Staple food, coarse grains, fruits, eggs, fish and shrimp, milk and tea	C-S	999 (345 with NAFLD) aged 45–60 yr	No association between traditional pattern and the risk of NAFLD	↔
		Animal food	Kelp/seaweed and mushroom, pork, beef, mutton, poultry, cooked meat, eggs, fish and shrimp, beans and grease			After controlling for potential confounders, animal food patterns had ↑ prevalence rate for NAFLD (PR: 1.35; 95%CI: 1.06–1.72; $P < 0.05$	↑
		Grains-vegetables (healthy pattern)	Coarse grains, tubers, vegetables, mushroom and kelp/seaweed, cooked meat and beans			After adjustment for BMI, a vegetable pattern had ↓ prevalence rate for NAFLD (PR: 0.78; 95%CI: 0.62–0.98, $P < 0.05$).	↓
		High-salt	Rice, pickled vegetables, processed meat, bacon, salted duck egg, salted fish and tea			No association between high salt and the risk of NAFLD	↔
Jia *et al*[65]	China	High-carbohydrate/sweet	Fruits, cakes and candied fruits	C-S	4365 (1339 with NAFLD: adults	↑ Adherence to a high-carbohydrate/sweet pattern was associated with ↑ the prevalence of NAFLD in females but not in males	↑ only in females not in males
Kalafati *et al*[55]	Greece	Fast food	Energy-dense foods rich in saturated fat and sugar and included fast foods, sweetened soft drinks, fried potatoes and savory and puff pastry snacks	C-C	351 (134 with NAFLD) Case: 50.0 ± 10.5 yr; Control 44.0 ± 11.0 yr	↑ Adherence to a fast-food pattern was associated with ↑ odds for NAFLD after adjustment for age, sex, EI, PA, pack-yr smoked, education, MS ($P < 0.01$)	↑
		Prudent (healthy pattern)	Oil-based cooked vegetables, legumes, potatoes, fruits, vegetables and fatty fish			↑ Adherence to the prudent pattern was associated with ↓ TG and uric acid levels (β: -5.96; $P < 0.05$; β: -0.15; $P < 0.05$, respectively)	↓
		High-protein	Red meat, poultry, eggs			The high protein pattern was not associated with any NAFLD-related biomarker	↔
		The unsaturated FA	Nuts, chocolate and other foods rich in unsaturated FA			Individuals in the second quartile of the unsaturated FA pattern had ↓ odds of developing NAFLD *vs* the first quartile after being adjusted for mentioned confounders ($P < 0.05$)	↓
Tutunchi *et al*[56]	Iran	Healthy	Vegetables, legumes, fruits and low-fat dairy products	C-C	210 (105 with NAFLD) Cases 46 ± 9 yr; Controls 45 ± 9 yr	A healthy pattern was associated with ↓ odds of NAFLD (OR: 0.34; 95%CI: 0.16–0.81) after controlling for sex, education, PA, BMI,	↓

						WC	
		Western	Sweet, hydrogenated fat, red and processed meat and soft drink dietary patterns			↑ Adherence to the western pattern was related to ↑ risk of NAFLD (OR: 2.68; 95%CI: 1.31–4.16), after controlling to mentioned confounders	↑
Zhang *et al*[61]	China	Sugar-rich	Strawberry, kiwi fruit, persimmon, sweets, candied fruits, Chinese cakes	P	17360 free from NAFLD at baseline; During a median follow-up of 4.2 yr, 4034 with NAFLD, aged > 18 yr	After adjusting for age, sex, BMI, smoking, alcohol, education, occupation, income, PA, EI, personal and family history of the disease, depressive symptoms, dietary supplement use, inflammation markers, WHR and each other dietary pattern score, the sugar-rich pattern was associated with ↑ risk of NAFLD (HR: 1.11; 95%CI 1.01, 1.23)	↑
		Vegetable (healthy pattern)	Cucumber, green leafy vegetables, Chinese cabbage, celery, pumpkin			After adjusting for mentioned confounders, vegetable diet was associated with ↓ risk of NAFLD (HR 0.96; 95%CI: 0.86, 1.07)	↓
		Animal food	Animal organs, animal blood, preserved eggs, instant noodles, pork skin, sausage			After adjusting for mentioned confounders, animal food diet was associated with ↑ risk of NAFLD (HR: 1.22; 95%CI: 1.10, 1.36)	↑
Alferink *et al* [62]	The Netherlands	Vegetable and fish (healthy pattern)	Vegetables, poultry, fish and fruit	P	963 (343 with NAFLD) Baseline: 71.0 yr; Follow-up: 75 yr	No associations between vegetable and fish diet and NAFLD	↔
		Red meat and alcohol	Red, refined or organ meat, salty snacks and beer or spirits and low intake of fruit and tea			No associations between red meat and alcohol pattern and NAFLD	↔
		Traditional	Vegetable oils and stanols and margarine or butter, potatoes, whole grains and sweet snacks or desserts			↑ Adherence to the Traditional pattern was associated with ↓ risk of NAFLD (OR: 0.40; 95%CI 0.15–1.00) adjustment for sex, age, baseline education level, PA, EI, alcohol intake and follow-up time, BMI, baseline type 2 diabetes mellitus and baseline hypertension	↓
		Salty snacks and sauces	Savory food groups such as nuts, legumes, salty snacks and sauces			No associations between salty snacks and sauces pattern and NAFLD	↔
		High-fat dairy and refined grain	Fruit juice, refined grains, high-fat dairy products and sweet snacks or desserts			No associations between high-fat dairy and refined grain pattern and NAFLD	↔
Fakhoury-Sayegh *et al*[64]	Lebanon	Traditional	Vegetables, chickpeas, red beans, lentils, peas, vegetable oil/olives	C-C	222 (112 with NAFLD) Cases: 40 ± 6 yr; Controls: 39 ± 13 yr	↑ Adherence to traditional pattern ↓ the odds of NAFLD (OR: 0.30; CI 95%: 0.11–0.86; $P < 0.05$) adjusted for MS, EI, education, PA, family history, smoking, place of residence and profession	↓

		High fruits	Fruits and fruit juices			↑ Adherence to high fruits pattern ↑ the odds of NAFLD (OR: 4.061; 95%CI: 1.320–12.100, $P < 0.05$, adjusted for mentioned confounders	↑
		The high meat and fast food diet: (Western-like dietary pattern)	Meat such as pork, chicken, beef meat and hotdog			↑ Adherence to Western pattern ↑ the odds of NAFLD (OR: 4.081; 95%CI: 1.36–12.28, $P < 0.05$) adjusted for mentioned confounders	↑
Nakashita *et al* [58]	Japan	Healthy	Seaweeds, vegetables, mushrooms, pulses, potatoes and starches	C-S	281 men (89 with NAFLD) NAFLD: 62 (57–67) yr; Controls: 61 (56–67) yr	A healthy pattern was correlated with the ↓ risk of NAFLD	↓
		Western	Fats and oils, meat, seasonings, spices			No correlation between western pattern and NAFLD	↔
		Snacks	Sugars and starches, beverages (tea, coffee, fruit juice, soft drinks), fruits			No correlation between snacks pattern and NAFLD	↔
Adriano *et al* [59]	Brazil	Healthy	Fruits, vegetables/legumes, white meat, olive oil, margarine, bread/toast (with significant negative loading for beef)	C-S	229 older adults (74.7% women) NAFLD: 67.0 ± 5.0 yr; Controls: 70.1 ± 7.0 yr	↑ Adherence to the healthy pattern was associated with ↓ prevalence of NAFLD (PR: 0.70; 95%CI: 0.50, 0.98, $P < 0.05$) after adjustment for sex, age, EI, BMI, smoking status, PA, family income and use of hypoglycemic drugs	↓
		Regional snacks (Northeast of Brazil)	Tea/coffee, dairy products, cassava flour/tapioca/cuscus, butter and olive oil			↑ Adherence to the regional snacks pattern was associated with the ↑ prevalence of NAFLD (PR: 1.42; 95%CI: 1.02, 1.92, $P < 0.05$) after adjustment for mentioned confounders	↑
		Energy-dense	Processed cold meats, beef, viscera, sweet products/desserts/sugar, soft drinks, tubers/spaghetti/pastries			No association between energy density pattern and NAFLD	↔
		Traditional	Rice, beans, bread/toast, tea/coffee, sweet products/desserts/sugar			No association between traditional pattern and NAFLD	↔

BMI: Body mass index; C-C: Case-control; C-S: Cross-sectional; CI: Confidence interval; EI: Energy intake; FA: Fatty acid; FFQ: Food frequency questionnaire; HR: Hazard ratio; NAFLD: Nonalcoholic fatty liver disease; MS: Metabolic syndrome; OR: Odds ratio; P: Prospective; PA: Physical activity; PR: Prevalence ratio; SES: Socioeconomic status; TG: Triglyceride; WC: Waist circumference; WHR: Waist-to-hip ratio.

fruits[53,64,65]; as well as, snacks and energy-dense dietary pattern[58,59,62]. The majority of these dietary patterns increased the risk of NAFLD. Although high-carbohydrate/sweet/sugar/high fruits dietary pattern was associated with a significantly higher risk of NAFLD, Jia *et al*[65] found that this diet was positively associated with the prevalence of NAFLD only in females but not in males. Overall, Hassani Zadeh *et al*[43], in their meta-analysis, found that Western dietary patterns increased the risk of NAFLD by 56%.

The Western dietary pattern rich in saturated and trans-fatty acids may affect the hepatic cell steatosis *via* chylomicron uptake[34]. This dietary pattern, due to high amounts of refined grains, white bread and sugar-sweetened beverages has been also strongly associated with IR, diabetes and obesity. Soft drinks, the main constituents of the Western diet, contain substantial amounts of added sugars and fructose[66]. It was indicated that a higher intake of fructose induces hepatic IR and inflammation, thereby fueling the development of NAFLD. In addition, fructose metabolism could promote hepatic lipogenesis by inhibiting the DNL pathway and regulating lipogenic gene expression in the liver[67]. It should be noted that moderate consumption of fruits due to the presence of other dietary components such as dietary fiber and antioxidant vitamins can have a protective effect against NAFLD. On the other hand, excessive fruit consumption, as was seen in a study by Fakhoury-Sayegh *et al*[64], may increase

the risk for NAFLD, due to the high content of simple sugars (especially fructose).

The traditional diet may differ depending on the region or country and encompasses the common foods eaten there. Since this pattern comprises both healthy and unhealthy food items in different proportions, in collected studies we can observe the different influences of this pattern on the risk of NAFLD. For example, in a Korean study[60] the traditional diet was characterized by high intake of vegetables, fermented vegetables, such as kimchi, fish and seafood, mushrooms and fermented, processed and natural soybeans and was associated with a higher risk of NAFLD independent of several confounders added to this model. A traditional Iranian dietary pattern characterized by intake of red and organ meats, dairy products, condiments, salt, tea and coffee and low fruits consumption was related to an increased risk of NAFLD[54]. However, in another Iranian study[34], a traditional diet, represented by a high intake of red meat organ meats, skinless poultry, eggs, yogurt drink, tea, legumes, tomato sauce, sugars sweets-desserts, potato, condiments, salt, pickles and broth, was not associated with risk of NAFLD. Similar observations were reported by Yang *et al*[57] and Adriano *et al*[59] where traditional Chinese food items (staple food, coarse grains, fruits, eggs, fish and shrimp, milk and tea) and traditional Brazilian foods (rice, beans, bread/toast, tea/coffee, and sweet products/desserts/sugar) were not associated with a risk of NAFLD. In turn, Alferink *et al*[62] found that traditional Dutch dietary patterns consisting of vegetable oils, stanols and margarine or butter, potatoes, whole grains, and sweet snacks or desserts were associated with regression of NAFLD. Similar observations revealed that the traditional Lebanon diet (characterized by high intake of vegetables, chickpeas, red beans, lentils, peas, and vegetable oil/olives) was also related to a lower risk of NAFLD [64].

DIETARY INTERVENTION STUDIES IN NAFLD PATIENTS

Lifestyle modification, including a change in diet, weight loss target and structured exercise/physical intervention is the first-line and a cornerstone therapy for the NAFLD condition. It is implemented to reduce the cardiometabolic risk factors and cardiovascular disease events and to resolve NAFLD. Table 3 displays the NAFLD diet treatment recommendations/guidelines of The European Association for the Study of the Liver[48] and the European Society for Clinical Nutrition and Metabolism[68], in addition to the American Association for the Study of Liver Diseases[69,70], the Asian Pacific Association for the Study of the Liver[71], the American Gastroenterological Association[7] and the World Gastroenterology Organization[72].

The primary dietary goal for patients with NAFLD is to implement a hypocaloric diet due to a caloric deficit. Most often, low-calorie diets lead to an energy deficit of 500-1000 calories. Ordinarily, overweight NAFLD patients are advised to have a deficit of at least 500 calories/d for weight loss[10,48,73,74]. A weight loss of 3%-5% of body weight is necessary to improve liver steatosis[10]. To improve most of the histopathological characteristics in NAFLD, hepatocyte ballooning, lobular inflammation and fibrosis, a greater loss of body weight of 7%-10% is required[75]. Meta-analysis of 8 randomized controlled trials confirm that a 7% reduction in body weight was associated with improvement of the NAFLD Activity Score[76]. But, it should be noted that 94% of patients who lost 5% of initial body weight stabilized/or improved liver fibrosis[77]. Meta-analyses of 22 randomized controlled trials with 2588 participants reported that weight-loss interventions were significantly associated with improvements in alanine aminotransferase (ALT), ultrasonography pronounced liver steatosis, NAFLD Activity Score and presence of steatohepatitis[11]. Caloric restriction alone or in combination with physical activity encourages the loss of body weight and reduces hepatic steatosis and subsequently promotes fat mobilization from the liver[70]. In adults with NAFLD, exercise alone may prevent, reduce and cured liver steatosis. However, the ability of physical activity to improve other NAFLD spectrum histological parameters remains unknown.

Based on the current evidence, there is no consensus on the ideal macronutrient composition of the diet for NAFLD patients. The best nutrition recommendation is a traceable diet, based on individual preferences, eating habits and behaviors[74]. Also, there is no solid evidence to support a particular macronutrient composition of a hypocaloric diet unique for use in NAFLD patients. Independent of weight loss, a diet low in carbohydrates and higher in protein intake is associated with improvements of metabolic parameters in NAFLD patients[73,78]. A recent meta-analysis 32 controlled isocaloric feeding studies with a constant proportion of protein in the diet and varying ratios of carbohydrate and fat indicates that diet differences are too small, which implies the importance of caloric intake in NAFLD patients[79]. Overall, more future studies on macronutrient composition in diet are needed.

As previously stated, Mediterranean dietary patterns prevent the onset of NAFLD. The MD is also the most recommended diet for the treatment of NAFLD patients[12]. It improves liver steatosis, as indicated by the results of several studies, regardless of whether there is a calorie restriction in the diet. Independent of weight loss, patients have greater reductions in intrahepatic lipid content and insulin sensitivity after following the MD compared to a low-fat/high-carbohydrate diet. Consumption of a MD with calories less than the required daily energy allowed male NAFLD patients to reduce body weight, lipid accumulation, visceral adiposity index, fatty liver index, hepatic steatosis index and IR, as well as a

Table 3 Summary of international guidelines on diet for nonalcoholic fatty liver disease patients

	EASL/EASD/EASO clinical practice guidelines for the management of NAFLD [48]	ESPEN guideline on clinical nutrition in liver disease[68]	AASLD practice guidance: The diagnosis and management of NAFLD[69,70]	APASL clinical practice guidelines for the management of MAFLD[71]	AGA clinical practice guidelines for diagnosis and management of NAFLD[7]	WGO guidance for NAFLD/NASH [72]
Target for weight loss	7%-10%	7%-10% (in obese patient); > 10% to improve fibrosis	3%-5% (to improve steatosis); 7%-10% for histological improvement	7%-10%	≥ 5% if steatosis; ≥ 7% if NASH; ≥ 10% if fibrosis	5%-10%
Macronutrient composition	Low to moderate fat and moderate to higher carbohydrate; low carbohydrate, ketogenic diets or high protein	Irrespective of macronutrient composition, MD to improve steatosis and IR	Less relevant	Low-carbohydrate, low-fat and Mediterranean-type diets	Minimize SFA, ↓ red and processed meat	Avoid trans-fats; ↑ omega 3/omega 6 PUFA
Energy restriction	Hypocaloric: Reduction of 500-1000 kcal/d target weight loss of 0.5-1.0 kg/wk	Hypocaloric diet according to obesity guidance	Hypocaloric diet reduction of 500-1000 kcal/d	Hypocaloric diet reduction of 500-1000 kcal/d	Hypocaloric: 1200-1500 kcal/d or ↓ from baseline 500-1000 kcal/d	Hypocaloric: ↓ calories intake 25%
Fructose intake	Avoid fructose-containing beverages and foods				Avoid fructose commercially produced	Avoid fructose and soft drinks
Coffee intake	No liver-related limitations	"More likely to benefit health than harm"		"More likely to benefit health than harm"		
Alcohol intake	Risk below (< 30 g men, < 20 g women)	Abstain	Not consume heavy amounts		Restrict	

AGA: American Gastroenterological Association; AASLD: American Association for the Study of the Liver; APASL: Asian Pacific Association for the Study of the Liver; EASL: European Association for the Study of the Liver; EASD: European Association for the Study of Diabetes; EASO: European Association for the Study of Obesity; ESPEN: European Society for Clinical Nutrition and Metabolism; IR: Insulin resistance; MAFLD: Metabolic associated fatty liver disease; MD: Mediterranean diet; NAFLD: Nonalcoholic fatty liver disease; NASH: Nonalcoholic steatohepatitis; PUFA: Polyunsaturated fatty acid; SFA: Saturated fatty acid; WGO: World Gastroenterology Organization.

reduced share of SFA in the serum fatty acid profile decreased serum levels of SFAs and increased serum levels of MUFAs and n-3 PUFA[80]. The MD has well-documented metabolic benefits to reduce cardiovascular risk and thus is well valued in the medical community[81]. This observation is important because NAFLD patients have an increased risk of cardiovascular disease.

A systematic review and meta-analysis of randomized controlled trials presented that Mediterranean and hypocaloric dietary interventions favoring unsaturated fatty acids led to improved intrahepatic lipid content and transaminases levels (ALT, aspartate aminotransferase) in NAFLD patients[82]. The gamma-glutamyl transferase level does not change significantly during the Mediterranean dietary interventions[82]. Diet compositions in randomized controlled trials used in these meta-analyses can be considered comparable. Based on the calculated NAFLD fibrosis score, the composite score of age, glucose levels, platelet count, albumin and aspartate aminotransferase/ALT ratio, indicated that risk for advanced hepatic fibrosis was 11% among NAFLD patients with incidentally discovered hepatic steatosis[76]. In patients with NAFLD, gamma-glutamyl transferase levels decreased only after low glycemic index-MD intervention[83]. Hence, it is confirmed that MD without caloric restriction reduced the liver fat. Since there are only a few studies examining dietary interventions in clinically advanced stages of NAFLD (active and fibrotic NASH), the optimal dietary recommendation for nutrition intervention in NAFLD remains to be defined.

Well-discussed risk factors for hepatic steatosis are high SFA intake and overconsumption of carbohydrates, such as fructose. This type of diet leads to obesity. Intervention studies provide clear and strong evidence of a link between excessive calorie intake and NAFLD development as well as being linked to excess energy intake with increased lipolysis, induced IR and increased harmful ceramides in plasma[15,16]. Excessive intake of SFA (1000 extra kcal/d) conducted in obese patients for 3 wk increased intrahepatic TG content more than the intake of unsaturated fats (+ 55% *vs* + 15%, respectively)[16]. Also, overconsumption of simple sugars increased the intrahepatic TG content (+ 33%) by stimulating DNL (+ 98%). In a review by Stokes *et al*[84], short-term hypocaloric diets (up to 16 wk) have shown beneficial effects in reducing intrahepatic lipid content. Also, research supports that carbohydrate restriction and consumption of unsaturated fatty acids have efficacious metabolic effects in NAFLD[12,81,84]. Obesity is closely related to low levels of n-3 PUFA in plasma phospholipids[85].

Dietary modifications including n-3 PUFA supplementation are considered to be suitable therapeutic strategies for obese NAFLD patients, though further clinical trials are required.

However, among NAFLD patients, weight loss is largely unsuccessful in the real world in the ambulatory and clinical settings[86]. However, more frequent clinical encounters and controls are associated with an increased likelihood of weight loss (enhanced probability of weight reduction). Therefore, national strategies are needed for targeted success in weight loss success in high-risk populations.

Time-restricted feeding and intermittent fasting

The newest popular dietary intervention in the past few years is time-restricted feeding as a form of daily intermittent fasting (IF). This dietary approach restricts the time between the first and last food intake, without emphasizing calorie restriction. IF implies a > 60% energy restriction on > 2 d/wk. In time-restricted eating, daily food intake is limited to 8-10 h. These diets with a limited eating window appear to be safe in the NAFLD population. Patients tolerate this diet well. The key feature of this dietetic approach is the so-called "metabolic switch" that occurs 12 h after the cessation of food intake, where glycogen stores in the liver are depleted, and adipose tissue lipolysis increases[87]. This type of diet seems to be effective for weight loss, whereas many authors denied that the effect is still the result of a real calorie restriction. Patients with NAFLD follow the IF diet based on metabolic changes that are presented among overweight/obese individuals. A recent meta-analysis, involving patients with NAFLD, has shown that IF is beneficial in weight loss and liver enzyme levels[88]. However, no additional metabolic benefit has been shown compared to calorie-restricted diets[89]. In patients with NAFLD improvement in fatty liver index correlates with the number of fasting days and with the degree reduction in body mass index[90].

In a study performed by Cai *et al*[91], 271 NAFLD patients were randomized to time-restricted feeding, alternate-day fasting and control groups and were followed for 12 wk[91]. Findings from this study indicated that alternate-day fasting could be an effective diet method for weight loss and amelioration of lipid metabolism, with no direct effect in steatosis regression. In one Malaysian randomized controlled trial, 8 wk of IF with alternate-day calorie restriction resulted in the reduction of body weight and liver enzymes as well as hepatic steatosis compared to a habitual diet[92]. 8 wk of IF with limited caloric intake on alternating days led to a decrease in body weight and liver enzymes, as well as hepatic steatosis compared to the usual diet. Additional evidence for the benefit of IF to diminish hepatic steatosis and body weight compared to common lifestyle modification has been reported by 5:2 diet (intermittent calorie restriction: 600 kcal/d for men and 500 kcal/d for women for 2 non-consecutive days per week). But, the same effect was obtained in another group of participants on a low-carbohydrate high-fat diet (daily caloric intake: 1900 kcal/d for men and 1600 kcal/d for women) [89]. Data regarding IF efficacy in the steatosis/fibrosis regression are lacking. For now, it is important for medical practitioners not to advise this diet to patients with cirrhosis caused by NAFLD due to the well-known effect of starvation on the development of sarcopenia.

DASH diet

Evidence from two observational studies revealed that high adherence to the DASH-style diet is inversely associated with the risk of developing NAFLD[93,94]. It is indicated that subjects who fully adhered to the DASH diet were 30% less likely to have NAFLD. DASH is a low-glycemic index and low energy-dense diet, emphasizing low sodium intake and minimal consumption of processed foods. It is well known that the DASH diet is associated with a reduction in cardiovascular risk, as originally intended for hypertension patients. A randomized controlled trial including 60 overweight/obese adults, with ultrasonography proven NAFLD showed that the DASH diet over 8 wk led to more effective weight loss, improvement of aminotransferases and markers of IR, TG and total-C/HDL-C ratio compared to a contemporary control diet[95]. The DASH diet may be a promising dietary option for NAFLD patients, as weight loss, improved cardiometabolic factors and regression of steatosis are surrogate markers of liver disease status and the main goals of NAFLD treatment. This diet has aroused interest among specialists who care for patients with NAFLD. Further studies are essential to assess the effects of the DASH diet on liver histology and the clinical outcome of patients with NAFLD.

Ketogenic diet

Ketogenic diet (KD) is the most popular low-carbohydrate eating plan based on a strict restriction in carbohydrates (less than 20-50 g/d) consumption. The KD became a popular weight loss intervention among obese patients due to its effectiveness despite safety concerns of this diet plan if dyslipidemia is present[96]. Therefore, KD could have a positive impact on NAFLD, due to very low content of carbohydrates in the diet. However, it is not known if ketosis plays an additional role. Several mechanisms may be proposed links between ketosis and improvement of NAFLD. First, a ketogenic diet decreases insulin levels that lead to increased rate of fatty acid oxidation and decreased lipogenesis [97]. Then, restriction of carbohydrates encourages the formation of ketone bodies, which cause satiety by a still-unknown mechanism[98]. In turn, reduced calorie intake leads to weight loss.

Few studies have tested KD as a treatment strategy for NAFLD patients. Based on fat content, KD can be a normocaloric, hypocaloric or non-restricted caloric diet. Pérez-Guisado *et al*[99] conducted a pilot study on 14 overweight male patients with MetS and with ultrasonography-proven NAFLD. Patients fed unrestricted Mediterranean high-fat KD, high in unsaturated fats (*i.e.* olive oil and fish oil rich with omega-3 fatty acids). Adherence to Mediterranean high-fat KD showed a significant improvement in body weight, aminotransferases and LDL-C levels, and steatosis degree (21% of the patients had complete fatty liver regression)[99].

Mardinoglu *et al*[100] reported a 2-wk KD intervention (carbohydrate 20–30 g/d, fat 241 g/d, 3115 kcal/d) in 17 obese patients with NAFLD. Despite a slight weight loss, liver fat content (assessed by magnetic resonance spectroscopy) was reduced by 43.8% in obese patients in this study. At the same time, a concomitant decrease in *de novo* gene for liver lipogenesis was obtained[100]. Moreover, literature data indicated that normocaloric high-fat KD inhibits DNL and induces fatty acid oxidation, caused sustained weight loss and reduced hepatic fat accumulation[16,101]. Based on the above findings KD could be a potential therapeutic dietary intervention for addressing steatosis regression and weight loss. Future studies are needed on the KD effect on fibrosis regression and resolution of inflammation. Because ketosis may have beneficial effects independently of the diet composition, studies aiming to identify the specific role that ketone bodies play in the pathophysiology of NAFLD are warranted.

Added sugars

Study evidence from cross-sectional trials pronounced a directly proportional association between the intake of refined sugar (especially high fructose corn syrup) due to the consumption of sweet sugar beverages with the risk of developing NAFLD[81,102]. Patients with NAFLD consume 2-3 times more fructose. Higher fructose consumption is also related to an increased risk of having steatohepatitis and advanced fibrosis in NAFLD patients. Based on current evidence, fructose supplementation was linked with higher adiposity and enhanced visceral fat, hypertriglyceridemia and IR, occurs due to increase DNL in liver, in spite of similar weight gain when compared to glucose[103]. Increasing the frequency of the snacks with added sugar consumption led to a prominent increase in the hepatic fat content. The augmented hepatic steatosis was proportional to visceral fat accumulation and to the rise in DNL.

Fructose-rich diets, based on sugar-sweetened beverages increase hepatic synthesis of TG and are recognized as a major mediator of NAFLD[73]. It was observed that carbohydrate overfeeding in overweight persons consumed 1000 kcal/d from simple carbohydrates (sugar-sweetened soft drinks, candy, pineapple juice) for 3 wk caused a 10-times greater relative increase in fat content in the liver than in body weight (27% *vs* 2%, respectively)[104]. The recommendation to avoid sweet sugar beverages reduced the intake of extra empty calories and supported a caloric deficit for weight loss. Notably, high fructose consumption in NAFLD patients was compiled, with an increase in hepatic fructokinase and fatty acid synthase mRNA when compared to healthy persons[105]. Fructose can advance hepatic steatosis both directly *via* DNL and indirectly *via* DNL feedback inhibition of fatty acids. Overconsumption of fructose may increase the risk of developing NASH and advanced fibrosis, although the relationship may be confounded by excess energy intake or by unhealthy dietary patterns and sedentary lifestyle, which are common in NAFLD patients[106].

Current literature evidence suggests that higher fructose intake (> 20E% or 100–220 g/d) may adversely affect disease onset and progression[81]. Meta-analyses reported that moderate fructose consumption lower than 10% of energy (< 50 g/d for a 2000 kcal diet) does not induce weight gain or dyslipidemia. Sugar-sweetened beverage intake of ≥ 1 serving/d rises the risk of having NAFLD by 50% [33] and liver fibrosis by 250%[107]. It seems that artificially sweetened beverages and defined 100% fruit juices have similar effects as sugar-sweetened beverages. The results of a systematic review indicated that fructose in the diet isocalorically replaced with other carbohydrate sources for 1-10 wk did not affect NAFLD biomarkers[108]. Fructose overconsumption increases intrahepatic lipids and ALT levels. This effect results from excess energy intake rather than fructose consumption[108]. In the future, long-term prospective clinical trials are essential to understand and confirm a link between NAFLD progression and fructose consumption.

Coffee consumption

NAFLD patients who drink three to four cups of coffee per day will have more health benefits than harm, with the reduction in risk for various health outcome[109]. Nevertheless, a recent meta-analysis of 11 epidemiological studies confirmed association with regular coffee consumption and decreased risk of NAFLD[110]. Moreover in patients already diagnosed with NAFLD, coffee consumption reduced risk for the development of liver fibrosis[97,110]. A case-control study showed involvement of coffee in the fatty liver score, pronounced by ultrasound in all coffee consumers[111]. A systematic review determined that coffee consumption was inversely related to the severity of steatohepatitis in NAFLD patients[112]. Prohibitive effects on fibrosis progression were determined by the FibroTest based on fasting biochemical markers presented in a prospective study in the general population[113]. It was noted that decaffeinated coffee has the same helpful effect on NAFLD[114]. It was considered that two cups of coffee/day helped in the prevention of hepatocellular carcinoma[115], while three cups of coffee/day prevented steatohepatitis and fibrosis[109]. As observations have so far been based on epidemiological studies, future clinical studies need to confirm whether coffee consumption can be

considered a preventative factor for NAFLD. Until then, routine prescription of coffee for NAFLD prevention/treatment is not recommended.

CONCLUSION

In conclusion, the Western dietary pattern characterized by high intake of soft drinks, red and processed meat and refined cereals with coincidentally low intake of fish, fruit and vegetables as well as whole grains tended to increase the risk of NAFLD. The healthy and Mediterranean dietary patterns characterized by high consumption of vegetables, fruits, nuts, olive oil, low-fat dairy products and fish were linked with a reduced NAFLD risk. More prospective cohort studies are needed to confirm the association between dietary patterns and NAFLD risk. Macronutrient composition and excessive caloric intake are critical determinates of obesity and liver health. DASH, IF and KD have aroused interest among specialists who care for patients with NAFLD. Further well-designed studies are needed to assess the effects of these diets on liver-related outcomes and liver histology. Dietary advice should be provided by a multidisciplinary team with a specialized dietitian as an individual approach, as we already know that our genetics and gut microbiota cause differences in the effects of the diet to our metabolism. Future research in field interaction overfeeding and genomics are warranted, as are of the inter-individual difference of liver steatoses.

FOOTNOTES

Author contributions: Ristic-Medic D designed the review; Ristic-Medic D and Bajerska J analyzed and interpreted the data and drafted the manuscript; Vucic V critically revised the paper.

Supported by Ministry of Education, Science and Technological Development of the Republic of Serbia, No. 451-03-68/2022-14/200042.

Conflict-of-interest statement: All the authors report no relevant conflicts of interest for this article.

Country/Territory of origin: Serbia

ORCID number: Danijela Ristic-Medic 0000-0002-7041-4220; Joanna Bajerska 0000-0002-2268-9326; Vesna Vucic 0000-0002-8563-594X.

S-Editor: Fan JR
L-Editor: A
P-Editor: Fan JR

REFERENCES

1 **Benedict M**, Zhang X. Non-alcoholic fatty liver disease: An expanded review. *World J Hepatol* 2017; **9**: 715-732 [PMID: 28652891 DOI: 10.4254/wjh.v9.i16.715]
2 **Wong MCS**, Huang JLW, George J, Huang J, Leung C, Eslam M, Chan HLY, Ng SC. The changing epidemiology of liver diseases in the Asia-Pacific region. *Nat Rev Gastroenterol Hepatol* 2019; **16**: 57-73 [PMID: 30158570 DOI: 10.1038/s41575-018-0055-0]
3 **Cotter TG**, Rinella M. Nonalcoholic Fatty Liver Disease 2020: The State of the Disease. *Gastroenterology* 2020; **158**: 1851-1864 [PMID: 32061595 DOI: 10.1053/j.gastro.2020.01.052]
4 **Adibi A**, Maleki S, Adibi P, Etminani R, Hovsepian S. Prevalence of Nonalcoholic Fatty Liver Disease and its Related Metabolic Risk Factors in Isfahan, Iran. *Adv Biomed Res* 2017; **6**: 47 [PMID: 28503502 DOI: 10.4103/2277-9175.204590]
5 **Wong MCS**, Huang J. The growing burden of liver cirrhosis: implications for preventive measures. *Hepatol Int* 2018; **12**: 201-203 [PMID: 29679258 DOI: 10.1007/s12072-018-9865-y]
6 **Godoy-Matos AF**, Silva Júnior WS, Valerio CM. NAFLD as a continuum: from obesity to metabolic syndrome and diabetes. *Diabetol Metab Syndr* 2020; **12**: 60 [PMID: 32684985 DOI: 10.1186/s13098-020-00570-y]
7 **Younossi ZM**, Corey KE, Lim JK. AGA Clinical Practice Update on Lifestyle Modification Using Diet and Exercise to Achieve Weight Loss in the Management of Nonalcoholic Fatty Liver Disease: Expert Review. *Gastroenterology* 2021; **160**: 912-918 [PMID: 33307021 DOI: 10.1053/j.gastro.2020.11.051]

8 **Ristic-Medic D**, Petrovic S, Arsic A, Vucic V. Liver disease and COVID-19: The link with oxidative stress, antioxidants and nutrition. *World J Gastroenterol* 2021; **27**: 5682-5699 [PMID: 34629794 DOI: 10.3748/wjg.v27.i34.5682]

9 **Polyzos SA**, Kountouras J, Mantzoros CS. Obesity and nonalcoholic fatty liver disease: From pathophysiology to therapeutics. *Metabolism* 2019; **92**: 82-97 [PMID: 30502373 DOI: 10.1016/j.metabol.2018.11.014]

10 **Sanyal AJ**. Putting non-alcoholic fatty liver disease on the radar for primary care physicians: how well are we doing? *BMC Med* 2018; **16**: 148 [PMID: 30139362 DOI: 10.1186/s12916-018-1149-9]

11 **Koutoukidis DA**, Astbury NM, Tudor KE, Morris E, Henry JA, Noreik M, Jebb SA, Aveyard P. Association of Weight Loss Interventions With Changes in Biomarkers of Nonalcoholic Fatty Liver Disease: A Systematic Review and Meta-analysis. *JAMA Intern Med* 2019; **179**: 1262-1271 [PMID: 31260026 DOI: 10.1001/jamainternmed.2019.2248]

12 **Pugliese N**, Plaz Torres MC, Petta S, Valenti L, Giannini EG, Aghemo A. Is there an 'ideal' diet for patients with NAFLD? *Eur J Clin Invest* 2022; **52**: e13659 [PMID: 34309833 DOI: 10.1111/eci.13659]

13 **Eslam M**, Valenti L, Romeo S. Genetics and epigenetics of NAFLD and NASH: Clinical impact. *J Hepatol* 2018; **68**: 268-279 [PMID: 29122391 DOI: 10.1016/j.jhep.2017.09.003]

14 **Mota M**, Banini BA, Cazanave SC, Sanyal AJ. Molecular mechanisms of lipotoxicity and glucotoxicity in nonalcoholic fatty liver disease. *Metabolism* 2016; **65**: 1049-1061 [PMID: 26997538 DOI: 10.1016/j.metabol.2016.02.014]

15 **Rosqvist F**, Kullberg J, Ståhlman M, Cedernaes J, Heurling K, Johansson HE, Iggman D, Wilking H, Larsson A, Eriksson O, Johansson L, Straniero S, Rudling M, Antoni G, Lubberink M, Orho-Melander M, Borén J, Ahlström H, Risérus U. Overeating Saturated Fat Promotes Fatty Liver and Ceramides Compared With Polyunsaturated Fat: A Randomized Trial. *J Clin Endocrinol Metab* 2019; **104**: 6207-6219 [PMID: 31369090 DOI: 10.1210/jc.2019-00160]

16 **Luukkonen PK**, Sädevirta S, Zhou Y, Kayser B, Ali A, Ahonen L, Lallukka S, Pelloux V, Gaggini M, Jian C, Hakkarainen A, Lundbom N, Gylling H, Salonen A, Orešič M, Hyötyläinen T, Orho-Melander M, Rissanen A, Gastaldelli A, Clément K, Hodson L, Yki-Järvinen H. Saturated Fat Is More Metabolically Harmful for the Human Liver Than Unsaturated Fat or Simple Sugars. *Diabetes Care* 2018; **41**: 1732-1739 [PMID: 29844096 DOI: 10.2337/dc18-0071]

17 **Meex RCR**, Blaak EE. Mitochondrial Dysfunction is a Key Pathway that Links Saturated Fat Intake to the Development and Progression of NAFLD. *Mol Nutr Food Res* 2021; **65**: e1900942 [PMID: 32574416 DOI: 10.1002/mnfr.201900942]

18 **Satapati S**, Kucejova B, Duarte JA, Fletcher JA, Reynolds L, Sunny NE, He T, Nair LA, Livingston KA, Fu X, Merritt ME, Sherry AD, Malloy CR, Shelton JM, Lambert J, Parks EJ, Corbin I, Magnuson MA, Browning JD, Burgess SC. Mitochondrial metabolism mediates oxidative stress and inflammation in fatty liver. *J Clin Invest* 2016; **126**: 1605 [PMID: 27035816 DOI: 10.1172/JCI86695]

19 **Sullivan EM**, Fix A, Crouch MJ, Sparagna GC, Zeczycki TN, Brown DA, Shaikh SR. Murine diet-induced obesity remodels cardiac and liver mitochondrial phospholipid acyl chains with differential effects on respiratory enzyme activity. *J Nutr Biochem* 2017; **45**: 94-103 [PMID: 28437736 DOI: 10.1016/j.jnutbio.2017.04.004]

20 **Donnelly KL**, Smith CI, Schwarzenberg SJ, Jessurun J, Boldt MD, Parks EJ. Sources of fatty acids stored in liver and secreted *via* lipoproteins in patients with nonalcoholic fatty liver disease. *J Clin Invest* 2005; **115**: 1343-1351 [PMID: 15864352 DOI: 10.1172/JCI23621]

21 **Nati M**, Haddad D, Birkenfeld AL, Koch CA, Chavakis T, Chatzigeorgiou A. The role of immune cells in metabolism-related liver inflammation and development of non-alcoholic steatohepatitis (NASH). *Rev Endocr Metab Disord* 2016; **17**: 29-39 [PMID: 26847547 DOI: 10.1007/s11154-016-9339-2]

22 **Zorena K**, Jachimowicz-Duda O, Ślęzak D, Robakowska M, Mrugacz M. Adipokines and Obesity. Potential Link to Metabolic Disorders and Chronic Complications. *Int J Mol Sci* 2020; **21** [PMID: 32443588 DOI: 10.3390/ijms21103570]

23 **Monda V**, Polito R, Lovino A, Finaldi A, Valenzano A, Nigro E, Corso G, Sessa F, Asmundo A, Nunno ND, Cibelli G, Messina G. Short-Term Physiological Effects of a Very Low-Calorie Ketogenic Diet: Effects on Adiponectin Levels and Inflammatory States. *Int J Mol Sci* 2020; **21** [PMID: 32370212 DOI: 10.3390/ijms21093228]

24 **Flehmig G**, Scholz M, Klöting N, Fasshauer M, Tönjes A, Stumvoll M, Youn BS, Blüher M. Identification of adipokine clusters related to parameters of fat mass, insulin sensitivity and inflammation. *PLoS One* 2014; **9**: e99785 [PMID: 24968098 DOI: 10.1371/journal.pone.0099785]

25 **Morioka T**, Emoto M, Yamazaki Y, Kawano N, Imamura S, Numaguchi R, Urata H, Motoyama K, Mori K, Fukumoto S, Koyama H, Shoji T, Inaba M. Leptin is associated with vascular endothelial function in overweight patients with type 2 diabetes. *Cardiovasc Diabetol* 2014; **13**: 10 [PMID: 24410779 DOI: 10.1186/1475-2840-13-10]

26 **Jung CH**, Kim BY, Mok JO, Kang SK, Kim CH. Association between serum adipocytokine levels and microangiopathies in patients with type 2 diabetes mellitus. *J Diabetes Investig* 2014; **5**: 333-339 [PMID: 24843783 DOI: 10.1111/jdi.12144]

27 **Zhang Q**, Wang J, Huang F, Yao Y, Xu L. Leptin induces NAFLD progression through infiltrated CD8+ T lymphocytes mediating pyroptotic-like cell death of hepatocytes and macrophages. *Dig Liver Dis* 2021; **53**: 598-605 [PMID: 33172809 DOI: 10.1016/j.dld.2020.10.025]

28 **Käräjämäki AJ**, Bloigu R, Kauma H, Kesäniemi YA, Koivurova OP, Perkiömäki J, Huikuri H, Ukkola O. Non-alcoholic fatty liver disease with and without metabolic syndrome: Different long-term outcomes. *Metabolism* 2017; **66**: 55-63 [PMID: 27423871 DOI: 10.1016/j.metabol.2016.06.009]

29 **Ballestri S**, Zona S, Targher G, Romagnoli D, Baldelli E, Nascimbeni F, Roverato A, Guaraldi G, Lonardo A. Nonalcoholic fatty liver disease is associated with an almost twofold increased risk of incident type 2 diabetes and metabolic syndrome. Evidence from a systematic review and meta-analysis. *J Gastroenterol Hepatol* 2016; **31**: 936-944 [PMID: 26667191 DOI: 10.1111/jgh.13264]

30 **Loomba R**, Abraham M, Unalp A, Wilson L, Lavine J, Doo E, Bass NM; Nonalcoholic Steatohepatitis Clinical Research Network. Association between diabetes, family history of diabetes, and risk of nonalcoholic steatohepatitis and fibrosis. *Hepatology* 2012; **56**: 943-951 [PMID: 22505194 DOI: 10.1002/hep.25772]

31 **Ghorpade DS**, Ozcan L, Zheng Z, Nicoloro SM, Shen Y, Chen E, Blüher M, Czech MP, Tabas I. Hepatocyte-secreted DPP4 in obesity promotes adipose inflammation and insulin resistance. *Nature* 2018; **555**: 673-677 [PMID: 29562231 DOI: 10.1038/nature26138]

32 **Barchetta I**, Ceccarelli V, Cimini FA, Barone E, Sentinelli F, Coluzzi M, Chiappetta C, Bertoccini L, Tramutola A,

Labbadia G, Di Cristofano C, Silecchia G, Leonetti F, Cavallo MG. Circulating dipeptidyl peptidase-4 is independently associated with the presence and severity of NAFLD/NASH in individuals with and without obesity and metabolic disease. *J Endocrinol Invest* 2021; **44**: 979-988 [PMID: 32852705 DOI: 10.1007/s40618-020-01392-5]

33 **Zelber-Sagi S**, Salomone F, Mlynarsky L. The Mediterranean dietary pattern as the diet of choice for non-alcoholic fatty liver disease: Evidence and plausible mechanisms. *Liver Int* 2017; **37**: 936-949 [PMID: 28371239 DOI: 10.1111/liv.13435]

34 **Salehi-Sahlabadi A**, Sadat S, Beigrezaei S, Pourmasomi M, Feizi A, Ghiasvand R, Hadi A, Clark CCT, Miraghajani M. Dietary patterns and risk of non-alcoholic fatty liver disease. *BMC Gastroenterol* 2021; **21**: 41 [PMID: 33509112 DOI: 10.1186/s12876-021-01612-z]

35 **Pérez-Martínez P**, Mikhailidis DP, Athyros VG, Bullo M, Couture P, Covas MI, de Koning L, Delgado-Lista J, Díaz-López A, Drevon CA, Estruch R, Esposito K, Fitó M, Garaulet M, Giugliano D, García-Ríos A, Katsiki N, Kolovou G, Lamarche B, Maiorino MI, Mena-Sánchez G, Muñoz-Garach A, Nikolic D, Ordovás JM, Pérez-Jiménez F, Rizzo M, Salas-Salvadó J, Schröder H, Tinahones FJ, de la Torre R, van Ommen B, Wopereis S, Ros E, López-Miranda J. Lifestyle recommendations for the prevention and management of metabolic syndrome: an international panel recommendation. *Nutr Rev* 2017; **75**: 307-326 [PMID: 28521334 DOI: 10.1093/nutrit/nux014]

36 **Bajerska J**, Chmurzynska A, Muzsik A, Krzyżanowska P, Mądry E, Malinowska AM, Walkowiak J. Weight loss and metabolic health effects from energy-restricted Mediterranean and Central-European diets in postmenopausal women: A randomized controlled trial. *Sci Rep* 2018; **8**: 11170 [PMID: 30042488 DOI: 10.1038/s41598-018-29495-3]

37 **Gosal H**, Kaur H, Chakwop Ngassa H, Elmenawi KA, Anil V, Mohammed L. The Significance of the Mediterranean Diet in the Management of Non-Alcoholic Fatty Liver Disease: A Systematic Review. *Cureus* 2021; **13**: e15618 [PMID: 34277236 DOI: 10.7759/cureus.15618]

38 **Gil A**, Gil F. Fish, a Mediterranean source of n-3 PUFA: benefits do not justify limiting consumption. *Br J Nutr* 2015; **113** Suppl 2: S58-S67 [PMID: 26148923 DOI: 10.1017/S0007114514003742]

39 **Kastorini CM**, Milionis HJ, Esposito K, Giugliano D, Goudevenos JA, Panagiotakos DB. The effect of Mediterranean diet on metabolic syndrome and its components: a meta-analysis of 50 studies and 534,906 individuals. *J Am Coll Cardiol* 2011; **57**: 1299-1313 [PMID: 21392646 DOI: 10.1016/j.jacc.2010.09.073]

40 **Entezari MR**, Talenezhad N, Mirzavandi F, Rahimpour S, Mozaffari-Khosravi H, Fallahzadeh H, Hosseinzadeh M. Mediterranean dietary pattern and non-alcoholic fatty liver diseases: a case-control study. *J Nutr Sci* 2021; **10**: e55 [PMID: 34367629 DOI: 10.1017/jns.2021.43]

41 **Giraldi L**, Miele L, Aleksovska K, Manca F, Leoncini E, Biolato M, Arzani D, Pirro MA, Marrone G, Cefalo C, Racco S, Liguori A, Rapaccini G, Miggiano GA, Gasbarrini A, Boccia S, Grieco A. Mediterranean diet and the prevention of non-alcoholic fatty liver disease: results from a case-control study. *Eur Rev Med Pharmacol Sci* 2020; **24**: 7391-7398 [PMID: 32706078 DOI: 10.26355/eurrev_202007_21907]

42 **Baratta F**, Pastori D, Polimeni L, Bucci T, Ceci F, Calabrese C, Ernesti I, Pannitteri G, Violi F, Angelico F, Del Ben M. Adherence to Mediterranean Diet and Non-Alcoholic Fatty Liver Disease: Effect on Insulin Resistance. *Am J Gastroenterol* 2017; **112**: 1832-1839 [PMID: 29063908 DOI: 10.1038/ajg.2017.371]

43 **Hassani Zadeh S**, Mansoori A, Hosseinzadeh M. Relationship between dietary patterns and non-alcoholic fatty liver disease: A systematic review and meta-analysis. *J Gastroenterol Hepatol* 2021; **36**: 1470-1478 [PMID: 33269500 DOI: 10.1111/jgh.15363]

44 **Kontogianni MD**, Tileli N, Margariti A, Georgoulis M, Deutsch M, Tiniakos D, Fragopoulou E, Zafiropoulou R, Manios Y, Papatheodoridis G. Adherence to the Mediterranean diet is associated with the severity of non-alcoholic fatty liver disease. *Clin Nutr* 2014; **33**: 678-683 [PMID: 24064253 DOI: 10.1016/j.clnu.2013.08.014]

45 **Aller R**, Izaola O, de la Fuente B, De Luis Román DA. Mediterranean diet is associated with liver histology in patients with non alcoholic fatty liver disease. *Nutr Hosp* 2015; **32**: 2518-2524 [PMID: 26667698 DOI: 10.3305/nh.2015.32.6.10074]

46 **Park SY**, Noureddin M, Boushey C, Wilkens LR, Setiawan VW. Diet Quality Association with Nonalcoholic Fatty Liver Disease by Cirrhosis Status: The Multiethnic Cohort. *Curr Dev Nutr* 2020; **4**: nzaa024 [PMID: 32190810 DOI: 10.1093/cdn/nzaa024]

47 **Chan R**, Wong VW, Chu WC, Wong GL, Li LS, Leung J, Chim AM, Yeung DK, Sea MM, Woo J, Chan FK, Chan HL. Diet-Quality Scores and Prevalence of Nonalcoholic Fatty Liver Disease: A Population Study Using Proton-Magnetic Resonance Spectroscopy. *PLoS One* 2015; **10**: e0139310 [PMID: 26418083 DOI: 10.1371/journal.pone.0139310]

48 **European Association for the Study of the Liver (EASL)**; European Association for the Study of Diabetes (EASD); European Association for the Study of Obesity (EASO). EASL-EASD-EASO Clinical Practice Guidelines for the management of non-alcoholic fatty liver disease. *J Hepatol* 2016; **64**: 1388-1402 [PMID: 27062661 DOI: 10.1016/j.jhep.2015.11.004]

49 **Anania C**, Perla FM, Olivero F, Pacifico L, Chiesa C. Mediterranean diet and nonalcoholic fatty liver disease. *World J Gastroenterol* 2018; **24**: 2083-2094 [PMID: 29785077 DOI: 10.3748/wjg.v24.i19.2083]

50 **Paniagua JA**, Gallego de la Sacristana A, Romero I, Vidal-Puig A, Latre JM, Sanchez E, Perez-Martinez P, Lopez-Miranda J, Perez-Jimenez F. Monounsaturated fat-rich diet prevents central body fat distribution and decreases postprandial adiponectin expression induced by a carbohydrate-rich diet in insulin-resistant subjects. *Diabetes Care* 2007; **30**: 1717-1723 [PMID: 17384344 DOI: 10.2337/dc06-2220]

51 **Assy N**, Nassar F, Nasser G, Grosovski M. Olive oil consumption and non-alcoholic fatty liver disease. *World J Gastroenterol* 2009; **15**: 1809-1815 [PMID: 19370776 DOI: 10.3748/wjg.15.1809]

52 **Oddy WH**, Herbison CE, Jacoby P, Ambrosini GL, O'Sullivan TA, Ayonrinde OT, Olynyk JK, Black LJ, Beilin LJ, Mori TA, Hands BP, Adams LA. The Western dietary pattern is prospectively associated with nonalcoholic fatty liver disease in adolescence. *Am J Gastroenterol* 2013; **108**: 778-785 [PMID: 23545714 DOI: 10.1038/ajg.2013.95]

53 **Zhang S**, Gu Y, Bian S, Górska MJ, Zhang Q, Liu L, Meng G, Yao Z, Wu H, Wang Y, Zhang T, Wang X, Sun S, Zhou M, Jia Q, Song K, Qi L, Niu K. Dietary patterns and risk of non-alcoholic fatty liver disease in adults: A prospective cohort study. *Clin Nutr* 2021; **40**: 5373-5382 [PMID: 34560608 DOI: 10.1016/j.clnu.2021.08.021]

54 **Dehghanseresht N**, Jafarirad S, Alavinejad SP, Mansoori A. Association of the dietary patterns with the risk of non-alcoholic fatty liver disease among Iranian population: a case-control study. *Nutr J* 2020; **19**: 63 [PMID: 32605646 DOI: 10.1186/s12937-020-00580-6]

55 **Kalafati IP**, Borsa D, Dimitriou M, Revenas K, Kokkinos A, Dedoussis GV. Dietary patterns and non-alcoholic fatty liver disease in a Greek case-control study. *Nutrition* 2019; **61**: 105-110 [PMID: 30708259 DOI: 10.1016/j.nut.2018.10.032]

56 **Tutunchi H**, Saghafi-Asl M, Asghari-Jafarabadi M, Ostadrahimi A. Association between Dietary Patterns and Non-alcoholic Fatty Liver Disease: Results from a Case-Control Study. *Arch Iran Med* 2021; **24**: 35-42 [PMID: 33588566 DOI: 10.34172/aim.2021.06]

57 **Yang CQ**, Shu L, Wang S, Wang JJ, Zhou Y, Xuan YJ, Wang SF. Dietary Patterns Modulate the Risk of Non-Alcoholic Fatty Liver Disease in Chinese Adults. *Nutrients* 2015; **7**: 4778-4791 [PMID: 26083112 DOI: 10.3390/nu7064778]

58 **Nakashita C**, Xi L, Inoue Y, Kabura R, Masuda S, Yamano Y, Katoh T. Impact of dietary compositions and patterns on the prevalence of nonalcoholic fatty liver disease in Japanese men: a cross-sectional study. *BMC Gastroenterol* 2021; **21**: 342 [PMID: 34481454 DOI: 10.1186/s12876-021-01919-x]

59 **Adriano LS**, Sampaio HA, Arruda SP, Portela CL, de Melo MLP, Carioca AA, Soares NT. Healthy dietary pattern is inversely associated with non-alcoholic fatty liver disease in elderly. *Br J Nutr* 2016; **115**: 2189-2195 [PMID: 27102566 DOI: 10.1017/S0007114516001410]

60 **Chung GE**, Youn J, Kim YS, Lee JE, Yang SY, Lim JH, Song JH, Doo EY, Kim JS. Dietary patterns are associated with the prevalence of nonalcoholic fatty liver disease in Korean adults. *Nutrition* 2019; **62**: 32-38 [PMID: 30826597 DOI: 10.1016/j.nut.2018.11.021]

61 **Zhang Q**, Ma X, Xing J, Shi H, Yang R, Jiao Y, Chen S, Wu S, Zhang S, Sun X. Serum Uric Acid Is a Mediator of the Association Between Obesity and Incident Nonalcoholic Fatty Liver Disease: A Prospective Cohort Study. *Front Endocrinol (Lausanne)* 2021; **12**: 657856 [PMID: 34054728 DOI: 10.3389/fendo.2021.657856]

62 **Alferink LJM**, Erler NS, de Knegt RJ, Janssen HLA, Metselaar HJ, Darwish Murad S, Kiefte-de Jong JC. Adherence to a plant-based, high-fibre dietary pattern is related to regression of non-alcoholic fatty liver disease in an elderly population. *Eur J Epidemiol* 2020; **35**: 1069-1085 [PMID: 32323115 DOI: 10.1007/s10654-020-00627-2]

63 **Drake I**, Sonestedt E, Ericson U, Wallström P, Orho-Melander M. A Western dietary pattern is prospectively associated with cardio-metabolic traits and incidence of the metabolic syndrome. *Br J Nutr* 2018; **119**: 1168-1176 [PMID: 29759108 DOI: 10.1017/S000711451800079X]

64 **Fakhoury-Sayegh N**, Younes H, Heraoui GNHA, Sayegh R. Nutritional Profile and Dietary Patterns of Lebanese Non-Alcoholic Fatty Liver Disease Patients: A Case-Control Study. *Nutrients* 2017; **9** [PMID: 29135945 DOI: 10.3390/nu9111245]

65 **Jia Q**, Xia Y, Zhang Q, Wu H, Du H, Liu L, Wang C, Shi H, Guo X, Liu X, Li C, Sun S, Wang X, Zhao H, Song K, Huang G, Wu Y, Cui N, Niu K. Dietary patterns are associated with prevalence of fatty liver disease in adults. *Eur J Clin Nutr* 2015; **69**: 914-921 [PMID: 25649235 DOI: 10.1038/ejcn.2014.297]

66 **Zhang S**, Gu Y, Bian S, Lu Z, Zhang Q, Liu L, Meng G, Yao Z, Wu H, Wang Y, Zhang T, Wang X, Sun S, Zhou M, Jia Q, Song K, Qi L, Niu K. Soft drink consumption and risk of nonalcoholic fatty liver disease: results from the Tianjin Chronic Low-Grade Systemic Inflammation and Health (TCLSIH) cohort study. *Am J Clin Nutr* 2021; **113**: 1265-1274 [PMID: 33564868 DOI: 10.1093/ajcn/nqaa380]

67 **Softic S**, Cohen DE, Kahn CR. Role of Dietary Fructose and Hepatic De Novo Lipogenesis in Fatty Liver Disease. *Dig Dis Sci* 2016; **61**: 1282-1293 [PMID: 26856717 DOI: 10.1007/s10620-016-4054-0]

68 **Bischoff SC**, Austin P, Boeykens K, Chourdakis M, Cuerda C, Jonkers-Schuitema C, Lichota M, Nyulasi I, Schneider SM, Stanga Z, Pironi L. ESPEN guideline on home enteral nutrition. *Clin Nutr* 2020; **39**: 5-22 [PMID: 31255350 DOI: 10.1016/j.clnu.2019.04.022]

69 The diagnosis and management of nonalcoholic fatty liver disease: Practice guidance from the American Association for the Study of Liver Diseases. *Clin Liver Dis (Hoboken)* 2018; **11**: 81 [PMID: 30992795 DOI: 10.1002/cld.722]

70 **Chalasani N**, Younossi Z, Lavine JE, Charlton M, Cusi K, Rinella M, Harrison SA, Brunt EM, Sanyal AJ. The diagnosis and management of nonalcoholic fatty liver disease: Practice guidance from the American Association for the Study of Liver Diseases. *Hepatology* 2018; **67**: 328-357 [PMID: 28714183 DOI: 10.1002/hep.29367]

71 **Eslam M**, Sarin SK, Wong VW, Fan JG, Kawaguchi T, Ahn SH, Zheng MH, Shiha G, Yilmaz Y, Gani R, Alam S, Dan YY, Kao JH, Hamid S, Cua IH, Chan WK, Payawal D, Tan SS, Tanwandee T, Adams LA, Kumar M, Omata M, George J. The Asian Pacific Association for the Study of the Liver clinical practice guidelines for the diagnosis and management of metabolic associated fatty liver disease. *Hepatol Int* 2020; **14**: 889-919 [PMID: 33006093 DOI: 10.1007/s12072-020-10094-2]

72 **Review Team**. , LaBrecque DR, Abbas Z, Anania F, Ferenci P, Khan AG, Goh KL, Hamid SS, Isakov V, Lizarzabal M, Peñaranda MM, Ramos JF, Sarin S, Stimac D, Thomson AB, Umar M, Krabshuis J, LeMair A; World Gastroenterology Organisation. World Gastroenterology Organisation global guidelines: Nonalcoholic fatty liver disease and nonalcoholic steatohepatitis. *J Clin Gastroenterol* 2014; **48**: 467-473 [PMID: 24921212 DOI: 10.1097/MCG.0000000000000116]

73 **Barrera F**, George J. The role of diet and nutritional intervention for the management of patients with NAFLD. *Clin Liver Dis* 2014; **18**: 91-112 [PMID: 24274867 DOI: 10.1016/j.cld.2013.09.009]

74 **Raynor HA**, Champagne CM. Position of the Academy of Nutrition and Dietetics: Interventions for the Treatment of Overweight and Obesity in Adults. *J Acad Nutr Diet* 2016; **116**: 129-147 [PMID: 26718656 DOI: 10.1016/j.jand.2015.10.031]

75 **Hohenester S**, Christiansen S, Nagel J, Wimmer R, Artmann R, Denk G, Bischoff M, Bischoff G, Rust C. Lifestyle intervention for morbid obesity: effects on liver steatosis, inflammation, and fibrosis. *Am J Physiol Gastrointest Liver Physiol* 2018; **315**: G329-G338 [PMID: 29878845 DOI: 10.1152/ajpgi.00044.2018]

76 **Musso G**, Cassader M, Rosina F, Gambino R. Impact of current treatments on liver disease, glucose metabolism and cardiovascular risk in non-alcoholic fatty liver disease (NAFLD): a systematic review and meta-analysis of randomised trials. *Diabetologia* 2012; **55**: 885-904 [PMID: 22278337 DOI: 10.1007/s00125-011-2446-4]

77 **Hsu CC**, Ness E, Kowdley KV. Nutritional Approaches to Achieve Weight Loss in Nonalcoholic Fatty Liver Disease.

Adv Nutr 2017; **8**: 253-265 [PMID: 28298270 DOI: 10.3945/an.116.013730]
78 **Miller EF**. Nutrition Management Strategies for Nonalcoholic Fatty Liver Disease: Treatment and Prevention. *Clin Liver Dis (Hoboken)* 2020; **15**: 144-148 [PMID: 32395240 DOI: 10.1002/cld.918]
79 **Hall KD**, Guo J. Obesity Energetics: Body Weight Regulation and the Effects of Diet Composition. *Gastroenterology* 2017; **152**: 1718-1727.e3 [PMID: 28193517 DOI: 10.1053/j.gastro.2017.01.052]
80 **Ristic-Medic D**, Kovacic M, Takic M, Arsic A, Petrovic S, Paunovic M, Jovicic M, Vucic V. Calorie-Restricted Mediterranean and Low-Fat Diets Affect Fatty Acid Status in Individuals with Nonalcoholic Fatty Liver Disease. *Nutrients* 2020; **13** [PMID: 33374554 DOI: 10.3390/nu13010015]
81 **George ES**, Forsyth A, Itsiopoulos C, Nicoll AJ, Ryan M, Sood S, Roberts SK, Tierney AC. Practical Dietary Recommendations for the Prevention and Management of Nonalcoholic Fatty Liver Disease in Adults. *Adv Nutr* 2018; **9**: 30-40 [PMID: 29438460 DOI: 10.1093/advances/nmx007]
82 **Houttu V**, Csader S, Nieuwdorp M, Holleboom AG, Schwab U. Dietary Interventions in Patients With Non-alcoholic Fatty Liver Disease: A Systematic Review and Meta-Analysis. *Front Nutr* 2021; **8**: 716783 [PMID: 34368214 DOI: 10.3389/fnut.2021.716783]
83 **Misciagna G**, Del Pilar Díaz M, Caramia DV, Bonfiglio C, Franco I, Noviello MR, Chiloiro M, Abbrescia DI, Mirizzi A, Tanzi M, Caruso MG, Correale M, Reddavide R, Inguaggiato R, Cisternino AM, Osella AR. Effect of a Low Glycemic Index Mediterranean Diet on Non-Alcoholic Fatty Liver Disease. A Randomized Controlled Clinici Trial. *J Nutr Health Aging* 2017; **21**: 404-412 [PMID: 28346567 DOI: 10.1007/s12603-016-0809-8]
84 **Stokes CS**, Lammert F, Krawczyk M. Short-term Dietary Interventions for the Management of Nonalcoholic Fatty Liver. *Curr Med Chem* 2019; **26**: 3483-3496 [PMID: 28482789 DOI: 10.2174/0929867324666170508144409]
85 **Arsic A**, Takic M, Kojadinovic M, Petrovic S, Paunovic M, Vucic V, Ristic Medic D. Metabolically healthy obesity: is there a link with polyunsaturated fatty acid intake and status? *Can J Physiol Pharmacol* 2021; **99**: 64-71 [PMID: 32822561 DOI: 10.1139/cjpp-2020-0317]
86 **Dudekula A**, Rachakonda V, Shaik B, Behari J. Weight loss in nonalcoholic Fatty liver disease patients in an ambulatory care setting is largely unsuccessful but correlates with frequency of clinic visits. *PLoS One* 2014; **9**: e111808 [PMID: 25375228 DOI: 10.1371/journal.pone.0111808]
87 **Kang J**, Ratamess NA, Faigenbaum AD, Bush JA, Beller N, Vargas A, Fardman B, Andriopoulos T. Effect of Time-Restricted Feeding on Anthropometric, Metabolic, and Fitness Parameters: A Systematic Review. *J Am Coll Nutr* 2021; 1-16 [PMID: 34491139 DOI: 10.1080/07315724.2021.1958719]
88 **Yin C**, Li Z, Xiang Y, Peng H, Yang P, Yuan S, Zhang X, Wu Y, Huang M, Li J. Effect of Intermittent Fasting on Non-Alcoholic Fatty Liver Disease: Systematic Review and Meta-Analysis. *Front Nutr* 2021; **8**: 709683 [PMID: 34322514 DOI: 10.3389/fnut.2021.709683]
89 **Holmer M**, Lindqvist C, Petersson S, Moshtaghi-Svensson J, Tillander V, Brismar TB, Hagström H, Stål P. Treatment of NAFLD with intermittent calorie restriction or low-carb high-fat diet - a randomised controlled trial. *JHEP Rep* 2021; **3**: 100256 [PMID: 33898960 DOI: 10.1016/j.jhepr.2021.100256]
90 **Wilhelmi de Toledo F**, Grundler F, Sirtori CR, Ruscica M. Unravelling the health effects of fasting: a long road from obesity treatment to healthy life span increase and improved cognition. *Ann Med* 2020; **52**: 147-161 [PMID: 32519900 DOI: 10.1080/07853890.2020.1770849]
91 **Cai H**, Qin YL, Shi ZY, Chen JH, Zeng MJ, Zhou W, Chen RQ, Chen ZY. Effects of alternate-day fasting on body weight and dyslipidaemia in patients with non-alcoholic fatty liver disease: a randomised controlled trial. *BMC Gastroenterol* 2019; **19**: 219 [PMID: 31852444 DOI: 10.1186/s12876-019-1132-8]
92 **Johari MI**, Yusoff K, Haron J, Nadarajan C, Ibrahim KN, Wong MS, Hafidz MIA, Chua BE, Hamid N, Arifin WN, Ma ZF, Lee YY. A Randomised Controlled Trial on the Effectiveness and Adherence of Modified Alternate-day Calorie Restriction in Improving Activity of Non-Alcoholic Fatty Liver Disease. *Sci Rep* 2019; **9**: 11232 [PMID: 31375753 DOI: 10.1038/s41598-019-47763-8]
93 **Hekmatdoost A**, Shamsipour A, Meibodi M, Gheibizadeh N, Eslamparast T, Poustchi H. Adherence to the Dietary Approaches to Stop Hypertension (DASH) and risk of Nonalcoholic Fatty Liver Disease. *Int J Food Sci Nutr* 2016; **67**: 1024-1029 [PMID: 27436528 DOI: 10.1080/09637486.2016.1210101]
94 **Xiao ML**, Lin JS, Li YH, Liu M, Deng YY, Wang CY, Chen YM. Adherence to the Dietary Approaches to Stop Hypertension (DASH) diet is associated with lower presence of non-alcoholic fatty liver disease in middle-aged and elderly adults. *Public Health Nutr* 2020; **23**: 674-682 [PMID: 31566148 DOI: 10.1017/S1368980019002568]
95 **Razavi Zade M**, Telkabadi MH, Bahmani F, Salehi B, Farshbaf S, Asemi Z. The effects of DASH diet on weight loss and metabolic status in adults with non-alcoholic fatty liver disease: a randomized clinical trial. *Liver Int* 2016; **36**: 563-571 [PMID: 26503843 DOI: 10.1111/liv.12990]
96 **Moreno B**, Bellido D, Sajoux I, Goday A, Saavedra D, Crujeiras AB, Casanueva FF. Comparison of a very low-calorie-ketogenic diet with a standard low-calorie diet in the treatment of obesity. *Endocrine* 2014; **47**: 793-805 [PMID: 24584583 DOI: 10.1007/s12020-014-0192-3]
97 **Watanabe M**, Tozzi R, Risi R, Tuccinardi D, Mariani S, Basciani S, Spera G, Lubrano C, Gnessi L. Beneficial effects of the ketogenic diet on nonalcoholic fatty liver disease: A comprehensive review of the literature. *Obes Rev* 2020; **21**: e13024 [PMID: 32207237 DOI: 10.1111/obr.13024]
98 **Westerbacka J**, Lammi K, Häkkinen AM, Rissanen A, Salminen I, Aro A, Yki-Järvinen H. Dietary fat content modifies liver fat in overweight nondiabetic subjects. *J Clin Endocrinol Metab* 2005; **90**: 2804-2809 [PMID: 15741262 DOI: 10.1210/jc.2004-1983]
99 **Pérez-Guisado J**, Muñoz-Serrano A. A pilot study of the Spanish Ketogenic Mediterranean Diet: an effective therapy for the metabolic syndrome. *J Med Food* 2011; **14**: 681-687 [PMID: 21612461 DOI: 10.1089/jmf.2010.0137]
100 **Mardinoglu A**, Wu H, Bjornson E, Zhang C, Hakkarainen A, Räsänen SM, Lee S, Mancina RM, Bergentall M, Pietiläinen KH, Söderlund S, Matikainen N, Ståhlman M, Bergh PO, Adiels M, Piening BD, Granér M, Lundbom N, Williams KJ, Romeo S, Nielsen J, Snyder M, Uhlén M, Bergström G, Perkins R, Marschall HU, Bäckhed F, Taskinen MR, Borén J. An Integrated Understanding of the Rapid Metabolic Benefits of a Carbohydrate-Restricted Diet on Hepatic

Steatosis in Humans. *Cell Metab* 2018; **27**: 559-571.e5 [PMID: 29456073 DOI: 10.1016/j.cmet.2018.01.005]

101 **Lundsgaard AM**, Holm JB, Sjøberg KA, Bojsen-Møller KN, Myrmel LS, Fjære E, Jensen BAH, Nicolaisen TS, Hingst JR, Hansen SL, Doll S, Geyer PE, Deshmukh AS, Holst JJ, Madsen L, Kristiansen K, Wojtaszewski JFP, Richter EA, Kiens B. Mechanisms Preserving Insulin Action during High Dietary Fat Intake. *Cell Metab* 2019; **29**: 50-63.e4 [PMID: 30269983 DOI: 10.1016/j.cmet.2018.08.022]

102 **Ouyang X**, Cirillo P, Sautin Y, McCall S, Bruchette JL, Diehl AM, Johnson RJ, Abdelmalek MF. Fructose consumption as a risk factor for non-alcoholic fatty liver disease. *J Hepatol* 2008; **48**: 993-999 [PMID: 18395287 DOI: 10.1016/j.jhep.2008.02.011]

103 **Stanhope KL**, Schwarz JM, Keim NL, Griffen SC, Bremer AA, Graham JL, Hatcher B, Cox CL, Dyachenko A, Zhang W, McGahan JP, Seibert A, Krauss RM, Chiu S, Schaefer EJ, Ai M, Otokozawa S, Nakajima K, Nakano T, Beysen C, Hellerstein MK, Berglund L, Havel PJ. Consuming fructose-sweetened, not glucose-sweetened, beverages increases visceral adiposity and lipids and decreases insulin sensitivity in overweight/obese humans. *J Clin Invest* 2009; **119**: 1322-1334 [PMID: 19381015 DOI: 10.1172/JCI37385]

104 **Sevastianova K**, Santos A, Kotronen A, Hakkarainen A, Makkonen J, Silander K, Peltonen M, Romeo S, Lundbom J, Lundbom N, Olkkonen VM, Gylling H, Fielding BA, Rissanen A, Yki-Järvinen H. Effect of short-term carbohydrate overfeeding and long-term weight loss on liver fat in overweight humans. *Am J Clin Nutr* 2012; **96**: 727-734 [PMID: 22952180 DOI: 10.3945/ajcn.112.038695]

105 **Roeb E**, Weiskirchen R. Fructose and Non-Alcoholic Steatohepatitis. *Front Pharmacol* 2021; **12**: 634344 [PMID: 33628193 DOI: 10.3389/fphar.2021.634344]

106 **Meng G**, Zhang B, Yu F, Li C, Zhang Q, Liu L, Wu H, Xia Y, Bao X, Shi H, Su Q, Gu Y, Fang L, Yang H, Yu B, Sun S, Wang X, Zhou M, Jia Q, Jiao H, Wang B, Guo Q, Carvalhoa LA, Sun Z, Song K, Yu M, Niu K. Soft drinks consumption is associated with nonalcoholic fatty liver disease independent of metabolic syndrome in Chinese population. *Eur J Nutr* 2018; **57**: 2113-2121 [PMID: 28702720 DOI: 10.1007/s00394-017-1485-0]

107 **Abdelmalek MF**, Suzuki A, Guy C, Unalp-Arida A, Colvin R, Johnson RJ, Diehl AM; Nonalcoholic Steatohepatitis Clinical Research Network. Increased fructose consumption is associated with fibrosis severity in patients with nonalcoholic fatty liver disease. *Hepatology* 2010; **51**: 1961-1971 [PMID: 20301112 DOI: 10.1002/hep.23535]

108 **Chiu S**, Sievenpiper JL, de Souza RJ, Cozma AI, Mirrahimi A, Carleton AJ, Ha V, Di Buono M, Jenkins AL, Leiter LA, Wolever TM, Don-Wauchope AC, Beyene J, Kendall CW, Jenkins DJ. Effect of fructose on markers of non-alcoholic fatty liver disease (NAFLD): a systematic review and meta-analysis of controlled feeding trials. *Eur J Clin Nutr* 2014; **68**: 416-423 [PMID: 24569542 DOI: 10.1038/ejcn.2014.8]

109 **Kositamongkol C**, Kanchanasurakit S, Auttamalang C, Inchai N, Kabkaew T, Kitpark S, Chaiyakunapruk N, Duangjai A, Saokaew S, Phisalprapa P. Coffee Consumption and Non-alcoholic Fatty Liver Disease: An Umbrella Review and a Systematic Review and Meta-analysis. *Front Pharmacol* 2021; **12**: 786596 [PMID: 34966282 DOI: 10.3389/fphar.2021.786596]

110 **Hayat U**, Siddiqui AA, Okut H, Afroz S, Tasleem S, Haris A. The effect of coffee consumption on the non-alcoholic fatty liver disease and liver fibrosis: A meta-analysis of 11 epidemiological studies. *Ann Hepatol* 2021; **20**: 100254 [PMID: 32920163 DOI: 10.1016/j.aohep.2020.08.071]

111 **Catalano D**, Martines GF, Tonzuso A, Pirri C, Trovato FM, Trovato GM. Protective role of coffee in non-alcoholic fatty liver disease (NAFLD). *Dig Dis Sci* 2010; **55**: 3200-3206 [PMID: 20165979 DOI: 10.1007/s10620-010-1143-3]

112 **Saab S**, Mallam D, Cox GA 2nd, Tong MJ. Impact of coffee on liver diseases: a systematic review. *Liver Int* 2014; **34**: 495-504 [PMID: 24102757 DOI: 10.1111/liv.12304]

113 **Zelber-Sagi S**, Salomone F, Webb M, Lotan R, Yeshua H, Halpern Z, Santo E, Oren R, Shibolet O. Coffee consumption and nonalcoholic fatty liver onset: a prospective study in the general population. *Transl Res* 2015; **165**: 428-436 [PMID: 25468486 DOI: 10.1016/j.trsl.2014.10.008]

114 **Kennedy OJ**, Fallowfield JA, Poole R, Hayes PC, Parkes J, Roderick PJ. All coffee types decrease the risk of adverse clinical outcomes in chronic liver disease: a UK Biobank study. *BMC Public Health* 2021; **21**: 970 [PMID: 34154561 DOI: 10.1186/s12889-021-10991-7]

115 **Bravi F**, Tavani A, Bosetti C, Boffetta P, La Vecchia C. Coffee and the risk of hepatocellular carcinoma and chronic liver disease: a systematic review and meta-analysis of prospective studies. *Eur J Cancer Prev* 2017; **26**: 368-377 [PMID: 27111112 DOI: 10.1097/CEJ.0000000000000252]

World Journal of Gastroenterology

Submit a Manuscript: https://www.f6publishing.com

World J Gastroenterol 2022 July 21; 28(27): 3334-3345

DOI: 10.3748/wjg.v28.i27.3334

ISSN 1007-9327 (print) ISSN 2219-2840 (online)

MINIREVIEWS

Application of intravoxel incoherent motion diffusion-weighted imaging in hepatocellular carcinoma

Yi Zhou, Jing Zheng, Cui Yang, Juan Peng, Ning Liu, Lin Yang, Xiao-Ming Zhang

Specialty type: Radiology, nuclear medicine and medical imaging

Provenance and peer review: Invited article; Externally peer reviewed.

Peer-review model: Single blind

Peer-review report's scientific quality classification

Grade A (Excellent): 0
Grade B (Very good): B, B, B
Grade C (Good): C, C
Grade D (Fair): 0
Grade E (Poor): 0

P-Reviewer: Marusic M, Croatia; Nath L, India; Sato T, Japan

Received: December 30, 2021
Peer-review started: December 30, 2021
First decision: April 16, 2022
Revised: April 26, 2022
Accepted: June 23, 2022
Article in press: June 23, 2022
Published online: July 21, 2022

Yi Zhou, Jing Zheng, Cui Yang, Juan Peng, Ning Liu, Lin Yang, Xiao-Ming Zhang, Medical Imaging Key Laboratory of Sichuan Province, Department of Radiology, Medical Research Center, The Affiliated Hospital of North Sichuan Medical College, Nanchong 637000, Sichuan Province, China

Yi Zhou, Department of Radiology, People's Hospital of Deyang City, Deyang 618000, Sichuan Province, China

Cui Yang, Department of Radiology, Panzhihua Central Hospital, Panzhihua 617000, Sichuan Province, China

Juan Peng, Department of Radiology, Sichuan Provincial People's Hospital Jinniu Hospital, Chengdu Jinniu District People's Hospital, Chengdu 610007, Sichuan Province, China

Corresponding author: Lin Yang, MD, Professor, Medical Imaging Key Laboratory of Sichuan Province, Department of Radiology, Medical Research Center, The Affiliated Hospital of North Sichuan Medical College, No. 63 Wenhua Road, Nanchong 637000, Sichuan Province, China. linyangmd@163.com

Abstract

The morbidity and mortality of hepatocellular carcinoma (HCC) rank 6th and 4th, respectively, among malignant tumors worldwide. Traditional diffusion-weighted imaging (DWI) uses the apparent diffusion coefficient (ADC) obtained by applying the monoexponential model to reflect water molecule diffusion in active tissue; however, the value of ADC is affected by microcirculation perfusion. Using a biexponential model, intravoxel incoherent motion (IVIM)-DWI quantitatively measures information related to pure water molecule diffusion and microcirculation perfusion, thus compensating for the shortcomings of DWI. The number of studies examining the application of IVIM-DWI in patients with HCC has gradually increased over the last few years, and many results show that IVIM-DWI has vital value for HCC differentiation, pathological grading, and predicting and evaluating the treatment response. The present study principally reviews the principle of IVIM-DWI and its research progress in HCC differentiation, pathological grading, predicting and evaluating the treatment response, predicting postoperative recurrence and predicting gene expression prediction.

Key Words: Hepatocellular carcinoma; Intravoxel incoherent motion; Differentiation; Pathological grading; Treatment response; Gene expression

Core Tip: Intravoxel incoherent motion (IVIM) diffusion-weighted imaging (DWI) quantitatively measures information related to pure water molecule diffusion and microcirculation perfusion using a biexponential model, thus compensating for the shortcomings of traditional DWI. The number of studies assessing IVIM-DWI in patients with hepatocellular carcinoma (HCC) has gradually increased over the last few years. This review, which is based on the literature, identified an imaging biomarker for HCC differentiation, pathological grading, predicting and evaluating the treatment response, predicting postoperative recurrence and predicting gene expression prediction. The results of this analysis show that IVIM-DWI has important value in the treatment and diagnosis of HCC.

Citation: Zhou Y, Zheng J, Yang C, Peng J, Liu N, Yang L, Zhang XM. Application of intravoxel incoherent motion diffusion-weighted imaging in hepatocellular carcinoma. *World J Gastroenterol* 2022; 28(27): 3334-3345
URL: https://www.wjgnet.com/1007-9327/full/v28/i27/3334.htm
DOI: https://dx.doi.org/10.3748/wjg.v28.i27.3334

INTRODUCTION

The morbidity and mortality of hepatocellular carcinoma (HCC) rank 6th and 4th, respectively, among malignant tumors worldwide[1,2]. The apparent diffusion coefficient (ADC) obtained using traditional diffusion-weighted imaging (DWI) reflects water molecule diffusion in tissue[3]. However, many studies have shown that a voxel contains other diffusion information in addition to the diffusion movement of pure water molecules, namely, the microcirculation perfusion of the capillary network in tissue[3-6]. One limitation of traditional DWI is that it is unable to distinguish water molecule diffusion and microcirculation perfusion information. Le Bihan *et al*[6,7] proposed that intravoxel incoherent motion (IVIM) quantitatively obtains information on both pure water molecule diffusion and diffusion related to microcirculation perfusion, thus compensating for the shortcoming of traditional DWI. Therefore, IVIM has become a research hotspot in recent years. The liver is suitable for IVIM research because of its relatively large blood supply. Since the first application of IVIM-DWI for the study of liver disease by Yamada *et al*[8], the number of studies assessing IVIM-DWI in patients with HCC has progressively increased, and significant progress has been achieved. This study mainly reviews IVIM-DWI research progress in the diagnosis and treatment of HCC.

THE BASIC PRINCIPLES OF IVIM-DWI

DWI is currently the only functional magnetic resonance imaging (MRI) technology that noninvasively measures water molecule diffusion in living tissue[3]. According to the theory of traditional DWI, the movement of free water molecules is considered to conform to a Gaussian distribution. However, due to the presence of complex cell structures and multiple diffusion barriers, such as cell membranes, in biological tissues, the diffusion behavior of water in biological tissues is more complicated. Therefore, the displacement of water in tissue may substantially deviate from a Gaussian distribution, challenging the validity of the monoexponential model to varying degrees. Additionally, the ADC, which reflects the water molecule diffusion, is affected simultaneously by microcirculation perfusion[3,5,7]. IVIM-DWI uses sufficient b values and biexponential models for the acquisition and analysis of images and distinguishes information regarding the pure tissue diffusion of water molecules and diffusion related to microcirculation perfusion. Among IVIM-DWI parameters, the simple diffusion coefficient, which is also referred to as the slow apparent diffusion coefficient (D), reflects the diffusion movement of pure water molecules in the tissue in a region of interest (ROI). The false diffusion coefficient, which is also called the fast apparent diffusion coefficient (D*), reflects diffusion movement related to microcirculation perfusion in the capillary network in an ROI. The fraction of the fast apparent diffusion coefficient (f) represents the volume ratio of the local microcirculation perfusion-related effect to the total diffusion effect, which may reflect the blood volume in an ROI. The formula for determining the relationship between IVIM-DWI signal attenuation and b values in tissue is as follows:

$S_b/S_0 = (1 - f) \times \exp(-bD) + f \times \exp[-b(D + D^*)]$

Where b is the diffusion sensitivity coefficient with units of s/mm^2, while the unit for both D and D* is mm^2/s, and S represents intravoxel signal intensity, with S_0 and S_b representing the signal intensities when b = 0 and b has other values, respectively. The b value determines the effect of microcirculation perfusion on DWI signal attenuation[6]. When the b value is low (b < 200 s/mm^2), the effect of microcir-

culation perfusion accounts for a large proportion of the total diffusion effect, whereas when the b value is high (b ≥ 200 s/mm^2), signal attenuation basically reflects only the pure water molecule diffusion in a voxel.

HCC DIFFERENTIATION

To date, many studies have shown that IVIM-DWI has important value in differentiating HCC from other liver lesions[8-22]. In theory, malignant tumors restrict the movement of water molecules to a significantly greater extent than benign tumors; thus, the ADC and D values of malignant tumors are lower than those of benign tumors[23]. Studies have confirmed that the ADC and D values of malignant liver lesions are remarkably lower than those of benign liver lesions and are useful to distinguish benign from malignant liver lesions, with the D value showing higher differentiation efficiency[8,10-15,17]. Yoon *et al*[14] conducted an IVIM study on 169 lesions in 142 patients. The values of ADC and D in malignant liver lesions [1.14 ± 0.24, 0.95 ± 0.21, (× 10^{-3} mm^2/s), respectively] were significantly lower than those in benign liver lesions (1.72 ± 0.37, 1.61 ± 0.34, (× 10^{-3} mm^2/s), respectively). The area under the receiver operating characteristic (ROC) curve (AUC) values for the ADC value and D value in differentiating liver malignancies and hypervascular malignancies were 0.933 and 0.971, respectively, and 0.919 and 0.961, respectively (all $P < 0.0005$).

However, research results for D* values and f values in differentiating benign and malignant liver nodules are inconsistent. A study by Ichikawa *et al*[16] showed that the D* value of malignant liver lesions was significantly lower than that of benign lesions, but no difference in f values was observed between benign and malignant lesions. A study by Luo *et al*[10] also revealed that the D* values of HCC were obviously lower than those of focal nodular hyperplasia, with no significant difference in the f value between the two groups. However, another study[11] by the same group showed that the f value in the malignant group was significantly lower than that in the benign group, and the D* value did not differ significantly between the two groups. The studies by Klauss *et al*[12] and Doblas *et al*[18] both showed no significant differences in the D* and f values between benign and malignant liver lesions and no significance in the values of D* and f in differentiating those two types of liver lesions. Recently, Podgórska *et al*[24] reported that the perfusion-diffusion ratio was more effective than IVIM-DWI parameters in differentiating solid benign and malignant primary liver lesions.

The inconsistencies in the results described above may be related to the following factors: (1) D* and f values not only reflect blood perfusion information but may also reflect other information, such as particle or gland excretion[10,15,25]; (2) the D* values of hepatic hemangioma with different blood supply types exhibit a range of fluctuation range[13]; and (3) interference from other factors, such as the b value distribution, ROI settings, and differences in tumor composition, may occur[16,23,26] (Figures 1 and 2).

Relatively few studies assessing the differentiation of malignant nodules with different pathological characteristics in the liver have been published. The few available studies have involved differentiating HCC from intrahepatic cholangiocarcinoma (ICC) and/or metastasis[9,27-29]. Our previous study[27] showed significantly lower ADC and D values for HCC than for ICC, a significantly higher D* value for HCC than for ICC, higher diagnostic efficiency for D* [AUC = 0.896], and no significant difference in f values between the two groups. According to other studies, ADC and D for HCC are obviously lower than those for ICC. However, the results for the IVIM-DWI parameters D* and f are not consistent. Choi *et al*[9] and Shao *et al*[28] reported that the f values of HCC were higher than those of ICC, while the D* values did not differ significantly between the two studied groups. Wei *et al*[29] did not document significant differences in either D* or f values between HCC and ICC groups.

The results of studies analyzing the differentiation between HCC and liver metastases differ substantially. Choi *et al*[9] found that the f value of HCC was significantly higher than that of liver metastases, but no significant differences were detected in other IVIM-DWI parameters. The study by Wu *et al*[30] indicated no obvious differences in the values of ADC, D, D*, and f for HCC from those for hepatic metastases, which may be due to changes in microcirculation and cell density caused by metastatic tumors of different origins. Dividing liver metastases into different subgroups according to different origins may be a more reasonable approach.

PREDICTION OF PATHOLOGICAL GRADING

Preoperative prediction of the pathological grade of HCC has important value in formulating guidelines for individualized treatments. Studies have shown that IVIM helps predict the pathological grade of HCC before surgery[23,26,31-44]. A meta-analysis by Yang *et al*[32] included 16 studies (1428 cases of HCC) using IVIM-DWI for pathological grading and found that ADC and D values showed high accuracy for the pathological grading of noninvasive HCC and better differentiation efficiency for D values than for ADC values. The explanation for this result may be that a higher tumor pathological

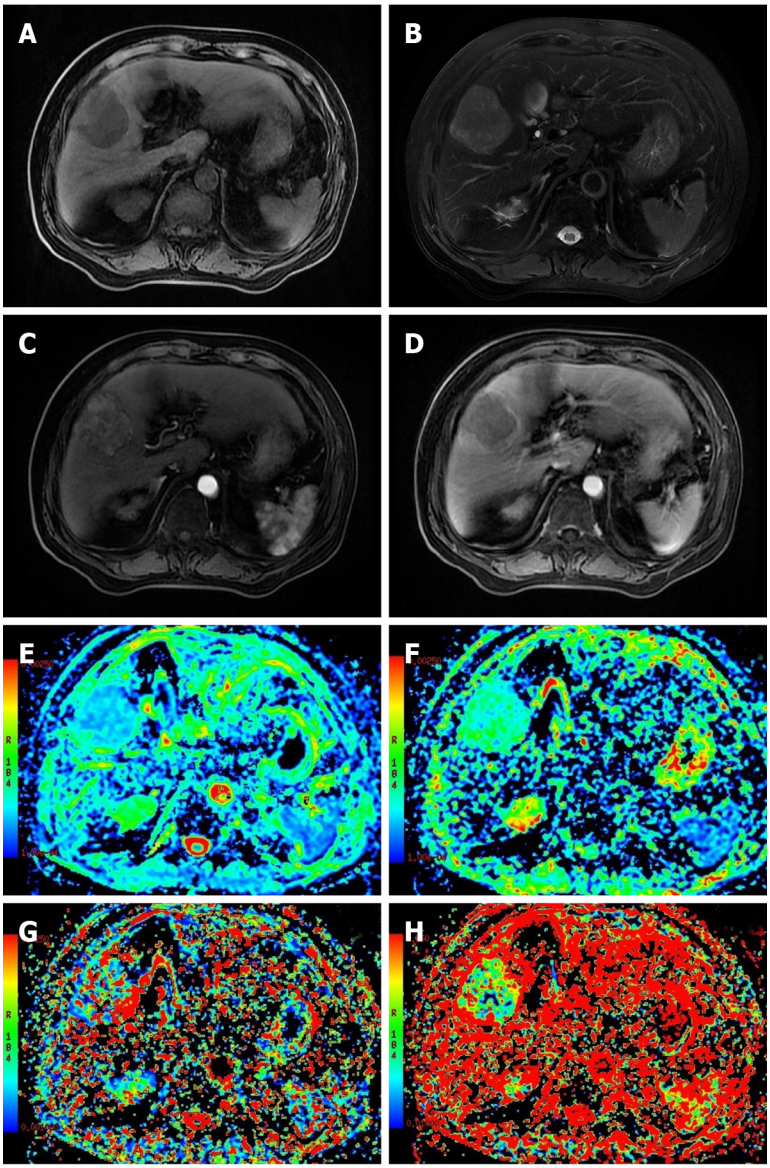

DOI: 10.3748/wjg.v28.i27.3334

Figure 1 Moderately differentiated hepatocellular carcinoma in an 85-year-old male. A 6.1-cm-sized mass in the right hepatic section shows hypointensity on unenhanced T1-weighted image, hyperintensity on unenhanced T2-weighted image, hyperenhancement in the image of the arterial phase, and wash-out in the image of the portal venous phase. A: Unenhanced T1-weighted image; B: Unenhanced T2-weighted image; C: Image of the arterial phase; D: Image of the portal venous phase; E: Image showing the apparent diffusion coefficient; F: Image showing D; G: Image showing D*; H: Image showing f.

grade indicates greater cellularity, a higher nuclear-to-cytoplasmic ratio, and a smaller extracellular space, resulting in more restricted water diffusion, which ultimately leads to lower ADC and D values [23,33,35]. A potential explanation for the superiority of D values compared to ADC values may be that D values theoretically avoid the effect of microcirculation perfusion information. The results for the correlation between D* and f values and pathological grading are inconsistent. In addition to reporting results for ADC and D values and tumor tissue grading consistent with those of previous studies, Li *et al* [36] used rat models and showed that the D* and f values of higher-grade lesions were higher than those of lower-grade lesions and that D* and f values were positively correlated with the tumor tissue grade. Sokmen *et al*[26] and Granata *et al*[38] found that f values were significantly correlated with the HCC pathological grade, while a significant correlation was not identified between D* values and the pathological grade. On the other hand, multiple studies by Zhu *et al*[23,33,35] showed that neither D* values nor f values were significantly correlated with the HCC pathological grade.

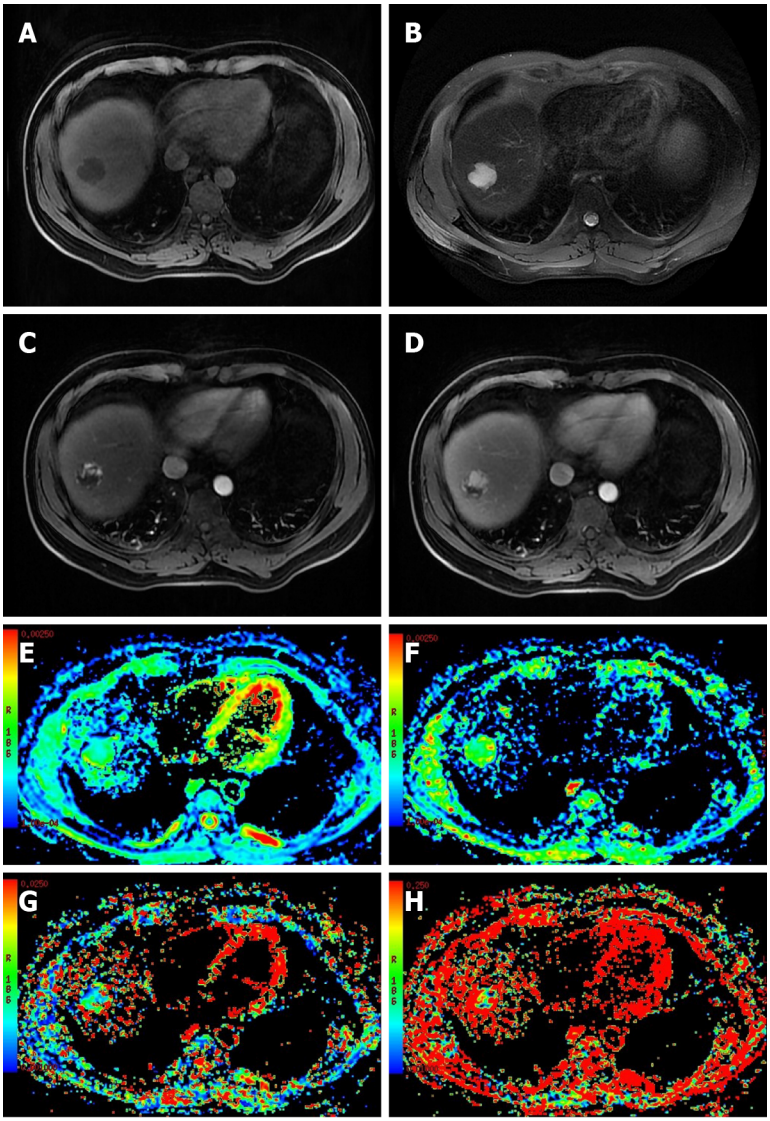

DOI: 10.3748/wjg.v28.i27.3334

Figure 2 Hepatic hemangiomas in a 35-year-old male. A 3.0-cm-sized mass in the right hepatic section shows hypointensity on the unenhanced T1-weighted image, hyperintensity on the unenhanced T2-weighted image, peripheral globular enhancement in the image of the arterial phase and centripetal fill-in in the image of the portal venous phase. A: Unenhanced T1-weighted image; B: Unenhanced T2-weighted image; C: Image of the arterial phase; D: Image of the portal venous phase; E: Image showing the apparent diffusion coefficient; F: Image showing the D; G: Image showing the D*; H: Image showing the f.

PREDICTION AND EVALUATION OF TREATMENT RESPONSES

Locoregional therapy

IVIM-DWI accurately reflects microstructures and blood perfusion changes before and after tumor treatment and is particularly suitable for the prediction and evaluation of the responses to and efficacy of tumor locoregional therapy (LRT)[45]. Many researchers have investigated the value of IVIM-DWI in the prediction and evaluation of transarterial chemoembolization (TACE) efficacy in patients with HCC [46-52]. Park *et al*[50] reported that the preoperative D* value of HCC with better lipiodol deposition was markedly higher than that of HCC with poor lipiodol deposition, suggesting that the D* value may predict lipiodol deposition after TACE for patients with HCC. As shown in our previous study[46], the ADC and D values of HCC were obviously elevated four weeks after TACE treatment, the D* value was significantly reduced, and the f value did not change significantly.

Hectors *et al*[53] investigated the effect of yttrium 90 radioembolization on diffusion and perfusion in HCC. The authors performed multiparametric MRI including IVIM-DWI on 24 patients with HCC before (n = 24) and six weeks (n = 21) after radioembolization. The ADC and D values of HCC were significantly increased at six weeks after radioembolization (P < 0.0004), while the D* values were significantly reduced (P = 0.014), and no significant change was detected in f values (P = 0.765).

Server *et al*[54] administered LRT to 15 patients with HCC (11 patients underwent transarterial radioembolization, and four patients underwent TACE, and IVIM-DWI was performed before and eight

weeks after LRT). Their results indicated that the ADC and D values obtained after LRT were significantly higher than those recorded before treatment, but the f values were significantly lower than those recorded before LRT. In the responder group, the ADC and D values were significantly increased, and the f values were significantly reduced after LRT. No significant differences were detected in the nonresponder group. Based on these findings, IVIM effectively predicts and evaluates the response to and efficacy of LRT. In these studies, the potential explanation for the inconsistency in the blood perfusion parameters D* and f may be that they represent different types of perfusion in various aspects, with the former usually reflecting the blood flow rate in capillaries and the latter mainly reflecting blood volume (Table 1).

Systemic therapy

Changes in volume are often not obvious in the early stage of targeted therapy for HCC. Compared to traditional imaging methods, IVIM-DWI has more advantages in the early evaluation of the HCC response to targeted therapy[55-59]. Wagner *et al*[56] revealed that the D value of viable tumor regions in malignant liver tumors was significantly lower than that of necrotic tumor tissue but higher than that of fibrotic tumor regions. Joo *et al*[55] used IVIM-DWI to evaluate the efficacy of the vascular blocker CKD-516 against rabbit VX2 liver tumors and found that the D* and f values of the treatment group were noticeably reduced at four hours. Based on these studies, IVIM-DWI is useful to assess early responses to tumor vascular blockers[56]. Yang *et al*[57] investigated the values of IVIM-DWI in evaluating the response of 35 nude mice with HCC to sorafenib. Compared to the values recorded at baseline and in the control group, the ADC and D values of the treatment group at each time point were significantly higher, while the f value was significantly decreased at 7 d and increased at 21 d. The values of ADC, D, and f were significantly correlated with the necrotic fraction. Lewin *et al*[58] used IVIM parameters to evaluate the efficacy of sorafenib treatment in patients with advanced HCC. The f values of responder patients were obviously increased at two weeks and two months after treatment, while these values decreased in nonresponder patients. Therefore, the authors propose that the f value is useful as a reliable marker to evaluate sorafenib treatment efficacy in patients with advanced HCC. Shirota *et al*[59] used IVIM-DWI to evaluate the responses of patients with HCC undergoing sorafenib treatment and found that the D value at baseline was significantly higher in the responder group than in the nonresponder group. The sensitivity and specificity of the D value for evaluating the treatment response were 100% and 67%, respectively (Table 2).

Immunotherapy for HCC is an emerging method with promising results; it exerts an antitumor effect without affecting tumor size. Functional imaging methods will play an important role in evaluating the response to immunotherapy. Andersson *et al*[60] evaluated the response of patients with HCC to intratumoral injections of the immune primer ilixadencel using IVIM-DWI and a histogram analysis. Seventeen patients with HCC were enrolled in this study. Their results showed that the 10th percentile of D* decreased significantly after treatment to baseline, and significant correlations were identified between the 10th percentile and median D value. Chen *et al*[61] reported that both pretreatment IVIM-DWI and DCE-MRI parameters, especially ADC and slope, may predict progression-free survival and overall survival in patients with HCC receiving lenalidomide (a dual antiangiogenic and immunomodulatory agent) as second-line therapy. Recently, the application of immune checkpoint inhibitors in tumors has become a new research hotspot. Subsequently, IVIM-DWI will inevitably play a valuable role in predicting the response to and evaluating the efficacy of tumor immunotherapy.

PREDICTION OF POSTOPERATIVE RECURRENCE

Some researchers have reported the value of IVIM-DWI in predicting recurrence and prognosis after the surgical resection of HCC. Microvascular invasion (MVI) is one of the main factors affecting postoperative recurrence or survival among patients with HCC. IVIM-DWI predicts HCC MVI prior to surgery[62]. Wei *et al*[63] prospectively studied the predictive value of preoperative IVIM-DWI and conventional imaging characteristics for MVI. The results of the univariate analysis showed that the characteristics that were significantly correlated with HCC MVI were decreased ADC values, decreased D values, and irregular circumferential enhancement. In the multivariate analysis, only the D value was an independent risk factor for HCC MVI (the AUC was 0.815). Zhao *et al*[64] and Li *et al*[65] reported similar results. Zhang *et al*[66] studied 157 patients undergoing HCC resection and found that D values might serve as a marker for predicting HCC recurrence after hepatectomy and that the predictive capability would be improved if it was combined with age and the alpha-fetoprotein level.

PREDICTING GENE EXPRESSION

Recently, some studies have indicated that IVIM-DWI predicts gene expression in patients with HCC [67-69]. We recently investigated the correlations of HCC IVIM-DWI parameters with angiopoietin-2

Table 1 Summary of locoregional therapy studies

Ref.	Country	Subject number	Key findings
Juan *et al* [46], 2019	China	20	After TACE, the ADC and Dslow values of HCC increased significantly, and the value of Dfast decreased significantly; the f value did not change markedly.
Wu *et al* [47], 2019	China	55	Compared with nonresponders, the mean, median, and 25th percentile of the PF, ADC, and ADCtotal were higher in responders, while the skewness and kurtosis of PF, kurtosis of ADC and ADCtotal were lower
Lin *et al* [48], 2016	China	118	Before TACE, significant differences in ADC, Dslow and Dfast were observed between the effective and ineffective groups. After TACE, the effective group exhibited lower Dfast and higher ADC and Dslow values than the ineffective group. The tumor regression rate was negatively correlated with Dfast but positively correlated with ADC and Dslow
Park *et al* [50], 2014	Korea	44	The preoperative D* value was significantly increased in the good lipiodol uptake group compared with the poor uptake group after TACE, while the ADC, D, and f values were not significantly different between these two groups
Jia F *et al* [51], 2020	China	56	ROC curve analyses revealed that the combined model including APT SIs and D values was better able to predict the tumor response to TACE than the individual parameters
Wu L *et al* [52], 2017	China	30	The ADCtotal ratio and D ratio measured 24-48 h after TACE were independent predictors of the response to TACE of patients with HCC and showed stronger associations with PFS than mRECIST criteria
Hectors *et al*[53], 2020	United States	24	The ADC and D values of HCC were significantly increased at six weeks after radioembolization, while the D* values were significantly reduced, with no significant change in f values
Server *et al* [54], 2019	Turkey	15	The ADC and D values after LRT were significantly higher than those measured before treatment, while the f values were significantly lower than those recorded before LRT. In the responder group, the ADC and D values were significantly increased after LRT, whereas the f values were significantly reduced

TACE: Transarterial chemoembolization; ADC: Apparent diffusion coefficient; HCC: Hepatocellular carcinoma; PF: Perfusion fraction; ROC: Receiver operating characteristic; APT: Amide proton transfer; SIs: Signal intensities; PFS: Progression-free survival; LRT: Locoregional therapy.

Table 2 Summary of systemic therapy studies

Ref.	Country	Subject number	Key findings
Joo *et al*[55], 2014	Korea	21	The D* and f values of the treatment group were significantly decreased at four hours. The sizes of the decreases in f and fD* at four hours were negatively correlated with the tumor size at 7 d of follow-up
Wagner *et al* [56], 2012	France	48	The D values of viable tumor regions in malignant liver tumors were significantly lower than those of necrotic tumor tissue but higher than those of fibrotic tumor regions
Yang *et al* [57], 2017	China	35	Compared with the values at baseline and those recorded in the control group, the ADC and D values in the treatment group were significantly higher at each time point, whereas the f values decreased significantly at 7 d and increased at 21 d
Lewin *et al* [58], 2011	France	12	The f values increased significantly in responder patients at two weeks and two months after treatment but decreased in nonresponder patients. The f value was useful as a reliable marker to evaluate sorafenib treatment efficacy in patients with advanced HCC
Shirota *et al* [59], 2016	Japan	9	The D values at baseline were significantly higher in the responder group than in the nonresponder group. The sensitivity and specificity of the D values for evaluating treatment response were 100% and 67%, respectively

ADC: Apparent diffusion coefficient; HCC: Hepatocellular carcinoma.

(Ang-2) and transketolase (TKT) expression[67]. We observed significantly higher D* and f values in the high Ang-2 expression group than in the low Ang-2 expression group, and the values of D* and f were positively correlated with the Ang-2 expression levels . On the other hand, the ADC and D values of the TKT high expression group were significantly lower than those of the TKT low expression group, and the ADC and D values were negatively correlated with TKT expression. Based on this result, IVIM-DWI noninvasively predicts Ang-2 and TKT expression in HCC before surgery. Shi *et al*[68] performed IVIM-DWI of 52 patients with HCC and identified four IVIM-derived histogram metrics with the capability for differentiating Ki67 expression, with *P* values less than 0.05. By establishing a diagnostic model based on a logistic regression model, the AUC value for diagnosing high Ki67 expression was 0.861. The results of this study suggest that the histogram indicators obtained from IVIM-DWI scanning can accurately predict the Ki67 expression status.

CONCLUSION

IVIM-DWI accurately and precisely reflects tissue structures and pathophysiological changes and has important application value for HCC differentiation, pathological grading, and predicting and evaluating the treatment response. However, the factors affecting IVIM-DWI measurement results are complicated and diverse[8,20,25,70-76]. Factors including the number, distribution, and fitting methods of b values, other physiological activities (such as gland secretion and flow), ROI settings, scanning devices and field strength, imaging acquisition methods, and motion artifacts all affect data quality[23,25,34,41]. Increased standardization of data acquisition and analysis is imperative to facilitate the generation of reliable IVIM-DWI biomarker measures that are broadly applicable[74,77,78]. In addition, recent studies have shown that IVIM-DWI modeling of the perfusion component is constrained by the diffusion component, and a reduced D slow measure leads to artificially higher PF and D fast measures [75,76]. These results should also be considered in the design of future IVIM-DWI studies. We postulate that with advances in imaging technology and further in-depth research, IVIM-DWI will certainly play a more prominent role in the diagnosis and treatment of HCC.

FOOTNOTES

Author contributions: Zhou Y wrote the paper; Zheng J, Yang C, Peng J and Liu N collected the data; Yang L revised the paper; Zhang XM designed the research project.

Supported by the Project of Department of Science and Technology of Sichuan Province, No. 2016JY0105; Project of Medical Association of Sichuan Province, No. S20070; and the Project of City-University Science and Technology Strategic Cooperation of Nanchong City (North Sichuan Medical College), No. 20SXQT0324.

Conflict-of-interest statement: The authors have no conflicts of interest related to this article to declare.

Country/Territory of origin: China

ORCID number: Yi Zhou 0000-0002-1911-5380; Jing Zheng 0000-0002-2031-0845; Cui Yang 0000-0001-6751-9075; Juan Peng 0000-0002-7961-3533; Ning Liu 0000-0003-3587-5440; Lin Yang 0000-0001-8746-9255; Xiao-Ming Zhang 0000-0001-5327-8506.

S-Editor: Zhang H
L-Editor: A
P-Editor: Zhang H

REFERENCES

1 **Yang JD**, Hainaut P, Gores GJ, Amadou A, Plymoth A, Roberts LR. A global view of hepatocellular carcinoma: trends, risk, prevention and management. *Nat Rev Gastroenterol Hepatol* 2019; **16**: 589-604 [PMID: 31439937 DOI: 10.1038/s41575-019-0186-y]

2 **Global Burden of Disease Cancer Collaboration**, Fitzmaurice C, Allen C, Barber RM, Barregard L, Bhutta ZA, Brenner H, Dicker DJ, Chimed-Orchir O, Dandona R, Dandona L, Fleming T, Forouzanfar MH, Hancock J, Hay RJ, Hunter-Merrill R, Huynh C, Hosgood HD, Johnson CO, Jonas JB, Khubchandani J, Kumar GA, Kutz M, Lan Q, Larson HJ, Liang X, Lim SS, Lopez AD, MacIntyre MF, Marczak L, Marquez N, Mokdad AH, Pinho C, Pourmalek F, Salomon JA, Sanabria JR, Sandar L, Sartorius B, Schwartz SM, Shackelford KA, Shibuya K, Stanaway J, Steiner C, Sun J, Takahashi K, Vollset SE, Vos T, Wagner JA, Wang H, Westerman R, Zeeb H, Zoeckler L, Abd-Allah F, Ahmed MB, Alabed S, Alam NK, Aldhahri SF, Alem G, Alemayohu MA, Ali R, Al-Raddadi R, Amare A, Amoako Y, Artaman A, Asayesh H, Atnafu N, Awasthi A, Saleem HB, Barac A, Bedi N, Bensenor I, Berhane A, Bernabé E, Betsu B, Binagwaho A, Boneya D, Campos-Nonato I, Castañeda-Orjuela C, Catalá-López F, Chiang P, Chibueze C, Chitheer A, Choi JY, Cowie B, Damtew S, das Neves J, Dey S, Dharmaratne S, Dhillon P, Ding E, Driscoll T, Ekwueme D, Endries AY, Farvid M, Farzadfar F, Fernandes J, Fischer F, G/Hiwot TT, Gebru A, Gopalani S, Hailu A, Horino M, Horita N, Husseini A, Huybrechts I, Inoue M, Islami F, Jakovljevic M, James S, Javanbakht M, Jee SH, Kasaeian A, Kedir MS, Khader YS, Khang YH, Kim D, Leigh J, Linn S, Lunevicius R, El Razek HMA, Malekzadeh R, Malta DC, Marcenes W, Markos D, Melaku YA, Meles KG, Mendoza W, Mengiste DT, Meretoja TJ, Miller TR, Mohammad KA, Mohammadi A, Mohammed S, Moradi-Lakeh M, Nagel G, Nand D, Le Nguyen Q, Nolte S, Ogbo FA, Oladimeji KE, Oren E, Pa M, Park EK, Pereira DM, Plass D, Qorbani M, Radfar A, Rafay A, Rahman M, Rana SM, Søreide K, Satpathy M, Sawhney M, Sepanlou SG, Shaikh MA, She J, Shiue I, Shore HR, Shrime

MG, So S, Soneji S, Stathopoulou V, Stroumpoulis K, Sufiyan MB, Sykes BL, Tabarés-Seisdedos R, Tadese F, Tedla BA, Tessema GA, Thakur JS, Tran BX, Ukwaja KN, Uzochukwu BSC, Vlassov VV, Weiderpass E, Wubshet Terefe M, Yebyo HG, Yimam HH, Yonemoto N, Younis MZ, Yu C, Zaidi Z, Zaki MES, Zenebe ZM, Murray CJL, Naghavi M. Global, Regional, and National Cancer Incidence, Mortality, Years of Life Lost, Years Lived With Disability, and Disability-Adjusted Life-years for 32 Cancer Groups, 1990 to 2015: A Systematic Analysis for the Global Burden of Disease Study. *JAMA Oncol* 2017; **3**: 524-548 [PMID: 27918777 DOI: 10.1001/jamaoncol.2016.5688]

3 **Taouli B**, Koh DM. Diffusion-weighted MR imaging of the liver. *Radiology* 2010; **254**: 47-66 [PMID: 20032142 DOI: 10.1148/radiol.09090021]

4 **Lewis S**, Dyvorne H, Cui Y, Taouli B. Diffusion-weighted imaging of the liver: techniques and applications. *Magn Reson Imaging Clin N Am* 2014; **22**: 373-395 [PMID: 25086935 DOI: 10.1016/j.mric.2014.04.009]

5 **Bammer R**. Basic principles of diffusion-weighted imaging. *Eur J Radiol* 2003; **45**: 169-184 [PMID: 12595101 DOI: 10.1016/s0720-048x(02)00303-0]

6 **Le Bihan D**, Breton E, Lallemand D, Aubin ML, Vignaud J, Laval-Jeantet M. Separation of diffusion and perfusion in intravoxel incoherent motion MR imaging. *Radiology* 1988; **168**: 497-505 [PMID: 3393671 DOI: 10.1148/radiology.168.2.3393671]

7 **Le Bihan D**, Breton E, Lallemand D, Grenier P, Cabanis E, Laval-Jeantet M. MR imaging of intravoxel incoherent motions: application to diffusion and perfusion in neurologic disorders. *Radiology* 1986; **161**: 401-407 [PMID: 3763909 DOI: 10.1148/radiology.161.2.3763909]

8 **Yamada I**, Aung W, Himeno Y, Nakagawa T, Shibuya H. Diffusion coefficients in abdominal organs and hepatic lesions: evaluation with intravoxel incoherent motion echo-planar MR imaging. *Radiology* 1999; **210**: 617-623 [PMID: 10207458 DOI: 10.1148/radiology.210.3.r99fe17617]

9 **Choi IY**, Lee SS, Sung YS, Cheong H, Lee H, Byun JH, Kim SY, Lee SJ, Shin YM, Lee MG. Intravoxel incoherent motion diffusion-weighted imaging for characterizing focal hepatic lesions: Correlation with lesion enhancement. *J Magn Reson Imaging* 2017; **45**: 1589-1598 [PMID: 27664970 DOI: 10.1002/jmri.25492]

10 **Luo M**, Zhang L, Jiang XH, Zhang WD. Intravoxel incoherent motion: application in differentiation of hepatocellular carcinoma and focal nodular hyperplasia. *Diagn Interv Radiol* 2017; **23**: 263-271 [PMID: 28703102 DOI: 10.5152/dir.2017.16595]

11 **Luo M**, Zhang L, Jiang XH, Zhang WD. Intravoxel Incoherent Motion Diffusion-weighted Imaging: Evaluation of the Differentiation of Solid Hepatic Lesions. *Transl Oncol* 2017; **10**: 831-838 [PMID: 28866259 DOI: 10.1016/j.tranon.2017.08.003]

12 **Klauss M**, Mayer P, Maier-Hein K, Laun FB, Mehrabi A, Kauczor HU, Stieltjes B. IVIM-diffusion-MRI for the differentiation of solid benign and malign hypervascular liver lesions-Evaluation with two different MR scanners. *Eur J Radiol* 2016; **85**: 1289-1294 [PMID: 27235876 DOI: 10.1016/j.ejrad.2016.04.011]

13 **Zhu L**, Cheng Q, Luo W, Bao L, Guo G. A comparative study of apparent diffusion coefficient and intravoxel incoherent motion-derived parameters for the characterization of common solid hepatic tumors. *Acta Radiol* 2015; **56**: 1411-1418 [PMID: 25422515 DOI: 10.1177/0284185114559426]

14 **Yoon JH**, Lee JM, Yu MH, Kiefer B, Han JK, Choi BI. Evaluation of hepatic focal lesions using diffusion-weighted MR imaging: comparison of apparent diffusion coefficient and intravoxel incoherent motion-derived parameters. *J Magn Reson Imaging* 2014; **39**: 276-285 [PMID: 23633178 DOI: 10.1002/jmri.24158]

15 **Watanabe H**, Kanematsu M, Goshima S, Kajita K, Kawada H, Noda Y, Tatahashi Y, Kawai N, Kondo H, Moriyama N. Characterizing focal hepatic lesions by free-breathing intravoxel incoherent motion MRI at 3.0 T. *Acta Radiol* 2014; **55**: 1166-1173 [PMID: 24316660 DOI: 10.1177/0284185113514966]

16 **Ichikawa S**, Motosugi U, Ichikawa T, Sano K, Morisaka H, Araki T. Intravoxel incoherent motion imaging of focal hepatic lesions. *J Magn Reson Imaging* 2013; **37**: 1371-1376 [PMID: 23172819 DOI: 10.1002/jmri.23930]

17 **Penner AH**, Sprinkart AM, Kukuk GM, Gütgemann I, Gieseke J, Schild HH, Willinek WA, Mürtz P. Intravoxel incoherent motion model-based liver lesion characterisation from three b-value diffusion-weighted MRI. *Eur Radiol* 2013; **23**: 2773-2783 [PMID: 23666233 DOI: 10.1007/s00330-013-2869-z]

18 **Doblas S**, Wagner M, Leitao HS, Daire JL, Sinkus R, Vilgrain V, Van Beers BE. Determination of malignancy and characterization of hepatic tumor type with diffusion-weighted magnetic resonance imaging: comparison of apparent diffusion coefficient and intravoxel incoherent motion-derived measurements. *Invest Radiol* 2013; **48**: 722-728 [PMID: 23669588 DOI: 10.1097/RLI.0b013e3182915912]

19 **Regini F**, Colagrande S, Mazzoni LN, Busoni S, Matteuzzi B, Santini P, Wyttenbach R. Assessment of Liver Perfusion by IntraVoxel Incoherent Motion (IVIM) Magnetic Resonance-Diffusion-Weighted Imaging: Correlation With Phase-Contrast Portal Venous Flow Measurements. *J Comput Assist Tomogr* 2015; **39**: 365-372 [PMID: 25700227 DOI: 10.1097/RCT.0000000000000220]

20 **Dyvorne H**, Jajamovich G, Kakite S, Kuehn B, Taouli B. Intravoxel incoherent motion diffusion imaging of the liver: optimal b-value subsampling and impact on parameter precision and reproducibility. *Eur J Radiol* 2014; **83**: 2109-2113 [PMID: 25277521 DOI: 10.1016/j.ejrad.2014.09.003]

21 **Ai Z**, Han Q, Huang Z, Wu J, Xiang Z. The value of multiparametric histogram features based on intravoxel incoherent motion diffusion-weighted imaging (IVIM-DWI) for the differential diagnosis of liver lesions. *Ann Transl Med* 2020; **8**: 1128 [PMID: 33240977 DOI: 10.21037/atm-20-5109]

22 **Granata V**, Fusco R, Amato DM, Albino V, Patrone R, Izzo F, Petrillo A. Beyond the vascular profile: conventional DWI, IVIM and kurtosis in the assessment of hepatocellular carcinoma. *Eur Rev Med Pharmacol Sci* 2020; **24**: 7284-7293 [PMID: 32706066 DOI: 10.26355/eurrev_202007_21883]

23 **Woo S**, Lee JM, Yoon JH, Joo I, Han JK, Choi BI. Intravoxel incoherent motion diffusion-weighted MR imaging of hepatocellular carcinoma: correlation with enhancement degree and histologic grade. *Radiology* 2014; **270**: 758-767 [PMID: 24475811 DOI: 10.1148/radiol.13130444]

24 **Podgórska J**, Pasicz K, Skrzyński W, Gołębiewski B, Kuś P, Jasieniak J, Kiliszczyk A, Rogowska A, Benkert T, Pałucki J, Grabska I, Fabiszewska E, Jagielska B, Kukołowicz P, Cieszanowski A. Perfusion-Diffusion Ratio: A New IVIM Approach

in Differentiating Solid Benign and Malignant Primary Lesions of the Liver. *Biomed Res Int* 2022; **2022**: 2957759 [PMID: 35075424 DOI: 10.1155/2022/2957759]

25 **Kakite S**, Dyvorne H, Besa C, Cooper N, Facciuto M, Donnerhack C, Taouli B. Hepatocellular carcinoma: short-term reproducibility of apparent diffusion coefficient and intravoxel incoherent motion parameters at 3.0T. *J Magn Reson Imaging* 2015; **41**: 149-156 [PMID: 24415565 DOI: 10.1002/jmri.24538]

26 **Sokmen BK**, Sabet S, Oz A, Server S, Namal E, Dayangac M, Dogusoy GB, Tokat Y, Inan N. Value of Intravoxel Incoherent Motion for Hepatocellular Carcinoma Grading. *Transplant Proc* 2019; **51**: 1861-1866 [PMID: 31399170 DOI: 10.1016/j.transproceed.2019.02.027]

27 **Peng J**, Zheng J, Yang C, Wang R, Zhou Y, Tao YY, Gong XQ, Wang WC, Zhang XM, Yang L. Intravoxel incoherent motion diffusion-weighted imaging to differentiate hepatocellular carcinoma from intrahepatic cholangiocarcinoma. *Sci Rep* 2020; **10**: 7717 [PMID: 32382050 DOI: 10.1038/s41598-020-64804-9]

28 **Shao S**, Shan Q, Zheng N, Wang B, Wang J. Role of Intravoxel Incoherent Motion in Discriminating Hepatitis B Virus-Related Intrahepatic Mass-Forming Cholangiocarcinoma from Hepatocellular Carcinoma Based on Liver Imaging Reporting and Data System v2018. *Cancer Biother Radiopharm* 2019; **34**: 511-518 [PMID: 31314589 DOI: 10.1089/cbr.2019.2799]

29 **Wei Y**, Gao F, Zheng D, Huang Z, Wang M, Hu F, Chen C, Duan T, Chen J, Cao L, Song B. Intrahepatic cholangiocarcinoma in the setting of HBV-related cirrhosis: Differentiation with hepatocellular carcinoma by using Intravoxel incoherent motion diffusion-weighted MR imaging. *Oncotarget* 2018; **9**: 7975-7983 [PMID: 29487707 DOI: 10.18632/oncotarget.23807]

30 **Wu H**, Liang Y, Jiang X, Wei X, Liu Y, Liu W, Guo Y, Tang W. Meta-analysis of intravoxel incoherent motion magnetic resonance imaging in differentiating focal lesions of the liver. *Medicine (Baltimore)* 2018; **97**: e12071 [PMID: 30142864 DOI: 10.1097/MD.0000000000012071]

31 **Shan Q**, Kuang S, Zhang Y, He B, Wu J, Zhang T, Wang J. A comparative study of monoexponential versus biexponential models of diffusion-weighted imaging in differentiating histologic grades of hepatitis B virus-related hepatocellular carcinoma. *Abdom Radiol (NY)* 2020; **45**: 90-100 [PMID: 31595327 DOI: 10.1007/s00261-019-02253-3]

32 **Yang D**, She H, Wang X, Yang Z, Wang Z. Diagnostic accuracy of quantitative diffusion parameters in the pathological grading of hepatocellular carcinoma: A meta-analysis. *J Magn Reson Imaging* 2020; **51**: 1581-1593 [PMID: 31654537 DOI: 10.1002/jmri.26963]

33 **Wei Y**, Gao F, Wang M, Huang Z, Tang H, Li J, Wang Y, Zhang T, Wei X, Zheng D, Song B. Intravoxel incoherent motion diffusion-weighted imaging for assessment of histologic grade of hepatocellular carcinoma: comparison of three methods for positioning region of interest. *Eur Radiol* 2019; **29**: 535-544 [PMID: 30027411 DOI: 10.1007/s00330-018-5638-1]

34 **Ichikawa S**, Motosugi U, Hernando D, Morisaka H, Enomoto N, Matsuda M, Onishi H. Histological Grading of Hepatocellular Carcinomas with Intravoxel Incoherent Motion Diffusion-weighted Imaging: Inconsistent Results Depending on the Fitting Method. *Magn Reson Med Sci* 2018; **17**: 168-173 [PMID: 28819085 DOI: 10.2463/mrms.mp.2017-0047]

35 **Zhu SC**, Liu YH, Wei Y, Li LL, Dou SW, Sun TY, Shi DP. Intravoxel incoherent motion diffusion-weighted magnetic resonance imaging for predicting histological grade of hepatocellular carcinoma: Comparison with conventional diffusion-weighted imaging. *World J Gastroenterol* 2018; **24**: 929-940 [PMID: 29491686 DOI: 10.3748/wjg.v24.i8.929]

36 **Li M**, Zheng XJ, Huang ZX, Song B. [Predicting Histological Grade of HCC in Rats using Intravoxel Incoherent Motion Imaging]. *Sichuan Da Xue Xue Bao Yi Xue Ban* 2018; **49**: 243-247 [PMID: 29737069]

37 **Shan Q**, Chen J, Zhang T, Yan R, Wu J, Shu Y, Kang Z, He B, Zhang Z, Wang J. Evaluating histologic differentiation of hepatitis B virus-related hepatocellular carcinoma using intravoxel incoherent motion and AFP levels alone and in combination. *Abdom Radiol (NY)* 2017; **42**: 2079-2088 [PMID: 28337521 DOI: 10.1007/s00261-017-1107-6]

38 **Granata V**, Fusco R, Catalano O, Guarino B, Granata F, Tatangelo F, Avallone A, Piccirillo M, Palaia R, Izzo F, Petrillo A. Intravoxel incoherent motion (IVIM) in diffusion-weighted imaging (DWI) for Hepatocellular carcinoma: correlation with histologic grade. *Oncotarget* 2016; **7**: 79357-79364 [PMID: 27764817 DOI: 10.18632/oncotarget.12689]

39 **Nakanishi M**, Chuma M, Hige S, Omatsu T, Yokoo H, Nakanishi K, Kamiyama T, Kubota K, Haga H, Matsuno Y, Onodera Y, Kato M, Asaka M. Relationship between diffusion-weighted magnetic resonance imaging and histological tumor grading of hepatocellular carcinoma. *Ann Surg Oncol* 2012; **19**: 1302-1309 [PMID: 21927976 DOI: 10.1245/s10434-011-2066-8]

40 **Koh DM**, Collins DJ, Orton MR. Intravoxel incoherent motion in body diffusion-weighted MRI: reality and challenges. *AJR Am J Roentgenol* 2011; **196**: 1351-1361 [PMID: 21606299 DOI: 10.2214/AJR.10.5515]

41 **Granata V**, Fusco R, Filice S, Catalano O, Piccirillo M, Palaia R, Izzo F, Petrillo A. The current role and future prospectives of functional parameters by diffusion weighted imaging in the assessment of histologic grade of HCC. *Infect Agent Cancer* 2018; **13**: 23 [PMID: 29988667 DOI: 10.1186/s13027-018-0194-5]

42 **Wu B**, Jia F, Li X, Li L, Wang K, Han D. Comparative Study of Amide Proton Transfer Imaging and Intravoxel Incoherent Motion Imaging for Predicting Histologic Grade of Hepatocellular Carcinoma. *Front Oncol* 2020; **10**: 562049 [PMID: 33194630 DOI: 10.3389/fonc.2020.562049]

43 **Zhou Y**, Yang G, Gong XQ, Tao YY, Wang R, Zheng J, Yang C, Peng J, Yang L, Li JD, Zhang XM. A study of the correlations between IVIM-DWI parameters and the histologic differentiation of hepatocellular carcinoma. *Sci Rep* 2021; **11**: 10392 [PMID: 34001962 DOI: 10.1038/s41598-021-89784-2]

44 **Song Q**, Guo Y, Yao X, Rao S, Qian C, Ye D, Zeng M. Comparative study of evaluating the microcirculatory function status of primary small HCC between the CE (DCE-MRI) and Non-CE (IVIM-DWI) MR Perfusion Imaging. *Abdom Radiol (NY)* 2021; **46**: 2575-2583 [PMID: 33483778 DOI: 10.1007/s00261-020-02945-1]

45 **Hussein RS**, Tantawy W, Abbas YA. MRI assessment of hepatocellular carcinoma after locoregional therapy. *Insights Imaging* 2019; **10**: 8 [PMID: 30694398 DOI: 10.1186/s13244-019-0690-1]

46 **Peng J**, Yang C, Zheng J, Wang R, Zhou Y, Wang WC, Yang L, Zhang XM, Miao ND, Ren YJ, Xu H and Min XL. Intravoxel Incoherent Motion Diffusion Weighted Imaging for the Therapeutic Response of Transarterial

Chemoembolization for Hepatocellular Carcinoma. *J Cancer Ther* 2019; **10**: 591-601 [DOI: 10.4236/jct.2019.107048]

47 **Wu LF**, Rao SX, Xu PJ, Yang L, Chen CZ, Liu H, Huang JF, Fu CX, Halim A, Zeng MS. Pre-TACE kurtosis of ADC_{total} derived from histogram analysis for diffusion-weighted imaging is the best independent predictor of prognosis in hepatocellular carcinoma. *Eur Radiol* 2019; **29**: 213-223 [PMID: 29922932 DOI: 10.1007/s00330-018-5482-3]

48 **Lin M**, Tian MM, Zhang WP, Xu L, Jin P. Predictive values of diffusion-weighted imaging and perfusion-weighted imaging in evaluating the efficacy of transcatheter arterial chemoembolization for hepatocellular carcinoma. *Onco Targets Ther* 2016; **9**: 7029-7037 [PMID: 27895495 DOI: 10.2147/OTT.S112555]

49 **Yang K**, Zhang XM, Yang L, Xu H, Peng J. Advanced imaging techniques in the therapeutic response of transarterial chemoembolization for hepatocellular carcinoma. *World J Gastroenterol* 2016; **22**: 4835-4847 [PMID: 27239110 DOI: 10.3748/wjg.v22.i20.4835]

50 **Park YS**, Lee CH, Kim JH, Kim IS, Kiefer B, Seo TS, Kim KA, Park CM. Using intravoxel incoherent motion (IVIM) MR imaging to predict lipiodol uptake in patients with hepatocellular carcinoma following transcatheter arterial chemoembolization: a preliminary result. *Magn Reson Imaging* 2014; **32**: 638-646 [PMID: 24703575 DOI: 10.1016/j.mri.2014.03.003]

51 **Jia F**, Wu B, Yan R, Li L, Wang K, Han D. Prediction Model for Intermediate-Stage Hepatocellular Carcinoma Response to Transarterial Chemoembolization. *J Magn Reson Imaging* 2020; **52**: 1657-1667 [PMID: 32424881 DOI: 10.1002/jmri.27189]

52 **Wu L**, Xu P, Rao S, Yang L, Chen C, Liu H, Fu C, Zeng M. ADC_{total} ratio and D ratio derived from intravoxel incoherent motion early after TACE are independent predictors for survival in hepatocellular carcinoma. *J Magn Reson Imaging* 2017; **46**: 820-830 [PMID: 28276105 DOI: 10.1002/jmri.25617]

53 **Hectors SJ**, Lewis S, Kennedy P, Bane O, Said D, Segall M, Schwartz M, Kim E, Taouli B. Assessment of Hepatocellular Carcinoma Response to ^{90}Y Radioembolization Using Dynamic Contrast Material-enhanced MRI and Intravoxel Incoherent Motion Diffusion-weighted Imaging. *Radiol Imaging Cancer* 2020; **2**: e190094 [PMID: 32803165 DOI: 10.1148/rycan.2020190094]

54 **Server S**, Sabet S, Bilgin R, Inan N, Yuzer Y, Tokat Y. Intravoxel Incoherent Motion Parameters for Assessing the Efficiency of Locoregional Bridging Treatments before Liver Transplantation. *Transplant Proc* 2019; **51**: 2391-2396 [PMID: 31474296 DOI: 10.1016/j.transproceed.2019.01.161]

55 **Joo I**, Lee JM, Han JK, Choi BI. Intravoxel incoherent motion diffusion-weighted MR imaging for monitoring the therapeutic efficacy of the vascular disrupting agent CKD-516 in rabbit VX2 liver tumors. *Radiology* 2014; **272**: 417-426 [PMID: 24697148 DOI: 10.1148/radiol.14131165]

56 **Wagner M**, Doblas S, Daire JL, Paradis V, Haddad N, Leitão H, Garteiser P, Vilgrain V, Sinkus R, Van Beers BE. Diffusion-weighted MR imaging for the regional characterization of liver tumors. *Radiology* 2012; **264**: 464-472 [PMID: 22692032 DOI: 10.1148/radiol.12111530]

57 **Yang SH**, Lin J, Lu F, Han ZH, Fu CX, Lv P, Liu H, Gao DM. Evaluation of antiangiogenic and antiproliferative effects of sorafenib by sequential histology and intravoxel incoherent motion diffusion-weighted imaging in an orthotopic hepatocellular carcinoma xenograft model. *J Magn Reson Imaging* 2017; **45**: 270-280 [PMID: 27299302 DOI: 10.1002/jmri.25344]

58 **Lewin M**, Fartoux L, Vignaud A, Arrivé L, Menu Y, Rosmorduc O. The diffusion-weighted imaging perfusion fraction f is a potential marker of sorafenib treatment in advanced hepatocellular carcinoma: a pilot study. *Eur Radiol* 2011; **21**: 281-290 [PMID: 20683597 DOI: 10.1007/s00330-010-1914-4]

59 **Shirota N**, Saito K, Sugimoto K, Takara K, Moriyasu F, Tokuuye K. Intravoxel incoherent motion MRI as a biomarker of sorafenib treatment for advanced hepatocellular carcinoma: a pilot study. *Cancer Imaging* 2016; **16**: 1 [PMID: 26822946 DOI: 10.1186/s40644-016-0059-3]

60 **Andersson M**, Jalnefjord O, Montelius M, Rizell M, Sternby Eilard M, Ljungberg M. Evaluation of response in patients with hepatocellular carcinoma treated with intratumoral dendritic cell vaccination using intravoxel incoherent motion (IVIM) MRI and histogram analysis. *Acta Radiol* 2021; 2841851211065935 [PMID: 34904868 DOI: 10.1177/02841851211065935]

61 **Chen BB**, Shao YY, Lin ZZ, Hsu CH, Cheng AL, Hsu C, Liang PC, Shih TT. Dynamic Contrast-Enhanced and Intravoxel Incoherent Motion MRI Biomarkers Are Correlated to Survival Outcome in Advanced Hepatocellular Carcinoma. *Diagnostics (Basel)* 2021; **11** [PMID: 34441274 DOI: 10.3390/diagnostics11081340]

62 **Zeng Q**, Liu B, Xu Y, Zhou W. An attention-based deep learning model for predicting microvascular invasion of hepatocellular carcinoma using an intra-voxel incoherent motion model of diffusion-weighted magnetic resonance imaging. *Phys Med Biol* 2021; **66** [PMID: 34469880 DOI: 10.1088/1361-6560/ac22db]

63 **Wei Y**, Huang Z, Tang H, Deng L, Yuan Y, Li J, Wu D, Wei X, Song B. IVIM improves preoperative assessment of microvascular invasion in HCC. *Eur Radiol* 2019; **29**: 5403-5414 [PMID: 30877465 DOI: 10.1007/s00330-019-06088-w]

64 **Zhao W**, Liu W, Liu H, Yi X, Hou J, Pei Y, Feng D, Liu L, Li W. Preoperative prediction of microvascular invasion of hepatocellular carcinoma with IVIM diffusion-weighted MR imaging and Gd-EOB-DTPA-enhanced MR imaging. *PLoS One* 2018; **13**: e0197488 [PMID: 29771954 DOI: 10.1371/journal.pone.0197488]

65 **Li H**, Zhang J, Zheng Z, Guo Y, Chen M, Xie C, Zhang Z, Mei Y, Feng Y, Xu Y. Preoperative histogram analysis of intravoxel incoherent motion (IVIM) for predicting microvascular invasion in patients with single hepatocellular carcinoma. *Eur J Radiol* 2018; **105**: 65-71 [PMID: 30017300 DOI: 10.1016/j.ejrad.2018.05.032]

66 **Zhang Y**, Kuang S, Shan Q, Rong D, Zhang Z, Yang H, Wu J, Chen J, He B, Deng Y, Roberts N, Shen J, Venkatesh SK, Wang J. Can IVIM help predict HCC recurrence after hepatectomy? *Eur Radiol* 2019; **29**: 5791-5803 [PMID: 30972544 DOI: 10.1007/s00330-019-06180-1]

67 **Zheng J**, Gong XQ, Tao YY, Wang R, Yang G, Li JD, Ren T, Li ZM, Yang C, Wang WC, Yang L, Zhang XM. A Correlative Study Between IVIM-DWI Parameters and the Expression Levels of Ang-2 and TKT in Hepatocellular Carcinoma. *Front Oncol* 2020; **10**: 594366 [PMID: 33520706 DOI: 10.3389/fonc.2020.594366]

68 **Shi G**, Han X, Wang Q, Ding Y, Liu H, Zhang Y, Dai Y. Evaluation of Multiple Prognostic Factors of Hepatocellular Carcinoma with Intra-Voxel Incoherent Motions Imaging by Extracting the Histogram Metrics. *Cancer Manag Res* 2020;

12: 6019-6031 [PMID: 32765101 DOI: 10.2147/CMAR.S262973]

69 **Guo Y**, Chen J, Zhang Y, Guo Y, Jiang M, Dai Y, Yao X. Differentiating Cytokeratin 19 expression of hepatocellular carcinoma by using multi-b-value diffusion-weighted MR imaging with mono-exponential, stretched exponential, intravoxel incoherent motion, diffusion kurtosis imaging and fractional order calculus models. *Eur J Radiol* 2022; **150**: 110237 [PMID: 35278979 DOI: 10.1016/j.ejrad.2022.110237]

70 **Andreou A**, Koh DM, Collins DJ, Blackledge M, Wallace T, Leach MO, Orton MR. Measurement reproducibility of perfusion fraction and pseudodiffusion coefficient derived by intravoxel incoherent motion diffusion-weighted MR imaging in normal liver and metastases. *Eur Radiol* 2013; **23**: 428-434 [PMID: 23052642 DOI: 10.1007/s00330-012-2604-1]

71 **Dyvorne HA**, Galea N, Nevers T, Fiel MI, Carpenter D, Wong E, Orton M, de Oliveira A, Feiweier T, Vachon ML, Babb JS, Taouli B. Diffusion-weighted imaging of the liver with multiple b values: effect of diffusion gradient polarity and breathing acquisition on image quality and intravoxel incoherent motion parameters--a pilot study. *Radiology* 2013; **266**: 920-929 [PMID: 23220895 DOI: 10.1148/radiol.12120686]

72 **Patel J**, Sigmund EE, Rusinek H, Oei M, Babb JS, Taouli B. Diagnosis of cirrhosis with intravoxel incoherent motion diffusion MRI and dynamic contrast-enhanced MRI alone and in combination: preliminary experience. *J Magn Reson Imaging* 2010; **31**: 589-600 [PMID: 20187201 DOI: 10.1002/jmri.22081]

73 **Luciani A**, Vignaud A, Cavet M, Nhieu JT, Mallat A, Ruel L, Laurent A, Deux JF, Brugieres P, Rahmouni A. Liver cirrhosis: intravoxel incoherent motion MR imaging--pilot study. *Radiology* 2008; **249**: 891-899 [PMID: 19011186 DOI: 10.1148/radiol.2493080080]

74 **Wang YXJ**, Huang H, Zheng CJ, Xiao BH, Chevallier O, Wang W. Diffusion-weighted MRI of the liver: challenges and some solutions for the quantification of apparent diffusion coefficient and intravoxel incoherent motion. *Am J Nucl Med Mol Imaging* 2021; **11**: 107-142 [PMID: 34079640]

75 **Wáng YXJ**. Mutual constraining of slow component and fast component measures: some observations in liver IVIM imaging. *Quant Imaging Med Surg* 2021; **11**: 2879-2887 [PMID: 34079748 DOI: 10.21037/qims-21-187]

76 **Wáng YXJ**. Observed paradoxical perfusion fraction elevation in steatotic liver: An example of intravoxel incoherent motion modeling of the perfusion component constrained by the diffusion component. *NMR Biomed* 2021; **34**: e4488 [PMID: 33559161 DOI: 10.1002/nbm.4488]

77 **Tao YY**, Zhou Y, Wang R, Gong XQ, Zheng J, Yang C, Yang L, Zhang XM. Progress of intravoxel incoherent motion diffusion-weighted imaging in liver diseases. *World J Clin Cases* 2020; **8**: 3164-3176 [PMID: 32874971 DOI: 10.12998/wjcc.v8.i15.3164]

78 **Tramontano L**, Cavaliere C, Salvatore M, Brancato V. The Role of Non-Gaussian Models of Diffusion Weighted MRI in Hepatocellular Carcinoma: A Systematic Review. *J Clin Med* 2021; **10** [PMID: 34203995 DOI: 10.3390/jcm10122641]

World Journal of Gastroenterology

Submit a Manuscript: https://www.f6publishing.com

World J Gastroenterol 2022 July 21; 28(27): 3346-3358

DOI: 10.3748/wjg.v28.i27.3346

ISSN 1007-9327 (print) ISSN 2219-2840 (online)

MINIREVIEWS

Regulatory T cells and their associated factors in hepatocellular carcinoma development and therapy

Chun-Ye Zhang, Shuai Liu, Ming Yang

Specialty type: Gastroenterology and hepatology

Provenance and peer review: Invited article; Externally peer reviewed.

Peer-review model: Single blind

Peer-review report's scientific quality classification
Grade A (Excellent): 0
Grade B (Very good): B
Grade C (Good): C
Grade D (Fair): 0
Grade E (Poor): 0

P-Reviewer: Grassi G, Italy; Lu G, China

Received: January 3, 2022
Peer-review started: January 3, 2022
First decision: January 23, 2022
Revised: January 27, 2022
Accepted: June 23, 2022
Article in press: June 23, 2022
Published online: July 21, 2022

Chun-Ye Zhang, Department of Veterinary Pathobiology, University of Missouri, Columbia, MO 65211, United States

Shuai Liu, The First Affiliated Hospital, Zhejiang University, Hangzhou 310006, Zhejiang Province, China

Ming Yang, Department of Surgery, University of Missouri, Columbia, MO 65211, United States

Corresponding author: Ming Yang, DVM, PhD, Postdoctoral Fellow, Department of Surgery, University of Missouri, Room 2203, NexGen Precision Building, 1030 Hitt Street, Columbia, MO 65211, United States. yangmin@health.missouri.edu

Abstract

Liver cancer is the third leading cause of cancer-related death worldwide with primary type hepatocellular carcinoma (HCC). Factors, including carcinogens, infection of hepatitis viruses, alcohol abuse, and non-alcoholic fatty liver disease (NAFLD), can induce HCC initiation and promote HCC progression. The prevalence of NAFLD accompanying the increased incidence of obesity and type 2 diabetes becomes the most increasing factor causing HCC worldwide. However, the benefit of current therapeutic options is still limited. Intrahepatic immunity plays critically important roles in HCC initiation, development, and progression. Regulatory T cells (Tregs) and their associated factors such as metabolites and secreting cytokines mediate the immune tolerance of the tumor microenvironment in HCC. Therefore, targeting Tregs and blocking their mediated factors may prevent HCC progression. This review summarizes the functions of Tregs in HCC-inducing factors including alcoholic and NAFLD, liver fibrosis, cirrhosis, and viral infections. Overall, a better understanding of the role of Tregs in the development and progression of HCC provides treatment strategies for liver cancer treatment.

Key Words: Hepatocellular carcinoma; Regulatory T cells; Alcoholic fatty liver disease; Non-alcoholic fatty liver disease; Treatment; Clinical trials

Core Tip: Liver cancer is the third leading cause of cancer-related death worldwide. Hepatocellular carcinoma (HCC) is the primary type of liver cancer. Factors, including carcinogenic infection of hepatitis viruses, alcohol abuse, and non-alcoholic fatty liver disease (NAFLD), can induce HCC initiation and promote HCC progression. The prevalence of NAFLD accompanying the increased incidence of obesity and type 2 diabetes becomes the most increasing factor causing HCC worldwide. However, the benefit of current therapeutic options is still limited. Intrahepatic immunity plays critically important roles in HCC initiation, development, and progression. Regulatory T cells (Tregs) and their associated factors such as metabolites and secreting cytokines mediate the immune tolerance of the tumor microenvironment in HCC. Therefore, targeting Tregs and blocking their mediated factors may prevent HCC progression. A better understanding of the role of Tregs in intrahepatic immunity is helpful to develop novel HCC treatment options.

Citation: Zhang CY, Liu S, Yang M. Regulatory T cells and their associated factors in hepatocellular carcinoma development and therapy. *World J Gastroenterol* 2022; 28(27): 3346-3358
URL: https://www.wjgnet.com/1007-9327/full/v28/i27/3346.htm
DOI: https://dx.doi.org/10.3748/wjg.v28.i27.3346

INTRODUCTION

Liver cancer is the third leading cause of cancer-related death worldwide with 8.3% of death ratio, following lung and colorectal cancers[1]. The most common type of primary liver cancer is hepatocellular carcinoma (HCC) and the second type is cholangiocarcinoma[2]. Factors, including carcinogens (*e.g.*, aflatoxin B1), infection of hepatitis viruses, alcohol abuse, and non-alcoholic fatty liver disease (NAFLD), can induce HCC and promote HCC progression[3-5]. In addition, accompanying the increasing incidence of obesity and type 2 diabetes (T2D), NAFLD becomes an increasing factor that causes HCC worldwide[6,7].

Surgical resection is a curative treatment option for the early stage of HCC. However, most cases in HCC were found in the late stage. In addition, other minimally invasive local therapies, such as radiofrequency ablation and microwave ablation, and systemic therapy, such as tyrosine kinase inhibitors, are treatment options for patients who are not suitable for surgery[8]. Furthermore, immunotherapy by targeting checkpoint inhibitors [*e.g.*, anti-programmed cell death protein 1 (PD-1)/programmed death-ligand 1 (PD-L1) antibodies] shows benefits against advanced HCC in the clinic. A combination treatment by blocking both PD-L1 (*e.g.*, atezolizumab) and vascular endothelial growth factor (VEGF) (*e.g.*, bevacizumab) is one of the best first-line treatments for advanced HCC[9]. Other potential immunotherapy options including T cell-mediated therapy such as chimeric antigen receptor-engineered T cells[10-12], peptide-based vaccines[13-15], and micro ribonucleic acids (miRNAs)-mediated therapies[16], are undergoing investigations for HCC treatment.

Intrahepatic immunity including both innate and adaptive immune responses plays pivotal roles in the development and progression of HCC, especially for T cells[17]. Among them, the imbalance between effector CD4 and/or CD8 T cells and regulatory T cells (Tregs) induces immunotolerance and promotes HCC progression[18,19]. Factors impacting the balance of effector T cells and Tregs include gut microbiota, transforming growth factor-beta (TGF-β), and treatments such as trans-arterial chemoembolization[18-20], *etc.* The expression of cytokines such as interleukin (IL)-2, IL-5, interferon (IFN)-γ was increased with an increased ratio of cytotoxic T lymphocytes (CTLs)/Tregs with the treatment of Lenvatinib, a multiple kinase inhibitor, while the expression of T-cell immunoglobulin mucin-3 (Tim-3) and CTL-associated antigen-4 (CTLA-4) was decreased on Treg cells[21]. Therefore, modulating the Treg frequency and the expression of related cytokines are critically important for anti-tumor immunotherapy.

In this review, functions of Tregs on HCC causing factors such as alcoholic liver disease (ALD), NAFLD, liver fibrosis, and cirrhosis are discussed. In addition, molecules mediated Treg functions and therapeutic options by targeting Tregs are summarized. Moreover, clinical trials by targeting Tregs to modulate immune response were analyzed.

TREGS IN CHRONIC LIVER DISEASE

Tregs in ALD

As immunosuppressive cells, Tregs play a pivotal role in chronic liver diseases, including ALD. For example, chronic-binge alcohol exposure in C57BL/6 mice induced the reduction of Treg cells, but increased T helper 17 cells (Th17) cells and the production of IL-17[22]. Treatment with ginsenoside F2

can ameliorate ALD by increasing the frequency of Foxp3$^+$Tregs and decreasing IL-17-producing Th17 cells compared to control groups[23]. However, the molecular mechanism of how Tregs impact the progression of ALD except for modulation of liver inflammation remains unclear.

Tregs in NAFLD and nonalcoholic steatohepatitis

The balance Th17 cells/Tregs plays an essential role in metabolic diseases by regulating immune response and glucose and lipid metabolism[8]. The lower Treg (forkhead box P3$^+$/FOXP3$^+$) and higher Th17 cell (IL-17-producing cells) numbers were found in portal or periportal tract in livers of adult NAFLD patients, whereas more Tregs were shown in pediatric NAFLD patients[24]. In addition, severe liver inflammation was positively associated with intralobular expression of FOXP3 in pediatric patients but was positively associated with higher expression of IL-17 and lower expression of FOXP3 in adult patients, indicating the role of Tregs in NAFLD is age-dependent. Intrahepatic imbalance of Th17/Treg cells promotes the progression of NAFLD, accompanying higher expression of inflammatory cytokines such as IL-6, IL-17, and IL-23 in both serum and liver[25]. Feeding a high-fat diet (HFD) can impact the balance of Th17/Treg cells and Th1/Th2 cells of CD4 T cells in mesenteric lymph nodes (MLN). In addition, those CD4 T cells can potentially migrate into the liver to promote liver inflammation to result in NAFLD progression[26]. The effects of CD4 T cells in MLN on liver inflammation and fat accumulation can be ameliorated by administration of antibiotics and probiotics, indicating an important role of gut microbiota in NAFLD pathogenesis[26].

Dywicki *et al*[27] showed intrahepatic Tregs were increased in high-fat high-carbohydrate (HF-HC) diet-induced nonalcoholic steatohepatitis (NASH) in BALB/c mice. In addition, depletion of adaptive immunity aggregated HF-HC diet-induced NASH in recombination activating 1-knockout BALB/c mice. Although Tregs showed an anti-inflammation effect in ALD[23], adoptive transfer of Tregs increased steatosis and serum level of alanine aminotransferase (ALT), indicating that Tregs enhance the progression of NAFLD[27]. Another study also showed that increasing Tregs in subcutaneous adipose tissue induced by adoptive transfer of Tregs from healthy C57BL/6J mice to high-fat HFD (HFHFD)-fed mice increased hepatic steatosis during NAFLD development[28].

Mechanistically, the formation of neutrophil extracellular traps during NASH progression can induce Treg differentiation from naïve CD4 T cells, which is dependent on Toll-like receptor 4 (TLR-4) and involved in NASH-HCC progression[29].

Tregs in liver fibrosis and cirrhosis

Progression of chronic liver disease, including ALD and NAFLD, can promote the development of liver fibrosis and its advanced stage liver cirrhosis. However, there are no currently available therapies that can treat or reverse liver cirrhosis. Deng *et al*[30] reported that co-infusion with human amniotic mesenchymal stromal cells (hAMSCs) and Tregs can prevent mild liver fibrosis. Tregs play a critical role in the secretion of hepatocyte growth factor (HGF) and cell differentiation of hAMSCs.

Furthermore, an imbalance of Th17 cells/Tregs was also shown in cirrhotic patients with hepatitis B virus (HBV) infection. The frequency of Tregs was reduced in peripheral blood, while the frequency of Th17 cells was increased, resulting in a decreased Treg/Th17 ratio as a potential diagnostic marker for decompensated liver cirrhosis[31]. Another study also showed that the frequencies of both Tregs and Th17 cells were increased in the blood of patients with HBV infection and cirrhotic livers but with a higher extent in Th17 cells, resulting in an increased ratio of Th17/Treg, compared to the control group [32]. In addition, the mRNA levels of proinflammatory cytokines IL-1β, IL-6, and tumor necrosis factor (TNF)-α, as well as the protein expression of nuclear factor κB in the liver were significantly increased in HBV-infected liver and cirrhotic liver compared to healthy controls. Another study also showed that HBV infection can induce IL-8/C-X-C motif chemokine receptor 1/TGF-β signaling to provoke Treg polarization, resulting in suppression of anti-tumor immunity and enhance of HCC metastasis[33]. Moreover, the frequency of Tregs in blood and plasma levels of IL-35 were increased and positively related to viral load in HCV infected patients with cirrhosis and HCC[34].

Tregs in HCC

A meta-analysis showed that a higher infiltration of CD3 T cells, CD8 T cells, and natural killer cells was associated with better overall survival (OS), disease-free survival (DFS), and recurrence-free survival (RFS). In contrast, a higher infiltration of Tregs and neutrophils indicated lower OS and DFS[35]. Another report also showed that an increase of Tregs or a decrease of M1 macrophages (proinflammatory phenotype) were associated with a poor prognosis of HCC patients[36]. C-C chemokine receptor type 4 (CCR4)$^+$Tregs are predominant Tregs that are recruited in tumor tissue of HCC associated infection of hepatitis viruses, which is associated with HCC resistance to sorafenib treatment[37]. The frequency of CD127^{low}, CD25$^+$, CD4$^+$, Tregs was increased significantly in the peripheral venous blood of HCC patients compared to healthy controls[38]. In addition, the serum levels of TGF-β1 and IL-10 in HCC patients were positively associated with the Treg population in the blood, which were decreased post-operation and chemotherapy treatments. C-C motif chemokine ligand (CCL) 5 expression on circulating tumor cells in HCC patients can attract Tregs to induce an immunosuppressive environment, one of the mechanisms for CTC escaping immune surveillance[39].

The expression of immune checkpoint proteins in the HCC microenvironment impacts Tregs and antitumor immunity. PD-L1^{+}neutrophils, Tregs, and neutrophil to lymphocyte ratio were significantly increased in peripheral blood of patients with poorly differentiated HCC with a worse prognosis compared to that in patients with highly-moderately differentiated HCC[40]. Zhou *et al*[41] reported that tumor-associated neutrophils can induce the infiltration of the macrophages and Tregs from HCC mice or patients *via* producing CCL2 and CCL17, resulting in HCC progression and resistance to sorafenib. CTLA-4 on Tregs in HCC impacts dendritic cell function by downregulating CD80/CD86 on dendritic cells (DCs)[42]. Therefore, blockade of CTLA-4 in HCC can improve DC-mediated anti-tumor immunity.

Treatment with tivozanib, a tyrosine kinase inhibitor, can suppress Tregs by inhibiting receptor tyrosine kinase c-Kit (CD117)/stem cell factor (SCF) axis and increased CD4^{+}PD-1^{+}T cells, resulting in a significant improvement in OS of HCC patients[43]. Treatment with Lenvatinib also can inhibit IL-2 mediated Treg differentiation except for decreasing PD-L1 expression in HCC cells[44]. Overall, the balance between Tregs with other T cells plays a vital in liver diseases, including the initiation and progression of HCC (Figure 1).

Furthermore, alteration of intrahepatic immunity is associated with HCC prognosis and treatment (Figure 2). An increase of Tregs, Th2, and Th17 T cells, as well as M2 macrophages, is usually and positively associated with HCC progression in patients, whereas an abundance of CD8 T cells, Th1 T cells, and M1 macrophages is associated with HCC therapy and good prognosis for HCC patients[45]. Single-cell RNA sequencing technologies have been applied to investigate the immune landscape of HCC samples to illustrate the subtypes of immune cells in HCC and their gene expressing profiles, as well as immune cell interactions, such as DCs with Tregs or CD8 T cells[46].

IMPORTANT MOLECULES MEDIATED TREG FUNCTION AND METABOLISM

HIF-1α

Hypoxia-inducible transcription factors (HIFs) regulate cell metabolism, proliferation, and migration in low oxygen or hypoxic environment, as well as angiogenesis[47]. It has been reported that the expression of HIF-1 alpha (HIF-1α) was higher in HCC tissues compared to that in corresponding adjacent tissues. In addition, overexpression of HIF-1α was associated with poor outcomes of HCC in human patients[48]. Chronic intermittent hypoxia can promote NASH progression *via* regulating the balance of Th17/Treg by inducing the expression of HIF-1α[49].

Gal-9

Tregs can be subclassified into inflamed-tissue related memory Tregs (mTregs) and non-related resting Treg (rTregs). During HBV infection, mTregs were increased accompanying liver inflammation and liver injury evidenced by an increase of serum ALT level, but not rTregs[50]. The S-type lectin galectin-9 (Gal-9) was increased in the HBV-infected liver, contributing to T cell depletion and exhaustion by binding Tim-3[51]. For example, activation of Gal-9/Tim-3 signaling in concanavalin A-induced mouse hepatitis suppressed the induction of effector T (Teff) cells and the production of IFN-γ[52]. In addition, the Gal-9/Tim-3 signaling pathway plays an important role in the expansion of mTregs[50].

GDF15

The expression of growth differentiation factor 15 (GDF15) was positively related to the frequency of Tregs in HCC. GDF15 can promote the suppressive effect of natural Tregs *via* binding with its unrecognized receptor CD48 on T cells to inhibit the function of homology and U-box containing protein 1, which can degrade FOXP3[53]. Thus, neutralizing GDF15 by an antibody can eradicate HCC and enhance anti-tumor immunity.

microRNAs

Hepatic expression of microRNA-195 (miR-195) was reduced in NAFLD development, accompanying an increased ratio of Th17/Treg ratio in the blood, as well as the expression IL-17, CD40, and TNF-α in rat liver[54]. Overexpression of miR-195 can maintain the balance of Th17/Treg to ameliorate NAFLD and liver inflammation. Many miRNAs can regulate Th17/Treg cell balance in NAFLD such as miR-29c *via* interacting with insulin-like growth factor binding protein 1/IGFBP1)[55]. In addition, other microRNAs such as miR-155[56,57], miR-423-5p[58], and miR-1246[59] play important roles in modulating the balance of Tregs with Th17 cells and their functions in liver disease.

TLRs

Activation of TLR signaling pathway can suppress the effect of Tregs on adaptive immune response, which is in part dependent on microbial production-induced expression of IL-6[60]. TLR9-deficiency increased the frequency of Treg cells in the intestine, resulting in a decrease of IL-17 and IFN-γ producing Teff cells[61]. The imbalance of Treg/Teff cells compromised immune response to oral

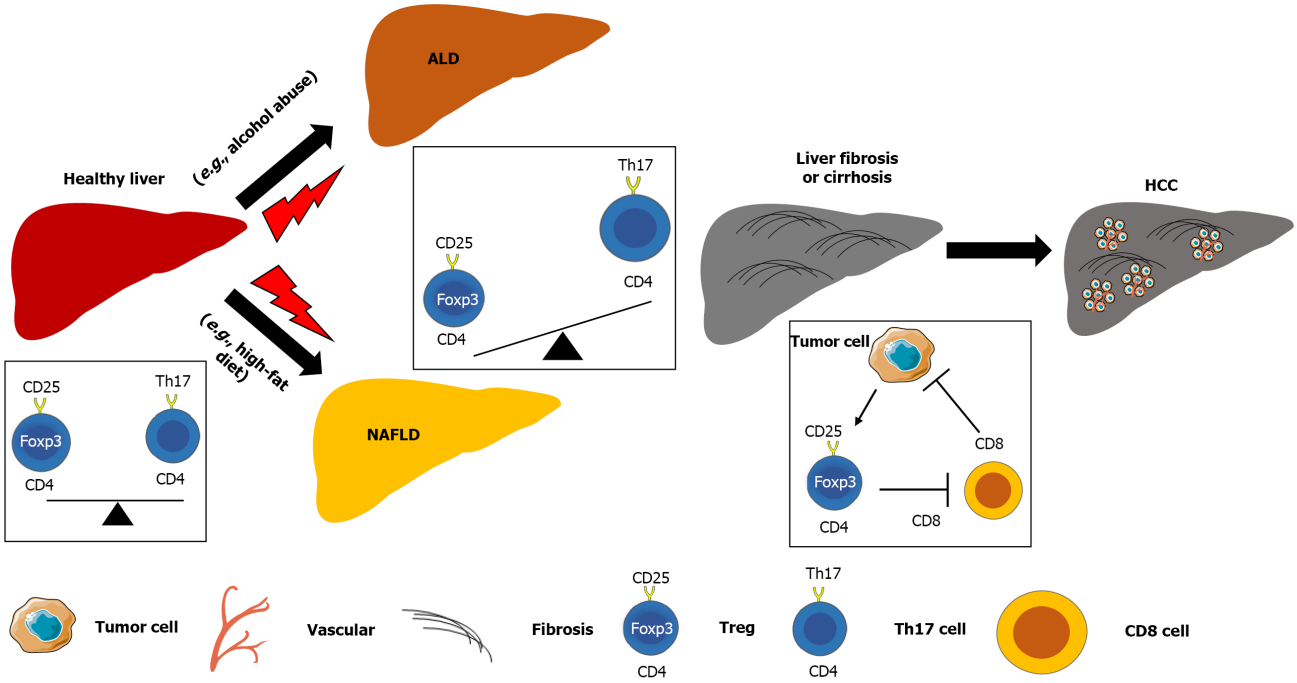

DOI: 10.3748/wjg.v28.i27.3346

Figure 1 The imbalance of regulatory T cells and effector T cells promotes the progression of chronic liver diseases and hepatocellular carcinoma. Chronic liver diseases such as alcoholic liver disease and non-alcoholic fatty liver disease induced by factors such as alcohol abuse and high-fat diet, respectively, can induce liver fibrosis, cirrhosis, and even hepatocellular carcinoma. The imbalance of regulatory T cells with T helper 17 cells or CD8 T cells is involved in the pathogenesis of liver inflammation, fibrosis, and cancer progression. ALD: Alcoholic liver disease; HCC: Hepatocellular carcinoma; NAFLD: Non-alcoholic fatty liver disease; Treg: Regulatory T cells; Th: T helper.

infection, which can be reversed by reconstitution of gut flora deoxyribonucleic acid (DNA)[61]. In addition, the antibiotic treatment caused gut microbiota dysbiosis and recapitulated TLR9 deficiency-induced impaired immune response.

Yes-associated protein (YAP)

Yes-associated protein (YAP), a coactivator and a corepressor of the Hippo signaling pathway, plays a vital role in Tregs *in vivo* and *in vitro*[62]. Blocking YAP-mediated activation of activin can improve anti-tumor immunity *via* regulating TGF-β/mothers against decapentaplegic homolog (SMAD)[62]. Similarly, blockage of TGF-β signaling can compromise Treg function to improve anti-tumor immune response[63], which may expand the population of quiescent Tregs, $CD4^+CD25^-Foxp3^+$.

The above-mentioned molecules can modulate Treg metabolism and function as potential molecular targets for HCC treatment. In addition, modulation of these molecules can potentially recover the balance of Tregs with other tumor-infiltrating immune cells to activate anti-tumor immunity (Figure 3).

TREATMENT OPTIONS

Modulation of microRNAs

Administration of miR-26a can reduce the frequency of Tregs and the concentrations of alpha-fetoprotein, des-gamma carboxyprothrombin, and VEGF in Balb/c mice with diethylnitrosamine-induced HCC[64]. The suppressive effects of miR-26a on HCC growth and angiogenesis are mediated by targeting IL-6/signal transducer and activator of transcription 3 (Stat3) signaling[65] and HGF/HGF receptor (HGFR/c-Met) signaling[66], respectively. In addition, miR-26a inversely regulated the expression of F-box protein 11 (FBXO11), which was upregulated and played an oncogenic role in HCC [67].

Adoptive transfer of cells

Adoptive transfer of Tregs attenuated triptolide-induced liver injury, while depletion of Tregs showed the opposite effect, indicating that Tregs contribute to the progression of liver injury[68]. Another study showed that adoptive transfer of hepatic stellate cell (HSC)-stimulated Tregs can significantly decrease liver injury in mice with autoimmune hepatitis by inducing the balance of Treg/Th17 ratio[69]. In addition, the adoptive transfer of HSCs promoted the differentiation of Tregs and decreased Th17 cells,

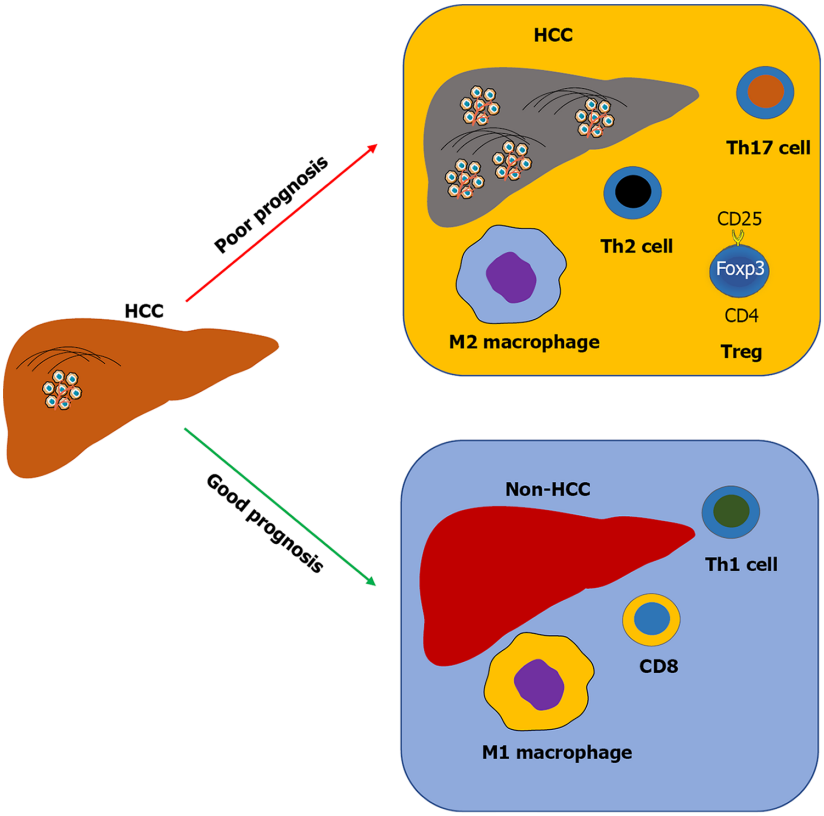

DOI: 10.3748/wjg.v28.i27.3346

Figure 2 The alteration of intrahepatic immunity predicts the prognosis of hepatocellular carcinoma patients. Usually, an increase of regulatory T cells, T helper (Th) 2 cells, and Th17 cells, as well as M2 macrophages is positively associated with hepatocellular carcinoma (HCC) progression in patients, whereas an abundance of CD8 T cells, Th1 T cells, and M1 macrophages is associated with HCC therapy and good prognosis for HCC patients. HCC: Hepatocellular carcinoma; Treg: Regulatory T cells; Th: T helper.

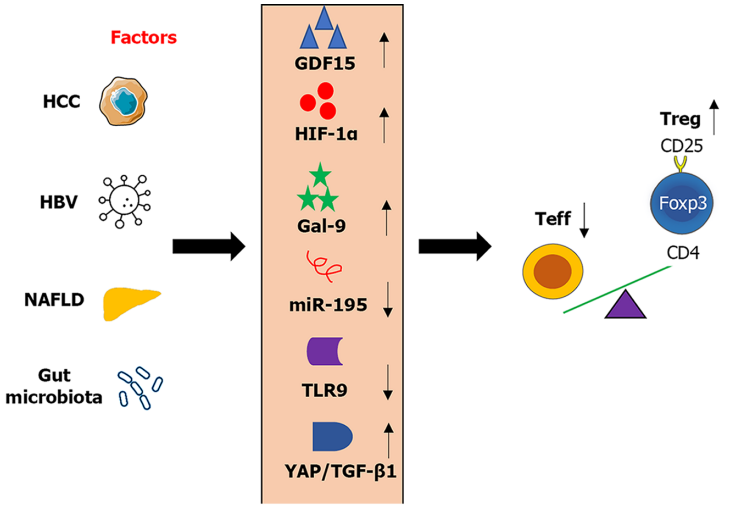

DOI: 10.3748/wjg.v28.i27.3346

Figure 3 Factors mediated the imbalance of regulatory T cells/effector T cells. Factor such as Hepatitis B virus, gut microbiota, and non-alcoholic fatty liver disease, as well as hepatocellular carcinoma tumor cells, can modulate several important molecules produced in the liver. Alteration of these molecules has been associated with the change of frequency and/or function of regulatory T cells in chronic liver disease, resulting in an imbalance of regulatory T cells/effector T cells. HCC: Hepatocellular carcinoma; HBV: Hepatitis B virus; NAFLD: Non-alcoholic fatty liver disease; Teff: Effector T cells; Treg: Regulatory T cells; GDF: Growth differentiation factor; HIF: Hypoxia-inducible transcription factors; Gal: Galectin; miR: micro ribonucleic acid; TLR: Toll-like receptor; YAP: Yes-associated protein; TGF-β: Transforming growth factor-beta.

resulting in amelioration of liver injury[70]. Deng *et al*[30] reported that co-infusion with hAMSCs and Tregs can prevent mild liver fibrosis. Tregs play a critical role in the secretion of HGF and cell differentiation of hAMSCs.

Table 1 Treatment options for hepatocellular carcinoma by targeting regulatory T cells and relative signaling pathways

Treatment	Targets	Functions	Ref.
CCR4 antagonist	CCR4	Administration of a CCR4 antagonist or N-CCR4-Fc, a neutralizing pseudo-receptor that can block Tregs accumulation in HCC, can enhance therapeutic efficacy to PD-1 blockade and sorafenib	Gao *et al*[37], 2022
miR-26a	IL6/Stat3 and HGF/c-Met	The suppressive effects of miR-26a on HCC growth and angiogenesis are mediated by targeting IL-6/signal transducer and activator of transcription 3 signaling and HGF/HGFR/c-Met signaling, respectively	Yang *et al*[65], 2013; Yang *et al*[66], 2014
GDF15 neutralizing antibody	GDF15/CD48	Inhibiting GDF15 function by a neutralizing antibody can effectively eradicate HCC and promote a tumoricidal immune response in mice	Wang *et al*[53], 2021
Supplementation of *Lactobacillus rhamnosus* GG or its culture supernatant	The ratio of Treg and Th17 cells	Supplementation of *Lactobacillus rhamnosus* GG or its culture supernatant can ameliorate chronic alcohol-induced liver injury by reducing hepatic inflammation, enhancing intestinal barrier integrity, and inducing balance in the ratio of Treg and Th17 cells to reduce alcoholic-induced liver injury	Chen *et al*[22], 2016; Wang *et al*[72], 2013; Wang *et al*[73], 2012
Prohep, a novel probiotic mixture	Gut microbiota and Treg differentiation	Probiotic treatment regulated T-cell differentiation in the gut by reducing Th17 polarization and increasing the differentiation of anti-inflammatory Treg cells, by increasing the abundance of beneficial bacteria, such as *Prevotella* and *Oscillibacter*	Li *et al*[74], 2016
Anti-PD-1 and anti-PD-L1 antibodies	PD-1 and PD-L1	Another study also showed that Treg-mediated inhibition of IFN-γ production and cytotoxicity of CD8 T cells can be partially reduced by anti-PD-1 and anti-PD-L1 antibodies in HCC	Langhans *et al*[76], 2019
Dual anti-PD-1/VEGFR-2 therapy	VEGFR-2 and PD-1	Dual therapies increased CD8 T cell infiltration and activation, reduced Tregs and infiltration of $CCR2^{+}$monocytes, as well as the phenotype of tumor-associated macrophages (the M1/M2 ratio) in HCC tissue	Shigeta *et al*[75], 2020
Anti-CTLA-4 monoclonal antibody	Tregs	Treg depletion-mediated by anti-CTLA-4 monoclonal antibody (clone 9H10) restored the function of tumor antigen-specific CD8 T cells, with a synergistic effect with anti-PD-1 treatment	Lee *et al*[77], 2020
Resveratrol	Tregs and immunosuppressive cytokines including TGF-β1 and IL-10	Treatment with resveratrol, a natural phenol, can inhibit H22 (a mouse HCC cell line)-induced orthotopic HCC tumor growth *via* decreasing the frequency of $CD8^{+}CD122^{+}$Tregs and M2-like macrophages in mice	Zhang *et al*[79], 2020

CCR: C-C chemokine receptor; HGF: Hepatocyte growth factor; HGFR: Hepatocyte growth factor receptor; HCC: Hepatocellular carcinoma; PD-1: Programmed cell death protein 1; miR: micro ribonucleic acid; IL: Interleukin; GDF: Growth differentiation factor; Treg: Regulatory T cells; Th: T helper; IFN: Interferon; VEGFR: Vascular endothelial growth factor receptor; CTLA: Cytotoxic T lymphocyte-associated antigen; TGF-β: Transforming growth factor-beta.

Modulation of gut microbiota

Depletion of Tregs in the intestine caused an increase in the abundance of *Firmicutes* and intestinal inflammation[71]. Supplementation of *Lactobacillus rhamnosus* GG or its culture supernatant can ameliorate chronic alcohol-induced liver injury by reducing TNF-α expression *via* inhibition of TLR4- and TLR5-mediated hepatic inflammation[72], as well as amelioration of intestinal barrier integrity and suppression of alcohol-induced endotoxemia[73]. In addition, the culture supernatant can balance the ratio of Treg and Th17 cells to reduce alcoholic-induced liver injury[22].

Treatment with Prohep, a novel probiotic mixture, significantly inhibited the HCC growth compared to the control group, resulting in an abundance of beneficial bacteria, such as *Prevotella* and *Oscillibacter* [74]. This study also showed that probiotic treatment regulated T-cell differentiation in the gut by reducing Th17 polarization and increasing the differentiation of anti-inflammatory Treg cells.

Blockade of immune checkpoints

Dual anti-PD-1/VEGF receptor-2 therapy increased CD8 T cell infiltration and activation, reduced Tregs and infiltration of $CCR2^{+}$monocytes, as well as the phenotype of tumor-associated macrophages (the M1/M2 ratio) in HCC tissue[75]. Another study also showed that Treg-mediated inhibition of IFN-γ production and cytotoxicity of CD8 T cells can be partially reduced by anti-PD-1 and anti-PD-L1 antibodies in HCC[76].

Treg depletion-mediated by anti-CTLA-4 monoclonal antibody (clone 9H10) restored the function of tumor antigen-specific CD8 T cells, with a synergetic effect with anti-PD-1 treatment[77].

Other treatments

CCR4 expression in Tregs accompanied with an increased expression IL-10 and IL-35, resulting in suppression of CD8 T cells and HCC progression. Administration of a CCR4 antagonist or N-CCR4-Fc, a

Table 2 Clinical trials by targeting regulatory T cells to modulate the immune response

Trial	Phase	Treatment	Results	Ref.
NCT02476123	I	Anti-CCR4 antibody mogamulizumab	Treg depletion induced by anti-CCR4 antibody (mogamulizumab), in combination with anti-PD-1 antibody (nivolumab) showed antitumor activity and increased $CD8^+$ T cell infiltration	Doi *et al*[78], 2019; Sánchez-Fueyo *et al*[83], 2020
NCT02166177	I	Intravenous infusion of ex vivo expanded Tregs	Treg transfer can transiently increase circulating Tregs and inhibit anti-donor T cell responses in patients with liver transplants	Fueyo *et al*[83], 2020
NCT02166177	I	Autologous Treg therapy	To defect safety and efficacy study of regulatory T cell therapy in liver transplant patients	Whitehouse *et al* [84], 2017
NCT01624077	I	Injection of Tregs	To defect safety and efficacy study of regulatory T cell therapy in liver transplant patients	Whitehouse *et al* [84], 2017
NCT03654040	I	A single dose of alloantigen-reactive Tregs (arTreg) (≥ 90 × 10^6 total cells)	It is a single-center, prospective, open-label, non-randomized clinical trial exploring cellular therapy to facilitate immunosuppression withdrawal in liver transplant recipients	Cvetkovski *et al* [85], 2021
NCT03577431		arTreg-CSB (2.5 × 10^6 cells)		
NCT02260375	I	Infusion of mesenchymal stromal cells	MSC infusion in liver transplant recipients slightly increased circulating Treg/memory Treg over baseline, without a statistically significant, but not in the control group	Casiraghi *et al* [86], 2021
NCT02027116	I	DNA vaccine GLS-6150	GLS-6150 decreases Treg cell frequency and enhances HCV-specific T cell responses without significant side effects	Han *et al*[87], 2020
NCT02174276	II	GS-4774, a yeast-based therapeutic vaccine	Treatment with GS-4774 increased T-cell functions by increasing the production of IFN-γ and TNF and reducing the cell number of Tregs	Boni *et al*[88], 2019
NCT02360592	IV	Combined therapy with interferon plus IL-1 and hepatitis B Vaccine	Combination therapy increased the level of hepatitis B surface antigen with partial restoration of Tregs and NK cells	Wu *et al*[89], 2019
NCT02072486	None	Sorafenib, a multiple kinase inhibitor	Treatment with sorafenib can significantly suppress extracellular signal-regulated $kinases^+$ FMS-like tyrosine $kinase\ 3^+$ Tregs and myeloid-derived suppressor cells to benefit the survival of HCC patients	Kalathil *et al* [90], 2019

CCR: C-C chemokine receptor; CSB: Co-stimulatory blockade; PD-1: Programmed cell death protein 1; Treg: Regulatory T cells; MSC: Mesenchymal stromal cells; DNA: Deoxyribonucleic acid; GLS: Glutaminase; IFN: Interferon; TNF: Tumor necrosis factor; IL: Interleukin; NK: Natural killer; FMS: Feline McDonough sarcoma.

neutralizing pseudo-receptor that can block Tregs accumulation in HCC, can enhance therapeutic efficacy to PD-1 blockade and sorafenib[37]. Treg depletion induced by anti-CCR4 antibody (mogamulizumab), in combination with anti-PD-1 antibody (nivolumab) showed antitumor activity and increased CD8+ T cell infiltration[78].

Treatment with resveratrol, a natural phenol, can inhibit H22 (a mouse HCC cell line)-induced orthotopic HCC tumor growth *via* decreasing the frequency of $CD8^+CD122^+$Tregs and M2-like macrophages in mice[79].

Ren *et al*[80] reported that Tregs were further increased in HCC patients compared to healthy and cirrhosis controls, as well as in HCC patients with Barcelona clinic liver cancer (BCLC) stage C compared to that in HCC patients with BCLC stage B. The authors also showed that treatment with microparticles-transarterial chemoembolization dramatically decreased Treg cell proportion at 1-2 wk post-treatment. Overall, the treatment options for HCC associated with Treg regulation were summarized in Table 1.

CLINICAL TRIALS

Tregs display multiple roles in the development and progression of HCC. The ratio of Treg/Th17 cells in peripheral blood can be applied to monitor immune tolerance as immune markers in liver transplantation[81]. The balance of Treg/Th17 cells or other effector T cells is essential for suppressing autoimmune diseases and cancers[82]. Therefore, treatments including diverse immunomodulatory therapies can regulate Tregs to enhance the antitumor immune response. In Table 2, potential therapies in clinical trials were summarized. Treatments including infusion of Tregs[83-85] and mesenchymal stromal cells (MSCs)[86], vaccines[87-89], and kinase inhibitors[90].

CONCLUSION

Tregs modulate the intestinal and intrahepatic immune response, contributing critically important roles in the gut-liver axis. Functional changes of Tregs are involved in the pathogenesis of chronic liver diseases, such as ALD and NAFLD, causing factors for HCC. Several important molecules investigated in recent studies are summarized and targeting them may potentially treat HCC by modulating Treg function and/or frequency. Clinical trials are undergoing to further explore the new treatments for HCC, which modulate the function of the frequency of Tregs. In the future, multi-omic analysis including metabolic and proteomic data for Treg metabolism and function during the progression of HCC is critical to illustrate the underlying mechanisms of Tregs in HCC pathogenesis and find out new therapeutic targets.

FOOTNOTES

Author contributions: Zhang CY, Liu S, and Yang M designed and collected data, wrote, revised, and finalized the manuscript; all authors contributed equally, and shared the first authorship.

Conflict-of-interest statement: There are no conflicts of interest to report.

Country/Territory of origin: United States

ORCID number: Chun-Ye Zhang 0000-0003-2567-029X; Shuai Liu 0000-0001-9695-2492; Ming Yang 0000-0002-4895-5864.

S-Editor: Chen YL
L-Editor: A
P-Editor: Chen YL

REFERENCES

1 **Sung H**, Ferlay J, Siegel RL, Laversanne M, Soerjomataram I, Jemal A, Bray F. Global Cancer Statistics 2020: GLOBOCAN Estimates of Incidence and Mortality Worldwide for 36 Cancers in 185 Countries. *CA Cancer J Clin* 2021; **71**: 209-249 [PMID: 33538338 DOI: 10.3322/caac.21660]
2 **Zhang C**, Yang M. The Emerging Factors and Treatment Options for NAFLD-Related Hepatocellular Carcinoma. *Cancers (Basel)* 2021; **13** [PMID: 34359642 DOI: 10.3390/cancers13153740]
3 **Qi X**, Yang M, Stenberg J, Dey R, Fogwe L, Alam MS, Kimchi ET, Staveley-O'Carroll KF, Li G. Gut microbiota mediated molecular events and therapy in liver diseases. *World J Gastroenterol* 2020; **26**: 7603-7618 [PMID: 33505139 DOI: 10.3748/wjg.v26.i48.7603]
4 **De Battista D**, Zamboni F, Gerstein H, Sato S, Markowitz TE, Lack J, Engle RE, Farci P. Molecular Signature and Immune Landscape of HCV-Associated Hepatocellular Carcinoma (HCC): Differences and Similarities with HBV-HCC. *J Hepatocell Carcinoma* 2021; **8**: 1399-1413 [PMID: 34849372 DOI: 10.2147/JHC.S325959]
5 **Zhu Q**, Ma Y, Liang J, Wei Z, Li M, Zhang Y, Liu M, He H, Qu C, Cai J, Wang X, Zeng Y, Jiao Y. AHR mediates the aflatoxin B1 toxicity associated with hepatocellular carcinoma. *Signal Transduct Target Ther* 2021; **6**: 299 [PMID: 34373448 DOI: 10.1038/s41392-021-00713-1]
6 **Bertot LC**, Adams LA. Trends in hepatocellular carcinoma due to non-alcoholic fatty liver disease. *Expert Rev Gastroenterol Hepatol* 2019; **13**: 179-187 [PMID: 30791782 DOI: 10.1080/17474124.2019.1549989]
7 **Zhang C**, Liu S, Yang M. Hepatocellular Carcinoma and Obesity, Type 2 Diabetes Mellitus, Cardiovascular Disease: Causing Factors, Molecular Links, and Treatment Options. *Front Endocrinol (Lausanne)* 2021; **12**: 808526 [PMID: 35002979 DOI: 10.3389/fendo.2021.808526]
8 **Zhang C**, Yang M, Ericsson AC. The Potential Gut Microbiota-Mediated Treatment Options for Liver Cancer. *Front Oncol* 2020; **10**: 524205 [PMID: 33163393 DOI: 10.3389/fonc.2020.524205]
9 **Sangro B**, Sarobe P, Hervás-Stubbs S, Melero I. Advances in immunotherapy for hepatocellular carcinoma. *Nat Rev Gastroenterol Hepatol* 2021; **18**: 525-543 [PMID: 33850328 DOI: 10.1038/s41575-021-00438-0]
10 **Pang N**, Shi J, Qin L, Chen A, Tang Y, Yang H, Huang Y, Wu Q, Li X, He B, Li T, Liang B, Zhang J, Cao B, Liu M, Feng Y, Ye X, Chen X, Wang L, Tian Y, Li H, Li J, Hu H, He J, Hu Y, Zhi C, Tang Z, Gong Y, Xu F, Xu L, Fan W, Zhao M, Chen D, Lian H, Yang L, Li P, Zhang Z. IL-7 and CCL19-secreting CAR-T cell therapy for tumors with positive glypican-3 or mesothelin. *J Hematol Oncol* 2021; **14**: 118 [PMID: 34325726 DOI: 10.1186/s13045-021-01128-9]
11 **Li D**, Li N, Zhang YF, Fu H, Feng M, Schneider D, Su L, Wu X, Zhou J, Mackay S, Kramer J, Duan Z, Yang H, Kolluri A, Hummer AM, Torres MB, Zhu H, Hall MD, Luo X, Chen J, Wang Q, Abate-Daga D, Dropulic B, Hewitt SM, Orentas RJ,

Greten TF, Ho M. Persistent Polyfunctional Chimeric Antigen Receptor T Cells That Target Glypican 3 Eliminate Orthotopic Hepatocellular Carcinomas in Mice. *Gastroenterology* 2020; **158**: 2250-2265.e20 [PMID: 32060001 DOI: 10.1053/j.gastro.2020.02.011]

12 **Batra SA**, Rathi P, Guo L, Courtney AN, Fleurence J, Balzeau J, Shaik RS, Nguyen TP, Wu MF, Bulsara S, Mamonkin M, Metelitsa LS, Heczey A. Glypican-3-Specific CAR T Cells Coexpressing IL15 and IL21 Have Superior Expansion and Antitumor Activity against Hepatocellular Carcinoma. *Cancer Immunol Res* 2020; **8**: 309-320 [PMID: 31953246 DOI: 10.1158/2326-6066.CIR-19-0293]

13 **Tsuchiya N**, Yoshikawa T, Fujinami N, Saito K, Mizuno S, Sawada Y, Endo I, Nakatsura T. Immunological efficacy of glypican-3 peptide vaccine in patients with advanced hepatocellular carcinoma. *Oncoimmunology* 2017; **6**: e1346764 [PMID: 29123959 DOI: 10.1080/2162402X.2017.1346764]

14 **Charneau J**, Suzuki T, Shimomura M, Fujinami N, Nakatsura T. Peptide-Based Vaccines for Hepatocellular Carcinoma: A Review of Recent Advances. *J Hepatocell Carcinoma* 2021; **8**: 1035-1054 [PMID: 34513746 DOI: 10.2147/JHC.S291558]

15 **Zhang C**, Yang M, Ericsson AC. Antimicrobial Peptides: Potential Application in Liver Cancer. *Front Microbiol* 2019; **10**: 1257 [PMID: 31231341 DOI: 10.3389/fmicb.2019.01257]

16 **Roy B**, Ghose S, Biswas S. Therapeutic strategies for miRNA delivery to reduce hepatocellular carcinoma. *Semin Cell Dev Biol* 2022; **124**: 134-144 [PMID: 33926792 DOI: 10.1016/j.semcdb.2021.04.006]

17 **Zhang C**, Yang M. Targeting T Cell Subtypes for NAFLD and NAFLD-Related HCC Treatment: An Opinion. *Front Med (Lausanne)* 2021; **8**: 789859 [PMID: 34869507 DOI: 10.3389/fmed.2021.789859]

18 **Behary J**, Amorim N, Jiang XT, Raposo A, Gong L, McGovern E, Ibrahim R, Chu F, Stephens C, Jebeili H, Fragomeli V, Koay YC, Jackson M, O'Sullivan J, Weltman M, McCaughan G, El-Omar E, Zekry A. Gut microbiota impact on the peripheral immune response in non-alcoholic fatty liver disease related hepatocellular carcinoma. *Nat Commun* 2021; **12**: 187 [PMID: 33420074 DOI: 10.1038/s41467-020-20422-7]

19 **Dituri F**, Mancarella S, Serino G, Chaoul N, Lupo LG, Villa E, Fabregat I, Giannelli G. Direct and Indirect Effect of TGFβ on Treg Transendothelial Recruitment in HCC Tissue Microenvironment. *Int J Mol Sci* 2021; **22** [PMID: 34769191 DOI: 10.3390/ijms222111765]

20 **Pinato DJ**, Murray SM, Forner A, Kaneko T, Fessas P, Toniutto P, Mínguez B, Cacciato V, Avellini C, Diaz A, Boyton RJ, Altmann DM, Goldin RD, Akarca AU, Marafioti T, Mauri FA, Casagrande E, Grillo F, Giannini E, Bhoori S, Mazzaferro V. Trans-arterial chemoembolization as a loco-regional inducer of immunogenic cell death in hepatocellular carcinoma: implications for immunotherapy. *J Immunother Cancer* 2021; **9** [PMID: 34593621 DOI: 10.1136/jitc-2021-003311]

21 **Zhu J**, Fang P, Wang C, Gu M, Pan B, Guo W, Yang X, Wang B. The immunomodulatory activity of lenvatinib prompts the survival of patients with advanced hepatocellular carcinoma. *Cancer Med* 2021; **10**: 7977-7987 [PMID: 34605616 DOI: 10.1002/cam4.4312]

22 **Chen RC**, Xu LM, Du SJ, Huang SS, Wu H, Dong JJ, Huang JR, Wang XD, Feng WK, Chen YP. Lactobacillus rhamnosus GG supernatant promotes intestinal barrier function, balances Treg and TH17 cells and ameliorates hepatic injury in a mouse model of chronic-binge alcohol feeding. *Toxicol Lett* 2016; **241**: 103-110 [PMID: 26617183 DOI: 10.1016/j.toxlet.2015.11.019]

23 **Kim MH**, Kim HH, Jeong JM, Shim YR, Lee JH, Kim YE, Ryu T, Yang K, Kim KR, Jeon BM, Kim SC, Jung JK, Choi JK, Lee YS, Byun JS, Jeong WI. Ginsenoside F2 attenuates chronic-binge ethanol-induced liver injury by increasing regulatory T cells and decreasing Th17 cells. *J Ginseng Res* 2020; **44**: 815-822 [PMID: 33192125 DOI: 10.1016/j.jgr.2020.03.002]

24 **Cairoli V**, De Matteo E, Rios D, Lezama C, Galoppo M, Casciato P, Mullen E, Giadans C, Bertot G, Preciado MV, Valva P. Hepatic lymphocytes involved in the pathogenesis of pediatric and adult non-alcoholic fatty liver disease. *Sci Rep* 2021; **11**: 5129 [PMID: 33664397 DOI: 10.1038/s41598-021-84674-z]

25 **He B**, Wu L, Xie W, Shao Y, Jiang J, Zhao Z, Yan M, Chen Z, Cui D. The imbalance of Th17/Treg cells is involved in the progression of nonalcoholic fatty liver disease in mice. *BMC Immunol* 2017; **18**: 33 [PMID: 28646856 DOI: 10.1186/s12865-017-0215-y]

26 **Su L**, Wu Z, Chi Y, Song Y, Xu J, Tan J, Cong X, Liu Y. Mesenteric lymph node $CD4^+$ T lymphocytes migrate to liver and contribute to non-alcoholic fatty liver disease. *Cell Immunol* 2019; **337**: 33-41 [PMID: 30770094 DOI: 10.1016/j.cellimm.2019.01.005]

27 **Dywicki J**, Buitrago-Molina LE, Noyan F, Davalos-Misslitz AC, Hupa-Breier KL, Lieber M, Hapke M, Schlue J, Falk CS, Raha S, Prinz I, Koenecke C, Manns MP, Wedemeyer H, Hardtke-Wolenski M, Jaeckel E. The Detrimental Role of Regulatory T Cells in Nonalcoholic Steatohepatitis. *Hepatol Commun* 2022; **6**: 320-333 [PMID: 34532981 DOI: 10.1002/hep4.1807]

28 **Van Herck MA**, Vonghia L, Kwanten WJ, Vanwolleghem T, Ebo DG, Michielsen PP, De Man JG, Gama L, De Winter BY, Francque SM. Adoptive Cell Transfer of Regulatory T Cells Exacerbates Hepatic Steatosis in High-Fat High-Fructose Diet-Fed Mice. *Front Immunol* 2020; **11**: 1711 [PMID: 32849604 DOI: 10.3389/fimmu.2020.01711]

29 **Wang H**, Zhang H, Wang Y, Brown ZJ, Xia Y, Huang Z, Shen C, Hu Z, Beane J, Ansa-Addo EA, Huang H, Tian D, Tsung A. Regulatory T-cell and neutrophil extracellular trap interaction contributes to carcinogenesis in non-alcoholic steatohepatitis. *J Hepatol* 2021; **75**: 1271-1283 [PMID: 34363921 DOI: 10.1016/j.jhep.2021.07.032]

30 **Deng Z**, Zhou J, Mu X, Gu J, Li X, Shao Q, Li J, Yang C, Han G, Zhao J, Xia Y. Regulatory T Cells Improved the Anti-cirrhosis Activity of Human Amniotic Mesenchymal Stem Cell in the Liver by Regulating the TGF-β-Indoleamine 2,3-Dioxygenase Signaling. *Front Cell Dev Biol* 2021; **9**: 737825 [PMID: 34712665 DOI: 10.3389/fcell.2021.737825]

31 **Lan YT**, Wang ZL, Tian P, Gong XN, Fan YC, Wang K. Treg/Th17 imbalance and its clinical significance in patients with hepatitis B-associated liver cirrhosis. *Diagn Pathol* 2019; **14**: 114 [PMID: 31639000 DOI: 10.1186/s13000-019-0891-4]

32 **Mou H**, Wu S, Zhao G, Wang J. Changes of Th17/Treg ratio in the transition of chronic hepatitis B to liver cirrhosis and correlations with liver function and inflammation. *Exp Ther Med* 2019; **17**: 2963-2968 [PMID: 30936966 DOI: 10.3892/etm.2019.7299]

33 **Zhang C**, Gao Y, Du C, Markowitz GJ, Fu J, Zhang Z, Liu C, Qin W, Wang H, Wang F, Yang P. Hepatitis B-Induced IL8 Promotes Hepatocellular Carcinoma Venous Metastasis and Intrahepatic Treg Accumulation. *Cancer Res* 2021; **81**: 2386-

2398 [PMID: 33653774 DOI: 10.1158/0008-5472.CAN-20-3453]
34 **Abd El-Ghani EH**, Afifi NA, Ibrahim MA, Zahran AM, El-Mokhtar MA, Mekky MA, Hetta HF. Regulatory T Cells and IL35 in Chronic Hepatitis C Related Cirrhosis and Hepatocellular Carcinoma. *Egypt J Immunol* 2021; **28**: 46-52 [PMID: 34147053]
35 **Schoenberg MB**, Li X, Han Y, Hao J, Miksch RC, Koch D, Börner N, Beger NT, Bucher JN, Schiergens TS, Guba MO, Werner J, Bazhin AV. The predictive value of tumor infiltrating leukocytes in Hepatocellular Carcinoma: A systematic review and meta-analysis. *Eur J Surg Oncol* 2021; **47**: 2561-2570 [PMID: 33966947 DOI: 10.1016/j.ejso.2021.04.042]
36 **Yu S**, Wang Y, Hou J, Li W, Wang X, Xiang L, Tan D, Wang W, Jiang L, Claret FX, Jiao M, Guo H. Tumor-infiltrating immune cells in hepatocellular carcinoma: Tregs is correlated with poor overall survival. *PLoS One* 2020; **15**: e0231003 [PMID: 32240238 DOI: 10.1371/journal.pone.0231003]
37 **Gao Y**, You M, Fu J, Tian M, Zhong X, Du C, Hong Z, Zhu Z, Liu J, Markowitz GJ, Wang FS, Yang P. Intratumoral stem-like CCR4+ regulatory T cells orchestrate the immunosuppressive microenvironment in HCC associated with hepatitis B. *J Hepatol* 2022; **76**: 148-159 [PMID: 34689996 DOI: 10.1016/j.jhep.2021.08.029]
38 **Zhou W**, Deng J, Chen Q, Li R, Xu X, Guan Y, Li W, Xiong X, Li H, Li J, Cai X. Expression of CD4+CD25+CD127^{Low} regulatory T cells and cytokines in peripheral blood of patients with primary liver carcinoma. *Int J Med Sci* 2020; **17**: 712-719 [PMID: 32218692 DOI: 10.7150/ijms.44088]
39 **Sun YF**, Wu L, Liu SP, Jiang MM, Hu B, Zhou KQ, Guo W, Xu Y, Zhong Y, Zhou XR, Zhang ZF, Liu G, Liu S, Shi YH, Ji Y, Du M, Li NN, Li GB, Zhao ZK, Huang XY, Xu LQ, Yu QC, Peng DH, Qiu SJ, Sun HC, Dean M, Wang XD, Chung WY, Dennison AR, Zhou J, Hou Y, Fan J, Yang XR. Dissecting spatial heterogeneity and the immune-evasion mechanism of CTCs by single-cell RNA-seq in hepatocellular carcinoma. *Nat Commun* 2021; **12**: 4091 [PMID: 34215748 DOI: 10.1038/s41467-021-24386-0]
40 **Zhou L**, Wang J, Lyu SC, Pan LC, Shi XJ, Du GS, He Q. PD-L1^{+}NEUT, Foxp3^{+}Treg, and NLR as New Prognostic Marker with Low Survival Benefits Value in Hepatocellular Carcinoma. *Technol Cancer Res Treat* 2021; **20**: 15330338211045820 [PMID: 34605709 DOI: 10.1177/15330338211045820]
41 **Zhou SL**, Zhou ZJ, Hu ZQ, Huang XW, Wang Z, Chen EB, Fan J, Cao Y, Dai Z, Zhou J. Tumor-Associated Neutrophils Recruit Macrophages and T-Regulatory Cells to Promote Progression of Hepatocellular Carcinoma and Resistance to Sorafenib. *Gastroenterology* 2016; **150**: 1646-1658.e17 [PMID: 26924089 DOI: 10.1053/j.gastro.2016.02.040]
42 **Chen X**, Du Y, Hu Q, Huang Z. Tumor-derived CD4+CD25+regulatory T cells inhibit dendritic cells function by CTLA-4. *Pathol Res Pract* 2017; **213**: 245-249 [PMID: 28214198 DOI: 10.1016/j.prp.2016.12.008]
43 **Kalathil SG**, Wang K, Hutson A, Iyer R, Thanavala Y. Tivozanib mediated inhibition of c-Kit/SCF signaling on Tregs and MDSCs and reversal of tumor induced immune suppression correlates with survival of HCC patients. *Oncoimmunology* 2020; **9**: 1824863 [PMID: 33101775 DOI: 10.1080/2162402X.2020.1824863]
44 **Yi C**, Chen L, Lin Z, Liu L, Shao W, Zhang R, Lin J, Zhang J, Zhu W, Jia H, Qin L, Lu L, Chen J. Lenvatinib Targets FGF Receptor 4 to Enhance Antitumor Immune Response of Anti-Programmed Cell Death-1 in HCC. *Hepatology* 2021; **74**: 2544-2560 [PMID: 34036623 DOI: 10.1002/hep.31921]
45 **Lee YH**, Tai D, Yip C, Choo SP, Chew V. Combinational Immunotherapy for Hepatocellular Carcinoma: Radiotherapy, Immune Checkpoint Blockade and Beyond. *Front Immunol* 2020; **11**: 568759 [PMID: 33117354 DOI: 10.3389/fimmu.2020.568759]
46 **Zhang Q**, He Y, Luo N, Patel SJ, Han Y, Gao R, Modak M, Carotta S, Haslinger C, Kind D, Peet GW, Zhong G, Lu S, Zhu W, Mao Y, Xiao M, Bergmann M, Hu X, Kerkar SP, Vogt AB, Pflanz S, Liu K, Peng J, Ren X, Zhang Z. Landscape and Dynamics of Single Immune Cells in Hepatocellular Carcinoma. *Cell* 2019; **179**: 829-845.e20 [PMID: 31675496 DOI: 10.1016/j.cell.2019.10.003]
47 **Wilson GK**, Tennant DA, McKeating JA. Hypoxia inducible factors in liver disease and hepatocellular carcinoma: current understanding and future directions. *J Hepatol* 2014; **61**: 1397-1406 [PMID: 25157983 DOI: 10.1016/j.jhep.2014.08.025]
48 **Guo Y**, Xiao Z, Yang L, Gao Y, Zhu Q, Hu L, Huang D, Xu Q. Hypoxiainducible factors in hepatocellular carcinoma (Review). *Oncol Rep* 2020; **43**: 3-15 [PMID: 31746396 DOI: 10.3892/or.2019.7397]
49 **Liu J**, Li W, Zhu W, He W, Zhao H, Xiang Y, Liu C, Wu W. Chronic intermittent hypoxia promotes the development of experimental non-alcoholic steatohepatitis by modulating Treg/Th17 differentiation. *Acta Biochim Biophys Sin (Shanghai)* 2018; **50**: 1200-1210 [PMID: 30379980 DOI: 10.1093/abbs/gmy131]
50 **Hu CC**, Jeng WJ, Chen YC, Fang JH, Huang CH, Teng W, Hsieh YC, Lin YC, Chien RN, Sheen IS, Lin CY. Memory Regulatory T cells Increase Only In Inflammatory Phase of Chronic Hepatitis B Infection and Related to Galectin-9/Tim-3 interaction. *Sci Rep* 2017; **7**: 15280 [PMID: 29127350 DOI: 10.1038/s41598-017-15527-x]
51 **Nebbia G**, Peppa D, Schurich A, Khanna P, Singh HD, Cheng Y, Rosenberg W, Dusheiko G, Gilson R, ChinAleong J, Kennedy P, Maini MK. Upregulation of the Tim-3/galectin-9 pathway of T cell exhaustion in chronic hepatitis B virus infection. *PLoS One* 2012; **7**: e47648 [PMID: 23112829 DOI: 10.1371/journal.pone.0047648]
52 **Ju Y**, Shang X, Liu Z, Zhang J, Li Y, Shen Y, Liu Y, Liu C, Liu B, Xu L, Wang Y, Zhang B, Zou J. The Tim-3/galectin-9 pathway involves in the homeostasis of hepatic Tregs in a mouse model of concanavalin A-induced hepatitis. *Mol Immunol* 2014; **58**: 85-91 [PMID: 24333756 DOI: 10.1016/j.molimm.2013.11.001]
53 **Wang Z**, He L, Li W, Xu C, Zhang J, Wang D, Dou K, Zhuang R, Jin B, Zhang W, Hao Q, Zhang K, Wang S, Gao Y, Gu J, Shang L, Tan Z, Su H, Zhang Y, Zhang C, Li M. GDF15 induces immunosuppression *via* CD48 on regulatory T cells in hepatocellular carcinoma. *J Immunother Cancer* 2021; **9** [PMID: 34489334 DOI: 10.1136/jitc-2021-002787]
54 **Li Y**, Jiang HT, Han LB, Xiao L, Gan JH. MiR-195 regulates CD40 to maintain Th17/Treg balance in rats with non-alcoholic fatty liver disease. *Biomed Pharmacother* 2020; **124**: 109930 [PMID: 31991386 DOI: 10.1016/j.biopha.2020.109930]
55 **Cai C**, Chen DZ, Tu HX, Chen WK, Ge LC, Fu TT, Tao Y, Ye SS, Li J, Lin Z, Wang XD, Xu LM, Chen YP. MicroRNA-29c Acting on FOS Plays a Significant Role in Nonalcoholic Steatohepatitis Through the Interleukin-17 Signaling Pathway. *Front Physiol* 2021; **12**: 597449 [PMID: 33927635 DOI: 10.3389/fphys.2021.597449]
56 **Xia G**, Wu S, Wang X, Fu M. Inhibition of microRNA-155 attenuates concanavalin-A-induced autoimmune hepatitis by regulating Treg/Th17 cell differentiation. *Can J Physiol Pharmacol* 2018; **96**: 1293-1300 [PMID: 30290123 DOI:

10.1139/cjpp-2018-0467]
57 **Liu N**, Chang CW, Steer CJ, Wang XW, Song G. MicroRNA-15a/16-1 Prevents Hepatocellular Carcinoma by Disrupting the Communication Between Kupffer Cells and Regulatory T Cells. *Gastroenterology* 2022; **162**: 575-589 [PMID: 34678217 DOI: 10.1053/j.gastro.2021.10.015]
58 **Yu Z**, Zhao H, Feng X, Li H, Qiu C, Yi X, Tang H, Zhang J. Long Non-coding RNA FENDRR Acts as a miR-423-5p Sponge to Suppress the Treg-Mediated Immune Escape of Hepatocellular Carcinoma Cells. *Mol Ther Nucleic Acids* 2019; **17**: 516-529 [PMID: 31351327 DOI: 10.1016/j.omtn.2019.05.027]
59 **Xie K**, Liu L, Chen J, Liu F. Exosomal miR-1246 derived from human umbilical cord blood mesenchymal stem cells attenuates hepatic ischemia reperfusion injury by modulating T helper 17/regulatory T balance. *IUBMB Life* 2019; **71**: 2020-2030 [PMID: 31433911 DOI: 10.1002/iub.2147]
60 **Pasare C**, Medzhitov R. Toll pathway-dependent blockade of CD4+CD25+ T cell-mediated suppression by dendritic cells. *Science* 2003; **299**: 1033-1036 [PMID: 12532024 DOI: 10.1126/science.1078231]
61 **Hall JA**, Bouladoux N, Sun CM, Wohlfert EA, Blank RB, Zhu Q, Grigg ME, Berzofsky JA, Belkaid Y. Commensal DNA limits regulatory T cell conversion and is a natural adjuvant of intestinal immune responses. *Immunity* 2008; **29**: 637-649 [PMID: 18835196 DOI: 10.1016/j.immuni.2008.08.009]
62 **Ni X**, Tao J, Barbi J, Chen Q, Park BV, Li Z, Zhang N, Lebid A, Ramaswamy A, Wei P, Zheng Y, Zhang X, Wu X, Vignali P, Yang CP, Li H, Pardoll D, Lu L, Pan D, Pan F. YAP Is Essential for Treg-Mediated Suppression of Antitumor Immunity. *Cancer Discov* 2018; **8**: 1026-1043 [PMID: 29907586 DOI: 10.1158/2159-8290.CD-17-1124]
63 **Polanczyk MJ**, Walker E, Haley D, Guerrouahen BS, Akporiaye ET. Blockade of TGF-β signaling to enhance the antitumor response is accompanied by dysregulation of the functional activity of $CD4^+CD25^+Foxp3^+$ and $CD4^+CD25^-Foxp3^+$ T cells. *J Transl Med* 2019; **17**: 219 [PMID: 31288845 DOI: 10.1186/s12967-019-1967-3]
64 **Badr AM**, El-Ahwany E, Goda L, Nagy F, Helal N, El Deeb S. MicroRNA-26a systemic administration attenuates tumor formation in hepatocellular carcinoma mouse model. *Pak J Pharm Sci* 2021; **34**: 925-932 [PMID: 34602415]
65 **Yang X**, Liang L, Zhang XF, Jia HL, Qin Y, Zhu XC, Gao XM, Qiao P, Zheng Y, Sheng YY, Wei JW, Zhou HJ, Ren N, Ye QH, Dong QZ, Qin LX. MicroRNA-26a suppresses tumor growth and metastasis of human hepatocellular carcinoma by targeting interleukin-6-Stat3 pathway. *Hepatology* 2013; **58**: 158-170 [PMID: 23389848 DOI: 10.1002/hep.26305]
66 **Yang X**, Zhang XF, Lu X, Jia HL, Liang L, Dong QZ, Ye QH, Qin LX. MicroRNA-26a suppresses angiogenesis in human hepatocellular carcinoma by targeting hepatocyte growth factor-cMet pathway. *Hepatology* 2014; **59**: 1874-1885 [PMID: 24259426 DOI: 10.1002/hep.26941]
67 **Ma Y**, Deng F, Li P, Chen G, Tao Y, Wang H. The tumor suppressive miR-26a regulation of FBXO11 inhibits proliferation, migration and invasion of hepatocellular carcinoma cells. *Biomed Pharmacother* 2018; **101**: 648-655 [PMID: 29518611 DOI: 10.1016/j.biopha.2018.02.118]
68 **Wang X**, Sun L, Zhang L, Jiang Z. Effect of Adoptive Transfer or Depletion of Regulatory T Cells on Triptolide-induced Liver Injury. *Front Pharmacol* 2016; **7**: 99 [PMID: 27148057 DOI: 10.3389/fphar.2016.00099]
69 **Huang H**, Deng Z. Adoptive transfer of regulatory T cells stimulated by Allogeneic Hepatic Stellate Cells mitigates liver injury in mice with concanavalin A-induced autoimmune hepatitis. *Biochem Biophys Res Commun* 2019; **512**: 14-21 [PMID: 30853178 DOI: 10.1016/j.bbrc.2019.02.147]
70 **Feng M**, Wang Q, Jiang Z, Ding J, Wang H, Wang M, Lu L, Guan W. Adoptive transferred hepatic stellate cells attenuated drug-induced liver injury by modulating the rate of regulatory T cells/T helper 17 cells. *Clin Immunol* 2016; **165**: 12-18 [PMID: 26911201 DOI: 10.1016/j.clim.2016.02.006]
71 **Kehrmann J**, Effenberg L, Wilk C, Schoemer D, Ngo Thi Phuong N, Adamczyk A, Pastille E, Scholtysik R, Klein-Hitpass L, Klopfleisch R, Westendorf AM, Buer J. Depletion of $Foxp3^+$ regulatory T cells is accompanied by an increase in the relative abundance of Firmicutes in the murine gut microbiome. *Immunology* 2020; **159**: 344-353 [PMID: 31755554 DOI: 10.1111/imm.13158]
72 **Wang Y**, Liu Y, Kirpich I, Ma Z, Wang C, Zhang M, Suttles J, McClain C, Feng W. Lactobacillus rhamnosus GG reduces hepatic TNFα production and inflammation in chronic alcohol-induced liver injury. *J Nutr Biochem* 2013; **24**: 1609-1615 [PMID: 23618528 DOI: 10.1016/j.jnutbio.2013.02.001]
73 **Wang Y**, Liu Y, Sidhu A, Ma Z, McClain C, Feng W. Lactobacillus rhamnosus GG culture supernatant ameliorates acute alcohol-induced intestinal permeability and liver injury. *Am J Physiol Gastrointest Liver Physiol* 2012; **303**: G32-G41 [PMID: 22538402 DOI: 10.1152/ajpgi.00024.2012]
74 **Li J**, Sung CY, Lee N, Ni Y, Pihlajamäki J, Panagiotou G, El-Nezami H. Probiotics modulated gut microbiota suppresses hepatocellular carcinoma growth in mice. *Proc Natl Acad Sci U S A* 2016; **113**: E1306-E1315 [PMID: 26884164 DOI: 10.1073/pnas.1518189113]
75 **Shigeta K**, Datta M, Hato T, Kitahara S, Chen IX, Matsui A, Kikuchi H, Mamessier E, Aoki S, Ramjiawan RR, Ochiai H, Bardeesy N, Huang P, Cobbold M, Zhu AX, Jain RK, Duda DG. Dual Programmed Death Receptor-1 and Vascular Endothelial Growth Factor Receptor-2 Blockade Promotes Vascular Normalization and Enhances Antitumor Immune Responses in Hepatocellular Carcinoma. *Hepatology* 2020; **71**: 1247-1261 [PMID: 31378984 DOI: 10.1002/hep.30889]
76 **Langhans B**, Nischalke HD, Krämer B, Dold L, Lutz P, Mohr R, Vogt A, Toma M, Eis-Hübinger AM, Nattermann J, Strassburg CP, Gonzalez-Carmona MA, Spengler U. Role of regulatory T cells and checkpoint inhibition in hepatocellular carcinoma. *Cancer Immunol Immunother* 2019; **68**: 2055-2066 [PMID: 31724091 DOI: 10.1007/s00262-019-02427-4]
77 **Lee JC**, Mehdizadeh S, Smith J, Young A, Mufazalov IA, Mowery CT, Daud A, Bluestone JA. Regulatory T cell control of systemic immunity and immunotherapy response in liver metastasis. *Sci Immunol* 2020; **5** [PMID: 33008914 DOI: 10.1126/sciimmunol.aba0759]
78 **Doi T**, Muro K, Ishii H, Kato T, Tsushima T, Takenoyama M, Oizumi S, Gemmoto K, Suna H, Enokitani K, Kawakami T, Nishikawa H, Yamamoto N. A Phase I Study of the Anti-CC Chemokine Receptor 4 Antibody, Mogamulizumab, in Combination with Nivolumab in Patients with Advanced or Metastatic Solid Tumors. *Clin Cancer Res* 2019; **25**: 6614-6622 [PMID: 31455681 DOI: 10.1158/1078-0432.CCR-19-1090]
79 **Zhang Q**, Huang H, Zheng F, Liu H, Qiu F, Chen Y, Liang CL, Dai Z. Resveratrol exerts antitumor effects by downregulating $CD8^+CD122^+$ Tregs in murine hepatocellular carcinoma. *Oncoimmunology* 2020; **9**: 1829346 [PMID:

33150044 DOI: 10.1080/2162402X.2020.1829346]

80 **Ren Z**, Yue Y, Zhang Y, Dong J, Liu Y, Yang X, Lin X, Zhao X, Wei Z, Zheng Y, Wang T. Changes in the Peripheral Blood Treg Cell Proportion in Hepatocellular Carcinoma Patients After Transarterial Chemoembolization With Microparticles. *Front Immunol* 2021; **12**: 624789 [PMID: 33717135 DOI: 10.3389/fimmu.2021.624789]

81 **Jhun J**, Lee SH, Lee SK, Kim HY, Jung ES, Kim DG, Choi J, Bae SH, Yoon SK, Chung BH, Yang CW, Cho ML, Choi JY. Serial Monitoring of Immune Markers Being Represented Regulatory T Cell/T Helper 17 Cell Ratio: Indicating Tolerance for Tapering Immunosuppression after Liver Transplantation. *Front Immunol* 2018; **9**: 352 [PMID: 29545795 DOI: 10.3389/fimmu.2018.00352]

82 **Knochelmann HM**, Dwyer CJ, Bailey SR, Amaya SM, Elston DM, Mazza-McCrann JM, Paulos CM. When worlds collide: Th17 and Treg cells in cancer and autoimmunity. *Cell Mol Immunol* 2018; **15**: 458-469 [PMID: 29563615 DOI: 10.1038/s41423-018-0004-4]

83 **Sánchez-Fueyo A**, Whitehouse G, Grageda N, Cramp ME, Lim TY, Romano M, Thirkell S, Lowe K, Fry L, Heward J, Kerr A, Ali J, Fisher C, Lewis G, Hope A, Kodela E, Lyne M, Farzaneh F, Kordasti S, Rebollo-Mesa I, Jose Lozano J, Safinia N, Heaton N, Lechler R, Martínez-Llordella M, Lombardi G. Applicability, safety, and biological activity of regulatory T cell therapy in liver transplantation. *Am J Transplant* 2020; **20**: 1125-1136 [PMID: 31715056 DOI: 10.1111/ajt.15700]

84 **Whitehouse GP**, Hope A, Sanchez-Fueyo A. Regulatory T-cell therapy in liver transplantation. *Transpl Int* 2017; **30**: 776-784 [PMID: 28608637 DOI: 10.1111/tri.12998]

85 **Cvetkovski F**, Hexham JM, Berglund E. Strategies for Liver Transplantation Tolerance. *Int J Mol Sci* 2021; **22** [PMID: 33668238 DOI: 10.3390/ijms22052253]

86 **Casiraghi F**, Perico N, Podestà MA, Todeschini M, Zambelli M, Colledan M, Camagni S, Fagiuoli S, Pinna AD, Cescon M, Bertuzzo V, Maroni L, Introna M, Capelli C, Golay JT, Buzzi M, Mister M, Ordonez PYR, Breno M, Mele C, Villa A, Remuzzi G; MSC-LIVER Study Group. Third-party bone marrow-derived mesenchymal stromal cell infusion before liver transplantation: A randomized controlled trial. *Am J Transplant* 2021; **21**: 2795-2809 [PMID: 33370477 DOI: 10.1111/ajt.16468]

87 **Han JW**, Sung PS, Hong SH, Lee H, Koh JY, White S, Maslow JN, Weiner DB, Park SH, Jeong M, Heo J, Ahn SH, Shin EC. IFNL3-adjuvanted HCV DNA vaccine reduces regulatory T cell frequency and increases virus-specific T cell responses. *J Hepatol* 2020; **73**: 72-83 [PMID: 32088322 DOI: 10.1016/j.jhep.2020.02.009]

88 **Boni C**, Janssen HLA, Rossi M, Yoon SK, Vecchi A, Barili V, Yoshida EM, Trinh H, Rodell TC, Laccabue D, Alfieri A, Brillo F, Fisicaro P, Acerbi G, Pedrazzi G, Andreone P, Cursaro C, Margotti M, Santoro R, Piazzolla V, Brunetto MR, Coco B, Cavallone D, Zhao Y, Joshi A, Woo J, Lau AH, Gaggar A, Subramanian GM, Massetto B, Fung S, Ahn SH, Ma X, Mangia A, Ferrari C. Combined GS-4774 and Tenofovir Therapy Can Improve HBV-Specific T-Cell Responses in Patients With Chronic Hepatitis. *Gastroenterology* 2019; **157**: 227-241.e7 [PMID: 30930022 DOI: 10.1053/j.gastro.2019.03.044]

89 **Wu D**, Wang P, Han M, Chen Y, Chen X, Xia Q, Yan W, Wan X, Zhu C, Xie Q, Jiang J, Wei L, Tan D, Dou X, Yu Y, Hou J, Luo X, Ning Q. Sequential combination therapy with interferon, interleukin-2 and therapeutic vaccine in entecavir-suppressed chronic hepatitis B patients: the Endeavor study. *Hepatol Int* 2019; **13**: 573-586 [PMID: 31172415 DOI: 10.1007/s12072-019-09956-1]

90 **Kalathil SG**, Hutson A, Barbi J, Iyer R, Thanavala Y. Augmentation of IFN-γ+ CD8+ T cell responses correlates with survival of HCC patients on sorafenib therapy. *JCI Insight* 2019; **4** [PMID: 31391334 DOI: 10.1172/jci.insight.130116]

World Journal of Gastroenterology

Submit a Manuscript: https://www.f6publishing.com

World J Gastroenterol 2022 July 21; 28(27): 3359-3369

DOI: 10.3748/wjg.v28.i27.3359

ISSN 1007-9327 (print) ISSN 2219-2840 (online)

MINIREVIEWS

Single-incision laparoscopic surgery to treat hepatopancreatobiliary cancer: A technical review

Shu-Hung Chuang, Shih-Chang Chuang

Specialty type: Surgery

Provenance and peer review: Invited article; Externally peer reviewed.

Peer-review model: Single blind

Peer-review report's scientific quality classification

Grade A (Excellent): 0
Grade B (Very good): B, B
Grade C (Good): 0
Grade D (Fair): 0
Grade E (Poor): 0

P-Reviewer: A JD, China; Hiep LT, Viet Nam

Received: January 17, 2022
Peer-review started: January 17, 2022
First decision: March 9, 2022
Revised: March 20, 2022
Accepted: June 16, 2022
Article in press: June 16, 2022
Published online: July 21, 2022

Shu-Hung Chuang, Shih-Chang Chuang, Division of General and Digestive Surgery, Department of Surgery, Kaohsiung Medical University Hospital, Kaohsiung Medical University, Kaohsiung 80708, Taiwan

Shu-Hung Chuang, Shih-Chang Chuang, School of Medicine, College of Medicine, Kaohsiung Medical University, Kaohsiung 80708, Taiwan

Corresponding author: Shih-Chang Chuang, MD, PhD, Associate Professor, Director, Surgeon, Surgical Oncologist, Division of General and Digestive Surgery, Department of Surgery, Kaohsiung Medical University Hospital, Kaohsiung Medical University, No. 100 Shih-Chuan 1st Road, Sanmin District, Kaohsiung 80708, Taiwan. chuangsc@cc.kmu.edu.tw

Abstract

Single-incision laparoscopic surgery (SILS), or laparoendoscopic single-site surgery, was launched to minimize incisional traumatic effects in the 1990s. Minor SILS, such as cholecystectomies, have been gaining in popularity over the past few decades. Its application in complicated hepatopancreatobiliary (HPB) surgeries, however, has made slow progress due to instrumental and technical limitations, costs, and safety concerns. While minimally invasive abdominal surgery is pushing the boundaries, advanced laparoscopic HPB surgeries have been shown to be comparable to open operations in terms of patient and oncologic safety, including hepatectomies, distal pancreatectomies (DP), and pancreaticoduodenectomies (PD). In contrast, advanced SILS for HPB malignancy has only been reported in a few small case series. Most of the procedures involved minor liver resections and DP; major hepatectomies were rarely described. Single-incision laparoscopic PD has not yet been reported. We herein review the published SILS for HPB cancer in the literature and our three-year experience focusing on the technical aspects.

Key Words: Hepatectomy; Hepatopancreatobiliary cancer; Laparoendoscopic single-site surgery; Pancreatectomy; Pancreaticoduodenectomy; Single-incision laparoscopic surgery

Core Tip: Single-incision laparoscopic surgery (SILS), or laparoendoscopic single-site surgery, has been introduced to minimize incisional traumatic effects over the past few decades. As minor SILS, such as cholecystectomies, have been gaining in popularity, major SILS for complicated hepatopancreatobiliary (HPB) surgeries have made slow progress due to instrumental and technical limitations, costs, and safety concerns. We herein review the published SILS for HPB cancer in the literature and our three-year experience focusing on the technical aspects.

Citation: Chuang SH, Chuang SC. Single-incision laparoscopic surgery to treat hepatopancreatobiliary cancer: A technical review. *World J Gastroenterol* 2022; 28(27): 3359-3369
URL: https://www.wjgnet.com/1007-9327/full/v28/i27/3359.htm
DOI: https://dx.doi.org/10.3748/wjg.v28.i27.3359

INTRODUCTION

Single-incision laparoscopic surgery (SILS), also known as laparoendoscopic single-site surgery, is an advanced minimally invasive procedure that leaves a single small incision after surgery. Since it was introduced in the 1990s, numerous studies regarding SILS for minor procedures have been published, such as for cholecystectomy[1]. In contrast, its application in advanced hepatopancreatobiliary (HPB) surgeries is rarely reported[2-8].

By minimizing the incision number, SILS has the potential advantages of less pain, fewer wound complications, faster recovery, and favorable cosmesis. Nevertheless, the existing literature regarding minor SILS fails to reach a conclusion. For example, single-incision laparoscopic cholecystectomies (SILC), the most published SILS to date, have been shown to be superior in marginal benefits such as less pain and shorter hospital stays, while incisional hernia and bile duct injury are considerable drawbacks[9-11]. Nevertheless, it is always necessary to remove a sizable specimen during advanced HPB surgeries. One of the small incisions in standard multi-incision laparoscopic surgeries (MILS) has to be enlarged to fit the specimen size as well as the only incision in SILS. Since incisional hernia has become a minor issue, patient and oncologic safety has attracted more concern in advanced single-incision laparoscopic HPB surgeries. MILS has been shown to be comparable to open operations for HPB malignancy, including hepatectomies, distal pancreatectomies (DP), and pancreaticoduodenectomies (PD), in recent years[12-24]. The fact that only a few case series of SILS for HPB cancer have been reported reflects the limitations of surgical techniques, instrumental technology, and adequate training. Although our previous study showed that practicing minor SILS helps to achieve competence in this technique for complicated diseases[25], there is still a long way to go. In this review, we conducted an updated literature search for SILS to treat malignant HPB diseases that were reported in English. Studies involving robotic technology were excluded. Meanwhile, a summary of our three-year experience focusing on the technical aspects was described.

SINGLE-INCISION LAPAROSCOPIC HEPATECTOMY (SILH) FOR MALIGNANCY

Literature review

Eight original studies[26-33] and 20 case reports[34-47] were identified with a cutoff value of 10 malignant cases. The outdated reports of sequential studies from the same groups were excluded. Nearly all the case reports involved minor liver resections [partial hepatectomies, monosegmentectomies, and left lateral sectionectomies (LLS)]. Three of the eight original articles described major hepatectomies (resection of over two segments), including nine right hemihepatectomies (RHs), 34 left hemihepatectomies, and seven right posterior sectionectomies (RPSs)[27,29,32] (Table 1). Most procedures were performed for malignant diseases. Five nonrandomized comparative studies between SILH and multi-incision laparoscopic hepatectomies (MILHs) were conducted[26-28,30,32]. Hyun *et al*[26] reported a shorter postoperative hospital stay and comparable pathologic features for minor SILH compared with minor MILH; long-term survival outcomes were absent. Mittermair *et al*[27] showed less blood loss, a lower number of patients with blood loss > 25 mL, and more blood transfusions in the major SILH group; no local tumor recurrence occurred during a median follow-up of 61 mo. Tsai *et al*[28] reported a shorter operative time and shorter postoperative hospital stays in the SILH group for LLS but not partial hepatectomies of segment 5-6; the 1-, 3-, and 5-year overall and recurrence-free survival rates for hepatocellular carcinoma were similar in both the SILH and MILH groups. Wang *et al*[30] showed shorter postoperative hospital stays for patients without cirrhosis undergoing LLS in the SILH group; the 1-year recurrence-free survival rates for hepatocellular carcinoma were similar in both the SILH and MILH groups. Han *et al*[32] reported a shorter operative time, less blood loss, and earlier

Table 1 English original researches of single-incision laparoscopic hepatectomies for malignancy retrieved online till December 2021

Ref.	Journal (year of publication)	SILH	Control group	RH	LH	RAS	RPS	LLS + MR
Hyun *et al*[26]	*J Gastrointest Surg* (2021)	15	MILH	0	0	0	0	15
Mittermair *et al*[27]	*J Clin Med* (2021)	34	MILH	4	6	0	7	17
Tsai *et al*[28]	*Surg Endosc* (2020)	54	MILH	0	0	0	0	54
Saad *et al*[29]	*ANZ J Surg* (2020)	54	No	0	11	0	0	43
Wang *et al*[30]	*Int J Surg* (2020)	33	MILH	0	0	0	0	33
Pan *et al*[31]	*Surg Laparosc Endosc Percutan Tech* (2019)	37	No	0	0	0	0	37
Han *et al*[32]	*World J Gastroenterol* (2018)	155	MILH	5	17	0	0	133
Weiss *et al*[33]	*J Hepatobiliary Pancreat Sci* (2015)	21	No	0	0	0	0	21
Our study	Under submission	31	No	3	2	3	3	20

SILH: Single-incision laparoscopic hepatectomies; MILH: Multi-incision laparoscopic hepatectomies; RH: Right hemihepatectomies; LH: Left hemihepatectomies; RAS: Right anterior sectionectomies; RPS: Right posterior sectionectomies; LLS: Left lateral sectionectomies; MR: Minor resections including monosegmentectomies and partial hepatectomies.

enteral feeding in the SILH group; the safety resection margins were similar in both the SILH and MILH groups. However, long-term survival outcomes were not presented.

In summary, SILH was superior to MILH in terms of shorter postoperative hospital stays in three comparative studies of minor liver resections[26,28,30]. For major hepatectomies, the two related studies came to a different conclusion. While Mittermair C *et al*[27] declared more substantial blood loss requiring transfusion in SILH, Han *et al*[32] reported a shorter operative time, less blood loss, and earlier enteral feeding for the single port technique.

Our experience and technical review

While SILC[25] and single-incision laparoscopic common bile duct exploration (SILCBD)[48] have become our standard of care for cholelithiasis over the past decade, we have developed more advanced SILS for malignant HPB diseases since 2016. The principles of standard MILS and surgical oncology were strictly followed to maintain a high standard of patient safety and prognosis. From July 2018 to July 2021, 31 SILH procedures were performed by the first author to treat malignant diseases (Table 1). Eleven (35.5%) major liver resections involved three RHs, two left hemohepatectomies (LHs), three right anterior sectionectomies (RASs), and three RPSs. The others were 20 (64.5%) minor resections. An additional port was needed in five (16.1%) procedures, and no open conversion occurred. There was one case of surgery-related 90-d mortality due to pulmonary infection.

Patient position

During formal hepatic surgery, the patient was placed in a reverse Trendelenburg position with arms abducted and legs split. The surgeon stood between the patient's legs to facilitate hepatic hilar management. The assistant held the laparoscope at the patient's left/right side (between the left/right limbs) during right/Left hepatic resections. For LLS, the operative table could be tilted toward the patient's right side. In contrast, it should be tilted toward the patient's left side during RPS. Lateral decubitus positions were not favored because of impaired access to the hepatic hilum.

Port and instrument

By using conventional laparoscopic ports and straight instruments through a 1.5-2.5 cm skin incision and multiple nearby punctures on the deep fascia, the costs can be reduced to a minimum. This single-incision multipuncture approach is only suitable for short-duration procedures such as SILC[25], SILCBDE[48], and minor SILH because of its inherent problem of air leakage. Otherwise, a 3-6 cm single skin and deep fascia incision with a homemade (surgical glove) or commercial multichannel port is recommended for major liver resections to remove a sizable specimen at the end of surgery.

We recommended 30° rigid laparoscopes and conventional straight instruments, as the latter could be manipulated more intuitively than curved or articulated instruments. A 5-mm 30° bariatric laparoscope can effectively prevent "sword fighting" between the light cable of the laparoscope and the instrument handles (Figure 1). The port configuration was arranged in a reverse triangular pattern (Figure 2). The 30° laparoscope passed through the lower port and the fulcrum to the upper part of the operative field to provide an overlooking view, and the two working instruments reached the lower part of the

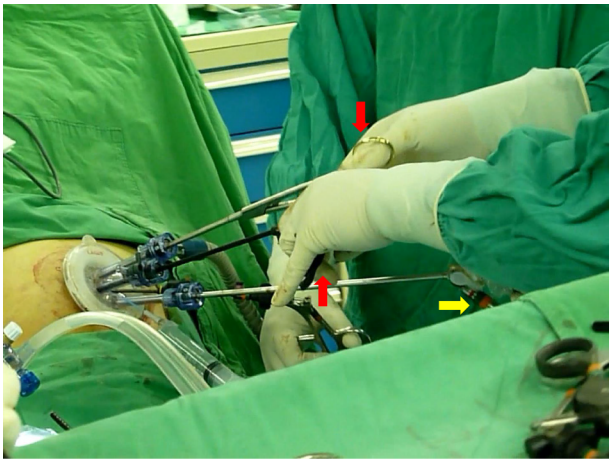

DOI: 10.3748/wjg.v28.i27.3359 **Copyright** ©The Author(s) 2022.

Figure 1 The 5-mm 30° bariatric laparoscope effectively prevented "sword fighting" between the light cable (yellow arrow) of the laparoscope and the instrument handles (red arrows) in single-incision laparoscopic surgery.

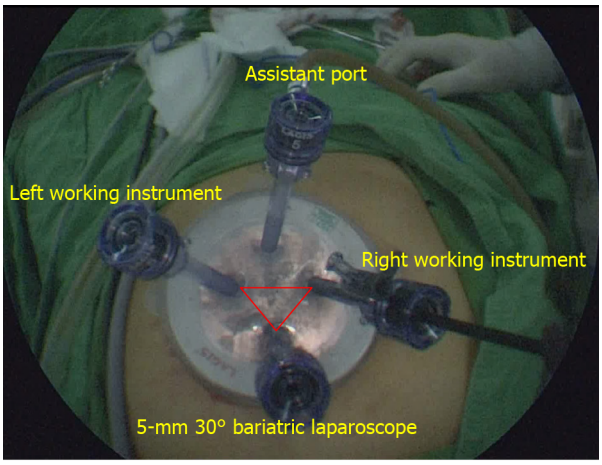

DOI: 10.3748/wjg.v28.i27.3359 **Copyright** ©The Author(s) 2022.

Figure 2 The port configuration was arranged in a reverse triangular pattern on a commercial multichannel port in a single-incision laparoscopic surgery. The upper port served as an assistant port for additional traction or suction/irrigation.

operative field to perform the procedure. This configuration decreased collisions between the laparoscope and the working instruments. Finally, a fourth port could be used to perform traction or suction.

Abdominal incision

Considering that upper abdominal incisions induce more pain, we avoided making incisions above the umbilical level. A praumbilical incision with downward extension is good for performing single-incision laparoscopic LH or RH. Otherwise, a transverse incision at the same level of the umbilicus is suitable to perform single-incision laparoscopic RAS or RPS. The incision should be tailored to the specimen size for its removal.

Hepatic inflow control

For temporary hepatic inflow control (Pringle maneuver), we favored the use of a 14-French Foley catheter (Figure 3), which was introduced by Huang *et al*[49] in 2018. During selective inflow control for major SILH, such as the extra Glissonian approach or individual dissection, a laparoscopic right angle dissector or a goldfinger retractor is useful. As the working instruments were kept aligned with the laparoscope in SILH, it was difficult to see the distal ends of the instruments. Laparoscopic working instruments with curved or flexible ends were easier to manipulate under limited vision.

Parenchymal transection

To avoid interinstrumental collisions, auxiliary traction devices substituted for assistant tractions. We preferred EndoGrab™ (Virtual Ports Ltd., Hod Hasharon, Israel), while gravity would provide counter-

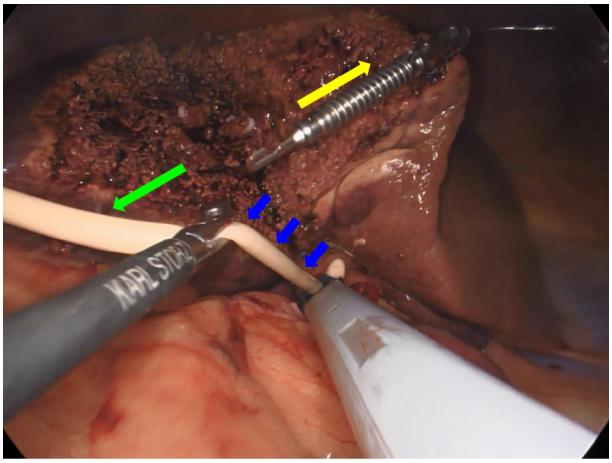

DOI: 10.3748/wjg.v28.i27.3359

Figure 3 The hepatoduodenal ligament was encircled by a 14-French Foley catheter (blue arrows) for temporary hepatic inflow control (Pringle maneuver) in a single-incision laparoscopic right posterior sectionectomy. An EndoGrab™ (Virtual Ports Ltd., Hod Hasharon, Israel) provided traction in the direction of the yellow arrow, while gravity created countertraction (green arrow).

traction in some instances (Figure 3). The transection line should be kept aligned with the laparoscopic view at all times.

Single-incision laparoscopic suturing technique

Suturing is the last line of defense in patient safety for not only open but also laparoscopic surgeries. It can be applied in various difficult situations to stop bleeding or biliary leakage. While performing single-incision laparoscopic suturing technique (SILST), forward-backward, vertical, and rotational movements are frequently used rather than transverse movements. The curved tip of a Maryland dissector helps to form a loop made by two instruments nearly parallel to each other (Figure 4). In addition, monofilament threads make loops more easily in SILST due to their high elasticity.

SINGLE-INCISION LAPAROSCOPIC PANCREATECTOMY FOR MALIGNANCY

Literature review

While most reported single-incision laparoscopic DP (SILDP) was used to treat benign lesions, only three original studies[50-52] (Table 2) and three case reports[53-55] of SILDP for cancer were identified with a cutoff value of 10 cases. Series containing neoplasms with uncertain behavior were excluded, as well as outdated reports of sequential studies from the same groups. All three original studies were nonrandomized comparative studies. SILDP was compared with multi-incision laparoscopic DP (MILDP) in two studies and the robotic approach in the remaining study. SILDP was associated with a longer operative time, reduced postoperative pain, and lower spleen/splenic vessel preservation rates than MILDP[50,51]. Robotic DP and splenectomies required a longer operating room time than SILDP and splenectomies, but the operative durations were similar[52]. All the patients except one undergoing DP for neoplasms had R0 resections, and six (7 ± 6.6) lymph nodes were noted according to the pathologic reports. However, long-term survival outcomes were not provided.

For PD, one of the most complicated abdominal surgeries, we could not find any report of applying a single-incision laparoscopic technique.

Our experience and technical review

We have no experience in performing SILDP for malignancy. Two patients with benign lesions (serous cystadenoma) underwent this procedure in the last two years. However, we have performed single-incision laparoscopic PD (SILPD) on three patients since May 2020. All procedures were accomplished successfully without conversion to MILS or open operations. No major complications, such as postoperative pancreatic fistula, occurred, and there was no 90-day mortality. The pathology report was distal cholangiocarcinoma in the first patient and pancreatic ductal adenocarcinoma in the other two. Routine D2 Lymph node dissections and intraoperative frozen sections for checking resection margins were carried out for oncologic safety. To the best of our knowledge, this report is the first experience of SILPD in the world and is now under submission.

Table 2 English original researches of single-incision laparoscopic pancreatectomies for malignancy retrieved online till December 2021

Ref.	Journal (year of publication)	Procedure	Case number	Control group	Spleen preservation
Park *et al*[50]	*Hepatobiliary Pancreat Sci* (2019)	SILDP	26	MILDP	0[1]
Ağcaoğlu *et al*[51]	*Sisli Etfal Hastan Tip Bul* (2019)	SILDP	10	MILDP	1
Ryan *et al*[52]	*JSLS* (2015)	SILDPS	16	RDPS	N/A

[1]Splenic vessel preservation.

SILDP: Single-incision laparoscopic distal pancreatectomies; MILDP: Multi-incision laparoscopic distal pancreatectomies; SILDPS: Single-incision laparoscopic distal pancreatectomies and splenectomies; RDPS: Robotic distal pancreatectomies and splenectomies; N/A: Not applicable.

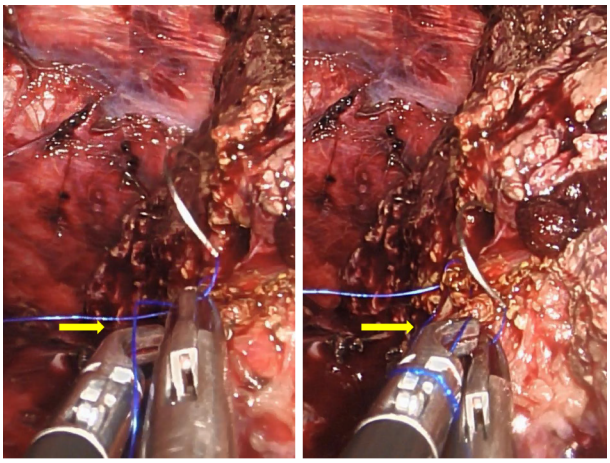

DOI: 10.3748/wjg.v28.i27.3359

Figure 4 The curved tip of a Maryland dissector (yellow arrow) helped to form a loop made by two instruments nearly parallel to each other in a single-incision laparoscopic surgery. A monofilament thread was used in this case.

Patient position

During a single-incision laparoscopic pancreatectomy, the patient was placed in a reverse Trendelenburg position with the surgeon standing between their legs. The operative table could be tilted toward the patient's right side for SILDP. The assistant held the laparoscope at the patient's left side (between the left limbs) during the resection phase and hepaticojejunostomy during SILPD. In contrast, the assistant held the laparoscope at the patient's right side (between the right limbs) during SILDP and pancreaticojejunostomy/gastrojejunostomy in SILPD.

Port and instrument

Major pancreatic and hepatic resections shared the same port configuration and instrument selection. Sometimes the surgeon had to cross the instruments to achieve an adequate approaching angle (the angle between the two working instruments) or solve a handedness problem, such as suturing a left target with a right-handed instrument.

Abdominal incision

In order to achieve less pain and better cosmesis, a several centimeter praumbilical incision with downward extension is good for performing a SILDP or a SILPD. The incision should be enlarged to facilitate specimen removal in a retrieval bag at the end of surgery if necessary.

Auxiliary traction

EndoGrab™ (Virtual Ports Ltd., Hod Hasharon, Israel) could be applied on the duodenum to be resected during the uncinate process dissection in a SILPD (Figure 5A). It was very useful for liver retraction during SILDP or SILPD (Figure 5B).

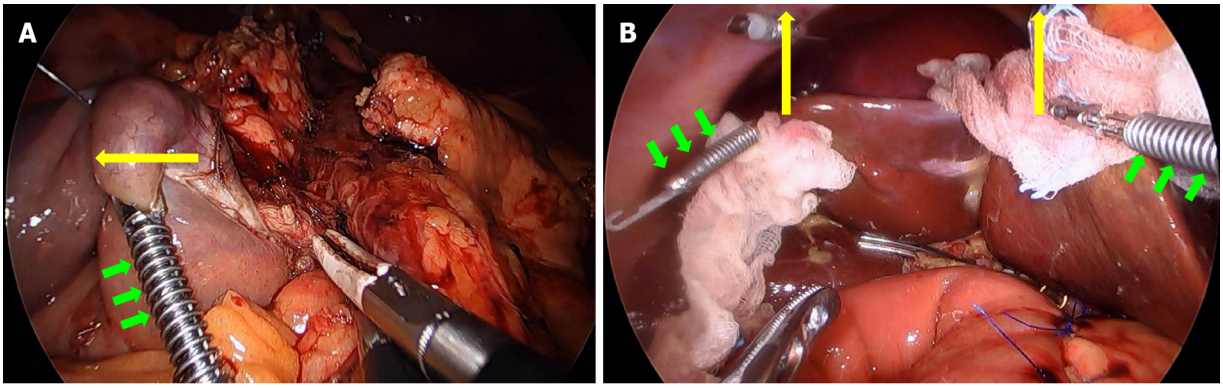

DOI: 10.3748/wjg.v28.i27.3359

Figure 5 EndoGrab™ (Virtual Ports Ltd., Hod Hasharon, Israel) provided auxiliary traction during single-incision laparoscopic pancreatectomies. A: EndoGrab™ (green arrows) was applied on the duodenal 3rd portion to provide lateral traction (yellow arrow) during the uncinate process dissection in a single-incision laparoscopic pancreaticoduodenectomy (SILPD); B: Two EndoGrabs™ (green arrows) facilitated upward traction (yellow arrows) of the liver edges during the reconstruction phase in a SILPD. Two pieces of gauze served as cushions to minimize the traumatic effect of EndoGrabs™ (green arrows) on the liver.

SILST

Unlike hepatectomies, suturing constituted a major component in pancreatic resections, such as hemostasis (Video 1), closure of the pancreatic stump in a DP and creation of the three anastomoses (pancreaticojejunostomy, hepaticojejunostomy, and gastrojejunostomy) in a PD. During critical duct-to-mucosa pancreaticojejunostomy, we recommend interrupted suturing for the inner layer to prevent anastomotic stricture caused by a "purse-string effect". Holding the interrupted stitches with metallic clips before tying them helped to gain adequate space for the anastomosis. In our experience, up to three metallic clips could be used simultaneously during anastomosis without confusing the surgeon (Figure 6). While performing SILST, all the principles of suturing in open surgery and MILS should be followed on the basis of high quality. Otherwise, additional port(s) should be utilized to minimize anastomotic leakage.

Step-by-step procedures in SILPD

While the laparoscopic view was unchanged during SILPD, the procedural steps were standardized to shorten the operative time as well as the learning curve. These steps include division of the gastrocolic ligament, release of the hepatic flexure of the transverse colon, Kocher maneuver (Station 13 Lymph nodes harvest), division of Treitz's ligament, pulling of the proximal jejunum to the patient's right side, creation of the tunnel under the pancreatic neck, division of the proximal jejunum and its mesentery, division of the lesser omentum and distal stomach (Station 5 and 6 Lymph node harvest), division of the pancreatic neck, dissection of the uncinate process (Station 14 Lymph nodes harvest), Station 8 and 12 Lymph node harvest, division of the common hepatic duct, removal of the gallbladder from the liver bed, specimen extraction, pancreaticojejunostomy, hepaticojejunostomy, gastrojejunostomy, and peritoneal irrigation with drainage.

SINGLE-INCISION LAPAROSCOPIC BILE DUCT RESECTION (SILBDR) FOR MALIGNANCY

Literature review

We only found one case report of SILBDR in the literature[56]. Two patients with Bismuth–Corlette type I perihilar cholangiocarcinoma underwent the procedure, including hepatoduodenal ligament lymphadenectomy, successfully with good recovery. The resection margins of the proximal and distal bile ducts were free from tumor invasion, but long-term follow-up was pending. The authors concluded that SILBDR can be optional in strictly selected patients with Bismuth–Corlette type I perihilar cholangiocarcinoma.

As perihilar cholangiocarcinoma is relatively rare to diagnose in an early stage, more advanced procedures, such as hemihepatectomies, caudate lobectomies, or PD, are usually performed in addition to bile duct resections for a better prognosis. The feasibility of SILS for resecting advanced-stage perihilar cholangiocarcinoma, an extremely complicated, demanding, and time-consuming procedure, should be considered with caution.

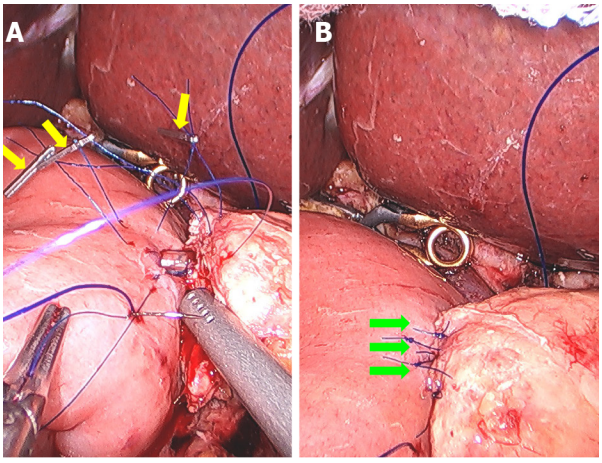

DOI: 10.3748/wjg.v28.i27.3359

Figure 6 Single-incision laparoscopic suturing technique was applied to a pancreatiojejunostomy. A: Three metallic clips (yellow arrows) were used at the same time during the inner duct-to-mucosa anastomosis of the pancreatiojejunostomy (PJ) in a single-incision laparoscopic pancreaticoduodenectomy; B: Completed inner duct-to-mucosa anastomosis (green arrows) of the PJ.

CONCLUSION

Minor SILH, such as LLS, monosegmentectomies, and partial liver resections, are feasible and safe to treat selected patients with cancer by experienced laparoscopic surgeons. Although the evidence level is low, minor SILH seems to be superior to minor MILH in terms of shorter postoperative hospital stay. The oncologic outcome is comparable for both procedures. Large-scale randomized controlled clinical trials are necessary to address this issue.

Major SILH might be feasible for highly selected patients by experienced laparoscopic surgeons in high-volume centers. The current evidence is limited and fails to determine its position compared with major MILH. Surgical skill refinement and technology advancement are anticipated to overcome this demanding procedure.

Although technically feasible, SILDP has been shown to be associated with longer operative time and lower spleen/splenic vessel preservation rates. Strict patient selection is mandatory for the possible accompanying splenectomy. Well-designed randomized controlled studies are needed to compare this procedure with MILDP. Robotic technology may have a positive effect on minimally invasive DP.

SILPD is just in its infancy, and this is also true for SILBDR. While developing these techniques, patient and oncologic safety should be prioritized. A low threshold to convert the procedures should always be kept in mind.

ACKNOWLEDGEMENTS

We gratefully acknowledge the work of Dr. Hsu JW in assisting with the surgical procedures and the data collection.

FOOTNOTES

Author contributions: Chuang SH drafted the manuscript; Chuang SC revised the manuscript; Both authors have read and approve the final manuscript.

Conflict-of-interest statement: The authors report no conflict of interest.

Country/Territory of origin: Taiwan

ORCID number: Shu-Hung Chuang 0000-0002-2007-0415; Shih-Chang Chuang 0000-0003-1481-1632.

S-Editor: Yan JP
L-Editor: A
P-Editor: Yan JP

REFERENCES

1 **Morales-Conde S**, Peeters A, Meyer YM, Antoniou SA, Del Agua IA, Arezzo A, Arolfo S, Yehuda AB, Boni L, Cassinotti E, Dapri G, Yang T, Fransen S, Forgione A, Hajibandeh S, Mazzola M, Migliore M, Mittermair C, Mittermair D, Morandeira-Rivas A, Moreno-Sanz C, Morlacchi A, Nizri E, Nuijts M, Raakow J, Sánchez-Margallo FM, Sánchez-Margallo JA, Szold A, Weiss H, Weiss M, Zorron R, Bouvy ND. European association for endoscopic surgery (EAES) consensus statement on single-incision endoscopic surgery. *Surg Endosc* 2019; **33**: 996-1019 [PMID: 30771069 DOI: 10.1007/s00464-019-06693-2]

2 **Machairas N**, Papaconstantinou D, Gaitanidis A, Hasemaki N, Paspala A, Stamopoulos P, Kykalos S, Sotiropoulos GC. Is Single-Incision Laparoscopic Liver Surgery Safe and Efficient for the Treatment of Malignant Hepatic Tumors? *J Gastrointest Cancer* 2020; **51**: 425-432 [PMID: 31388921 DOI: 10.1007/s12029-019-00285-y]

3 **Wang YB**, Xia J, Zhang JY, Gong JP, Wang XM. Effectiveness and safety of single-port versus multi-port laparoscopic surgery for treating liver diseases: a meta-analysis. *Surg Endosc* 2017; **31**: 1524-1537 [PMID: 27553801 DOI: 10.1007/s00464-016-5199-9]

4 **Karabicak I**, Karabulut K. Single port laparoscopic liver surgery: A minireview. *World J Gastrointest Endosc* 2016; **8**: 444-450 [PMID: 27358670 DOI: 10.4253/wjge.v8.i12.444]

5 **Benzing C**, Krenzien F, Atanasov G, Seehofer D, Sucher R, Zorron R, Pratschke J, Schmelzle M. Single incision laparoscopic liver resection (SILL) - a systematic review. *GMS Interdiscip Plast Reconstr Surg DGPW* 2015; **4**: Doc17 [PMID: 26734538 DOI: 10.3205/iprs000076]

6 **Ban D**, Kudo A, Irie T, Ochiai T, Aihara A, Matsumura S, Tanaka S, Tanabe M. Advances in reduced port laparoscopic liver resection. *Asian J Endosc Surg* 2015; **8**: 11-15 [PMID: 25510567 DOI: 10.1111/ases.12164]

7 **Chang SK**, Lee KY. Therapeutic advances: single incision laparoscopic hepatopancreatobiliary surgery. *World J Gastroenterol* 2014; **20**: 14329-14337 [PMID: 25339820 DOI: 10.3748/wjg.v20.i39.14329]

8 **Gkegkes ID**, Iavazzo C. Single incision laparoscopic hepatectomy: A systematic review. *J Minim Access Surg* 2014; **10**: 107-112 [PMID: 25013325 DOI: 10.4103/0972-9941.134872]

9 **Yao D**, Wu S, Tian Y, Fan Y, Kong J, Li Y. Transumbilical single-incision laparoscopic distal pancreatectomy: primary experience and review of the English literature. *World J Surg* 2014; **38**: 1196-1204 [PMID: 24357245 DOI: 10.1007/s00268-013-2404-z]

10 **Chatzizacharias NA**, Dajani K, Koong JK, Jah A. The Role of the Single Incision Laparoscopic Approach in Liver and Pancreatic Resectional Surgery. *Minim Invasive Surg* 2016; **2016**: 1454026 [PMID: 27891251 DOI: 10.1155/2016/1454026]

11 **Chuang SH**, Lin CS. Single-incision laparoscopic surgery for biliary tract disease. *World J Gastroenterol* 2016; **22**: 736-747 [PMID: 26811621 DOI: 10.3748/wjg.v22.i2.736]

12 **Hildebrand N**, Verkoulen K, Dewulf M, Heise D, Ulmer F, Coolsen M. Short-term outcomes of laparoscopic versus open hepatectomy in the elderly patient: systematic review and meta-analysis. *HPB (Oxford)* 2021; **23**: 984-993 [PMID: 33632653 DOI: 10.1016/j.hpb.2021.01.016]

13 **Machairas N**, Kostakis ID, Schizas D, Kykalos S, Nikiteas N, Sotiropoulos GC. Meta-analysis of laparoscopic versus open liver resection for intrahepatic cholangiocarcinoma. *Updates Surg* 2021; **73**: 59-68 [PMID: 33219937 DOI: 10.1007/s13304-020-00930-3]

14 **Cipriani F**, Ratti F, Fiorentini G, Reineke R, Aldrighetti L. Systematic review of perioperative and oncologic outcomes of minimally-invasive surgery for hilar cholangiocarcinoma. *Updates Surg* 2021; **73**: 359-377 [PMID: 33615423 DOI: 10.1007/s13304-021-01006-6]

15 **Lyu Y**, Cheng Y, Wang B, Zhao S, Chen L. Assessment of laparoscopic versus open distal pancreatectomy: a systematic review and meta-analysis. *Minim Invasive Ther Allied Technol* 2022; **31**: 350-358 [PMID: 32903097 DOI: 10.1080/13645706.2020.1812664]

16 **Gavriilidis P**, Roberts KJ, Sutcliffe RP. Laparoscopic versus open distal pancreatectomy for pancreatic adenocarcinoma: a systematic review and meta-analysis. *Acta Chir Belg* 2018; **118**: 278-286 [PMID: 29996721 DOI: 10.1080/00015458.2018.1492212]

17 **van Hilst J**, Korrel M, de Rooij T, Lof S, Busch OR, Groot Koerkamp B, Kooby DA, van Dieren S, Abu Hilal M, Besselink MG; DIPLOMA study group. Oncologic outcomes of minimally invasive versus open distal pancreatectomy for pancreatic ductal adenocarcinoma: A systematic review and meta-analysis. *Eur J Surg Oncol* 2019; **45**: 719-727 [PMID: 30579652 DOI: 10.1016/j.ejso.2018.12.003]

18 **Yang DJ**, Xiong JJ, Lu HM, Wei Y, Zhang L, Lu S, Hu WM. The oncological safety in minimally invasive versus open distal pancreatectomy for pancreatic ductal adenocarcinoma: a systematic review and meta-analysis. *Sci Rep* 2019; **9**: 1159 [PMID: 30718559 DOI: 10.1038/s41598-018-37617-0]

19 **Nickel F**, Haney CM, Kowalewski KF, Probst P, Limen EF, Kalkum E, Diener MK, Strobel O, Müller-Stich BP, Hackert T. Laparoscopic Versus Open Pancreaticoduodenectomy: A Systematic Review and Meta-analysis of Randomized Controlled Trials. *Ann Surg* 2020; **271**: 54-66 [PMID: 30973388 DOI: 10.1097/SLA.0000000000003309]

20 **Wang M**, Li D, Chen R, Huang X, Li J, Liu Y, Liu J, Cheng W, Chen X, Zhao W, Tan Z, Huang H, Zhu F, Qin T, Ma J, Yu G, Zhou B, Zheng S, Tang Y, Han W, Meng L, Ke J, Feng F, Chen B, Yin X, Chen W, Ma H, Xu J, Lin R, Dong Y, Yu Y, Zhang H, Qin R; Minimally Invasive Treatment Group in the Pancreatic Disease Branch of China's International Exchange and Promotion Association for Medicine and Healthcare (MITG-P-CPAM). Laparoscopic versus open

pancreatoduodenectomy for pancreatic or periampullary tumours: a multicentre, open-label, randomised controlled trial. *Lancet Gastroenterol Hepatol* 2021; **6**: 438-447 [PMID: 33915091 DOI: 10.1016/S2468-1253(21)00054-6]

21 **Katsuki R**, Jo T, Yasunaga H, Kumazawa R, Uda K. Outcomes of laparoscopic versus open pancreatoduodenectomy: A nationwide retrospective cohort study. *Surgery* 2021; **169**: 1427-1433 [PMID: 33487433 DOI: 10.1016/j.surg.2020.12.018]

22 **Yin Z**, Jian Z, Hou B, Jin H. Surgical and Oncological Outcomes of Laparoscopic Versus Open Pancreaticoduodenectomy in Patients With Pancreatic Duct Adenocarcinoma. *Pancreas* 2019; **48**: 861-867 [PMID: 31306305 DOI: 10.1097/MPA.0000000000001363]

23 **Jiang YL**, Zhang RC, Zhou YC. Comparison of overall survival and perioperative outcomes of laparoscopic pancreaticoduodenectomy and open pancreaticoduodenectomy for pancreatic ductal adenocarcinoma: a systematic review and meta-analysis. *BMC Cancer* 2019; **19**: 781 [PMID: 31391085 DOI: 10.1186/s12885-019-6001-x]

24 **Peng L**, Zhou Z, Cao Z, Wu W, Xiao W, Cao J. Long-Term Oncological Outcomes in Laparoscopic Versus Open Pancreaticoduodenectomy for Pancreatic Cancer: A Systematic Review and Meta-Analysis. *J Laparoendosc Adv Surg Tech A* 2019; **29**: 759-769 [PMID: 30835156 DOI: 10.1089/lap.2018.0683]

25 **Chuang SH**, Yang WJ, Chang CM, Lin CS, Yeh MC. Is routine single-incision laparoscopic cholecystectomy feasible? *Am J Surg* 2015; **210**: 315-321 [PMID: 25916613 DOI: 10.1016/j.amjsurg.2014.12.032]

26 **Hyun IG**, Choi Y, Han HS, Yoon YS, Cho JY, Kim KH, Han S. Feasibility of Solo Single-Incision Laparoscopic Surgery in Non-anatomical Minor Liver Resection: a Propensity Score-Matched Analysis. *J Gastrointest Surg* 2021; **25**: 681-687 [PMID: 32157607 DOI: 10.1007/s11605-020-04527-4]

27 **Mittermair C**, Weiss M, Schirnhofer J, Brunner E, Fischer K, Obrist C, de Cillia M, Kemmetinger V, Gollegger E, Hell T, Weiss H. The Shift from Multiport to Single Port Increases the Amount of Bleeding in Laparoscopic Major Hepatectomy. *J Clin Med* 2021; **10** [PMID: 33498169 DOI: 10.3390/jcm10030374]

28 **Tsai KY**, Chen HA, Wang WY, Huang MT. Long-term and short-term surgical outcomes of single-incision laparoscopic hepatectomy on anterolateral liver segments. *Surg Endosc* 2020; **34**: 2969-2979 [PMID: 31482356 DOI: 10.1007/s00464-019-07080-7]

29 **Saad MR**, Choi Y, Han HS, Yoon YS, Cho JY, Lee JS, Lee BR. Solo single-incision laparoscopic liver resection: a cohort series. *ANZ J Surg* 2020; **90**: 1108-1111 [PMID: 32378778 DOI: 10.1111/ans.15941]

30 **Wang JC**, Pan Y, Chen J, Hu D, Tuoheti Y, Zhou Z, Xu L, Chen M, Zhang Y. Single versus multiple port laparoscopic left lateral sectionectomy for hepatocellular carcinoma: A retrospective comparative study. *Int J Surg* 2020; **77**: 15-21 [PMID: 32179178 DOI: 10.1016/j.ijsu.2020.03.003]

31 **Pan Y**, Chen J, Xu L, Zhou Z, Chen M, Zhang Y. Single-Port Laparoscopic Hepatectomy for Liver Tumor: Operative Steps (With Video). *Surg Laparosc Endosc Percutan Tech* 2019; **29**: e98-e101 [PMID: 31567784 DOI: 10.1097/SLE.0000000000000724]

32 **Han JH**, You YK, Choi HJ, Hong TH, Kim DG. Clinical advantages of single port laparoscopic hepatectomy. *World J Gastroenterol* 2018; **24**: 379-386 [PMID: 29391760 DOI: 10.3748/wjg.v24.i3.379]

33 **Weiss M**, Mittermair C, Brunner E, Schirnhofer J, Obrist C, Pimpl K, Hell T, Weiss H. Inline radiofrequency pre-coagulation simplifies single-incision laparoscopic minor liver resection. *J Hepatobiliary Pancreat Sci* 2015; **22**: 831-836 [PMID: 26510122 DOI: 10.1002/jhbp.295]

34 **Tayar C**, Subar D, Salloum C, Malek A, Laurent A, Azoulay D. Single incision laparoscopic hepatectomy: Advances in laparoscopic liver surgery. *J Minim Access Surg* 2014; **10**: 14-17 [PMID: 24501503 DOI: 10.4103/0972-9941.124454]

35 **Pan M**, Jiang Z, Cheng Y, Xu X, Zhang Z, Zhou C, He G, Xu T, Liu H, Gao Y. Single-incision laparoscopic hepatectomy for benign and malignant hepatopathy: initial experience in 8 Chinese patients. *Surg Innov* 2012; **19**: 446-451 [PMID: 22474017 DOI: 10.1177/1553350612438412]

36 **Toyama Y**, Yoshida S, Okui N, Kitamura H, Yanagisawa S, Yanaga K. Transumbilical single-incision laparoscopic hepatectomy using precoagulation and clipless technique in a patient with combined hepatocellular-cholangiocarcinoma: a case report. *Surg Laparosc Endosc Percutan Tech* 2013; **23**: e194-e199 [PMID: 24105295 DOI: 10.1097/SLE.0b013e31828b8602]

37 **Camps Lasa J**, Cugat Andorrà E, Herrero Fonollosa E, García Domingo MI, Sánchez Martínez R, Vargas Pierola H, Rodríguez Campos A. Single-port laparoscopic approach of the left liver: initial experience. *Cir Esp* 2014; **92**: 589-594 [PMID: 24999088 DOI: 10.1016/j.ciresp.2014.05.009]

38 **Kim G**, Lau AC, Chang SK. Single-incision laparoscopic hepatic resection in patients with previous hepatic resections: a mini case series. *Asian J Endosc Surg* 2014; **7**: 63-66 [PMID: 24450347 DOI: 10.1111/ases.12072]

39 **Karabicak I**, Karabulut K, Yuruker S, Kesicioglu T, Ozen N. Single-Port Laparoscopic Liver Resection: Largest Turkish Experience. *Indian J Surg* 2017; **79**: 111-115 [PMID: 28442836 DOI: 10.1007/s12262-015-1435-0]

40 **Inoue Y**, Asakuma M, Hirokawa F, Hayashi M, Shimizu T, Uchiyama K. Single port access for laparoscopic lateral segmentectomy. *Wideochir Inne Tech Maloinwazyjne* 2017; **12**: 357-365 [PMID: 29362650 DOI: 10.5114/wiitm.2017.70260]

41 **Tzanis D**, Lainas P, Tranchart H, Pourcher G, Devaquet N, Perlemuter G, Naveau S, Dagher I. Atypical as well as anatomical liver resections are feasible by laparoendoscopic single-site surgery. *Int J Surg Case Rep* 2014; **5**: 580-583 [PMID: 25108073 DOI: 10.1016/j.ijscr.2013.11.009]

42 **Struecker B**, Haber P, Öllinger R, Bahra M, Pascher A, Pratschke J, Schmelzle M. Comparison of Single-Port Versus Standard Multiport Left Lateral Liver Sectionectomy. *Surg Innov* 2018; **25**: 136-141 [PMID: 29303066 DOI: 10.1177/1553350617752010]

43 **Belli G**, Fantini C, D'Agostino A, Cioffi L, Russo G, Belli A, Limongelli P. Laparoendoscopic single site liver resection for recurrent hepatocellular carcinoma in cirrhosis: first technical note. *Surg Laparosc Endosc Percutan Tech* 2011; **21**: e166-e168 [PMID: 21857451 DOI: 10.1097/SLE.0b013e3182207d3a]

44 **Wu S**, Yu XP, Tian Y, Siwo EA, Li Y, Yu H, Yao D, Lv C. Transumbilical single-incision laparoscopic resection of focal hepatic lesions. *JSLS* 2014; **18** [PMID: 25392646 DOI: 10.4293/JSLS.2014.00397]

45 **Dapri G**, Dimarco L, Cadière GB, Donckier V. Initial experience in single-incision transumbilical laparoscopic liver resection: indications, potential benefits, and limitations. *HPB Surg* 2012; **2012**: 921973 [PMID: 23082044 DOI:

10.1155/2012/921973]
46 **Røsok BI**, Edwin B. Single-Incision Laparoscopic Liver Resection for Colorectal Metastasis through Stoma Site at Time of Reversal of Diversion Ileostomy: A Case Report. *Minim Invasive Surg* 2011; **2011**: 502176 [PMID: 22091359 DOI: 10.1155/2011/502176]
47 **Cantos-Pallares M**, Mir-Labrador J, Rafael Redondo-Cano C, Nuñez-Ronda R, Artigues-Sanchez de Rojas E, Fabra-Ramis R. Single-port Laparoscopic Liver Resection in Patients with Previous Abdominal Surgeries: Is it a Feasible Approach? *J Coll Physicians Surg Pak* 2022; **32**: 96-98 [PMID: 34983156 DOI: 10.29271/jcpsp.2022.01.96]
48 **Chuang SH**, Chen PH, Chang CM, Tsai YF, Lin CS. Single-incision laparoscopic common bile duct exploration with conventional instruments: an innovative technique and a comparative study. *J Gastrointest Surg* 2014; **18**: 737-743 [PMID: 24347312 DOI: 10.1007/s11605-013-2420-1]
49 **Huang JW**, Su WL, Wang SN. Alternative Laparoscopic Intracorporeal Pringle Maneuver by Huang's Loop. *World J Surg* 2018; **42**: 3312-3315 [PMID: 29589115 DOI: 10.1007/s00268-018-4584-z]
50 **Park P**, Han HJ, Song TJ, Choi SB, Kim WB, Yoo YD, Kim DS, Cha JH. Single-port versus conventional laparoscopic distal pancreatectomy: a propensity score matched analysis and a learning curve of single-port approach. *J Hepatobiliary Pancreat Sci* 2019; **26**: 401-409 [PMID: 31211913 DOI: 10.1002/jhbp.646]
51 **Ağcaoğlu O**, Aksakal N, Azamat İF, Doğan S, Mercan S, Barbaros U. Comparison of Clinical Outcomes of Single-Incision Versus Conventional Multiport Laparoscopic Distal Pancreatectomy: A Single Institution Experience. *Sisli Etfal Hastan Tip Bul* 2019; **53**: 114-119 [PMID: 32377068 DOI: 10.14744/SEMB.2019.37880]
52 **Ryan CE**, Ross SB, Sukharamwala PB, Sadowitz BD, Wood TW, Rosemurgy AS. Distal pancreatectomy and splenectomy: a robotic or LESS approach. *JSLS* 2015; **19**: e2014.00246 [PMID: 25848192 DOI: 10.4293/JSLS.2014.00246]
53 **Kuroki T**, Kitasato A, Adachi T, Soyama A, Takatsuki M, Eguchi S. Single-incision laparoscopic distal pancreatectomy: our initial experience. *Hepatogastroenterology* 2014; **61**: 212-214 [PMID: 24895823 DOI: 10.1002/hep.24089]
54 **Misawa T**, Ito R, Futagawa Y, Fujiwara Y, Kitamura H, Tsutsui N, Shiba H, Wakiyama S, Ishida Y, Yanaga K. Single-incision laparoscopic distal pancreatectomy with or without splenic preservation: how we do it. *Asian J Endosc Surg* 2012; **5**: 195-199 [PMID: 23095300 DOI: 10.1111/j.1758-5910.2012.00155.x]
55 **Haugvik SP**, Røsok BI, Waage A, Mathisen O, Edwin B. Single-incision versus conventional laparoscopic distal pancreatectomy: a single-institution case-control study. *Langenbecks Arch Surg* 2013; **398**: 1091-1096 [PMID: 24177746 DOI: 10.1007/s00423-013-1133-y]
56 **Yu H**, Wu SD, Tian Y, Su Y, Li YN. Single-incision laparoscopic resection of Bismuth I hilar cholangiocarcinoma. *Surg Innov* 2013; **20**: 209-213 [PMID: 22393076 DOI: 10.1177/1553350612438414]

World Journal of Gastroenterology

Submit a Manuscript: https://www.f6publishing.com

World J Gastroenterol 2022 July 21; 28(27): 3370-3382

DOI: 10.3748/wjg.v28.i27.3370

ISSN 1007-9327 (print) ISSN 2219-2840 (online)

MINIREVIEWS

Probiotics and postbiotics in colorectal cancer: Prevention and complementary therapy

Monika Kvakova, Anna Kamlarova, Jana Stofilova, Veronika Benetinova, Izabela Bertkova

Specialty type: Gastroenterology and hepatology

Provenance and peer review: Invited article; Externally peer reviewed.

Peer-review model: Single blind

Peer-review report's scientific quality classification

Grade A (Excellent): 0
Grade B (Very good): B, B
Grade C (Good): 0
Grade D (Fair): 0
Grade E (Poor): 0

P-Reviewer: Ros J, Spain; Wen XL, China

Received: January 18, 2022
Peer-review started: January 18, 2022
First decision: March 8, 2022
Revised: March 22, 2022
Accepted: June 16, 2022
Article in press: June 16, 2022
Published online: July 21, 2022

Monika Kvakova, Anna Kamlarova, Jana Stofilova, Veronika Benetinova, Izabela Bertkova, Center of Clinical and Preclinical Research MEDIPARK, Faculty of Medicine, P.J. Safarik University in Kosice, Kosice 04011, Slovakia

Corresponding author: Monika Kvakova, PhD, Research Fellow, Research Scientist, Center of Clinical and Preclinical Research MEDIPARK, Faculty of Medicine, P.J. Safarik University in Kosice, Trieda SNP 1, Kosice 04011, Slovakia. monika.kvakova@upjs.sk

Abstract

Colorectal cancer (CRC) is a leading cause of human mortality worldwide. As conventional anticancer therapy not always being effective, there is growing interest in innovative "drug-free" cancer treatments or interventions that improve the efficacy of established therapy. CRC is associated with microbiome alterations, a process known as dysbiosis that involves depletion and/or enrichment of particular gut bacterial species and their metabolic functions. Supplementing patient treatment with traditional probiotics (with or without prebiotics), next-generation probiotics (NGP), or postbiotics represents a potentially effective and accessible complementary anticancer strategy by restoring gut microbiota composition and/or by signaling to the host. In this capacity, restoration of the gut microbiota in cancer patients can stabilize and enhance intestinal barrier function, as well as promote anticarcinogenic, anti-inflammatory, antimutagenic or other biologically important biochemical pathways that show high specificity towards tumor cells. Potential benefits of traditional probiotics, NGP, and postbiotics include modulating gut microbiota composition and function, as well as the host inflammatory response. Their application in CRC prevention is highlighted in this review, where we consider supportive *in vitro*, animal, and clinical studies. Based on emerging research, NGP and postbiotics hold promise in establishing innovative treatments for CRC by conferring physiological functions *via* the production of dominant natural products and metabolites that provide new host-microbiota signals to combat CRC. Although favorable results have been reported, further investigations focusing on strain and dose specificity are required to ensure the efficacy and safety of traditional probiotics, NGP, and postbiotics in CRC prevention and treatment.

Key Words: Colorectal cancer; Traditional probiotics; Next-generation probiotics; Postbiotics; Gut microbiota

Core Tip: The effects of traditional probiotics, next-generation probiotics (NGP), or postbiotics in colorectal cancer (CRC) prevention and complementary therapy can be associated independently or in mutual cooperation with several mechanisms, including suppression of inflammation, enhancing apoptosis of tumor cells, restoring intestinal barrier function, competition with pathogens and by promoting healthy gut microbiota composition and function. Traditional probiotics, NGP, or postbiotics supplementation is also a potential strategy to boost the effectiveness of chemotherapy and immunotherapy, reduce the rate of postoperative complications, and improve the quality of lives of CRC patients.

Citation: Kvakova M, Kamlarova A, Stofilova J, Benetinova V, Bertkova I. Probiotics and postbiotics in colorectal cancer: Prevention and complementary therapy. *World J Gastroenterol* 2022; 28(27): 3370-3382
URL: https://www.wjgnet.com/1007-9327/full/v28/i27/3370.htm
DOI: https://dx.doi.org/10.3748/wjg.v28.i27.3370

INTRODUCTION

Colorectal cancer (CRC) is the third most commonly diagnosed cancer in males and the second in females worldwide; thus a significant change in lifestyle is required to facilitate effective CRC prevention[1]. CRC is a heterogeneous disease of the intestinal epithelium, comprising the colon, rectum, and anus. It is characterized by a dysregulated immune response, accumulation of stem cell mutations, intestinal barrier disruption, and dysbiosis, which is often regarded as an unfavorable alteration in gut microbiota composition and function. Up to 90% of CRC risk is thought to be lifestyle-dependent, primarily due to dietary or environmental factors including feeding patterns that modulate consumption of fiber, red and processed meat or alcohol consumption, and low omega-3 fatty acids and vitamin D intake. Obesity, lack of physical activity, and smoking are also significant risk factors that promote CRC-associated microbiota changes[2]. CRC is linked with microbiome alterations, which include depletion and/or enrichment in particular bacterial species that are present in CRC patients (extensively reviewed by Torres-Maravilla *et al*[3], Ternes *et al*[4], Janney *et al*[2], Fong *et al*[5], and Wirbel *et al*[6]).

The human microbiota is a complex ecosystem of bacteria, viruses, eukaryotes, and archea, which can regulate a variety of host physiological functions including digestion, immune response, metabolism, disease pathogenesis, elimination of toxins, and biosynthesis of key compounds such as essential vitamins and cofactors. Microbiota can even modulate gut-brain axis function to alter, for example, anxiety and mood. Symbiotic bacteria that colonize the human gut can be classified into several phyla comprising Bacteroidetes and Firmicutes, followed by Proteobacteria, Fusobacteria, Actinobacteria, Verrucomicrobia, and Spirochaetes. Microbiome composition varies between healthy individuals, as well as in CRC patients[7]. CRC-associated bacteria that have been identified to date include enrichment of *Fusobacterium nucleatum*, *Enterococcus faecalis*, *Streptococcus gallolyticus*, entero-toxigenic *Bacteroides fragilis*, *Escherichia coli*, *Peptostreptococcus* spp., and *Ruminococcus* spp. By contrast, *Lactobacillus* spp., *Bifidobacterium* spp., *Faecalibacterium* spp., *Roseburia* spp., *Clostridium* spp., *Granulicatella* spp., *Streptococcus thermophilus*, and other species of *Lachnospiraceae* family are depleted in CRC (Table 1)[2-5]. These altered microbiota signatures can potentially be used to provide future diagnostics, and their presence/absence may contribute to the pathogenesis or prevention/treatment of CRC. However, the pathophysiological role of dysbiosis in CRC still remains unclear, since microbiota changes may reflect changes in host health status and some bacteria may even confer protection as a compensatory response to disease progression. This complexity is clearly evident by the report of specific bacteria associated with tumor initiation phase (driver bacteria) whereas other bacteria are associated with tumor development during progressive stages of CRC (passenger bacteria). Driver bacteria reportedly contribute to the formation of a tumor microenvironment that is comprised of normal epithelial cells and cancer cells. In this milieu, secreted microbial metabolites trigger damage to normal host cells, thus reprograming their metabolism to change the intestinal microenvironment and microbiome profile towards a more "CRC supportive" composition[8-10]. Potential driver bacteria include *Bacteroides fragilis*, *Escherichia coli*, *Enterococcus Faecalis*, *Bacillus*, *Bradyrhizobium*, *Methylobacterium*, *Streptomyces*, *Shigella*, *Citrobacter*, *Salmonella*, *Intrasporangiaceae*, and *Sinobacteraceae*. On the other hand, passenger bacteria occupy an existing tumor microenvironment where they are thought to either promote or inhibit CRC progression. Reported passenger bacteria include species *Fusobacterium*, *Parvimonas*, *Peptostreptococcus*, *Campylobacter*, *Streptococcus*, *Schwartzia*, *Burkholderiales*, *Caulobacteraceae*, *Delftia*, *Oxalobacteraceae*, *Faecalibacterium*, and *Sutterella*[8-11]. The host gut microbiota and immune system play important roles in CRC prevention and development. Therefore, probiotics, next-generation probiotics

Table 1 Overview of the most relevant bacteria related to colorectal cancer

Enriched bacteria	Depleted bacteria	Ref.
Fusobacterium nucleatum, Peptostreptococcus spp., *Porphyromonas asaccharolytica, Prevotella* spp., *Parvimonas micra, Bacteroides fragilis, Streptococcus gallolyticus, Escherichia coli, Campylobacter* spp., *Shigella* spp., *Enterococcus faecalis*	*Blautia* spp., *Faecalibacterium prausnitzii, Clostridium butyricum, Streptococcus thermophilus, Roseburia* spp.	[4,55-57]

(NGP), or postbiotics could be used as weapons to prevent CRC, to support the treatment and to improve the clinical outcomes in CRC patients.

This minireview summarizes recent CRC findings from clinical, animal and *in vitro* studies, and discusses the efficiency of probiotics, NGP, and postbiotics in CRC prevention and therapy.

TRADITIONAL PROBIOTICS

Probiotics are defined as "live, non-pathogenic microorganisms that, when administered in adequate amounts, may confer a health benefit on the host"[12]. Probiotics have a centuries-long history of safe use as prevention and adjuvant therapy in combating human diseases. They are also promising candidates in modulating human gut microbiota composition and function in CRC patients. Traditional widely used probiotics mainly belong to *Bifidobacterium* spp., *Lactobacillus* spp. and other lactic-acid-producing bacteria, including species belonging to *Streptococcus, Enterococcus*, and *Lactococcus*, complemented by yeasts of the genus *Saccharomyces*. The beneficial effects of probiotics, functioning in a species and/or strain-specific manner, include sustaining a healthy microbiome, reversing dysbiosis, preventing pathogenic infections and mucosal adhesion of pathogens, stabilizing and enhancing intestinal barrier function. Probiotic bacteria may achieve these beneficial functions in part by producing anti-carcinogenic, anti-inflammatory, anti-mutagenic and other biologically important compounds such as short-chain fatty acids (SCFAs), vitamin K, or B-group vitamins[5,7,13,14].

Current research builds on a foundation of work demonstrating that gut microbiota modulation through administration of probiotics and/or prebiotics plays an important role in CRC prevention and therapy. In a randomized, double-blinded, placebo-controlled trial, 60 patients underwent surgical CRC resection, of whom 29 received the probiotic powder (*Bifidobacterium animalis* subsp. *lactis* HY8002 [1 × 10^8 CFU], *Lactobacillus casei* HY2782 [5 × 10^7 CFU], and *Lactobacillus plantarum* HY7712 [5 × 10^7 CFU]) and 31 placebo, for 4 wk, starting at 1 wk preoperatively. The treatment group receiving probiotic powder showed an increase in abundance of *Bifidobacterium*, *Akkermansia*, *Parabacteroides*, *Veillonella*, *Lactobacillus*, *Erysipelatoclostridium* and a reduction in bacteria associated with CRC, such as *Prevotella*, *Alloprevotella*, *Fusobacterium*, and *Porphyromonas*. Lower serum zonulin, improved postoperative bowel function, and postoperative recovery were evident in the probiotic group compared with placebo[15]. In another randomized clinical trial, a group of 31 CRC patients received probiotic supplement *Bifidobacterium longum* BB536 (5 × 10^{10} CFU/2 g/daily) preoperatively for 7–14 d and postoperatively for 2 wk. Attenuated postoperative inflammatory responses (high-sensitivity C-Reactive protein), reduced risk of postoperative infectious complications, and accelerated health recovery after colorectal resection were evident in the treatment group. Hospital stay was significantly shortened and correlated significantly with increased Actinobacteria and decreased Firmicutes after probiotic intervention[16]. Aisu *et al*[17] administered BIO THREE® 2 mg *Enterococcus faecalis* T110, 10 mg *Clostridium butyricum* TO-A, and 10 mg *Bacillus mesentericus* TO-A to 75 CRC patients 15 d prior to the surgery. Incidence of postoperative complications and superficial incisional infections were lower, and these health effects were as shown to associate with an increased mean proportion of beneficial *Bifidobacterium*, postoperatively, even though this organism was not administered as part of the probiotic regime. The change in microbial diversity and improved integrity of the mucosal barrier were also observed by Liu *et al*[18] after *Lactobacillus plantarum* CGMCC 1258, *Lactobacillus acidophilus* LA-11, *Bifidobacterium longum* BL-88 (2.6 × 10^{14} CFU/2 g/daily) administration 6 d preoperatively and 10 d postoperatively to CRC patients. The numbers of beneficial bacteria, including *Bifidobacteria* and *Lactobacilli*, increased in the probiotic group after surgery, whereas they decreased in the placebo group. By contrast, Enterobacteriales and *Pseudomonas*, were decreased in the probiotic group whereas they increased in the placebo group. Based on a number of clinical trials, the preoperative oral intake of probiotics combined with the postoperative treatment in patients who need gastrointestinal surgery is potentially recommended. Larger rigorously controlled clinical trials are required to endorse these preliminary positive outcome studies since avoidance of probiotic use has also been recommended in patients with immunodeficiency and dysbiosis. More studies and the key outcomes are listed in Table 2.

Table 2 Efficiency of probiotics in colorectal cancer prevention and therapy-clinical trials

Probiotic strain/synbiotics	Dose/length of the study	Trial type/sample size	Microbial changes/key outcomes	Ref.
Lactobacillus rhamnosus GG, *Bifidobacterium lactis* Bb12 + inulin enriched with oligofructose	10^{10} CFU and 10 g of prebiotic, 12 wk	Human prevention study-CRC patients (*n* = 15 placebo, *n* = 19 synbiotics), polypectomized patients (*n* =19 placebo, *n* = 21 synbiotics)	↑*Bifidobacterium*, ↑*Lactobacillus*, ↓*Clostridium perfringens*; ↓proliferation rate of colorectal cells and stimulation of peripheral blood mononuclear cells (↑IFNg, ↓IL-2)	Rafter *et al*[58]
Bifidobacterium longum BB536, *Lactobacillus johnsonii* La1	2×10^7 CFU or 2×10^9 CFU, 3 d preoperatively and 3 d postoperatively	CRC patients undergoing elective colorectal resection- Randomized double blind, placebo-controlled study (*n* = 10 placebo, *n* = 21 probiotics)	*B. longum* BB536 did not adhere to colonic mucosa only La1, ↓*Enterobacteriaceae* ↓*Enterococcus*, modulation of local immunity (↑CD3+, CD4+, CD8+, activity of dendritic cells); no clinical effect	Gianotti *et al*[59]
Bifidobacterium longum, *Lactobacillus acidophilus*, *Enterococcus faecalis*	3×10^8 CFU, 3 d (from -5 to -3 d) preoperatively	Single-center prospective randomized control study (*n* = 30 placebo, *n* = 30 probiotics)	↑*Bifidobacterium* and ↓*Escherichia*; ↓endotoxins, D-lactic acid, serum IL-6 and C-reactive protein; ↑serum IgG and IgA; ↓postoperative occurrence of infectious complications of CRC	Zhang *et al*[60]
Bifidobacterium longum, *Lactobacillus acidophilus* and *Enterococcus faecalis*	1:1:1 daily 6×10^7 CFU, 5 d	Perioperative intake of probiotics in CRC patients (*n* = 11 placebo, *n* = 11 probiotics)	↑richness and diversity of mucosal microbes, ↓*Peptostreptococcus*, ↓*Comamonas*, ↓*Fusobacterium*, ↑*Enterococcus*, ↑Proteobacteria; no clinical effect	Gao *et al*[61]
LactoLevure (*Lactobacillus acidophilus* LA-5, *Lacobacillus plantarum*, *Bifidobacterium lactis* BB-12, *Saccharomyces boulardii*)	1.75×10^9 CFU, 0.5×10^9 CFU, 1.75×10^9 CFU, 1.5×10^9 CFU, respectively, 1 d preoperatively and 15 d postoperatively	CRC patients undergoing surgery- Randomized, double-blind, placebo-controlled study (*n* = 80 placebo, *n* = 84 probiotics)	Reduction of the postoperative pneumonia rate, anastomotic leakage and surgical site infections; ↑gene expression of SOCS3; ↑circulating IL-6, TNF-α	Kotzampassi *et al*[62] (NCT02313519)
Colon Dophilus™ [*Bifidobacterium breve* HA-129 (25%), *Bifidobacterium bifidum* HA-132 HA (20%), *Bifidobacterium longum* HA-135 (14.5%), *Lactobacillus rhamnosus* HA-111 (8%), *Lactobacillus acidophilus* HA-122 (8%), *Lactobacillus casei* HA-108 (8%), *Lactobacillus plantarum* HA-119 (8%), *Streptococcus thermopilus* HA-110 (6%), *Lactobacillus brevis* HA-112 (2%), *Bifidobacterium infantis* HA-116 (0.5%)]	10×10^9CFU/ daily, 12 wk	Patients with CRC, concomitantly with irinotecan chemotherapy- Randomized, placebo-controlled study (*n* = 23 placebo, *n* = 23 probiotics)	Reduction in the incidence and severity of chemotherapy induced diarrhea and incidence of enterocolitis.	Mego *et al*[63] (NCT01410955)
Saccharomyces boulardii	7 d preoperatively	Randomized study (*n* = 18 conventional treatment, *n* = 15 probiotics)	↓mucosal IL-1β, IL-10, and IL-23A mRNA levels; no statistical impact on postoperative infection rates	Consoli *et al*[64]
ProBion Clinica (*Bifidobacterium lactis* Bl-04 and *Lactobacillus acidophilus* NCFM + inulin)	1.4×10^{10} CFU, 7×10^9 CFU and 0.63 g of prebiotic, 8-78 d	Prospective randomized intervention (*n* = 7 placebo, *n* = 8 probiotics)	Increased abundance of butyrate producing bacteria ↑Firmicutes, ↑*Faecalibacterium*, ↑*Eubacterium*, ↑*Roseburia* ↑*Lachnospira*; ↓CRC associated bacteria- *Fusobacterium* and *Peptostreptococcus*	Hibberd *et al*[65] (NCT03072641)
Simbio-flora (*Lactobacillus acidophilus* NCFM, *Lactobacillus rhamnosus* HN001, *Lactobacillus casei* LPC-37, *Bifidobacterium lactis* HN019 and fructooligosaccharide)	10^9 CFU and 6 g of prebiotic, 7 d preoperatively	Patients with CRC subjected to colorectal resection- Prospective, randomized, double-blind, placebo-controlled study (*n* = 37 placebo, *n* = 36 synbiotic)	Reduced inflammatory state (C-reactive protein, IL-6), reductions in morbidity, hospital length of stay, and use of antibiotics. Stimulated bowel function, decreased complications and reduced cumulative duration of antibiotic usage	Polakowski *et al*[66]
Lactobacillus acidophilus BCMC® 12,130, *Lactobacillus lactis* BCMC® 12,451, *Lactobacillus casei* subsp BCMC® 12,313, *Bifidobacterium longum* BCMC® 02120, *Bifidobacterium bifidum* BCMC® 02290 and *Bifidobacterium infantis* BCMC® 02129	30 billion CFU, twice daily for 6 mo	Randomized double-blind placebo-controlled trial (*n* = 25 placebo, *n* = 27 probiotics)	Reduction in the levels of pro-inflammatory cytokines, TNF-α, IL-6, IL-10, IL-12, IL-17A, IL-17C and IL-22.	Zaharuddin *et al*[32] (NCT03782428)

CRC: Colorectal cancer; IFNg: Interferon-gamma; Ig: Immunoglobulin; IL: Interleukin; TNF-α: Tumor necrosis factor-alpha.

NGP

One potential approach to achieve CRC prevention and treatment is through NGP administration. As described above, the most frequently used probiotics belong to *Bifidobacterium* spp. and *Lactobacillus* spp. However, recent studies using metagenomic approaches have revealed the importance of further identification and characterization of commensal species, mainly anaerobic ones, residing in the gastrointestinal tract that play an important role in regulating the immune system and maintaining overall gut health. Growing evidence suggests that dysbiosis may contribute to CRC progression as well as several other diseases[19-22]. Although there is no official definition of NGP, it is generally defined as live microorganisms identified on the basis of comparative microbiota analyses between healthy and sick individuals/animals that, when administered with strain-specificity and in dose dependent manner, confer health benefits on the host[23,24]. Compared with healthy individuals, patients with CRC possess a different compositional structure and physiological activity of the gut microbiota with SCFAs-producing bacteria being depleted. This suggests that SCFAs-producing bacteria might potentially exhibit anti-inflammatory and anticarcinogenic properties, as well as being NGP candidates in CRC prevention and therapy. SCFAs, primarily acetate, propionate, and butyrate, are key physiological metabolites of the microbial fermentation of dietary fiber in the colon. Butyrate is the major energy source for colonocyte homeostasis, promoting growth stimulation and production of protective cytokines that maintain gut barrier integrity and function[14,25-27]. Furthermore, increasing levels of SCFAs in the gut helps to create a favorable microenvironment for beneficial bacteria by inhibiting the growth and adhesion of pathogens, and by enhancing vitamin bioavailability, mineral absorption and promoting mucosal integrity. Most butyrate-producing bacteria in the human colon belong to the Firmicutes phylum, clostridial clusters IV and XIVa, the most dominant species being *Faecalibacterium prausnitzii* and *Eubacterium rectale,* followed by *Eubacterium* spp. as well as *Anaerostipes* spp. and *Roseburia* spp. In addition to butyrate-producing bacteria, other NGP candidates with important regulatory effects on gut homeostasis include *Akkermansia muciniphila*, non-toxigenic *Bacteroides fragilis*, *Propionibacterium freudenreichii,* and some strains of *Bacillus* spp. and *Clostridium* spp., which belong to Generally Recognized As Safe microorganisms[7,28,29].

Chronic oral administration of *Butyricicoccus pullicaecorum* BCRC 81109 (butyrate producing bacteria) to BALB/cByJNarl male mice decreased colon tumor progression over 9 wk. This protection against CRC clinical outcomes was linked to activation of the SCFAs transporter solute carrier family 5 member 8 and/or G-protein-coupled receptor (GPR) 43[30]. Chen *et al*[25] also observed in an *in vivo* animal study that application of butyrate producing bacteria *Clostridium butyricum* ATCC 19398 (2×10^9 CFU/0.2 mL 3 times a week for 12 wk) inhibited intestinal tumor development by an increasing apoptosis of CRC cells, by modulating the Wnt/β-catenin signaling pathway. There was also a reduction in pathogenic bacteria and bile acid-biotransforming bacteria, whereas an increase in beneficial *Lactobacillus* spp. and SCFAs-producing *Rumincoccaceae* and *Eubacterium* spp. was evident. Thus, reduction in colonic secondary bile acids increased cecal SCFAs levels and activated G-protein coupled receptors, GPR43 and GPR109A, which were mechanistically implicated. Growth of CRC cell lines (HCT-116 and SW1116) was significantly inhibited by strains *Bacillus subtilis* ATCC 23857 and *Clostridium butyricum* ATCC 19398, and by their main metabolites bacitracin and butyrate. mRNA levels of important receptors and transcriptional factors related to inflammation for example, TLR4, MYD88, nuclear factor-kappa B (NF-κB), interleukin 22 (IL-22), and survivin were decreased and expression of $p21^{WAF1}$ was increased after treatment of SW1116 cells with *Bacillus subtilis* and *Clostridium butyricum* NGP[31]. Purified components produced by NGP cells were also studied and inhibition of human cancer cell proliferation by controlling the cell cycle was detected. Polysaccharide A purified from *Bacteroides fragilis* NCTC9343 (non-toxigenic) induced the production of the pro-inflammatory cytokine IL-8[32] and aspartic protease Amuc_1434 (recombinant enzyme) from *Akkermansia muciniphila* upregulated the expression of tumor protein 53, increased mitochondrial reactive oxygen species (ROS) levels and promoted apoptosis of LS174T cells[33]. Pahle *et al*[34] employed *Clostridium perfringens* enterotoxin (CPE) in CPE gene therapy to selectively target claudin-3 and claudin-4 expressing colon carcinomas *in vitro* and *in vivo* by using a translation optimized CPE expressing vector. Elevated toxicity of the optimized CPE expressing vector was evident in claudin-positive cells 48 h after the transfection, with toxicity rates of 76%–92% and rapid cytotoxic effects such as membrane disruption and necrosis. Further *in vivo* studies focused on the efficiency of NGP application in CRC are listed in Table 3 and postbiotics derived from NGP are considered below.

POSTBIOTICS

Postbiotics is an extensively researched subject that remains a largely understudied topic in CRC. Due to the phenomenal number and variety of metabolites produced by bacteria, it has been an enormous challenge to isolate and characterize the specific compound/s responsible for the therapeutic efficacy. Moreover, defining safety profiles and appropriate application doses of particular postbiotics in the preclinical and clinical settings may require regulatory guidelines and approvals[5]. The International

Table 3 Efficiency of next-generation probiotics in colorectal cancer *in vivo*

NGP strain	Application	Study/ cohort	Mechanism/effect(s)	Ref.
Akkermansia muciniphila MucT ATCC BAA-835	pasteurized culture 1.5 × 10^8 CFU/100 μL or recombinant Amuc_1100 3 μg (specific outer membrane protein)/2 wk before AOM injection until sacrifice	23-wk *in vivo* animal study, acute colitis was induced by AOM (10 mg/kg) (intraperitoneally) + 2% DSS (in water)-male C57BL/6J mice	Prevention of AOM/DSS-induced tumorigenesis by DNA damage attenuation, cell apoptosis and abnormal proliferation. Significant amelioration of acute colitis, relieved colon shortening and splenomegaly, delayed tumor formation and reduced expression of γH2AX, cleaved caspase 3 and Ki67. Blunted CAC through the expansion and activation of cytotoxic T lymphocytes, indicated by TNF-α induction and PD-1 downregulation	Wang *et al* [67]
Akkermansia muciniphila ATCC BAA-835	1 × 10^8 CFU/mouse every other day (day 7-12), gavage administration	4-wk *in vivo* animal study, CRC induced by mice colon cancer cells CT-26 (1 × 10^6) (subcutaneously)-*n* = 70, male BALB/c mice	*A. muciniphila* colonization significantly increased inhibition rate/anti-cancer effect of FOLFOX (from 48% to 76%) and significantly decreased marker of proliferation-Ki67 (% of positively stained cells)	Hou *et al*[68]
Clostridium butyricum (powder by Kexing Biopharm CO., LTD)	2 × 10^8 CFU/0.2 mL/3 times *per* week, gavage administration	78 d *in vivo* animal study, CAC induced by intraperitoneal AOM (12.5 mg/kg) + 2.5% DSS (in water)-*n* = 30, C57BL/6 mice	Inhibition of NF-κB pathway and apoptosis promotion. Change in the microbiome composition-reduction of Firmicutes to Bacteroidetes ratio. Reduction of incidence and size of CRC and increase of tumor cells apoptosis. Reduction in cytokines including TNF-α, IL-6 and level of COX-2. Decrease in phosphorylation of NF-κB and level of Bcl-2. Increase in Bax expression	Liu *et al*[69]
Clostridium butyricum ATCC 19398 or *Bacillus subtilis* ATCC 23857	2.5 × 10^8 CFU/0.3 mL/3 times *per* week for 28 wk, oral administration	28 wk *in vivo* animal study. CRC induced with DMH (20 mg/kg body weight)/weekly (intraperitoneally)-*n* = 72, male C57BL/6 mice	Inhibition of intestinal tumorigenesis and modulation of immunity and inflammation. Reduction in tumor size and incidence. After supplementation with probiotics, mice showed decreased Th2 and Th17 expression and increased CD4/CD8 expression compared to DMH-treated mice. Reduced gene expression of TLR4–MYD88–NF-κB, IL-22 and increase of $P21^{waf1}$ and Tlr3 mRNA levels in intestinal mucosa	Chen *et al* [31]

AOM: Azoxymethane; CAC: Colitis-associated cancer; CRC: Colorectal cancer; DMH: 1,2-dimethylhydrazine; DSS: Dextran sulfate sodium; FOLFOX: Oxaliplatin, fluorouracil and calcium folinate; IL: Interleukin; NF-κB: Nuclear factor-kappa B; TNF-α: Tumor necrosis factor-alpha.

Scientific Association for Probiotics and Prebiotics (ISAPP) offers expertise in microbiology, microbial physiology, gastroenterology, nutrition, food science and pediatrics. ISAPP recently provided the clear definition and scope of postbiotics to include "preparation of inanimate microorganisms and/or their components that confer a health benefit on the host"[35]. Postbiotics, which exert desired physiological effects to the host, include inactivated microbial cells or cell components (cell surface proteins, endo- or exo-polysaccharides, peptidoglycan-derived muropeptides and teichoic acids) or important metabolites secreted by gut microbiota through a fermentation process or released under certain conditions such as a change in intestinal environment or after lysis (SCFAs including acetate, propionate and butyrate; enzymes; bacteriocins; reuterin; acetoin; organic acids, *etc*)[5,35,36]. Therefore, the isolation and characterization of new postbiotics is a growing field and requires careful biochemical characterization of beneficial mechanisms. Supplementation with postbiotics, can in some cases be an effective and safer strategy to prevent and/or treat diseases, compared with ingestion of viable probiotic bacteria[5].

Microbial metabolites undoubtedly play an important role in CRC pathogenesis. Certain postbiotics exert antitumor activity, including selective cytotoxicity against tumor cells suggesting their therapeutic potential (Figure 1)[5]. For example, SCFAs are well-known inhibitors of epigenetic enzymes histone deacetylases, which play a central role in gene regulation; thus, SCFAs have the ability to induce cell cycle arrest, and/or apoptosis in many cancer cell lines[37]. Cell-free supernatants (CFS) of different *Lactobacillus* and *Bifidobacterium* strains have been shown to induce apoptosis or inhibit proliferation of CRC cell lines[38-40]. Chen *et al*[41] demonstrated that supernatants of *Lactobacillus johnsonii* BCRC17010 and *Lactobacillus reuteri* BCRC14625 strains in high concentrations were able to damage HT-29 cell membranes causing elevated lactate dehydrogenase release. A recent study has reported a potent selective cytotoxicity effect of postbiotic metabolites from *Lactobacillus plantarum* strains *via* anti-proliferative effects and induction of apoptosis in HT-29 cells whilst sparing the normal cells[42]. Cousin *et al* [43] showed that metabolites from *Propionibacterium freudenreichii* ITG-P9, namely propionate and acetate, had induced intrinsic apoptosis of CRC cells, *via* the production and release of SCFAs acting on mitochondria. Moreover, CFS or SCFAs in combination with Tumor Necrosis Factor-Related Apoptosis-Inducing Ligand (TRAIL), increased the pro-apoptotic gene expression (TRAIL-R2/DR5), decreased the anti-apoptotic gene expression of FLIP and XIAP in HT-29 cancer cells and enhanced the cytotoxicity in CRC cells compared to human healthy intestinal epithelial cells. Further control studies are required to delineate specific molecular targets in these models since enhanced toxicity to fermentation induced acidic pH shifts remains a potential protective mechanism.

As inflammation is undeniably linked to carcinogenesis, any postbiotic that inhibits inflammation is also an important candidate acting as anti-tumor agent. It was shown that *Lactobacillus rhamnosus* GG-

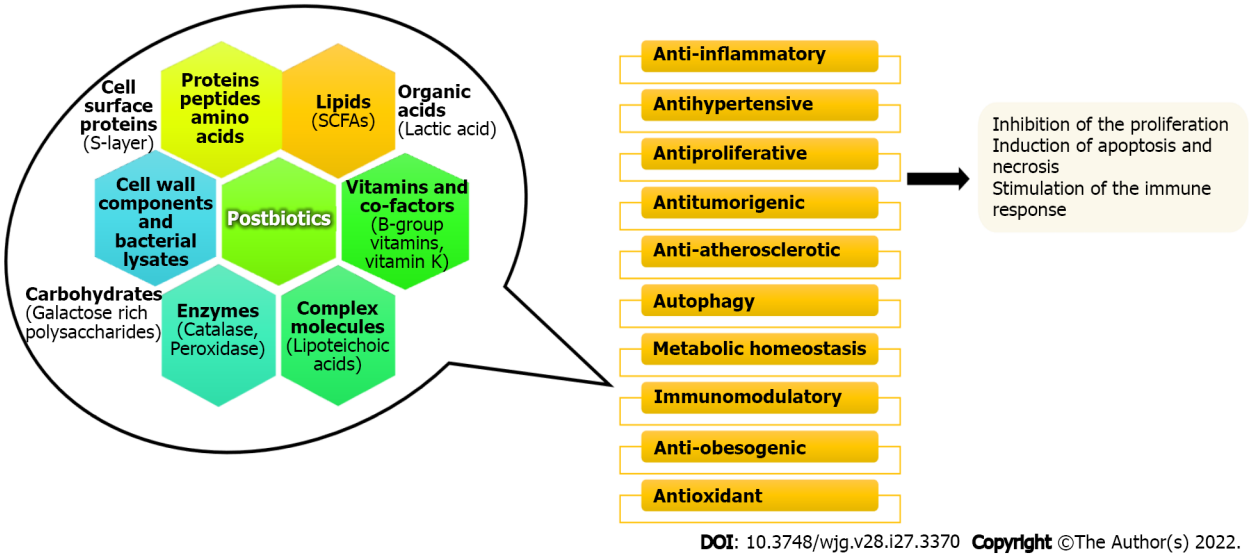

Figure 1 Examples of postbiotics and their proposed activity in patients with colorectal cancer. SCFAs: Short-chain fatty acids.

derived protein p40 can play a role in the prevention of CRC by suppressing intestinal epithelial inflammation, inhibiting epithelial cells apoptosis and by promoting IgA production[44-46]. CFS derived from several other probiotic strains, such as, *Lactobacillus acidophilus*, *Lactobacillus casei*, *Lactobacillus rhamnosus* GG and *Bifidobacterium breve*, were able to downregulate inflammation, exhibit antioxidant activity or maintained intestinal barrier integrity[47-49].

To date, only a few animal studies have been performed to evaluate the effectiveness of postbiotics in CRC prevention and therapy *in vivo*. The stage is now set to expand this work with the use of translational *in vivo* models and clinical trials, which are essential to demonstrate efficacy. Sharma and Shukla [50] observed that CFS from *Lactobacillus rhamnosus* MD 14 MH656799 containing acetamide, acetate, propionate, butyrate, thiocyanic acid and oxalic acid attenuated early colon carcinogenesis in Sprague–Dawley rats (n = 36). The protective mechanism was linked to reduced fecal procarcinogenic enzymes, oxidants, aberrant crypt foci, vis-à-vis downregulating oncogenes (β-catenin, K-ras, Cox-2, NF-κB) and upregulating tumor suppressor p53 gene leading to an almost healthy colon histology. De Moreno de LeBlanc *et al*[51] evaluated the effect of the enzyme catalase as a postbiotic from catalase-producing *Lactococcus lactis* htrA-NZ9000 on the prevention/regression of 1,2-dimethylhydrazine (DMH) induced CRC in BALB/c mice (n = 180-210). Catalase-producing *Lactococcus lactis* increased catalase activity in DMH-treated mice and reduced H_2O_2 levels compared with the control group. Using the histopathological grading scale of chemically induced CRC, mice that received catalase-producing *Lactococcus lactis* had significantly less colonic damage and inflammation (2.0 ± 0.4) compared to control animals that received non-catalase-producing *Lactococcus lactis* (4.0 ± 0.3) or placebo-treated animals (4.7 ± 0.5). Increased antioxidant activity reduced levels of H_2O_2 and ROS involved in CRC onset and progression.

There are also promising results from studies of postbiotics derived from NGP. Recently, numerous *in vitro* studies showed that supernatant from SCFAs-producing bacteria, such as *Butyricicoccus pullicaecorum* BCRC 81109[30], *Clostridium butyricum* ATCC 19398[25], *Propionibacterium freudenreichii* TL142[52], *Propionibacterium acidipropionici* CNRZ80, *Propionibacterium freudenreichii* subsp. *freudenreichii* ITG18, *Propionibacterium freudenreichii* subsp. *shermanii* SI41[53] suppressed CRC cells proliferation and induced apoptosis. The same results were documented by Zhao *et al*[54], where single strain CFS from human *Bacillus* strains BY38, BY40, BY43, BY45 exhibited inhibitory effects on the proliferation of CRC cells in a dose-dependent manner through the induction of cell apoptosis. These results suggest that NGP could represent novel and promising anti-tumor agents against CRC. Further *in vitro* studies focused on the activity of postbiotics derived from different probiotic strains in CRC cell lines are listed in Table 4.

CONCLUSION

Traditional probiotics have utility in the management of CRC as adjuvant treatment, mainly to reduce postoperative complications and to alleviate the side effects of chemotherapy. Antitumorigenic mechanisms of probiotics include the modification of intestinal microbiome, improvement of intestinal barrier integrity, immune potentiation and maintaining gut homeostasis. However, it is well known that the efficiency of probiotics is strain specific. The available clinical data indicate that CRC patients most

Table 4 Efficiency of postbiotics on cancer cells *in vitro*

Probiotic strain	Derived postbiotic	Cell line	Mechanism/effect(s)	Ref.
Lactobacilus casei ATCC334	CFS (ferrichrome)	Caco-2/bbe, SKCO-1, SW620	In CFS, ferrichrome subsequently identified as the responsible molecule that induced apoptosis *via* JNK-DDTI3 signaling axis, thus having tumor-suppressive effect and exerted minimal effect on normal intestinal epithelial cells	Konishi *et al*[70]
Lactobacillus rhamnosus MD 14 MH 656799	CFS (acetate, butyrate, propionate, acetamide, thiocyanic acid, and oxalic acid)	Caco-2, HT-29	CFS with metabolites exhibited both anti-genotoxic and cytotoxic potential against CRC cells	Sharma *et al*[71]
Bifidobacterium adolescentis SPM0212	CFS	Caco-2, HT-29, SW480	CFS significantly inhibited the proliferation of cancer cells	Kim *et al*[39]
Lactobacillus fermentum KCTC 3112	CFS	CCD18-Co, HCT-116, HT-29	Induction of cancer cells apoptosis by CFS up-regulating Caspase-3, Bax, Bak, Noxa, and Bid mRNA expressions	Lee *et al*[38]
Lactobacillus casei (ATCC 334), *Lactobacillus rhamnosus* (GG ATCC 53103)	CFS	HCT-116	Anti-metastatic effects of high molecular weight fractions	Escamilla *et al*[40]
Lactobacillus acidophilus ATCC 4356, *Lactococcus lactis* ATCC 11454, *Lactobacillus casei* ATCC 334, *Lactobacillus reuteri* ATCC 55148, *Saccharomyces boulardii* ATCC MYA-796	CFS	HT-29	Downregulation of the expression of PGE-2 and IL-8 in cancer cells by metabolites of probiotics. CFS differently modulated IL-1β, IL-6, TNF-α, and IL-10 production by human macrophages, suggesting a peculiar anti-inflammatory activity	De Marco *et al*[48]
Lactobacillus casei ATCC 393	Sonicated-cell suspension	CT26, HT-29	Inhibition of cancer cells proliferation and induction of apoptosis	Tiptiri-Kourpeti *et al* [72]
Lactobacillus reuteri PTCC 1655	Sonicated-cell suspension	HT-29-ShE	Anti-metastatic and anti-proliferative effects	Maghsood *et al*[73]
Lactococcus lactis PTCC 1336	Nisin, cell wall, cytoplasmic extract of nisin	SW480	Anti-proliferative effects, associated with the decreased expression of cyclin D1 in SW480 cell line	Hosseini *et al*[74]
Pediococcus pentosaceus FP3, *Lactobacillus salivarius* FP25/FP35, *Enterococcus faecium* FP51	SCFAs (butyrate and propionate)	Caco-2	Significant proliferation inhibition of Caco-2 cells and activation of apoptosis	Thirabunyanon and Hongwittayakorn [75]
Streptomyces levis ABRIINW111	Extracted metabolites	SW480	SW480 growth inhibition, increased Caspase-3 and reduced Ki67 expression in a concentration/time-dependent manner; subG$_1$ phase (apoptosis) increased by metabolites and cell cycle arrest in G$_1$, G$_2$/M and S phase; *p53* gene expression followed SW480 cells treatment significantly	Faramarzian Azimi Maragheh *et al*[76]
Streptomyces sp. MUM256	MUM256 extract	HT-29, Caco-2	Antioxidant properties, cytotoxicity against CRC cells by reduction in viability and induction of apoptosis (depolarization of mitochondrial membrane potential and arrest in subG$_1$ phase)	Tan *et al*[77]
Clostridium butyricum ATCC 19398	SCFAs	HCT-116, HCT-8, Caco-2	Suppression of the Wnt/b-catenin signaling pathway and modulation of the gut microbiota composition.	Chen *et al*[25]

CFS: Cell-free supernatant; CRC: Colorectal cancer; IL: Interleukin; SCFAs: Short-chain fatty acids; TNF-α: Tumor necrosis factor-alpha.

often benefit from combined administration of strains *Lactobacillus acidophilus*, *Lactobacillus casei*, *Bifidobacterium lactis*, and *Bifidobacterium longum*. Use of their combination or in combination with other species is more effective than individual supplementation. Nevertheless, consideration of each CRC patient's health status is still strictly recommended before administering viable probiotics. The gut microbiota is emerging as a contributing factor in the etiopathology of CRC. It is necessary to consider gut microbiota-drug interactions, including composition and metabolic activity of gut microbiota, which can both positively and negatively affect the outcome of CRC therapy. And even though research in this area is still in its infancy, it can be assumed that future clinical treatment and prevention of CRC will focus on supplementing the microbiome with commensal species (NGP candidates) that are predominantly anaerobic. Recent studies indicate that SCFAs-producing bacteria, especially butyrate producers, such as *Akkermansia muciniphila*, *Propionibacterium freudenreichi*, and *Butyricicoccus pullicaecorum* belong to

beneficial NGP that may have applicability in CRC therapy. Furthermore, it was discovered that strains previously defined as potential pathogens appear to possess probiotic properties when these lack key virulence factors, for example non-toxigenic *Bacteroides fragilis* NCTC9343 has positive effects on patient's health. A significant disadvantage of NGP is, above all, their safety as this has not yet been sufficiently confirmed in animal and clinical studies. Safety validation is of particular importance before administering NGP to oncology patients. Although NGP research is experimentally demanding, emerging data shows great potential. Therefore, it is necessary to continue and explore new possibilities of NGP use in the therapy or prevention of diseases, including CRC, especially through clinical trials. Supplementation with postbiotics should be favorable in CRC therapy, because postbiotics have the ability to stimulate immune responses, inhibit cancer cell proliferation, induce apoptosis and necrosis, and they can shape microbiome composition in CRC patients. The advantage of postbiotics is that they do not pose a risk of unwanted infection to the patient, although screening for product contamination will be important. Moreover, it is possible to accurately determine and verify administered doses of a particular postbiotic. However, this emerging research area currently lack *in vivo* or clinical data to assess feasibility. In conclusion, the administration of traditional probiotics, NGP or postbiotics, supported by various experimental studies, is an efficient complementary therapeutic approach to combat CRC. A protective effect of probiotics and postbiotics against CRC onset is also indicated, however, lifestyle changes are recommended as a first line of defense in CRC prevention.

ACKNOWLEDGEMENTS

We are thankful to Tor C Savidge, PhD for the editorial assistance.

FOOTNOTES

Author contributions: All authors contributed equally to the conceptualization and design of the manuscript; Kvakova M prepared and finalized the manuscript; Kamlarova A, Stofilova J, and Benetinova V reviewed the literature, and prepared the tables and figure; Bertkova I as senior author revised the manuscript; all authors approved the final manuscript.

Supported by Scientific Grant Agency of the Ministry of Education of Slovak Republic and Academy of Sciences VEGA, No. 1/0393/20; and the Operational Program Integrated Infrastructure Within the Project: Demand-Driven Research for the Sustainable and Innovative Food, Co-financed by the European Regional Development Fund, No. Drive4SIFood 313011V336.

Conflict-of-interest statement: All the authors report no relevant conflicts of interest for this article.

Country/Territory of origin: Slovakia

ORCID number: Monika Kvakova 0000-0002-9659-5584; Anna Kamlarova 0000-0001-7871-5338; Jana Stofilova 0000-0002-9409-4153; Veronika Benetinova 0000-0001-9523-8203; Izabela Bertkova 0000-0003-3076-2711.

S-Editor: Fan JR
L-Editor: Filipodia
P-Editor: Fan JR

REFERENCES

1 **Sung H**, Ferlay J, Siegel RL, Laversanne M, Soerjomataram I, Jemal A, Bray F. Global Cancer Statistics 2020: GLOBOCAN Estimates of Incidence and Mortality Worldwide for 36 Cancers in 185 Countries. *CA Cancer J Clin* 2021; **71**: 209-249 [PMID: 33538338 DOI: 10.3322/caac.21660]

2 **Janney A**, Powrie F, Mann EH. Host-microbiota maladaptation in colorectal cancer. *Nature* 2020; **585**: 509-517 [PMID: 32968260 DOI: 10.1038/s41586-020-2729-3]

3 **Torres-Maravilla E**, Boucard AS, Mohseni AH, Taghinezhad-S S, Cortes-Perez NG, Bermúdez-Humarán LG. Role of Gut Microbiota and Probiotics in Colorectal Cancer: Onset and Progression. *Microorganisms* 2021; **9** [PMID: 34068653 DOI: 10.3390/microorganisms9051021]

4 **Ternes D**, Karta J, Tsenkova M, Wilmes P, Haan S, Letellier E. Microbiome in Colorectal Cancer: How to Get from Meta-omics to Mechanism? *Trends Microbiol* 2020; **28**: 401-423 [PMID: 32298617 DOI: 10.1016/j.tim.2020.01.001]

5 **Fong W**, Li Q, Yu J. Gut microbiota modulation: a novel strategy for prevention and treatment of colorectal cancer. *Oncogene* 2020; **39**: 4925-4943 [PMID: 32514151 DOI: 10.1038/s41388-020-1341-1]

6 **Wirbel J**, Pyl PT, Kartal E, Zych K, Kashani A, Milanese A, Fleck JS, Voigt AY, Palleja A, Ponnudurai R, Sunagawa S, Coelho LP, Schrotz-King P, Vogtmann E, Habermann N, Niméus E, Thomas AM, Manghi P, Gandini S, Serrano D, Mizutani S, Shiroma H, Shiba S, Shibata T, Yachida S, Yamada T, Waldron L, Naccarati A, Segata N, Sinha R, Ulrich CM, Brenner H, Arumugam M, Bork P, Zeller G. Meta-analysis of fecal metagenomes reveals global microbial signatures that are specific for colorectal cancer. *Nat Med* 2019; **25**: 679-689 [PMID: 30936547 DOI: 10.1038/s41591-019-0406-6]

7 **Kvakova M**, Bertkova I, Stofilova J, Savidge TC. Co-Encapsulated Synbiotics and Immobilized Probiotics in Human Health and Gut Microbiota Modulation. *Foods* 2021; **10** [PMID: 34200108 DOI: 10.3390/foods10061297]

8 **Zhang M**, Lv Y, Hou S, Liu Y, Wang Y, Wan X. Differential Mucosal Microbiome Profiles across Stages of Human Colorectal Cancer. *Life (Basel)* 2021; **11** [PMID: 34440574 DOI: 10.3390/Life11080831]

9 **Wang Y**, Zhang C, Hou S, Wu X, Liu J, Wan X. Analyses of Potential Driver and Passenger Bacteria in Human Colorectal Cancer. *Cancer Manag Res* 2020; **12**: 11553-11561 [PMID: 33209059 DOI: 10.2147/CMAR.S275316]

10 **Xu S**, Yin W, Zhang Y, Lv Q, Yang Y, He J. Foes or Friends? *Cancers (Basel)* 2020; **12** [PMID: 32041122 DOI: 10.3390/cancers12020372]

11 **Tjalsma H**, Boleij A, Marchesi JR, Dutilh BE. A bacterial driver-passenger model for colorectal cancer: beyond the usual suspects. *Nat Rev Microbiol* 2012; **10**: 575-582 [PMID: 22728587 DOI: 10.1038/nrmicro2819]

12 **FAO/WHO**. Health and Nutritional Properties of Probiotics in Food Including Powder Milk with Live Lactic Acid Bacteria. 2006. [cited 20 December 2021]. Available from: www.fao.org

13 **Tripathy A**, Dash J, Kancharla S, Kolli P, Mahajan D, Senapati S, Jena MK. Probiotics: A Promising Candidate for Management of Colorectal Cancer. *Cancers (Basel)* 2021; **13** [PMID: 34202265 DOI: 10.3390/cancers13133178]

14 **Zhao Y**, Wang C, Goel A. Role of gut microbiota in epigenetic regulation of colorectal Cancer. *Biochim Biophys Acta Rev Cancer* 2021; **1875**: 188490 [PMID: 33321173 DOI: 10.1016/j.bbcan.2020.188490]

15 **Park IJ**, Lee JH, Kye BH, Oh HK, Cho YB, Kim YT, Kim JY, Sung NY, Kang SB, Seo JM, Sim JH, Lee JL, Lee IK. Effects of PrObiotics on the Symptoms and Surgical ouTComes after Anterior REsection of Colon Cancer (POSTCARE): A Randomized, Double-Blind, Placebo-Controlled Trial. *J Clin Med* 2020; **9** [PMID: 32664289 DOI: 10.3390/jcm9072181]

16 **Mizuta M**, Endo I, Yamamoto S, Inokawa H, Kubo M, Udaka T, Sogabe O, Maeda H, Shirakawa K, Okazaki E, Odamaki T, Abe F, Xiao JZ. Perioperative supplementation with bifidobacteria improves postoperative nutritional recovery, inflammatory response, and fecal microbiota in patients undergoing colorectal surgery: a prospective, randomized clinical trial. *Biosci Microbiota Food Health* 2016; **35**: 77-87 [PMID: 27200261 DOI: 10.12938/bmfh.2015-017]

17 **Aisu N**, Tanimura S, Yamashita Y, Yamashita K, Maki K, Yoshida Y, Sasaki T, Takeno S, Hoshino S. Impact of perioperative probiotic treatment for surgical site infections in patients with colorectal cancer. *Exp Ther Med* 2015; **10**: 966-972 [PMID: 26622423 DOI: 10.3892/etm.2015.2640]

18 **Liu Z**, Qin H, Yang Z, Xia Y, Liu W, Yang J, Jiang Y, Zhang H, Wang Y, Zheng Q. Randomised clinical trial: the effects of perioperative probiotic treatment on barrier function and post-operative infectious complications in colorectal cancer surgery - a double-blind study. *Aliment Pharmacol Ther* 2011; **33**: 50-63 [PMID: 21083585 DOI: 10.1111/j.1365-2036.2010.04492.x]

19 **Gautier T**, David-Le Gall S, Sweidan A, Tamanai-Shacoori Z, Jolivet-Gougeon A, Loréal O, Bousarghin L. Next-Generation Probiotics and Their Metabolites in COVID-19. *Microorganisms* 2021; **9** [PMID: 33925715 DOI: 10.3390/microorganisms9050941]

20 **Osman MA**, Neoh HM, Ab Mutalib NS, Chin SF, Mazlan L, Raja Ali RA, Zakaria AD, Ngiu CS, Ang MY, Jamal R. Parvimonas micra, Peptostreptococcus stomatis, Fusobacterium nucleatum and Akkermansia muciniphila as a four-bacteria biomarker panel of colorectal cancer. *Sci Rep* 2021; **11**: 2925 [PMID: 33536501 DOI: 10.1038/s41598-021-82465-0]

21 **Lv Y**, Ye T, Wang HP, Zhao JY, Chen WJ, Wang X, Shen CX, Wu YB, Cai YK. Suppression of colorectal tumorigenesis by recombinant *Bacteroides fragilis* enterotoxin-2 *in vivo*. *World J Gastroenterol* 2017; **23**: 603-613 [PMID: 28216966 DOI: 10.3748/wjg.v23.i4.603]

22 **Dai Z**, Coker OO, Nakatsu G, Wu WKK, Zhao L, Chen Z, Chan FKL, Kristiansen K, Sung JJY, Wong SH, Yu J. Multi-cohort analysis of colorectal cancer metagenome identified altered bacteria across populations and universal bacterial markers. *Microbiome* 2018; **6**: 70 [PMID: 29642940 DOI: 10.1186/s40168-018-0451-2]

23 **Martín R**, Langella P. Emerging Health Concepts in the Probiotics Field: Streamlining the Definitions. *Front Microbiol* 2019; **10**: 1047 [PMID: 31164874 DOI: 10.3389/fmicb.2019.01047]

24 **Lin TL**, Shu CC, Lai WF, Tzeng CM, Lai HC, Lu CC. Investiture of next generation probiotics on amelioration of diseases – Strains do matter. *Med Microecol* 2019; **1-2**: 100002 [DOI: 10.1016/j.medmic.2019.100002]

25 **Chen D**, Jin D, Huang S, Wu J, Xu M, Liu T, Dong W, Liu X, Wang S, Zhong W, Liu Y, Jiang R, Piao M, Wang B, Cao H. Clostridium butyricum, a butyrate-producing probiotic, inhibits intestinal tumor development through modulating Wnt signaling and gut microbiota. *Cancer Lett* 2020; **469**: 456-467 [PMID: 31734354 DOI: 10.1016/j.canlet.2019.11.019]

26 **Hu S**, Liu L, Chang EB, Wang JY, Raufman JP. Butyrate inhibits pro-proliferative miR-92a by diminishing c-Myc-induced miR-17-92a cluster transcription in human colon cancer cells. *Mol Cancer* 2015; **14**: 180 [PMID: 26463716 DOI: 10.1186/s12943-015-0450-x]

27 **Chen HM**, Yu YN, Wang JL, Lin YW, Kong X, Yang CQ, Yang L, Liu ZJ, Yuan YZ, Liu F, Wu JX, Zhong L, Fang DC, Zou W, Fang JY. Decreased dietary fiber intake and structural alteration of gut microbiota in patients with advanced colorectal adenoma. *Am J Clin Nutr* 2013; **97**: 1044-1052 [PMID: 23553152 DOI: 10.3945/ajcn.112.046607]

28 **Gu ZY**, Pei WL, Zhang Y, Zhu J, Li L, Zhang Z. Akkermansia muciniphila in inflammatory bowel disease and colorectal cancer. *Chin Med J (Engl)* 2021; **134**: 2841-2843 [PMID: 34711719 DOI: 10.1097/CM9.0000000000001829]

29 **Rivière A**, Selak M, Lantin D, Leroy F, De Vuyst L. Bifidobacteria and Butyrate-Producing Colon Bacteria: Importance and Strategies for Their Stimulation in the Human Gut. *Front Microbiol* 2016; **7**: 979 [PMID: 27446020 DOI:

10.3389/fmicb.2016.00979]
30 **Chang SC**, Shen MH, Liu CY, Pu CM, Hu JM, Huang CJ. A gut butyrate-producing bacterium *Butyricicoccus pullicaecorum* regulates short-chain fatty acid transporter and receptor to reduce the progression of 1,2-dimethylhydrazine-associated colorectal cancer. *Oncol Lett* 2020; **20**: 327 [PMID: 33101496 DOI: 10.3892/ol.2020.12190]
31 **Chen ZF**, Ai LY, Wang JL, Ren LL, Yu YN, Xu J, Chen HY, Yu J, Li M, Qin WX, Ma X, Shen N, Chen YX, Hong J, Fang JY. Probiotics Clostridium butyricum and Bacillus subtilis ameliorate intestinal tumorigenesis. *Future Microbiol* 2015; **10**: 1433-1445 [PMID: 26346930 DOI: 10.2217/fmb.15.66]
32 **Zaharuddin L**, Mokhtar NM, Muhammad Nawawi KN, Raja Ali RA. A randomized double-blind placebo-controlled trial of probiotics in post-surgical colorectal cancer. *BMC Gastroenterol* 2019; **19**: 131 [PMID: 31340751 DOI: 10.1186/s12876-019-1047-4]
33 **Meng X**, Zhang J, Wu H, Yu D, Fang X. *Akkermansia muciniphila* Aspartic Protease Amuc_1434* Inhibits Human Colorectal Cancer LS174T Cell Viability *via* TRAIL-Mediated Apoptosis Pathway. *Int J Mol Sci* 2020; **21** [PMID: 32403433 DOI: 10.3390/ijms21093385]
34 **Pahle J**, Menzel L, Niesler N, Kobelt D, Aumann J, Rivera M, Walther W. Rapid eradication of colon carcinoma by Clostridium perfringens Enterotoxin suicidal gene therapy. *BMC Cancer* 2017; **17**: 129 [PMID: 28193196 DOI: 10.1186/s12885-017-3123-x]
35 **Salminen S**, Collado MC, Endo A, Hill C, Lebeer S, Quigley EMM, Sanders ME, Shamir R, Swann JR, Szajewska H, Vinderola G. The International Scientific Association of Probiotics and Prebiotics (ISAPP) consensus statement on the definition and scope of postbiotics. *Nat Rev Gastroenterol Hepatol* 2021; **18**: 649-667 [PMID: 33948025 DOI: 10.1038/s41575-021-00440-6]
36 **Wegh CAM**, Geerlings SY, Knol J, Roeselers G, Belzer C. Postbiotics and Their Potential Applications in Early Life Nutrition and Beyond. *Int J Mol Sci* 2019; **20** [PMID: 31547172 DOI: 10.3390/ijms20194673]
37 **King J**, Patel M, Chandrasekaran S. Metabolism, HDACs, and HDAC Inhibitors: A Systems Biology Perspective. *Metabolites* 2021; **11** [PMID: 34822450 DOI: 10.3390/metabo11110792]
38 **Lee YP**, Chiu CC, Lin TJ, Hung SW, Huang WC, Chiu CF, Huang YT, Chen YH, Chen TH, Chuang HL. The germ-free mice monocolonization with *Bacteroides fragilis* improves azoxymethane/dextran sulfate sodium induced colitis-associated colorectal cancer. *Immunopharmacol Immunotoxicol* 2019; **41**: 207-213 [PMID: 30706742 DOI: 10.1080/08923973.2019.1569047]
39 **Kim Y**, Lee D, Kim D, Cho J, Yang J, Chung M, Kim K, Ha N. Inhibition of proliferation in colon cancer cell lines and harmful enzyme activity of colon bacteria by Bifidobacterium adolescentis SPM0212. *Arch Pharm Res* 2008; **31**: 468-473 [PMID: 18449504 DOI: 10.1007/s12272-001-1180-y]
40 **Escamilla J**, Lane MA, Maitin V. Cell-free supernatants from probiotic Lactobacillus casei and Lactobacillus rhamnosus GG decrease colon cancer cell invasion in vitro. *Nutr Cancer* 2012; **64**: 871-878 [PMID: 22830611 DOI: 10.1080/01635581.2012.700758]
41 **Chen ZY**, Hsieh YM, Huang CC, Tsai CC. Inhibitory Effects of Probiotic Lactobacillus on the Growth of Human Colonic Carcinoma Cell Line HT-29. *Molecules* 2017; **22** [PMID: 28075415 DOI: 10.3390/molecules22010107]
42 **Chuah LO**, Foo HL, Loh TC, Mohammed Alitheen NB, Yeap SK, Abdul Mutalib NE, Abdul Rahim R, Yusoff K. Postbiotic metabolites produced by Lactobacillus plantarum strains exert selective cytotoxicity effects on cancer cells. *BMC Complement Altern Med* 2019; **19**: 114 [PMID: 31159791 DOI: 10.1186/s12906-019-2528-2]
43 **Cousin FJ**, Jouan-Lanhouet S, Théret N, Brenner C, Jouan E, Le Moigne-Muller G, Dimanche-Boitrel MT, Jan G. The probiotic Propionibacterium freudenreichii as a new adjuvant for TRAIL-based therapy in colorectal cancer. *Oncotarget* 2016; **7**: 7161-7178 [PMID: 26771233 DOI: 10.18632/oncotarget.6881]
44 **Wang Y**, Liu L, Moore DJ, Shen X, Peek RM, Acra SA, Li H, Ren X, Polk DB, Yan F. An LGG-derived protein promotes IgA production through upregulation of APRIL expression in intestinal epithelial cells. *Mucosal Immunol* 2017; **10**: 373-384 [PMID: 27353252 DOI: 10.1038/mi.2016.57]
45 **Wang L**, Cao H, Liu L, Wang B, Walker WA, Acra SA, Yan F. Activation of epidermal growth factor receptor mediates mucin production stimulated by p40, a Lactobacillus rhamnosus GG-derived protein. *J Biol Chem* 2014; **289**: 20234-20244 [PMID: 24895124 DOI: 10.1074/jbc.M114.553800]
46 **Yan F**, Polk DB. Characterization of a probiotic-derived soluble protein which reveals a mechanism of preventive and treatment effects of probiotics on intestinal inflammatory diseases. *Gut Microbes* 2012; **3**: 25-28 [PMID: 22356855 DOI: 10.4161/gmic.19245]
47 **Gao J**, Li Y, Wan Y, Hu T, Liu L, Yang S, Gong Z, Zeng Q, Wei Y, Yang W, Zeng Z, He X, Huang SH, Cao H. A Novel Postbiotic From *Lactobacillus rhamnosus* GG With a Beneficial Effect on Intestinal Barrier Function. *Front Microbiol* 2019; **10**: 477 [PMID: 30923519 DOI: 10.3389/fmicb.2019.00477]
48 **De Marco S**, Sichetti M, Muradyan D, Piccioni M, Traina G, Pagiotti R, Pietrella D. Probiotic Cell-Free Supernatants Exhibited Anti-Inflammatory and Antioxidant Activity on Human Gut Epithelial Cells and Macrophages Stimulated with LPS. *Evid Based Complement Alternat Med* 2018; **2018**: 1756308 [PMID: 30069221 DOI: 10.1155/2018/1756308]
49 **Bermudez-Brito M**, Muñoz-Quezada S, Gomez-Llorente C, Matencio E, Bernal MJ, Romero F, Gil A. Cell-free culture supernatant of Bifidobacterium breve CNCM I-4035 decreases pro-inflammatory cytokines in human dendritic cells challenged with Salmonella typhi through TLR activation. *PLoS One* 2013; **8**: e59370 [PMID: 23555025 DOI: 10.1371/journal.pone.0059370]
50 **Sharma M**, Shukla G. Administration of Metabiotics Extracted From Probiotic *Lactobacillus rhamnosus* MD 14 Inhibit Experimental Colorectal Carcinogenesis by Targeting Wnt/β-Catenin Pathway. *Front Oncol* 2020; **10**: 746 [PMID: 32670864 DOI: 10.3389/fonc.2020.00746]
51 **de Moreno de LeBlanc A**, LeBlanc JG, Perdigón G, Miyoshi A, Langella P, Azevedo V, Sesma F. Oral administration of a catalase-producing Lactococcus lactis can prevent a chemically induced colon cancer in mice. *J Med Microbiol* 2008; **57**: 100-105 [PMID: 18065674 DOI: 10.1099/jmm.0.47403-0]
52 **Lan A**, Lagadic-Gossmann D, Lemaire C, Brenner C, Jan G. Acidic extracellular pH shifts colorectal cancer cell death from apoptosis to necrosis upon exposure to propionate and acetate, major end-products of the human probiotic

propionibacteria. *Apoptosis* 2007; **12**: 573-591 [PMID: 17195096 DOI: 10.1007/s10495-006-0010-3]
53 **Jan G**, Belzacq AS, Haouzi D, Rouault A, Métivier D, Kroemer G, Brenner C. Propionibacteria induce apoptosis of colorectal carcinoma cells *via* short-chain fatty acids acting on mitochondria. *Cell Death Differ* 2002; **9**: 179-188 [PMID: 11840168 DOI: 10.1038/sj.cdd.4400935]
54 **Zhao MF**, Liang GD, Zhou YJ, Chi ZP, Zhuang H, Zhu SL, Wang Y, Liu GR, Zhao JB, Liu SL. Novel Bacillus strains from the human gut exert anticancer effects on a broad range of malignancy types. *Invest New Drugs* 2020; **38**: 1373-1382 [PMID: 32734371 DOI: 10.1007/s10637-020-00906-5]
55 **Cheng Y**, Ling Z, Li L. The Intestinal Microbiota and Colorectal Cancer. *Front Immunol* 2020; **11**: 615056 [PMID: 33329610 DOI: 10.3389/fimmu.2020.615056]
56 **Zhao L**, Cho WC, Nicolls MR. Colorectal Cancer-Associated Microbiome Patterns and Signatures. *Front Genet* 2021; **12**: 787176 [PMID: 35003221 DOI: 10.3389/fgene.2021.787176]
57 **Rebersek M**. Gut microbiome and its role in colorectal cancer. *BMC Cancer* 2021; **21**: 1325 [PMID: 34895176 DOI: 10.1186/s12885-021-09054-2]
58 **Rafter J**, Bennett M, Caderni G, Clune Y, Hughes R, Karlsson PC, Klinder A, O'Riordan M, O'Sullivan GC, Pool-Zobel B, Rechkemmer G, Roller M, Rowland I, Salvadori M, Thijs H, Van Loo J, Watzl B, Collins JK. Dietary synbiotics reduce cancer risk factors in polypectomized and colon cancer patients. *Am J Clin Nutr* 2007; **85**: 488-496 [PMID: 17284748 DOI: 10.1093/ajcn/85.2.488]
59 **Gianotti L**, Morelli L, Galbiati F, Rocchetti S, Coppola S, Beneduce A, Gilardini C, Zonenschain D, Nespoli A, Braga M. A randomized double-blind trial on perioperative administration of probiotics in colorectal cancer patients. *World J Gastroenterol* 2010; **16**: 167-175 [PMID: 20066735 DOI: 10.3748/wjg.v16.i2.167]
60 **Zhang JW**, Du P, Gao J, Yang BR, Fang WJ, Ying CM. Preoperative probiotics decrease postoperative infectious complications of colorectal cancer. *Am J Med Sci* 2012; **343**: 199-205 [PMID: 22197980 DOI: 10.1097/MAJ.0b013e31823aace6]
61 **Gao Z**, Guo B, Gao R, Zhu Q, Wu W, Qin H. Probiotics modify human intestinal mucosa-associated microbiota in patients with colorectal cancer. *Mol Med Rep* 2015; **12**: 6119-6127 [PMID: 26238090 DOI: 10.3892/mmr.2015.4124]
62 **Kotzampassi K**, Stavrou G, Damoraki G, Georgitsi M, Basdanis G, Tsaousi G, Giamarellos-Bourboulis EJ. A Four-Probiotics Regimen Reduces Postoperative Complications After Colorectal Surgery: A Randomized, Double-Blind, Placebo-Controlled Study. *World J Surg* 2015; **39**: 2776-2783 [PMID: 25894405 DOI: 10.1007/s00268-015-3071-z]
63 **Mego M**, Chovanec J, Vochyanova-Andrezalova I, Konkolovsky P, Mikulova M, Reckova M, Miskovska V, Bystricky B, Beniak J, Medvecova L, Lagin A, Svetlovska D, Spanik S, Zajac V, Mardiak J, Drgona L. Prevention of irinotecan induced diarrhea by probiotics: A randomized double blind, placebo controlled pilot study. *Complement Ther Med* 2015; **23**: 356-362 [PMID: 26051570 DOI: 10.1016/j.ctim.2015.03.008]
64 **Consoli ML**, da Silva RS, Nicoli JR, Bruña-Romero O, da Silva RG, de Vasconcelos Generoso S, Correia MI. Randomized Clinical Trial: Impact of Oral Administration of Saccharomyces boulardii on Gene Expression of Intestinal Cytokines in Patients Undergoing Colon Resection. *JPEN J Parenter Enteral Nutr* 2016; **40**: 1114-1121 [PMID: 25917895 DOI: 10.1177/0148607115584387]
65 **Hibberd AA**, Lyra A, Ouwehand AC, Rolny P, Lindegren H, Cedgård L, Wettergren Y. Intestinal microbiota is altered in patients with colon cancer and modified by probiotic intervention. *BMJ Open Gastroenterol* 2017; **4**: e000145 [PMID: 28944067 DOI: 10.1136/bmjgast-2017-000145]
66 **Polakowski CB**, Kato M, Preti VB, Schieferdecker MEM, Ligocki Campos AC. Impact of the preoperative use of synbiotics in colorectal cancer patients: A prospective, randomized, double-blind, placebo-controlled study. *Nutrition* 2019; **58**: 40-46 [PMID: 30278428 DOI: 10.1016/j.nut.2018.06.004]
67 **Wang L**, Tang L, Feng Y, Zhao S, Han M, Zhang C, Yuan G, Zhu J, Cao S, Wu Q, Li L, Zhang Z. A purified membrane protein from *Akkermansia muciniphila* or the pasteurised bacterium blunts colitis associated tumourigenesis by modulation of $CD8^+$ T cells in mice. *Gut* 2020; **69**: 1988-1997 [PMID: 32169907 DOI: 10.1136/gutjnl-2019-320105]
68 **Hou X**, Zhang P, Du H, Chu W, Sun R, Qin S, Tian Y, Zhang Z, Xu F. *Akkermansia Muciniphila* Potentiates the Antitumor Efficacy of FOLFOX in Colon Cancer. *Front Pharmacol* 2021; **12**: 725583 [PMID: 34603035 DOI: 10.3389/fphar.2021.725583]
69 **Liu M**, Xie W, Wan X, Deng T. Clostridium butyricum modulates gut microbiota and reduces colitis associated colon cancer in mice. *Int Immunopharmacol* 2020; **88**: 106862 [PMID: 32771947 DOI: 10.1016/j.intimp.2020.106862]
70 **Konishi H**, Fujiya M, Tanaka H, Ueno N, Moriichi K, Sasajima J, Ikuta K, Akutsu H, Tanabe H, Kohgo Y. Probiotic-derived ferrichrome inhibits colon cancer progression *via* JNK-mediated apoptosis. *Nat Commun* 2016; **7**: 12365 [PMID: 27507542 DOI: 10.1038/ncomms12365]
71 **Sharma M**, Chandel D, Shukla G. Antigenotoxicity and Cytotoxic Potentials of Metabiotics Extracted from Isolated Probiotic, *Lactobacillus rhamnosus* MD 14 on Caco-2 and HT-29 Human Colon Cancer Cells. *Nutr Cancer* 2020; **72**: 110-119 [PMID: 31266374 DOI: 10.1080/01635581.2019.1615514]
72 **Tiptiri-Kourpeti A**, Spyridopoulou K, Santarmaki V, Aindelis G, Tompoulidou E, Lamprianidou EE, Saxami G, Ypsilantis P, Lampri ES, Simopoulos C, Kotsianidis I, Galanis A, Kourkoutas Y, Dimitrellou D, Chlichlia K. Lactobacillus casei Exerts Anti-Proliferative Effects Accompanied by Apoptotic Cell Death and Up-Regulation of TRAIL in Colon Carcinoma Cells. *PLoS One* 2016; **11**: e0147960 [PMID: 26849051 DOI: 10.1371/journal.pone.0147960]
73 **Maghsood F**, Johari B, Rohani M, Madanchi H, Saltanatpour Z, Kadivar M. Anti-proliferative and Anti-metastatic Potential of High Molecular Weight Secretory Molecules from Probiotic Lactobacillus Reuteri Cell-Free Supernatant Against Human Colon Cancer Stem-Like Cells (HT29-ShE). *Int J Pept Res Ther* 2020; **26**: 2619-2631 [DOI: 10.1007/s10989-020-10049-z]
74 **Hosseini SS**, Goudarzi H, Ghalavand Z, Hajikhani B, Rafeieiatani Z, Hakemi-Vala M. Anti-proliferative effects of cell wall, cytoplasmic extract of *Lactococcus lactis* and nisin through down-regulation of *cyclin D1* on SW480 colorectal cancer cell line. *Iran J Microbiol* 2020; **12**: 424-430 [PMID: 33603997 DOI: 10.18502/ijm.v12i5.4603]
75 **Thirabunyanon M**, Hongwittayakorn P. Potential probiotic lactic acid bacteria of human origin induce antiproliferation of colon cancer cells *via* synergic actions in adhesion to cancer cells and short-chain fatty acid bioproduction. *Appl Biochem*

Biotechnol 2013; **169**: 511-525 [PMID: 23239414 DOI: 10.1007/s12010-012-9995-y]

76 **Faramarzian Azimi Maragheh B**, Fatourachi P, Mohammadi SM, Valipour B, Behtari M, Dehnad A, Nozad Charoudeh H. *Streptomyces Levis ABRIINW111* Inhibits SW480 Cells Growth by Apoptosis Induction. *Adv Pharm Bull* 2018; **8**: 675-682 [PMID: 30607340 DOI: 10.15171/apb.2018.076]

77 **Tan LT**, Chan KG, Pusparajah P, Yin WF, Khan TM, Lee LH, Goh BH. Mangrove derived Streptomyces sp. MUM265 as a potential source of antioxidant and anticolon-cancer agents. *BMC Microbiol* 2019; **19**: 38 [PMID: 30760201 DOI: 10.1186/s12866-019-1409-7]

World Journal of Gastroenterology

Submit a Manuscript: https://www.f6publishing.com

World J Gastroenterol 2022 July 21; 28(27): 3383-3397

DOI: 10.3748/wjg.v28.i27.3383

ISSN 1007-9327 (print) ISSN 2219-2840 (online)

MINIREVIEWS

Interventional strategies in infected necrotizing pancreatitis: Indications, timing, and outcomes

Birte Purschke, Louisa Bolm, Max Nikolaus Meyer, Hiroki Sato

Specialty type: Gastroenterology and hepatology

Provenance and peer review: Invited article; Externally peer reviewed.

Peer-review model: Single blind

Peer-review report's scientific quality classification

Grade A (Excellent): 0
Grade B (Very good): B
Grade C (Good): C
Grade D (Fair): 0
Grade E (Poor): 0

P-Reviewer: Jiang M, China; Shalli K, United Kingdom

Received: January 20, 2022
Peer-review started: January 20, 2022
First decision: February 24, 2022
Revised: March 7, 2022
Accepted: June 15, 2022
Article in press: June 15, 2022
Published online: July 21, 2022

Birte Purschke, Louisa Bolm, Department of Gastrointestinal Surgery, Massachusetts General Hospital, Boston, MA 02114, United States

Max Nikolaus Meyer, Department of Radiation Oncology, Massachusetts General Hospital, Boston, MA 02114, United States

Hiroki Sato, Department of Medicine, Asahikawa Medical University, Asahikawa 0788510, Hokkaido, Japan

Hiroki Sato, Department of Gastroenterology, Asahikawa Kosei Hospital, Asahikawa 0788211, Hokkaido, Japan

Corresponding author: Hiroki Sato, MD, PhD, Academic Fellow, Chief Doctor, Research Fellow, Department of Medicine, Asahikawa Medical University, 1-1, Midorigaoka Higashi 2 Jyo 1 Chome, Asahikawa 0788510, Hokkaido, Japan. hirokisato@asahikawa-med.ac.jp

Abstract

Acute pancreatitis (AP) is one of the most common gastrointestinal diseases and remains a life-threatening condition. Although AP resolves to restitutio ad integrum in approximately 80% of patients, it can progress to necrotizing pancreatitis (NP). NP is associated with superinfection in a third of patients, leading to an increase in mortality rate of up to 40%. Accurate and early diagnosis of NP and associated complications, as well as state-of-the-art therapy are essential to improve patient prognoses. The emerging role of endoscopy and recent trials on multidisciplinary management of NP established the "step-up approach". This approach starts with endoscopic interventions and can be escalated to other interventional and ultimately surgical procedures if required. Studies showed that this approach decreases the incidence of new multiple-organ failure as well as the risk of interventional complications. However, the optimal interventional sequence and timing of interventional procedures remain controversial. This review aims to summarize the indications, timing, and treatment outcomes for infected NP and to provide guidance on multidisciplinary decision-making.

Key Words: Pancreatitis; Acute necrotizing pancreatitis; Necrosis; Superinfection; Endoscopy; Surgery

Core Tip: Acute pancreatitis remains a potentially life-threatening disease. Necrotizing pancreatitis (NP) is associated with superinfection and increases the mortality rate. We summarized the current evidence and clinical recommendations of multidisciplinary approaches focusing on conservative, interventional, and surgical treatment. The interventional approach is often required as a first step in treating infected NP, while further options include minimal invasive or an escalation to open surgical treatment. Although this "step-up approach" is well-established, the exact timing, sequence, and procedure choice remain controversial; this review aims to summarize current evidence and to provide guidance for decision making in clinical practice.

Citation: Purschke B, Bolm L, Meyer MN, Sato H. Interventional strategies in infected necrotizing pancreatitis: Indications, timing, and outcomes. *World J Gastroenterol* 2022; 28(27): 3383-3397
URL: https://www.wjgnet.com/1007-9327/full/v28/i27/3383.htm
DOI: https://dx.doi.org/10.3748/wjg.v28.i27.3383

INTRODUCTION

Acute pancreatitis (AP) is one of the most common and severe gastrointestinal diseases[1]. The rate of AP-related hospitalization in the United States increased from 65.38 to 81.88 per 100000 United States adults per year from 2001 to 2014[2].

The pathophysiology of AP is characterized by acinar cell injury leading to premature intrapancreatic activation of digestive proteases. ATP depletion and mixed lineage kinase domain-like protein phosphorylation lead to acinar cell necroptosis and necrosis[3]. This results in a cascade effect leading to autodigestion of the pancreatic parenchyma. The acinar cell injury and autodigestion can be induced by different mechanisms; recent publications discuss, for example, the role of hypercalcemia and organelle dysfunction. Cholecystokinin, biliary acids, and alcohol consumption can lead to increased Ca^{2+} efflux by the endoplasmic reticulum (ER). In turn, hypercalcemia can damage the mitochondrial membrane, reducing ATP production and hence the function of the Ca^{2+} efflux mechanisms of the cell itself, which increases the intracellular Ca^{2+} levels even further. This intracellular Ca^{2+} overload ultimately leads to the release and activation of digestive enzymes, which results in premature activation of trypsin. In addition, bile acids, alcohol, and other pancreatic toxic substances can trigger the acinar cells themselves, leading to higher secretion of trypsin[4-6].

AP can be classified as either interstitial edematous or necrotizing pancreatitis (NP). While inflammation and edema of the pancreatic parenchyma and peripancreatic tissues characterize intestinal edematous pancreatitis, further pancreatic or peripancreatic necrosis is known as NP[6], which is a potentially life-threatening disease associated with a 15% mortality rate. In approximately a third of patients with NP, superinfection (fungal or bacterial infection) of necrosis occurs during the clinical course, mostly within 2 to 4 wk after disease onset. Infected NP (INP) results in an even higher mortality rate of up to 30% to 39% (Figure 1)[7-9]. The major causes of INP are obstructing gallstones (up to 50%) and alcohol abuse (20%)[10].

Several scores were introduced in order to predict the severity of AP and its mortality. A retrospective study from 2013 comparing some of these scores revealed that especially the Bedside Index for Severity in Acute Pancreatitis (BISAP) and Acute Physiology and Chronic Health Evaluation (APACHE-II) score stand out compared to scores like the computed tomography (CT) severity index, Ranson Score, body mass index, or hematocrit in terms of predicting severity, organ failure, and death. The BISAP score is a combination of the following five parameters, each worth one point: Altered mental state, blood urea nitrogen > 25.2 mg/dL or more, positive systemic inflammatory response syndrome criteria, age over 60 years, and pleural effusion on CT scan. In comparison, the APACHE-II score uses 14 different parameters, ranging from age to the Glasgow Coma Scale[11].

Another applicable score in INP is the Marshall Score, which determines the presence of organ failure, which, according to the 2012 revised Atlanta Classification of AP, is a criterion that differentiates between mild (no organ failure), moderate (organ failure after less than 48 h), and severe (organ failure after more than 48 h) pancreatitis. The Marshall Score assesses the respiratory system on a scale from 0 to 4 using PaO_2/FIO_2, the renal system using serum creatinine in mg/dL, and the cardiovascular system using the systolic blood pressure in mmHg. A score of 2 or higher for any of the systems indicates organ failure[12].

The clinical management of INP is complex and involves a multidisciplinary team of intensive care specialists, gastroenterologists, and surgeons. Recent trials have provided important insight into the disease mechanisms and have optimized the treatment strategies. However, the indications, timing, and outcomes of different interventional strategies remain controversial.

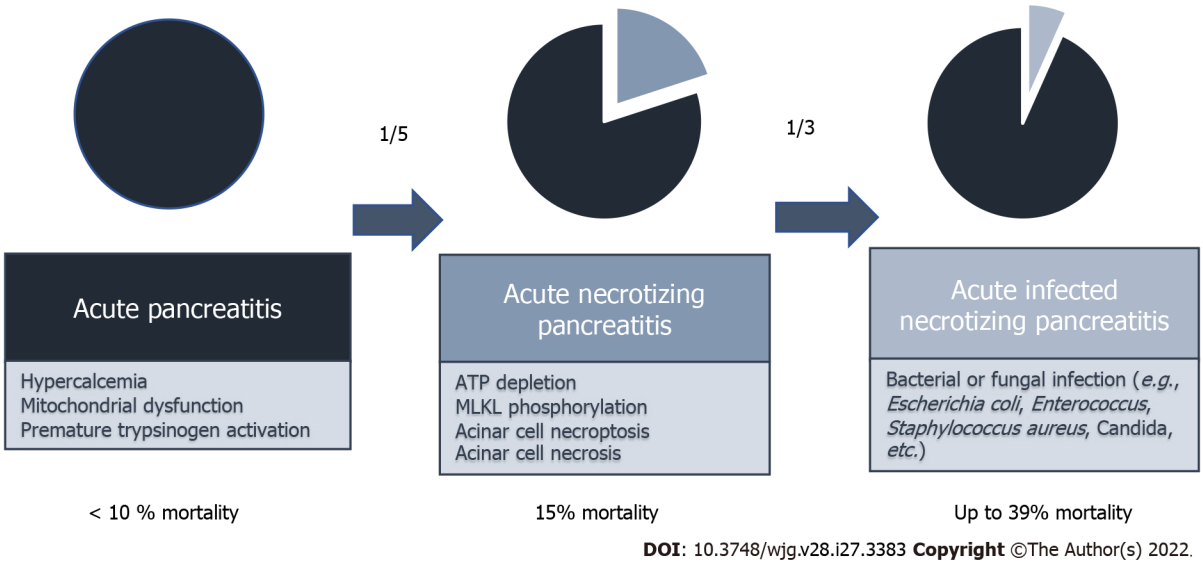

DOI: 10.3748/wjg.v28.i27.3383 **Copyright** ©The Author(s) 2022.

Figure 1 Mortality rates of acute pancreatitis and pathomechanisms. The mortality rate of all patients with acute pancreatitis (AP) is less than 10%. One-fifth of the patients developed necrotizing AP by ATP depletion, MLKL phosphorylation, acinar cell necroptosis, and/or acinar cell necrosis. One-third of the patients with necrotizing AP developed bacterial or fungal infection. The mortality rate of the infected necrotizing pancreatitis is up to 39%.

PHASES OF AP

According to the 2012 revised Atlanta classification of pancreatitis, two AP phases can be differentiated: the early (< 1 wk after onset) and late (> 1 wk after onset) phases. The early phase is characterized by the first clinical signs of pancreatitis: Abdominal pain, biochemical findings, and imaging findings consistent with pancreatitis. During this time, a pro-inflammatory sterile response occurs, which can lead to systemic inflammatory response syndrome (SIRS)[13]. Nevertheless, AP is self-limited in more than 80% of patients, and treatment in the early phase consists of supportive care instead of a curative intervention[14]. However, necrosis and acute necrotic collection (ANC) can occur in the late phase. ANC is considered a local complication of AP and is characterized by a collection of both fluid and necrosis without a defined wall[8]. ANC can resolve spontaneously or eventually become encapsulating, which allows the collection to become more organized within a well-defined inflammatory wall [15,16]. This process takes approximately 4-6 wk and the end-product is called a walled-off necrosis (WON)[17]. Once WON is diagnosed, whether the pancreatic or peripancreatic necrotic tissue and ANCs are sterile or infected must be determined to plan the subsequent treatment course. Superinfection of acute NP increases the mortality rate (24% *vs* 3.5%)[18,19]. In order to prevent SIRS, sepsis, and multiple (respiratory, cardiovascular, hepatic, and renal) organ failure, the treatment goal is to remove the infected non-vital tissue[13,18,20].

DIAGNOSIS OF ACUTE INP

The diagnosis of AP is mostly based on clinical symptoms; the major ones being abdominal pain, fever, nausea, and vomiting. The diagnosis is further narrowed by measuring the levels of serum amylase and/or lipase. As a diagnostic criterion for pancreatitis, these markers exceed the physiological range by approximately three times. Characteristic imaging findings, such as enlargement of the pancreas and hypodense areas within the parenchyma and/or the peripancreatic tissue, are radiological imaging criteria[8,17,21].

The primary imaging modality within the first 48 h is a transabdominal ultrasound, primarily to determine the need for cholecystectomy for biliary pancreatitis. If the diagnosis of AP remains uncertain, a CT scan can be performed. However, changes on CT are most evident approximately 72 h after AP onset[21].

To diagnose NP, contrast-enhanced CT (CECT) is the preferred imaging modality, as it can identify the presence of gas in the necrotic collection. Magnetic resonance imaging can also be used but is less sensitive than CECT[22]. The diagnosis of infected necrosis is based on clinical criteria including fever and rising serum inflammatory markers[23].

INP REQUIRES A MULTIDISCIPLINARY APPROACH

INP requires both closely monitored intensive care and interventional approaches to remove infected necrotic areas. Endoscopic interventional options involve endoscopic drainage and/or endoscopic necrosectomy. Further interventions are percutaneous transgastric drainage, minimally invasive or open necrosectomy. Using the acronym "PANCREAS", Gomes *et al*[24] summarized eight important steps in the management of severe AP: Perfusion, analgesia, nutrition, clinical and radiological assessment, endoscopy, antibiotics, and surgery.

Historically, INP patients have undergone early open debridement of necrotic tissue (median timing of the operation 21[25] to 28[26] d), mostly followed by local continuous lavage[26]. Recently, interventional strategies have shifted towards a so-called "step-up approach," which involves endoscopic or surgical interventions that comprise open and minimally invasive procedures. The approach starts with simple, less invasive interventions like endoscopic drainage, and escalates to more invasive and finally surgical procedures if these approaches fail.

CONSERVATIVE TREATMENT

INP patients require close monitoring and may need to be admitted to intensive care treatment due to the risk of sepsis and consequent organ failure[27]. The major components of conservative therapy are fluid administration, nutrition, and antibiotics.

FLUID ADMINISTRATION

Hypovolemia is a constant risk in AP patients; moreover, installing fluid infusions and closely monitoring patient circulation parameters is therefore essential. The duration of intravenous infusions as well as the total volume of fluids per day, are subject to ongoing debate[24].

A recent meta-analysis analyzed the impact of early aggressive fluid therapy (infusion rate of 3-5 mL/kg/h in the first 24 h) as compared to non-aggressive hydration. Eleven trials were included, and the authors could not detect a difference in mortality rate; however, aggressive fluid therapy increased the risk of acute kidney injury and pulmonary edema. Furthermore, there was no difference in overall outcomes such as incidence of SIRS, organ failure, or pancreatic necrosis for both therapeutic strategies [28]. Another study demonstrated that early rapid fluid therapy is associated with persistent organ failure, primarily of the respiratory system[29].

Recent studies have favored Ringer's lactate solution as the fluid of choice as opposed to saline solution, as the former reduced systemic inflammation[30]. Recent studies have concluded that the optimal AP regimen involves 3-4 L of Ringer's lactate solution every 24 h and predefined checkpoints at 6-8 h in order to tailor the fluid management to the condition of the patient. Furthermore, measuring urine output, intraabdominal pressure, and vital signs can help adjust the regimen of fluid therapy[31].

NUTRITION

While fasting was considered helpful in AP in the past, current evidence supports early oral or enteral nutrition even if patients experience AP-related complications. As patients with acute NP have increased energy requirements and sustained protein catabolism, an early start of enteral nutrition within the first 48 h of symptom onset is the current standard of care[32]. Regarding nutrition protocol, 25 kcal/kg/d up to a maximum of 30 kcal/kg/d with 1.2-1.5 g/kg of protein per day is recommended [24]. As compared to parenteral nutrition, enteral nutrition is associated with a lower rate of infectious complications and organ failure, shorter hospital stay, and reduced mortality rate[33,34].

ANTIBIOTICS AND PANCREATIC FUNGAL INFECTION

In contrast to patients with general AP, INP patients require immediate antibiotic therapy starting as soon as the diagnosis of INP is confirmed. INP should be initially treated with empirical antibiotics covering both aerobic and anaerobic Gram-negative and Gram-positive microorganisms, such as Imipenem or Ciprofloxacin[35]. A CT-guided fine-needle aspiration (FNA) can help design a more targeted treatment plan. The bacteria most frequently identified in IPN are *Escherichia coli*, *Enterococcus*, *Staphylococcus aureus*, *Staphylococcus epidermidis, Klebsiella pneumoniae, Pseudomonas spp*., and *Streptococcus spp*.[36].

Although antibiotic therapy is an essential tool in the treatment of INP patients, there is insufficient evidence to support the role of antibiotic prophylaxis after the diagnosis of sterile pancreatitis in order to prevent superinfection[36-38].

The use of prophylactic antibacterial therapy and duration of antibacterial therapy have been observed to increase the incidence of pancreatic fungal infection, which is a condition in patients with NP that is associated with increased mortality, intensive care unit admission rate, and length of stay. Its incidence was 26.6% in a study including 2151 patients with NP[39].

INVASIVE TREATMENT

Treatment planning and determining therapy concepts in INP patients should be performed within a multidisciplinary team of surgeons, interventional radiologists, and gastrointestinal endoscopists at experienced centers. Specialists should assess the feasibility of different access routes (transgastric, transduodenal, percutaneous, retroperitoneal, laparoscopic, or laparotomic) and weigh the treatment options, while considering the individual clinical condition of each patient (Table 1).

ENDOSCOPY

Endoscopy plays an emerging role in the treatment of INP[40]. Interventional approaches such as the placement of plastic or metal stents for endoscopic transluminal drainage (ETD) or direct necrosectomy are endoscopically feasible[41].

ETD AND STENT CHOICE

ETD is performed as the standard first step of endoscopic INP treatment. The aim of this procedure is to establish a temporary connection between the gastric cavity and necrotic cavity in the adjacent pancreas in order to drain necrotic collections.

ETD is performed with the assistance of endoscopic ultrasound, which helps avoid puncturing of vessels (*via* color doppler) or targets other than the necrotic collections[42]. The endoscopist then places either a plastic, double pigtail stent; a self-expandable metal stent (SEMS); or a lumen-apposing metal stent (LAMS). The metal stents are larger in diameter (15-20 mm) than the plastic stents (2.33–3.33 mm) and provide access for potential subsequent debridement (Figure 2). SEMS are not commonly used, as they have been reported to migrate into the collapsed fluid collection, posing a risk of major bleeding [43]. LAMS are designed to prevent migration and minimize the risk of leakage with their apposing features[44,45]. Another advantage of LAMS over plastic stents is the delivery system *via* a single-step platform, resulting in a shorter intervention time[46]. Retrospective studies comparing drainage with either LAMS or plastic stents found that the procedure time is significantly shorter for LAMS drainage [47,48]. One of these studies also shows that LAMS drainage results in increased clinical success, reduced need for surgery, and a lower recurrence rate[47].

A more recent randomized clinical trial, however, compared both stent types in a total of 60 patients (31 undergoing LAMS placement and 29 undergoing plastic stent placement) and found that LAMS was not superior to plastic stents. The authors detected no difference in treatment success, the number of procedures required, length of stay, adverse events (within < 3 wk of LAMS removal), readmissions, or overall treatment costs[49,50]. Moreover, the study showed significant stent-related adverse events if LAMS were left in place for more than 3 wk. Given these heterogeneous results, future studies are needed to further evaluate the outcomes of different ETD strategies. Nevertheless, the treating medical team should consider the different procedure duration, since the average time to place the LAMS is shorter compared to plastic stents (15 *vs* 40 min, $P < 0.001$)[51].

ENDOSCOPIC NECROSECTOMY

If the clinical condition of INP patients fails to improve 72 h after ETD, necrosectomy should be considered. Endoscopic transluminal necrosectomy (ETN) can be performed, using a LAMS as access route to the necrotic cavity. With help of forceps, nets, and lavage techniques with saline or hydrogen peroxide, the necrotic tissues are removed endoscopically. ETN can be performed several times if necroses cannot be removed in one procedure[52,53]. It is important to consider that multiple ETN attempts also cause an increased risk of procedure-related complications such as bleeding or perforation [42].

Table 1 Overview of possible interventions in infected necrotizing pancreatitis

		Indications	Contraindications	Most common complications	Ref.
Interventions	Endoscopic transluminal drainage	Standard first step for INP, standard for PFC treatment	Unencapsulated collections, distance from gastroduodenal duct (> 1 cm), vascular pseudoaneuryms	Major bleedings, perforation, post-procedure infection, recurrence, migration of the stent	[37, 38, 40]
	Endoscopic necrosectomy	No improvement in clinical condition within < 72 h after ETD, follow-up treatment	Large necrotic areas, dense necrosis, disconnected duct	Bleeding, perforation, pancreatic fistula, infections	[37, 48, 50]
	Percutaneous catheter drainage	Hardly accessible ANC, ETD not feasible, as combination with ETD	Intracystic haemorrhagia, pancreatic ascites	Intestinal fistula, infection	[36, 51]
	Open surgery	Infected necrosis, suspected perforation, abdominal compartment syndrome, ischemia, intrabadominal haemorrhagia, poorly walled off necrosis, final treatment option if other interventions fail	No clear contraindications reported	Bleeding, infection, perforation, multi-organ failure	[52, 53]
	Minimally invasive surgery	Infected necrosis	Extensive or hardly accessible collections	Bleeding, infection, perforation	[44, 57, 58]

INP: Infected necrotizing pancreatitis; ANC: Acute necrotic collection; ETD: Endoscopic transluminal drainage.

If a transgastric access is not possible or WONs are located in an inaccessible lateral position, a sinus tract endoscopy (STE) may be an option. In order to perform STE, a CT-guided percutaneous drainage catheter is placed 10 d prior to the procedure. The catheter causes the tract wall to mature, so the insertion of an adult gastroscope under fluoroscopic control can be performed safely. The necrotic cavity is lavaged and necrotic tissue is removed, as is done in the ETN procedure (Figure 3)[54].

Endoscopic necrosectomy reduces the rate of surgical interventions[55]. However, these interventions are limited to small necrotic areas and can be very time consuming (60-120 min)[56].

PERCUTANEOUS CATHETER DRAINAGE

Percutaneous catheter drainage (PCD) is often used prior to endoscopic necrosectomy if the ANC is located in the flank or pelvic region and access *via* ETD is not possible. An interventional radiologist places a general-purpose pigtail drainage catheter into the necrotic collection using the Seldinger technique *via* the most direct transperitoneal route. The preferred route for PCD is through the retroperitoneum. In this case, the drain can be used to guide potential further minimally invasive retroperitoneal necrosectomy (*i.e.*, video-assisted retroperitoneal debridement or STE). A combination of endoscopic transluminal and PCD (also known as dual-modality drainage) is a further option in patients with large collections extending into the paracolic gutters or pelvic region[57]. PCD is the least invasive intervention and was the only intervention needed for patients with INP in 35% (15 out of 43) patients in the randomized PANTER trial[40].

SURGERY

Larger, more complex, and endoscopically not accessible necrotic areas may require minimally invasive or open surgical approaches[16].

OPEN SURGERY

AP can lead to severe complications, such as hemorrhage, perforation, or ischemia. These complications may require immediate open surgical treatment. Abdominal compartment syndrome is a further severe potential complication of AP that must be managed *via* laparotomy. The drainage or debridement of ANCs and contacting the omental bursa should be avoided during these surgical emergency procedures [58]. Beside emergency indications, INP itself is a well-accepted indication for surgical treatment[59].

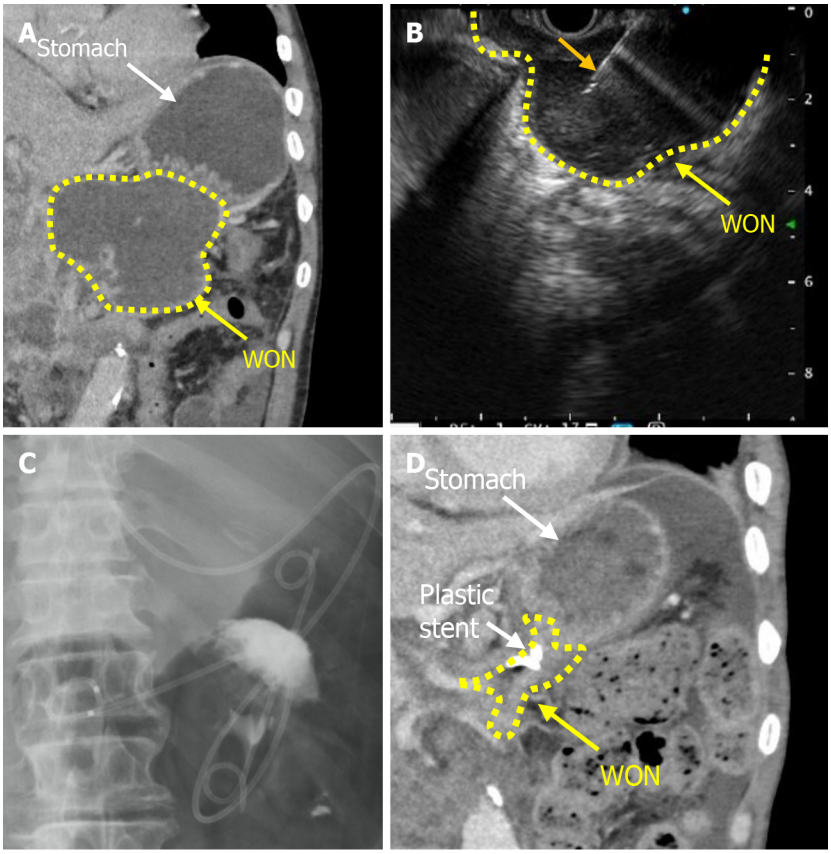

DOI: 10.3748/wjg.v28.i27.3383

Figure 2 Endoscopic transluminal drainage with plastic stenting. A: A typical computed tomography (CT) scan with walled-off necrosis (WON) formed by necrotizing pancreatitis (white arrow shows stomach and yellow dotted line is the demarcation line of the WON); B: Endoscopic ultrasonography (EUS)-guided drainage for WON was performed (orange arrow shows the needle of 22-gauge EUS needle); C: Two plastic stents and nasobiliary drainage tube was placed into the WON; D: The size of the WON was reduced in the CT scan one month after the procedure. WON: Walled-off necrosis.

Open surgical necrosectomy follows the main principle of exposing the necrotic area and bluntly debriding necrotic tissue: Necrosectomy can be performed with: (1) Open packing; (2) Closed packing; (3) Closed continuous lavage; and (4) Planned re-laparotomies. Open packing involves packing the necrotic cavity with non-adherent dressing after surgical necrosectomy. Readmissions follow every 48 h until the abdomen can be closed after inserting drains. Closed packing is performed when multiple, large, gauze-filled Penrose drains are placed in the residual cavity after necrosectomy and the abdomen is subsequently closed. Closed continuous lavage is performed with the help of two or more double-lumen Salem sump tubes and single-lumen silicone rubber tubes, which are inserted from each flank side and have an in- and outflow of the lavage. Up to 40 L of lavage fluids are used. Planned re-laparotomies provide continuous removal of necrotic tissue over several following days. Surgeons often incorporate zippers into the abdominal wall facilitating repetitive surgical intervention[59].

The standard surgical access is performed either as a transperitoneal or retroperitoneal access. Transgastric access has been added more recently and is considered a fast single-stage option for the treatment of symptomatic WON in severely ill patients[60]. A recent study suggested choosing surgical transgastric necrosectomy whenever feasible in the case of a disconnected pancreatic duct, for dense and large necrosis, and if cholecystectomy must be performed. If the transgastric access is not possible, the authors suggested video-assisted retroperitoneal debridement (VARD) as an alternative procedure[61].

MINIMALLY INVASIVE SURGERY

The main procedures of minimal invasive management of INP are minimal access retroperitoneal pancreatic necrosectomy (MARPN) and VARD. MARPN involves the placement of a 12-French catheter under CT guidance by an interventional radiologist prior to surgery. The preformed access tract is then dilated up to 30-French during the minimal invasive procedure, so that a rigid nephroscope can be entered. The nephroscope serves as visualization instrument and working channel for necrosectomy at the same time. An irrigation drainage system for continuous lavage is installed at the end of the procedure. MARPN can be done multiple times until the patient's condition improves.

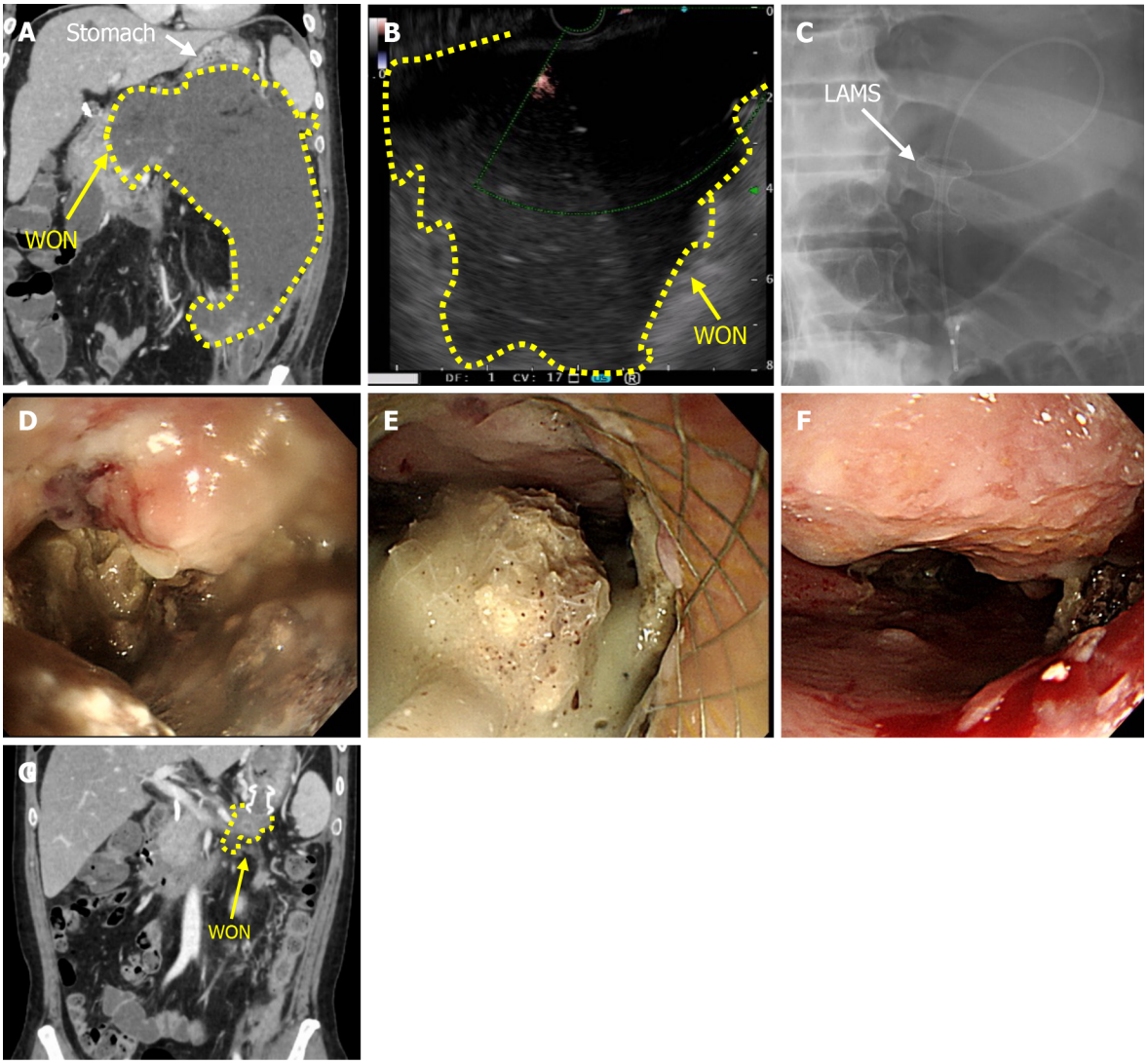

DOI: 10.3748/wjg.v28.i27.3383

Figure 3 A case with endoscopic transluminal drainage with lumen-apposing metal stent. A: Computed tomography (CT) scan before performing the endoscopic ultrasonography (EUS)-guided drainage (White arrow shows the stomach and the yellow arrow shows the walled-off necrosis (WON); the yellow dotted line is the demarcation line of the WON); B: EUS (with color doppler) picture shows marked echoic lesion without vessels; C: Lumen-apposing metal stent (LAMS) and nasobiliary drainage tube were placed (white arrow shows LAMS: Hot AXIOS™ 15 mm × 10 mm, Boston Scientific, Marlborough, MA, United States; Boston Scientific Japan, Tokyo, Japan); D: Esophagogastroduodenoscopy was inserted into necrotic cavity through LAMS; E: Necrosectomy was performed using endoscopic retrieval net; F: Endoscopic findings of the WON one month after the multiple necrosectomy sessions (2-3 times/wk); G: CT scan shows marked reduction of WON cavity one month after multiple necrosectomy sessions. WON: Walled-off necrosis; LAMS: Lumen-apposing metal stent.

VARD consists of combined manual and laparoscopical necrosectomy. It was first reported in 2007 by van Santvoort *et al*[62], who described it as "a hybrid between pure endoscopic retroperitoneal necrosectomy and the open translumbar approach." The procedure starts with a left flank subcostal incision facilitating direct manual debridement followed by a laparoscopic deeper inspection and debridement by laparoscopic instruments. The intervention ends with a continuous lavage.

COMPARISON BETWEEN OPEN AND MINIMALLY INVASIVE SURGERY

Open surgical necrosectomy in AP was historically associated with a mortality rate of 50% or higher[63, 64]. Improved intensive care management, as well as advances in surgical techniques, including minimally invasive options, and the availability of first line endoscopic and minimally invasive procedures have improved patient outcomes over the past decades[65].

A retrospective study compared outcomes of INP patients between 1997-2008 and 2009-2013 and revealed decreased mortality (23.8% *vs* 11.2%, $P = 0.001$) and overall complication rates (73.3% *vs* 64.4%, $P = 0.80$) in the more recent cohort. Minimal invasive approaches contribute to better treatment success rates and improved outcomes in INP as compared to open surgery. MARPN also reportedly results in decreased postoperative multiorgan failure compared to open pancreatic necrosectomy (35% *vs* 20.4%, *P*

= 0.001)[66].

A recent retrospective cohort study comparing 88 patients with open surgical necrosectomy to 91 patients who were treated with minimal invasive surgery (MIS) showed that MIS results in a fivefold decrease in mortality[49]. A meta-analysis published in 2018 reported lower risk of death rates in the very high-risk group when comparing minimally invasive necrosectomy to open surgery[67].

STEP-UP APPROACH

The therapeutic approach in INP patients has shifted from open surgical treatment to a less invasive management that can be summarized by "three Ds": Delay – drain – debride. This approach leads to the introduction of the so-called "step-up approach", which was first described in 2006 by the Dutch Pancreatitis Study group in their PANTER trial[40].

Delay refers to the solidification and complete encapsulation of the pancreatic collection when WON occurs. This is presumed to optimize conditions for intervention, with a lower risk of bleeding and less reinterventions. Drain alludes to using a percutaneous or endoscopic transgastric catheter drainage to mitigate sepsis. Finally, when patients fail to show clinical improvement, debridement is required; in such cases, performing endoscopic or surgical necrosectomy is the next step[40]. A multidisciplinary team of INP experts can choose from different treatment options for each step and decides on the most suitable approach for each individual patient. Re-evaluation periods of 72 h between steps should be maintained[49]. This therapeutic management is also referred to as the "step-up approach", which comprises both an endoscopic and a surgical approach. The overall paradigm is to start with the least invasive and harmful intervention with an option to escalate to more radical approaches with continuous evaluation. The step-up approach decreased the incidence of new multiple-organ failure from 40% to 12% when compared to primary laparotomy[40]. It is the current state-of-the-art approach and has been implemented in all major guidelines (Figure 4)[23,68].

ENDOSCOPIC OR SURGICAL STEP-UP APPROACH

The step-up approach can be performed using endoscopic or surgical necrosectomy. Comparing both approaches has been subject of several randomized trials. From 2008 to 2010, the first prospective, multicentric randomized controlled trial comparing the surgical and endoscopic step-up approaches was performed in the Netherlands. The so-called PENGUIN trial compared endoscopic transgastric necrosectomy with prior retroperitoneal drainage and different techniques of surgical necrosectomy (VARD or, if not feasible, laparotomy) in 10 INP patients per group. The results demonstrated reduced inflammatory response as measured by serum interleukin 6 Levels, reduced rates of pancreatic fistulas (10% *vs* 70%, P = 0.020), and no occurrence of new-onset multiorgan failure (0% *vs* 50%, P = 0.030) in patients in the endoscopic arm[69]. The authors concluded that the endoscopic approach was associated with reduced physiological stress, while surgical access was more invasive.

The multicentric TENSION trial was conducted during 2011-2015 in the Netherlands and compared the outcomes of 51 patients following the endoscopic step-up approach to 47 following the surgical step-up approach. The findings showed no significant difference in mortality and major morbidity between both groups (43% in the endoscopic step-up approach *vs*. 45% in the surgical step-up approach, P = 0.880). However, the mean hospital stay was shorter (53 *vs* 69 d, P = 0.014), fewer pancreatic fistulas occurred (5% *vs* 32%, P = 0.001), and there was a lower overall mean cost (60228 € *vs* 73883 € in the endoscopic step-up approach group[70]).

From 2014 to 2017, the monocentric MISER trial was performed in the United States, comparing minimally invasive surgery (laparoscopic debridement or VARD) to the endoscopic step-up approach in a total of 66 patients. They included severely ill patient cohorts and excluded patients who had improved clinically with only percutaneous drainage as treatment. Consistent with the findings of the TENSION trial, MISER showed no difference in mortality rates (8.8% with the endoscopic step-up approach *vs*. 6.3% with minimally invasive surgery, P = 0.999). However, patients assigned to the endoscopic approach were less likely to develop enteral and pancreatic-cutaneous fistulas (0% *vs* 28.1%, P = 0.001), experienced a lower rate of major complications (12% *vs*. 41%, P = 0.007), and had lower rates of SIRS (20.6% *vs* 65.6 %, P < 0.001). Six months after treatment, patients in the surgical group had significantly more disease-related adverse events than did those in the endoscopic group (43.8 % *vs* 5.9 %, P < 0.001). Finally, the physical health scores for quality of life at 3 mo were better with the endoscopic approach (P = 0.039) and the mean total cost were lower ($75830) compared with the surgical approach ($117492)[49].

The currently available randomized controlled trials point to the endoscopic step-up approach as the preferred treatment for INP patients. However, if the endoscopic treatment is unfeasible, or the necrotic collection extends to the flank or pelvic region (which is difficult to access endoscopically), surgical interventions constitute the alternative when performed as a step-up approach. Each INP patient should be assessed and treated by a multidisciplinary team with sufficient experience in both approaches.

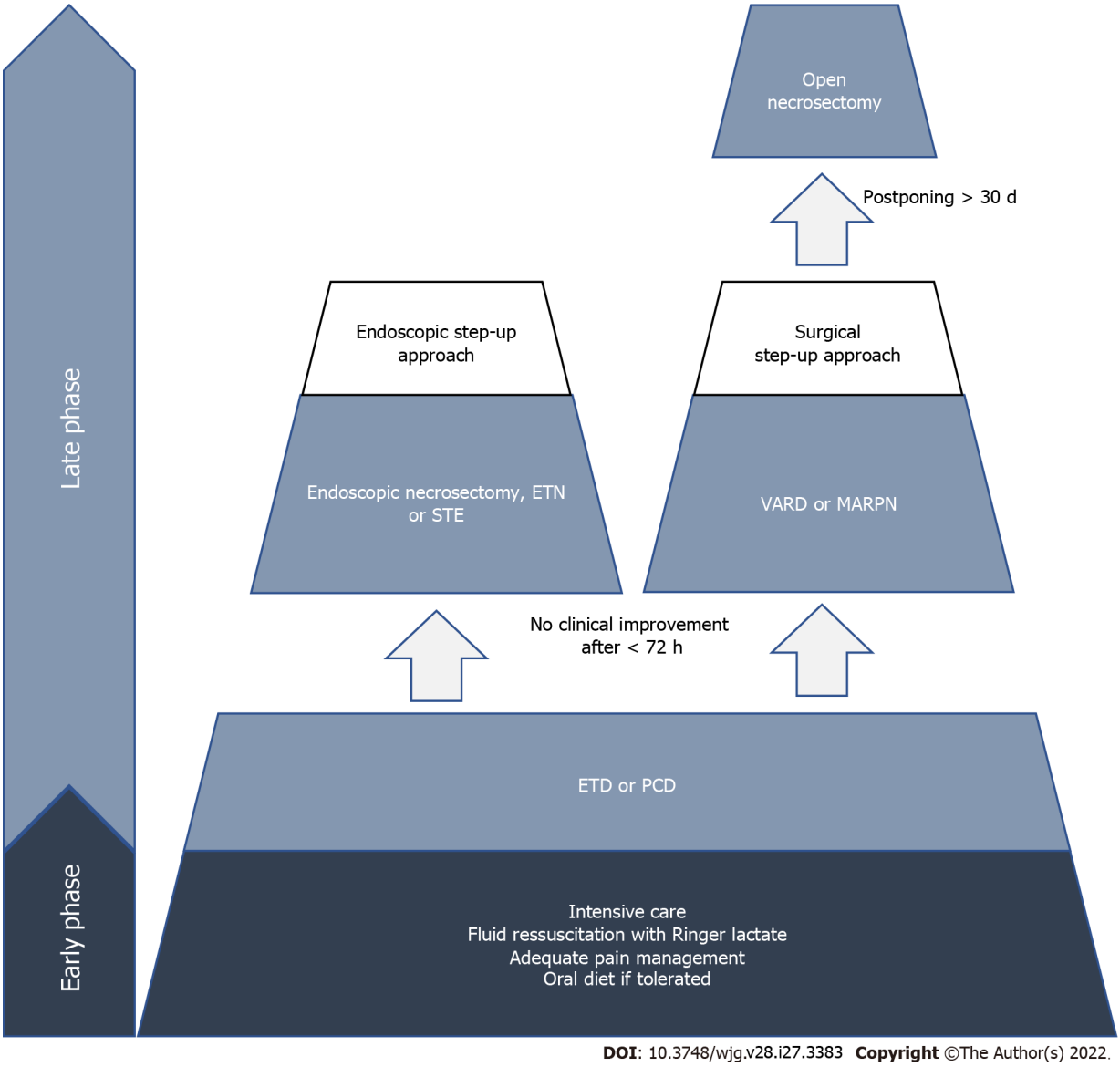

DOI: 10.3748/wjg.v28.i27.3383

Figure 4 Overview of the step-up approaches of infected necrotizing pancreatitis patients. In the acute phase, multidisciplinary treatment for acute pancreatitis is recommended. Endoscopic necrosectomy or surgical step-up should be considered if there no clinical improvement is observed within 72 h. Open necrosectomy should be considered after video-assisted retroperitoneal debridement or minimal access retroperitoneal pancreatic necrosectomy. ETN: Endoscopic transluminal necrosectomy; STE: Sinus tract endoscopy; ETD: Endoscopic transluminal drainage; PCD: Percutaneous catheter drainage; VARD: Video-assisted retroperitoneal debridement; MARPN: Minimal access retroperitoneal pancreatic necrosectomy.

TIMING OF INTERVENTIONS

The optimal timing of interventions remains a controversial topic and is subject to ongoing debate. An international survey performed in 2016 among 87 pancreatologists revealed that 55% of experts routinely postponed invasive interventions after diagnosing infected necrosis in AP and awaited the effect of antibiotics. However, 33% of pancreatologists preferred surgical necrosectomy as early as possible in infected necrosis, while the remaining 67% would select that route only in the case of WON [71].

A 2014 prospective study including 223 patients revealed that a postponed surgical intervention after 30 d was associated with a lower mortality rate compared to that associated with surgical intervention before day 30 [10% (9/87) *vs* 21% (28/136), $P = 0.040$][72]. This study followed up on a retrospective study from 2007 that also revealed that patients receiving a postponed surgical necrosectomy exhibited lower mortality rates as compared to those receiving surgical treatment after 15-29 d and 1-14 d (8% *vs* 45% *vs* 75%, $P < 0.001$)[26].

A recent study of the Dutch Pancreatic Study Group, the POINTER trial, determined whether the outcomes in INP patients could be improved by early catheter drainage. In the study, catheter drainage was performed immediately in 55 patients, while 49 received the treatment after waiting until WON occurred. Patients were included when there was gas reported on CECT, positive gram/culture FNA,

and clinical suspicion for INP. The rate of organ failure was comparable in both groups and there was no difference in mortality rates. The total number of interventions was 4:1 in the early intervention group compared to the group with delayed intervention, and the total number of necrosectomies in the whole number of patients was 28 (51%) in the immediate as compared to 11 (22%) in the postponed drainage group. Postponing the intervention led to conservative treatment in nearly 40% of patients. This trial could not detect a benefit of immediate drainage over postponed drainage. Conversely, postponing intervention may ultimately avoid necrosectomy and its potential complications[73].

CONCLUSION

Recent advances in endoscopic and minimally invasive therapy have led to a shift in the interventional strategy for INP. Although no standardized approach suits every patient, the "step-up approach" has emerged as a paradigm to treat this severe disease. The key is to start with the least invasive procedure and potentially escalate to more invasive interventions after continuous evaluation, if necessary. This approach highlights the importance of a multidisciplinary team to guide therapeutic approaches in INP patients. The strategy should be based on the individual patient and should allow for dynamic changes in regard to the patient's clinical condition. This claim is also backed by the studies presented in this review that demonstrate lower rates of new multiorgan failure and reduction of hospitalization days, among other preferred outcomes. Even with these recent advances, INP continues to elicit a high mortality rate and further research is required to optimize strategic approaches.

ACKNOWLEDGEMENTS

We thank Hiramatsu K at Asahikawa Kosei Hospital for providing percutaneous radiological drainage pictures; We also thank Okada T, Kawamoto T, Fujinaga A, and Goto M at Asahikawa Kosei Hospital, as well as Hayashi A, the member of Division of Metabolism and Biosystemic Science, Gastroenterology and Hematology/Oncology Department of Medicine, Asahikawa Medical University for providing endoscopic drainage pictures.

FOOTNOTES

Author contributions: Purschke B wrote and edited the manuscript, and collected the clinical data and evidence; Bolm L edited the manuscript and reviewed the discussion about interventional surgical strategies; Meyer MN reviewed the manuscript and provided recommendations on treatment strategies; Sato H reviewed the manuscript and provided strategies and recommendations on the endoscopic intervention part; all authors have read and approved the final manuscript.

Supported by Japan Society for the Promotion of Science KAKENHI, No. 19K17480 and No. 21KK0283 (to Sato H).

Conflict-of-interest statement: Authors declare no conflicts of interests for this article.

Country/Territory of origin: Japan

ORCID number: Birte Purschke 0000-0002-6885-6345; Louisa Bolm 0000-0002-1612-1857; Max Nikolaus Meyer 0000-0003-2970-5752; Hiroki Sato 0000-0002-6994-1840.

Corresponding Author's Membership in Professional Societies: Japan Gastroenterological Endoscopy Society, No. 20190318; Japanese Society of Gastroenterology, No. 39625; American Gastroenterological Association, No. 1156949; Japan Society of Human Genetics, No. 1517082360; Japanese Society of Internal Medicine, No. 99021; Japanese Association for Medical Artificial Intelligence, No. 388; Japanese Board of Cancer Therapy, No. 1810053; Japan Society of Medical Oncology, No. 20-0076; Japanese Society for Helicobacter Research; Japan Society of Hepatology, No. 8987; Royal Society of Medicine, No. 00723754.

S-Editor: Yan JP
L-Editor: A
P-Editor: Yan JP

REFERENCES

1 **Peery AF**, Crockett SD, Murphy CC, Lund JL, Dellon ES, Williams JL, Jensen ET, Shaheen NJ, Barritt AS, Lieber SR, Kochar B, Barnes EL, Fan YC, Pate V, Galanko J, Baron TH, Sandler RS. Burden and Cost of Gastrointestinal, Liver, and Pancreatic Diseases in the United States: Update 2018. *Gastroenterology* 2019; **156**: 254-272.e11 [PMID: 30315778 DOI: 10.1053/j.gastro.2018.08.063]

2 **Gapp J**, Hall AG, Walters RW, Jahann D, Kassim T, Reddymasu S. Trends and Outcomes of Hospitalizations Related to Acute Pancreatitis: Epidemiology From 2001 to 2014 in the United States. *Pancreas* 2019; **48**: 548-554 [PMID: 30946239 DOI: 10.1097/MPA.0000000000001275]

3 **Zheng Z**, Ding YX, Qu YX, Cao F, Li F. A narrative review of acute pancreatitis and its diagnosis, pathogenetic mechanism, and management. *Ann Transl Med* 2021; **9**: 69 [PMID: 33553362 DOI: 10.21037/atm-20-4802]

4 **Mayerle J**, Sendler M, Hegyi E, Beyer G, Lerch MM, Sahin-Tóth M. Genetics, Cell Biology, and Pathophysiology of Pancreatitis. *Gastroenterology* 2019; **156**: 1951-1968.e1 [PMID: 30660731 DOI: 10.1053/j.gastro.2018.11.081]

5 **Habtezion A**, Gukovskaya AS, Pandol SJ. Acute Pancreatitis: A Multifaceted Set of Organelle and Cellular Interactions. *Gastroenterology* 2019; **156**: 1941-1950 [PMID: 30660726 DOI: 10.1053/j.gastro.2018.11.082]

6 **Mederos MA**, Reber HA, Girgis MD. Acute Pancreatitis: A Review. *JAMA* 2021; **325**: 382-390 [PMID: 33496779 DOI: 10.1001/jama.2020.20317]

7 **Werge M**, Novovic S, Schmidt PN, Gluud LL. Infection increases mortality in necrotizing pancreatitis: A systematic review and meta-analysis. *Pancreatology* 2016; **16**: 698-707 [PMID: 27449605 DOI: 10.1016/j.pan.2016.07.004]

8 **Colvin SD**, Smith EN, Morgan DE, Porter KK. Acute pancreatitis: an update on the revised Atlanta classification. *Abdom Radiol (NY)* 2020; **45**: 1222-1231 [PMID: 31494708 DOI: 10.1007/s00261-019-02214-w]

9 **van Santvoort HC**, Bakker OJ, Bollen TL, Besselink MG, Ahmed Ali U, Schrijver AM, Boermeester MA, van Goor H, Dejong CH, van Eijck CH, van Ramshorst B, Schaapherder AF, van der Harst E, Hofker S, Nieuwenhuijs VB, Brink MA, Kruyt PM, Manusama ER, van der Schelling GP, Karsten T, Hesselink EJ, van Laarhoven CJ, Rosman C, Bosscha K, de Wit RJ, Houdijk AP, Cuesta MA, Wahab PJ, Gooszen HG; Dutch Pancreatitis Study Group. A conservative and minimally invasive approach to necrotizing pancreatitis improves outcome. *Gastroenterology* 2011; **141**: 1254-1263 [PMID: 21741922 DOI: 10.1053/j.gastro.2011.06.073]

10 **Nesvaderani M**, Eslick GD, Vagg D, Faraj S, Cox MR. Epidemiology, aetiology and outcomes of acute pancreatitis: A retrospective cohort study. *Int J Surg* 2015; **23**: 68-74 [PMID: 26384834 DOI: 10.1016/j.ijsu.2015.07.701]

11 **Park JY**, Jeon TJ, Ha TH, Hwang JT, Sinn DH, Oh TH, Shin WC, Choi WC. Bedside index for severity in acute pancreatitis: comparison with other scoring systems in predicting severity and organ failure. *Hepatobiliary Pancreat Dis Int* 2013; **12**: 645-650 [PMID: 24322751 DOI: 10.1016/s1499-3872(13)60101-0]

12 **Foster BR**, Jensen KK, Bakis G, Shaaban AM, Coakley FV. Revised Atlanta Classification for Acute Pancreatitis: A Pictorial Essay. *Radiographics* 2016; **36**: 675-687 [PMID: 27163588 DOI: 10.1148/rg.2016150097]

13 **Zerem E**. Treatment of severe acute pancreatitis and its complications. *World J Gastroenterol* 2014; **20**: 13879-13892 [PMID: 25320523 DOI: 10.3748/wjg.v20.i38.13879]

14 **Kayar Y**, Senturk H, Tozlu M, Baysal B, Atay M, Ince AT. Prediction of Self-Limited Acute Pancreatitis Cases at Admission to Emergency Unit. *GE Port J Gastroenterol* 2019; **26**: 251-259 [PMID: 31328139 DOI: 10.1159/000493762]

15 **Yasuda I**, Takahashi K. Endoscopic management of walled-off pancreatic necrosis. *Dig Endosc* 2021; **33**: 335-341 [PMID: 32306430 DOI: 10.1111/den.13699]

16 **Heckler M**, Hackert T, Hu K, Halloran CM, Büchler MW, Neoptolemos JP. Severe acute pancreatitis: surgical indications and treatment. *Langenbecks Arch Surg* 2021; **406**: 521-535 [PMID: 32910276 DOI: 10.1007/s00423-020-01944-6]

17 **van Dijk SM**, Hallensleben NDL, van Santvoort HC, Fockens P, van Goor H, Bruno MJ, Besselink MG; Dutch Pancreatitis Study Group. Acute pancreatitis: recent advances through randomised trials. *Gut* 2017; **66**: 2024-2032 [PMID: 28838972 DOI: 10.1136/gutjnl-2016-313595]

18 **Büchler MW**, Gloor B, Müller CA, Friess H, Seiler CA, Uhl W. Acute necrotizing pancreatitis: treatment strategy according to the status of infection. *Ann Surg* 2000; **232**: 619-626 [PMID: 11066131 DOI: 10.1097/00000658-200011000-00001]

19 **da Costa DW**, Boerma D, van Santvoort HC, Horvath KD, Werner J, Carter CR, Bollen TL, Gooszen HG, Besselink MG, Bakker OJ. Staged multidisciplinary step-up management for necrotizing pancreatitis. *Br J Surg* 2014; **101**: e65-e79 [PMID: 24272964 DOI: 10.1002/bjs.9346]

20 **Werner J**, Feuerbach S, Uhl W, Büchler MW. Management of acute pancreatitis: from surgery to interventional intensive care. *Gut* 2005; **54**: 426-436 [PMID: 15710995 DOI: 10.1136/gut.2003.035907]

21 **Leppäniemi A**, Tolonen M, Tarasconi A, Segovia-Lohse H, Gamberini E, Kirkpatrick AW, Ball CG, Parry N, Sartelli M, Wolbrink D, van Goor H, Baiocchi G, Ansaloni L, Biffl W, Coccolini F, Di Saverio S, Kluger Y, Moore E, Catena F. 2019 WSES guidelines for the management of severe acute pancreatitis. *World J Emerg Surg* 2019; **14**: 27 [PMID: 31210778 DOI: 10.1186/s13017-019-0247-0]

22 **McPherson SJ**, O'Reilly DA, Sinclair MT, Smith N. The use of imaging in acute pancreatitis in United Kingdom hospitals: findings from a national quality of care study. *Br J Radiol* 2017; **90**: 20170224 [PMID: 28869389 DOI: 10.1259/bjr.20170224]

23 **Working Group IAP/APA Acute Pancreatitis Guidelines**. IAP/APA evidence-based guidelines for the management of acute pancreatitis. *Pancreatology* 2013; **13**: e1-15 [PMID: 24054878 DOI: 10.1016/j.pan.2013.07.063]

24 **Gomes CA**, Di Saverio S, Sartelli M, Segallini E, Cilloni N, Pezzilli R, Pagano N, Gomes FC, Catena F. Severe acute pancreatitis: eight fundamental steps revised according to the 'PANCREAS' acronym. *Ann R Coll Surg Engl* 2020; **102**: 555-559 [PMID: 32159357 DOI: 10.1308/rcsann.2020.0029]

25 **Fernández-del Castillo C**, Rattner DW, Makary MA, Mostafavi A, McGrath D, Warshaw AL. Débridement and closed packing for the treatment of necrotizing pancreatitis. *Ann Surg* 1998; **228**: 676-684 [PMID: 9833806 DOI: 10.1097/00000658-199811000-00007]

26 **Besselink MG**, Verwer TJ, Schoenmaeckers EJ, Buskens E, Ridwan BU, Visser MR, Nieuwenhuijs VB, Gooszen HG.

Timing of surgical intervention in necrotizing pancreatitis. *Arch Surg* 2007; **142**: 1194-1201 [PMID: 18086987 DOI: 10.1001/archsurg.142.12.1194]

27 **Schepers NJ**, Bakker OJ, Besselink MG, Ahmed Ali U, Bollen TL, Gooszen HG, van Santvoort HC, Bruno MJ; Dutch Pancreatitis Study Group. Impact of characteristics of organ failure and infected necrosis on mortality in necrotising pancreatitis. *Gut* 2019; **68**: 1044-1051 [PMID: 29950344 DOI: 10.1136/gutjnl-2017-314657]

28 **Gad MM**, Simons-Linares CR. Is aggressive intravenous fluid resuscitation beneficial in acute pancreatitis? *World J Gastroenterol* 2020; **26**: 1098-1106 [PMID: 32206000 DOI: 10.3748/wjg.v26.i10.1098]

29 **Li L**, Jin T, Wen S, Shi N, Zhang R, Zhu P, Lin Z, Jiang K, Guo J, Liu T, Philips A, Deng L, Yang X, Singh VK, Sutton R, Windsor JA, Huang W, Xia Q. Early Rapid Fluid Therapy Is Associated with Increased Rate of Noninvasive Positive-Pressure Ventilation in Hemoconcentrated Patients with Severe Acute Pancreatitis. *Dig Dis Sci* 2020; **65**: 2700-2711 [PMID: 31912265 DOI: 10.1007/s10620-019-05985-w]

30 **Wu BU**, Hwang JQ, Gardner TH, Repas K, Delee R, Yu S, Smith B, Banks PA, Conwell DL. Lactated Ringer's solution reduces systemic inflammation compared with saline in patients with acute pancreatitis. *Clin Gastroenterol Hepatol* 2011; **9**: 710-717.e1 [PMID: 21645639 DOI: 10.1016/j.cgh.2011.04.026]

31 **Garg PK**, Mahapatra SJ. Optimum Fluid Therapy in Acute Pancreatitis Needs an Alchemist. *Gastroenterology* 2021; **160**: 655-659 [PMID: 33412126 DOI: 10.1053/j.gastro.2020.12.017]

32 **Bakker OJ**, van Brunschot S, Farre A, Johnson CD, Kalfarentzos F, Louie BE, Oláh A, O'Keefe SJ, Petrov MS, Powell JJ, Besselink MG, van Santvoort HC, Rovers MM, Gooszen HG. Timing of enteral nutrition in acute pancreatitis: meta-analysis of individuals using a single-arm of randomised trials. *Pancreatology* 2014; **14**: 340-346 [PMID: 25128270 DOI: 10.1016/j.pan.2014.07.008]

33 **Li W**, Liu J, Zhao S, Li J. Safety and efficacy of total parenteral nutrition versus total enteral nutrition for patients with severe acute pancreatitis: a meta-analysis. *J Int Med Res* 2018; **46**: 3948-3958 [PMID: 29962261 DOI: 10.1177/0300060518782070]

34 **Oláh A**, Romics L Jr. Enteral nutrition in acute pancreatitis: a review of the current evidence. *World J Gastroenterol* 2014; **20**: 16123-16131 [PMID: 25473164 DOI: 10.3748/wjg.v20.i43.16123]

35 **Isenmann R**, Büchler MW, Friess H, Uhl W, Beger HG. Antibiotics in acute pancreatitis. *Dig Surg* 1996; **13**: 365-369 [DOI: 10.1159/000172465]

36 **Barie PS**. A critical review of antibiotic prophylaxis in severe acute pancreatitis. *Am J Surg* 1996; **172**: 38S-43S [PMID: 9003689 DOI: 10.1016/S0002-9610(96)00349-2]

37 **Villatoro E**, Mulla M, Larvin M. Antibiotic therapy for prophylaxis against infection of pancreatic necrosis in acute pancreatitis. *Cochrane Database Syst Rev* 2010; CD002941 [PMID: 20464721 DOI: 10.1002/14651858.CD002941.pub3]

38 **Jafri NS**, Mahid SS, Minor KS, Idstein SR, Hornung CA, Galandiuk S. Meta-analysis: antibiotic prophylaxis to prevent peristomal infection following percutaneous endoscopic gastrostomy. *Aliment Pharmacol Ther* 2007; **25**: 647-656 [PMID: 17311597 DOI: 10.1111/j.1365-2036.2007.03247.x]

39 **Singh RR**, Mitchell W, David Y, Cheesman A, Dixon RE, Nagula S, DiMaio CJ, Greenwald DA, Kumta NA. Pancreatic Fungal Infection in Patients With Necrotizing Pancreatitis: A Systematic Review and Meta-analysis. *J Clin Gastroenterol* 2021; **55**: 218-226 [PMID: 33252558 DOI: 10.1097/MCG.0000000000001467]

40 **Besselink MG**, van Santvoort HC, Nieuwenhuijs VB, Boermeester MA, Bollen TL, Buskens E, Dejong CH, van Eijck CH, van Goor H, Hofker SS, Lameris JS, van Leeuwen MS, Ploeg RJ, van Ramshorst B, Schaapherder AF, Cuesta MA, Consten EC, Gouma DJ, van der Harst E, Hesselink EJ, Houdijk LP, Karsten TM, van Laarhoven CJ, Pierie JP, Rosman C, Bilgen EJ, Timmer R, van der Tweel I, de Wit RJ, Witteman BJ, Gooszen HG; Dutch Acute Pancreatitis Study Group. Minimally invasive 'step-up approach' versus maximal necrosectomy in patients with acute necrotising pancreatitis (PANTER trial): design and rationale of a randomised controlled multicenter trial [ISRCTN13975868]. *BMC Surg* 2006; **6**: 6 [PMID: 16606471 DOI: 10.1186/1471-2482-6-6]

41 **Ruiz-Clavijo D**, de la Higuera BG, Vila JJ. Advances in the endoscopic management of pancreatic collections. *World J Gastrointest Endosc* 2015; **7**: 381-388 [PMID: 25901217 DOI: 10.4253/wjge.v7.i4.381]

42 **Trikudanathan G**, Attam R, Arain MA, Mallery S, Freeman ML. Endoscopic interventions for necrotizing pancreatitis. *Am J Gastroenterol* 2014; **109**: 969-81; quiz 982 [PMID: 24957157 DOI: 10.1038/ajg.2014.130]

43 **Talreja JP**, Shami VM, Ku J, Morris TD, Ellen K, Kahaleh M. Transenteric drainage of pancreatic-fluid collections with fully covered self-expanding metallic stents (with video). *Gastrointest Endosc* 2008; **68**: 1199-1203 [PMID: 19028232 DOI: 10.1016/j.gie.2008.06.015]

44 **Mussetto A**, Fugazza A, Fuccio L, Triossi O, Repici A, Anderloni A. Current uses and outcomes of lumen-apposing metal stents. *Ann Gastroenterol* 2018; **31**: 535-540 [PMID: 30174389 DOI: 10.20524/aog.2018.0287]

45 **Dalsania R**, Willingham FF. Treatment of walled-off pancreatic necrosis. *Curr Opin Gastroenterol* 2019; **35**: 478-482 [PMID: 31313686 DOI: 10.1097/MOG.0000000000000564]

46 **Bang JY**, Varadarajulu S. Lumen-apposing metal stents for endoscopic ultrasonography-guided interventions. *Dig Endosc* 2019; **31**: 619-626 [PMID: 31050068 DOI: 10.1111/den.13428]

47 **Chen YI**, Yang J, Friedland S, Holmes I, Law R, Hosmer A, Stevens T, Franco MC, Jang S, Pawa R, Mathur N, Sejpal DV, Inamdar S, Trindade AJ, Nieto J, Berzin TM, Sawhney M, DeSimone ML, DiMaio C, Kumta NA, Gupta S, Yachimski P, Anderloni A, Baron TH, James TW, Jamil LH, Ona MA, Lo SK, Gaddam S, Dollhopf M, Bukhari MA, Moran R, Gutierrez OB, Sanaei O, Fayad L, Ngamruengphong S, Kumbhari V, Singh V, Repici A, Khashab MA. Lumen apposing metal stents are superior to plastic stents in pancreatic walled-off necrosis: a large international multicenter study. *Endosc Int Open* 2019; **7**: E347-E354 [PMID: 30834293 DOI: 10.1055/a-0828-7630]

48 **Rana SS**, Sharma R, Dhalaria L, Gupta R. Efficacy and safety of plastic versus lumen-apposing metal stents for transmural drainage of walled-off necrosis: a retrospective single-center study. *Ann Gastroenterol* 2020; **33**: 426-432 [PMID: 32624665 DOI: 10.20524/aog.2020.0499]

49 **Bang JY**, Arnoletti JP, Holt BA, Sutton B, Hasan MK, Navaneethan U, Feranec N, Wilcox CM, Tharian B, Hawes RH, Varadarajulu S. An Endoscopic Transluminal Approach, Compared With Minimally Invasive Surgery, Reduces Complications and Costs for Patients With Necrotizing Pancreatitis. *Gastroenterology* 2019; **156**: 1027-1040.e3 [PMID:

30452918 DOI: 10.1053/j.gastro.2018.11.031]
50 **Bang JY**, Hasan MK, Navaneethan U, Sutton B, Frandah W, Siddique S, Hawes RH, Varadarajulu S. Lumen-apposing metal stents for drainage of pancreatic fluid collections: When and for whom? *Dig Endosc* 2017; **29**: 83-90 [PMID: 27199157 DOI: 10.1111/den.12681]
51 **Bang JY**, Navaneethan U, Hasan MK, Sutton B, Hawes R, Varadarajulu S. Non-superiority of lumen-apposing metal stents over plastic stents for drainage of walled-off necrosis in a randomised trial. *Gut* 2019; **68**: 1200-1209 [PMID: 29858393 DOI: 10.1136/gutjnl-2017-315335]
52 **Arvanitakis M**, Dumonceau JM, Albert J, Badaoui A, Bali MA, Barthet M, Besselink M, Deviere J, Oliveira Ferreira A, Gyökeres T, Hritz I, Hucl T, Milashka M, Papanikolaou IS, Poley JW, Seewald S, Vanbiervliet G, van Lienden K, van Santvoort H, Voermans R, Delhaye M, van Hooft J. Endoscopic management of acute necrotizing pancreatitis: European Society of Gastrointestinal Endoscopy (ESGE) evidence-based multidisciplinary guidelines. *Endoscopy* 2018; **50**: 524-546 [PMID: 29631305 DOI: 10.1055/a-0588-5365]
53 **Baron TH**. Endoscopic pancreatic necrosectomy. *Gastroenterol Hepatol (N Y)* 2008; **4**: 617-620 [PMID: 22798744 DOI: 10.1016/s0016-5085(08)60559-4]
54 **Goenka MK**, Goenka U, Mujoo MY, Tiwary IK, Mahawar S, Rai VK. Pancreatic Necrosectomy through Sinus Tract Endoscopy. *Clin Endosc* 2018; **51**: 279-284 [PMID: 29301065 DOI: 10.5946/ce.2017.066]
55 **Gardner TB**, Coelho-Prabhu N, Gordon SR, Gelrud A, Maple JT, Papachristou GI, Freeman ML, Topazian MD, Attam R, Mackenzie TA, Baron TH. Direct endoscopic necrosectomy for the treatment of walled-off pancreatic necrosis: results from a multicenter U.S. series. *Gastrointest Endosc* 2011; **73**: 718-726 [PMID: 21237454 DOI: 10.1016/j.gie.2010.10.053]
56 **Voermans RP**, Besselink MG, Fockens P. Endoscopic management of walled-off pancreatic necrosis. *J Hepatobiliary Pancreat Sci* 2015; **22**: 20-26 [PMID: 25345777 DOI: 10.1002/jhbp.180]
57 **Boxhoorn L**, Voermans RP, Bouwense SA, Bruno MJ, Verdonk RC, Boermeester MA, van Santvoort HC, Besselink MG. Acute pancreatitis. *Lancet* 2020; **396**: 726-734 [PMID: 32891214 DOI: 10.1016/S0140-6736(20)31310-6]
58 **Trikudanathan G**, Wolbrink DRJ, van Santvoort HC, Mallery S, Freeman M, Besselink MG. Current Concepts in Severe Acute and Necrotizing Pancreatitis: An Evidence-Based Approach. *Gastroenterology* 2019; **156**: 1994-2007.e3 [PMID: 30776347 DOI: 10.1053/j.gastro.2019.01.269]
59 **Werner J**, Hartwig W, Hackert T, Büchler MW. Surgery in the treatment of acute pancreatitis--open pancreatic necrosectomy. *Scand J Surg* 2005; **94**: 130-134 [PMID: 16111095 DOI: 10.1177/145749690509400209]
60 **Driedger M**, Zyromski NJ, Visser BC, Jester A, Sutherland FR, Nakeeb A, Dixon E, Dua MM, House MG, Worhunsky DJ, Munene G, Ball CG. Surgical Transgastric Necrosectomy for Necrotizing Pancreatitis: A Single-stage Procedure for Walled-off Pancreatic Necrosis. *Ann Surg* 2020; **271**: 163-168 [PMID: 30216220 DOI: 10.1097/SLA.0000000000003048]
61 **Luckhurst CM**, El Hechi M, Elsharkawy AE, Eid AI, Maurer LR, Kaafarani HM, Thabet A, Forcione DG, Fernández-Del Castillo C, Lillemoe KD, Fagenholz PJ. Improved Mortality in Necrotizing Pancreatitis with a Multidisciplinary Minimally Invasive Step-Up Approach: Comparison with a Modern Open Necrosectomy Cohort. *J Am Coll Surg* 2020; **230**: 873-883 [PMID: 32251846 DOI: 10.1016/j.jamcollsurg.2020.01.038]
62 **van Santvoort HC**, Besselink MG, Horvath KD, Sinanan MN, Bollen TL, van Ramshorst B, Gooszen HG; Dutch Acute Pancreatis Study Group. Videoscopic assisted retroperitoneal debridement in infected necrotizing pancreatitis. *HPB (Oxford)* 2007; **9**: 156-159 [PMID: 18333133 DOI: 10.1080/13651820701225688]
63 **Mier J**, León EL, Castillo A, Robledo F, Blanco R. Early versus late necrosectomy in severe necrotizing pancreatitis. *Am J Surg* 1997; **173**: 71-75 [PMID: 9074366 DOI: 10.1016/S0002-9610(96)00425-4]
64 **Götzinger P**, Sautner T, Kriwanek S, Beckerhinn P, Barlan M, Armbruster C, Wamser P, Függer R. Surgical treatment for severe acute pancreatitis: extent and surgical control of necrosis determine outcome. *World J Surg* 2002; **26**: 474-478 [PMID: 11910483 DOI: 10.1007/s00268-001-0252-8]
65 **Szeliga J**, Jackowski M. Minimally invasive procedures in severe acute pancreatitis treatment - assessment of benefits and possibilities of use. *Wideochir Inne Tech Maloinwazyjne* 2014; **9**: 170-178 [PMID: 25097683 DOI: 10.5114/wiitm.2014.41628]
66 **Gomatos IP**, Halloran CM, Ghaneh P, Raraty MG, Polydoros F, Evans JC, Smart HL, Yagati-Satchidanand R, Garry JM, Whelan PA, Hughes FE, Sutton R, Neoptolemos JP. Outcomes From Minimal Access Retroperitoneal and Open Pancreatic Necrosectomy in 394 Patients With Necrotizing Pancreatitis. *Ann Surg* 2016; **263**: 992-1001 [PMID: 26501713 DOI: 10.1097/SLA.0000000000001407]
67 **van Brunschot S**, Hollemans RA, Bakker OJ, Besselink MG, Baron TH, Beger HG, Boermeester MA, Bollen TL, Bruno MJ, Carter R, French JJ, Coelho D, Dahl B, Dijkgraaf MG, Doctor N, Fagenholz PJ, Farkas G, Castillo CFD, Fockens P, Freeman ML, Gardner TB, Goor HV, Gooszen HG, Hannink G, Lochan R, McKay CJ, Neoptolemos JP, Oláh A, Parks RW, Peev MP, Raraty M, Rau B, Rösch T, Rovers M, Seifert H, Siriwardena AK, Horvath KD, van Santvoort HC. Minimally invasive and endoscopic versus open necrosectomy for necrotising pancreatitis: a pooled analysis of individual data for 1980 patients. *Gut* 2018; **67**: 697-706 [PMID: 28774886 DOI: 10.1136/gutjnl-2016-313341]
68 **Tenner S**, Baillie J, DeWitt J, Vege SS; American College of Gastroenterology. American College of Gastroenterology guideline: management of acute pancreatitis. *Am J Gastroenterol* 2013; **108**: 1400-15; 1416 [PMID: 23896955 DOI: 10.1038/ajg.2013.218]
69 **Bakker OJ**, van Santvoort HC, van Brunschot S, Geskus RB, Besselink MG, Bollen TL, van Eijck CH, Fockens P, Hazebroek EJ, Nijmeijer RM, Poley JW, van Ramshorst B, Vleggaar FP, Boermeester MA, Gooszen HG, Weusten BL, Timmer R; Dutch Pancreatitis Study Group. Endoscopic transgastric vs surgical necrosectomy for infected necrotizing pancreatitis: a randomized trial. *JAMA* 2012; **307**: 1053-1061 [PMID: 22416101 DOI: 10.1001/jama.2012.276]
70 **van Brunschot S**, van Grinsven J, Voermans RP, Bakker OJ, Besselink MG, Boermeester MA, Bollen TL, Bosscha K, Bouwense SA, Bruno MJ, Cappendijk VC, Consten EC, Dejong CH, Dijkgraaf MG, van Eijck CH, Erkelens GW, van Goor H, Hadithi M, Haveman JW, Hofker SH, Jansen JJ, Laméris JS, van Lienden KP, Manusama ER, Meijssen MA, Mulder CJ, Nieuwenhuis VB, Poley JW, de Ridder RJ, Rosman C, Schaapherder AF, Scheepers JJ, Schoon EJ, Seerden T, Spanier BW, Straathof JW, Timmer R, Venneman NG, Vleggaar FP, Witteman BJ, Gooszen HG, van Santvoort HC, Fockens P; Dutch Pancreatitis Study Group. Transluminal endoscopic step-up approach versus minimally invasive surgical step-up

approach in patients with infected necrotising pancreatitis (TENSION trial): design and rationale of a randomised controlled multicenter trial [ISRCTN09186711]. *BMC Gastroenterol* 2013; **13**: 161 [PMID: 24274589 DOI: 10.1186/1471-230X-13-161]

71 **van Grinsven J**, van Brunschot S, Bakker OJ, Bollen TL, Boermeester MA, Bruno MJ, Dejong CH, Dijkgraaf MG, van Eijck CH, Fockens P, van Goor H, Gooszen HG, Horvath KD, van Lienden KP, van Santvoort HC, Besselink MG; Dutch Pancreatitis Study Group. Diagnostic strategy and timing of intervention in infected necrotizing pancreatitis: an international expert survey and case vignette study. *HPB (Oxford)* 2016; **18**: 49-56 [PMID: 26776851 DOI: 10.1016/j.hpb.2015.07.003]

72 **Guo Q**, Li A, Xia Q, Lu H, Ke N, Du X, Zhang Z, Hu W. Timing of intervention in necrotizing pancreatitis. *J Gastrointest Surg* 2014; **18**: 1770-1776 [PMID: 25091844 DOI: 10.1007/s11605-014-2606-1]

73 **Boxhoorn L**, van Dijk SM, van Grinsven J, Verdonk RC, Boermeester MA, Bollen TL, Bouwense SAW, Bruno MJ, Cappendijk VC, Dejong CHC, van Duijvendijk P, van Eijck CHJ, Fockens P, Francken MFG, van Goor H, Hadithi M, Hallensleben NDL, Haveman JW, Jacobs MAJM, Jansen JM, Kop MPM, van Lienden KP, Manusama ER, Mieog JSD, Molenaar IQ, Nieuwenhuijs VB, Poen AC, Poley JW, van de Poll M, Quispel R, Römkens TEH, Schwartz MP, Seerden TC, Stommel MWJ, Straathof JWA, Timmerhuis HC, Venneman NG, Voermans RP, van de Vrie W, Witteman BJ, Dijkgraaf MGW, van Santvoort HC, Besselink MG; Dutch Pancreatitis Study Group. Immediate versus Postponed Intervention for Infected Necrotizing Pancreatitis. *N Engl J Med* 2021; **385**: 1372-1381 [PMID: 34614330 DOI: 10.1056/NEJMoa2100826]

World Journal of Gastroenterology

Submit a Manuscript: https://www.f6publishing.com

World J Gastroenterol 2022 July 21; 28(27): 3398-3409

DOI: 10.3748/wjg.v28.i27.3398

ISSN 1007-9327 (print) ISSN 2219-2840 (online)

MINIREVIEWS

Artificial intelligence in liver ultrasound

Liu-Liu Cao, Mei Peng, Xiang Xie, Gong-Quan Chen, Shu-Yan Huang, Jia-Yu Wang, Fan Jiang, Xin-Wu Cui, Christoph F Dietrich

Specialty type: Gastroenterology and hepatology

Provenance and peer review: Invited article; Externally peer reviewed.

Peer-review model: Single blind

Peer-review report's scientific quality classification

Grade A (Excellent): 0
Grade B (Very good): 0
Grade C (Good): C, C
Grade D (Fair): 0
Grade E (Poor): 0

P-Reviewer: Hussain J, Oman; Li L, China

Received: February 7, 2022
Peer-review started: February 7, 2022
First decision: April 10, 2022
Revised: April 18, 2022
Accepted: June 19, 2022
Article in press: June 19, 2022
Published online: July 21, 2022

Liu-Liu Cao, Mei Peng, Xiang Xie, Fan Jiang, Department of Medical Ultrasound, The Second Hospital of Anhui Medical University, Hefei 230601, Anhui Province, China

Gong-Quan Chen, Department of Medical Ultrasound, Minda Hospital of Hubei Minzu University, Enshi 445000, Hubei Province, China

Shu-Yan Huang, Department of Medical Ultrasound, The First People's Hospital of Huaihua, Huaihua 418000, Hunan Province, China

Jia-Yu Wang, Xin-Wu Cui, Department of Medical Ultrasound, Tongji Hospital of Tongji Medical College, Huazhong University of Science and Technology, Wuhan 430030, Hubei Province, China

Christoph F Dietrich, Department Allgemeine Innere Medizin, Kliniken Hirslanden Beau Site, Salem und Permanence, Bern 3626, Switzerland

Corresponding author: Fan Jiang, MD, Associate Professor, Department of Medical Ultrasound, The Second Hospital of Anhui Medical University, No. 678 Furong Road, Economic and Technological Development Zone, Hefei 230601, Anhui Province, China.
ahultrasound2005@126.com

Abstract

Artificial intelligence (AI) is playing an increasingly important role in medicine, especially in the field of medical imaging. It can be used to diagnose diseases and predict certain statuses and possible events that may happen. Recently, more and more studies have confirmed the value of AI based on ultrasound in the evaluation of diffuse liver diseases and focal liver lesions. It can assess the severity of liver fibrosis and nonalcoholic fatty liver, differentially diagnose benign and malignant liver lesions, distinguish primary from secondary liver cancers, predict the curative effect of liver cancer treatment and recurrence after treatment, and predict microvascular invasion in hepatocellular carcinoma. The findings from these studies have great clinical application potential in the near future. The purpose of this review is to comprehensively introduce the current status and future perspectives of AI in liver ultrasound.

Key Words: Machine learning; Deep learning; Radiomics; Diffuse liver diseases; Focal liver diseases; Ultrasound

Core Tip: Artificial intelligence (AI) is playing an increasingly important role in medicine, especially in the field of medical imaging. Currently, there is a need of a comprehensive review to introduce the application of AI based on ultrasound in diffuse and focal liver lesions. In this article, we introduce the application of AI in the assessment of liver fibrosis and nonalcoholic fatty liver and the differentiation of focal liver lesions. In addition, we discuss the performance of AI based on ultrasound in predicting curative effect, prognosis and microvascular invasion in hepatocellular carcinoma. Lastly, we illustrate the future prospect of AI in liver ultrasound.

Citation: Cao LL, Peng M, Xie X, Chen GQ, Huang SY, Wang JY, Jiang F, Cui XW, Dietrich CF. Artificial intelligence in liver ultrasound. *World J Gastroenterol* 2022; 28(27): 3398-3409
URL: https://www.wjgnet.com/1007-9327/full/v28/i27/3398.htm
DOI: https://dx.doi.org/10.3748/wjg.v28.i27.3398

INTRODUCTION

In the past several years, liver diseases have affected millions of lives and became one of the main causes of illness and death in the world[1]. It is reported that more than one-fifth of the Chinese population are affected by liver diseases, such as liver fibrosis, liver cancer and nonalcoholic fatty liver disease (NAFLD), contributing unambiguously to health loss. Therefore, paying more attention to liver diseases is of great significance.

Artificial intelligence (AI) is defined as the research of algorithms that enable machines to have the ability of reasoning and performing functions such as solving problems, recognizing object and word, inferring world states, and making decisions[2]. AI is a precise prediction technique that automates learning and recognizes patterns in data. Apart from this, AI has been extensively applied to medical diagnosis, especially in medical image analysis. This application mainly relies on deep learning, a subfield of machine learning. Deep learning is on the frontier of AI, which is based on deep neural networks (DNNs) with more than one hidden layer. Convolutional neural networks (CNNs) are a branch of DNNs that are particularly useful for recognizing images and have stimulated a large amount of interest from industry, academia and clinicians[3].

Compared to other medical imaging techniques, ultrasound is noninvasive, portable and can provide real-time imaging. In recent years, AI-powered ultrasound has become more developed and been implemented in clinical applications in order to reduce the subjectivity and improve the efficiency of ultrasound diagnosis[4]. Many studies have confirmed the value of AI in the evaluation of thyroid nodule, breast lesion and liver lesion classification by ultrasound. In addition to these applications, other AI applications in ultrasound have also been explored and achieved great progress.

In liver medical imaging, AI can make a quantitative assessment by recognizing imaging information automatically to aid physicians in making more precise and comprehensive imaging diagnoses[5]. This technique has been extensively applied to computed tomography (CT), positron emission tomography-CT, magnetic resonance imaging and ultrasound to diagnose liver lesions. For instance, deep learning based on CT and positron emission tomography-CT can be used to detect new liver tumors and metastatic liver malignancy, and to predict the primary origin of liver metastasis[6-8].

There are also many studies that have illustrated the application of AI in liver ultrasound, while a comprehensive review of AI in this field is lacking. In this review, we will introduce the application of AI based on ultrasound in diffuse liver diseases, including liver fibrosis and steatosis, and focal liver lesions (FLLs), including their differential diagnosis, prediction of a curative effect and prognosis and microvascular invasion (MVI) of hepatocellular carcinoma (HCC). The main structure of this review was illustrated in Figure 1.

APPLICATION OF AI IN DIFFUSE LIVER DISEASE

There are a variety of diffuse liver diseases that can be asymptomatic or cause severe liver dysfunction, and many of them may lead to cirrhosis, hepatic carcinoma, and death. We will introduce the applications of AI based on ultrasound in two common diffuse liver diseases, *i.e.* liver fibrosis and steatosis.

Liver fibrosis

Liver fibrosis is the early step of cirrhosis and an important pathological basis of HCC[9]. Therefore, the early detection and prevention of liver fibrosis is essential in the clinical setting. However, although liver biopsy is the gold standard for classifying liver fibrosis using the Metavir score[10] or New Inuyama classification[11] to distribute the score ranging from F0 (no fibrosis) to F4 (cirrhosis). The use

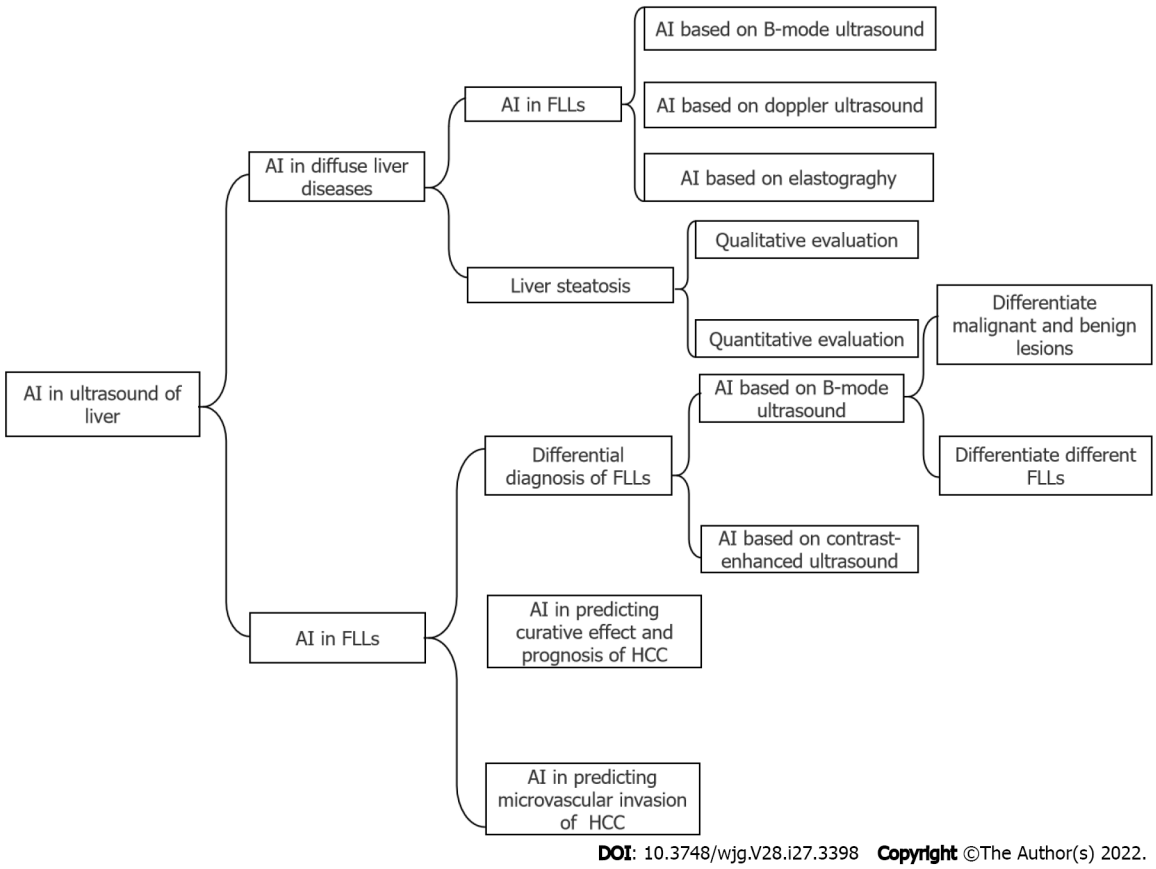

DOI: 10.3748/wjg.V28.i27.3398

Figure 1 Main structure of this review. AI: Artificial intelligence; FLLs: Focal liver lesions; HCC: Hepatocellular carcinoma.

of tissue examination for the assessment of liver fibrosis is controversial because liver biopsy is invasive and liver fibrosis is not equably distributed throughout the liver. There are an increasing number of credible, noninvasive and available approaches being widely applied in clinical practice. Recently, a large number of noninvasive techniques have been used to prevent adverse outcomes through the application of AI based on ultrasound.

AI based on B-mode ultrasound: As early as 20 years ago, AI was used to assist the diagnosis of liver fibrosis. Badawi *et al*[12] creatively proposed an approach that employed fuzzy reasoning techniques to identify diffuse liver diseases automatically by using digital quantitative features measured from the ultrasound images. They extracted parameters only from B-mode images, and the results revealed that this approach had higher specificity and sensitivity for the diagnosis of liver fibrosis than the statistical classification techniques, which had a certain effect but could not help much.

Apart from this, a novel deep multi-scale texture network based entirely on B-mode ultrasound images that was proposed recently seems to be more convenient[13]. The area under the receiver operating characteristic curve of this approach was 0.92 for significant fibrosis (≥ F2) and 0.89 for cirrhosis (F4) in the validation group, which outperformed the ultrasonographers and three serum biomarkers during diagnosis. Although it cannot be used for liver fibrosis staging now, it has excellent potential in the future workflow.

AI based on Doppler ultrasound: On the basis of grey-scale parameters from B-mode images, Doppler parameters of intrahepatic blood vasculature were added as essential parameters. Eventually, five ultrasonographic variables, including the liver parenchyma, thickness of the spleen, the hepatic vein waveform, hepatic artery pulsatile index and damping index, were selected as the input neurons. A data optimization procedure was used in an artificial neural network for the diagnosis of liver fibrosis, which achieved an area under the curve of 0.92[14]. Although this model proved to predict liver cirrhosis accurately, it still could not provide a specific grading.

AI based on elastography: In recent years, with the development of ultrasound, studies have proposed computer-aided techniques based on elastography that is of great importance in ultrasound images to identify and stage liver fibrosis. Real-time tissue elastography (RTE) is one of the recently developed elastography techniques. In a study, 11 image features were extracted directly from the RTE software that was installed in the ultrasound system to quantify the patterns of the RTE images[15]. Then, the data were processed and divided among four classical classifiers. The results showed that the

performance of the adopted classifiers was much better than the previous liver fibrosis index method, which predicted the stage of fibrosis using RTE images and multiple regression analyses. The good performance in this study demonstrated that machine learning had the potential to perform as powerful tools for staging liver fibrosis.

Nowadays, most applications of AI in evaluating the stage of liver fibrosis are based on shear wave elastography. An automated approach including the image quality check, region of interest (ROI) selection and CNN classification based on shear wave elastography showed a more accurate detection of ≥ F2 fibrosis levels than a previously published baseline approach, with an area under curve of 0.89 *vs* 0.74[16]. The deep learning radiomics also presented the potential diagnostic performance in chronic hepatitis B patients compared with two-dimensional shear wave elastography[17]. AI could help stage liver fibrosis more accurately with the assistance of elastography.

Liver steatosis

Hepatic steatosis, characterized by the accumulation of fat droplets in hepatocytes, can develop into nonalcoholic fibrosis, steatohepatitis, cirrhosis, and even HCC[18,19]. Early detection and treatment may halt or reverse NAFLD progression[19]. As a consequence, there is a critical need to develop noninvasive imaging methods to assess hepatic steatosis. Noninvasive liver imaging methods including CT, magnetic resonance imaging and ultrasound have been extensively investigated[20].

Ultrasound is the first-line examination for identifying liver steatosis. It shows an enlarged liver with a greater number of echoes caused by fat droplets, and the liver is brighter and more hyperechoic compared with the right kidney. The image is qualitative and relies on the subjective judgement of the operator, which definitely leads to variable results and low reproducibility[21]. To overcome the observer bias, a series of quantitative and semi-quantitative parameters, including attenuation and backscatter coefficients, the hepato-renal index (HRI) and ultrasound envelope statistic parametric imaging (known as speckle statistics), have been implemented, some of which represent excellent reproducibility and reliability[21-24]. At present, almost all the studies published have concentrated on NAFLD.

It was reported that the detection of moderate and severe steatosis based on ultrasound has an 84.8% sensitivity and a 93.6% specificity, while mild steatosis has an even lower sensitivity[25]. Recently, some researchers applied AI to improve the ultrasound detection rate of NAFLD, and the results were promising. Table 1 shows the studies using AI based on ultrasound to identify steatosis. The studies showed that AI had tremendous potential in helping diagnose liver steatosis. Some studies attempted to optimize CNN models. In the future, classifying the degree of liver steatosis with the assistance of the AI could be a trend.

Qualitative evaluation: Deep learning has been applied to qualitatively evaluate NAFLD. An approach of assessing fatty liver disease by utilizing deep learning based on CNNs with B-mode images was proposed[26]. The study recruited 135 participants with known or suspected NAFLD to investigate the function of four liver views (three views in the transverse plane, including hepatic veins at the confluence with the inferior vena cava, right portal vein and right posterior portal vein, and one view in the sagittal plane, *i.e.* the liver and kidney view) in the assessment[27]. The study assessed attention maps for liver assessment based on CNNs, which illustrated that the available image features provided by each view could assess liver fat. Unlike the previous study, magnetic resonance imaging proton density fat fraction was used as a reference standard, which was not precise enough compared with liver biopsy.

A novel framework combining transfer learning with fine-tuning was proposed[28]. Although this study revealed that the new framework outperformed CNN, this conclusion was not entirely convincing because the radiologists' qualitative scores were the reference standard. This framework was also utilized in other studies and achieved a good performance.

With the development of deep learning, Chou *et al*[29] established two-class, three-class and four-class prediction models to classify the severity of steatosis by using B-mode ultrasound images from 2070 patients. Although liver biopsy is the gold standard, the deep learning model could select eligible patients for a liver biopsy by evaluating the severity of fatty liver preliminarily, which would reduce unnecessary tests.

Different deep learning algorithms tend to have different performances. The combined deep learning algorithm based on B-mode images had an area under the receiver operating characteristic curve of 0.9999 and accuracy of 0.9864 compared with other algorithms[30]. Therefore, in future studies selecting an optimal algorithm is important.

Quantitative evaluation: AI has also been applied to quantitatively evaluate NAFLD. Radiofrequency signals may negate the loss or change of data during translation to B-mode ultrasound images. A study acquired the diagnosis and fat fraction of NAFLD by inputting the original data based on one-dimensional algorithms[31]. The investigators obtained a 97% sensitivity and 94% specificity, and the positive predictive value was up to 97%, which demonstrated that the utilization of original ultrasound radiofrequency could be applied in diagnosing NAFLD and to quantifying liver fat fraction. Similarly, in an animal experiment, a CNN model based on radiofrequency signals was shown to have a better

Table 1 Studies using artificial intelligence based on ultrasound for fatty liver disease diagnosis

Task	Reference standard	Sample size	Method	Results	Ref.
Fatty liver disease diagnosis	Liver biopsy	55 patients with severe obesity, 38 of whom had fatty liver disease	Deep learning with B-mode image ultrasound	Sensitivity: 100%; specificity: 88%; accuracy: 96%; AUC: 0.98	[26]
Fatty liver disease diagnosis	Radiologist qualitative score	157 ultrasound liver images from unknown number of participants	Deep learning with B-mode image ultrasound	Sensitivity: 95%; specificity: 85%; accuracy: 90.6%; AUC: 0.96	[28]
NAFLD assessment	MRI proton density fat fraction	204 participants, 140 of whom had NAFLD, 64 control participants	One-dimensional CNNs	Sensitivity: 97%; specificity: 94%; accuracy: 96%; AUC: 0.98	[31]
NAFLD assessment	MRI proton density fat fraction	135 adult participants with known or suspected NAFLD	Transfer learning with a pretrained CNN by four ultrasound views of liver routinely obtained	SCC: 0.81; AUC: 0.91 (PDFF ≥ 5%)	[27]
NAFLD assessment	Liver biopsy	295 subjects, 198 mild fatty liver, one moderate degree of fatty liver	DCNN-based organ segmentation with Gaussian mixture modeling for automated quantification of the HRI	ICC of two radiologists and DCNN were 0.919, 0.916, 0.734	[33]
The severity of fatty liver	Abdominal ultrasound	21855 B-mode ultrasound images, 2070 patients with different severities from none to severe fatty liver	Pretrained CNN models with B-mode ultrasound images	The areas under the receiver operating characteristic curves were 0.974 (mild steatosis *vs* others), 0.971 (moderate steatosis *vs* others), 0.981 (severe steatosis *vs* others), 0.985 (any severity *vs* normal) and 0.996 (moderate-to-severe steatosis clinically abnormal *vs* normal-to-mild steatosis clinically normal)	[29]

AUC: Area under curve; CNN: Convolutional neural network; DCNN: Deep convolutional neural network; HRI: Hepato-renal index; ICC: Intraclass correlation; MRI: Magnetic resonance image; NAFLD: Nonalcoholic fatty liver disease; PDFF: Proton density fat fraction; SCC: Spearman correlation coefficient.

performance than the traditional quantitative ultrasound when classifying steatosis[32].

An HRI model based on CNNs was also tested for NAFLD evaluation. Cha *et al*[33] reported that an automated approach had no significant difference in hepatic measurements and HRI calculations compared with experienced radiologists, which indicated that the aid of deep learning could reduce a radiologist's workload and improve the residents' diagnostic accuracy. In this study, an automated HRI calculation algorithm was used, including liver and kidney segmentation, kidney ROI extraction, liver ROI extraction, and calculation of the HRI.

APPLICATION OF AI IN FLLS

HCC is the most conventional original malignant FLL, which is the sixth most common cancer in human beings as well as the fourth cause of cancer-related deaths in the world[1]. Hence, early accurate differential diagnosis of malignant and benign FLL is important for the management and prognosis of patients[34].

Ultrasound is the first-line imaging modality to identify FLLs in the clinical workflow. The development of AI provides a new method to improve the accuracy of ultrasound in diagnosing FLLs. Compared with radiologists viewing anatomical images, AI can better reflect monolithic tumor morphology as well as capture both granular and radiological patterns in a specific task, which is difficult by normal human vision[35]. Figure 2 illustrates the flowchart of the application of deep learning and radiomics in FLLs. Studies have confirmed that the application of AI can improve the diagnostic performance of ultrasound for FLLs (Table 2).

Differential diagnosis of FLLs

AI based on B-mode ultrasound: AI has been widely used in differentiating malignant and benign FLLs based on B-mode ultrasound. Gray level co-occurrence matrix could be used in extracting features from B-mode images, which has been used in differentiating malignant and benign FLLs combined with a fuzzy support vector machine[36]. This study achieved an area under the curve of 0.984 and 0.971 in database 1 and database 2, respectively, which confirmed the feasibility of AI in this field.

Table 2 Studies using artificial intelligence based on ultrasound for focal liver lesion diagnosis

Modality and task	Approach	Target disease: number of the case	Performance	Ref.
Classifying different FLLs based on B-mode	ANN	Cyst: 29; hemangioma: 37; malignant tumor: 33	Cyst *vs* hemangioma accuracy: 99.7%; cyst *vs* malignant tumor accuracy: 98.7%; hemangioma *vs* malignant tumor accuracy: 96.1%	[40]
Differentiating benign and malignant lesions based on B-mode	CNN	Benign lesions: 300; malignant lesions: 296	All lesion accuracy: 84%; uncertain set of lesion accuracy: 79%	[37]
Classifying different FLLs based on B-mode	ANN (sparse autoencoder)	Normal liver: 16; cyst: 44; hemangioma: 18; HCC: 30	overall accuracy: 97.2%; overall sensitivity: 98%; overall specificity: 95.7%	[41]
Differentiating benign and malignant lesions based on B-mode	FSVM	training set; DS1: benign lesions: 132, malignant lesions: 68; DS2: malignant liver cancer: 50, hepatocellular adenoma: 150, hemangioma: 35, focal nodular hyperplasia: 145, lipoma: 70	DS1: accuracy: 97%, sensitivity: 100%, specificity: 95.5%, AUC: 0.984; DS2: accuracy: 95.1%, sensitivity: 92.0%, specificity: 95.5%, AUC: 0.971	[36]
Classifying different FLLs based on B-mode	CNN	Non-tumorous liver: 258, hemangioma: 17, HCC: 6, cyst: 30, focal nodular hyperplasia: 8	AUC for tumor detection: 0.935; AUC for tumor discrimination (mean): 0.916	[42]
Diagnosing HCC based on B-mode	CNN	Malignant tumor: 1786; benign tumor: 427	AUC for EV: 0.924	[38]
Differentiating benign and malignant lesions based on B-mode	CNN	HCC: 6; cyst: 6600; hemangioma: 5374; focal fatty sparing: 5110; focal fatty infiltration: 934	IV: overall sensitivity: 83.9%; overall specificity: 97.1%; HCC detection rate: 85.3%; EV: overall sensitivity: 84.9%; overall specificity: 97.1%; HCC detection rate: 78.3%	[39]
Classifying different FLLs based on CEUS	ANN	hemangioma: 16; focal fatty liver: 23; HCC: 41; metastatic tumor: 32 (hypervascular: 20 hypovascular: 12)	Accuracy: 94.5%; sensitivity: 93.2%; specificity: 89.7%	[47]
Differentiating benign and malignant lesions based on CEUS	Deep belief networks	HCC: 6; hemangioma: 10; liver abscess: 4; metastases: 3; focal fatty sparing: 3	Accuracy: 83.4%; sensitivity: 83.3%; specificity: 87.5%	[59]
Differentiating benign and malignant lesions based on CEUS	SVM	Benign tumor: 30; malignant tumor: 22	Accuracy: 90.3%; sensitivity: 93.1%; specificity: 86.9%	[45]
Differentiating benign and malignant lesions based on CEUS	SVM	Benign tumor, HCC or metastatic tumor: 98	Benign *vs* malignant accuracy: 91.8%, sensitivity: 93.1%, specificity: 86.9%; benign *vs* HCC *vs* metastatic carcinoma: accuracy: 85.7%; sensitivity: 84.4%; specificity: 87.7%	[46]
Differentiating benign and malignant lesions based on CEUS	Deep canonical correlation analysis + multiple kernel learning	Benign tumor: 46; malignant tumor: 47	Accuracy: 90.4%; sensitivity: 93.6%; specificity: 86.9%	[43]
Differentiating benign and malignant lesions based on CEUS	3D-CNN	HCC: 2110; focal nodular hyperplasia: 2310	Accuracy: 93.1%; sensitivity: 94.5%; specificity: 93.6%	[44]
Differentiating benign and malignant lesions based on CEUS	Deep neural network	Focal nodular hyperplasia: 16; HCC: 30; hemangioma: 23; hypervascular metastasis: 11; hypovascular metastasis: 11	Top accuracy: 88%	[48]
Differentiating benign and malignant lesions based on CEUS	CNN	Development set: malignant tumor: 281, benign tumor: 82; testing set: malignant tumor: 164, benign tumor: 47	Accuracy: 91.0%; sensitivity: 92.7%; specificity: 85.1%; AUC: 0.934	[49]

ANN: Artificial neural network; AUC: Area under curve; CEUS: Contrast-enhanced ultrasound; CNN: Convolutional neural network; DS1: Database 1; DS2: Database 2; EV: External validation; FLL: Focal liver lesion; FSVM: Fuzzy support vector machine; HCC: Hepatocellular carcinoma; IV: Internal validation; SVM: Support vector machine; 3D: Three-dimensional.

With the development of AI, deep learning plays a more vital role in the differential diagnosis of FLLs. A CNN with ResNet50 was utilized to recognize benign from malignant solid liver lesions through ultrasonography. The performance was comparable to that of expert radiologists[37]. However, this study did not involve other information such as clinical factors. In another (multicenter) study, after adding seven clinical factors, a higher accuracy, sensitivity and specificity was obtained, compared with those from radiologists with 15 years of experience. The area under the curve for recognizing malignant from benign lesions reached up to 0.924 in the external validation cohort[38].

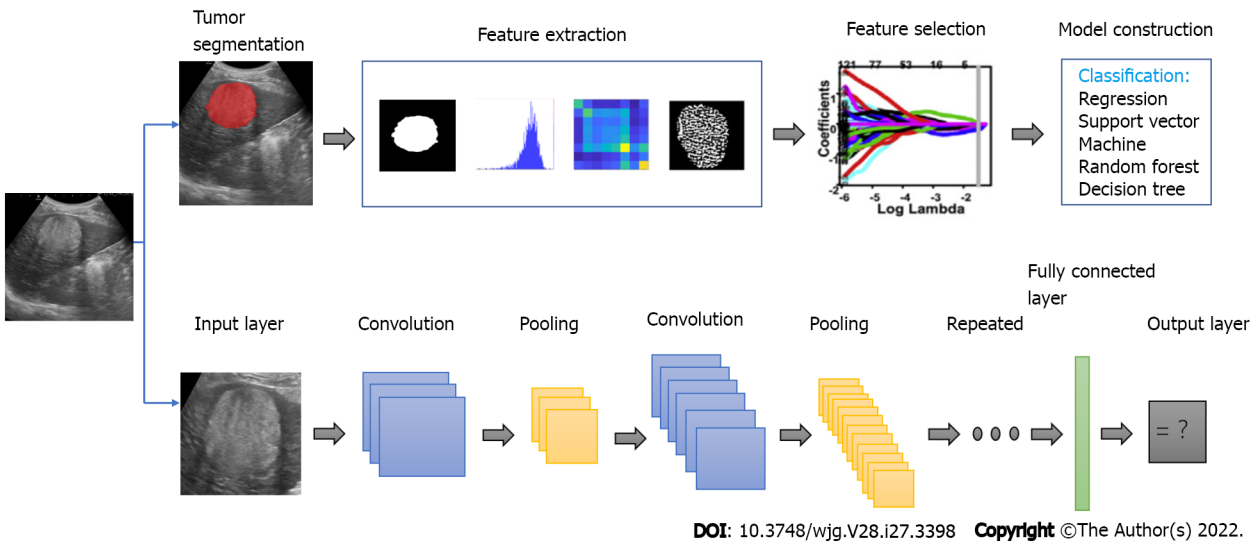

Figure 2 Illustration of the flowchart of the application of deep learning and radiomics in focal liver lesions. These two methods were based on big data, which contained image preprocessing, feature extraction and model construction.

However, the aforementioned studies only included common FLLs. Increasing the types of FLLs may confuse the diagnosis and reduce the accuracy. Similar to the previous study, a multicenter study estimating internal validation and external validation cohorts had a larger volume of training data and involved more varieties of FLLs, including cysts, HCC, hemangiomas, focal fatty infiltration and focal fatty sparing[39]. Although they obtained a lower sensitivity due to more types of diseases, the performance in the external validation cohorts was still satisfactory. In addition, they utilized videos as training materials to achieve real-time analysis in the future workflow. This novel approach would offer great convenience to radiologists in helping differentiate FLLs.

AI could also be used in the classification of FLLs. In order to optimize feature sets, a hybrid textural feature extraction system was proposed by Hwang *et al*[40]. In their preliminary study, a high accuracy was observed in classifying cysts *vs* hemangiomas and cysts *vs* malignant lesions. However, when classifying hemangiomas *vs* malignant lesions by extracting multiple ROI, the accuracy was only 80%. The proposed approach exhibited a better accuracy in all classification groups by quantifying the key features in ultrasound images, especially in classifying hemangioma *vs* malignant, with an accuracy of 96.13%.

Later, a sparse autoencoder system based on deep learning was proposed in diagnosing cysts, hemangiomas and malignant lesions, and it outperformed the three progressive techniques, including K-enarest neighbor, multi-support vector machine and naive Bayes, with an overall accuracy of 97.2% [41].

These two studies[40,41] focused on three kinds of FLLs. An algorithm that could simultaneously detect and characterize FLLs based on deep learning was proposed in diagnosing HCC, focal nodular hyperplasia, cysts, hemangiomas and metastasis, and it achieved an average area under the curve of 0.916[42]. That study yielded promising results by using a small amount of data. Larger databases would increase the accuracy of this model.

AI based on contrast-enhanced ultrasound: It is reported that contrast-enhanced ultrasound (CEUS) images had better sensitivity and specificity for differentiating between malignant and benign tumors compared with B-mode images, which indicated CEUS had a superior diagnostic performance. Combining AI with CEUS could differentiate benign and malignant FLLs and classify different kinds of malignant lesions.

AI could be used to differentiate malignant and benign FLLs based on three-phase CEUS images. A two-stage multiple view learning that represented the integration of deep canonical correlation analysis and multiple kernel learning was used to fuse the characteristics of three-phase patterns in CEUS, presenting an accuracy of 90.41%[43]. The proposed algorithm had both a low computational complex and a high predictive accuracy. For multiview CEUS images, utilizing a multimodal feature fusion algorithm is necessary.

Compared with deep canonical correlation analysis-multiple kernel learning, the use of a three-dimensioned CNN, which integrated the relationship between two temporally adjacent frames to extract features spatially and temporally, achieved a higher accuracy of 93.1%, sensitivity of 94.5% and specificity of 93.6%[44]. However, this algorithm still needs to be validated.

These two studies above[43,44] exploited heterogeneous visual morphology to describe the difference between liver masses. Apart from this method, time-intensity curve (TIC), which represents the contrast

intensity constantly and generates the fitted curve of enhanced intensity during the process, was used in many studies.

Support vector machine[45,46] and deep learning[47,48] based on TICs have presented good performances in differentiating FLLs. A support vector machine-based image analysis system was used for FLL classification and presented an area under the curve of 0.89[45]. An artificial neural network diagnostic system based on TICs was shown to have a similar accuracy and specificity in classifying five different liver tumors 10 years ago[47]. Later, deep learning became more mature, and TICs of the arterial and the portal vein phases of CEUS videos were extracted on the basis of the deep belief networks, a kind of neural network that was composed of layers of Boltzmann machines, to analyze the extracted TICs[48]. The accuracy of this deep learning method for classifying benign from malignant lesions was 83.36%. A novel evaluation procedure named 'leave-one-patient-out' and custom DNNs were creatively presented. That study involved various types of liver lesions and compared the custom DNN designs with the state-of-the-art architectures and obtained a maximal accuracy of 88% by utilizing the proposed evaluation procedure in both pretrained and trained-from-scratch models. This novel approach has a magnificent prospect for development, and it is worth further investigation.

AI based on CEUS was shown to assist in clinical settings as the reference and improve the performance of residents in the differentiation of benign and malignant FLLs[49]. In the future, it will likely play a supporting role in clinical work. However, AI based on TICs tends to complicate the calculation because generating TICs is a time-consuming process. Therefore, developing new approaches to extract features from CEUS images is important.

Application of AI in predicting curative effect and prognosis of HCC

It was reported that the Edmondson-Steiner grade is a vital preoperation predictor of tumor survival and recurrence after undergoing surgical resection[50,51]. Because preoperative pathological differentiation grade can only be obtained by an invasive biopsy[52], it is necessary to explore a noninvasive method to predict therapeutic effect, recurrence and metastasis to achieve personalized treatment.

Some studies[53-55] demonstrated the superiority of AI based on CEUS in predicting a curative effect and prognosis in HCC. Although the results revealed a better performance of AI models compared with a single clinical or ultrasound model, a better performance may be obtained by adding clinical factors in the future studies.

Predicting curative effect of HCC: Transarterial chemoembolization (TACE) is the first-line therapy in patients who are diagnosed with mid-stage HCC, and the response to the first TACE treatment is related to the subsequent curative effect and survival. Therefore, it is necessary to predict the personalized responses to the first TACE treatment. A deep learning radiomics-based CEUS model, machine learning radiomics-based B-mode image model and machine learning radiomics-based TIC of the CEUS model were established to achieve this function[53]. These models presented a better performance compared with the hepatoma arterial embolization prognostic score based on three indexes concerning liver function and tumor load, which will be of great benefit in selecting both first treatment and subsequent therapies after the first TACE treatment.

Predicting prognosis of patients with HCC: Radiofrequency ablation and surgical resection are recommended for early-stage HCC. Deep learning could also be used to predict the progression-free survival of these two therapies in HCC patients[54]. Two models based on these two kinds of therapies provided a satisfactory prediction accuracy and calibration of 2-year progression-free survival. In another study[55], a three dimensional-CNN model, which avoided missing information from CEUS images compared with extracting features from four-phase images, was used. It was observed that predicting prognosis of different treatments in advance and timely swapping of treatment would increase the 2-year progression-free survival, which could contribute to a better prognosis.

Application of AI in predicting MVI of HCC

MVI has shown to be the independent predictor of recurrence and poor outcomes of HCC. Therefore, making a noninvasive and accurate preoperative identification of MVI would be of great significance for HCC patients. The application of AI in predicting MVI achieved good performance based on gray-scale ultrasound images and CEUS.

The radiomics score based on ultrasound of HCC was established and shown to be an independent predictor of MVI[56]. The performance of the clinical nomogram improved significantly with the aid of a radiomics score, which demonstrated the important role of this technique.

Features of the peritumoral area have been shown to be more accurate recently[56]. The radiomic signatures from the gross and peritumoral region showed the best performance compared with the gross-tumoral region and the peritumoral region[57]. The area under the curves were 0.726 based on features of the gross and peritumoral region and 0.744 after the incorporation of essential clinical information.

These studies[56,57] mentioned above have confirmed the application of AI based on gray-scale ultrasound, and AI could be applied to CEUS in predicting MVI as well. Zhang *et al*[58] extracted radiomics features from the B-mode, artery phase, portal venous phase and delay phase images of

preoperative CEUS to construct four radiomics scores based on the primary dataset. Then, they used four radiomic scores and clinical factors for multivariate logistic regression analysis, which demonstrated that the portal venous phase and delay phase radiomics score, tumor size and alpha-fetoprotein level were independent risk factors in predicting MVI. The radiomics nomogram based on these four predictors indicated a better discrimination and a good calibration compared with the clinical model (based on tumor size and alpha-fetoprotein level) in both the primary dataset (area under the curve: 0.849 *vs* 0.690) and the validation dataset (area under the curve: 0.788 *vs* 0.661). This study developed a new noninvasive predictive nomogram based on CEUS that could provide useful information in predicting MVI preoperatively, thus facilitating the choice of a more appropriate surgical option.

CONCLUSION

In conclusion, AI can provide great assistance in the evaluation of diffuse liver diseases (including liver fibrosis and liver steatosis) and FLLs. First, it could be applied to identify and stage liver fibrosis on the basis of B-mode ultrasound, Doppler ultrasound, and elastography. Second, the application of deep learning could be used to make qualitative evaluation based entirely on B-mode images and quantitative evaluation based on radiofrequency signals and HRI, which would improve the ultrasound detection rate of NAFLD. Third, AI has the ability to differentiate malignant FLLs from benign FLLs as well as classify different kinds of FLLs with a better performance compared with clinical indexes. Fourth, the curative effect and prognosis of HCC treatment can be predicted, and an optimal personalized treatment can be chosen. Last, AI based on B-mode ultrasound and CEUS could predict MVI of HCC preoperatively, which could be helpful for more appropriate surgical planning. These applications had good specificity, accuracy and a comparable or even better performance compared with experts in the diagnosis and differentiation of diffuse and focal liver lesions.

There are also some limitations in the applications of AI using ultrasound. First, it is difficult to prepare a large-scale dataset, especially for medical images. Second, although deep learning is the widest used algorithm and has good performance in various studies, its interpretability and generalization is low. Third, the input data may vary from different equipment and operators, which would influence the performance of AI. Last, because a large amount of data is needed to train and validate the established algorithms, the conclusions of many single-center studies are not convincing. Therefore, researchers are expected to conduct more multicenter studies and incorporate more samples, as much as possible. At the same time, optimizing algorithms and creating standards for medical images are also necessary. Despite medical images, researchers could also build the database containing important clinical factors to establish a more comprehensive AI model for future work.

FOOTNOTES

Author contributions: Jiang F, Cui XW and Dietrich CF conceived and established the design of the paper; Cao LL, Peng M, Xie X, Chen GQ, Huang SY, Wang JY, Dietrich CF, Jiang F and Cui XW explored the literature data; Cao LL provided the first draft of the manuscript, which was discussed and revised critically for intellectual content by Peng M, Xie X, Dietrich CF, Jiang F and Cui XW; all authors discussed the statements and conclusions, and approved the final version to be published.

Supported by National Natural Science Foundation of China, No. 82071953; and 2020 Hunan Province Clinical Medical Technology Innovation Guidance Project.

Conflict-of-interest statement: All the authors report no relevant conflicts of interest for this article.

Country/Territory of origin: China

ORCID number: Liu-Liu Cao 0000-0001-8078-5634; Mei Peng 0000-0001-7809-9440; Xiang Xie 0000-0001-5514-2362; Gong-Quan Chen 0000-0002-4204-6133; Shu-Yan Huang 0000-0002-7050-9553; Jia-Yu Wang 0000-0001-9902-0666; Fan Jiang 0000-0001-8896-2009; Xin-Wu Cui 0000-0003-3890-6660; Christoph F Dietrich 0000-0001-6015-6347.

S-Editor: Fan JR
L-Editor: A
P-Editor: Fan JR

REFERENCES

1 **Xiao J**, Wang F, Wong NK, He J, Zhang R, Sun R, Xu Y, Liu Y, Li W, Koike K, He W, You H, Miao Y, Liu X, Meng M, Gao B, Wang H, Li C. Global liver disease burdens and research trends: Analysis from a Chinese perspective. *J Hepatol* 2019; **71**: 212-221 [PMID: 30871980 DOI: 10.1016/j.jhep.2019.03.004]

2 **Bellman RE**. An Introduction to Artificial Intelligence: Can Computers Think? Spring: 1978

3 **Chan HP**, Samala RK, Hadjiiski LM, Zhou C. Deep Learning in Medical Image Analysis. *Adv Exp Med Biol* 2020; **1213**: 3-21 [PMID: 32030660 DOI: 10.1007/978-3-030-33128-3_1]

4 **Akkus Z**, Cai J, Boonrod A, Zeinoddini A, Weston AD, Philbrick KA, Erickson BJ. A Survey of Deep-Learning Applications in Ultrasound: Artificial Intelligence-Powered Ultrasound for Improving Clinical Workflow. *J Am Coll Radiol* 2019; **16**: 1318-1328 [PMID: 31492410 DOI: 10.1016/j.jacr.2019.06.004]

5 **Ambinder EP**. A history of the shift toward full computerization of medicine. *J Oncol Pract* 2005; **1**: 54-56 [PMID: 20871680 DOI: 10.1200/jop.2005.1.2.54]

6 **Vivanti R**, Szeskin A, Lev-Cohain N, Sosna J, Joskowicz L. Automatic detection of new tumors and tumor burden evaluation in longitudinal liver CT scan studies. *Int J Comput Assist Radiol Surg* 2017; **12**: 1945-1957 [PMID: 28856515 DOI: 10.1007/s11548-017-1660-z]

7 **Preis O**, Blake MA, Scott JA. Neural network evaluation of PET scans of the liver: a potentially useful adjunct in clinical interpretation. *Radiology* 2011; **258**: 714-721 [PMID: 21339347 DOI: 10.1148/radiol.10100547]

8 **Ben-Cohen A**, Klang E, Diamant I, Rozendorn N, Raskin SP, Konen E, Amitai MM, Greenspan H. CT Image-based Decision Support System for Categorization of Liver Metastases Into Primary Cancer Sites: Initial Results. *Acad Radiol* 2017; **24**: 1501-1509 [PMID: 28778512 DOI: 10.1016/j.acra.2017.06.008]

9 **Yoo S**, Wang W, Wang Q, Fiel MI, Lee E, Hiotis SP, Zhu J. A pilot systematic genomic comparison of recurrence risks of hepatitis B virus-associated hepatocellular carcinoma with low- and high-degree liver fibrosis. *BMC Med* 2017; **15**: 214 [PMID: 29212479 DOI: 10.1186/s12916-017-0973-7]

10 **Bedossa P**, Poynard T. An algorithm for the grading of activity in chronic hepatitis C. The METAVIR Cooperative Study Group. *Hepatology* 1996; **24**: 289-293 [PMID: 8690394 DOI: 10.1002/hep.510240201]

11 **Yamada G**. [Histopathological characteristics and clinical significance of New Inuyama Classification in chronic hepatitis B]. *Nihon Rinsho* 2004; **62** Suppl 8: 290-292 [PMID: 15453332]

12 **Badawi AM**, Derbala AS, Youssef AM. Fuzzy logic algorithm for quantitative tissue characterization of diffuse liver diseases from ultrasound images. *Int J Med Inform* 1999; **55**: 135-147 [PMID: 10530829 DOI: 10.1016/s1386-5056(99)00010-6]

13 **Ruan D**, Shi Y, Jin L, Yang Q, Yu W, Ren H, Zheng W, Chen Y, Zheng N, Zheng M. An ultrasound image-based deep multi-scale texture network for liver fibrosis grading in patients with chronic HBV infection. *Liver Int* 2021; **41**: 2440-2454 [PMID: 34219353 DOI: 10.1111/liv.14999]

14 **Zhang L**, Li QY, Duan YY, Yan GZ, Yang YL, Yang RJ. Artificial neural network aided non-invasive grading evaluation of hepatic fibrosis by duplex ultrasonography. *BMC Med Inform Decis Mak* 2012; **12**: 55 [PMID: 22716936 DOI: 10.1186/1472-6947-12-55]

15 **Chen Y**, Luo Y, Huang W, Hu D, Zheng RQ, Cong SZ, Meng FK, Yang H, Lin HJ, Sun Y, Wang XY, Wu T, Ren J, Pei SF, Zheng Y, He Y, Hu Y, Yang N, Yan H. Machine-learning-based classification of real-time tissue elastography for hepatic fibrosis in patients with chronic hepatitis B. *Comput Biol Med* 2017; **89**: 18-23 [PMID: 28779596 DOI: 10.1016/j.compbiomed.2017.07.012]

16 **Brattain LJ**, Telfer BA, Dhyani M, Grajo JR, Samir AE. Objective Liver Fibrosis Estimation from Shear Wave Elastography. *Annu Int Conf IEEE Eng Med Biol Soc* 2018; **2018**: 1-5 [PMID: 30440285 DOI: 10.1109/EMBC.2018.8513011]

17 **Wang K**, Lu X, Zhou H, Gao Y, Zheng J, Tong M, Wu C, Liu C, Huang L, Jiang T, Meng F, Lu Y, Ai H, Xie XY, Yin LP, Liang P, Tian J, Zheng R. Deep learning Radiomics of shear wave elastography significantly improved diagnostic performance for assessing liver fibrosis in chronic hepatitis B: a prospective multicentre study. *Gut* 2019; **68**: 729-741 [PMID: 29730602 DOI: 10.1136/gutjnl-2018-316204]

18 **Loomba R**, Sanyal AJ. The global NAFLD epidemic. *Nat Rev Gastroenterol Hepatol* 2013; **10**: 686-690 [PMID: 24042449 DOI: 10.1038/nrgastro.2013.171]

19 **Friedman SL**, Neuschwander-Tetri BA, Rinella M, Sanyal AJ. Mechanisms of NAFLD development and therapeutic strategies. *Nat Med* 2018; **24**: 908-922 [PMID: 29967350 DOI: 10.1038/s41591-018-0104-9]

20 **Lăpădat AM**, Jianu IR, Ungureanu BS, Florescu LM, Gheonea DI, Sovaila S, Gheonea IA. Non-invasive imaging techniques in assessing non-alcoholic fatty liver disease: a current status of available methods. *J Med Life* 2017; **10**: 19-26 [PMID: 28255371]

21 **Lee DH**. Imaging evaluation of non-alcoholic fatty liver disease: focused on quantification. *Clin Mol Hepatol* 2017; **23**: 290-301 [PMID: 28994271 DOI: 10.3350/cmh.2017.0042]

22 **Ballestri S**, Nascimbeni F, Lugari S, Lonardo A, Francica G. A critical appraisal of the use of ultrasound in hepatic steatosis. *Expert Rev Gastroenterol Hepatol* 2019; **13**: 667-681 [PMID: 31104523 DOI: 10.1080/17474124.2019.1621164]

23 **Pirmoazen AM**, Khurana A, El Kaffas A, Kamaya A. Quantitative ultrasound approaches for diagnosis and monitoring hepatic steatosis in nonalcoholic fatty liver disease. *Theranostics* 2020; **10**: 4277-4289 [PMID: 32226553 DOI: 10.7150/thno.40249]

24 **Xia MF**, Yan HM, He WY, Li XM, Li CL, Yao XZ, Li RK, Zeng MS, Gao X. Standardized ultrasound hepatic/renal ratio and hepatic attenuation rate to quantify liver fat content: an improvement method. *Obesity (Silver Spring)* 2012; **20**: 444-452 [PMID: 22016092 DOI: 10.1038/oby.2011.302]

25 **Kotronen A**, Peltonen M, Hakkarainen A, Sevastianova K, Bergholm R, Johansson LM, Lundbom N, Rissanen A, Ridderstråle M, Groop L, Orho-Melander M, Yki-Järvinen H. Prediction of non-alcoholic fatty liver disease and liver fat using metabolic and genetic factors. *Gastroenterology* 2009; **137**: 865-872 [PMID: 19524579 DOI: 10.1053/j.gastro.2009.06.005]

26 **Byra M**, Styczynski G, Szmigielski C, Kalinowski P, Michałowski Ł, Paluszkiewicz R, Ziarkiewicz-Wróblewska B, Zieniewicz K, Sobieraj P, Nowicki A. Transfer learning with deep convolutional neural network for liver steatosis assessment in ultrasound images. *Int J Comput Assist Radiol Surg* 2018; **13**: 1895-1903 [PMID: 30094778 DOI: 10.1007/s11548-018-1843-2]

27 **Byra M**, Han A, Boehringer AS, Zhang YN, O'Brien WD Jr, Erdman JW Jr, Loomba R, Sirlin CB, Andre M. Liver Fat Assessment in Multiview Sonography Using Transfer Learning With Convolutional Neural Networks. *J Ultrasound Med* 2022; **41**: 175-184 [PMID: 33749862 DOI: 10.1002/jum.15693]

28 **Reddy DS**, Bharath R, Rajalakshmi P. A Novel Computer-Aided Diagnosis Framework Using Deep Learning for Classification of Fatty Liver Disease in Ultrasound Imaging. *Int Confer e-Health Network App Ser* 2018; 1-5

29 **Chou TH**, Yeh HJ, Chang CC, Tang JH, Kao WY, Su IC, Li CH, Chang WH, Huang CK, Sufriyana H, Su EC. Deep learning for abdominal ultrasound: A computer-aided diagnostic system for the severity of fatty liver. *J Chin Med Assoc* 2021; **84**: 842-850 [PMID: 34282076 DOI: 10.1097/JCMA.0000000000000585]

30 **Zamanian H**, Mostaar A, Azadeh P, Ahmadi M. Implementation of Combinational Deep Learning Algorithm for Non-alcoholic Fatty Liver Classification in Ultrasound Images. *J Biomed Phys Eng* 2021; **11**: 73-84 [PMID: 33564642 DOI: 10.31661/jbpe.v0i0.2009-1180]

31 **Han A**, Byra M, Heba E, Andre MP, Erdman JW Jr, Loomba R, Sirlin CB, O'Brien WD Jr. Noninvasive Diagnosis of Nonalcoholic Fatty Liver Disease and Quantification of Liver Fat with Radiofrequency Ultrasound Data Using One-dimensional Convolutional Neural Networks. *Radiology* 2020; **295**: 342-350 [PMID: 32096706 DOI: 10.1148/radiol.2020191160]

32 **Nguyen TN**, Podkowa AS, Park TH, Miller RJ, Do MN, Oelze ML. Use of a convolutional neural network and quantitative ultrasound for diagnosis of fatty liver. *Ultrasound Med Biol* 2021; **47**: 556-568 [PMID: 33358553 DOI: 10.1016/j.ultrasmedbio.2020.10.025]

33 **Cha DI**, Kang TW, Min JH, Joo I, Sinn DH, Ha SY, Kim K, Lee G, Yi J. Deep learning-based automated quantification of the hepatorenal index for evaluation of fatty liver by ultrasonography. *Ultrasonography* 2021; **40**: 565-574 [PMID: 33966363 DOI: 10.14366/usg.20179]

34 **Amarapurkar D**, Han KH, Chan HL, Ueno Y; Asia-Pacific Working Party on Prevention of Hepatocellular Carcinoma. Application of surveillance programs for hepatocellular carcinoma in the Asia-Pacific Region. *J Gastroenterol Hepatol* 2009; **24**: 955-961 [PMID: 19383082 DOI: 10.1111/j.1440-1746.2009.05805.x]

35 **Kumar V**, Gu Y, Basu S, Berglund A, Eschrich SA, Schabath MB, Forster K, Aerts HJ, Dekker A, Fenstermacher D, Goldgof DB, Hall LO, Lambin P, Balagurunathan Y, Gatenby RA, Gillies RJ. Radiomics: the process and the challenges. *Magn Reson Imaging* 2012; **30**: 1234-1248 [PMID: 22898692 DOI: 10.1016/j.mri.2012.06.010]

36 **Xian GM**. An identification method of malignant and benign liver tumors from ultrasonography based on GLCM texture features and fuzzy SVM. *Expert System App* 2010; **37**: 6737-6741 [DOI: 10.1016/J.ESWA.2010.02.067]

37 **Xi IL**, Wu J, Guan J, Zhang PJ, Horii SC, Soulen MC, Zhang Z, Bai HX. Deep learning for differentiation of benign and malignant solid liver lesions on ultrasonography. *Abdom Radiol (NY)* 2021; **46**: 534-543 [PMID: 32681268 DOI: 10.1007/s00261-020-02564-w]

38 **Yang Q**, Wei J, Hao X, Kong D, Yu X, Jiang T, Xi J, Cai W, Luo Y, Jing X, Yang Y, Cheng Z, Wu J, Zhang H, Liao J, Zhou P, Song Y, Zhang Y, Han Z, Cheng W, Tang L, Liu F, Dou J, Zheng R, Yu J, Tian J, Liang P. Improving B-mode ultrasound diagnostic performance for focal liver lesions using deep learning: A multicentre study. *EBioMedicine* 2020; **56**: 102777 [PMID: 32485640 DOI: 10.1016/j.ebiom.2020.102777]

39 **Tiyarattanachai T**, Apiparakoon T, Marukatat S, Sukcharoen S, Geratikornsupuk N, Anukulkarnkusol N, Mekaroonkamol P, Tanpowpong N, Sarakul P, Rerknimitr R, Chaiteerakij R. Development and validation of artificial intelligence to detect and diagnose liver lesions from ultrasound images. *PLoS One* 2021; **16**: e0252882 [PMID: 34101764 DOI: 10.1371/journal.pone.0252882]

40 **Hwang YN**, Lee JH, Kim GY, Jiang YY, Kim SM. Classification of focal liver lesions on ultrasound images by extracting hybrid textural features and using an artificial neural network. *Biomed Mater Eng* 2015; **26** Suppl 1: S1599-S1611 [PMID: 26405925 DOI: 10.3233/BME-151459]

41 **Hassan TM**, Elmogy M, Sallam ES. Diagnosis of Focal Liver Diseases Based on Deep Learning Technique for Ultrasound Images. *J Sci Engi* 2017; **42**: 3127-3140 [DOI: 10.1007/S13369-016-2387-9]

42 **Schmauch B**, Herent P, Jehanno P, Dehaene O, Saillard C, Aubé C, Luciani A, Lassau N, Jégou S. Diagnosis of focal liver lesions from ultrasound using deep learning. *Diagn Interv Imaging* 2019; **100**: 227-233 [PMID: 30926443 DOI: 10.1016/j.diii.2019.02.009]

43 **Guo LH**, Wang D, Qian YY, Zheng X, Zhao CK, Li XL, Bo XW, Yue WW, Zhang Q, Shi J, Xu HX. A two-stage multi-view learning framework based computer-aided diagnosis of liver tumors with contrast enhanced ultrasound images. *Clin Hemorheol Microcirc* 2018; **69**: 343-354 [PMID: 29630528 DOI: 10.3233/CH-170275]

44 **Pan F**, Huang Q, Li X. Classification of liver tumors with CEUS based on 3D-CNN. *Int Confer Adv Rob Mechat* 2019; 845-849

45 **Gatos I**, Tsantis S, Spiliopoulos S, Skouroliakou A, Theotokas I, Zoumpoulis P, Hazle JD, Kagadis GC. A new automated quantification algorithm for the detection and evaluation of focal liver lesions with contrast-enhanced ultrasound. *Med Phys* 2015; **42**: 3948-3959 [PMID: 26133595 DOI: 10.1118/1.4921753]

46 **Kondo S**, Takagi K, Nishida M, Iwai T, Kudo Y, Ogawa K, Kamiyama T, Shibuya H, Kahata K, Shimizu C. Computer-Aided Diagnosis of Focal Liver Lesions Using Contrast-Enhanced Ultrasonography With Perflubutane Microbubbles. *IEEE Trans Med Imaging* 2017; **36**: 1427-1437 [PMID: 28141517 DOI: 10.1109/TMI.2017.2659734]

47 **Streba CT**, Ionescu M, Gheonea DI, Sandulescu L, Ciurea T, Saftoiu A, Vere CC, Rogoveanu I. Contrast-enhanced ultrasonography parameters in neural network diagnosis of liver tumors. *World J Gastroenterol* 2012; **18**: 4427-4434 [PMID: 22969209 DOI: 10.3748/wjg.v18.i32.4427]

48 **Căleanu CD**, Sîrbu CL, Simion G. Deep Neural Architectures for Contrast Enhanced Ultrasound (CEUS) Focal Liver Lesions Automated Diagnosis. *Sensors (Basel)* 2021; **21** [PMID: 34208548 DOI: 10.3390/s21124126]

49 **Hu HT**, Wang W, Chen LD, Ruan SM, Chen SL, Li X, Lu MD, Xie XY, Kuang M. Artificial intelligence assists

identifying malignant *vs* benign liver lesions using contrast-enhanced ultrasound. *J Gastroenterol Hepatol* 2021; **36**: 2875-2883 [PMID: 33880797 DOI: 10.1111/jgh.15522]

50 **Zhou L**, Rui JA, Zhou WX, Wang SB, Chen SG, Qu Q. Edmondson-Steiner grade: A crucial predictor of recurrence and survival in hepatocellular carcinoma without microvascular invasio. *Pathol Res Pract* 2017; **213**: 824-830 [PMID: 28554743 DOI: 10.1016/j.prp.2017.03.002]

51 **Zhou L**, Rui JA, Wang SB, Chen SG, Qu Q, Chi TY, Wei X, Han K, Zhang N, Zhao HT. Factors predictive for long-term survival of male patients with hepatocellular carcinoma after curative resection. *J Surg Oncol* 2007; **95**: 298-303 [PMID: 17326130 DOI: 10.1002/jso.20678]

52 **Court CM**, Harlander-Locke MP, Markovic D, French SW, Naini BV, Lu DS, Raman SS, Kaldas FM, Zarrinpar A, Farmer DG, Finn RS, Sadeghi S, Tomlinson JS, Busuttil RW, Agopian VG. Determination of hepatocellular carcinoma grade by needle biopsy is unreliable for liver transplant candidate selection. *Liver Transpl* 2017; **23**: 1123-1132 [PMID: 28688158 DOI: 10.1002/lt.24811]

53 **Liu D**, Liu F, Xie X, Su L, Liu M, Kuang M, Huang G, Wang Y, Zhou H, Wang K, Lin M, Tian J. Accurate prediction of responses to transarterial chemoembolization for patients with hepatocellular carcinoma by using artificial intelligence in contrast-enhanced ultrasound. *Eur Radiol* 2020; **30**: 2365-2376 [PMID: 31900703 DOI: 10.1007/s00330-019-06553-6]

54 **Liu F**, Liu D, Wang K, Xie X, Su L, Kuang M, Huang G, Peng B, Wang Y, Lin M, Tian J. Deep Learning Radiomics Based on Contrast-Enhanced Ultrasound Might Optimize Curative Treatments for Very-Early or Early-Stage Hepatocellular Carcinoma Patients. *Liver Cancer* 2020; **9**: 397-413 [PMID: 32999867 DOI: 10.1159/000505694]

55 **Wang W**, Wu SS, Zhang JC, Xian MF, Huang H, Li W, Zhou ZM, Zhang CQ, Wu TF, Li X, Xu M, Xie XY, Kuang M, Lu MD, Hu HT. Preoperative Pathological Grading of Hepatocellular Carcinoma Using Ultrasomics of Contrast-Enhanced Ultrasound. *Acad Radiol* 2021; **28**: 1094-1101 [PMID: 32622746 DOI: 10.1016/j.acra.2020.05.033]

56 **Hu HT**, Wang Z, Huang XW, Chen SL, Zheng X, Ruan SM, Xie XY, Lu MD, Yu J, Tian J, Liang P, Wang W, Kuang M. Ultrasound-based radiomics score: a potential biomarker for the prediction of microvascular invasion in hepatocellular carcinoma. *Eur Radiol* 2019; **29**: 2890-2901 [PMID: 30421015 DOI: 10.1007/s00330-018-5797-0]

57 **Dong Y**, Zhou L, Xia W, Zhao XY, Zhang Q, Jian JM, Gao X, Wang WP. Preoperative Prediction of Microvascular Invasion in Hepatocellular Carcinoma: Initial Application of a Radiomic Algorithm Based on Grayscale Ultrasound Images. *Front Oncol* 2020; **10**: 353 [PMID: 32266138 DOI: 10.3389/fonc.2020.00353]

58 **Zhang D**, Wei Q, Wu GG, Zhang XY, Lu WW, Lv WZ, Liao JT, Cui XW, Ni XJ, Dietrich CF. Preoperative Prediction of Microvascular Invasion in Patients With Hepatocellular Carcinoma Based on Radiomics Nomogram Using Contrast-Enhanced Ultrasound. *Front Oncol* 2021; **11**: 709339 [PMID: 34557410 DOI: 10.3389/fonc.2021.709339]

59 **Wu K**, Chen X, Ding M. Deep learning based classification of focal liver lesions with contrast-enhanced ultrasound. *Optik* 2014; **125**: 4057-4063 [DOI: 10.1016/J.IJLEO.2014.01.114]

World Journal of Gastroenterology

Submit a Manuscript: https://www.f6publishing.com

World J Gastroenterol 2022 July 21; 28(27): 3410-3421

DOI: 10.3748/wjg.v28.i27.3410

ISSN 1007-9327 (print) ISSN 2219-2840 (online)

MINIREVIEWS

Risk factors and diagnostic biomarkers for nonalcoholic fatty liver disease-associated hepatocellular carcinoma: Current evidence and future perspectives

Masayuki Ueno, Haruhiko Takeda, Atsushi Takai, Hiroshi Seno

Specialty type: Gastroenterology and hepatology

Provenance and peer review: Invited article; Externally peer reviewed.

Peer-review model: Single blind

Peer-review report's scientific quality classification

Grade A (Excellent): 0
Grade B (Very good): B
Grade C (Good): C
Grade D (Fair): 0
Grade E (Poor): 0

P-Reviewer: Ulasoglu C, Turkey; Wang YL, China

Received: February 2, 2022
Peer-review started: February 2, 2022
First decision: April 10, 2022
Revised: April 24, 2022
Accepted: June 15, 2022
Article in press: June 15, 2022
Published online: July 21, 2022

Masayuki Ueno, Haruhiko Takeda, Atsushi Takai, Hiroshi Seno, Department of Gastroenterology and Hepatology, Kyoto University Graduate School of Medicine, Kyoto 6068507, Japan

Corresponding author: Atsushi Takai, MD, PhD, Assistant Professor, Department of Gastroenterology and Hepatology, Kyoto University Graduate School of Medicine, 54 Shogoin-Kawahara-cho, Sakyo-ku, Kyoto 6068507, Japan. atsushit@kuhp.kyoto-u.ac.jp

Abstract

High rates of excessive calorie intake diets and sedentary lifestyles have led to a global increase in nonalcoholic fatty liver disease (NAFLD). As a result, this condition has recently become one of the leading causes of hepatocellular carcinoma (HCC). Furthermore, the incidence of NAFLD-associated HCC (NAFLD-HCC) is expected to increase in the near future. Advanced liver fibrosis is the most common risk factor for NAFLD-HCC. However, up to 50% of NAFLD-HCC cases develop without underlying liver cirrhosis. Epidemiological studies have revealed many other risk factors for this condition; including diabetes, other metabolic traits, obesity, old age, male sex, Hispanic ethnicity, mild alcohol intake, and elevated liver enzymes. Specific gene variants, such as single-nucleotide polymorphisms of patatin-like phospholipase domain 3, transmembrane 6 superfamily member 2, and membrane-bound O-acyl-transferase domain-containing 7, are also associated with an increased risk of HCC in patients with NAFLD. This clinical and genetic information should be interpreted together for accurate risk prediction. Alpha-fetoprotein (AFP) is the only biomarker currently recommended for HCC screening. However, it is not sufficiently sensitive in addressing this diagnostic challenge. The GALAD score can be calculated based on sex, age, lectin-bound AFP, AFP, and des-carboxyprothrombin and is reported to show better diagnostic performance for HCC. In addition, emerging studies on genetic and epigenetic biomarkers have also yielded promising diagnostic potential. However, further research is needed to establish an effective surveillance program for the early diagnosis of NAFLD-HCC.

Key Words: Nonalcoholic fatty liver disease; Hepatocellular carcinoma; Risk factors; Biomarkers; Tumor markers; Genetics

Core Tip: This review summarizes the risk factors and diagnostic biomarkers for nonalcoholic fatty liver disease (NAFLD)-associated hepatocellular carcinoma (HCC). The highlighted risk factors include liver fibrosis, diabetes, age, sex, race, alcohol intake, elevated liver enzymes, and specific genetic variants. Currently available diagnostic biomarkers include alpha-fetoprotein (AFP), des-carboxyprothrombin, and the AFP isoform L3. The combined use of these biomarkers may increase the diagnostic sensitivity of NAFLD-HCC detection. However, more discussion will be necessary on the cost-effectiveness of these approaches. This review also summarizes emerging means of discovering novel biomarkers using omics techniques. A better understanding of these risk factors and diagnostic biomarkers will facilitate the effective surveillance of NAFLD-HCC.

Citation: Ueno M, Takeda H, Takai A, Seno H. Risk factors and diagnostic biomarkers for nonalcoholic fatty liver disease-associated hepatocellular carcinoma: Current evidence and future perspectives. *World J Gastroenterol* 2022; 28(27): 3410-3421
URL: https://www.wjgnet.com/1007-9327/full/v28/i27/3410.htm
DOI: https://dx.doi.org/10.3748/wjg.v28.i27.3410

INTRODUCTION

Hepatocellular carcinoma (HCC) accounts for the majority of primary liver cancers[1]. It is the sixth most common form of cancer and the fourth leading cause of worldwide cancer-related deaths[2]. By contrast to the declining trends for other major cancers, mortality rates from liver cancer have increased by almost 3% *per* year[3]. Chronic liver infection from hepatitis B or C virus (HBV or HCV, respectively) and alcohol abuse are the most common causes of HCC[1,4]. However, there is a growing concern about the rapid increase in nonalcoholic fatty liver disease (NAFLD) as another cause of HCC.

NAFLD is a spectrum of chronic liver diseases characterized by excess fat accumulation in hepatocytes[5]. The prevalence of NAFLD is rapidly increasing worldwide, with recent studies reporting a global percentage of approximately 25%[6]. Unsurprisingly, the incidence of NAFLD-associated HCC (NAFLD-HCC) is also increasing in many areas of the world. In the United States, the proportion of NAFLD-HCC among all HCC patients has significantly increased from 9.3% to 13.6% over the past decade[7]. In a French cohort of patients who underwent liver resection, the prevalence of NAFLD-HCC increased from 2.6% (1995-1999) to 19.5% (2010-2014)[8]. Similar trends are also seen in Asian countries. According to a nationwide survey conducted in Japan, the proportion of nonalcoholic steatohepatitis (NASH)-related HCC has increased from 1.5% (2007 or before) to 7.2% (2014–2016)[9]. Universal HBV vaccination and widespread use of direct-acting antiviral agents for HCV are expected to decrease the number of virus-related HCC cases. Nonetheless, NAFLD-HCC is expected to continue to rise in the future[10,11].

NAFLD-HCC is often diagnosed at an advanced stage due to a lack of efficient surveillance policies [11]. In the Veteran Affairs population, only 40% of NAFLD-HCC patients underwent HCC surveillance compared to more than 80% of patients with HCV-related HCC[12]. From the perspective of cost-effectiveness, HCC screening should be considered when the annual risk of HCC exceeds 0.4–2.0%[13,14]. However, in a large-scale retrospective cohort study, out of 2382289 person-years of follow-up, only 490 patients with NAFLD were diagnosed with HCC (0.21/1000 person-years)[15]. Thus, it is necessary to more effectively identify high-risk patients who will benefit from HCC surveillance. Additionally, the diagnostic performance of the implemented examination is important for effective surveillance. Although ultrasonography with or without alpha-fetoprotein (AFP) is recommended for HCC screening [16], the sensitivity and specificity of these examinations are insufficient in patients with NAFLD. The high prevalence of obesity in patients with NAFLD impairs ultrasonography performance[17]. Therefore, many researchers have been searching for alternative NAFLD-HCC surveillance tools to increase the chances of early diagnosis. Recent advances in omics technology have enabled easier genetic and epigenetic benchmark analysis. Thus, many potential biomarkers are currently under investigation.

In this review, we discuss the current evidence for clinical and genetic HCC risk factors. We also summarize previous reports on the diagnostic biomarkers of NAFLD-HCC, including those under development. Finally, we briefly address future perspectives on HCC surveillance for NAFLD patients.

CLINICAL RISK FACTORS

Liver fibrosis

Liver fibrosis is the most important risk factor for the development of HCC in patients with NAFLD[18,

19]. In a large retrospective cohort study, the annual HCC incidence rates amongst NAFLD patients with and without cirrhosis were 10.6 and 0.08 *per* 1000 person-years, respectively[15]. This indicates that the presence of liver cirrhosis increases the risk of NAFLD-HCC by more than 10-fold (Table 1).

Liver biopsy is the gold standard for evaluating the fibrotic stage of the liver[20]. However, noninvasive examinations are more widely used in clinical practice. Available serum biomarkers for assessing fibrosis include the aspartate transaminase (AST)-to-platelet ratio index, Fibrosis-4 (FIB-4) index, and enhanced liver fibrosis score[21]. The FIB-4 index is calculated using various factors; including age, AST, alanine aminotransferase (ALT), and platelet count. Furthermore, a significant association between the FIB-4 index and HCC risk in NAFLD patients has been reported[15,22]. The Mac-2-binding protein glycosylation isomer is a novel serum biomarker that shows relatively high efficacy at assessing liver fibrosis[23]. It may also be useful in predicting the risk of hepatocarcinogenesis among NAFLD patients[24].

Additionally, elastography techniques using ultrasound or magnetic resonance imaging are useful tools for noninvasive evaluation of degree of fibrosis[21]. A retrospective study from Japan suggested that shear wave velocity measurements can be used for HCC risk assessment in NAFLD patients[25].

Diabetes mellitus and other metabolic traits

Several studies have demonstrated that (mostly type 2) diabetes mellitus is associated with an increased risk of HCC development in NAFLD patients. The hazard ratio for HCC in diabetic patients has been reported to be around 2.2–4.2[22,26,27] (Table 1). In a nationwide Japanese study, the annual incidence of HCC was only 0.11% in diabetes patients overall. However, it increased to 1.0% when they had an FIB-4 index of 3.5 or more[14]. Therefore, the degree of liver fibrosis, together with presence or absence of diabetes, should be assessed to predict the risk of NAFLD-HCC.

There have been conflicting reports regarding the association between other metabolic traits such as hypertension, dyslipidemia, with NAFLD-HCC[28]. However, a recent study showed that these conditions were also risk factors for NAFLD-HCC (Table 1). Furthermore, the hazard ratio for HCC was 5.6 in patients with diabetes, hypertension, and dyslipidemia[27,29].

Obesity

Regardless of underlying liver diseases, obesity is associated with an increased risk of HCC[30]. This relationship has also been confirmed in patients with NAFLD[29,31]. In a cohort of NAFLD-HCC patients treated with curative radiofrequency ablation, the degree of visceral fat accumulation, but not body mass index (BMI), was independently associated with an increased risk of HCC recurrence[32]. A propensity score-matched study showed that the incidence of both NASH and HCC were significantly lower in patients who underwent bariatric surgery, indicating a protective role of sustained weight loss by bariatric surgery[33].

Age, sex, and race

Old age, male sex, and Hispanic ethnicity are also known risk factors for NAFLD-HCC (Table 1); the details are described in another review article[31]. In the United States, a multicenter case-control study showed that old age (*per* year) and male sex were independently associated with a higher NAFLD-HCC risk [odds ratios (OR), 1.08 and 4.34, respectively][34]. In another study, age ≥ 65 years was associated with a 1.83 times higher NAFLD-HCC risk compared to age < 65 years[15]. Regarding ethnicity, a previous study showed that Hispanic patients had a lower NAFLD-HCC risk (OR, 0.3). By contrast, another study showed the opposite result (hazard ratio, 1.59)[15,34]. Several other studies have shown that Hispanic ethnicity is, in itself, a risk factor for NAFLD, partly because of the high prevalence of patatin-like phospholipase domain 3 (*PNPLA3*) variants among Hispanic people[35,36].

Alcohol intake and smoking

NAFLD is defined as hepatic steatosis without harmful alcohol intake (more than 30 g/day for men and 20 g/day for women). However, mild alcohol intake can also be a risk factor for NAFLD-HCC[37]. Previous studies have shown that mild drinking habits were associated with 3.6–4.8 times higher risk of HCC in NAFLD patients compared to no habits of drinking[38,39] (Table 1). No study has specifically investigated the association between smoking and NAFLD-HCC. However, smoking is associated with an increased risk of HCC. Additionally, it has been reported to be associated with advanced liver fibrosis in NAFLD patients[31,40]. Because these factors are modifiable, NAFLD patients should be informed that cessation of alcohol intake and smoking may reduce the risk of future HCC development.

Elevated liver enzymes

Patients with NASH are thought to have a higher risk of HCC than those with NAFLD[18]. However, liver biopsy is required to accurately distinguish these conditions. Therefore, elevated liver enzyme levels are often used as surrogate markers for NASH in clinical practice. Several studies have shown that elevated liver enzymes in NAFLD patients are significantly associated with an increased risk of HCC (hazard ratio, 2.07–8.20)[41-43] (Table 1). At the same time, however, normal transaminase levels do not exclude the possibility of advanced liver fibrosis[44].

Table 1 Clinical risk factors for nonalcoholic fatty liver disease-associated hepatocellular carcinoma

Risk factors	Reported evidence	Ref.
Liver fibrosis	The annual incidence rate of HCC in NAFLD patients with cirrhosis was more than 10 times higher than in those without	[15,22,24,25]
	Non-invasive fibrosis markers (*e.g.*, FIB-4 index, M2BPGi, and shear wave velocity in VTQ) also had significant associations with the risk of NAFLD-HCC	
Diabetes	Associated with increased risk of HCC in NAFLD patients (hazard ratio: 2.2–4.2)	[22,26,27]
Hypertension	May be an independent risk factor for NAFLD-HCC	[29]
Dyslipidemia	May be an independent risk factor for NAFLD-HCC	[29]
Age	Increased age was an independent risk factor for HCC in patients with NASH-related cirrhosis	[15,34]
	NAFLD patients aged ≥ 65 had 1.83 times higher risk of HCC than those aged < 65	
Male sex	Male patients with NASH-related cirrhosis had 4.34 times higher risk of HCC than female patients	[34]
Ethnicity	Hispanic ethnicity was associated with 1.59 times higher risk of HCC in NAFLD patients compared to white ethnicity (however, there have been conflicting results)	[15]
Mild alcohol intake	Associated with increased risk of HCC in NAFLD patients (hazard ratio: 3.6–4.8)	[38,39]
Elevated liver enzymes	Associated with increased risk of HCC in NAFLD patients (hazard ratio: 2.1–8.2)	[41-43]

HCC: Hepatocellular carcinoma; NAFLD: Nonalcoholic fatty liver disease; FIB-4: Fibrosis-4; M2BPGi: Mac-2-binding protein glycosylation isomer; VTQ: Virtual touch quantification; NASH: Nonalcoholic steatohepatitis.

Combined risk assessment

As we described above, many factors influence the risk of HCC in NAFLD patients. Therefore, integrating multiple factors will improve the accuracy of risk assessment. Lee *et al*[45] proposed a risk prediction model consisting of age, platelet count, and liver stiffness. This showed relatively good prediction performance in the validation cohort (*i.e.*, area under the receiver operating characteristic curve (AUROC), 0.78)[45]. Ioannou *et al*[46] reported another prediction model with a similar predictive value (AUROC, 0.75), consisting of age, sex, diabetes, BMI, platelet count, serum albumin, and AST/√ALT ratio[46].

GENETIC RISK FACTORS

Although NAFLD development and progression is largely determined by environmental factors, several genetic factors are involved in NAFLD pathogenesis. These genes included *PNPLA3*, transmembrane 6 superfamily member 2 (*TM6SF2*), glucokinase regulator (*GCKR*), membrane-bound O-acyl-transferase domain-containing 7 (*MBOAT7*), and 17-beta-hydroxysteroid dehydrogenase 13 (*HSD17B13*)[5,47]. Epigenetic factors, such as DNA methylation, histone modification, and non-coding RNAs, also play roles in the progression of NAFLD and hepatocarcinogenesis[48]. The risk of severe liver fibrosis has been reported to be 12.5-fold higher in patients with first-degree relatives with NAFLD-related cirrhosis than those without[49].

Single-nucleotide polymorphisms (SNPs) of *PNPLA3* have been the most studied for its association with HCC[50]. In a cohort of European Caucasian patients with NAFLD, the *PNPLA3* rs738409 polymorphism was significantly associated with HCC risk. GG carriers were found to evince a 5-fold increased risk compared to CC carriers[51]. This association was confirmed by subsequent studies[52,53]. The *TM6SF2* rs58542926 polymorphism has been reported to be another risk factor for HCC and advanced fibrosis/cirrhosis[54,55]. In addition, the *MBOAT7* rs641738 variant has also been reported as a risk factor for NAFLD-HCC. Furthermore, in an Italian cohort, the rs6417338 C-to-T variant was associated with a 1.65-fold increased risk of HCC[56]. Other reported SNPs associated with NAFLD-HCC risk include Toll-like receptor 5 rs5744174[57], signal transducer transcription 6 rs167769[58] activator, yes-associated protein 1 rs11225163[58], *HSD17B13* rs72613567[55], and dystrophy-associated fer-1-like protein rs17007417[59] (Table 2).

Zhang *et al*[55] reported a combined risk assessment model consisting of *PNPLA3*, *TM6SF2*, and *HSD17B13* variants[55]. In this study, patients with the highest score had a 29-fold higher risk of developing HCC. Bianco *et al*[60] reported another polygenic risk assessment model consisting of *PNPLA3*, *TM6SF2*, *GCKR*, *MBOAT7*, and *HSD17B13*[60]. The sensitivity and specificity for diagnosing HCC were 0.43 and 0.79%, respectively (AUROC, 0.65).

Table 2 Genetic risk factors for nonalcoholic fatty liver disease-associated hepatocellular carcinoma

Risk factors	Reported evidence	Ref.
PNPLA3	Carriage of rs738409 GG polymorphism is associated with 5.1–6.4-fold increased risk of HCC in NAFLD patients	[51-53,60]
	PNPLA3 G variant (GG *vs* CG *vs* CC) was not significantly associated with the risk of cardiovascular events extrahepatic cancers or overall death, but was associated with HCC (HR: 2.66) and liver-related death (HR: 2.42)	
	Used for developing polygenic risk scores	
TM6SF2	*TM6SF2* minor allele carriage (rs58542926 C>T) was associated with advanced fibrosis/cirrhosis and HCC (OR, 2.8) in NAFLD patients	[54,55,60]
	Combined assessment with *PNPLA3* and *HSD17B13* variants were useful for risk stratification of NAFLD-HCC	
	Used for developing polygenic risk scores	
MBOAT7	*MBOAT7* rs641738 C>T variants were associated with higher risk of HCC in NAFLD patients (OR, 1.65–2.10)	[56,60]
	Used for developing polygenic risk scores	
TLR5	*TLR5* rs5744174 TT genotype was a risk factor of HCC in patients with steatohepatitis-related cirrhosis (OR, 1.9)	[57]
STAT6	*STAT6* rs167769 CC genotype was inversely associated with the risk of HCC in NASH patients (OR, 0.015)	[58]
YAP1	Carriage of *YAP1* rs11225163 C allele was inversely associated with the risk of HCC in NASH patients (OR, 0.047)	[58]
HSD17B13	Combined assessment with *PNPLA3* and *TM6SF2* variants were useful for risk stratification of NAFLD-HCC	[55]
DYSF	*DYSF* rs17007417 T allele carriage was associated with increased risk of HCC in NAFLD patients (OR, 2.74)	[59]
GCKR	*GCKR* rs1260326 T allele carriage was associated with increased risk of HCC in NAFLD patients (OR, 1.38)	[59,60]
	Used for developing polygenic risk scores	

PNPLA3: Patatin-like phospholipase domain 3; HCC: Hepatocellular carcinoma; NAFLD: Nonalcoholic fatty liver disease; HR: Hazard ratio; TM6SF2: Transmembrane 6 superfamily member 2; HSD17B13: 7-beta-Hydroxysteroid dehydrogenase 13; OR: Odds ratio; MBOAT7: Membrane-bound O-acyltransferase domain-containing 7; TLR5: Toll-like receptor 5; STAT6: Signal transducer activator of transcription 6; NASH: Nonalcoholic steatohepatitis; YAP1: Yes-associated protein 1; DYSF: Dystrophy-associated fer-1-like protein; GCKR: Glucokinase regulator.

DIAGNOSTIC BIOMARKERS

Currently available biomarkers

The currently available serum biomarkers for diagnosing HCC include AFP, des-carboxyprothrombin (DCP), and AFP isoform L3 (AFP-L3) (Table 3). Only AFP is recommended for HCC surveillance as *per* the major guidelines[31]. However, patients with NAFLD-HCC tend to have lower AFP levels than those with viral HCC[12,61]. Thus, the combined use of multiple tumor markers may be considered to increase the detection rate of HCC[62]. The GALAD score is a scoring system for the diagnosis of HCC. This score can be calculated by sex, age, lectin-bound AFP, AFP, and DCP. In a German cohort of NASH patients with and without HCC, the GALAD score exhibited excellent diagnostic performance (AUROC, 0.96). This was significantly better than AFP (AUROC, 0.88), DCP (AUROC, 0.87), and AFP-L3 (AUROC, 0.86) alone[63]. However, it must be noted that that only 20% of the HCC patients included in this study were within the Milan criteria. In addition, further research is needed from the perspective of cost effectiveness to determine whether this scoring system should be recommended for routine HCC screening in patients with NAFLD.

Potential biomarkers under investigation

Many serum biomarkers are under investigation for more accurate diagnosis of NAFLD-HCC without imaging. These biomarkers include iron and transferrin saturation[64], glypican-3 and adiponectin[65], midkine[66], apoptosis inhibitor of macrophages[67,68], glycosylation patterns of glycoproteins[69], and specific types of glycopeptides[70,71] (Table 3). Recently, Kozumi *et al*[72] showed that intrahepatic and serum thrombospondin 2 (*THBS2*) expression levels are strongly associated with advanced fibrosis in patients with NASH[72]. In their study, HCC was observed only in patients with high serum levels of

Table 3 Currently available and potential diagnostic biomarkers for nonalcoholic fatty liver disease-associated hepatocellular carcinoma

Biomarkers	Reported evidence	Ref.
Currently available		
AFP	Modest diagnostic ability for HCC in NAFLD patients (AUROC, 0.71–0.88)	[63,84]
DCP	The diagnostic ability for NAFLD-HCC was similar to that of AFP	[63,84]
	Combined use with AFP improved the diagnostic performance	
	Used for calculation of GALAD score	
AFP-L3	The diagnostic ability for NAFLD-HCC was similar to that of AFP	[63]
	Used for calculation of GALAD score	
Under development		
Iron status	Elevations of serum iron levels and transferrin saturation were associated with increased risk of HCC in NAFLD patients (HR, 2.91 and 2.02, respectively)	[64]
Proteins	Midkine increased the diagnostic yield in AFP-negative HCC in NAFLD patients; 59.2% of AFP-negative NAFLD-HCC patients had elevation of serum midkine levels	[65-67,72]
	IgM-free AIM had better diagnostic performance for NASH-HCC than AFP or DCP (AUROC, 0.905–0.929)	
	Serum TSP-2 levels were significantly associated with advanced fibrosis in NASH patients. Among 164 patients with NAFLD, HCC occurred only in patients with high serum levels of TSP-2	
Glycoprotein	Glycosylation patterns of alpha-1 acid glycoprotein may serve as a diagnostic biomarker for AFP-negative HCC in NAFLD patients	[69]
Proteoglycan	Glypican-3 had modest diagnostic ability (AUROC, 0.759), similar to AFP (AUROC, 0.763). When combined with age, sex, DCP and adiponectin, the AUROC increased to 0.948	[65]
Glycopeptide	Site-specific N-glycopeptides from vitronectin may serve as diagnostic biomarkers for NASH-HCC. When used together with AFP, the AUROC were 0.834 and 0.847, compared to 0.791 of AFP alone	[70,71]
	Site-specific N-glycopeptides from serum haptoglobin showed better diagnostic accuracy for NASH-HCC than AFP	
Cytokine (adipokine)	Adiponectin had slightly better diagnostic ability (AUROC, 0.770) than AFP (AUROC, 0.763). When combined with age, sex, DCP and glypican-3, the AUROC increased to 0.948	[65]
Cell-free DNA	*TERT* promoter mutation (C228T) in serum cfDNA showed better diagnostic ability for early NAFLD-HCC than AFP and DCP	[76,78]
	Methylation biomarkers in cfDNA improved the diagnostic performance when combined with AFP	
microRNA	The expression levels of exosomal miR-182, miR-301a and miR-373 in both serum and ascetic fluid were higher in NASH-cirrhosis patients with HCC than in those without HCC	[77]

AFP: Alpha-fetoprotein; HCC: Hepatocellular carcinoma; NAFLD: Nonalcoholic fatty liver disease; AUROC: Area under receiver operating characteristic curve; DCP: Des-carboxyprothrombin; AFP-L3: AFP isoform L3; HR: Hazard ratio; IgM: Immunoglobulin M; AIM: Apoptosis inhibitor of macrophages; TSP-2: Thrombospondin-2; NASH: Nonalcoholic steatohepatitis; TERT: Telomerase reverse transcriptase; cfDNA: Cell-free DNA; miR: microRNA.

thrombospondin-2 (TSP-2). Thus, serum TSP-2 testing may also be useful for NAFLD-HCC surveillance.

Genetic and epigenetic biomarkers have attracted increasing attention in recent years (Table 3). For example, telomerase reverse transcriptase (*TERT*) promoter mutations, the most common form of HCC genetic alteration[73-75], can be analyzed using cell-free DNA (cfDNA). Akuta *et al*[76] reported that *TERT* C228T mutation could be detected in 63.9% of NAFLD-HCC patients by analyzing cfDNA[76]. Notably, it can be positive, even in patients with normal AFP and DCP levels. Another example of circulating biomarkers is non-coding RNAs, especially microRNAs. In a preliminary study, the serum expression levels of miR-182, miR-301a, and miR-373 were significantly higher in NASH-HCC patients than in NASH patients without HCC[77]. DNA methylation can also be analyzed using peripheral blood. In a recent study, methylation cfDNA biomarkers provided a modest diagnostic value for NAFLD-HCC with a sensitivity of 87.5% and specificity of 39.4%[78]. The combination of this DNA methylation panel and AFP led to a better cohort wide diagnostic performance than either of them used

alone. Although the utility of these biomarkers is yet to be validated, in the near future, advances in omics technology will surely provide better diagnostic tools for NAFLD-HCC than conventional tumor markers.

FUTURE PERSPECTIVES

A more effective surveillance approach is strongly desired to reduce the number of deaths due to NAFLD-HCC. As advanced liver fibrosis is the most common risk factor for NAFLD-HCC, current screening recommendations primarily focus on patients with cirrhosis. However, in a French study, only 37% of patients undergoing liver resection for NAFLD-HCC had bridging fibrosis or cirrhosis; with a frequency significantly lower than that of other etiologies[8]. Similar results were observed in a Japanese multicenter study; in which only 49% of patients with NAFLD-HCC had underlying cirrhosis [79]. Therefore, more than half of patients with NAFLD-HCC will lose the chance of early detection if no other risk factors are considered. As discussed above, other clinical factors and specific genetic variants have robust associations with NAFLD-HCC risk. We should make the best use of this evidence to enhance effective HCC surveillance. In addition, more accurate diagnostic biomarkers for NAFLD-HCC are needed. Among the currently available biomarkers, the GALAD score seems to be the most reliable. However, advances in omics technology will certainly provide more powerful diagnostic tools in the future. For instance, a recent study showed that fragmentomic cfDNA analysis offered excellent accuracy in detecting primary liver tumors (AUROC, 0.995), regardless of the underlying liver disease [80]. Moreover, it showed a sensitivity of over 95%, even for stage I tumors. Thus, further research on genetic and epigenetic biomarkers is very much needed.

Novel conceptional criteria for metabolic dysfunction-associated fatty liver disease (MAFLD) were proposed in 2020[81]. Although MAFLD has been reported as a more practical definition for identifying patients with fatty liver disease with high risk of disease progression[82], it remains unclear whether the evidence of risk factors and diagnostic markers for NAFLD-HCC can be extended to MAFLD-HCC. A nationwide cohort study conducted in Taiwan revealed that patients with NAFLD/MAFLD overlap had similar risk of HCC compared to those with NAFLD alone[83]. Nonetheless, further studies are warranted on this topic.

CONCLUSION

The incidence of NAFLD-HCC is increasing rapidly worldwide. Thus, an effective surveillance approach is required to reduce the number of deaths due to this condition. Although advanced fibrosis is the most important risk factor for NAFLD-HCC, other clinical risk factors such as diabetes, old age, male sex, and elevated liver enzymes should also be considered. Recent advances in omics technology have revealed that genetic factors such as the SNP of *PNPLA3* also affect the risk of hepatocarcinogenesis in patients with NAFLD. With regards to the diagnostic biomarkers for NAFLD-HCC, only AFP is recommended for surveillance as *per* major guidelines. A recent study showed that the GALAD score evinced a more effective diagnostic performance than when AFP was used alone. However, clinical implementation should be discussed from the perspective of cost-effectiveness. Specific gene mutations and DNA methylation can be detected in cfDNA and are expected to be novel biomarkers for the early NAFLD-HCC diagnosis, as well as specific proteins, glycopeptides, and adipokines.

ACKNOWLEDGEMENTS

We would like to thank Drs. Ken Takahashi, Takahiro Shimizu, Yuji Eso, Eriko Iguchi, Ken Kumagai, Masako Mishima, Mari Teramura, Shigeharu Nakano, Takahiko Ito, Haruka Amino, and Takahiro Inoue for their helpful discussions and comments on the manuscript.

FOOTNOTES

Author contributions: Ueno M drafted the manuscript and prepared the tables; Takeda H and Takai A designed the outline and coordinated the writing of the manuscript; Seno H supervised data interpretation and revised the manuscript.

Conflict-of-interest statement: All the authors report no relevant conflicts of interest for this article.

Country/Territory of origin: Japan

ORCID number: Masayuki Ueno 0000-0002-2497-9327; Haruhiko Takeda 0000-0002-8954-9133; Atsushi Takai 0000-0002-5233-4120; Hiroshi Seno 0000-0002-8509-8128.

S-Editor: Fan JR
L-Editor: A
P-Editor: Fan JR

REFERENCES

1 **Villanueva A**. Hepatocellular Carcinoma. *N Engl J Med* 2019; **380**: 1450-1462 [PMID: 30970190 DOI: 10.1056/NEJMra1713263]
2 **Bray F**, Ferlay J, Soerjomataram I, Siegel RL, Torre LA, Jemal A. Global cancer statistics 2018: GLOBOCAN estimates of incidence and mortality worldwide for 36 cancers in 185 countries. *CA Cancer J Clin* 2018; **68**: 394-424 [PMID: 30207593 DOI: 10.3322/caac.21492]
3 **Miller KD**, Fidler-Benaoudia M, Keegan TH, Hipp HS, Jemal A, Siegel RL. Cancer statistics for adolescents and young adults, 2020. *CA Cancer J Clin* 2020; **70**: 443-459 [PMID: 32940362 DOI: 10.3322/caac.21637]
4 **Takeda H**, Takai A, Inuzuka T, Marusawa H. Genetic basis of hepatitis virus-associated hepatocellular carcinoma: linkage between infection, inflammation, and tumorigenesis. *J Gastroenterol* 2017; **52**: 26-38 [PMID: 27714455 DOI: 10.1007/s00535-016-1273-2]
5 **Brunt EM**, Wong VW, Nobili V, Day CP, Sookoian S, Maher JJ, Bugianesi E, Sirlin CB, Neuschwander-Tetri BA, Rinella ME. Nonalcoholic fatty liver disease. *Nat Rev Dis Primers* 2015; **1**: 15080 [PMID: 27188459 DOI: 10.1038/nrdp.2015.80]
6 **Younossi Z**, Anstee QM, Marietti M, Hardy T, Henry L, Eslam M, George J, Bugianesi E. Global burden of NAFLD and NASH: trends, predictions, risk factors and prevention. *Nat Rev Gastroenterol Hepatol* 2018; **15**: 11-20 [PMID: 28930295 DOI: 10.1038/nrgastro.2017.109]
7 **Hester D**, Golabi P, Paik J, Younossi I, Mishra A, Younossi ZM. Among Medicare Patients With Hepatocellular Carcinoma, Non-alcoholic Fatty Liver Disease is the Most Common Etiology and Cause of Mortality. *J Clin Gastroenterol* 2020; **54**: 459-467 [PMID: 30672817 DOI: 10.1097/MCG.0000000000001172]
8 **Pais R**, Fartoux L, Goumard C, Scatton O, Wendum D, Rosmorduc O, Ratziu V. Temporal trends, clinical patterns and outcomes of NAFLD-related HCC in patients undergoing liver resection over a 20-year period. *Aliment Pharmacol Ther* 2017; **46**: 856-863 [PMID: 28857208 DOI: 10.1111/apt.14261]
9 **Enomoto H**, Ueno Y, Hiasa Y, Nishikawa H, Hige S, Takikawa Y, Taniai M, Ishikawa T, Yasui K, Takaki A, Takaguchi K, Ido A, Kurosaki M, Kanto T, Nishiguchi S; Japan Etiology of Liver Cirrhosis Study Group in the 54th Annual Meeting of JSH. The transition in the etiologies of hepatocellular carcinoma-complicated liver cirrhosis in a nationwide survey of Japan. *J Gastroenterol* 2021; **56**: 158-167 [PMID: 33219410 DOI: 10.1007/s00535-020-01748-x]
10 **Estes C**, Anstee QM, Arias-Loste MT, Bantel H, Bellentani S, Caballeria J, Colombo M, Craxi A, Crespo J, Day CP, Eguchi Y, Geier A, Kondili LA, Kroy DC, Lazarus JV, Loomba R, Manns MP, Marchesini G, Nakajima A, Negro F, Petta S, Ratziu V, Romero-Gomez M, Sanyal A, Schattenberg JM, Tacke F, Tanaka J, Trautwein C, Wei L, Zeuzem S, Razavi H. Modeling NAFLD disease burden in China, France, Germany, Italy, Japan, Spain, United Kingdom, and United States for the period 2016-2030. *J Hepatol* 2018; **69**: 896-904 [PMID: 29886156 DOI: 10.1016/j.jhep.2018.05.036]
11 **Degasperi E**, Colombo M. Distinctive features of hepatocellular carcinoma in non-alcoholic fatty liver disease. *Lancet Gastroenterol Hepatol* 2016; **1**: 156-164 [PMID: 28404072 DOI: 10.1016/S2468-1253(16)30018-8]
12 **Mittal S**, Sada YH, El-Serag HB, Kanwal F, Duan Z, Temple S, May SB, Kramer JR, Richardson PA, Davila JA. Temporal trends of nonalcoholic fatty liver disease-related hepatocellular carcinoma in the veteran affairs population. *Clin Gastroenterol Hepatol* 2015; **13**: 594-601.e1 [PMID: 25148760 DOI: 10.1016/j.cgh.2014.08.013]
13 **Parikh ND**, Singal AG, Hutton DW, Tapper EB. Cost-Effectiveness of Hepatocellular Carcinoma Surveillance: An Assessment of Benefits and Harms. *Am J Gastroenterol* 2020; **115**: 1642-1649 [PMID: 32530829 DOI: 10.14309/ajg.0000000000000715]
14 **Tateishi R**, Matsumura T, Okanoue T, Shima T, Uchino K, Fujiwara N, Senokuchi T, Kon K, Sasako T, Taniai M, Kawaguchi T, Inoue H, Watada H, Kubota N, Shimano H, Kaneko S, Hashimoto E, Watanabe S, Shiota G, Ueki K, Kashiwabara K, Matsuyama Y, Tanaka H, Kasuga M, Araki E, Koike K; LUCID study investigators. Hepatocellular carcinoma development in diabetic patients: a nationwide survey in Japan. *J Gastroenterol* 2021; **56**: 261-273 [PMID: 33427937 DOI: 10.1007/s00535-020-01754-z]
15 **Kanwal F**, Kramer JR, Mapakshi S, Natarajan Y, Chayanupatkul M, Richardson PA, Li L, Desiderio R, Thrift AP, Asch SM, Chu J, El-Serag HB. Risk of Hepatocellular Cancer in Patients With Non-Alcoholic Fatty Liver Disease. *Gastroenterology* 2018; **155**: 1828-1837.e2 [PMID: 30144434 DOI: 10.1053/j.gastro.2018.08.024]
16 **Kim TH**, Kim SY, Tang A, Lee JM. Comparison of international guidelines for noninvasive diagnosis of hepatocellular carcinoma: 2018 update. *Clin Mol Hepatol* 2019; **25**: 245-263 [PMID: 30759967 DOI: 10.3350/cmh.2018.0090]
17 **Harris PS**, Hansen RM, Gray ME, Massoud OI, McGuire BM, Shoreibah MG. Hepatocellular carcinoma surveillance: An evidence-based approach. *World J Gastroenterol* 2019; **25**: 1550-1559 [PMID: 30983815 DOI: 10.3748/wjg.v25.i13.1550]
18 **Younossi ZM**, Henry L. Epidemiology of non-alcoholic fatty liver disease and hepatocellular carcinoma. *JHEP Rep* 2021;

3: 100305 [PMID: 34189448 DOI: 10.1016/j.jhepr.2021.100305]
19 **Ito T**, Ishigami M, Ishizu Y, Kuzuya T, Honda T, Hayashi K, Nishimura D, Toyoda H, Kumada T, Goto H, Hirooka Y. Utility and limitations of noninvasive fibrosis markers for predicting prognosis in biopsy-proven Japanese non-alcoholic fatty liver disease patients. *J Gastroenterol Hepatol* 2019; **34**: 207-214 [PMID: 30144360 DOI: 10.1111/jgh.14448]
20 **Berger D**, Desai V, Janardhan S. Con: Liver Biopsy Remains the Gold Standard to Evaluate Fibrosis in Patients With Nonalcoholic Fatty Liver Disease. *Clin Liver Dis (Hoboken)* 2019; **13**: 114-116 [PMID: 31061705 DOI: 10.1002/cld.740]
21 **Castera L**, Friedrich-Rust M, Loomba R. Noninvasive Assessment of Liver Disease in Patients With Nonalcoholic Fatty Liver Disease. *Gastroenterology* 2019; **156**: 1264-1281.e4 [PMID: 30660725 DOI: 10.1053/j.gastro.2018.12.036]
22 **Alexander M**, Loomis AK, van der Lei J, Duarte-Salles T, Prieto-Alhambra D, Ansell D, Pasqua A, Lapi F, Rijnbeek P, Mosseveld M, Waterworth DM, Kendrick S, Sattar N, Alazawi W. Risks and clinical predictors of cirrhosis and hepatocellular carcinoma diagnoses in adults with diagnosed NAFLD: real-world study of 18 million patients in four European cohorts. *BMC Med* 2019; **17**: 95 [PMID: 31104631 DOI: 10.1186/s12916-019-1321-x]
23 **Kamada Y**, Ono M, Hyogo H, Fujii H, Sumida Y, Yamada M, Mori K, Tanaka S, Maekawa T, Ebisutani Y, Yamamoto A, Takamatsu S, Yoneda M, Kawada N, Chayama K, Saibara T, Takehara T, Miyoshi E; Japan Study Group of Nonalcoholic Fatty Liver Disease (JSG-NAFLD). Use of Mac-2 binding protein as a biomarker for nonalcoholic fatty liver disease diagnosis. *Hepatol Commun* 2017; **1**: 780-791 [PMID: 29404494 DOI: 10.1002/hep4.1080]
24 **Kawanaka M**, Tomiyama Y, Hyogo H, Koda M, Shima T, Tobita H, Hiramatsu A, Nishino K, Okamoto T, Sato S, Hara Y, Nishina S, Kawamoto H, Chayama K, Okanoue T, Hino K. Wisteria floribunda agglutinin-positive Mac-2 binding protein predicts the development of hepatocellular carcinoma in patients with non-alcoholic fatty liver disease. *Hepatol Res* 2018; **48**: 521-528 [PMID: 29316028 DOI: 10.1111/hepr.13054]
25 **Takamura M**, Kanefuji T, Suda T, Yokoo T, Kamimura H, Tsuchiya A, Kamimura K, Tamura Y, Igarashi M, Kawai H, Yamagiwa S, Nomoto M, Aoyagi Y. Value of shear wave velocity measurements for the risk assessment of hepatocellular carcinoma development in patients with nonalcoholic fatty liver disease : HCC risk assessment by VTTQ. *Hepatol Int* 2014; **8**: 240-249 [PMID: 26202505 DOI: 10.1007/s12072-014-9517-9]
26 **Grgurevic I**, Bozin T, Mikus M, Kukla M, O'Beirne J. Hepatocellular Carcinoma in Non-Alcoholic Fatty Liver Disease: From Epidemiology to Diagnostic Approach. *Cancers (Basel)* 2021; **13** [PMID: 34830997 DOI: 10.3390/cancers13225844]
27 **Fassio E**, Barreyro FJ, Pérez MS, Dávila D, Landeira G, Gualano G, Ruffillo G. Hepatocellular carcinoma in patients with metabolic dysfunction-associated fatty liver disease: Can we stratify at-risk populations? *World J Hepatol* 2022; **14**: 354-371 [PMID: 35317172 DOI: 10.4254/wjh.v14.i2.354]
28 **Benhammou JN**, Lin J, Hussain SK, El-Kabany M. Emerging risk factors for nonalcoholic fatty liver disease associated hepatocellular carcinoma. *Hepatoma Res* 2020; **6** [PMID: 32685690 DOI: 10.20517/2394-5079.2020.16]
29 **Jarvis H**, Craig D, Barker R, Spiers G, Stow D, Anstee QM, Hanratty B. Metabolic risk factors and incident advanced liver disease in non-alcoholic fatty liver disease (NAFLD): A systematic review and meta-analysis of population-based observational studies. *PLoS Med* 2020; **17**: e1003100 [PMID: 32353039 DOI: 10.1371/journal.pmed.1003100]
30 **Chen Y**, Wang X, Wang J, Yan Z, Luo J. Excess body weight and the risk of primary liver cancer: an updated meta-analysis of prospective studies. *Eur J Cancer* 2012; **48**: 2137-2145 [PMID: 22446023 DOI: 10.1016/j.ejca.2012.02.063]
31 **Huang DQ**, El-Serag HB, Loomba R. Global epidemiology of NAFLD-related HCC: trends, predictions, risk factors and prevention. *Nat Rev Gastroenterol Hepatol* 2021; **18**: 223-238 [PMID: 33349658 DOI: 10.1038/s41575-020-00381-6]
32 **Ohki T**, Tateishi R, Shiina S, Goto E, Sato T, Nakagawa H, Masuzaki R, Goto T, Hamamura K, Kanai F, Yoshida H, Kawabe T, Omata M. Visceral fat accumulation is an independent risk factor for hepatocellular carcinoma recurrence after curative treatment in patients with suspected NASH. *Gut* 2009; **58**: 839-844 [PMID: 19174415 DOI: 10.1136/gut.2008.164053]
33 **Kwak M**, Mehaffey JH, Hawkins RB, Hsu A, Schirmer B, Hallowell PT. Bariatric surgery is associated with reduction in non-alcoholic steatohepatitis and hepatocellular carcinoma: A propensity matched analysis. *Am J Surg* 2020; **219**: 504-507 [PMID: 31575419 DOI: 10.1016/j.amjsurg.2019.09.006]
34 **Corey KE**, Gawrieh S, deLemos AS, Zheng H, Scanga AE, Haglund JW, Sanchez J, Danford CJ, Comerford M, Bossi K, Munir S, Chalasani N, Wattacheril J. Risk factors for hepatocellular carcinoma in cirrhosis due to nonalcoholic fatty liver disease: A multicenter, case-control study. *World J Hepatol* 2017; **9**: 385-390 [PMID: 28321274 DOI: 10.4254/wjh.v9.i7.385]
35 **Romeo S**, Kozlitina J, Xing C, Pertsemlidis A, Cox D, Pennacchio LA, Boerwinkle E, Cohen JC, Hobbs HH. Genetic variation in PNPLA3 confers susceptibility to nonalcoholic fatty liver disease. *Nat Genet* 2008; **40**: 1461-1465 [PMID: 18820647 DOI: 10.1038/ng.257]
36 **Thandra KC**, Barsouk A, Saginala K, Aluru JS, Rawla P. Epidemiology of non-alcoholic fatty liver disease and risk of hepatocellular carcinoma progression. *Clin Exp Hepatol* 2020; **6**: 289-294 [PMID: 33511275 DOI: 10.5114/ceh.2020.102153]
37 **Petroni ML**, Brodosi L, Marchignoli F, Musio A, Marchesini G. Moderate Alcohol Intake in Non-Alcoholic Fatty Liver Disease: To Drink or Not to Drink? *Nutrients* 2019; **11** [PMID: 31847199 DOI: 10.3390/nu11123048]
38 **Kimura T**, Tanaka N, Fujimori N, Sugiura A, Yamazaki T, Joshita S, Komatsu M, Umemura T, Matsumoto A, Tanaka E. Mild drinking habit is a risk factor for hepatocarcinogenesis in non-alcoholic fatty liver disease with advanced fibrosis. *World J Gastroenterol* 2018; **24**: 1440-1450 [PMID: 29632425 DOI: 10.3748/wjg.v24.i13.1440]
39 **Protopapas AA**, Cholongitas E, Chrysavgis L, Tziomalos K. Alcohol consumption in patients with nonalcoholic fatty liver disease: yes, or no? *Ann Gastroenterol* 2021; **34**: 476-486 [PMID: 34276185 DOI: 10.20524/aog.2021.0641]
40 **Ou H**, Fu Y, Liao W, Zheng C, Wu X. Association between Smoking and Liver Fibrosis among Patients with Nonalcoholic Fatty Liver Disease. *Can J Gastroenterol Hepatol* 2019; **2019**: 6028952 [PMID: 31737583 DOI: 10.1155/2019/6028952]
41 **Kawamura Y**, Arase Y, Ikeda K, Seko Y, Imai N, Hosaka T, Kobayashi M, Saitoh S, Sezaki H, Akuta N, Suzuki F, Suzuki Y, Ohmoto Y, Amakawa K, Tsuji H, Kumada H. Large-scale long-term follow-up study of Japanese patients with non-alcoholic Fatty liver disease for the onset of hepatocellular carcinoma. *Am J Gastroenterol* 2012; **107**: 253-261 [PMID: 22008893 DOI: 10.1038/ajg.2011.327]
42 **Natarajan Y**, Kramer JR, Yu X, Li L, Thrift AP, El-Serag HB, Kanwal F. Risk of Cirrhosis and Hepatocellular Cancer in

Patients With NAFLD and Normal Liver Enzymes. *Hepatology* 2020; **72**: 1242-1252 [PMID: 32022277 DOI: 10.1002/hep.31157]

43 **Lee TY**, Wu JC, Yu SH, Lin JT, Wu MS, Wu CY. The occurrence of hepatocellular carcinoma in different risk stratifications of clinically noncirrhotic nonalcoholic fatty liver disease. *Int J Cancer* 2017; **141**: 1307-1314 [PMID: 28509327 DOI: 10.1002/ijc.30784]

44 **Makker J**, Tariq H, Kumar K, Ravi M, Shaikh DH, Leung V, Hayat U, Hassan MT, Patel H, Nayudu S, Chilimuri S. Prevalence of advanced liver fibrosis and steatosis in type-2 diabetics with normal transaminases: A prospective cohort study. *World J Gastroenterol* 2021; **27**: 523-533 [PMID: 33642826 DOI: 10.3748/wjg.v27.i6.523]

45 **Lee JS**, Sinn DH, Park SY, Shin HJ, Lee HW, Kim BK, Park JY, Kim DY, Ahn SH, Oh JH, Lee JI, Kim SU. Liver Stiffness-Based Risk Prediction Model for Hepatocellular Carcinoma in Patients with Nonalcoholic Fatty Liver Disease. *Cancers (Basel)* 2021; **13** [PMID: 34572795 DOI: 10.3390/cancers13184567]

46 **Ioannou GN**, Green P, Kerr KF, Berry K. Models estimating risk of hepatocellular carcinoma in patients with alcohol or NAFLD-related cirrhosis for risk stratification. *J Hepatol* 2019; **71**: 523-533 [PMID: 31145929 DOI: 10.1016/j.jhep.2019.05.008]

47 **Carlsson B**, Lindén D, Brolén G, Liljeblad M, Bjursell M, Romeo S, Loomba R. Review article: the emerging role of genetics in precision medicine for patients with non-alcoholic steatohepatitis. *Aliment Pharmacol Ther* 2020; **51**: 1305-1320 [PMID: 32383295 DOI: 10.1111/apt.15738]

48 **Tian Y**, Wong VW, Chan HL, Cheng AS. Epigenetic regulation of hepatocellular carcinoma in non-alcoholic fatty liver disease. *Semin Cancer Biol* 2013; **23**: 471-482 [PMID: 24018165 DOI: 10.1016/j.semcancer.2013.08.010]

49 **Caussy C**, Soni M, Cui J, Bettencourt R, Schork N, Chen CH, Ikhwan MA, Bassirian S, Cepin S, Gonzalez MP, Mendler M, Kono Y, Vodkin I, Mekeel K, Haldorson J, Hemming A, Andrews B, Salotti J, Richards L, Brenner DA, Sirlin CB, Loomba R; Familial NAFLD Cirrhosis Research Consortium. Nonalcoholic fatty liver disease with cirrhosis increases familial risk for advanced fibrosis. *J Clin Invest* 2017; **127**: 2697-2704 [PMID: 28628033 DOI: 10.1172/JCI93465]

50 **Anstee QM**, Day CP. The Genetics of Nonalcoholic Fatty Liver Disease: Spotlight on PNPLA3 and TM6SF2. *Semin Liver Dis* 2015; **35**: 270-290 [PMID: 26378644 DOI: 10.1055/s-0035-1562947]

51 **Oda K**, Uto H, Mawatari S, Ido A. Clinical features of hepatocellular carcinoma associated with nonalcoholic fatty liver disease: a review of human studies. *Clin J Gastroenterol* 2015; **8**: 1-9 [PMID: 25575848 DOI: 10.1007/s12328-014-0548-5]

52 **Seko Y**, Sumida Y, Tanaka S, Mori K, Taketani H, Ishiba H, Hara T, Okajima A, Umemura A, Nishikawa T, Yamaguchi K, Moriguchi M, Kanemasa K, Yasui K, Imai S, Shimada K, Itoh Y. Development of hepatocellular carcinoma in Japanese patients with biopsy-proven non-alcoholic fatty liver disease: Association between PNPLA3 genotype and hepatocarcinogenesis/fibrosis progression. *Hepatol Res* 2017; **47**: 1083-1092 [PMID: 27862719 DOI: 10.1111/hepr.12840]

53 **Wang Z**, Budhu AS, Shen Y, Wong LL, Hernandez BY, Tiirikainen M, Ma X, Irwin ML, Lu L, Zhao H, Lim JK, Taddei T, Mishra L, Pawlish K, Stroup A, Brown R, Nguyen MH, Koshiol J, Hernandez MO, Forgues M, Yang HI, Lee MH, Huang YH, Iwasaki M, Goto A, Suzuki S, Matsuda K, Tanikawa C, Kamatani Y, Mann D, Guarnera M, Shetty K, Thomas CE, Yuan JM, Khor CC, Koh WP, Risch H, Wang XW, Yu H. Genetic susceptibility to hepatocellular carcinoma in chromosome 22q13.31, findings of a genome-wide association study. *JGH Open* 2021; **5**: 1363-1372 [PMID: 34950780 DOI: 10.1002/jgh3.12682]

54 **Liu YL**, Reeves HL, Burt AD, Tiniakos D, McPherson S, Leathart JB, Allison ME, Alexander GJ, Piguet AC, Anty R, Donaldson P, Aithal GP, Francque S, Van Gaal L, Clement K, Ratziu V, Dufour JF, Day CP, Daly AK, Anstee QM. TM6SF2 rs58542926 influences hepatic fibrosis progression in patients with non-alcoholic fatty liver disease. *Nat Commun* 2014; **5**: 4309 [PMID: 24978903 DOI: 10.1038/ncomms5309]

55 **Zhang HB**, Su W, Xu H, Zhang XY, Guan YF. HSD17B13: A Potential Therapeutic Target for NAFLD. *Front Mol Biosci* 2021; **8**: 824776 [PMID: 35071330 DOI: 10.3389/fmolb.2021.824776]

56 **Donati B**, Dongiovanni P, Romeo S, Meroni M, McCain M, Miele L, Petta S, Maier S, Rosso C, De Luca L, Vanni E, Grimaudo S, Romagnoli R, Colli F, Ferri F, Mancina RM, Iruzubieta P, Craxi A, Fracanzani AL, Grieco A, Corradini SG, Aghemo A, Colombo M, Soardo G, Bugianesi E, Reeves H, Anstee QM, Fargion S, Valenti L. MBOAT7 rs641738 variant and hepatocellular carcinoma in non-cirrhotic individuals. *Sci Rep* 2017; **7**: 4492 [PMID: 28674415 DOI: 10.1038/s41598-017-04991-0]

57 **Nischalke HD**, Fischer J, Klüners A, Matz-Soja M, Krämer B, Langhans B, Goeser F, Soyka M, Stickel F, Spengler U, Nattermann J, Strassburg CP, Berg T, Lutz P. A genetic variant in toll-like receptor 5 is linked to chemokine levels and hepatocellular carcinoma in steatohepatitis. *Liver Int* 2021; **41**: 2139-2148 [PMID: 34051061 DOI: 10.1111/liv.14980]

58 **El-Derany MO**. Polymorphisms in Interleukin 13 Signaling and Interacting Genes Predict Advanced Fibrosis and Hepatocellular Carcinoma Development in Non-Alcoholic Steatohepatitis. *Biology (Basel)* 2020; **9** [PMID: 32283835 DOI: 10.3390/biology9040075]

59 **Kawaguchi T**, Shima T, Mizuno M, Mitsumoto Y, Umemura A, Kanbara Y, Tanaka S, Sumida Y, Yasui K, Takahashi M, Matsuo K, Itoh Y, Tokushige K, Hashimoto E, Kiyosawa K, Kawaguchi M, Itoh H, Uto H, Komorizono Y, Shirabe K, Takami S, Takamura T, Kawanaka M, Yamada R, Matsuda F, Okanoue T. Risk estimation model for nonalcoholic fatty liver disease in the Japanese using multiple genetic markers. *PLoS One* 2018; **13**: e0185490 [PMID: 29385134 DOI: 10.1371/journal.pone.0185490]

60 **Bianco C**, Jamialahmadi O, Pelusi S, Baselli G, Dongiovanni P, Zanoni I, Santoro L, Maier S, Liguori A, Meroni M, Borroni V, D'Ambrosio R, Spagnuolo R, Alisi A, Federico A, Bugianesi E, Petta S, Miele L, Vespasiani-Gentilucci U, Anstee QM, Stickel F, Hampe J, Fischer J, Berg T, Fracanzani AL, Soardo G, Reeves H, Prati D, Romeo S, Valenti L. Non-invasive stratification of hepatocellular carcinoma risk in non-alcoholic fatty liver using polygenic risk scores. *J Hepatol* 2021; **74**: 775-782 [PMID: 33248170 DOI: 10.1016/j.jhep.2020.11.024]

61 **Than NN**, Ghazanfar A, Hodson J, Tehami N, Coldham C, Mergental H, Manas D, Shah T, Newsome PN, Reeves H, Shetty S. Comparing clinical presentations, treatments and outcomes of hepatocellular carcinoma due to hepatitis C and non-alcoholic fatty liver disease. *QJM* 2017; **110**: 73-81 [PMID: 27634970 DOI: 10.1093/qjmed/hcw151]

62 **Ertle JM**, Heider D, Wichert M, Keller B, Kueper R, Hilgard P, Gerken G, Schlaak JF. A combination of α-fetoprotein and

des-γ-carboxy prothrombin is superior in detection of hepatocellular carcinoma. *Digestion* 2013; **87**: 121-131 [PMID: 23406785 DOI: 10.1159/000346080]

63 **Best J**, Bechmann LP, Sowa JP, Sydor S, Dechêne A, Pflanz K, Bedreli S, Schotten C, Geier A, Berg T, Fischer J, Vogel A, Bantel H, Weinmann A, Schattenberg JM, Huber Y, Wege H, von Felden J, Schulze K, Bettinger D, Thimme R, Sinner F, Schütte K, Weiss KH, Toyoda H, Yasuda S, Kumada T, Berhane S, Wichert M, Heider D, Gerken G, Johnson P, Canbay A. GALAD Score Detects Early Hepatocellular Carcinoma in an International Cohort of Patients With Nonalcoholic Steatohepatitis. *Clin Gastroenterol Hepatol* 2020; **18**: 728-735.e4 [PMID: 31712073 DOI: 10.1016/j.cgh.2019.11.012]

64 **Yu YC**, Luu HN, Wang R, Thomas CE, Glynn NW, Youk AO, Behari J, Yuan JM. Serum Biomarkers of Iron Status and Risk of Hepatocellular Carcinoma Development in Patients with Nonalcoholic Fatty Liver Disease. *Cancer Epidemiol Biomarkers Prev* 2022; **31**: 230-235 [PMID: 34649958 DOI: 10.1158/1055-9965.EPI-21-0754]

65 **Caviglia GP**, Armandi A, Rosso C, Gaia S, Aneli S, Rolle E, Abate ML, Olivero A, Nicolosi A, Guariglia M, Ribaldone DG, Carucci P, Saracco GM, Bugianesi E. Biomarkers of Oncogenesis, Adipose Tissue Dysfunction and Systemic Inflammation for the Detection of Hepatocellular Carcinoma in Patients with Nonalcoholic Fatty Liver Disease. *Cancers (Basel)* 2021; **13** [PMID: 34064999 DOI: 10.3390/cancers13102305]

66 **Vongsuvanh R**, van der Poorten D, Iseli T, Strasser SI, McCaughan GW, George J. Midkine Increases Diagnostic Yield in AFP Negative and NASH-Related Hepatocellular Carcinoma. *PLoS One* 2016; **11**: e0155800 [PMID: 27219517 DOI: 10.1371/journal.pone.0155800]

67 **Sumida Y**, Yoneda M, Seko Y, Ishiba H, Hara T, Toyoda H, Yasuda S, Kumada T, Hayashi H, Kobayashi T, Imajo K, Tada T, Kawaguchi T, Eguchi Y, Oeda S, Takahashi H, Tomita E, Okanoue T, Nakajima A; Japan Study Group Of Nafld Jsg-Nafld. Surveillance of Hepatocellular Carcinoma in Nonalcoholic Fatty Liver Disease. *Diagnostics (Basel)* 2020; **10** [PMID: 32785100 DOI: 10.3390/diagnostics10080579]

68 **Shimizu T**, Sawada T, Asai T, Kanetsuki Y, Hirota J, Moriguchi M, Nakajima T, Miyazaki T, Okanoue T. Hepatocellular carcinoma diagnosis using a novel electrochemiluminescence immunoassay targeting serum IgM-free AIM. *Clin J Gastroenterol* 2022; **15**: 41-51 [PMID: 34981443 DOI: 10.1007/s12328-021-01567-4]

69 **Liang J**, Zhu J, Wang M, Singal AG, Odewole M, Kagan S, Renteria V, Liu S, Parikh ND, Lubman DM. Evaluation of AGP Fucosylation as a Marker for Hepatocellular Carcinoma of Three Different Etiologies. *Sci Rep* 2019; **9**: 11580 [PMID: 31399619 DOI: 10.1038/s41598-019-48043-1]

70 **Zhu J**, Huang J, Zhang J, Chen Z, Lin Y, Grigorean G, Li L, Liu S, Singal AG, Parikh ND, Lubman DM. Glycopeptide Biomarkers in Serum Haptoglobin for Hepatocellular Carcinoma Detection in Patients with Nonalcoholic Steatohepatitis. *J Proteome Res* 2020; **19**: 3452-3466 [PMID: 32412768 DOI: 10.1021/acs.jproteome.0c00270]

71 **Lin Y**, Zhu J, Pan L, Zhang J, Tan Z, Olivares J, Singal AG, Parikh ND, Lubman DM. A Panel of Glycopeptides as Candidate Biomarkers for Early Diagnosis of NASH Hepatocellular Carcinoma Using a Stepped HCD Method and PRM Evaluation. *J Proteome Res* 2021; **20**: 3278-3289 [PMID: 33929864 DOI: 10.1021/acs.jproteome.1c00175]

72 **Kozumi K**, Kodama T, Murai H, Sakane S, Govaere O, Cockell S, Motooka D, Kakita N, Yamada Y, Kondo Y, Tahata Y, Yamada R, Hikita H, Sakamori R, Kamada Y, Daly AK, Anstee QM, Tatsumi T, Morii E, Takehara T. Transcriptomics Identify Thrombospondin-2 as a Biomarker for NASH and Advanced Liver Fibrosis. *Hepatology* 2021; **74**: 2452-2466 [PMID: 34105780 DOI: 10.1002/hep.31995]

73 **Totoki Y**, Tatsuno K, Covington KR, Ueda H, Creighton CJ, Kato M, Tsuji S, Donehower LA, Slagle BL, Nakamura H, Yamamoto S, Shinbrot E, Hama N, Lehmkuhl M, Hosoda F, Arai Y, Walker K, Dahdouli M, Gotoh K, Nagae G, Gingras MC, Muzny DM, Ojima H, Shimada K, Midorikawa Y, Goss JA, Cotton R, Hayashi A, Shibahara J, Ishikawa S, Guiteau J, Tanaka M, Urushidate T, Ohashi S, Okada N, Doddapaneni H, Wang M, Zhu Y, Dinh H, Okusaka T, Kokudo N, Kosuge T, Takayama T, Fukayama M, Gibbs RA, Wheeler DA, Aburatani H, Shibata T. Trans-ancestry mutational landscape of hepatocellular carcinoma genomes. *Nat Genet* 2014; **46**: 1267-1273 [PMID: 25362482 DOI: 10.1038/ng.3126]

74 **Takeda H**, Takai A, Kumagai K, Iguchi E, Arasawa S, Eso Y, Shimizu T, Ueda Y, Taura K, Uemoto S, Kita R, Haga H, Marusawa H, Fujimoto A, Seno H. Multiregional whole-genome sequencing of hepatocellular carcinoma with nodule-in-nodule appearance reveals stepwise cancer evolution. *J Pathol* 2020; **252**: 398-410 [PMID: 32815153 DOI: 10.1002/path.5533]

75 **Ki Kim S**, Ueda Y, Hatano E, Kakiuchi N, Takeda H, Goto T, Shimizu T, Yoshida K, Ikura Y, Shiraishi Y, Chiba K, Tanaka H, Miyano S, Uemoto S, Chiba T, Ogawa S, Marusawa H. TERT promoter mutations and chromosome 8p loss are characteristic of nonalcoholic fatty liver disease-related hepatocellular carcinoma. *Int J Cancer* 2016; **139**: 2512-2518 [PMID: 27511114 DOI: 10.1002/ijc.30379]

76 **Akuta N**, Kawamura Y, Kobayashi M, Arase Y, Saitoh S, Fujiyama S, Sezaki H, Hosaka T, Suzuki Y, Suzuki F, Ikeda K, Kumada H. TERT Promoter Mutation in Serum Cell-Free DNA Is a Diagnostic Marker of Primary Hepatocellular Carcinoma in Patients with Nonalcoholic Fatty Liver Disease. *Oncology* 2021; **99**: 114-123 [PMID: 32998139 DOI: 10.1159/000510366]

77 **Muhammad Yusuf AN**, Raja Ali RA, Muhammad Nawawi KN, Mokhtar NM. Potential biomarkers in NASH-induced liver cirrhosis with hepatocellular carcinoma: A preliminary work on roles of exosomal miR-182, miR-301a, and miR-373. *Malays J Pathol* 2020; **42**: 377-384 [PMID: 33361718]

78 **Lewin J**, Kottwitz D, Aoyama J, deVos T, Garces J, Hasinger O, Kasielke S, Knaust F, Rathi P, Rausch S, Weiss G, Zipprich A, Mena E, Fong TL. Plasma cell free DNA methylation markers for hepatocellular carcinoma surveillance in patients with cirrhosis: a case control study. *BMC Gastroenterol* 2021; **21**: 136 [PMID: 33765926 DOI: 10.1186/s12876-021-01714-8]

79 **Yasui K**, Hashimoto E, Komorizono Y, Koike K, Arii S, Imai Y, Shima T, Kanbara Y, Saibara T, Mori T, Kawata S, Uto H, Takami S, Sumida Y, Takamura T, Kawanaka M, Okanoue T; Japan NASH Study Group, Ministry of Health, Labour, and Welfare of Japan. Characteristics of patients with nonalcoholic steatohepatitis who develop hepatocellular carcinoma. *Clin Gastroenterol Hepatol* 2011; **9**: 428-33; quiz e50 [PMID: 21320639 DOI: 10.1016/j.cgh.2011.01.023]

80 **Zhang X**, Wang Z, Tang W, Wang X, Liu R, Bao H, Chen X, Wei Y, Wu S, Wu X, Shao Y, Fan J, Zhou J. Ultra-Sensitive and Affordable Assay for Early Detection of Primary Liver Cancer Using Plasma cfDNA Fragmentomics. *Hepatology* 2021 [DOI: 10.1002/hep.32308]

81 **Eslam M**, Sanyal AJ, George J; International Consensus Panel. MAFLD: A Consensus-Driven Proposed Nomenclature for Metabolic Associated Fatty Liver Disease. *Gastroenterology* 2020; **158**: 1999-2014.e1 [PMID: 32044314 DOI: 10.1053/j.gastro.2019.11.312]

82 **Lin S**, Huang J, Wang M, Kumar R, Liu Y, Liu S, Wu Y, Wang X, Zhu Y. Comparison of MAFLD and NAFLD diagnostic criteria in real world. *Liver Int* 2020; **40**: 2082-2089 [PMID: 32478487 DOI: 10.1111/liv.14548]

83 **Chen YG**, Yang CW, Chung CH, Ho CL, Chen WL, Chien WC. The association between metabolic risk factors, nonalcoholic fatty liver disease, and the incidence of liver cancer: a nationwide population-based cohort study. *Hepatol Int* 2022 [PMID: 35064545 DOI: 10.1007/s12072-021-10281-9]

84 **Beale G**, Chattopadhyay D, Gray J, Stewart S, Hudson M, Day C, Trerotoli P, Giannelli G, Manas D, Reeves H. AFP, PIVKAII, GP3, SCCA-1 and follisatin as surveillance biomarkers for hepatocellular cancer in non-alcoholic and alcoholic fatty liver disease. *BMC Cancer* 2008; **8**: 200 [PMID: 18638391 DOI: 10.1186/1471-2407-8-200]

World Journal of Gastroenterology

Submit a Manuscript: https://www.f6publishing.com

World J Gastroenterol 2022 July 21; 28(27): 3422-3434

DOI: 10.3748/wjg.v28.i27.3422

ISSN 1007-9327 (print) ISSN 2219-2840 (online)

ORIGINAL ARTICLE

Basic Study

Accumulation of poly (adenosine diphosphate-ribose) by sustained supply of calcium inducing mitochondrial stress in pancreatic cancer cells

Keun-Yeong Jeong, Jae Jun Sim, Minhee Park, Hwan Mook Kim

Specialty type: Gastroenterology and hepatology

Provenance and peer review: Invited article; Externally peer reviewed.

Peer-review model: Single blind

Peer-review report's scientific quality classification

Grade A (Excellent): 0
Grade B (Very good): B
Grade C (Good): C, C
Grade D (Fair): 0
Grade E (Poor): 0

P-Reviewer: Prasetyo EP, Indonesia; Tang D, China; Zuo CJ, China

Received: January 11, 2022
Peer-review started: January 11, 2022
First decision: March 8, 2022
Revised: March 15, 2022
Accepted: June 26, 2022
Article in press: June 26, 2022
Published online: July 21, 2022

Keun-Yeong Jeong, Jae Jun Sim, Minhee Park, Hwan Mook Kim, Research and Development, Metimedi Pharmaceuticals, Incheon 22006, South Korea

Corresponding author: Keun-Yeong Jeong, PhD, Executive Vice President, Research Assistant Professor, Research and Development, Metimedi Pharmaceuticals, 263 Central-ro, Incheon 22006, South Korea. alvirus@naver.com

Abstract

BACKGROUND

The biochemical phenomenon defined as poly adenosine diphosphate (ADP)-ribosylation (PARylation) is essential for the progression of pancreatic cancer. However, the excessive accumulation of poly ADP-ribose (PAR) induces apoptosis-inducing factor (AIF) release from mitochondria and energy deprivation resulting in the caspase-independent death of cancer cells.

AIM

To investigate whether sustained calcium supply could induce an anticancer effect on pancreatic cancer by PAR accumulation.

METHODS

Two pancreatic cancer cell lines, AsPC-1 and CFPAC-1 were used for the study. Calcium influx and mitochondrial reactive oxygen species (ROS) were observed by fluorescence staining. Changes in enzyme levels, as well as PAR accumulation and energy metabolism, were measured using assay kits. AIF-dependent cell death was investigated followed by confirming *in vivo* anticancer effects by sustained calcium administration.

RESULTS

Mitochondrial ROS levels were elevated with increasing calcium influx into pancreatic cancer cells. Then, excess PAR accumulation, decreased PAR glycohydrolase and ADP-ribosyl hydrolase 3 levels, and energy deprivation were observed. *In vitro* and *in vivo* antitumor effects were confirmed to accompany elevated AIF levels.

CONCLUSION

This study visualized the potential anticancer effects of excessive PAR accumu-

lation by sustained calcium supply on pancreatic cancer, however elucidating a clear mode of action remains a challenge, and it should be accompanied by further studies to assess its potential for clinical application.

Key Words: Pancreatic cancer; Calcium; Reactive oxygen species; Poly adenosine diphosphate-ribose; Poly adenosine diphosphate-ribosylation; Poly adenosine diphosphate-ribose polymerase; Apoptosis-inducing factor; Nicotinamide adenine dinucleotide; Anticancer effect

Core Tip: Accumulation of poly adenosine diphosphate-ribose (PAR) was induced by an increase in reactive oxygen species following sustained calcium supply, which in turn led to the death of pancreatic cancer cells by energy deprivation and apoptosis-inducing factor expression. Although calcium-mediated accumulation of PAR would be a potential strategy for the treatment of pancreatic cancer, the association with the mechanical role of calcium in enabling the inactivation of PAR-degrading enzymes needs to be elucidated.

Citation: Jeong KY, Sim JJ, Park M, Kim HM. Accumulation of poly (adenosine diphosphate-ribose) by sustained supply of calcium inducing mitochondrial stress in pancreatic cancer cells. *World J Gastroenterol* 2022; 28(27): 3422-3434
URL: https://www.wjgnet.com/1007-9327/full/v28/i27/3422.htm
DOI: https://dx.doi.org/10.3748/wjg.v28.i27.3422

INTRODUCTION

Recent literature emphasizes that the biochemical phenomenon defined as poly adenosine diphosphate (ADP)-ribosylation (PARylation) is essential for the progression of cancer[1]. Poly ADP-ribose (PAR) is synthesized by the biochemical reaction of PAR polymerase-1 (PARP-1), which catalyzes the polymerization of ADP-ribose from the donor nicotinamide adenine dinucleotide (NAD+) to form a linear or branched PAR polymer[2]. Because PARylation is implicated in the multistep process involving various physiological maintenance factors and overcoming stress conditions for cancer cell survival, there might be connections between PARP-1 function and pancreatic cancer progression as a bridgehead linked by PARylation[1,2].

Although PARylation is essential for cancer survival, the excessive accumulation of PAR can mediate apoptosis-inducing factor (AIF) release from mitochondria and its nuclear translocation, resulting in the caspase-independent death of cancer cells[3]. The mode of action of the relationship between AIF and PAR involved in cell death has not been elucidated, but AIF translocation to the nucleus leading to chromatin condensation and large-scale DNA fragmentation is a well-established theory[3,4]. Cell death following PAR accumulation was recently defined as parthanatos, which is considered another death mechanism in a large category of apoptosis-type reactions[4]. Therefore, targeting ADP-ribosyl hydrolase 3 (ARH3), a type of PAR-degrading protein, and PAR glycohydrolase (PARG), a reversible covalent-modifier targeting PAR, might be potential methods to induce anticancer effects *via* PAR accumulation[5-7]. Although approaches to inhibit such enzymes through RNA interference or genetic manipulation have been tried, there have been few studies of the relevant mechanisms targeting pancreatic cancer[6,7].

Calcium is a key element in physiological signal transduction that enables the adjustment of energy production to cellular demand[8]; however, some reports indicated that cancer cells were affected during the influx of a high concentration of calcium resulting in excessive reactive oxygen species (ROS) produced from mitochondria[9]. Furthermore, there was an association between PARP-1 and an increase in ROS[1,10,11]. It was reported that the hyperactivation of PARP-1 was induced by an increase in ROS caused by intracellular calcium influx, the activation of PARP-1 as a response to DNA damage, or to drive an antioxidant program to protect cells from ROS[1,10,11]. This implies that excessive PAR accumulation can be induced as a result of PARP-1 hyperactivation followed by PARylation, suggesting the prospect of influencing pancreatic cancer cell survival by supplying high concentrations of calcium. The study aimed to investigate whether a sustained calcium supply induced intracellular PAR accumulation with an increase in ROS and to demonstrate the potential of this phenomenon to promote anticancer effects on pancreatic cancer.

MATERIALS AND METHODS

Cell lines and culture conditions

AsPC-1 and CFPAC-1 were obtained from the American Type Culture Collection (Manassas, VA, United States). The cells were grown in Roswell Park Memorial Institute 1640 and Iscove's Modified Dubecco's Medium supplemented with 10% fetal bovine serum (Welgene, Gyeongsan, Korea) and 1% penicillin/streptomycin (Welgene, Gyeongsan, Korea). All cells were cultured under a humidified atmosphere at 37 °C containing 5% CO_2.

Reagents

Lactate calcium salt (CaLac) and calpeptin were purchased from Sigma-Aldrich (St. Louis, MO, United States) and dissolved in distilled water. The solutions were stored at 4 °C until use.

Measurement of intracellular calcium

Calcium concentrations were measured using a confocal laser scanning microscope (Leica, Heidelberg, Germany). Cultured pancreatic cancer cells were loaded with 10 μM Fluo-3/AM (Invitrogen, Frederick, MD, United States) dissolved in dimethyl sulfoxide (Sigma-Aldrich). Then the cells were incubated for 30 min at 37 °C. Fluo-3/AM was excited at 488 nm and emitted fluorescence was measured at 515 nm.

Immunocytochemistry

Pancreatic cancer cells were fixed on bio-coated coverslips (BD bioscience, NJ, United States) using 4% paraformaldehyde, and incubated for 15 h with the primary antibody against AIF (1:200, Santa Cruz Biotechnology, Santa Cruz, CA, United States). Subsequently, the cells were incubated with an anti-rabbit secondary biotinylated anti-body (1:5000, Abcam) and visualized with streptavidin conjugated to fluorescein (Vector Laboratories, Burlingame, CA, United States). MitoSOX Red (Thermo Fisher Scientific, Waltham, MA, United States) was used to detect mitochondrial superoxide production. Fluorescence was measured using a confocal laser scanning microscope (Leica). Signal intensities were quantified and analyzed using the Xenogen Imaging System (IVIS® 100 series, Caliper Life Science, MA, United States).

Enzyme-linked immunosorbent assay

PARG, RNF-146, PAR, and AIF levels were quantified from 1×10^6 number of pancreatic cancer cells or 2 mm^3 volume of tumor tissues using each assay kit (PARG assay kit: Trevigen, Gaithersburg, MD, United States; RNF-146 ELISA kit: Abbexa, Houston, TX, United States; PAR ELISA kit: Cell Biolabs, San Diego, CA, United States; AIF ELISA kit: Abcam, Cambridge, England), according to the manufacturer's instructions.

Adenosine triphosphate assay

The cell culture medium was supplemented with CaLac, and cultures were incubated for 24 h. 1×10^6 cells were then sonicated. The cells were centrifuged at 1500 g for 20 min to remove insoluble material, and the supernatant was collected. Adenosine triphosphate (ATP) was measured by ATP colorimetric assay kit (Abcam) according to manufacturer's instructions.

NAD+ and NADH assay

The cell culture medium was supplemented with CaLac, and the cultures were incubated for 24 h. 1×10^6 cells were then sonicated. The cells were washed twice with phosphate buffer solution (PBS), and NAD+ and NADH levels were measured using the NAD/NADH quantitation kit (Sigma) according to the manufacturer's protocol.

Transferase-mediated dUTP nick end labeling assay

Pancreatic cancer cells were treated with CaLac for 24 h and then washed with cold PBS. The cells were fixed with 4% paraformaldehyde for 30 min and washed twice with PBS for 2 min. Fixed cells in permeabilization solution (0.1% Triton X-100 and 0.1% Sodium citrate) were washed. The tumors were fixed in 10% neutral buffered formalin and embedded in paraffin. Tissue sections (4 μm) were made from paraffin-embedded blocks on a microtome, and then the sections were deparaffinized and rehydrated. To detect cell death, the DeadEnd™ Fluorometric transferase-mediated dUTP nick end labeling (TUNEL) system kit (Promega, Madison, WI, United States) was used according to the manufacturer's instructions.

FACS analysis

Annexin V and propidium iodide (PI) staining was performed using an Annexin V-FITC Apoptosis Detection Kit (BD Biosciences). 2.5×10^6 of AsPC-1 and CFPAC-1 cells were exposed to CaLac for 24 h. The cells were resuspended in 100 μL of Annexin V-FITC binding buffer, and then 5 μL of Annexin V-FITC conjugate and 10 μL of PI buffer were added. Annexin V and PI were analyzed using a FACS

CaliburTM instrument (BD Biosciences).

Cell viability assay

Pancreatic cancer cells were cultured in a 96-well plate (3×10^3 cells/well) for 24 h, and then treated with CaLac for 24 h at 37 °C. Then, 10 μL of 3-(4,5-dimethylthiazol-2-yl)-2,5-diphenyltetrazolium bromide was added to each well, and the cells were incubated at 37 °C for 1 h in a humidified environment containing 5% CO_2. After the media was discarded, 200 μL of dimethyl sulfoxide (Cell Signaling Technology, Danvers, MA, United States) was added to each well. The absorbance was read at 570 nm using a microplate reader (iMark Microplate Absorbance Reader, Bio-Rad, CA, United States).

Xenograft animal model

Twenty-eight male Balb/c nude mice (5 wk of age) were purchased from the Charles River Breeding Laboratories (Wilmington, MA, United States). All animals were maintained on a 12 h light/dark cycle (light on, 08:00) at 22-25 °C, with free access to food and water. To investigate the antitumor activity of CaLac *in vivo*, a therapeutic strategy was devised to investigate its effect on the heterotopic xenograft animal model. Fourteen mice were used for establishing a heterotopic xenograft model using AsPC-1 cells (5×10^6) resuspended in 100 μL of phosphate-buffered saline. The cells were injected subcutaneously into the left flank of mice. Once the tumors reached a diameter of 8 mm, 7 mice were randomly divided into the untreated group, and 7 mice were divided into the CaLac-treated group. 20 mg/kg of CaLac was subcutaneously injected daily for 21 d. Tumor growth was monitored three times per week. To harvest tumors for histological and molecular biology analysis, carbon dioxide inhalation was used for euthanasia at the end of the experiments.

Immunohistochemistry

The tumors were fixed in 10% neutral buffered formalin and embedded in paraffin. Tissue sections (4 μm) were made from paraffin-embedded blocks on a microtome, and then the sections were deparaffinized and rehydrated. Endogenous peroxidase activity was blocked by 3% H_2O_2 in distilled water for 30 min. Antigen retrieval was induced by slide heating with 10 mmol/L citrate buffer (pH 6.0) using a microwave oven. The sections were blocked using a blocking agent (Invitrogen, Frederick, MD, United States) and incubated overnight with the primary antibodies at 4 °C. The primary antibodies were as follows: Ki-67 (1:200, Santa Cruz Biotechnology) and proliferating cell nuclear antigen (PCNA, 1:200, Santa Cruz Biotechnology). The sections were then incubated with biotinylated anti-mouse antibody (1:500, Vector Laboratories, Burlingame, CA, United States) for 1 h. After a PBST wash, the sections were treated with 3,3'-diaminobenzidine substrate (Dako, Carpentaria, CA, United States) and counterstained with hematoxylin (Thermo Fisher Scientific). A Leica DM 1000 LED microscope (Leica Microsystems, Wetzlar, Germany) was used for image analysis.

Statistical analysis

Data are presented as the means ± SD. Statistical significance was analyzed using the Student's *t*-test or one-way analysis of variance, depending on the normality of the data distribution. $P < 0.05$ was considered as statistically significant. All statistical analyses were performed by Sigma Stat v3.5 (Systat Software Inc., Chicago, IL, United States).

RESULTS

Calcium influx increases mitochondrial ROS in pancreatic cancer cells

The fluorescence intensity of fluo-3 by calcium reaction was increased in cells of both types of pancreatic cancer, AsPC-1 and CFPAC-1, following CaLac treatment (Figure 1A). In a quantitative analysis of fluorescence intensity, intracellular calcium levels were significantly increased by sustained calcium supply to about 2.1- and 1.9-fold in AsPC-1 and CFPAC-1, respectively, compared with the untreated group (Figure 1B). The increase in red fluorescence level in pancreatic cancer cells indicated increased ROS generation in pancreatic cancer cells by sustained calcium supply, indicating that ROS originated from mitochondria by the simultaneous use of a mitochondrial tracer showing green fluorescence (Figure 1C). In an analysis of the mean fluorescence intensity (MFI), mitochondrial ROS levels detected by MitoSOX™ were significantly increased by sustained calcium supply to about 2.33- and 2.63-fold in ASPC-1 and CFPAC-1, respectively, compared with the untreated group (Figures 1D and E).

An increase in ROS causes the excessive accumulation of PAR and energy deprivation

In addition to the immediate association of PAR accumulation by increased ROS levels, PARG and RNF-146 were supplementally investigated to confirm a change in the enzyme levels involved in PAR accumulation. A decrease in the enzymatic activity of PARG and ARH3 following calcium supply was observed (Figures 2A and B), accompanied by the accumulation of PAR in pancreatic cancer cells (Figure 2C). Changes in coenzyme factors involved in energy metabolism following the accumulation of

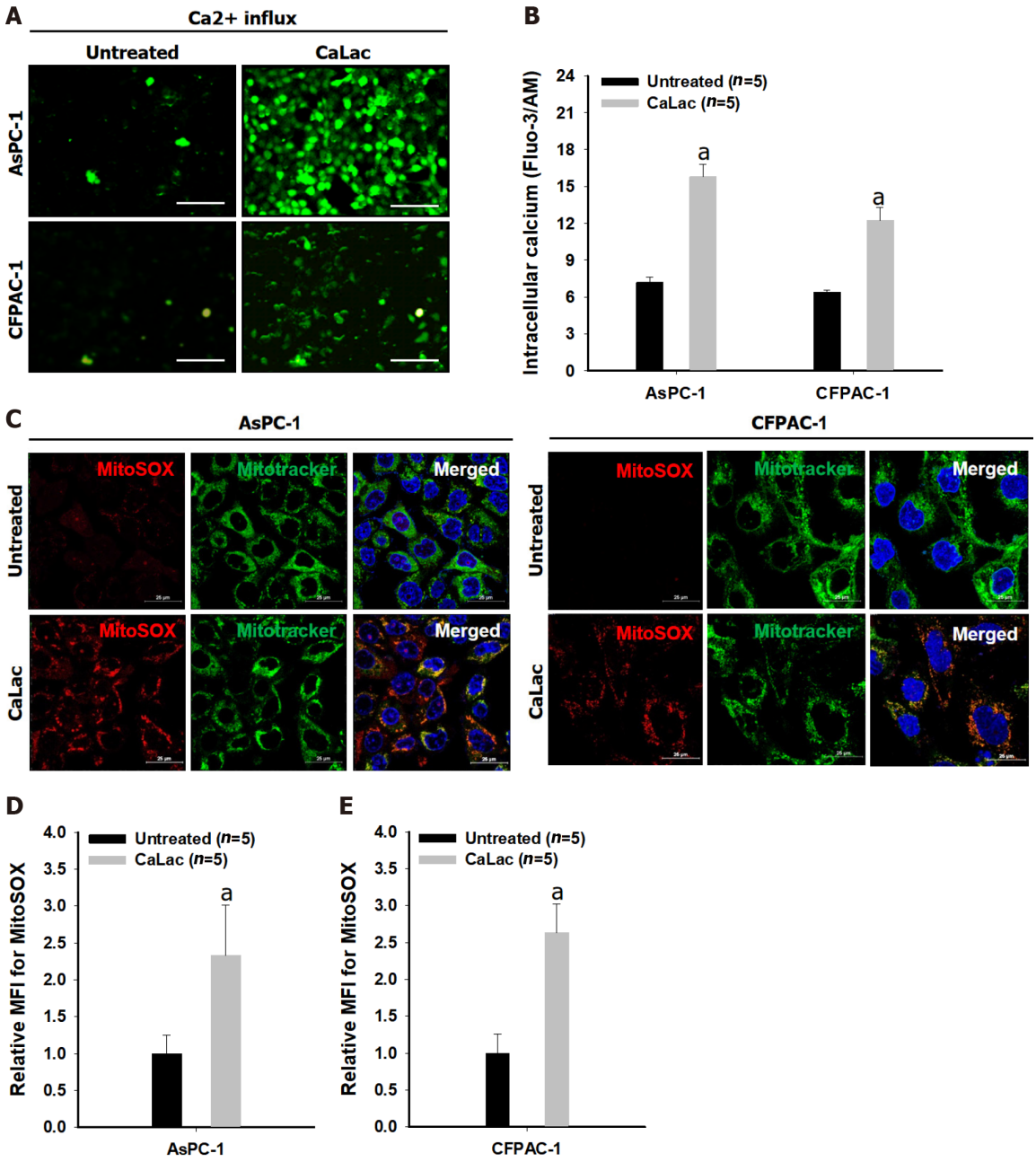

Figure 1 Confirmation of mitochondrial reactive oxygen species generation by sustained calcium supply. A: Fluorescent calcium imaging following lactate calcium salt (CaLac) treatment of pancreatic cancer cells (AsPC-1 and CFPAC-1). Scale bars: 100 μm; B: Quantitative analysis of the fluorescence intensity of calcium; C: Confocal imaging of mitochondrial reactive oxygen species (ROS) in pancreatic cancer cells. Red dye: Mitochondrial superoxide indicator; Green dye: Mitochondrial indicator. Scale bars: 25 μm; D: Quantitative analysis of the fluorescence intensity of mitochondrial ROS in AsPC-1; E: Quantitative analysis of the fluorescence intensity of mitochondrial ROS in CFPAC-1. The fluorescence intensity was calculated by the mean fluorescence intensity. The cells were treated with 2.5 mM CaLac for 72 h. Results represent the mean ± SD. $^{a}P < 0.001$ *vs* untreated. CaLac: Lactate calcium salt; MitoSOX: Mitochondrial superoxide indicator.

PAR were also identified (Figures 2D and E). These results indicated that the excessive synthesis of PAR resulted in reduced NAD+ levels (Figure 2D) and the increase of NADH levels (Figure 2E), which led to a depletion of ATP (Figure 2F).

An increase in AIF expression induces the death of pancreatic cancer cells

The results of immunocytochemical staining for the co-expression of AIF with the mitochondrial tracker in two types of pancreatic cancer cells indicated the calcium supply induced the translocation of AIF from the cytoplasm into the nucleus, whereas only cytoplasmic co-expression was observed in the untreated group (Figure 3A). Furthermore, it was quantitatively increased by calcium supply when the expression of AIF only was confirmed as a separate result through MFI analysis (Figures 3B and C). Then, the reaction ratio by TUNEL staining per total cells was significantly increased (Figures 3D and E), and Annexin V labeled cells increased from 6.61% to 37.61% and from 4.8% to 26.91% in AsPC-1 and CFPAC-1, respectively (Figure 3F). A decrease in cell viability by calcium supply was macroscopically

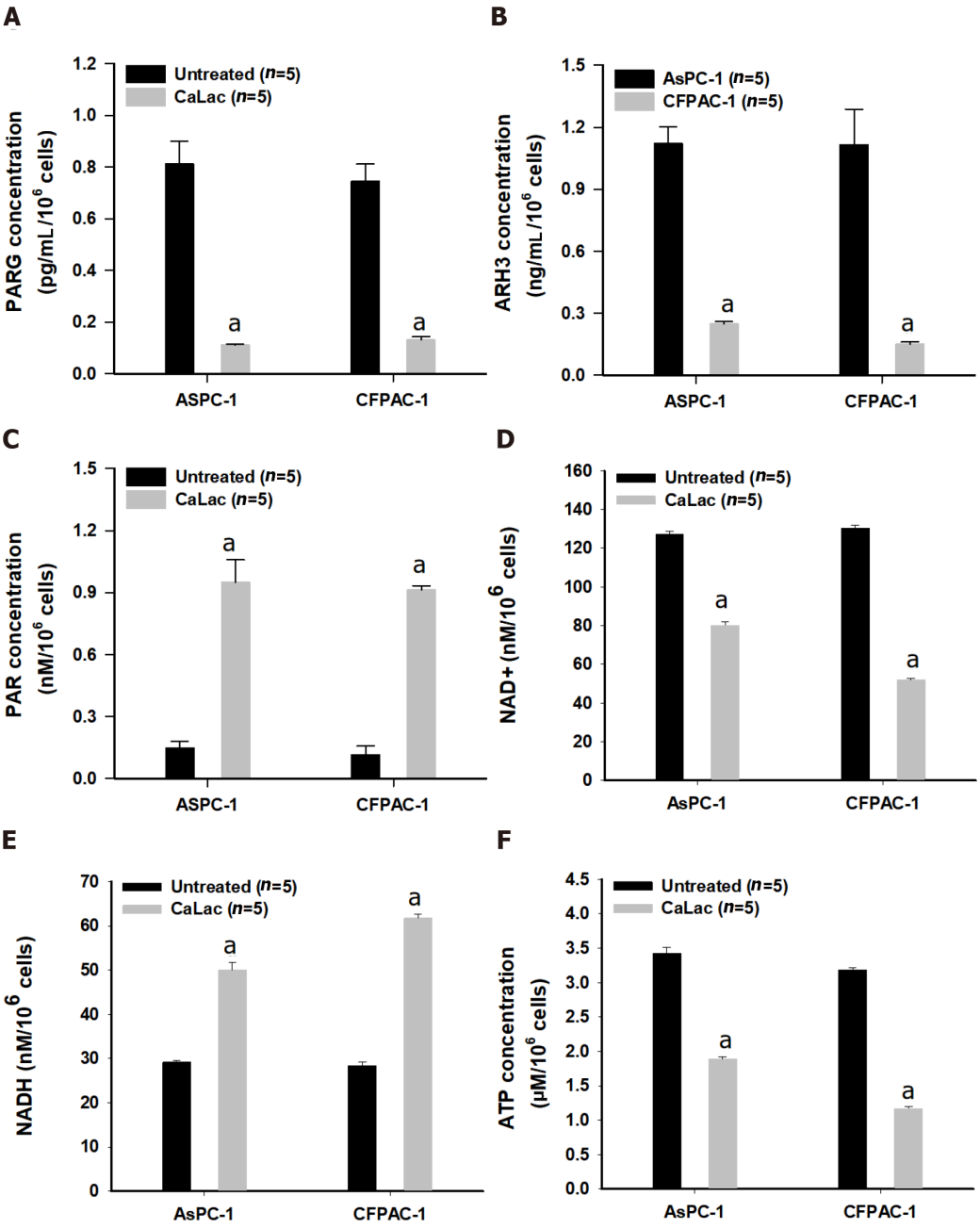

Figure 2 Confirmation of enzyme change and poly adenosine diphosphate-ribose accumulation by calcium supply resulting in energy crisis. A: Quantitative analysis of the enzyme levels of poly adenosine diphosphate (ADP)-ribose (PAR) glycohydrolase in pancreatic cancer cells (AsPC-1 and CFPAC-1); B: Quantitative analysis of the enzyme levels of ADP-ribosyl hydrolase 3 in AsPC-1 and CFPAC-1; C: Quantitative analysis of PAR levels; D: Quantitative analysis of nicotinamide adenine dinucleotide levels; E: Quantitative analysis of NADH levels; F: Quantitative analysis of adenosine triphosphate (ATP) levels. The cells were treated with 2.5 mM lactate calcium salt for 72 h. Results represent the mean ± SD. $^{a}P < 0.001$ *vs* untreated. CaLac: Lactate calcium salt; PARG: Poly adenosine diphosphate-ribose glycohydrolase; ARH3: Adenosine diphosphate-ribosyl hydrolase 3; NAD+: Nicotinamide adenine dinucleotide; ATP: Adenosine triphosphate.

observed by microphotographs (Figure 3G), and the CaLac group (calcium supply) showed low cell viability (mean 35.5%) when defining the total cell viability of the untreated group as 100% (Figure 3H).

An increase in PAR accumulation relates to calcium-dependent proteolytic enzyme activity in pancreatic cancer cells

To elucidate an increase in PAR accumulation by sustained calcium supply, the calpain inhibitor, calpeptin, was introduced. Changes in PARG, ARH3, PAR, and AIF were sequentially observed in pancreatic cancer cells (Figure 4). Although PARG levels were significantly decreased by sustained calcium supply, there was only a slight decrease (no significant difference) when combining calpeptin with calcium supply (Figures 4A and B). Calpeptin itself did not directly change the levels of PARG (Figures 4A and B) similar to that of ARH3 (Figures 4C and D). Furthermore, the levels of PAR and AIF

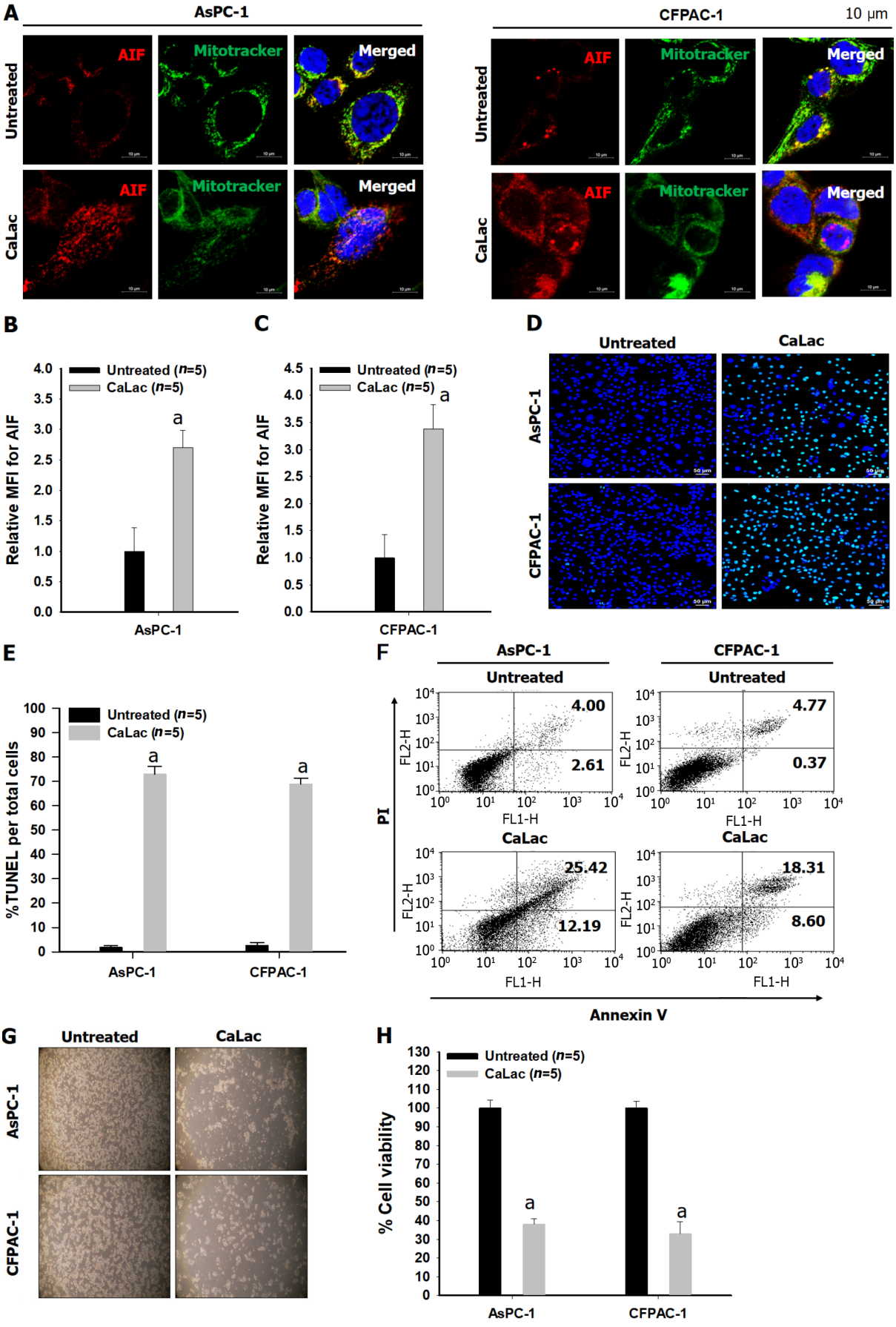

Figure 3 Confirmation of the expression of apoptosis-inducing factor followed by an increase in apoptosis in pancreatic cancer cells (AsPC-1 and CFPAC-1). A: Immunocytochemical staining for apoptosis-inducing factor (AIF) release from mitochondria and translocation into the nucleus. Red dye: AIF; Green dye: Mitochondrial indicator. Scale bars: 10 μm; B: Quantitative analysis of the mean fluorescence intensity (MFI) of AIF in CFPAC-1; C: Quantitative

analysis of the MFI of AIF in AsPC-1; D: Fluorescent microphotographs for colorimetric terminal deoxynucleotidyl transferase -mediated dUTP nick end labeling (TUNEL) detection. Green dye: TUNEL staining. Scale bars: 50 μm; E: Quantitative analysis of the % ratio of TUNEL detected cells per total pancreatic cancer cells; F: Representative flow cytometry plots using Annexin V-fluorescein-5-isothiocyanate/propidium iodide staining for apoptosis; G: Representative microphotographs to compare cell condition after calcium supply; H: Quantitative analysis of the percent cell viability following calcium supply. The cells were treated with 2.5 mM lactate calcium salt for 72 h. Results represent the mean ± SD. $^{a}P < 0.001$ *vs* untreated. CaLac: Lactate calcium salt; AIF: Apoptosis-inducing factor; MFI: Mean fluorescence intensity; TUNEL: Transferase-mediated dUTP nick end labeling.

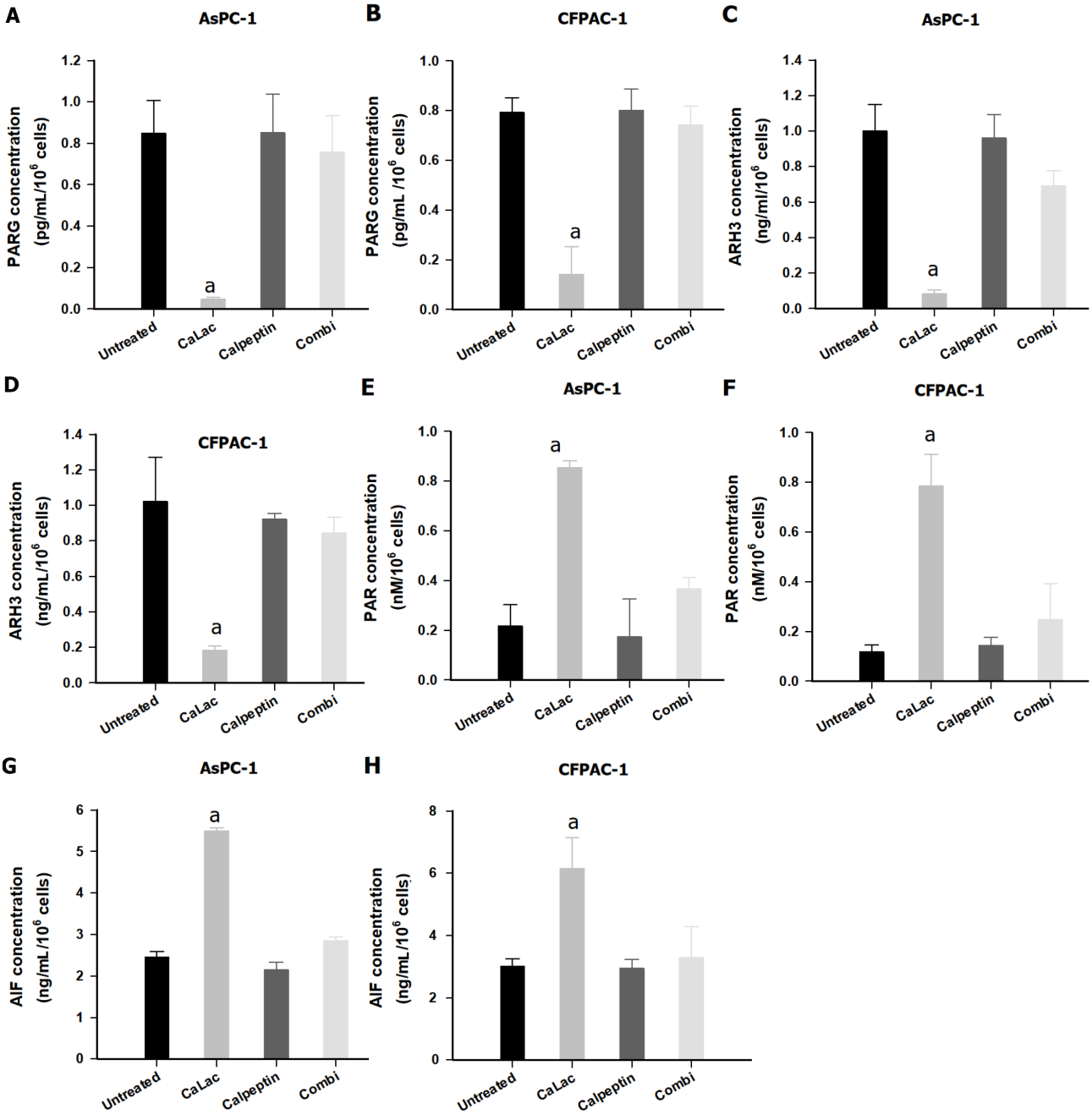

Figure 4 Confirmation of poly-adenosine diphosphate ribose accumulation in pancreatic cancer cells (AsPC-1 and CFPAC-1) by calcium-mediated proteasomal activity. A: Quantitative analysis of poly adenosine diphosphate-ribose glycohydrolase (PARG) levels in AsPC-1; B: Quantitative analysis of PARG levels in CFPAC-1; C: Quantitative analysis of ADP-ribosyl hydrolase 3 (ARH3) levels in AsPC-1; D: Quantitative analysis of ARH3 levels in CFPAC-1; E: Quantitative analysis of PAR levels in AsPC-1; F: Quantitative analysis of PAR levels in CFPAC-1; G: Quantitative analysis of apoptosis-inducing factor (AIF) levels in AsPC-1; H: Quantitative analysis of AIF levels in CFPAC-1. Calpeptin was used for proteasome inhibition. The cells were treated with 2.5 mM lactate calcium salt for 72 h. Results represent the mean ± SD. $^{a}P < 0.001$ *vs* untreated. CaLac: Lactate calcium salt; PARG: Poly adenosine diphosphate-ribose glycohydrolase; ARH3: Adenosine diphosphate-ribosyl hydrolase 3; AIF: Apoptosis-inducing factor.

were increased by calcium supply, which was restored to a level similar to that of the untreated group under culture conditions in which calpeptin was added (Figures 4E-H).

Sustained calcium administration induces anticancer effects on pancreatic cancer

Comparative results of tumor growth in heterotopic xenograft models demonstrated the inhibition of pancreatic cancer growth by calcium administration (Figures 5Aand B, Figure 6). The tumor volume on the last day of measurement was 830.37 ± 138.36 and 431.41 ± 91.98 in the untreated and the CaLac groups, respectively. Tumor volume was reduced by about 48.1% in the CaLac group compared with the untreated group (Figure 5B). There were few viable cells capable of discriminating the staining of nuclei in tumor tissues of the CaLac group (Figure 5C), indicating an increase in PAR-dependent AIF expression following sustained calcium-induced apoptosis (Figures 5D and E). The apoptotic signal in tumor tissues was increased 5.13-fold in the CaLac group compared with the untreated group (Figures 5F and G). As a result of apoptosis, the malignancy indicators of tumors were significantly reduced (Figure 5H) and the expressions of Ki-67 and PCNA were significantly reduced by about 64% and 68%, respectively in the CaLac group (Figures 5I and J).

DISCUSSION

This study demonstrated that the accumulation of PAR was induced by an increase in ROS following sustained calcium supply, which in turn led to the death of pancreatic cancer cells by energy deprivation and AIF expression. CaLac is a small molecule generated by the reaction of lactic acid with calcium carbonate and is characterized as a weak electrolyte with a neutralized charge[12]. Such a characteristic of CaLac suggests it might readily cross cell membranes as a bound form. Therefore, the accumulation of calcium was greatly increased in pancreatic cancer cells by the sustained treatment of CaLac, which was in line with our direction of research targeting intracellular calcium accumulation. It is well known that intracellular calcium uptake can promote ROS formation in mitochondria by stimulating tricarboxylic acid cycle enzymes and electron transport chain activity[9]. The results indicated that calcium accumulation by CaLac led to an increase in the mitochondrial ROS of pancreatic cancer cells. An active calcium signal must operate within physiological levels, but when intracellular calcium levels exceed this threshold, excessive ROS production can have a detrimental effect on cell survival by disrupting mitochondrial bioenergetic regulation and cellular functions[13]. The main reason for investigating an increase in PAR synthesis among the various biological phenomena mediated by calcium-dependent excessive ROS is its key function as a protective mechanism for cancer cell survival under hostile conditions[1,10,11,14]. ROS can be spontaneously generated during the ceaseless process of the rapid growth of cancer cells, but excessive ROS can cause DNA damage by irreversible oxidative stress[15]. PAR synthesis is defined as PARylation by PARP-1 recruits or modifies several nuclear proteins during the DNA damage response against harmful oxidative stress; however, the excessive synthesis of PAR can lead to cell death[1,14]. A sustained calcium supply causes the accumulation of PAR to cope with long-lasting DNA damage along with an increase of ROS in pancreatic cancer cells. Well-established phenomena induced by PAR accumulation include energy deprivation and AIF release from mitochondria[3,4,16]. Because PAR is catalyzed for synthesis from donor NAD+, excessive PAR accumulation causes a decrease in the intracellular level of NAD+, leading to energy deprivation[8,17]. Furthermore, an increase in AIF release induces cell death by large-scale DNA fragmentation defined as parthanatos, although a clear mechanism has not been elucidated[4,16]. The results indicated that AIF migrates from the mitochondria to the cytoplasm and nucleus in response to the accumulation of PAR followed by inducing the death of pancreatic cancer cells. Therefore, excessive PAR accumulation caused by an increase in ROS by sustained calcium supply can be considered to mediate anticancer activity as the main mechanism with energy deprivation and AIF release in pancreatic cancer cells. Cancer cells activate PAR erasing enzymes PARG and ARH3 to hydrolyze ribose-ribose bonds, PAR itself, or O-acetyl-ADP-ribose resulting in the prevention of excessive PAR accumulation[6,18]. These hydrolytic reactions form a biochemical mechanism to counter the PAR-mediated death of cancer cells[4,19,20]. In this study, it was confirmed that the enzymatic activities of PARG and ARH3 were significantly decreased after sustained calcium supply; however, the activity was restored by treatment with calpeptin, a potent, cell-permeable calpain inhibitor. Calpain is a break-down molecule and a calcium-dependent cysteine protease that can also induce ROS production depending on its activation, and it may also damage ion channels, cell adhesion molecules, and cell surface receptors as well as various enzymes[21,22]. On this basis, it is anticipated that calcium-dependent calpain activation would directly induce the enzymatic inactivity of PARG and ARH according to the results of calpeptin application on pancreatic cancer cells. However, the current research outcome was unable to provide a clear mechanistic basis for the enzymatic inactivation of PARG and ARH by calpain. Because PARG and ARH3 are directly related to the accumulation of PAR in pancreatic cancer cells, we wish to investigate this further in more detail.

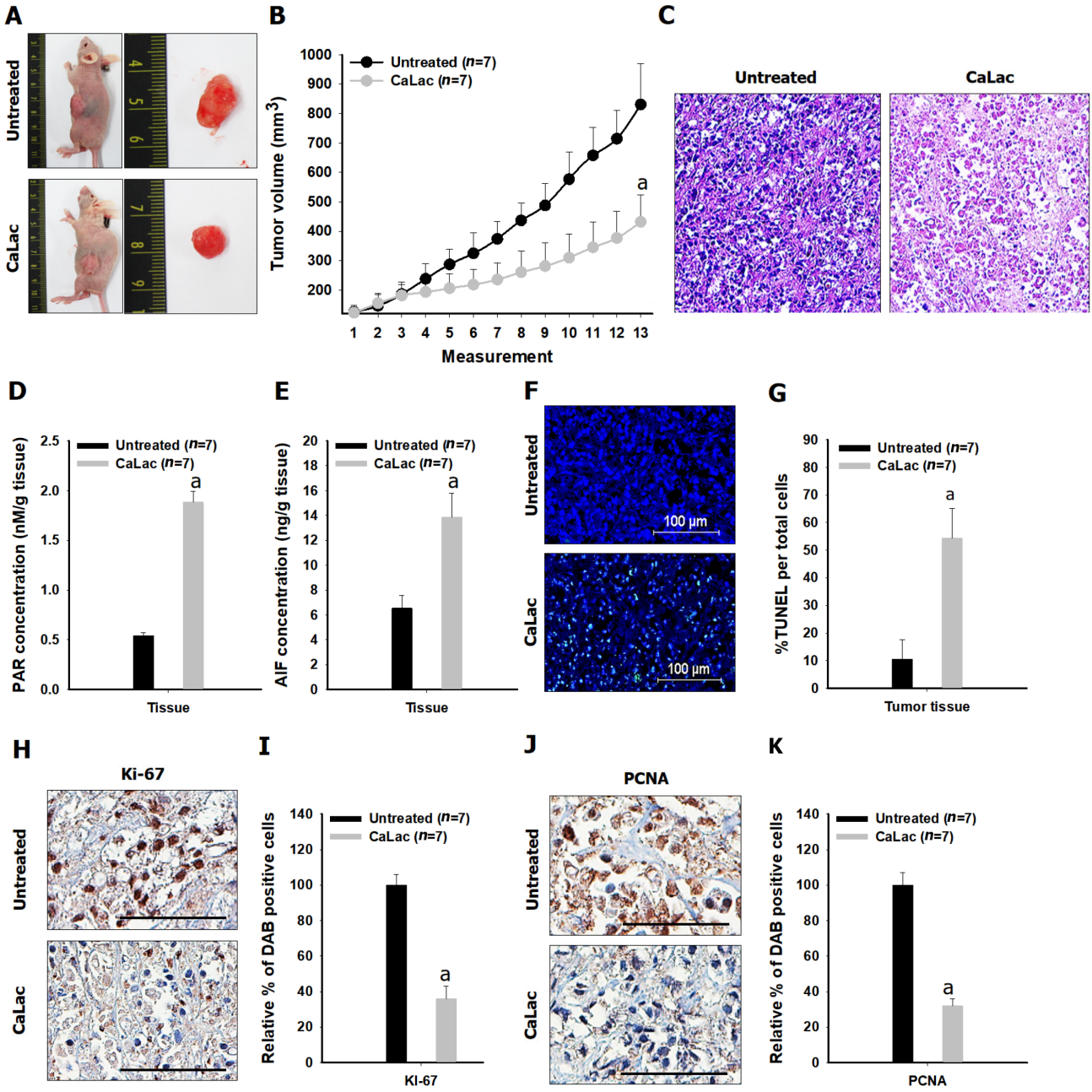

Figure 5 Confirmation of the *in vivo* antitumor effect on pancreatic cancer following sustained calcium administration. A: Macroscopic observation of the tumor mass; B: Comparison of tumor volume between the untreated and calcium-administered groups. Lactate calcium salt (CaLac): 20 mg/kg/mouse, subcutaneous injection, daily for 21 d; C: Hematoxylin and eosin staining. Scale bars: 100 μm; D: Comparison of poly adenosine diphosphate ribose expression in tumor tissues; E: Comparison of apoptosis-inducing factor expression in tumor tissues; F and G: % terminal deoxynucleotidyl transferase-mediated dUTP nick end labeling expression to compare increased apoptosis in tumor tissues. Scale bars: 100 μm; H and I: Comparison of Ki-67 expression in tumor tissues. Scale bars: 50 μm; J and K: Comparison of proliferating cell nuclear antigen in tumor tissues. Scale bars: 50 μm. $^{a}P < 0.001$ *vs* untreated. Results are the mean ± SD. PAR: Poly adenosine diphosphate ribose; AIF: Apoptosis-inducing factor; TUNEL: Transferase-mediated dUTP nick end labeling; PCNA: Proliferating cell nuclear antigen; CaLac: Lactate calcium salt.

CONCLUSION

This study focused on the accumulation of PAR to induce energy deprivation and AIF release by sustained calcium supply to investigate its potential anticancer effect on pancreatic cancer. We demonstrated that an increase in ROS and inhibition of PAR-erasing enzymes might be the main contributors to these effects. However, the connection to the mechanistic role of calcium in enabling the inactivation of PAR-degrading enzyme needs to be elucidated, and additional studies to explore the potential of clinical application are required.

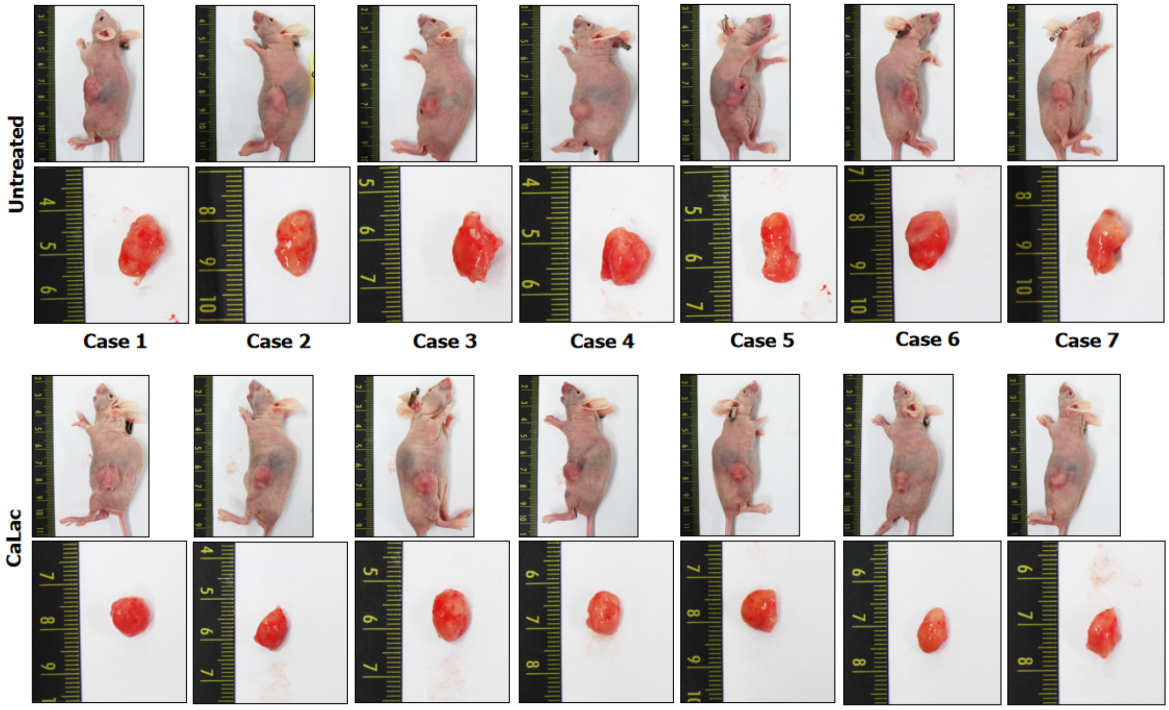

Figure 6 Tumor pictures of all xenograft mice following the end of 20 mg/kg lactate calcium salt administration for 21 d. CaLac: Lactate calcium salt.

ARTICLE HIGHLIGHTS

Research background

The excessive accumulation of poly adenosine diphosphate(ADP)-ribose (PAR) induces energy deprivation and apoptosis-inducing factor (AIF) release from mitochondria resulting in the caspase-independent death of cancer cells, and an increase in PAR is closely related to an increase in reactive oxygen species (ROS).

Research motivation

Increasing ROS can be induced in cancer cells by calcium influx. Therefore, it would be possible to expect the anticancer effect targeting pancreatic cancer through calcium-dependent PAR accumulation.

Research objectives

This study focused on the accumulation of PAR to induce energy deprivation and AIF release by sustained calcium supply to investigate its potential anticancer effect on pancreatic cancer.

Research methods

Two pancreatic cancer cell lines, AsPC-1 and CFPAC-1 were used for the study. Calcium influx and mitochondrial ROS were observed by fluorescence staining. Changes in enzyme levels, as well as PAR accumulation and energy metabolism, were measured using assay kits. AIF-dependent cell death was investigated followed by confirming *in vivo* anticancer effects by sustained calcium administration.

Research results

Mitochondrial ROS levels were elevated with increasing calcium influx into pancreatic cancer cells. Then, excess PAR accumulation, decreased PAR glycohydrolase and ADP-ribosyl hydrolase 3 levels, and energy crisis were observed. *In vitro* and *in vivo* antitumor effects were confirmed to accompany elevated AIF levels.

Research conclusions

Accumulation of PAR was induced by an increase in ROS following sustained calcium supply, which in turn led to the death of pancreatic cancer cells by energy deprivation and AIF expression. Calcium-mediated accumulation of PAR would be a potential strategy for the treatment of pancreatic cancer.

Research perspectives

Although this study visualized the potential anticancer effects of excessive PAR accumulation by sustained calcium supply on pancreatic cancer, elucidating a clear mode of action remains a challenge, and it should be accompanied by further studies to assess its potential for clinical application.

FOOTNOTES

Author contributions: Jeong KY conceived the project and wrote the paper; Jeong KY and Sim JJ designed the experiments; Jeong KY, Sim JJ, and Park MH performed the experiments; Jeong KY, Sim JJ, and Kim HM analyzed the data; and all authors discussed the results and revised the manuscript.

Institutional animal care and use committee statement: Animal care and experimental procedures were authorized by the Institutional Animal Care and Use Committee at Gachon University (IACUC-LCDI-2019-0102, 16 July 2019).

Conflict-of-interest statement: All the authors report no relevant conflicts of interest for this article.

Data sharing statement: No additional data are available.

ARRIVE guidelines statement: The authors have read the ARRIVE guidelines, and the manuscript was prepared and revised according to the ARRIVE guidelines.

Country/Territory of origin: South Korea

ORCID number: Keun-Yeong Jeong 0000-0002-4933-3493; Jae Jun Sim 0000-0002-3851-5689; Minhee Park 0000-0002-2513-2080; Hwan Mook Kim 0000-0001-7649-9790.

S-Editor: Wang JJ
L-Editor: A
P-Editor: Qi WW

REFERENCES

1 **Jeong KY**, Park MH. The Significance of Targeting Poly (ADP-Ribose) Polymerase-1 in Pancreatic Cancer for Providing a New Therapeutic Paradigm. *Int J Mol Sci* 2021; **22** [PMID: 33805293 DOI: 10.3390/ijms22073509]
2 **Alemasova EE**, Lavrik OI. Poly(ADP-ribosyl)ation by PARP1: reaction mechanism and regulatory proteins. *Nucleic Acids Res* 2019; **47**: 3811-3827 [PMID: 30799503 DOI: 10.1093/nar/gkz120]
3 **Kamaletdinova T**, Fanaei-Kahrani Z, Wang ZQ. The Enigmatic Function of PARP1: From PARylation Activity to PAR Readers. *Cells* 2019; **8** [PMID: 31842403 DOI: 10.3390/cells8121625]
4 **Wang Y**, Dawson VL, Dawson TM. Poly(ADP-ribose) signals to mitochondrial AIF: a key event in parthanatos. *Exp Neurol* 2009; **218**: 193-202 [PMID: 19332058 DOI: 10.1016/j.expneurol.2009.03.020]
5 **O'Sullivan J**, Tedim Ferreira M, Gagné JP, Sharma AK, Hendzel MJ, Masson JY, Poirier GG. Emerging roles of eraser enzymes in the dynamic control of protein ADP-ribosylation. *Nat Commun* 2019; **10**: 1182 [PMID: 30862789 DOI: 10.1038/s41467-019-08859-x]
6 **Harrision D**, Gravells P, Thompson R, Bryant HE. Poly(ADP-Ribose) Glycohydrolase (PARG) vs. Poly(ADP-Ribose) Polymerase (PARP) - Function in Genome Maintenance and Relevance of Inhibitors for Anti-cancer Therapy. *Front Mol Biosci* 2020; **7**: 191 [PMID: 33005627 DOI: 10.3389/fmolb.2020.00191]
7 **Jain A**, Agostini LC, McCarthy GA, Chand SN, Ramirez A, Nevler A, Cozzitorto J, Schultz CW, Lowder CY, Smith KM, Waddell ID, Raitses-Gurevich M, Stossel C, Gorman YG, Atias D, Yeo CJ, Winter JM, Olive KP, Golan T, Pishvaian MJ, Ogilvie D, James DI, Jordan AM, Brody JR. Poly (ADP) Ribose Glycohydrolase Can Be Effectively Targeted in Pancreatic Cancer. *Cancer Res* 2019; **79**: 4491-4502 [PMID: 31273064 DOI: 10.1158/0008-5472.CAN-18-3645]
8 **Rossi A**, Pizzo P, Filadi R. Calcium, mitochondria and cell metabolism: A functional triangle in bioenergetics. *Biochim Biophys Acta Mol Cell Res* 2019; **1866**: 1068-1078 [PMID: 30982525 DOI: 10.1016/j.bbamcr.2018.10.016]
9 **Bertero E**, Maack C. Calcium Signaling and Reactive Oxygen Species in Mitochondria. *Circ Res* 2018; **122**: 1460-1478 [PMID: 29748369 DOI: 10.1161/CIRCRESAHA.118.310082]
10 **Pazzaglia S**, Pioli C. Multifaceted Role of PARP-1 in DNA Repair and Inflammation: Pathological and Therapeutic Implications in Cancer and Non-Cancer Diseases. *Cells* 2019; **9** [PMID: 31877876 DOI: 10.3390/cells9010041]
11 **Martí JM**, Fernández-Cortés M, Serrano-Sáenz S, Zamudio-Martinez E, Delgado-Bellido D, Garcia-Diaz A, Oliver FJ. The Multifactorial Role of PARP-1 in Tumor Microenvironment. *Cancers (Basel)* 2020; **12** [PMID: 32245040 DOI:

10.3390/cancers12030739]
12 **Jeong KY**, Sim JJ, Park MH, Kim HM. Remodeling of Cancer-Specific Metabolism under Hypoxia with Lactate Calcium Salt in Human Colorectal Cancer Cells. *Cancers (Basel)* 2021; **13** [PMID: 33806179 DOI: 10.3390/cancers13071518]
13 **Hempel N**, Trebak M. Crosstalk between calcium and reactive oxygen species signaling in cancer. *Cell Calcium* 2017; **63**: 70-96 [PMID: 28143649 DOI: 10.1016/j.ceca.2017.01.007]
14 **Gupte R**, Liu Z, Kraus WL. PARPs and ADP-ribosylation: recent advances linking molecular functions to biological outcomes. *Genes Dev* 2017; **31**: 101-126 [PMID: 28202539 DOI: 10.1101/gad.291518.116]
15 **Perillo B**, Di Donato M, Pezone A, Di Zazzo E, Giovannelli P, Galasso G, Castoria G, Migliaccio A. ROS in cancer therapy: the bright side of the moon. *Exp Mol Med* 2020; **52**: 192-203 [PMID: 32060354 DOI: 10.1038/s12276-020-0384-2]
16 **Mashimo M**, Onishi M, Uno A, Tanimichi A, Nobeyama A, Mori M, Yamada S, Negi S, Bu X, Kato J, Moss J, Sanada N, Kizu R, Fujii T. The 89-kDa PARP1 cleavage fragment serves as a cytoplasmic PAR carrier to induce AIF-mediated apoptosis. *J Biol Chem* 2021; **296**: 100046 [PMID: 33168626 DOI: 10.1074/jbc.RA120.014479]
17 **Murata MM**, Kong X, Moncada E, Chen Y, Imamura H, Wang P, Berns MW, Yokomori K, Digman MA. NAD+ consumption by PARP1 in response to DNA damage triggers metabolic shift critical for damaged cell survival. *Mol Biol Cell* 2019; **30**: 2584-2597 [PMID: 31390283 DOI: 10.1091/mbc.E18-10-0650]
18 **Kassab MA**, Yu LL, Yu X. Targeting dePARylation for cancer therapy. *Cell Biosci* 2020; **10**: 7 [PMID: 32010441 DOI: 10.1186/s13578-020-0375-y]
19 **Liu L**, Li J, Ke Y, Zeng X, Gao J, Ba X, Wang R. The key players of parthanatos: opportunities for targeting multiple levels in the therapy of parthanatos-based pathogenesis. *Cell Mol Life Sci* 2022; **79**: 60 [PMID: 35000037 DOI: 10.1007/s00018-021-04109-w]
20 **Fatokun AA**, Dawson VL, Dawson TM. Parthanatos: mitochondrial-linked mechanisms and therapeutic opportunities. *Br J Pharmacol* 2014; **171**: 2000-2016 [PMID: 24684389 DOI: 10.1111/bph.12416]
21 **Randriamboavonjy V**, Kyselova A, Fleming I. Redox Regulation of Calpains: Consequences on Vascular Function. *Antioxid Redox Signal* 2019; **30**: 1011-1026 [PMID: 30266074 DOI: 10.1089/ars.2018.7607]
22 **Johnson DE**. Noncaspase proteases in apoptosis. *Leukemia* 2000; **14**: 1695-1703 [PMID: 10995018 DOI: 10.1038/sj.leu.2401879]

World Journal of Gastroenterology

Submit a Manuscript: https://www.f6publishing.com

World J Gastroenterol 2022 July 21; 28(27): 3435-3454

DOI: 10.3748/wjg.v28.i27.3435

ISSN 1007-9327 (print) ISSN 2219-2840 (online)

ORIGINAL ARTICLE

Basic Study

RING finger and WD repeat domain 3 regulates proliferation and metastasis through the Wnt/β-catenin signalling pathways in hepatocellular carcinoma

Ruo-Peng Liang, Xiao-Xue Zhang, Jie Zhao, Qin-Wei Lu, Rong-Tao Zhu, Wei-Jie Wang, Jian Li, Kai Bo, Chi-Xian Zhang, Yu-Ling Sun

Specialty type: Gastroenterology and hepatology

Provenance and peer review: Unsolicited article; Externally peer reviewed.

Peer-review model: Single blind

Peer-review report's scientific quality classification

Grade A (Excellent): 0
Grade B (Very good): B
Grade C (Good): C
Grade D (Fair): 0
Grade E (Poor): 0

P-Reviewer: Gupta T, India; Limaiem F, Tunisia
A-Editor: Morozov S, Russia

Received: February 7, 2022
Peer-review started: February 7, 2022
First decision: April 5, 2022
Revised: April 16, 2022
Accepted: June 3, 2022
Article in press: June 3, 2022
Published online: July 21, 2022

Ruo-Peng Liang, Jie Zhao, Qin-Wei Lu, Rong-Tao Zhu, Wei-Jie Wang, Jian Li, Kai Bo, Chi-Xian Zhang, Yu-Ling Sun, Department of Hepatobiliary and Pancreatic Surgery, The First Affiliated Hospital of Zhengzhou University, Zhengzhou 450052, Henan Province, China

Xiao-Xue Zhang, Department of Physical Examination, The First Affiliated Hospital of Zhengzhou University, Zhengzhou 450052, Henan Province, China

Corresponding author: Yu-Ling Sun, MD, PhD, Chief Doctor, Department of Hepatobiliary and Pancreatic Surgery, The First Affiliated Hospital of Zhengzhou University, No. 50 West Jianshe Road, Zhengzhou 450052, Henan Province, China. ylsun@zzu.edu.cn

Abstract

BACKGROUND

Hepatocellular carcinoma (HCC) exhibits high invasiveness and mortality rates, and the molecular mechanisms of HCC have gained increasing research interest. The abnormal DNA damage response has long been recognized as one of the important factors for tumor occurrence and development. Recent studies have shown the potential of the protein RING finger and WD repeat domain 3 (RFWD3) that positively regulates p53 stability in response to DNA damage as a therapeutic target in cancers.

AIM

To investigate the relationship between HCC and RFWD3 *in vitro* and *in vivo* and explored the underlying molecular signalling transduction pathways.

METHODS

RFWD3 gene expression was analyzed in HCC tissues and adjacent normal tissues. Lentivirus was used to stably knockdown RFWD3 expression in HCC cell lines. After verifying the silencing efficiency, Celigo/cell cycle/apoptosis and MTT assays were used to evaluate cell proliferation and apoptosis. Subsequently, cell migration and invasion were assessed by wound healing and transwell assays. In addition, transduced cells were implanted subcutaneously and injected into the tail vein of nude mice to observe tumor growth and metastasis. Next, we used lentiviral-mediated rescue of RFWD3 shRNA to verify the phenotype.

Finally, the microarray, ingenuity pathway analysis, and western blot analysis were used to analyze the regulatory network underlying HCC.

RESULTS

Compared with adjacent tissues, RFWD3 expression levels were significantly higher in clinical HCC tissues and correlated with tumor size and TNM stage ($P < 0.05$), which indicated a poor prognosis state. RFWD3 silencing in BEL-7404 and HCC-LM3 cells increased apoptosis, decreased growth, and inhibited the migration in shRNAi cells compared with those in shCtrl cells ($P < 0.05$). Furthermore, the *in vitro* results were supported by the findings of the *in vivo* experiments with the reduction of tumor cell invasion and migration. Moreover, the rescue of RFWD3 shRNAi resulted in the resumption of invasion and metastasis in HCC cell lines. Finally, gene expression profiling and subsequent experimental verification revealed that RFWD3 might influence the proliferation and metastasis of HCC *via* the Wnt/β-catenin signalling pathway.

CONCLUSION

We provide evidence for the expression and function of RFWD3 in HCC. RFWD3 affects the prognosis, proliferation, invasion, and metastasis of HCC by regulating the Wnt/β-catenin signalling pathway.

Key Words: RING finger and WD repeat domain 3; Hepatocellular carcinoma; Invasion; Proliferation; Metastasis; Wnt/β-catenin signaling pathways

Core Tip: The relationship between RING finger and WD repeat domain 3 (RFWD3) and tumorigenesis process has been reported occasionally, but the relationship between RFWD3 and hepatocellular carcinoma (HCC) is still unclear. This research reports the significant role of RFWD3 in HCC development by using bioinformatics databases, clinical samples, cell phenotypes, *in vivo* experiments, and microarray analyses. It provides evidence that RFWD3 expression might affect the tumorigenesis process of HCC by regulating the Wnt/β-catenin signalling pathways, laying a basic foundation for future relevant studies.

Citation: Liang RP, Zhang XX, Zhao J, Lu QW, Zhu RT, Wang WJ, Li J, Bo K, Zhang CX, Sun YL. RING finger and WD repeat domain 3 regulates proliferation and metastasis through the Wnt/β-catenin signalling pathways in hepatocellular carcinoma. *World J Gastroenterol* 2022; 28(27): 3435-3454
URL: https://www.wjgnet.com/1007-9327/full/v28/i27/3435.htm
DOI: https://dx.doi.org/10.3748/wjg.v28.i27.3435

INTRODUCTION

Hepatocellular carcinoma (HCC) is one of the most common malignant tumors and is highly invasive with a high mortality rate[1]. Reportedly, the incidence of HCC has increased rapidly by approximately 3%–4% *per* year in the United States[2]. Despite advances in medical research, early diagnosis of HCC remains difficult, and most patients are diagnosed with middle-or late-stage disease[3-5]. Moreover, even though some progress has been made in the clinical diagnosis and treatment of HCC, the long-term survival after treatment for patients diagnosed with early-stage HCC is low[6]. With the development of biomedicine, more basic studies have been carried out on HCC, but the underlying mechanism remains unclear, warranting promising interventions[7,8].

Multiple signal transduction pathways have been demonstrated to be involved in cellular responses to stress. For example, the ubiquitin-proteasome system (UPS) plays an important role in DNA damage repair, transcription regulation, cell cycle arrest, and apoptosis[9-11]. Several studies have focused on the role of the protein RING finger and WD repeat domain 3 (RFWD3) in the ataxia telangiectasia-mutated (ATM)/ATM-Rad3-related pathways of DNA damage response[12-16]. RFWD3 contains a RING finger domain and displays *in vitro* E3 ubiquitin ligase activity. It comprises an SQ-rich region in the N-terminus, a coiled-coil domain, and a WD40 domain in the C-terminus. In addition, sequence comparison revealed that the residues flanking serine 46 and serine 63 of RFWD3 are conserved[17]. According to the current literature, RFWD3 accumulates at stalled replication forks as part of the DNA damage response[18,19]. At these sites, RFWD3 co-localizes with replication protein A (RPA) and binds *via* its WD40 domain at the C-terminus to RPA2[20,21]. It functions in replication checkpoint signalling

upon replication stress and promotes replication fork restart after homologous recombination (HR)[22, 23]. RFWD3 is regarded as a tumor suppressor gene, and recent functional and mechanistic studies have indicated that it maintains the stability of p53[24]. Feeney *et al*[25] reported that it facilitates RPA-mediated DNA damage response[25]. Furthermore, RFWD3 is required for the proliferation of non-small-cell lung cancer, gastric carcinoma, and colorectal cancer cells and may have an important role[26-28]. However, the relationship between HCC and RFWD3 has not been explored.

In a preliminary experiment using a small number of HCC samples, our team found that RFWD3 expression was higher in HCC tissues than in adjacent non-cancerous tissues[29]. To rule out the effects of small sample numbers, the results were then verified using the open-source database. For this purpose, we chose RNA SEQ data (FPKM normalized) of liver cancer from The Cancer Genome Atlas (TCGA) database directly downloaded from the UCSC Xena database and further transformed it into log2 (TPM + 1) format. The results were concordant with our preliminary findings. Furthermore, the immunohistochemical analysis demonstrated that RFWD3 expression was associated with the clinical TNM stage (and with survival, according to the database). Therefore, in this study, we tested the hypothesis that RFWD3 plays a significant role in HCC development.

To test this hypothesis, in this study, we investigate the relationship between HCC and RFWD3 *in vitro* using human HCC cell lines and *in vivo* using HCC xenograft models in nude mice. Further, we unravel the underlying molecular signalling transduction pathways in HCC. The findings of this study provide evidence for the first time that RFWD3 plays a significant role in HCC cell proliferation and may serve as a potential therapeutic target for HCC.

MATERIALS AND METHODS

Tissue samples

Sixty tissue sample pairs (HCC and adjacent normal liver tissues) were obtained from clinical patients who underwent surgical HCC resection at the First Affiliated Hospital of Zhengzhou University (Zhengzhou, China). Before the operation, all patients were informed that the resected tissues could be used for research, and consent was obtained from each patient. After resection, the tissues were snap-frozen immediately and stored at −80 °C. All the experimental procedures were approved by the Ethics Committee of the First Affiliated Hospital of Zhengzhou University (Approval No. 10[2017]).

TCGA liver HCC cohort assessment

TCGA liver HCC cohort included 374 cancer tissues and 50 adjacent normal tissues. According to the expression level of *RFWD3* gene, we used the best cut-off value to divide the HCC patients into high and low expression groups by the Surv function of the survminer package. Then, the Kaplan-Meier method and log-rank test were used to evaluate the differences in overall survival and recurrence-free survival between the two groups. All data processing, statistical analyses, and graphical presentations (of this section) were carried out using R 4.0.5 software.

Immunohistochemical analysis of human HCC tissues

HCC tissue microarray data of 60 HCC and adjacent tissues, including some basic clinical data shown in Table 1, were obtained from BiochipTech (Zhengzhou, China). Immunohistochemistry (IHC) was performed using a 1:100 dilution of a primary antibody against *RFWD3* (Multi Sciences, Hangzhou, China), and all immunohistochemical procedures were performed according to a common standard protocol. First, the expression levels of RFWD3 between HCC and adjacent tissues were compared with a histochemical score (H-score). Then, a scoring system that combined the staining intensity (SI: 0, negative; 1, weak; 2, moderate; 3, strong) and the percentage of positive cells (PP: 0, < 5%; 1, 6%–25%; 2, 26%–50%; 3, 51%–75%; 4, > 75%) was used to compare the correlation of clinical data in patients with RFWD3 expression (SI × PP > 4 was considered high expression; SI × PP ≤ 4 was considered low expression).

Cell lines and culturing, lentivirus vector construction, and transduction

The human HCC cell lines BEL-7404 and HCC-LM3, maintained in our laboratory, were cultured (BEL-7404: 10% FBS, 90% RPMI-1640; HCC-LM3: 10% FBS, 90% DMEM; all purchased from Gibco, United States) according to the American type culture collection protocol. All cells were cultured in 50 ml/L CO_2 at 37°C in a moderately humid environment. The RFWD3 siRNA sequence (5-CAGAGAATGATG-GCAACAT-3) was synthesized and cloned into the AgeI/EcoRI sites of the lentivirus-based GV493-puromycin vector (shRNAi). The negative control lentiviral vector (5-TTCTCCGAACGTGTCACGT-3) was used as a control (shCtrl). The cells were divided into two groups (shCtrl and shRNAi), seeded in six-well plates, and allowed to grow until the logarithmic phase and less than 70% confluency. After verifying the transfection efficiency, the cells were harvested for subsequent *in vivo* and *in vitro* experiments. Additionally, the *RFWD3*-reverse mutation sequence (5-CTGAGAACGACGGAAATAT-3) was synthesized and cloned into the *BamHI*/*AgeI* sites of the lentivirus-based GV557-neomycin vector

Table 1 Clinicopathological features in hepatocellular carcinoma tissue microarrays

Clinicopathological parameters	Number	Expression of RFWD3		*P* value
		Low[1]	High[1]	
Total	60	25	35	
Gender				
Male	24	9	15	
Female	36	16	20	0.592
HBsAg				
Positive	39	17	22	
Negative	21	8	13	0.68
Age (yr)				
< 60	34	17	17	
≥ 60	26	8	18	0.134
Tumor size				
< 5 cm	27	15	12	
≥ 5 cm	33	10	23	0.048[a]
TNM stage[2]				
I–II	31	17	14	
III–IV	29	8	21	0.032[a]

[1]Staining intensity (SI) × percentage of positive (PP) > 4 was considered high expression; SI × PP < 4 was considered low expression.
[2]TNM stage was determined according to the guidelines of the American Joint Committee on Cancer (2010).
[a]$P < 0.05$.
RFWD3: RING finger and WD repeat domain 3.

(KD-OE). The virus without anti-Smad served as negative controls (KD-OE-NC) for subsequent phenotypic validation. The GV493-puromycin and GV557-neomycin vectors were obtained from GeneChem (Shanghai, China).

Quantitative reverse transcription-polymerase chain reaction

Quantitative reverse transcription-polymerase chain reaction (qRT-PCR) was used to detect the mRNA expression level of RFWD3 using the following primers: Forward: 5′-AGAGTATGGAGGGGT-TGTTGAC-3′ and reverse: 5′-TAGAAGCAGAAGGTAGCAGAGG-3′. Total RNA was extracted from tissues and cells using TRIzol reagent (Thermo Fisher Scientific, United States) and reverse transcribed into cDNA using a Prime-Script RT Reagent Kit with gDNA Eraser (Takara Bio, Japan). Following a common standard protocol, qRT-PCR was performed in a total volume of 10 μL on a 7900-HT Fast Real-time PCR System (Applied Biosystems Inc., United States) to evaluate RFWD3 expression in 60 pairs of HCC tissues and determine the RFWD3 knockdown efficiency in cells transduced with shCtrl and shRNAi.

Western blot analysis

To determine the RFWD3 virus transfection efficiency in cells transduced with shCtrl, shRNAi, KD-OE, and KD-OE-NC, the levels of RFWD3 protein expression were assessed by western blot (WB). Briefly, the total protein was extracted by incubating the cells in RIPA lysis buffer (Thermo Fisher Scientific, United States) supplemented with a protease inhibitor cocktail (Thermo Fisher Scientific, United States) for 1 h on ice, followed by sonication (Shanghai Experimental Instruments, China) for three 5 s cycles on ice. After centrifugation (14000 ×*g*, 4 °C, 15 min), the supernatant was collected for protein concentration measurement using a bicinchoninic acid protein assay kit (Pierce Biotechnology, United States). Denatured protein samples (30 μg/10 μL) were separated by SDS-PAGE (Invitrogen, United States) and transferred to polyvinylidene fluoride membranes (Bio-Rad, United States). Afterward, the membranes were blocked with 5% non-fat milk (BD Biosciences, United States) dissolved in 30 mL Tris-buffered saline with Tween-20 (TBST) for 2 h at common room temperature. The membranes were then incubated overnight at 4 °C with primary antibodies against GAPDH (1:1000; Abcam, United States) and RFWD3 (1:1000; Multi Sciences, Hangzhou, China). After three 5 min washes in TBST with agitation, the membranes were incubated for 1 h at room temperature with the appropriate secondary

horseradish peroxidase-linked antibodies, including goat anti-rabbit IgG for GAPDH (1:2000; Abcam, United States) and goat anti-rabbit IgG for RFWD3 (*1:2000*; Multi Sciences, Hangzhou, China). An ECL kit (Pierce Biotechnology, United States) was used to visualize the protein bands.

Cell growth and proliferation assays

A Celigo imaging cytometer (Celigo; Nexcelom Bioscience, United States) and MTT assays were used to detect the number of cells at each time point, and the growth status of the cells was analyzed. For the Celigo assay, cells in the logarithmic phase were digested with trypsin (Sangon Biotech, Shanghai, China), seeded in 96-well plates (2000 cells/well in 100 μL medium) with three wells *per* condition, and cultured in a 37 °C incubator with 50 mL/L CO_2. From the first day to the fifth day after seeding, the plate was subjected to high-throughput screening every day. GFP fluorescence was measured in each scan to generate a five days cell proliferation curve. For the MTT assay, two groups of cells were seeded in 96-well plates (2000 cells/well) with three wells *per* condition and incubated at 37 °C for six consecutive days. Cell viability was analyzed every 24 h by washing the cells twice with PBS and adding MTT solution (5 mg/mL) to each well. After 4 h of incubation, the supernatant in each well was removed, and 100 μL DMSO was added to solubilize the formazan crystals. After 10 min, the optical density (OD) was measured at an excitation wavelength of 490 nm and an emission wavelength of 570 nm using a microplate reader (VarioskanFlash; Thermo Fisher Scientific, United States).

Cell cycle assays

Cell cycle progression was examined using propidium iodide (PI; Sigma, United States) and RNase A (Thermo Fisher, United States). Cells in the logarithmic growth phase in six-well culture plates were digested with trypsin (Sangon Biotech, Shanghai, China) and diluted with the culture medium. Three replicate tubes were analyzed for both the shCtrl and shRNAi groups (1×10^6 cells/tube). The cells were centrifuged at 1300 rpm for 5 min, and the supernatant was discarded. The cell pellet was washed with pre-cooled D-Hanks equilibrium solution (4 °C with pH = 7.2–7.4), and the harvested cells were fixed with 70% cold ethanol at 4 °C overnight. Afterward, the cells were washed twice with 4 °C D-Hanks solution and incubated with 10 mg/mL RNase at 37 °C. Cell cycle progression was monitored by staining the nuclei with PI. The fluorescence of DNA-bound PI in cells was measured using flow cytometry (FCM; FC500 flow cytometer; Cytomics, United States). Finally, ModFit LT software (Windows version 4.0; Verity Software House, United States) was used to analyze the cell populations in different phases of the cell cycle.

Cell apoptosis assays

Cell apoptosis was assayed using an Annexin V-APC/PI apoptosis detection kit (Biosciences, Thermo Fisher, United States). Cells in the logarithmic phase were digested with trypsin (Sangon Biotech, Shanghai, China) and diluted with the culture medium. Three replicate tubes each were analyzed for the shCtrl, shRNAi, KD-OE, and KD-OE-NC groups of each cell line (1×10^4 cells/tube). The cells were centrifuged at 1300 rpm for 5 min, and the supernatant was discarded. The cell pellet was washed with a pre-cooled D-Hanks equilibrium solution (4 °C with pH = 7.2–7.4). The cells were then washed with 1 × binding buffer, centrifuged at 1300 rpm for 3 min, and resuspended in 200 μL 1 × binding buffer. Next, 10 μL Annexin V-APC staining solution was added, and the samples were incubated for 10–15 min at room temperature in the dark. Finally, apoptosis was detected in the samples.

Cell invasion and migration assays

Cell migration was assayed using wound healing and transwell assays. For the wound-healing assay, cells were plated in 6-well plates and scratched with a sterile pipette tip. The cells were then imaged using a microscope (Olympus, Japan) to observe migration after 12 and 24 h. For the invasion and migration assays, the upper surfaces of transwell chambers (Costar, Cambridge, MA, United States) were uncoated (for the migration experiments) or coated with Matrigel (1:4, BD, United States) (for the invasion experiments). Cells were then added to the upper chambers containing 200 μL serum-free medium (BEL-7404: RPMI-1640; HCC-LM3: DMEM) *per* well, and 500 μL medium (with 10% FBS) was added to the lower chambers. After 48 h, the chambers were cleaned, stained with hematoxylin, transferred to glass slides after the operation, and then observed under a microscope (Olympus, Japan). Six fields *per* chamber were used to quantify the invaded cell numbers with 100 × and 200 × magnifications.

Establishment of HCC xenograft models in nude mice

All animal experimental protocols were conducted following the ARRIVE (Animal Research: Reporting In Vivo Experiments) guidelines (https://www.nc3rs.org.uk/arrive-guidelines) and performed following protocols approved by the Research Ethics Committee of the First Affiliated Hospital of Zhengzhou University (Approval No. 10[2017]). Nude mice were purchased from Shanghai B&K Universal Group Limited (certificate number: SCXK 2013-0016; Shanghai, China). For the proliferation assay, 5×10^6 HCC-LM3 cells stably transduced with the lentiviral pSC-1-GFP vector carrying shCtrl or shRNAi were suspended in PBS and injected subcutaneously into the flank region of 6-week-old male

athymic nude mice (six mice in each group). For the metastasis assay, 2×10^6 HCC-LM3 cells transduced as described above were injected into the tail vein of nude mice. The animals were acclimatized to laboratory conditions (23 °C, 12 h/12 h light/dark, 50% humidity, ad libitum access to food and water). After four weeks, the mice were euthanized by barbiturate overdose (intravenous injection, 150 mg/kg pentobarbital sodium) for tissue collection and photographed.

Microarray-based gene expression analysis

To elucidate the molecular mechanisms involved in the association between RFWD3 and HCC, we performed microarray-based gene expression analysis to compare gene expression between the shCtrl and shRNAi groups. We then used ingenuity pathway analysis (IPA) to explore the molecular signal transduction pathways involved in HCC. All procedures were performed according to a common protocol, and assistance was provided by the Shanghai Biotechnology Corporation (SBC, Shanghai, China).

Statistical Analysis

Statistical analyses and related statistical illustrations were performed using SPSS (version 21.0; IBM, Armonk, NY, United States) and GraphPad Prism software (ver. *5.0* for Windows; GraphPad Software Inc., United States). The Pearson chi-square test was used to determine the correlation between clinical characteristics and immunohistochemical staining. Other results are expressed as mean ± SD. A t-test was used to compare the two groups, and a P value of < 0.05 was considered statistically significant.

RESULTS

RFWD3 is ppregulated in HCC and correlated with worse prognosis

RFWD3 expression was examined in HCC tissues and matched adjacent normal tissues. IHC analysis of 60 tissue pairs revealed that HCC tissues exhibited a higher H-score than non-tumor tissues (Figure 1A) [30]. This result was supported by the qRT-PCR analysis of 54 tissue sample pairs (some outlier value pairs were excluded) (Figure 1B). These results were concordant with the RFWD3 expression data obtained by analyzing the bioinformatics database (Figure 1C). In addition, the bioinformatics database showed that higher RFWD3 expression represents a worse prognosis in HCC (Figure 1D and E). These data indicate that high RFWD3 expression might predict poor HCC development and prognosis (Table 1).

Validation of lentiviral-mediated knockdown efficiency in cell lines

After verifying the high expression of RFWD3 in HCC tissues, we selected HCC cell lines for further *in vitro* experiments. BEL-7404, HCC-LM3, SMMC-7721, and BEL-7402 cells were evaluated for the stable expression of RFWD3. Based on qRT-PCR and cell growth analyses, we chose BEL-7404 and HCC-LM3 cells for lentiviral-mediated knockdown of RFWD3 expression (Figure 2A). After lentiviral transduction, compared with the shCtrl group, the shRNAi group showed obvious knockdown of RFWD3 (qRT-PCR: BEL-7404: $P < 0.01$; HCC-LM3: $P < 0.01$) (Figure 2B). These results were subsequently confirmed with WB analysis and GFP fluorescence imaging (Figure 2C and D).

RFWD3 knockdown inhibits HCC growth and proliferation in vitro

A high-content screening assay (Celigo) was performed to monitor cell growth for five days. The total cell count and growth rate were lower in the shRNAi group than in the shCtrl group (Figure 3A). To further verify these results, we used an MTT assay. After five days of incubation in the same environment, consistent with the Celigo results, the OD value was significantly lower in the shRNAi group than that in the shCtrl group (Figure 3B). Taken together, these results indicate that RFWD3 knockdown significantly reduced the proliferation of HCC cells.

RFWD3 knockdown induces cell cycle arrest

To determine whether RFWD3 affects cell proliferation by regulating the cell cycle, we used PI staining to evaluate cell cycle progression. In the shCtrl and shRNAi groups, the cell cycle distributions were as follows (presented as the mean value of three replicates). For BEL-7404 shCtrl cells, 40.09% were in G0/G1 phase, 35.01% were in the S phase, and 24.9% were in the G2/M phase, while for BEL-7404 shRNAi cells, 37.82% were in G0/G1 phase, 30.03% were in S phase, and 32.15% were in G2/M phase. For HCC-LM3 shCtrl cells, 55.07% were in G0/G1 phase, 36.98% were in the S phase, and 7.95% were in the G2/M phase, while for HCC-LM3 shRNAi cells, 54.98% were in G0/G1 phase, 29.84% were in S phase, and 15.18% were in G2/M phase. Compared with shCtrl cells, shRNAi cells showed a reduced percentage of cells in G0/G1 (BEL-7404: $P < 0.01$) and S phase (BEL-7404: $P < 0.01$; HCC-LM3: $P < 0.01$), and the fraction of cells in the G2/M phase was significantly increased (BEL-7404: $P < 0.01$; HCC-LM3: $P < 0.01$). These results indicated that RFWD3 knockdown blocked cell cycle progression through the G2/M phase (Figure 3C and D).

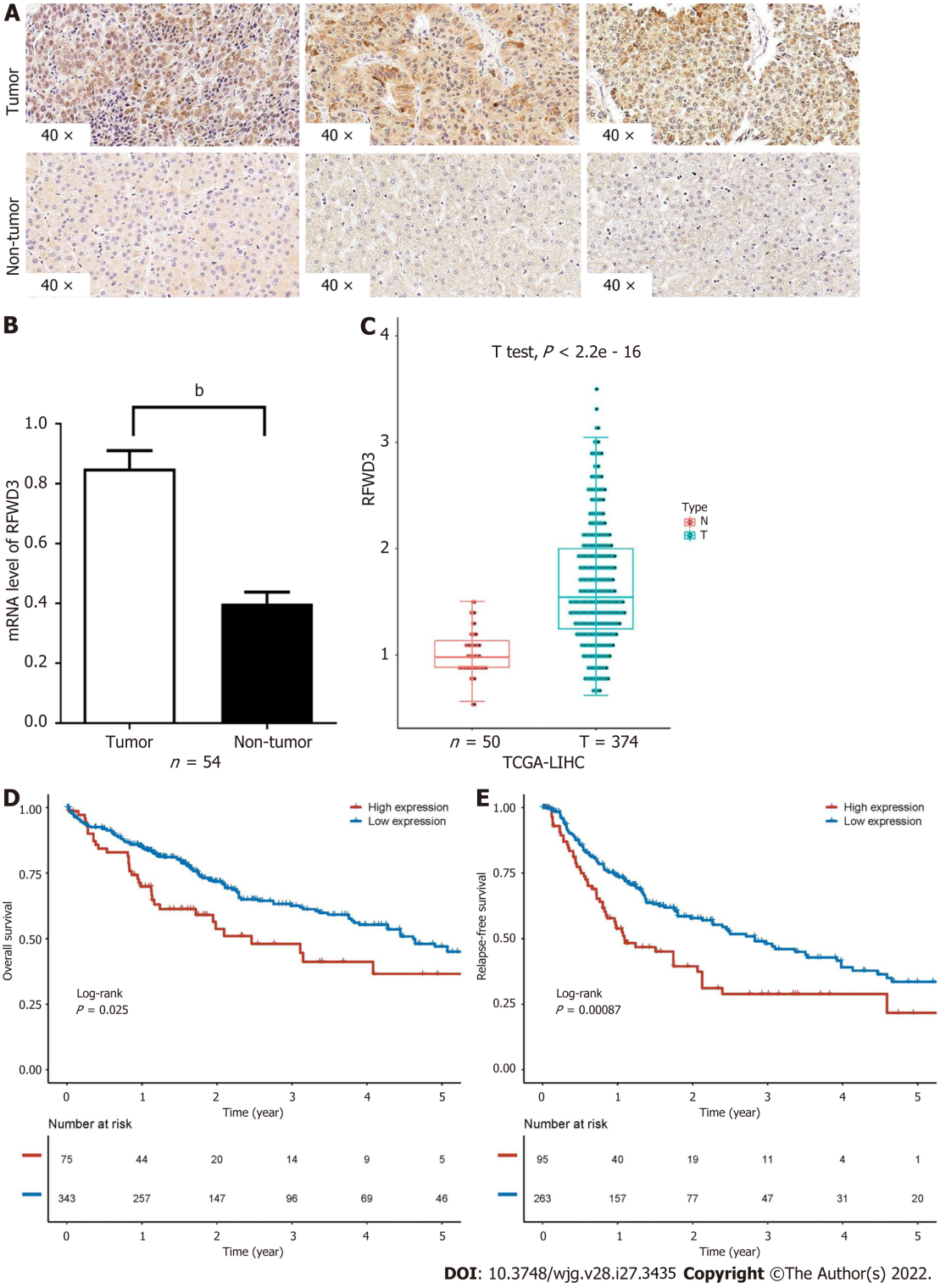

DOI: 10.3748/wjg.v28.i27.3435

Figure 1 Expression of RING finger and WD repeat domain 3 in hepatocellular carcinoma and its correlation with a worse prognosis. A: RING finger and WD repeat domain 3 (RFWD3) expression in hepatocellular carcinoma (HCC) tumor and non-tumor tissues detected using immunohistochemical staining; B: Expression analysis of RFWD3 in 54 tissue sample pairs (some invalid samples were removed) using quantitative reverse transcription-polymerase chain reaction ($^bP < 0.01$); C: Comparison of RFWD3 expression between tumor and non-tumor tissues in HCC patients (T = 374, *n* = 50, the data source is the Cancer Genome Atlas (TCGA) (TCGA) database); D and E: Kaplan-Meier survival curves of HCC patients with high and low expression of RFWD3 (*n* = 91, the data source is the TCGA database).

RFWD3 knockdown increased cell apoptosis

To determine whether RFWD3 affects cell proliferation by inducing apoptosis, an Annexin V-APC/PI apoptosis detection kit (AV/PI) was used to detect apoptosis in the two groups of cells by FCM. The apoptosis ratios were (presented as the mean value of three replicates) 4.47 ± 0.3748 for BEL-7404 shCtrl cells, 9.77 ± 0.1142 for BEL-7404 shRNAi cells, 2.14 ± 0.2234 for HCC-LM3 shCtrl cells, and 9.01 ± 0.2230

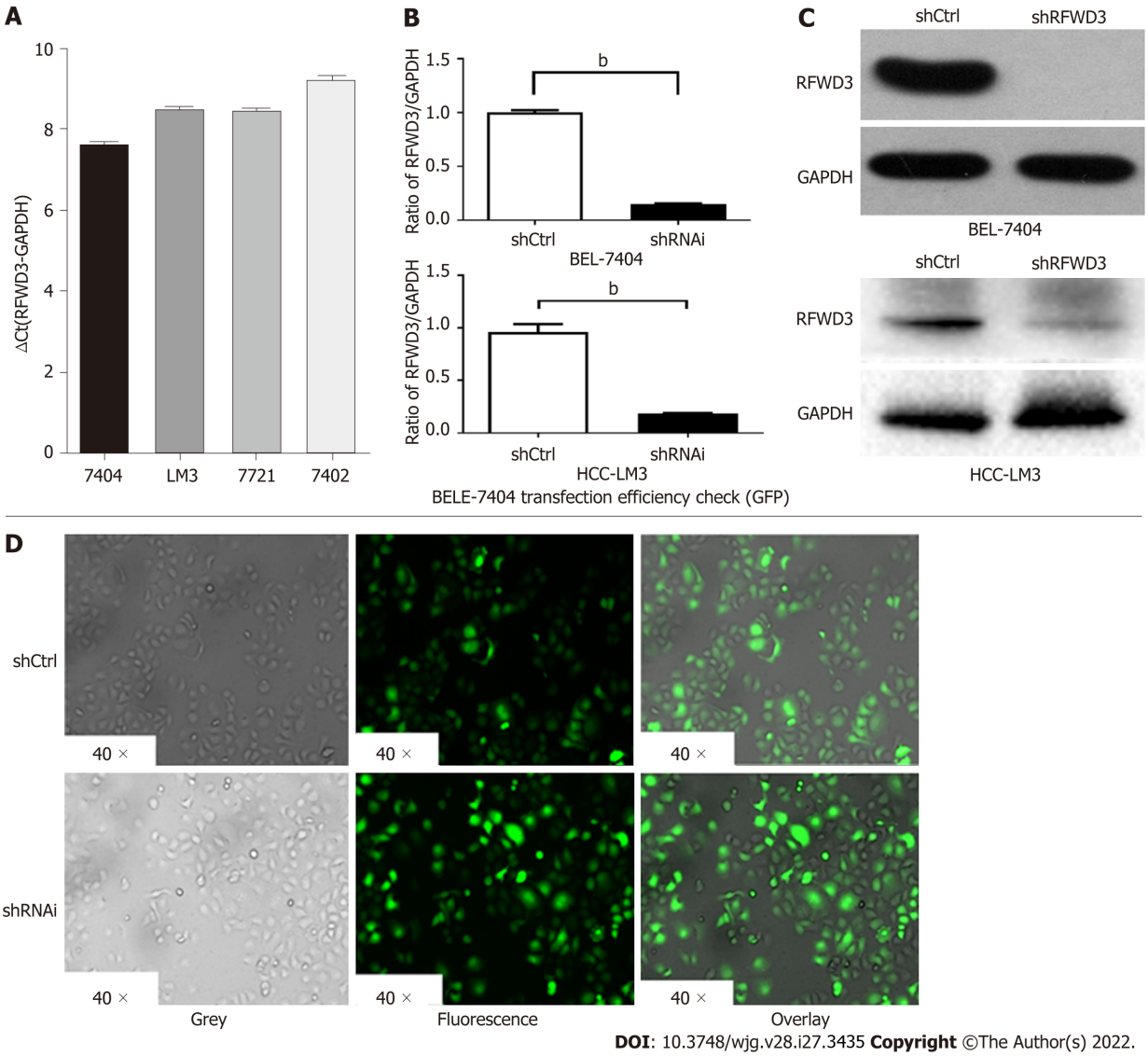

DOI: 10.3748/wjg.v28.i27.3435 **Copyright** ©The Author(s) 2022.

Figure 2 Validation of lentivirus knockdown efficiency in cell lines. A: RING finger and WD repeat domain 3 (RFWD3) expression in BEL-7404 and Hepatocellular carcinoma (HCC)-LM3 cells obtained using quantitative reverse transcription-polymerase chain reaction (qRT-PCR) analysis; B and C: The shRNAi group shows obvious knockdown of RFWD3 [BEL-7404: qRT-PCR: $^{b}P < 0.01$, western blot (WB): $^{b}P < 0.01$; HCC-LM3: qRT-PCR: $^{b}P < 0.01$, WB: $^{b}P < 0.01$]; D: Confirmation of the lentivirus transduction efficiency using GFP fluorescence imaging.

for HCC-LM3 shRNAi cells. Compared with shCtrl cells, shRNAi cells had a higher apoptosis rate (BEL-7404: $P < 0.01$; HCC-LM3: $P < 0.01$). This result demonstrated that RFWD3 knockdown increased the apoptosis ratio, thus affecting the proliferation of HCC cells (Figure 3E and F).

RFWD3 knockdown reduced HCC cell invasion and migration

Wound healing and transwell assays were used to evaluate HCC cell invasion and migration. In the wound healing assay, the shCtrl groups exhibited better healing ability ($P < 0.05$). After 12 h, the wound area was 103.40 ± 1.32 in BEL-7404 shCtrl cells, 125.90 ± 4.46 in BEL-7404 shRNAi cells, 145.40 ± 0.84 in HCC-LM3 shCtrl cells and 159.50 ± 2.21 in HCC-LM3 shRNAi cells. Over time, the difference in the size of the wound area between the two groups increased. After 24 h, the wound area was 22.97 ± 0.22 in BEL-7404 shCtrl cells, 60.94 ± 2.41 in BEL shRNAi cells, 60.22 ± 12.68 in HCC-LM3 shCtrl cells and 134.40 ± 0.84 in HCC-LM3 shRNAi cells (Figure 4A). We next examined cell migration and invasion with transwell assays. The migration of both BEL-7404 and HCC-LM3 shRNAi cells was attenuated compared with shCtrl cells ($P < 0.05$). Similar results were observed in the invasion assay (Figure 4B). These data revealed that RFWD3 knockdown reduced HCC cell invasion and migration.

RFWD3 knockdown decreased HCC cell proliferation, invasion, and metastasis in vivo

We established an HCC xenograft model in nude mice to verify the results *in vivo*. HCC-LM3 shCtrl and shRNAi cells were injected subcutaneously (Figure 5A) and into the tail vein (Figure 5B) of nude mice (six mice in each group). After four weeks, the mice were euthanized by cervical dislocation. The tumors

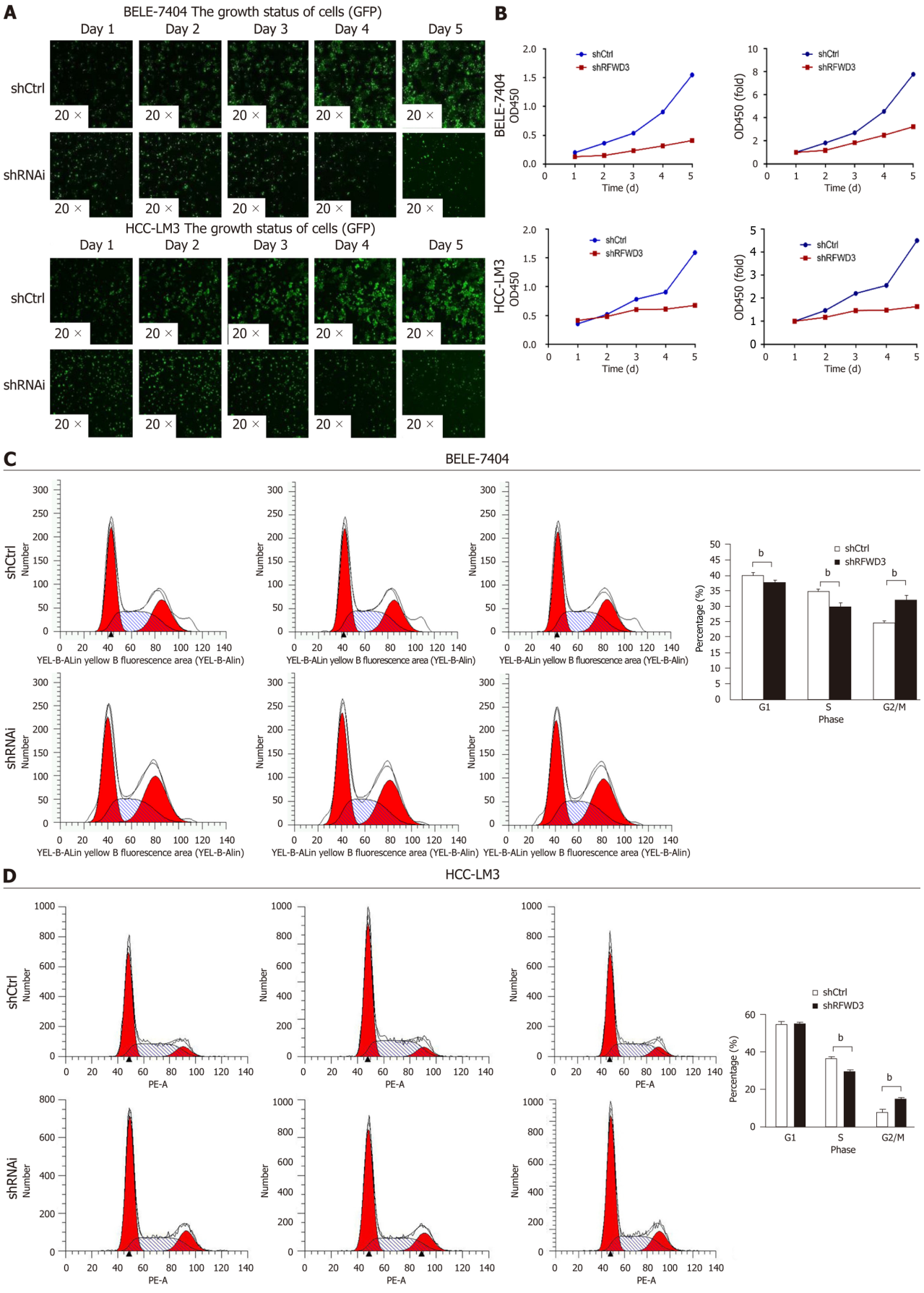
A
BELE-7404 The growth status of cells (GFP)
Day 1
Day 2
Day 3
Day 4
Day 5
shCtrl
shRNAi
20 ×
HCC-LM3 The growth status of cells (GFP)
B
BELE-7404 OD450
HCC-LM3 OD450
OD450 (fold)
shCtrl
shRFWD3
Time (d)
C
BELE-7404
shCtrl
shRNAi
Number
YEL-B-ALin yellow B fluorescence area (YEL-B-Alin)
Percentage (%)
G1
S
G2/M
Phase
D
HCC-LM3
PE-A

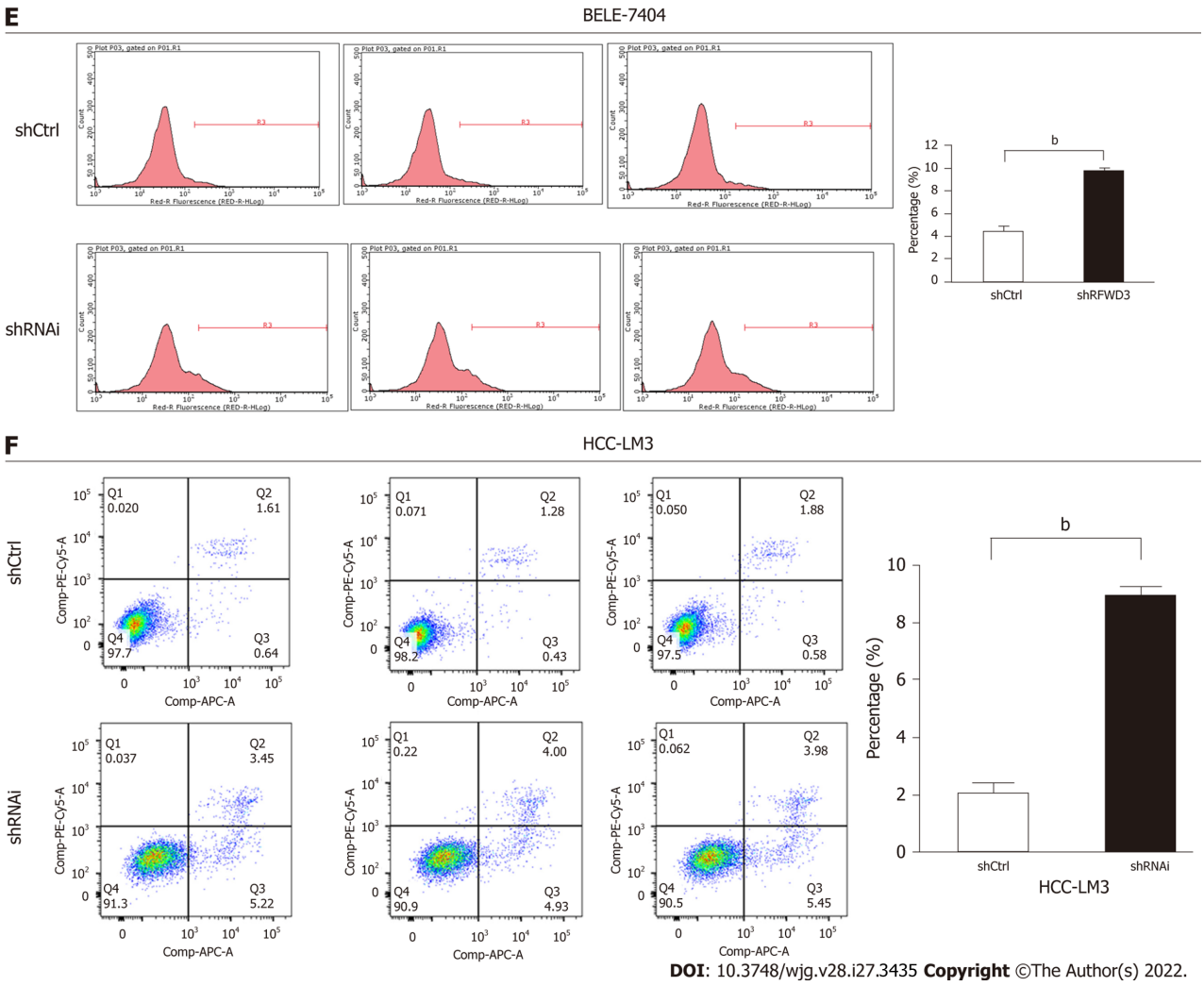

DOI: 10.3748/wjg.v28.i27.3435 **Copyright** ©The Author(s) 2022.

Figure 3 RING finger and WD repeat domain 3 knockdown inhibits cell growth and proliferation and induces cell cycle arrest and apoptosis. A: Cell growth and proliferation of BEL-7404, Hepatocellular carcinoma (HCC)-LM3 shRNAi, and shCtrl cells continuously monitored using a Celigo instrument for five days; B: MTT assay demonstrating that RING finger and WD repeat domain 3 siRNA significantly reduced the proliferation of HCC cells; C and D: The cell cycle progression evaluated by flow cytometry (FCM) with propidium iodide (PI) and RNase A ($^bP < 0.01$); E and F: FCM to assess the apoptosis in shRNAi and shCtrl groups of cells using Annexin V-APC/PI Apoptosis Detection Kit ($^bP < 0.01$).

(subcutaneous injection groups) and lung tissues (tail vein injection groups) were removed for imaging analysis. The growth and invasion ability of tumors was significantly lower in mice injected with shRNAi cells than in mice injected with shCtrl cells. These results show that silencing RFWD3 effectively reduced HCC tumor proliferation, invasion, and metastasis in vivo.

Validation of the efficiency of lentiviral-mediated rescue of RFWD3 shRNAi in cell lines

To rule out off-target effects and confirm the biological function of RFWD3 shRNAi, a rescue experiment was performed with RFWD3-KD-OE in HCC cells. After transfection with an LV-RFWD3 lentiviral vector, we used GFP fluorescence imaging to confirm transduction efficiency (Figure 6A). Compared with the RFWD3-KD-OE-NC group, the RFWD3-KD-OE group showed upregulation of RFWD3 in qRT-PCR (Figure 6B). WB analysis also confirmed the lentivirus transduction efficiency (Figure 6C).

RFWD3-KD-OE resume shRNAi HCC cells proliferation, invasion, and migration

In the MTT assay, the OD value of the RFWD3-KD-OE group was higher than that of the RFWD3-KD-OE-NC group. These results indicate that RFWD3-KD-OE rescued the proliferation of shRNAi BEL-7404 cells (Figure 7A). Furthermore, no difference was observed between the G1 and S phases in the two groups of cell cycle progression assays. However, in the G2/M phase, the fraction of RFWD3-KD-OE-NC cells was increased (the average value was 30.51% in RFWD3-KD-OE-NC cells, 29.74% in RFWD3-KD-OE cells, $P < 0.05$); however, the gap in data was diminished compared with previous BEL-7404 RNAi groups (24.9% in shCtrl cells, 32.15% in shRNAi cells, $P < 0.05$) (Figure 7B). In the subsequent apoptosis experiments, BEL-7404 RFWD3-KD-OE-NC cells had a higher apoptosis rate (the average

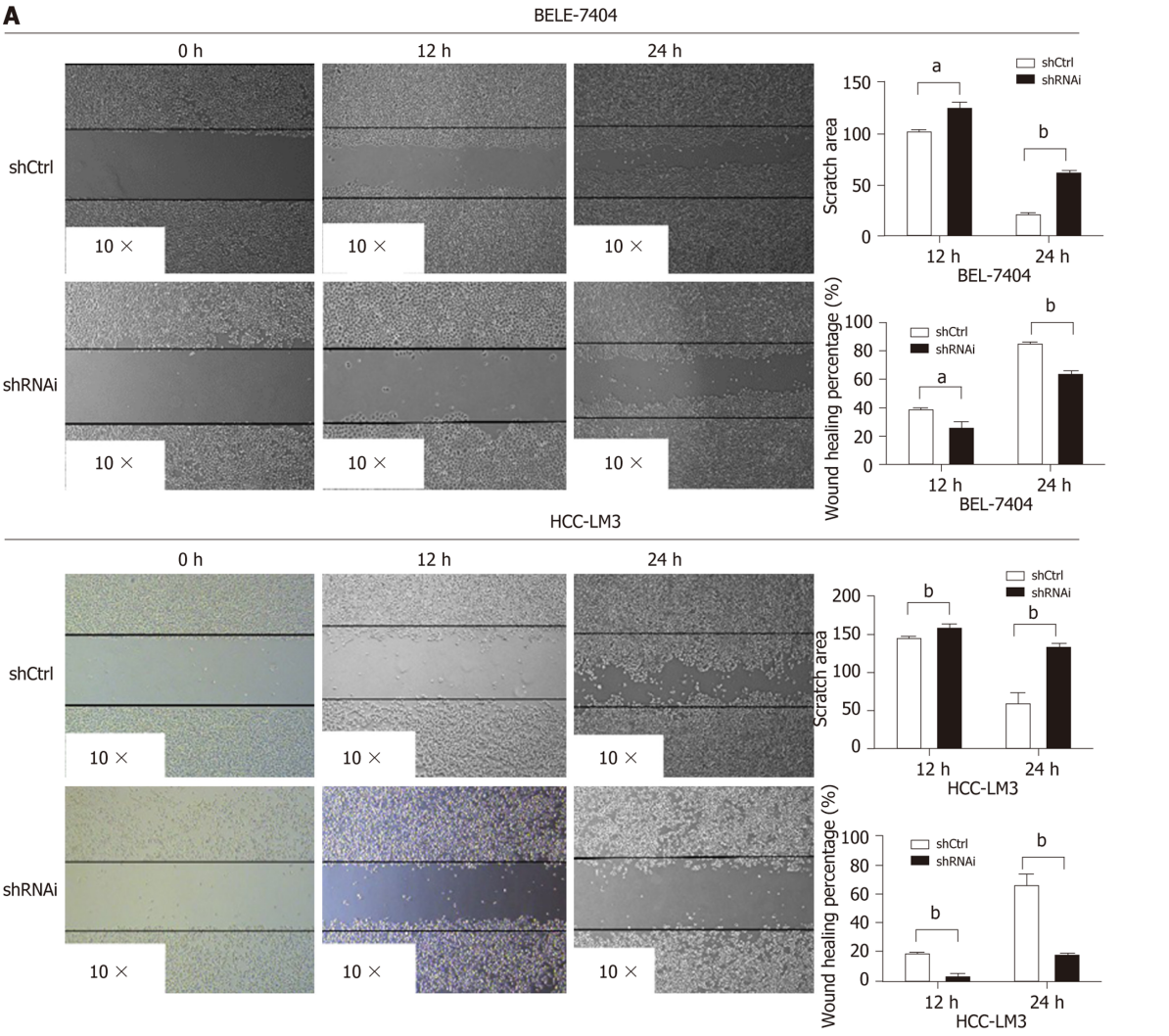
A
BELE-7404
0 h
12 h
24 h
shCtrl
shRNAi
10 ×
Scratch area
shCtrl
shRNAi
a
b
12 h
24 h
BEL-7404
Wound healing percentage (%)
HCC-LM3

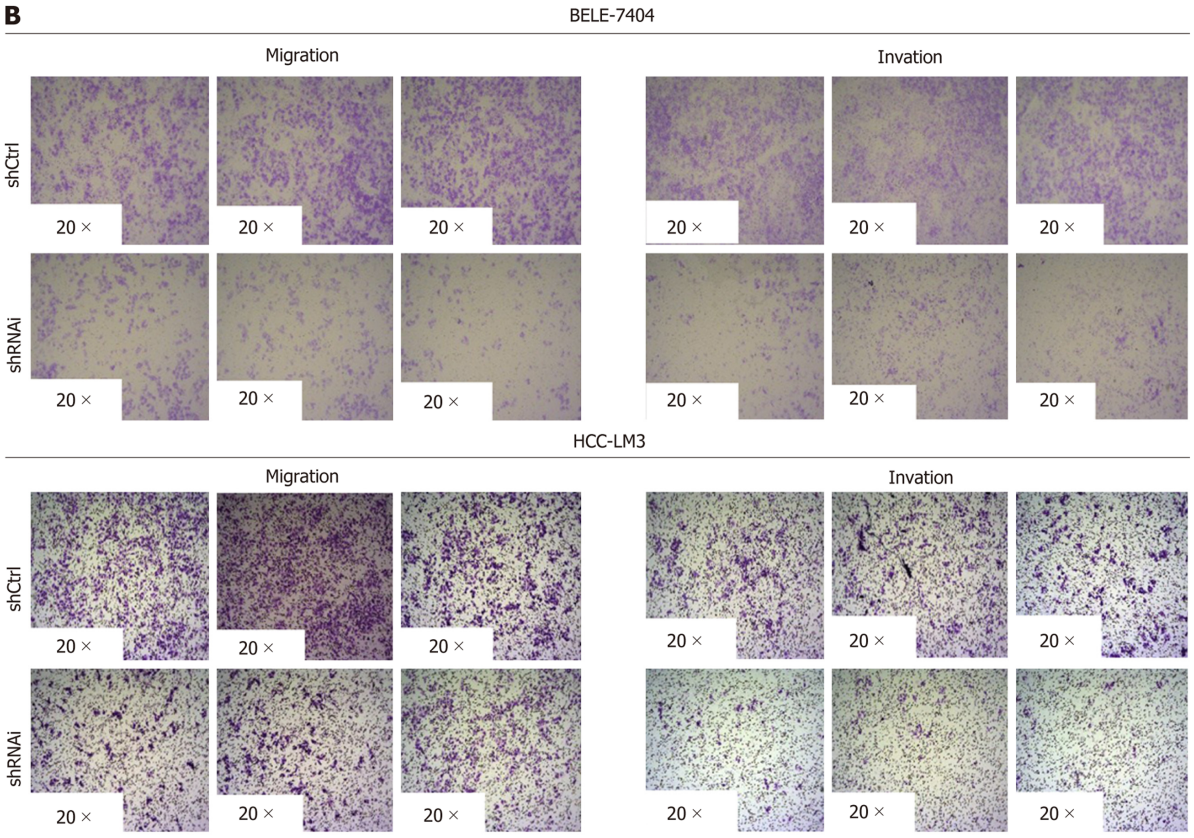
B
BELE-7404
Migration
Invation
shCtrl
shRNAi
20 ×
HCC-LM3

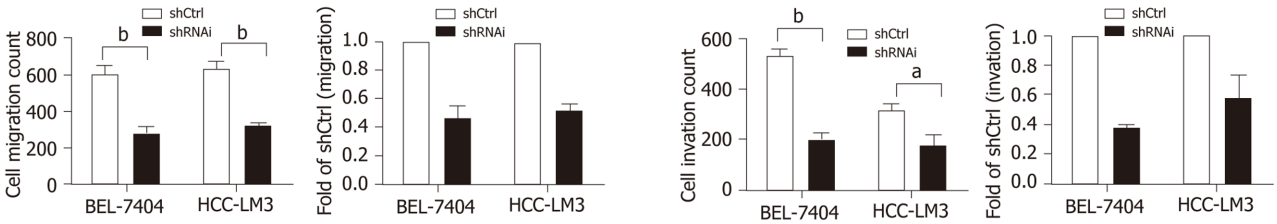

DOI: 10.3748/wjg.v28.i27.3435 **Copyright** ©The Author(s) 2022.

Figure 4 RING finger and WD repeat domain 3 knockdown reduces hepatocellular carcinoma cell invasion and migration. A: Wound-healing assay in the shCtrl and shRNAi groups ($^{a}P < 0.05$, $^{b}P < 0.01$); B: The migration ability of both BEL-7404 and hepatocellular carcinoma-LM3 shRNAi cells. Invasion assays demonstrating similar results ($^{a}P < 0.05$, $^{b}P < 0.01$).

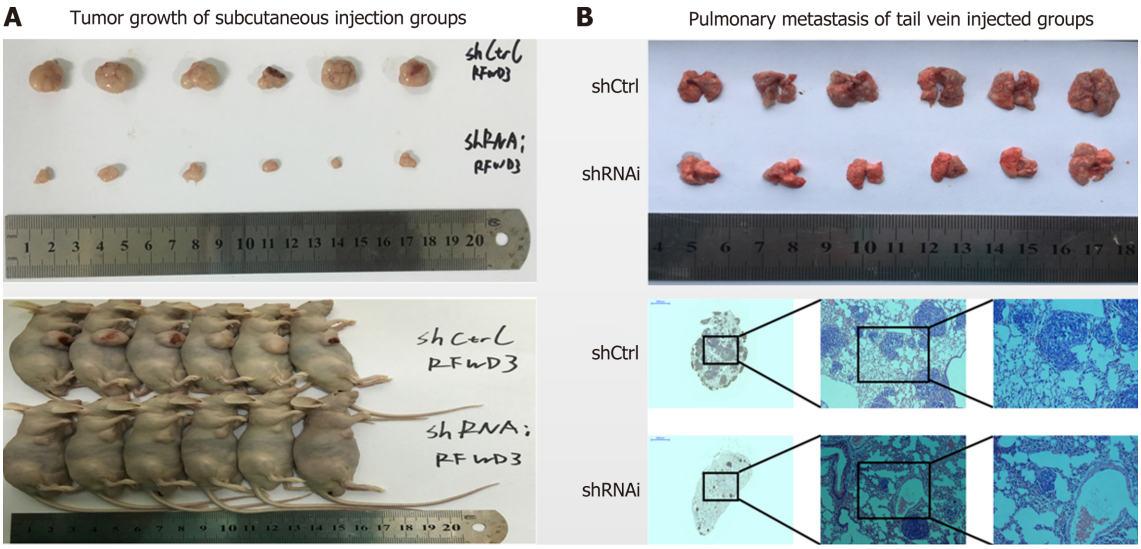

DOI: 10.3748/wjg.v28.i27.3435 **Copyright** ©The Author(s) 2022.

Figure 5 RING finger and WD repeat domain 3 knockdown reduces hepatocellular carcinoma cell growth *in vivo*. A: Imaging analysis of the tumor and lung tissues of mice injected with shRNAi and shCtrl cells; B: Imaging analysis of pulmonary metastasis of hepatocellular carcinoma cells in mice injected with shRNAi and shCtrl cells.

value was 20.47% in RFWD3-KD-OE-NC cells, 18.03% in RFWD3-KD-OE cells, $P < 0.01$) (Figure 7C). This result demonstrated that RFWD3-KD-OE reduced the apoptosis ratio, thus affecting the proliferation of shRNAi BEL-7404 cells. In transwell assays, the migration of BEL-7404 RFWD3-KD-OE cells was higher than that of RFWD3-KD-OE-NC cells ($P < 0.01$) (Figure 7D). Similar results were observed in the invasion assay ($P < 0.01$; Figure 7E). These data revealed that RFWD3-KD-OE rescued BEL-7404 shRNAi cell invasion and migration.

RFWD3 influence the progress of HCC via the Wnt/β-catenin signalling pathway

To further validate the results of the *in vitro* and *in vivo* experiments, we performed microarray analysis to explore the molecular mechanism underlying the differential RFWD3 expression between shCtrl and shRNAi HCC cells. A total of 454 genes (Figure 8A) exhibited differential mRNA expression between the two groups (> 2-fold, $P < 0.05$). We then analyzed the disease and function to determine the enriched gene sets. Genes involved in cell death, viability and survival, cell movement and invasion, cellular assembly and organization, DNA replication, recombination and repair, and cellular function and maintenance were significantly enriched ($P < 0.05$, Figure 8B). Classical pathway analysis revealed that, in addition to the previously reported p53 and cell cycle checkpoint control pathways, the Wnt/β-catenin signalling pathway was altered following RFWD3 silencing ($P < 0.05$, Figure 8C and D). Next, we used IPA to analyze the knowledge-based interactome associated with the regulation of these pathways (Figure 8E). Some genes involved in tumorigenesis were shown to be regulated by RFWD3, including *CREBBP*, *KREMEN-1*, *LRP6*, *JUN*, *WNT5A*, and *WNT7B*. Finally, we tested the protein expression between shCtrl and shRNAi and RFWD3-KD-OE *vs* RFWD3-KD-OE-NC groups and found that the expression of *CREBBP*, *WNT5A*, *JUN*, *WNT7B*, and *LRP6* were decreased, and the expression of *KREMEN-1* was increased in the shRNAi and RFWD3-KD-OE-NC groups than that in shCtrl and RFWD3-KD-OE groups (Figure 8F-I). These results indicate that the Wnt/β-catenin signalling pathway is involved in the RFWD3-mediated promotion of HCC tumorigenesis.

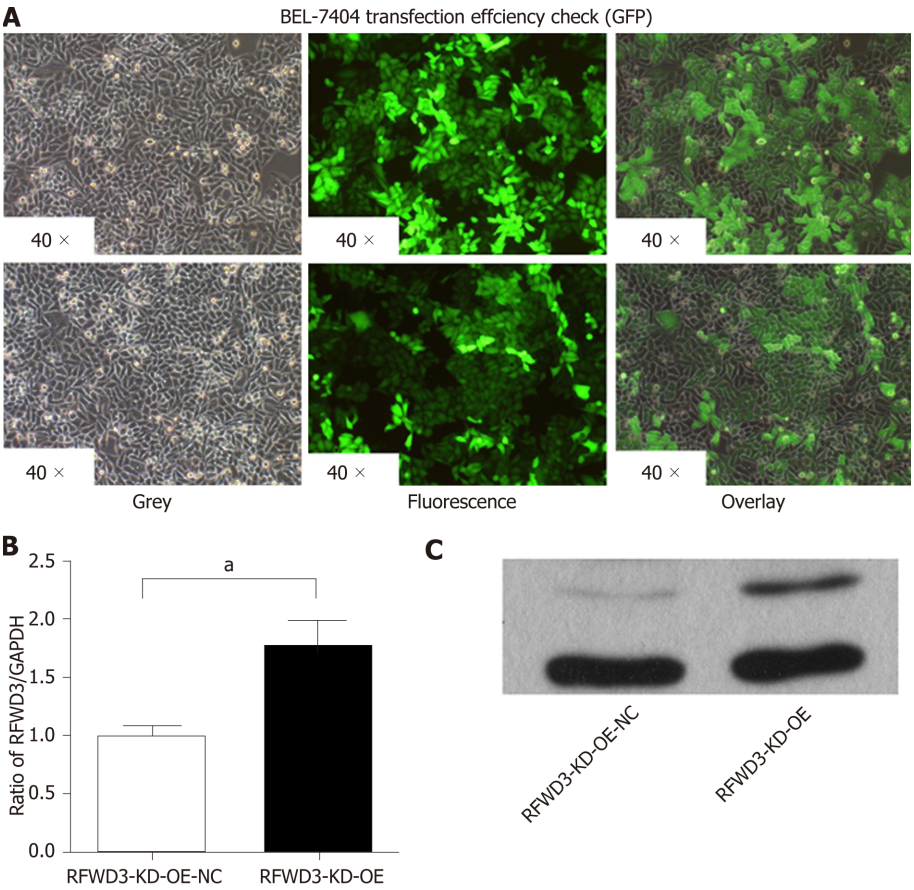

DOI: 10.3748/wjg.v28.i27.3435

Figure 6 Validation of lentiviral-mediated rescue RING finger and WD repeat domain 3 shRNAi efficiency in cell lines. A: GFP fluorescence imaging confirms the lentivirus transduction efficiency; B: Compared with the RING finger and WD repeat domain 3 (RFWD3)-KD-OE-NC group, the RFWD3-KD-OE group shows upregulated RFWD3 in the quantitative reverse transcription-polymerase chain reaction analysis ($^aP < 0.05$); C: Western blot analysis confirms the same upshot.

DISCUSSION

In this study, we demonstrated reduced growth and proliferation of HCC cells in the shRNAi group. Subsequent evaluation of cell cycle progression revealed disrupted cell cycle progression at the G2/M phase, whereas the FCM analysis showed a higher rate of apoptosis in the shRNAi group than in the ShCtrl group. These results confirmed that RFWD3 silencing caused both cell cycle arrest at the G2/M phase and apoptosis. Furthermore, the *in vitro* experiments revealed that shCtrl cells had better healing abilities than shRNAi cells. In the subsequent transwell experiments, we also found that the shRNAi cells had about half the metastatic capacity of the shCtrl cells. These results were validated *in vivo* using mice models, which showed that the tumor volumes in mice injected subcutaneously with shRNAi cells were significantly smaller than those in mice injected with shCtrl cells. Furthermore, the pulmonary metastasis group revealed that lung metastasis was significantly reduced in mice injected with shRNAi cells than in those injected with shCtrl cells.

To rule out off-target effects with RFWD3-shRNAi, we performed a rescue experiment. After verifying the transfection efficiency and screening of stable cell lines, we carried out phenotype verification. Compared with the control group, the cell growth state was restored in the RFWD3-KD-OE group. It also showed a higher OD value in the MTT assay, decreased fraction of G2/M phase, and diminution gap of data compared with RFWD3-KD-OE-NC group. Furthermore, in the apoptosis experiments, the RFWD3-KD-OE group had a lower apoptosis rate than the RFWD3-KD-OE-NC group. The same results were observed in the transwell assays, and the migration and invasion abilities of the RFWD3-KD-OE group were recovered. These data revealed that RFWD3-KD-OE resumed BEL-7404 shRNAi cell invasion and metastasis and proved that the previous RFWD3-shRNAi experimental results were not due to off-target effects.

Subsequently, we proved that RFWD3 silencing plays a positive role in inhibiting the proliferation, invasion, and metastasis of HCC. Previous studies have reported that the essential role of RFWD3 in HR makes it important for cell survival, as it promotes the repair of DNA damage. Therefore, the increased apoptosis could be attributed to the unrepaired DNA damage upon RFWD3 loss. On the contrary, the migration and metastasis phenotypes could be explained by decreased viability due to increased

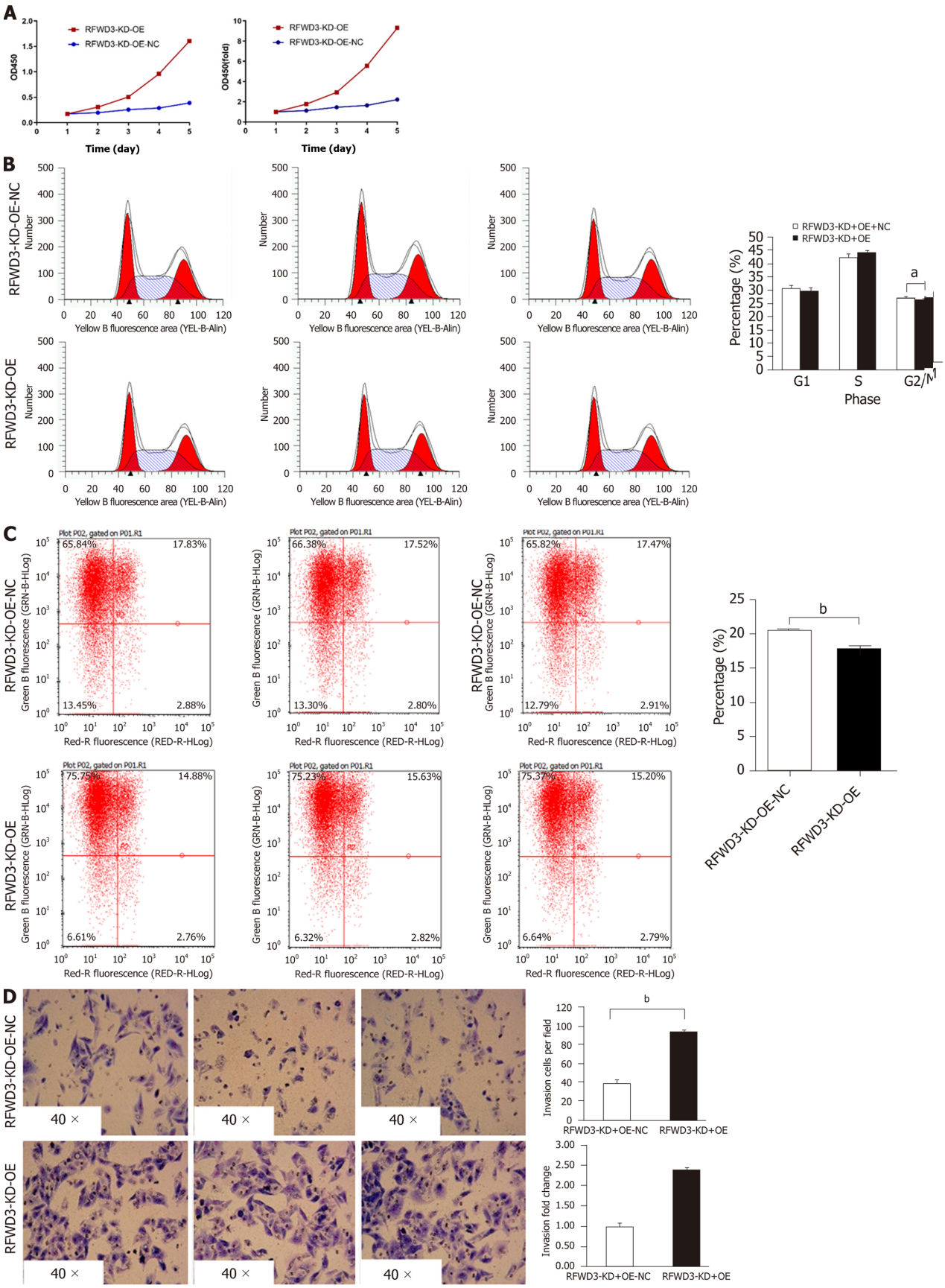
A
RFWD3-KD-OE
RFWD3-KD-OE-NC
OD450
OD450(fold)
Time (day)
B
RFWD3-KD-OE-NC
RFWD3-KD-OE
Number
Yellow B fluorescence area (YEL-B-Alin)
RFWD3-KD+OE+NC
RFWD3-KD+OE
Percentage (%)
G1
S
G2/M
Phase
a
C
Plot P02, gated on P01.R1
Green B fluorescence (GRN-B-HLog)
Red-R fluorescence (RED-R-HLog)
65.84%
17.83%
13.45%
2.88%
66.38%
17.52%
13.30%
2.80%
65.82%
17.47%
12.79%
2.91%
75.75%
14.88%
6.61%
2.76%
75.23%
15.63%
6.32%
2.82%
75.37%
15.20%
6.64%
2.79%
b
D
40 ×
Invasion cells per field
Invasion fold change

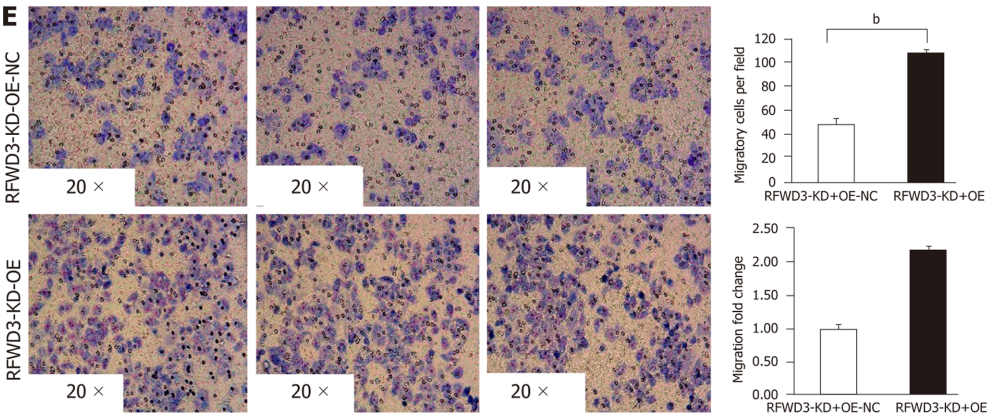

DOI: 10.3748/wjg.v28.i27.3435

Figure 7 RING finger and WD repeat domain 3-KD-OE reverses the cell phenotype of shRNAi BEL-7404 cells. A: MTT assay; B: The cell cycle distribution in RING finger and WD repeat domain 3 (RFWD3)-KD-OE-NC and RFWD3-KD-OE cells ($^aP < 0.05$); C: Rate of apoptosis in RFWD3-KD-OE-NC and RFWD3-KD-OE groups ($^bP < 0.01$); D and E: RFWD3-KD-OE resumes BEL-7404 shRNAi cell invasion and migration ability in transwell ($^bP < 0.01$) and invasion assays ($^bP < 0.01$).

RFWD3 function during DNA repair. In other words, this condition may be explained by a common theory: "There are more firefighters on the fire scene than ordinary people." However, the questions like whether the increased expression of RFWD3 in HCC is a compensatory mechanism to deal with increased genomic instability or whether RFWD3 is regulated by a Janus-faced regulator that plays other roles in HCC, consequently promoting the progression of HCC remained unanswered.

To answer these questions, we explored the mechanism underlying HCC and identified the molecular signalling transduction pathways using microarray-based gene expression analyses and IPA. The raw data (Supplementary materials 1) were verified with the uniformity, integrity and reliability (Supplementary materials 2). Gene expression profiling revealed that RFWD3 silencing enriched the expression of genes involved in cellular function and maintenance, cell death, viability, movement, invasion and survival, and DNA replication, recombination, and repair (Supplementary materials 3). In terms of the gene pathways involved, in addition to the p53 and cell replication cycle pathways that were previously reported in the literature, we found that the Wnt/β-catenin signalling pathway also had a significant impact. Further examination of the knowledge-based interactome associated with the regulation of Wnt/β-catenin *via* IPA analysis demonstrated that *CREMEN1, JUN, CREBBP, WNT5A, WNT7B,* and *LRP6*, which have been implicated in the proliferation and metastasis of various cancers, were differentially regulated by RFWD3 (> 2-fold, $P < 0.05$).

Reportedly, Wnt/β-catenin signalling plays an important role in embryonic liver development and regeneration and preserves liver health. An aberrant Wnt signalling activity has been implicated in several human cancers[31,32]. In normal tissues, only a small amount of β-catenin is found in the cytoplasm and is quickly degraded by the UPS. It is bound by a destruction complex containing *GSK3B, AXIN,* and *APC* and then ubiquitinated by β-transducin repeat-containing protein and subsequently degraded by the proteasome[33]. In the traditional Wnt/β-catenin pathway in tumors, the destruction complex is disassembled by the phosphorylation of *LRP6* and *GSK3β*, thereby preventing β-catenin degradation[34]. The accumulated β-catenin is transferred from the cytoplasm to the nucleus, where it competes with Groucho to form the *β-catenin-TCF/LEF* transcriptional complex. Finally, the Wnt signalling pathway is activated to regulate the transcription of target genes such as *cyclin D1*, *c-myc*, and *MMP9* under the synergistic effect of auxiliary factors, thus regulating tumor progression[35]. *KREMEN-1* is a transmembrane protein that contains a kringle domain. Studies have shown that it is a high-affinity receptor for *DKK*. *KREMEN-1, DKK*, and *LRP5/6* form a ternary complex that inhibits Wnt/β-catenin signalling, thus inducing head defects in Xenopus embryos[36,37]. Furthermore, *KREMEN-1* expression is prevalent in adult mammals but is often lacking in tumors. It has been shown that Wnt/β-catenin signalling maintains the low differentiation state of stem cells and undifferentiated cells, but *Dickkopf-KREMEN* blocks Wnt/β-catenin signalling causing cells to differentiate[38].

Collectively, the findings demonstrated that factors involved in Wnt/β-catenin signallings, such as *CREBBP, WNT5A, JUN, WNT7B,* and *LRP6*, were downregulated by RFWD3 silencing, and the expression of *KREMEN-1* was increased, indicating that RFWD3 might influence the progression of HCC *via* the Wnt/β-catenin signalling pathway. Based on these findings, it can be inferred that RFWD3 affects the Wnt/β-catenin signalling pathway and therefore affects HCC tumorigenesis. However, the detailed regulatory mechanism is still unclear and should be explored in future studies.

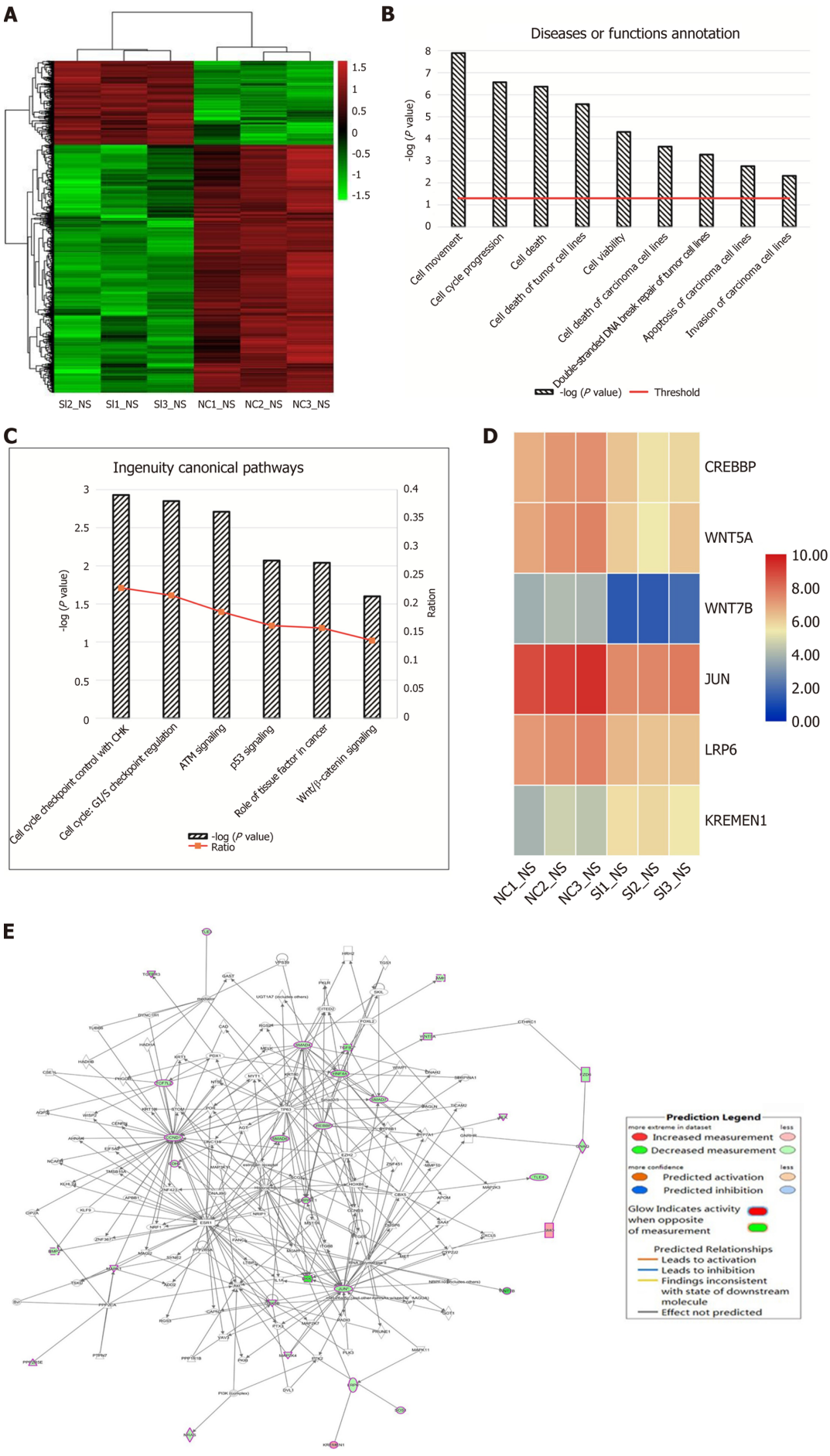
A
1.5
1
0.5
0
-0.5
-1
-1.5
SI2_NS
SI1_NS
SI3_NS
NC1_NS
NC2_NS
NC3_NS
B
Diseases or functions annotation
-log (P value)
Cell movement
Cell cycle progression
Cell death
Cell death of tumor cell lines
Cell viability
Cell death of carcinoma cell lines
Double-stranded DNA break repair of tumor cell lines
Apoptosis of carcinoma cell lines
Invasion of carcinoma cell lines
-log (P value)
Threshold
C
Ingenuity canonical pathways
-log (P value)
Ration
Cell cycle checkpoint control with CHK
Cell cycle: G1/S checkpoint regulation
ATM signaling
p53 signaling
Role of tissue factor in cancer
Wnt/β-catenin signaling
-log (P value)
Ratio
D
CREBBP
WNT5A
WNT7B
JUN
LRP6
KREMEN1
10.00
8.00
6.00
4.00
2.00
0.00
NC1_NS
NC2_NS
NC3_NS
SI1_NS
SI2_NS
SI3_NS
E
Prediction Legend
more extreme in dataset
less
Increased measurement
Decreased measurement
more confidence
less
Predicted activation
Predicted inhibition
Glow Indicates activity when opposite of measurement
Predicted Relationships
Leads to activation
Leads to inhibition
Findings inconsistent with state of downstream molecule
Effect not predicted

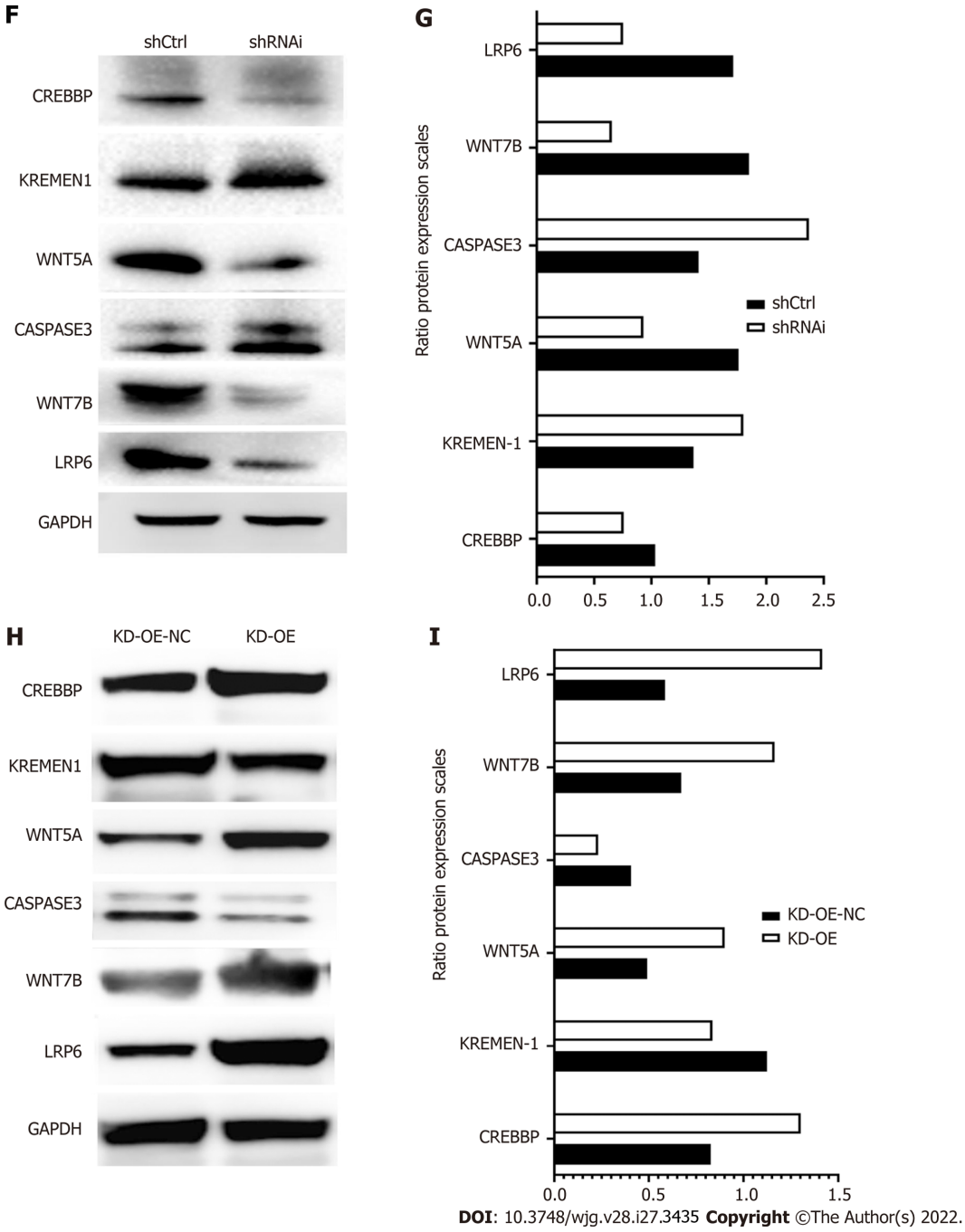

DOI: 10.3748/wjg.v28.i27.3435

Figure 8 shRFWD3i influences the progress of hepatocellular carcinoma through the Wnt/β-catenin signalling pathway. A: Heatmap analysis showing the gene expression changes after RING finger and WD repeat domain 3 (RFWD3) silencing (454 genes, above 2-fold); B: Disease and functional analysis to classify genes enriched after RFWD3 silencing; C: Classical pathway analysis indicates genes enriched after RFWD3 silencing; D: The microarray analysis reveals alteration in the Wnt/β-catenin signalling pathway following RFWD3 silencing; E: Knowledge-based interaction network of Wnt/β-catenin signalling targets (> 2-fold change, $P < 0.05$). The intensity of the node color indicates the degree of upregulation (red) or downregulation (green) following RFWD3 silencing in hepatocellular carcinoma cells; F-I: The expression of *CREBBP, Wnt5A, JUN, Wnt7B* and *LRP6* were decreased, and the expression of *KREMEN-1* was increased in the shRNAi group using western blot analysis, in rescue experiment, the results are reversed.

CONCLUSION

In this study, we validated the expression and function of RFWD3 in HCC and demonstrated that RFWD3 expression might affect the proliferation and metastasis of HCC by regulating the Wnt/β-catenin signalling pathway. The findings suggest that RFWD3 could be a potential therapeutic target for HCC; however, it warrants further investigations to ascertain these possibilities.

ARTICLE HIGHLIGHTS

Research background

Hepatocellular carcinoma (HCC) is one of the most common malignant tumors with a high mortality rate. The molecular biology research of HCC can reveal the potential mechanism and provide direction for its comprehensive treatment.

Research motivation

The relationship between RING finger and WD repeat domain 3 (RFWD3) and the tumorigenesis process has been reported occasionally; however, the relationship between RFWD3 and HCC is still unclear.

Research objectives

We aimed to investigate the relationship between HCC and RFWD3 and explore the underlying molecular signalling transduction pathways.

Research methods

We analyzed RFWD3 expression in HCC tissues and evaluated cell phenotypes such as proliferation, apoptosis, migration, and invasion using Lentivirus mediated RFWD3 knockdown. In addition, *in vivo* experiments were performed to observe tumor growth and metastasis. Next, the phenotype was verified using the lentiviral-mediated rescue of RFWD3 shRNA. Finally, we unraveled the regulatory network underlying HCC using microarray, bioinformatics, and western blot analyses.

Research results

RFWD3 expression levels were correlated with tumor size and TNM stage in clinical samples. RFWD3 silencing increased apoptosis, decreased growth, and inhibited migration in HCC cell lines and nude mice, which were resumed with RFWD3 shRNAi rescue. Subsequent experiments revealed that RFWD3 might influence the proliferation and metastasis of HCC *via* the Wnt/β-catenin signalling pathway.

Research conclusions

This study shows that RFWD3 affects the Wnt/β-catenin signalling pathway and therefore affects HCC tumorigenesis.

Research perspectives

The findings suggest that RFWD3 could be a potential therapeutic target for HCC. However, it warrants further investigations to ascertain these inferences.

ACKNOWLEDGEMENTS

We would like to thank Wen-Feng Song, Hao Chen, Liang-Jie Hong, Dan-Jing Guo, Rong Su, Hao-Hao Chen and Han-Wen Zhang for their technical assistance.

FOOTNOTES

Author contributions: Sun YL conceived the experiments; Liang RP, Zhang XX, Zhao J, Lu QW, Zhu RT, Wang WJ, Li J, Bo K and Zhang CX contributed sample collection/reagents/materials/analysis tools, performed all experiments, and analyzed the data; Liang RP, Zhang XX and Zhao J analyzed the results and wrote the paper; all authors have read and approve the final manuscript.

Supported by National Natural Science Foundation of China, No. 82172944 and No. 81900558; Co-operation Research Plan of Medical Science and Technology of Henan Province, No. LHGJ20190149; and The Key Scientific Research Projects of Universities of Henan Province, No. 21A320052.

Institutional review board statement: This study was reviewed and approved by the First Affiliated Hospital of Zhengzhou University, Zhengzhou, China, No. 10[2017].

Institutional animal care and use committee statement: All animal experimental protocols were conducted following the ARRIVE guidelines (Animal Research: Reporting In Vivo Experiments, https://www.nc3rs.org.uk/arrive-guidelines) and approved by Laboratory Animals and the Institutional Animal Care and Use Committee of the First Affiliated Hospital of Zhengzhou University (Approval Number: 10[2017]).

Conflict-of-interest statement: All the authors report no relevant conflicts of interest for this article.

Data sharing statement: The data are available from the corresponding author on reasonable request.

ARRIVE guidelines statement: The authors have read the ARRIVE guidelines, and the manuscript was prepared and revised according to the ARRIVE guidelines.

Country/Territory of origin: China

ORCID number: Ruo-Peng Liang 0000-0002-3789-1666; Xiao-Xue Zhang 0000-0003-2272-3405; Jie Zhao 0000-0001-7701-1654; Qin-Wei Lu 0000-0003-3801-8217; Rong-Tao Zhu 0000-0003-3655-9458; Wei-Jie Wang 0000-0003-3136-8628; Jian Li 0000-0001-7756-2312; Kai Bo 0000-0002-0039-0585; Chi-Xian Zhang 0000-0002-4387-7182; Yu-Ling Sun 0000-0001-5289-4673.

S-Editor: Fan JR
L-Editor: A
P-Editor: Zhang YL

REFERENCES

1 **Chen W**, Zheng R, Baade PD, Zhang S, Zeng H, Bray F, Jemal A, Yu XQ, He J. Cancer statistics in China, 2015. *CA Cancer J Clin* 2016; **66**: 115-132 [PMID: 26808342 DOI: 10.3322/caac.21338]
2 **Siegel RL**, Miller KD, Jemal A. Cancer statistics, 2020. *CA Cancer J Clin* 2020; **70**: 7-30 [PMID: 31912902 DOI: 10.3322/caac.21590]
3 **Li J**, Qiu X, Guo W, Yan B, Zhang S. Prospective analysis of tiopronin in prevention of sorafenib and antiviral therapy inducing liver toxicity in advanced hepatitis B virus-related hepatocellular carcinoma. *Med Oncol* 2015; **32**: 238 [PMID: 26330362 DOI: 10.1007/s12032-015-0684-x]
4 **Tsai CL**, Hsu FM, Cheng JC. How to Improve Therapeutic Ratio in Radiotherapy of HCC. *Liver Cancer* 2016; **5**: 210-220 [PMID: 27493896 DOI: 10.1159/000367767]
5 **Kim KI**, Chung HK, Park JH, Lee YJ, Kang JH. Alpha-fetoprotein-targeted reporter gene expression imaging in hepatocellular carcinoma. *World J Gastroenterol* 2016; **22**: 6127-6134 [PMID: 27468205 DOI: 10.3748/wjg.v22.i27.6127]
6 **Trojan J**, Zangos S, Schnitzbauer AA. Diagnostics and Treatment of Hepatocellular Carcinoma in 2016: Standards and Developments. *Visc Med* 2016; **32**: 116-120 [PMID: 27413729 DOI: 10.1159/000445730]
7 **Tang ZY**. Hepatocellular carcinoma--cause, treatment and metastasis. *World J Gastroenterol* 2001; **7**: 445-454 [PMID: 11819809 DOI: 10.3748/wjg.v7.i4.445]
8 **Hu L**, Lau SH, Tzang CH, Wen JM, Wang W, Xie D, Huang M, Wang Y, Wu MC, Huang JF, Zeng WF, Sham JS, Yang M, Guan XY. Association of Vimentin overexpression and hepatocellular carcinoma metastasis. *Oncogene* 2004; **23**: 298-302 [PMID: 14647434 DOI: 10.1038/sj.onc.1206483]
9 **Harper JW**, Elledge SJ. The DNA damage response: ten years after. *Mol Cell* 2007; **28**: 739-745 [PMID: 18082599 DOI: 10.1016/j.molcel.2007.11.015]
10 **Turnbull AP**, Ioannidis S, Krajewski WW, Pinto-Fernandez A, Heride C, Martin ACL, Tonkin LM, Townsend EC, Buker SM, Lancia DR, Caravella JA, Toms AV, Charlton TM, Lahdenranta J, Wilker E, Follows BC, Evans NJ, Stead L, Alli C, Zarayskiy VV, Talbot AC, Buckmelter AJ, Wang M, McKinnon CL, Saab F, McGouran JF, Century H, Gersch M, Pittman MS, Marshall CG, Raynham TM, Simcox M, Stewart LMD, McLoughlin SB, Escobedo JA, Bair KW, Dinsmore CJ, Hammonds TR, Kim S, Urbé S, Clague MJ, Kessler BM, Komander D. Molecular basis of USP7 inhibition by selective small-molecule inhibitors. *Nature* 2017; **550**: 481-486 [PMID: 29045389 DOI: 10.1038/nature24451]
11 **Hou CC**, Yang WX. New insights to the ubiquitin-proteasome pathway (UPP) mechanism during spermatogenesis. *Mol Biol Rep* 2013; **40**: 3213-3230 [PMID: 23268313 DOI: 10.1007/s11033-012-2397-y]
12 **Shiloh Y**. ATM and related protein kinases: safeguarding genome integrity. *Nat Rev Cancer* 2003; **3**: 155-168 [PMID: 12612651 DOI: 10.1038/nrc1011]
13 **Cimprich KA**, Cortez D. ATR: an essential regulator of genome integrity. *Nat Rev Mol Cell Biol* 2008; **9**: 616-627 [PMID: 18594563 DOI: 10.1038/nrm2450]
14 **Mu JJ**, Wang Y, Luo H, Leng M, Zhang J, Yang T, Besusso D, Jung SY, Qin J. A proteomic analysis of ataxia telangiectasia-mutated (ATM)/ATM-Rad3-related (ATR) substrates identifies the ubiquitin-proteasome system as a regulator for DNA damage checkpoints. *J Biol Chem* 2007; **282**: 17330-17334 [PMID: 17478428 DOI: 10.1074/jbc.C700079200]
15 **Matsuoka S**, Ballif BA, Smogorzewska A, McDonald ER 3rd, Hurov KE, Luo J, Bakalarski CE, Zhao Z, Solimini N, Lerenthal Y, Shiloh Y, Gygi SP, Elledge SJ. ATM and ATR substrate analysis reveals extensive protein networks responsive to DNA damage. *Science* 2007; **316**: 1160-1166 [PMID: 17525332 DOI: 10.1126/science.1140321]
16 **Smolka MB**, Albuquerque CP, Chen SH, Zhou H. Proteome-wide identification of *in vivo* targets of DNA damage

checkpoint kinases. *Proc Natl Acad Sci U S A* 2007; **104**: 10364-10369 [PMID: 17563356 DOI: 10.1073/pnas.0701622104]
17 **Fu X**, Yucer N, Liu S, Li M, Yi P, Mu JJ, Yang T, Chu J, Jung SY, O'Malley BW, Gu W, Qin J, Wang Y. RFWD3-Mdm2 ubiquitin ligase complex positively regulates p53 stability in response to DNA damage. *Proc Natl Acad Sci U S A* 2010; **107**: 4579-4584 [PMID: 20173098 DOI: 10.1073/pnas.0912094107]
18 **Elia AE**, Wang DC, Willis NA, Boardman AP, Hajdu I, Adeyemi RO, Lowry E, Gygi SP, Scully R, Elledge SJ. RFWD3-Dependent Ubiquitination of RPA Regulates Repair at Stalled Replication Forks. *Mol Cell* 2015; **60**: 280-293 [PMID: 26474068 DOI: 10.1016/j.molcel.2015.09.011]
19 **Zhang W**, Sidhu SS. Development of inhibitors in the ubiquitination cascade. *FEBS Lett* 2014; **588**: 356-367 [PMID: 24239534 DOI: 10.1016/j.febslet.2013.11.003]
20 **Knies K**, Inano S, Ramírez MJ, Ishiai M, Surrallés J, Takata M, Schindler D. Biallelic mutations in the ubiquitin ligase RFWD3 cause Fanconi anemia. *J Clin Invest* 2017; **127**: 3013-3027 [PMID: 28691929 DOI: 10.1172/JCI92069]
21 **Wolberger C**. Mechanisms for regulating deubiquitinating enzymes. *Protein Sci* 2014; **23**: 344-353 [PMID: 24403057 DOI: 10.1002/pro.2415]
22 **Gong Z**, Chen J. E3 Ligase RFWD3 participates in replication checkpoint control. *J Biol Chem* 2011; **286**: 22308-22313 [PMID: 21504906 DOI: 10.1074/jbc.M111.222869]
23 **Sokratous K**, Hadjisavvas A, Diamandis EP, Kyriacou K. The role of ubiquitin-binding domains in human pathophysiology. *Crit Rev Clin Lab Sci* 2014; **51**: 280-290 [PMID: 24901807 DOI: 10.3109/10408363.2014.915287]
24 **Liu S**, Chu J, Yucer N, Leng M, Wang SY, Chen BP, Hittelman WN, Wang Y. RING finger and WD repeat domain 3 (RFWD3) associates with replication protein A (RPA) and facilitates RPA-mediated DNA damage response. *J Biol Chem* 2011; **286**: 22314-22322 [PMID: 21558276 DOI: 10.1074/jbc.M111.222802]
25 **Feeney L**, Muñoz IM, Lachaud C, Toth R, Appleton PL, Schindler D, Rouse J. RPA-Mediated Recruitment of the E3 Ligase RFWD3 Is Vital for Interstrand Crosslink Repair and Human Health. *Mol Cell* 2017; **66**: 610-621.e4 [PMID: 28575657 DOI: 10.1016/j.molcel.2017.04.021]
26 **Zhang Y**, Zhao X, Zhou Y, Wang M, Zhou G. Identification of an E3 Ligase-encoding gene RFWD3 in non-small cell lung cancer. *Front Med* 2020; **14**: 318-326 [PMID: 31571161 DOI: 10.1007/s11684-019-0708-6]
27 **Jia J**, Yang Y, Yan T, Chen T, Lu G. Down-regulation of RFWD3 inhibits cancer cells proliferation and migration in gastric carcinoma. *Gen Physiol Biophys* 2020; **39**: 363-371 [PMID: 32902405 DOI: 10.4149/gpb_2020009]
28 **Xu F**, Xiao Z, Fan L, Ruan G, Cheng Y, Tian Y, Chen M, Chen D, Wei Y. RFWD3 Participates in the Occurrence and Development of Colorectal Cancer *via* E2F1 Transcriptional Regulation of BIRC5. *Front Cell Dev Biol* 2021; **9**: 675356 [PMID: 34712656 DOI: 10.3389/fcell.2021.675356]
29 **Wang WJ**, Jin WW, Pan J, Wang LB, Zhu RT, Li J, Zhang CX, Liang RP. The expression of ring finger and WD repeat domain 3 in hepatocellular carcinoma and its clinical relevance. *J Hepatopancreat Sur* 2019; **31**: 741-745 [DOI: 10.11952/j.issn.1007-1954.2019.12.009]
30 **Rutgers M**, van Pelt MJ, Dhert WJ, Creemers LB, Saris DB. Evaluation of histological scoring systems for tissue-engineered, repaired and osteoarthritic cartilage. *Osteoarthritis Cartilage* 2010; **18**: 12-23 [PMID: 19747584 DOI: 10.1016/j.joca.2009.08.009]
31 **McLin VA**, Rankin SA, Zorn AM. Repression of Wnt/beta-catenin signaling in the anterior endoderm is essential for liver and pancreas development. *Development* 2007; **134**: 2207-2217 [PMID: 17507400 DOI: 10.1242/dev.001230]
32 **Brafman D**, Willert K. Wnt/β-catenin signaling during early vertebrate neural development. *Dev Neurobiol* 2017; **77**: 1239-1259 [PMID: 28799266 DOI: 10.1002/dneu.22517]
33 **Fatima S**, Luk JM, Poon RT, Lee NP. Dysregulated expression of dickkopfs for potential detection of hepatocellular carcinoma. *Expert Rev Mol Diagn* 2014; **14**: 535-548 [PMID: 24809435 DOI: 10.1586/14737159.2014.915747]
34 **Murillo-Garzón V**, Kypta R. WNT signalling in prostate cancer. *Nat Rev Urol* 2017; **14**: 683-696 [PMID: 28895566 DOI: 10.1038/nrurol.2017.144]
35 **Lee HC**, Kim M, Wands JR. Wnt/Frizzled signaling in hepatocellular carcinoma. *Front Biosci* 2006; **11**: 1901-1915 [PMID: 16368566 DOI: 10.2741/1933]
36 **Nakamura T**, Aoki S, Kitajima K, Takahashi T, Matsumoto K, Nakamura T. Molecular cloning and characterization of Kremen, a novel kringle-containing transmembrane protein. *Biochim Biophys Acta* 2001; **1518**: 63-72 [PMID: 11267660 DOI: 10.1016/s0167-4781(01)00168-3]
37 **Mishra SK**, Funair L, Cressley A, Gittes GK, Burns RC. High-affinity Dkk1 receptor Kremen1 is internalized by clathrin-mediated endocytosis. *PLoS One* 2012; **7**: e52190 [PMID: 23251700 DOI: 10.1371/journal.pone.0052190]
38 **Nakamura T**, Nakamura T, Matsumoto K. The functions and possible significance of Kremen as the gatekeeper of Wnt signalling in development and pathology. *J Cell Mol Med* 2008; **12**: 391-408 [PMID: 18088386 DOI: 10.1111/j.1582-4934.2007.00201.x]

World Journal of Gastroenterology

Submit a Manuscript: https://www.f6publishing.com

World J Gastroenterol 2022 July 21; 28(27): 3455-3475

DOI: 10.3748/wjg.v28.i27.3455

ISSN 1007-9327 (print) ISSN 2219-2840 (online)

ORIGINAL ARTICLE

Basic Study

Associations of gut microbiota with dyslipidemia based on sex differences in subjects from Northwestern China

Lei Guo, Yang-Yang Wang, Ji-Han Wang, He-Ping Zhao, Yan Yu, Guo-Dong Wang, Kun Dai, Yu-Zhu Yan, Yan-Jie Yang, Jing Lv

Specialty type: Gastroenterology and hepatology

Provenance and peer review: Invited article; Externally peer reviewed.

Peer-review model: Single blind

Peer-review report's scientific quality classification

Grade A (Excellent): 0
Grade B (Very good): B, B
Grade C (Good): 0
Grade D (Fair): D
Grade E (Poor): 0

P-Reviewer: Amedei A, Italy; Panduro A, Mexico; Papazafiropoulou A, Greece

Received: February 18, 2022
Peer-review started: February 18, 2022
First decision: May 9, 2022
Revised: May 17, 2022
Accepted: June 20, 2022
Article in press: June, 20, 2022
Published online: July 21, 2022

Lei Guo, Department of Spine Surgery, Honghui Hospital, Xi'an Jiaotong University, Xi'an 710054, Shaanxi Province, China

Yang-Yang Wang, School of Electronics and Information, Northwestern Polytechnical University, Xi'an 710129, Shaanxi Province, China

Ji-Han Wang, Institute of Medical Research, Northwestern Polytechnical University, Xi'an 710072, Shaanxi Province, China

He-Ping Zhao, Yan Yu, Yu-Zhu Yan, Jing Lv, Department of Clinical Laboratory, Honghui Hospital, Xi'an Jiaotong University, Xi'an 710054, Shaanxi Province, China

Guo-Dong Wang, Department of Quality Control, Xi'an Mental Health Center, Xi'an 710100, Shaanxi Province, China

Kun Dai, Department of Clinical Laboratory, Yanliang Railway Hospital of Xi'an, Xi'an 710089, Shaanxi Province, China

Yan-Jie Yang, Department of Cardiology, The First Affiliated Hospital of Xi'an Jiaotong University, Xi'an 710061, Shaanxi Province, China

Corresponding author: Jing Lv, MD, Doctor, Department of Clinical Laboratory, Honghui Hospital, Xi'an Jiaotong University, No. 555 You Yi Dong Road, Xi'an 710054, Shaanxi Province, China. lvjing-1219@163.com

Abstract

BACKGROUND

The gut microbiota (GM) has been proven to play a role in the regulation of host lipid metabolism, which provides a new theory about the pathogenesis of dyslipidemia. However, the associations of GM with dyslipidemia based on sex differences remain unclear and warrant elucidation.

AIM

To investigate the associations of GM features with serum lipid profiles based on sex differences in a Chinese population.

METHODS

This study ultimately recruited 142 participants (73 females and 69 males) at

Honghui Hospital, Xi'an Jiaotong University. The anthropometric and blood metabolic parameters of all participants were measured. According to their serum lipid levels, female and male participants were classified into a high triglyceride (H_TG) group, a high total cholesterol (H_CHO) group, a low high-density lipoprotein cholesterol (L_HDL-C) group, and a control (CON) group with normal serum lipid levels. Fresh fecal samples were collected for 16S rRNA gene sequencing. UPARSE software, QIIME software, the RDP classifier and the FAPROTAX database were used for sequencing analyses.

RESULTS

The GM composition at the phylum level included Firmicutes and Bacteroidetes as the core GM. Different GM features were identified between females and males, and the associations between GM and serum lipid profiles were different in females and males. The GM features in different dyslipidemia subgroups changed in both female patients and male patients. Proteobacteria, Lactobacillaceae, *Lactobacillus* and *Lactobacillus_salivarius* were enriched in H_CHO females compared with CON females, while Coriobacteriia were enriched in L_HDL-C females. In the comparison among the three dyslipidemia subgroups in females, *Lactobacillus_salivarius* were enriched in H_CHO females, and Prevotellaceae were enriched in L_HDL-C females. Compared with CON or H_TG males, Prevotellaceae, *unidentified_Ruminococcaceae*, *Roseburia* and *Roseburia_inulinivorans* were decreased in L_HDL-C males (P value < 0.05), and linear discriminant analysis effect size analysis indicated an enrichment of the above GM taxa in H_TG males compared with other male subgroups. Additionally, *Roseburia_inulinivorans* abundance was positively correlated with serum TG and total cholesterol levels, and *Roseburia* were positively correlated with serum TG level. Furthermore, Proteobacteria (0.724, 95%CI: 0.567-0.849), Lactobacillaceae (0.703, 95%CI: 0.544-0.832), *Lactobacillus* (0.705, 95%CI: 0.547-0.834) and *Lactobacillus_salivarius* (0.706, 95%CI: 0.548-0.835) could distinguish H_CHO females from CON females, while Coriobacteriia (0.710, 95%CI: 0.547-0.841), Coriobacteriales (0.710, 95%CI: 0.547-0.841), Prevotellaceae (0.697, 95%CI: 0.534-0.830), *Roseburia* (0.697, 95%CI: 0.534-0.830) and *Roseburia_inulinivorans* (0.684, 95%CI: 0.520-0.820) could discriminate H_TG males from CON males. Based on the predictions of GM metabolic capabilities with the FAPROTAX database, a total of 51 functional assignments were obtained in females, while 38 were obtained in males. This functional prediction suggested that cellulolysis increased in L_HDL-C females compared with CON females, but decreased in L_HDL-C males compared with CON males.

CONCLUSION

This study indicates associations of GM with serum lipid profiles, supporting the notion that GM dysbiosis may participate in the pathogenesis of dyslipidemia, and sex differences should be considered.

Key Words: Dyslipidemia; Gut microbiota; 16S rRNA; Sequencing; Sex differences; Northwestern China

Core Tip: Dyslipidemia is the circulating lipid expression of metabolic syndrome, and alterations of gut microbiota (GM) are indicated to participate in the pathogenesis of dyslipidemia; however, little evidence was found in the literature on sex differences for these associations. Our results demonstrated the GM features in different dyslipidemia subgroups in females and males, suggesting a complex interaction between GM and lipid metabolism. Our observations may provide new evidence that different GM taxa may be associated with distinct lipids, and that GM may affect specific aspects of lipid metabolism. More studies are required to propose specific taxa that have the potential to ameliorate dyslipidemia.

Citation: Guo L, Wang YY, Wang JH, Zhao HP, Yu Y, Wang GD, Dai K, Yan YZ, Yang YJ, Lv J. Associations of gut microbiota with dyslipidemia based on sex differences in subjects from Northwestern China. *World J Gastroenterol* 2022; 28(27): 3455-3475

URL: https://www.wjgnet.com/1007-9327/full/v28/i27/3455.htm

DOI: https://dx.doi.org/10.3748/wjg.v28.i27.3455

INTRODUCTION

Obesity has become a worldwide public health challenge, with its prevalence nearly tripled since 1975 [1]. Obesity is defined as a chronic accumulation of excessive lipids in tissues[2], which is related to the disruption of lipid metabolism[3]. As a defect in lipid metabolism, dyslipidemia is defined as any abnormality in blood lipid levels, and is characterized by an elevation of circulating triglyceride (TG), total cholesterol (TC), and low-density lipoprotein cholesterol (LDL-C), or a decrease in high-density lipoprotein cholesterol (HDL-C). Since observational studies have shown that 60%-70% of adults have lipid levels outside the recommended range[4,5], it is essential to reveal the underlying mechanism of dyslipidemia. Circulating lipid levels are known to have an important genetic contribution from over 500 single-nucleotide polymorphisms in more than 150 Loci, explaining approximately 40% of the total individual variation[6]. However, the unexplained 60% variation has been attributed to undiscovered elements and unquantified environmental factors, such as dietary intake and physical activity[7,8]. In recent years, considerable progress has been made in elucidating the mechanism responsible for dyslipidemia, and accumulated evidence has shown that the gut microbiota (GM) may play a potential role in obesity and related metabolic diseases, such as dyslipidemia[9-12].

The human gastrointestinal tract harbors over 100 trillion microorganisms[13], and the gut bacteria having effects on human health are the most prevalent and well-studied. In humans, GM profiles vary among different ethnicities (host genetics) and between different sexes[14,15], and are mainly shaped by early life events and stabilize in adolescence[16]. However, its composition and activity can be dynamic, and may be altered dramatically by multiple factors, such as medications, chronic dietary patterns and other environmental exposures[15,17,18]. This "microbial organ" has been recognized to perform various physiological functions[19-21], and is often called "a new virtual metabolic organ"[22,23]. The first indication of associations between GM and disorder statuses were for inflammation[24], and altered GM community (dysbiosis) has now been established in the development of cardiometabolic phenotypes[25]. These lines of evidence have raised an interest in GM as an important candidate in accounting for the unexplained variation in serum lipid levels in humans, and as a target for the therapeutic benefit of dyslipidemia[26]. Recent studies have convincingly linked GM to dyslipidemia, and GM was reported to explain substantial variation in TG and HDL-C levels independent of genetic factors in a Dutch study[26]. In addition, accumulating data from animal studies demonstrate that GM can affect host lipid metabolism through multiple direct and indirect biological mechanisms[27,28]. Nevertheless, determining associations between GM and host lipid metabolism remains a challenge in humans. Furthermore, sex is an important factor that may influence GM profiles, and sex differences can be observed in serum lipid profiles[29-31]. However, the relationship between GM and dyslipidemia based on sex differences remains unclear.

Collectively, ethnicity, geography and sex are potent factors that could influence the GM community [14,15,32]. Thus, this study focused on the associations of GM features with dyslipidemia based on sex differences in a northwestern Chinese population. We first reveal sex differences regarding GM features and then introduce dyslipidemia, highlighting its intricate relationships with GM, and discuss possible altered GM functions.

MATERIALS AND METHODS

Study design

From July 2018 to January 2020, this study recruited 206 adult individuals (107 females and 99 males) from the outpatient clinics at Honghui Hospital, Xi'an Jiaotong University, China. Individuals were excluded if one of the following conditions existed: (1) With any gastrointestinal diseases, infectious or chronic diseases, serious systematic dysfunctions, or surgery histories of the gastrointestinal tract; (2) Taking any medications that could disrupt the original GM community, such as probiotics or prebiotics, antimicrobial therapies, anti-inflammatory drugs, acid-suppressing drugs, immunosuppressants, or anti-dyslipidemia/anti-dysglycemia/anti-hypertension drugs within the past month prior to sampling [33]; and (3) Females who were pregnant or lactating. The individuals who met the above conditions were included as participants in this study, and informed consent was obtained. Finally, 142 participants (73 females and 69 males) were recruited, including 81 dyslipidemia patients and 61 controls (CON) with normal serum lipid levels. Data privacy was ensured by using anonymized identifiers, and the study flow is shown in Figure 1. This study was approved by the Ethical Committee of Honghui Hospital, Xi'an Jiaotong University (Protocol Number: 201801022, approved January 8, 2018).

Measurement of anthropometric parameters

On their first visit, related medical information was documented for all participants. Body weight (W) and height (H) were measured without shoes and heavy clothing to the nearest 0.1 cm and 0.1 kg, respectively. Waist circumference (WC) was measured in the middle of the lower rib margin and the iliac crest with a nonexpandable tape to the nearest 0.1 cm in the standing position. Body mass index

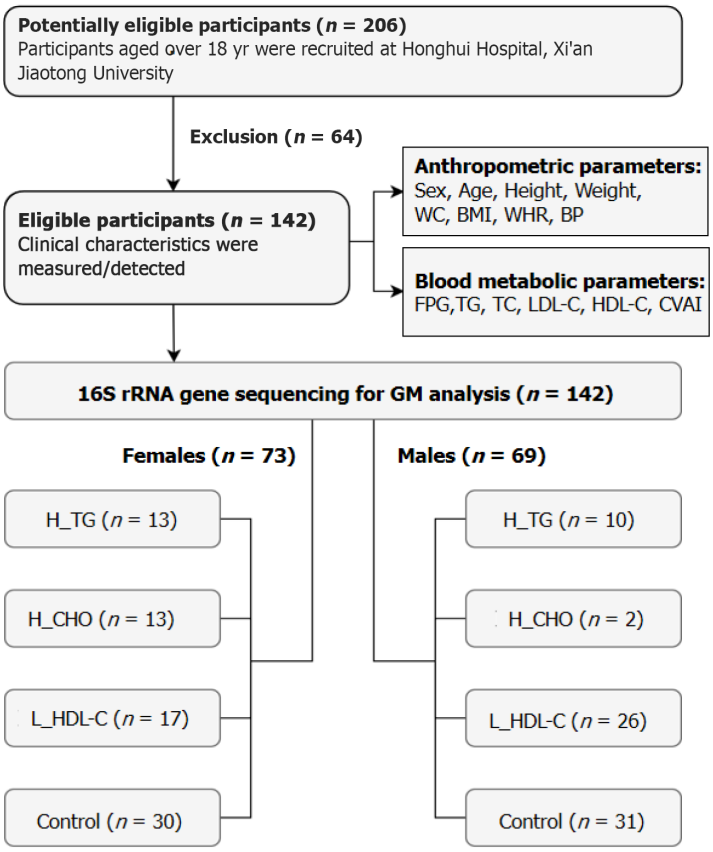

DOI: 10.3748/wjg.v28.i27.3455

Figure 1 Flow chart of this study. WC: Waist circumference; BMI: Body mass index; WHR: Waist circumference/height ratio; BP: Blood pressure; FPG: Fasting plasma glucose; TG: Triglyceride; TC: Total cholesterol; LDL-C: Low-density lipoprotein cholesterol; HDL-C: High-density lipoprotein cholesterol; CVAI: Chinese visceral adiposity index; GM: Gut microbiota; H_TG: High triglyceride group; H_CHO: High cholesterol group; L_HDL-C: Low high-density lipoprotein cholesterol group.

(BMI) and WC/height ratio (WHR) were calculated accordingly. Blood pressure (BP) was assessed using a medical electronic sphygmomanometer (HEM-7130 professional, OMRON, Dalian, China) on the left arm positioned at the heart level with palm face up in a sitting position. The participants were required to rest in a seated position for at least 5 min before BP assessment, with triplicate measurements at 1-min intervals. All equipment was calibrated at the beginning of the study.

Detection and computation of metabolic indicators

Venous blood samples were drawn from an antecubital vein in the morning following an overnight (at least 8 h) fast. Levels of fasting plasma glucose, TG, TC, LDL-C and HDL-C were detected by an automatic biochemical analyzer (Cobas c701, Roche, Mannheim, Germany). This instrument system was calibrated regularly. Moreover, the Chinese visceral adiposity index (CVAI) was calculated using the formula[34]: CVAI for females = -187.32 + 1.71 × age + 4.23 × BMI + 1.12 × WC (cm) + 39.76 × Log_{10}TG (mmol/L) - 11.66 × HDL-C (mmol/L), and CVAI for males = -267.93 + 0.68 × age + 0.03 × BMI + 4.00 × WC + 22.00 × Log_{10}TG - 16.32 × HDL-C.

Diagnostic criteria and grouping

In accordance with the "Guidelines for prevention and treatment of dyslipidemia in Chinese adults" (revised in 2016)[35] and the stratification standard of dyslipidemia in the primary prevention population of arteriosclerotic cardiovascular disease in China[36], dyslipidemia was defined as the presence of one or more abnormal serum lipid levels without any lipid-lowering medication: TG ≥ 1.7 mmol/L, TC ≥ 5.2 mmol/L, LDL-C ≥ 3.4 mmol/L, and/or HDL-C < 1.0 mmol/L. Subsequently, participants were divided into subgroups according to their serum lipid profiles. Specifically, patients were classified into the high TG (H_TG) group if only high TG level existed. Patients with increased serum TC and/or LDL-C levels and without HDL-C or TG abnormalities were classified into the high cholesterol (H_CHO) group. Patients were classified into the low HDL-C (L_HDL-C) group if only low serum HDL-C level existed. Participants with normal serum lipid profiles served as CON.

Fecal sample collection, DNA extraction, and 16S rRNA gene sequencing

Fresh fecal samples were collected from each participant at home, and stored in foam boxes with frozen cold packs[37]. Within 6 h after defecation, all fecal samples were transported to the Clinical Laboratory of Honghui Hospital, Xi'an Jiaotong University, and immediately stored at -80 °C until further processing. Genomic DNA was extracted from all samples using the QIAamp Fast DNA Stool Mini Kit (Qiagen, Hilden, Germany) following the manufacturer's instructions. After quality evaluation and concentration determination, DNA samples, greater than 1 μg and with an OD value between 1.8-2.0, were considered to be qualified for subsequent sequencing. Then, the V3-V4 regions of the 16S rRNA gene were amplified by universal primers (338F: 5'-ACT CCT ACG GGA GGC AGC AG-3'; 806R: 5'-GGA CTA CHV GGG TWT CTA AT-3') with barcodes, and all PCRs were performed using Phusion® High Fidelity PCR Master Mix (New England Biolabs, Ipswich, MA, United States). Next, the PCR products were mixed and purified using a GeneJET™ Gel Extraction Kit (Thermo Scientific, Waltham, MA, United States). The sequencing library for each sample was constructed with the NEB Next® Ultra ™ DNA Library Prep Kit for Illumina (New England Biolabs, Ipswich, MA, United States), and library quality was assessed on a Qubit® 2.0 Fluorometer (Thermo Scientific, Waltham, MA, United States). Finally, the generated libraries were pair-end (2 × 250 bp) sequenced on the Illumina NovaSeq 6000 platform (Illumina, San Diego, CA, United States).

16S rRNA gene sequencing analyses

UPARSE (v7.0.1001) and QIIME software (v1.7.0) were introduced for sequencing analyses. According to a similarity threshold of 97%, acquired clean reads with high quality were de novo clustered into the same operational taxonomic unit (OTU), and the representative sequence of each OTU was screened and used to annotate taxonomic information based on the RDP classifier (v2.2). The GM diversity and composition were assessed based on the annotated OTUs. The alpha diversity (α-diversity) of GM was estimated by four indices, including Chao1, abundance coverage-based estimator (Ace), Shannon and Simpson. The comparisons of these indices between groups were conducted by the Wilcoxon rank-sum test, using function *wilcox.test* from the R package stats. To investigate the significance of differences in the GM community, beta diversity (β-diversity) was estimated using the unweighted UniFrac method to calculate the distances between samples, and visualized by the principal coordinates analysis (PCoA) model. The "*WGCNA*", "*stats*" and "*ggplot2*" packages in R were utilized. The top ten GM taxa sorted by higher relative abundances at the six taxonomic levels, including phylum, class, order, family, genus and species, were identified and visualized in each group. The linear discriminant analysis (LDA) effect size (LEfSe) algorithm was applied to identify the enriched significant taxa in each group. The LDA score threshold was set to 2 on a log10 scale. The FAPROTAX (v1.2.2) database, containing 90 different types of metabolic assignments, was introduced to obtain the functional information of the GM community[38], and the differences between groups were assessed by the Wilcoxon rank-sum test, with a P value < 0.05 considered significant.

Statistical analysis

SPSS (v23.0.0.0, IBM SPSS Inc., Chicago, IL), R platform (v4.0.2, R Foundation, Vienna, Austria), GraphPad Prism (v8.4.3, GraphPad Software Inc., San Diego, CA, United States) and MedCalc (v19.0.4, MedCalc Software Bvba, Ostend, Belgium) were employed for statistical analysis and figure construction. The normal distribution of quantitative variables was assessed by the Shapiro-Wilk test. Clinical parameters are presented as the mean ± SD, and were analyzed among groups by the variance analysis (ANOVA) or Welch's ANOVA depending on the homogeneity of variance. In addition, the Games-Howell test was used for multiple comparisons if a P value < 0.05 existed. The "*ggcorrplot*" package in R was utilized for Spearman correlation analysis between clinical parameters. Moreover, Spearman correlation analysis was also applied to evaluate the potential associations between GM features and clinical parameters, using the function *cor.test (method = spearman)* in R. Receiver operating characteristic (ROC) curve analysis, with areas under the curve, was applied to evaluate the diagnostic performance of specific GM taxa. All statistical tests with a P value < 0.05 were considered significant.

The bioinformatics analyses and statistical methods/techniques mentioned in this study were conducted, verified and reviewed by our expert Ji-Han Wang, PhD, from Institute of Medical Research, Northwestern Polytechnical University, and Guo-Dong Wang, Master Degree, from Department of Quality Control, Xi'an Mental Health Center.

RESULTS

Basic information of the study population

The present study finally included 142 participants (73 females and 69 males), as shown in Figure 1. Table 1 shows the clinical characteristics of all the participants grouped by sex and serum lipid profiles. Serum lipid levels and CVAI showed differences among female subgroups as did height, WC and WHR (P value < 0.05). Serum lipid levels and CVAI showed differences among male subgroups as well (P

Table 1 Clinical characteristics of the study population

	Females					Males				
	High TG	High CHO	Low HDL-C	Control	*P* value	High TG	High CHO	Low HDL-C	Control	*P* value
Number	13	13	17	30		10	2	26	31	
Age (yr)	55 ± 8	56 ± 5	54 ± 16	52 ± 12	0.420	54 ± 12	58 ± 11	52 ± 12	56 ± 13	0.770
Height (cm)	155.0 ± 7.2	147.0 ± 5.8	153.6 ± 5.4	154.3 ± 4.8	0.001[a]	164.7 ± 6.2	160.0 ± 1.2	166.8 ± 5.4	164.8 ± 6.1	0.300
Weight (kg)	61.6 ± 9.3	53.6 ± 8.6	55.0 ± 9.2	55.3 ± 8.8	0.102	65.8 ± 9.0	56.2 ± 4.9	65.0 ± 8.3	61.0 ± 10.5	0.231
WC (cm)	90.2 ± 9.6	85.4 ± 7.2	82.3 ± 7.8	82.4 ± 8.6	0.035[a]	88.3 ± 6.1	75.2 ± 9.5	87.0 ± 8.2	83.1 ± 8.8	0.066
BMI (kg/m^2)	25.7 ± 3.7	24.7 ± 3.3	23.3 ± 3.2	23.2 ± 3.2	0.103	24.2 ± 3.0	22.0 ± 2.2	23.3 ± 2.8	22.4 ± 3.6	0.403
WHR	0.58 ± 0.07	0.58 ± 0.05	0.54 ± 0.06	0.53 ± 0.06	0.017[a]	0.54 ± 0.03	0.47 ± 0.06	0.52 ± 0.05	0.50 ± 0.50	0.153
SBP (mmHg)	141 ± 17	139 ± 17	125 ± 19	129 ± 25	0.127	137 ± 23	136 ± 12	128 ± 21	134 ± 18	0.569
DBP (mmHg)	82 ± 10	78 ± 8	73 ± 9	76 ± 11	0.110	84 ± 12	80 ± 5	78 ± 11	81 ± 10	0.509
FPG (mmol/L)	5.00 ± 1.33	4.96 ± 0.57	5.48 ± 1.17	4.90 ± 0.59	0.346	5.05 ± 0.73	4.85 ± 2.23	4.81 ± 0.80	4.97 ± 1.10	0.895
TG (mmol/L)	2.15 ± 0.48	1.40 ± 0.22	1.01 ± 0.31	1.21 ± 0.33	< 0.001[a]	4.04 ± 0.86	5.75 ± 0.65	3.07 ± 0.76	3.97 ± 0.55	0.012[a]
TC (mmol/L)	4.31 ± 0.50	5.58 ± 0.43	2.57 ± 0.63	0.41 ± 0.67	< 0.001[a]	2.01 ± 0.68	4.26 ± 0.95	1.77 ± 0.54	2.19 ± 0.45	< 0.001[a]
LDL-C (mmol/L)	2.16 ± 0.43	3.44±0.49	1.51 ± 0.56	2.25 ± 0.56	< 0.001[a]	1.13 ± 0.09	1.20 ± 0.27	0.79 ± 0.14	1.48 ± 0.32	0.001[a]
HDL-C (mmol/L)	1.29 ± 0.23	1.75±0.31	0.77 ± 0.15	1.50 ± 0.36	< 0.001[a]	2.98 ± 0.78	4.55 ± 0.92	2.28 ± 0.69	2.49 ± 0.54	< 0.001[a]
CVAI	113.63 ± 25.96	94.16 ± 19.92	86.84 ± 32.86	76.30 ± 37.05	0.008[a]	112.13 ± 26.62	54.08 ± 53.32	103.91 ± 36.87	78.76 ± 38.08	0.011[a]

[a]$P < 0.05$.

Data are presented as mean ± SD. *P* values are from the variance analysis (ANOVA) or Welch's ANOVA depending on the homogeneity of variance. CHO: Cholesterol; WC: Waist circumference; BMI: Body mass index; WHR: Waist circumference/height ratio; SBP: Systolic blood pressure; DBP: Diastolic blood pressure; FPG: Fasting plasma glucose; TG: Triglyceride; TC: Total cholesterol; LDL-C: Low-density lipoprotein cholesterol; HDL-C: High-density lipoprotein cholesterol; CVAI: Chinese visceral adiposity index.

value < 0.05). Please refer to Supplementary Table 1 for detailed information and differences between females and males. The correlation analysis between the clinical characteristics of females and males is shown in Figure 2, and indicates positive correlations between the serum lipid indicators.

Diversity analysis of GM in the study population

To identify the associations of GM features with serum lipid profiles, we performed 16S rRNA gene sequencing analyses of GM from fecal samples. After quality CON, sequencing reads from 142 fecal samples were processed to determine the OTUs. Our data indicated that females had more unique OTUs, and the number of common OTUs shared by the female subgroups was larger than that shared by the male subgroups (data not shown).

We evaluated the diversity of the GM community to assess the richness and evenness for females and males, and Shannon and Simpson indices suggested a higher α-diversity in females (*P* value < 0.05, Figure 3A). In addition, a dissimilarity between females and males was observed according to the visualized PCoA model for β-diversity analysis (Figure 3B). Since sex is an important determinant of GM and serum lipids[30,32,39], the study population was divided into a female group and a male group for the subsequent analyses.

To reveal the associations of GM diversity with serum lipid profiles based on sex differences, we conducted analogous analyses in the enrolled females and males. Our results showed that the α-diversity of GM was different in different dyslipidemia subgroups in females and males (Figure 3C and D). Of note, the α-diversity in L_HDL-C females was higher than that in CON females (*P* value < 0.05), while it was lower in L_HDL-C males than that in CON males (*P* value < 0.05). Additionally, the α-diversity of GM in H_TG males was higher than that in L_HDL-C males (*P* value < 0.05). The PCoA results suggested that the GM community in different dyslipidemia subgroups varied from that in the CON group in females and males, respectively, but could not be separated accurately and clearly (data not shown). Furthermore, the α-diversity of GM was found to be correlated with the serum lipid profiles and CVAI in males (Figure 3E). Specifically, the Chao1, Ace and Shannon indices were positively correlated with the serum HDL-C levels, while the Chao1 and Ace indices were negatively correlated

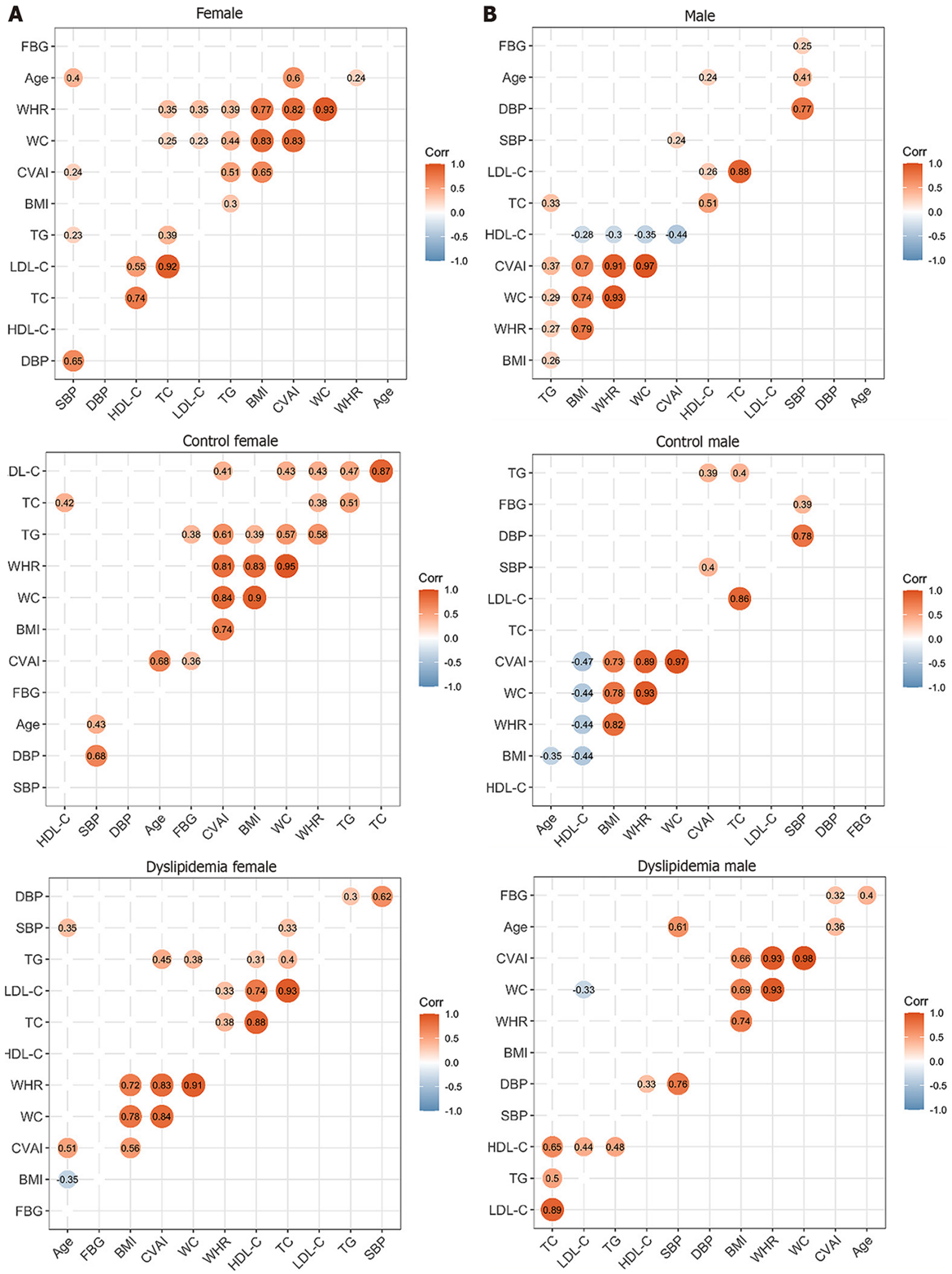

DOI: 10.3748/wjg.v28.i27.3455 **Copyright** ©The Author(s) 2022.

Figure 2 Correlations between the clinical characteristics in the study population. A: Correlations between the clinical characteristics of the enrolled females; B: Correlations between the clinical characteristics of the enrolled males. The circle represents the correlation coefficient of each two parameters (*P* value < 0.05). The number presented in the circle is the correlation coefficient. The larger the absolute value is, the stronger the correlation is. Blue indicates a negative correlation and orange indicates a positive correlation. The depth of the color represents the strength of the correlation. The deeper the color is, the stronger the correlation is. The "*ggcorrplot*" package in R was utilized for Spearman's correlation analysis. WC: Waist circumference; BMI: Body mass index; WHR: Waist circumference/height ratio; SBP: Systolic blood pressure; DBP: Diastolic blood pressure; TG: Triglyceride; TC: Total cholesterol; LDL-C: Low-density lipoprotein cholesterol; HDL-C: High-density lipoprotein cholesterol; CVAI: Chinese visceral adiposity index.

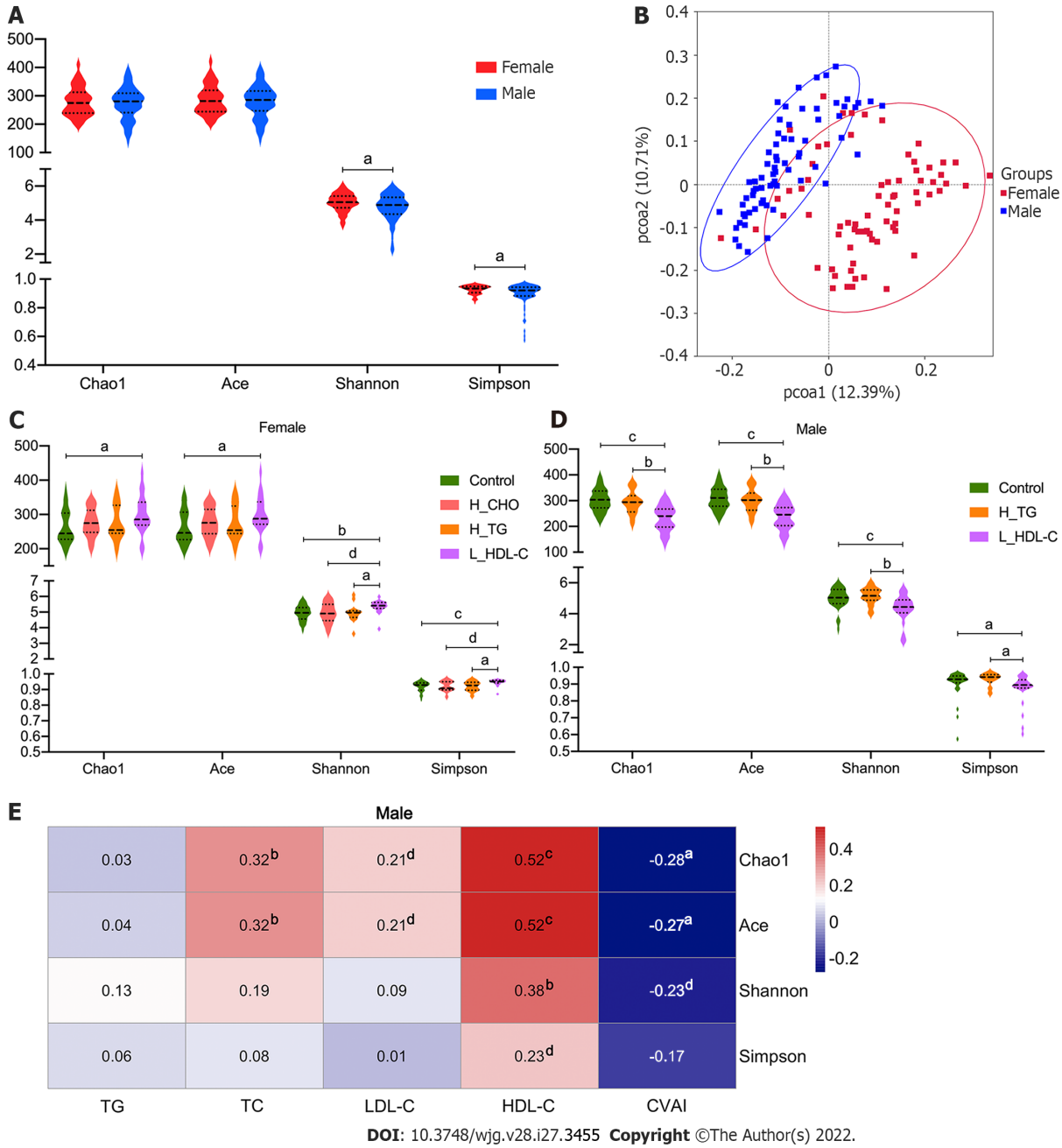

DOI: 10.3748/wjg.v28.i27.3455

Figure 3 Diversity analysis of gut microbiota in the study population. A: Violin plots of α-diversity analysis of gut microbiota (GM) in females and males of the study population. Each plot represents one index of the α-diversity distribution of GM, including Chao1, Ace, Shannon and Simpson indices, for each group. The Wilcoxon rank-sum test was used to evaluate the differences between groups; B: Plots of principal coordinate analysis (PCoA) based on the operational taxonomic unit level in females and males of the study population. Each square represents the GM community in one sample, and the axis title represents the percentage change of interpretation. The distance between squares represents the similarity or dissimilarity of the GM community in the study population, and PCoA analysis was conducted by unweighted UniFrac method; C: Violin plots of α-diversity analysis of GM in females of the study population; D: Violin plots of α-diversity analysis of GM in males of the study population; E: Correlations between GM diversity and serum lipid profiles in males of the study population. Spearman's correlation analysis was conducted. The number presented in each cell is the correlation coefficient. The larger the absolute value is, the stronger the correlation is. Blue indicates a negative correlation and red indicates a positive correlation. The depth of the color represents the strength of the correlation. The deeper the color is, the stronger the correlation is. $^{a}P < 0.05$, $^{b}P < 0.01$, $^{c}P < 0.001$, $^{d}P < 0.1$. TG: Triglyceride; TC: Total cholesterol; LDL-C: Low-density lipoprotein cholesterol; HDL-C: High-density lipoprotein cholesterol; CVAI: Chinese visceral adiposity index; H_CHO: High total cholesterol; H_TG: high triglyceride; L_HDL-C: Low high-density lipoprotein cholesterol.

with CVAI. However, similar results could not be observed in females. The bioinformatics analyses above revealed the associations between the general state of GM and the human serum lipid profiles.

Taxonomic composition of GM in the study population

After diversity analysis, we focused on the relative abundances of GM taxa at six different taxonomic levels in different groups, and the top ten taxa with higher relative abundances at each level are shown in Supplementary Figure 1 for females and males. Similarly, the top ten taxa at each level were

identified in the female subgroups (Figure 4). Consistent with previous data, the GM composition at the phylum level included Firmicutes and Bacteroidetes as the core GM, with lower relative abundances of Actinobacteria, Proteobacteria and others. The most abundant GM taxa were Clostridia, Bacteroidia, Clostridiales, Bacteroides, Ruminococcaceae, Lachnospiraceae, Bacteroidaceae, *Faecalibacterium* and *Bacteroides*. GM taxa with relative abundances of no less than 0.0001 at each level were included in the following analyses. The relative abundances of Proteobacteria, Lactobacillaceae and *Lactobacillus* were no less than 0.010 in H_CHO females, and were greater than those in CON females (P value < 0.05); while the relative abundance of Coriobacteriia was higher in L_HDL-C females than that in CON females (P value < 0.05). In the comparison of H_CHO and L_HDL-C females, Prevotellaceae abundance was greater in L_HDL-C females (P value < 0.05), and *Lactobacillus_salivarius* abundance was greater in H_CHO females (P value < 0.05). In the comparison of H_CHO and H_TG females, *Agathobacter* abundance was higher in H_TG females (P value < 0.05), while the relative abundances of *Ruminococcus_bromii* and *Lactobacillus_salivarius* were higher in H_CHO females (P value < 0.05). Additionally, Prevotellaceae abundance was greater in L_HDL-C females than that in H_TG females (P value < 0.05). Subsequently, analogous comparison analysis was conducted in the male subgroups (Figure 5). The most abundant taxa were Clostridia, Bacteroidia, Clostridiales, Bacteroidales, Ruminococcaceae, Lachnospiraceae, *Faecalibacterium*, *Bifidobacterium*, *Bifidobacterium_pseudocatenulatum* and *Clostridium_disporicum*. In the comparison of L_HDL-C and CON males, the relative abundances of Bacteroidetes, Bacteroidia, Bacteroidales, Prevotellaceae, *unidentified_Ruminococcaceae*, *Roseburia* and *Roseburia_inulinivorans* were lower in L_HDL-C males (P value < 0.05). Meanwhile, Coriobacteriia, Coriobacteriales, Prevotellaceae, *unidentified_Ruminococcaceae*, *Roseburia* and *Roseburia_inulinivorans* were lower in L_HDL-C males than those in H_TG males (P value < 0.05). Interestingly, no differences were observed in the comparison between the H_TG group and CON group (P value > 0.05) in females or males.

LEfSe analysis was conducted in different dyslipidemia subgroups and the CON group in females and males. Compared with CON females (Figure 6), LEfSe analysis revealed the enrichment of Proteobacteria, Lactobacillaceae, *Lactobacillus* and *Lactobacillus_salivarius* in H_CHO females, and the enrichment of Coriobacteriia in L_HDL-C females. In the comparison among the three dyslipidemia subgroups in females, *Lactobacillus_salivarius* were enriched in H_CHO females, and Prevotellaceae were enriched in L_HDL-C females. Simultaneously, LEfSe analysis revealed that Prevotellaceae, *unidentified_Ruminococcaceae*, *Roseburia*, *Roseburia_inulinivorans*, Coriobacteriia, Coriobacteriales and Verrucomicrobiae were enriched in H_TG males compared with other males (Figure 7).

Associations of GM taxa with serum lipid profiles in the study population

To further explore the clinical implications of GM in dyslipidemia, Spearman correlation analysis was introduced to assess the associations between differential GM taxa and the serum lipid profiles/CVAI, and a number of reliable correlations were revealed. In females, a positive correlation of *Bacteroides_coprocola* with serum TG level was observed, while negative correlations of Bacteroidetes, Bacteroidia and Bacteroidales with CVAI were noted (P value < 0.05, Figure 8A). Moreover, more correlations were identified in males (P value < 0.05, Figure 8B). Specifically, the relative abundances of Actinobacteria, unidentified_Actinobacteria, Bifidobacteriales, Bifidobacteriaceae and *Bifidobacterium* were negatively correlated with the serum TG and TC levels, the relative abundance of *Roseburia_inulinivorans* was positively correlated with the serum TG and TC levels, and the relative abundance of *Roseburia* was positively correlated with the serum TG level. In addition, the relative abundances of Leuconostocaceae, *Weissella* and *Weissella_cibaria* were correlated with increased serum TC and LDL-C levels, and the relative abundance of *Bacteroides_vulgatus* was correlated with decreased serum LDL-C level. Furthermore, we found that the relative abundances of Bacteroidetes, Bacteroidia, Bacteroidales, Coriobacteriales, Prevotellaceae, *unidentified_Ruminococcaceae* and *Roseburia_inulinivorans* were positively correlated with serum HDL-C level, and the relative abundances of Bacteroidetes, Bacteroidia, Bacteroidales and *Bacteroides_vulgatus* were negatively correlated with CVAI in males.

To search for the specific GM taxa that may facilitate the differentiation of lipid profiles in dyslipidemia patients from CON, ROC curve analysis was conducted in the female and male subgroups (P value < 0.05, Figure 9). The GM taxa, that effectively distinguished H_CHO females from CON females, were Proteobacteria (0.724, 95%CI: 0.567-0.849), Lactobacillaceae (0.703, 95%CI: 0.544-0.832), *Lactobacillus* (0.705, 95%CI: 0.547-0.834) and *Lactobacillus_salivarius* (0.706, 95%CI: 0.548-0.835). In addition, Coriobacteriia (0.697, 95%CI: 0.546-0.822) may help discriminate L_HDL-C females from CON females. Moreover, the GM taxa in favor of the differentiation of H_TG males from CON males were Coriobacteriia (0.710, 95%CI: 0.547-0.841), Coriobacteriales (0.710, 95%CI: 0.547-0.841), Prevotellaceae (0.697, 95%CI: 0.534-0.830), *Roseburia* (0.697, 95%CI: 0.534-0.830) and *Roseburia_inulinivorans* (0.684, 95%CI: 0.520-0.820). Additionally, seven GM taxa may play a role in distinguishing L_HDL-C males from CON males: Bacteroidetes (0.676, 95%CI: 0.539-0.794), Bacteroidia (0.676, 95%CI: 0.539-0.794), Bacteroidales (0.676, 95%CI: 0.538-0.793), Prevotellaceae (0.685, 95%CI: 0.548-0.802), *unidentified_Ruminococcaceae* (0.687, 95%CI: 0.551-0.804), *Roseburia* (0.662, 95%CI: 0.524-0.782) and *Roseburia_inulinivorans* (0.682, 95%CI: 0.545-0.799).

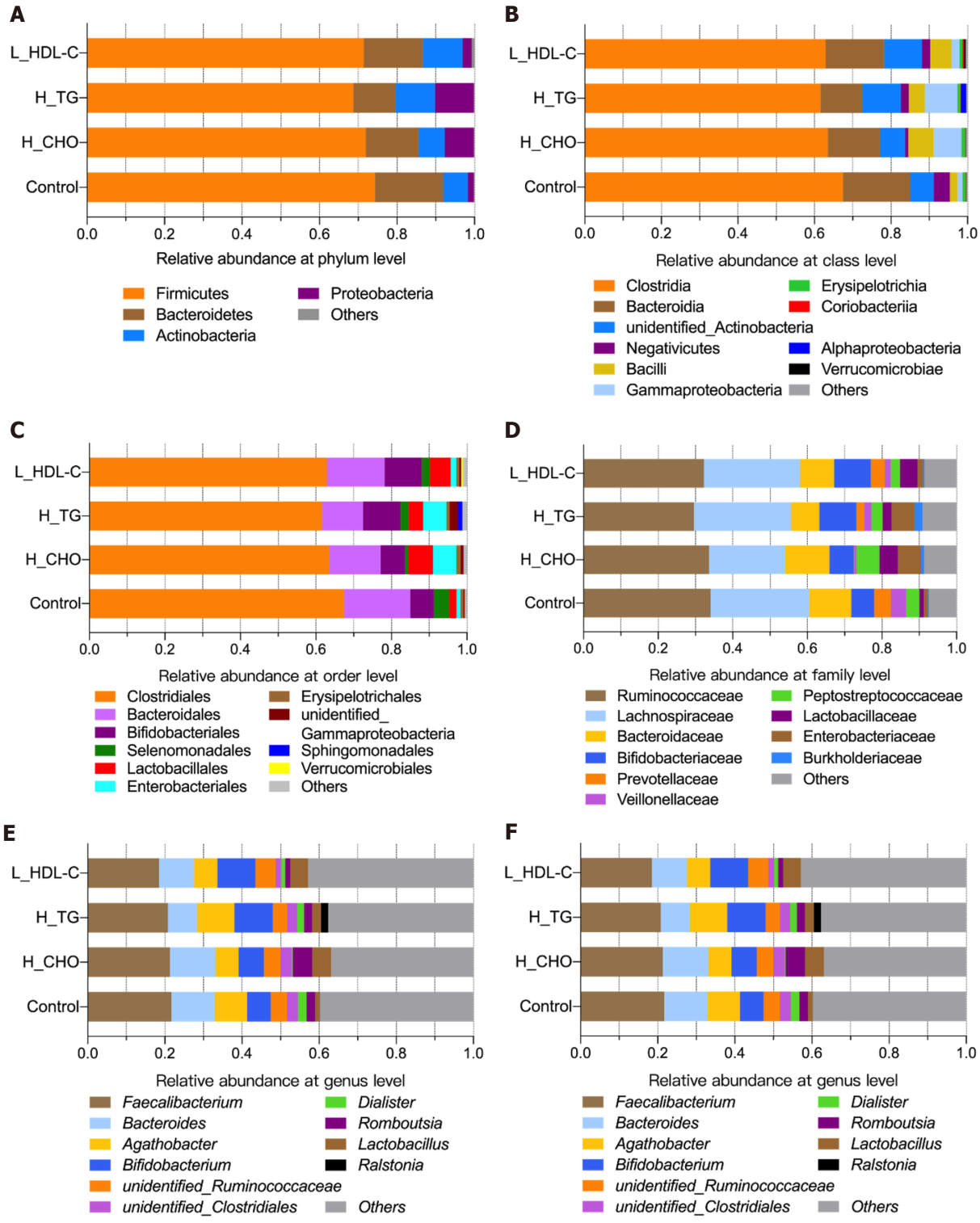

DOI: 10.3748/wjg.v28.i27.3455

Figure 4 The taxonomic composition of gut microbiota in females of the study population. Bar plots show the relative abundances of the top ten taxa at the six taxonomic levels, including phyla, class, orders, family, genus and species, in females. Each component of the cumulative bar chart indicates a phylum, a class, an order, a family, a genus or a species. A: Relative abundance at phylum level; B: Relative abundance at class level; C: Relative abundance at order level; D: Relative abundance at family level; E: Relative abundance at genus level; F: Relative abundance at species level. H_CHO: High total cholesterol; H_TG: high triglyceride; L_HDL-C: Low high-density lipoprotein cholesterol.

Functional analysis of GM in the study population

Finally, we evaluated the functions of the GM community using the FAPROTAX database, and obtained the main metabolic processes of microorganisms associated with different biogeochemical cycles. A total of 51 functional assignments, with relative abundances larger than 0.0001 of the average level, were obtained in females, and 38 assignments were obtained in males. Apparently, GM functions showed

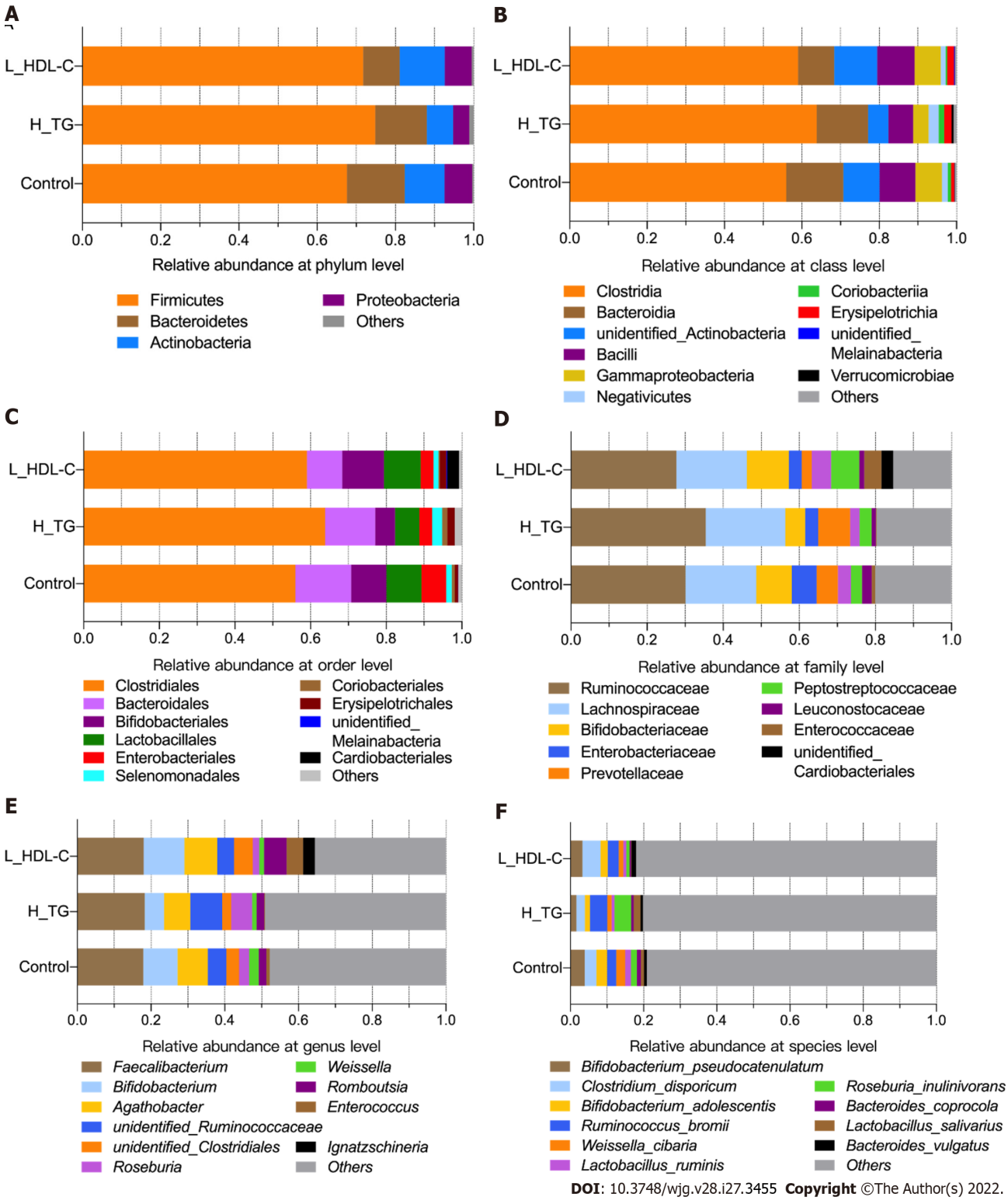

DOI: 10.3748/wjg.v28.i27.3455

Figure 5 The taxonomic composition of gut microbiota in males of the study population. Bar plots show the relative abundances of the top ten taxa at the six taxonomic levels, including phyla, class, orders, family, genus and species, in males. Each component of the cumulative bar chart indicates a phylum, a class, an order, a family, a genus or a species. A: Relative abundance at phylum level; B: Relative abundance at class level; C: Relative abundance at order level; D: Relative abundance at family level; E: Relative abundance at genus level; F: Relative abundance at species level. H_TG: high triglyceride; L_HDL-C: Low high-density lipoprotein cholesterol.

different patterns between females and males, further supporting our strategy of separation and independent analysis in females and males. The top twenty annotated functions with higher relative abundances in females and males are shown in Figure 10. Furthermore, comparison analysis between the different subgroups was conducted. Compared with CON females, the relative abundance of aerobic chemoheterotrophy was increased in H_CHO females (P value < 0.05), while cellulolysis

DOI: 10.3748/wjg.v28.i27.3455

Figure 6 Linear discriminant analysis effect size analysis in females of the study population. Linear discriminant analysis (LDA) scores indicate differentially represented gut microbiota taxa (biomarkers) in each female subgroups. The length of each bar represents the LDA score format with log 10, and the logarithmic threshold for discriminative features was set to 2.0. H_CHO: High total cholesterol; H_TG: high triglyceride; L_HDL-C: Low high-density lipoprotein cholesterol.

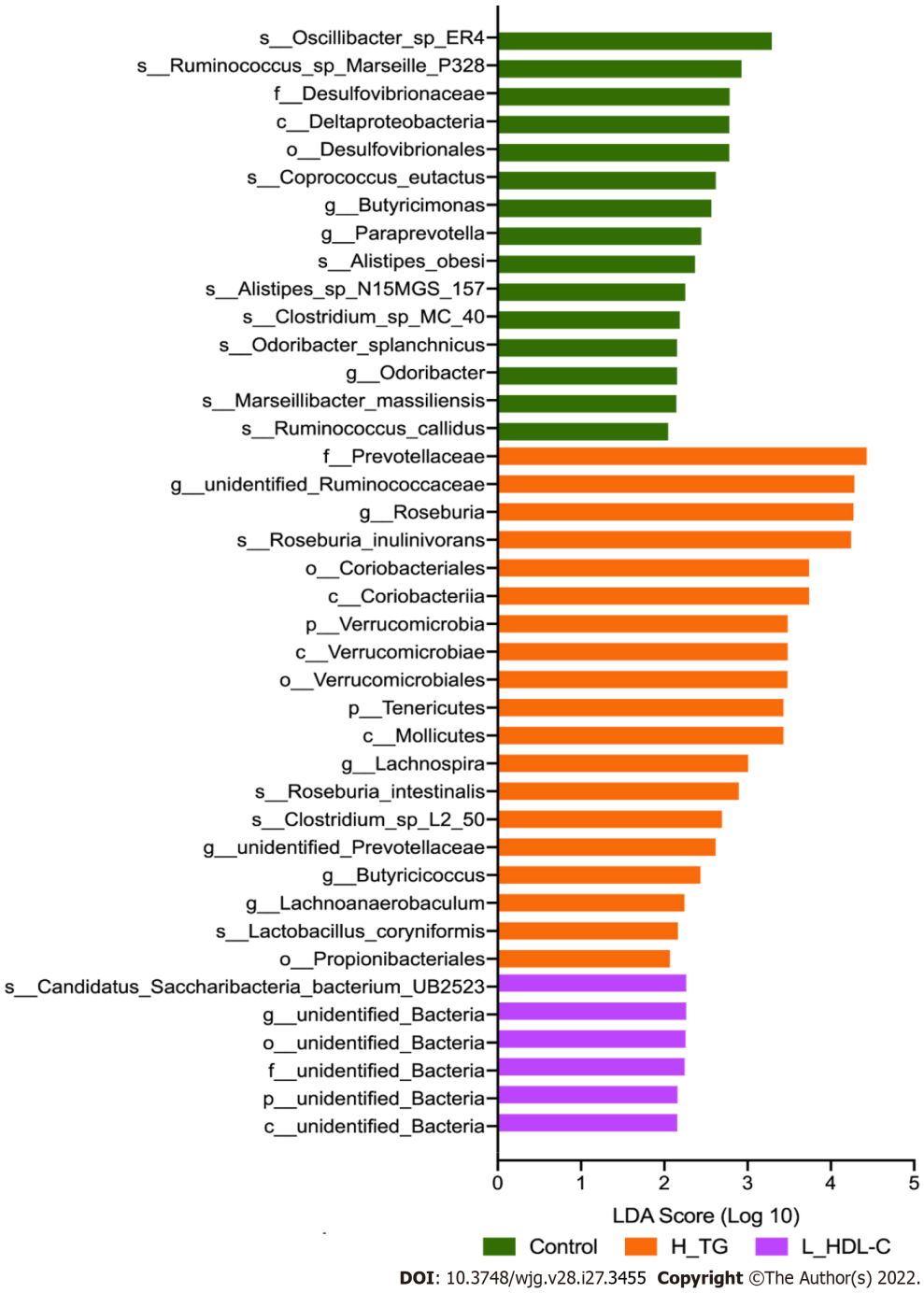

DOI: 10.3748/wjg.v28.i27.3455

Figure 7 Linear discriminant analysis effect size analysis in males of the study population. Linear discriminant analysis (LDA) scores indicate differentially represented gut microbiota taxa (biomarkers) in each male subgroups. The length of each bar represents the LDA score format with log 10, and the logarithmic threshold for discriminative features was set to 2.0. H_TG: high triglyceride; L_HDL-C: Low high-density lipoprotein cholesterol.

abundance was increased in L_HDL-C females (P value < 0.05). Additionally, cellulolysis abundance was increased in L_HDL-C females when compared with that in H_CHO females (P value < 0.05). Compared with CON males, the relative abundances of sulfate respiration, respiration of sulfur compounds and cellulolysis were decreased in L_HDL-C males (P value < 0.05), while the relative abundance of nitrate respiration was increased in L_HDL-C males (P value < 0.05).

DISCUSSION

Dyslipidemia is considered a defect of lipid metabolism in circulation, characterized by increased or decreased levels of serum lipids. Notably, alterations in the GM community may participate in the pathogenesis of dyslipidemia, and the GM composition could be influenced by sex, host genotype and

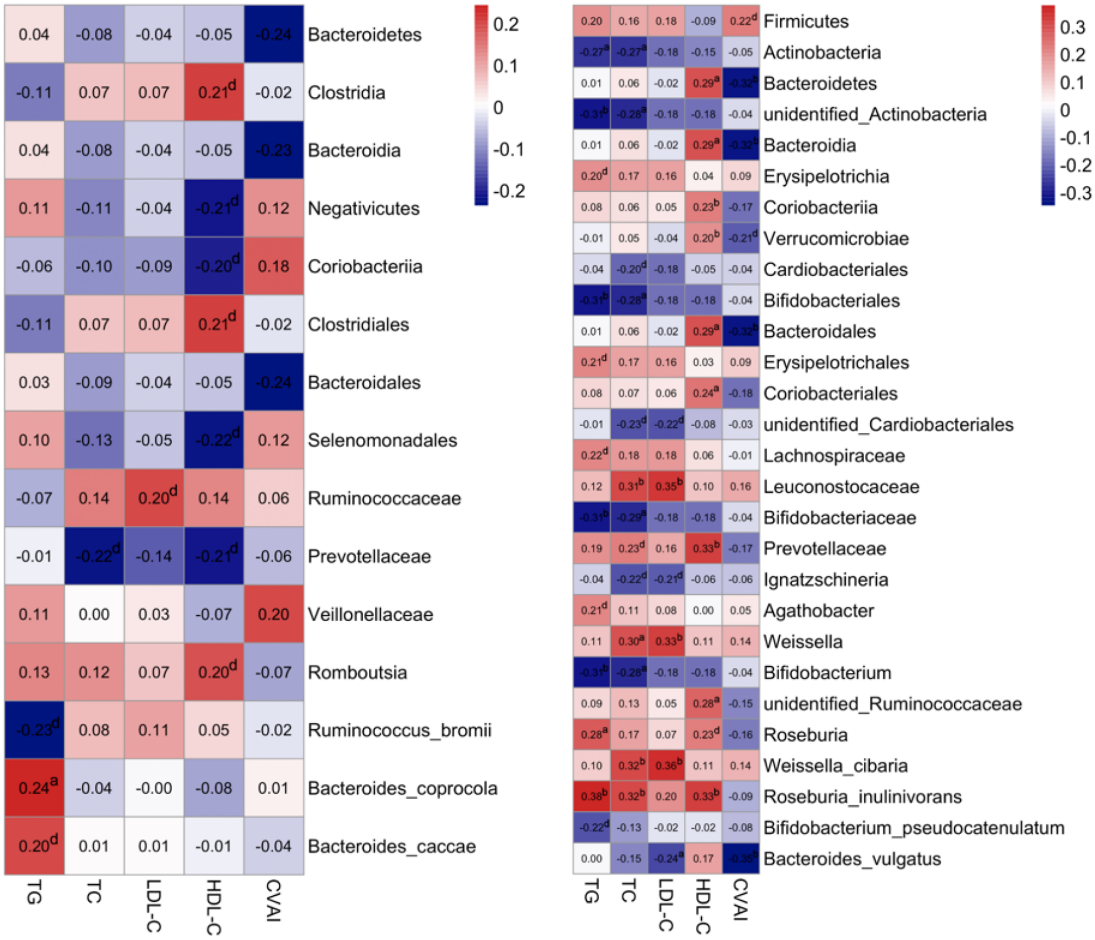

DOI: 10.3748/wjg.v28.i27.3455

Figure 8 Associations of gut microbiota taxa with serum lipid indicators in the study population. A: Correlations of gut microbiota (GM) taxa with serum lipid indicators in females. Spearman's correlation analysis was conducted. The number presented in each cell is the correlation coefficient. The larger the absolute value is, the stronger the correlation is. Blue indicates a negative correlation and red indicates a positive correlation. The depth of the color represents the strength of the correlation. The deeper the color is, the stronger the correlation is; B: Correlations of GM taxa with serum lipid indicators in males. $^{a}P < 0.05$, $^{b}P < 0.01$, $^{d}P < 0.1$. TG: Triglyceride; TC: Total cholesterol; LDL-C: Low-density lipoprotein cholesterol; HDL-C: High-density lipoprotein cholesterol; CVAI: Chinese visceral adiposity index.

geographic location. To our knowledge, little evidence is present in the literature on the correlations between GM and serum lipids based on sex differences[39]; hence, the initial objective of this study was to identify the associations of GM features with serum lipid profiles based on sex differences in a Chinese population.

Considered as a whole, there were significant differences in serum lipid profiles and GM features between females and males. Specifically, females have higher GM diversities, and the GM composition was quite different from that in males, which is consistent with previous data[40]. In addition, the functional analysis of GM also showed an obvious dissimilarity between females and males, further supporting our strategy of respective GM analysis in females and males[14]. Of note, the associations between GM and dyslipidemia in humans have been investigated and demonstrated by various studies, suggesting the alteration of GM in patients with impaired lipid metabolism[28,41]. For instance, Cotillard *et al*[42] noted that reduced GM richness, commonly observed in obese patients, was linked to increased serum TG and TC levels. Following that study, more studies have demonstrated negative correlations of circulating TG and LDL-C levels with GM diversity, and a positive correlation of HDL-C with GM richness[9,26,43,44]. Moreover, certain GM taxa were found to be correlated with specific lipid profiles, suggesting that different GM taxa may affect distinct classes of lipids[26,42,43]. Although the present data have not clearly defined the GM pattern of patients with dyslipidemia, these observations provide new avenues for validation and follow-up studies. Therefore, dyslipidemia female and male patients in this study were divided into a H_TG group, a H_CHO group and a L_HDL-C group, for a more targeted investigation and interpretation.

As an important indicator of the GM community and a general measure of gut health, higher GM diversities have been proposed to be associated with healthy lipid levels, such as increased HDL-C and decreased TG levels[26]. Our results showed a positive correlation between GM diversities and the serum HDL-C level in males, consistent with previous data[26]. Additionally, GM diversities were

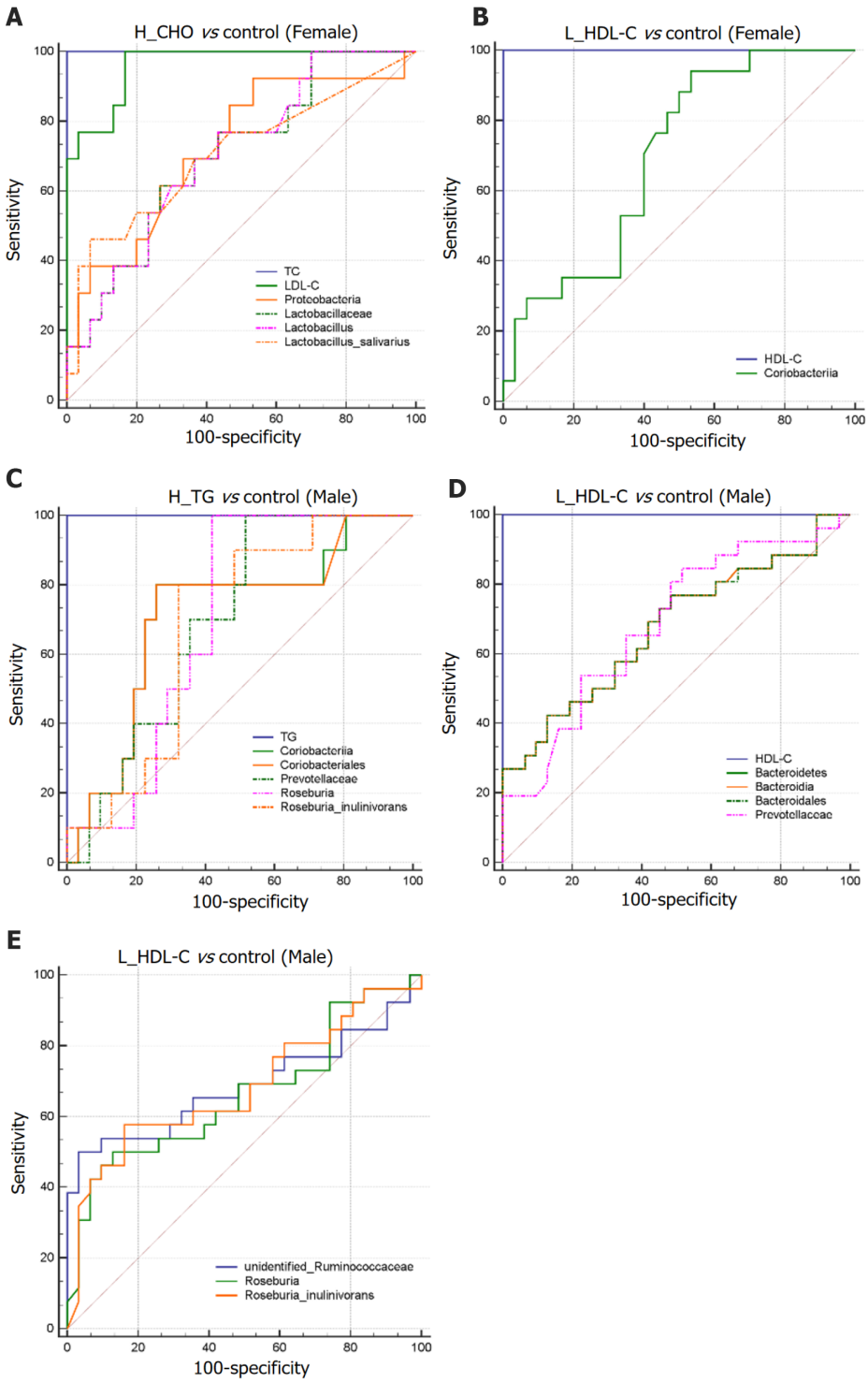

DOI: 10.3748/wjg.v28.i27.3455

Figure 9 Differential gut microbiota taxa-based classification of dyslipidemia in the study population. Receiver operating characteristic curve analysis for identifying dyslipidemia subgroup from controls by gut microbiota taxa in females and males. A: High total cholesterol *vs* control (Female); B: Low high-density lipoprotein cholesterol (L_HDL-C) *vs* control (Female); C: High triglyceride *vs* control (Male); D and E: L_HDL-C *vs* control (Male). H_CHO: High total cholesterol; H_TG: high triglyceride; L_HDL-C: Low high-density lipoprotein cholesterol.

negatively correlated with CVAI in males. As a valuable indicator of "adipose distribution and function", CVAI has been suggested to be a reliable and applicable indicator for the evaluation of visceral fat dysfunction in Chinese individuals, which is based on simple and obtainable clinical parameters and the serum lipid levels[34,45]. The CVAI is essentially correlated with lipid metabolism, and its negative correlation with GM diversities could further support the reliability of our data.

Butyrate has been suggested to facilitate the prevention and treatment of diet-induced obesity by reducing fat accumulation and insulin resistance[46,47], and the ability to produce butyrate is widely distributed among gram-positive anaerobic bacteria[48]. As members of the butyrate-producing bacteria

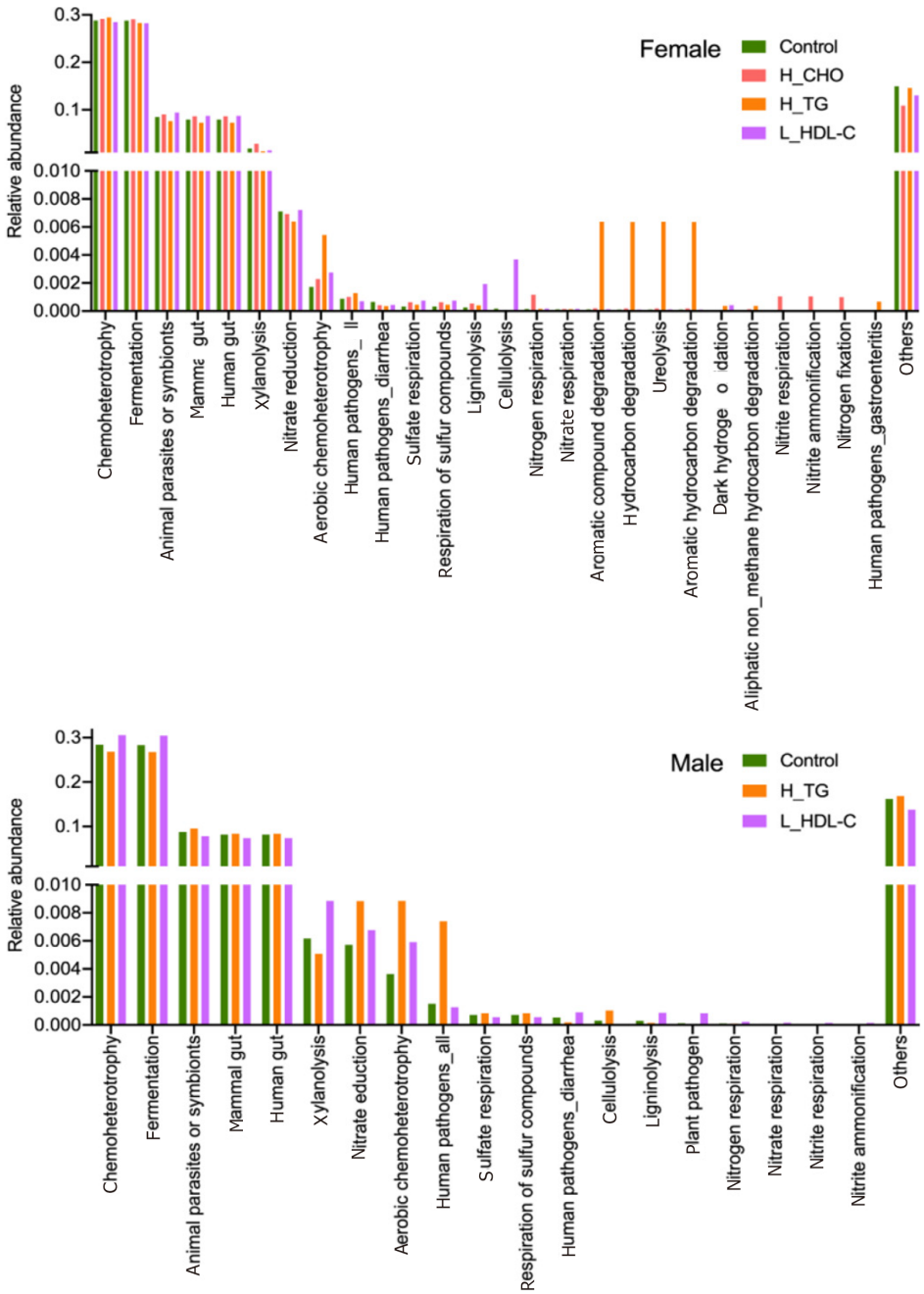

DOI: 10.3748/wjg.v28.i27.3455

Figure 10 The main functional annotations of gut microbiota in the study population. Bar plots show the relative abundances of top twenty annotated functions with higher relative abundances in female subgroups and male subgroups, respectively, using the FAPROTAX database. H_CHO: High total cholesterol; H_TG: high triglyceride; L_HDL-C: Low high-density lipoprotein cholesterol.

[48], *Roseburia* and *Roseburia_inulinivorans* have been investigated in certain diseases. By analyzing the GM composition of patients with symptomatic atherosclerosis, Karlsson *et al*[49] noted an enrichment of *Roseburia* in CVD patients, while a lower abundance of *Roseburia* was be observed in patients with diabetes[44]. In this study, we found that *Roseburia_inulinivorans* were positively correlated with the serum TG, TC and HDL-C levels, and *Roseburia* were positively correlated with the serum TG level in males. In addition, decreased *Roseburia* and *Roseburia_inulinivorans* abundances distinguished L_HDL-C males from CON males, while increased *Roseburia* and *Roseburia_inulinivorans* abundances distinguished H_TG males from CON males. Furthermore, strains of *Bifidobacterium* and *Lactobacillus* have potential therapeutic purposes[50]. An *et al*[51] once described a comparable, positive anti-obesity and lipid-lowering effect of *Bifidobacterium* spp. in obese rats fed a high-fat diet. Consistent with the evidence, our results demonstrated that the relative abundances of Bifidobacteriales, Bifidobacteriaceae and *Bifidobacterium* were negatively correlated with the serum TG and TC levels in males. However, certain favorable GM taxa, such as Lactobacillaceae, *Lactobacillus* and *Lactobacillus_salivarius*, were enriched in H_CHO females. As a probiotic supplement, *Lactobacillus* were noted to have a negative correlation with serum

lipid profiles[52]. An animal study, focused on mice fed a high-fat high-cholesterol diet and supplemented with *Lactobacillus curvatus* and/or *Lactobacillus plantarum*, revealed that these probiotic bacteria play important roles in normalizing lipid metabolism, such as decreasing TC levels in plasma and liver, and reducing the accumulation of hepatic TG[53]. Obviously, certain conflicting findings exist, which should be further investigated. Nevertheless, these observations indicate that different GM taxa associate with certain lipids, and may affect specific aspects of lipid metabolism[26,42,43].

A recent study on rats[54] demonstrated that a high-fat diet decreased the proportions of Bacteroidetes and its genera *Bacteroides* and *Prevotella*, and a study on swine indicated that decreased Bacteroidetes proportions were accompanied by decreases in the circulating TG level[55]; however, whether Bacteroidetes can alter cholesterol or TG levels in humans remains disputed. In humans, decreased Bacteroidetes proportions, including *Bacteroides_vulgatus* and *Bacteroides_dorei*, were observed in patients with coronary artery disease[56,57]. In addition, some species of *Bacteroides* were shown to be decreased in patients with CVDs[49], and may be used as biomarkers for evaluating the alleviation of obesity[54]. Our results showed that *Bacteroides_vulgatus* were negatively correlated with the serum LDL-C level but positively correlated with the serum TG level in females, while Bacteroidetes, Bacteroidia and Bacteroidales were negatively correlated with CVAI in females. Moreover, Bacteroidetes, Bacteroidia and Bacteroidales were positively correlated with the serum HDL-C level, differentiated L_HDL-C males from CON males, and were negatively correlated with CVAI in males. These observed associations may further support their roles in the favorable regulation of lipid metabolism. Interestingly, Prevotellaceae were enriched in L_HDL-C group in the comparison among the three dyslipidemia subgroups in females. However, the relative abundance of Prevotellaceae was decreased significantly in L_HDL-C males, and could distinguish L_HDL-C males from CON males. Additionally, increased Prevotellaceae also helped discriminate H_TG males from CON males in our study. Of note, Kelly *et al*[58] reported that genera within the family Prevotellaceae had different effects; some were associated with an increased and others with a decreased CVD risk profile. Meanwhile, Coriobacteriia were indicated to be enriched in L_HDL-C females, and could differentiate L_HDL-C females from CON females. Moreover, we identified that Coriobacteriales were correlated with the increased serum HDL-C level in males, and increased Coriobacteriia and Coriobacteriales could distinguish H_TG males from CON males. However, these taxa have not been studied thoroughly, and it is difficult to assess their metabolic functions in human lipid metabolism.

Different GM taxa may have distinct activities and modes of action[50,59], and certain taxa may exert synergistic and cooperative interactions[60], indicating the importance of balance in the GM community. Our results may suggest a complex interaction between GM and distinct lipid metabolisms based on sex differences, and provide new evidence of the involvement of GM in dyslipidemia. Nevertheless, more studies are required to determine which specific taxa have the potential to ameliorate dyslipidemia.

There were several limitations in this study, the most marked of which was the small sample size in each subgroup. This was a single-center study, recruiting Chinese participants near Xi'an, a central city in northwestern China. In addition, certain confounders, such as dietary habit, that could have influenced the GM composition[61], must be taken into consideration. However, elucidation of certain associations of GM taxa with host lipid metabolism in this study is still valuable. We hope that our observations will facilitate prospective studies investigating diverse aspects of GM influences on human dyslipidemia based on sex differences. In future studies, it is recommended that the sample size be increased, more confounders be considered, and various research methods be integrated to ascertain potential associations.

CONCLUSION

Based on the thorough analyses of GM features with dyslipidemia in females and males, potent associations of GM-host relations based on sex differences were revealed, and the potential of GM for dyslipidemia diagnosis was demonstrated. Although this study could not provide a conclusive association between GM and dyslipidemia, it may provide new insights into the pathogenesis of dyslipidemia.

ARTICLE HIGHLIGHTS

Research background

Dyslipidemia is a common chronic disorder, and is defined as any abnormality in blood lipid levels. In recent years, considerable progress has been made in elucidating the mechanisms of dyslipidemia, and the gut microbiota (GM) has been indicated to play a pivotal role in its pathophysiology. However, the associations between GM and dyslipidemia remain to be elucidated.

Research motivation

Although recent studies have convincingly linked GM to dyslipidemia, proving the associations between GM and host lipid metabolism remains a challenge in humans. In addition, ethnicity, geography and sex are potent factors that could influence the GM community. Therefore, it is important to clarify the relationship between GM and dyslipidemia, and to explore the importance of sex differences. In this study, we first revealed sex differences regarding the GM features, and then introduced dyslipidemia, highlighting its intricate relationships with GM and possible altered GM functions.

Research objectives

This study focused on the associations of GM features with dyslipidemia based on sex differences in a northwestern Chinese population.

Research methods

This study finally recruited 142 participants (73 females and 69 males) at Honghui Hospital, Xi'an Jiaotong University, who fulfilled the criteria for the diagnosis of dyslipidemia according to the "Guidelines for prevention and treatment of dyslipidemia in Chinese adults". The anthropometric and blood metabolic parameters of all participants were measured. According to their detected serum lipid levels, female and male participants were classified into a high triglyceride (H_TG) group, a high total cholesterol (H_CHO) group, a low high-density lipoprotein cholesterol (L_HDL-C) group, and a control (CON) group with normal serum lipid levels. Fresh fecal samples were collected for 16S rRNA gene sequencing, and UPARSE software, QIIME software, the RDP classifier tool and the FAPROTAX database were used for sequencing analyses.

Research results

Different GM features were identified between females and males, and the associations between GM and serum lipid profiles were different between females and males. In the comparison of the three dyslipidemia subgroups in females, *Lactobacillus_salivarius* were enriched in H_CHO females, and Prevotellaceae were enriched in L_HDL-C females. Compared with CON or H_TG males, Prevotellaceae, *unidentified_Ruminococcaceae*, *Roseburia* and *Roseburia_inulinivorans* were decreased in L_HDL-C males; while linear discriminant analysis effect size analysis indicated an enrichment of these above GM taxa in H_TG males in comparison to other male subgroups. Additionally, *Roseburia_inulinivorans* abundance was positively correlated with the serum TG and total cholesterol levels, and *Roseburia* were positively correlated with the serum TG level. Furthermore, Proteobacteria, Lactobacillaceae, *Lactobacillus* and *Lactobacillus_salivarius* distinguished H_CHO females from CON females, while Coriobacteriia, Coriobacteriales, Prevotellaceae, *Roseburia* and *Roseburia_inulinivorans* distinguished H_TG males from CON males. Based on the predictions of GM metabolic capabilities from the FAPROTAX database, cellulolysis was increased in L_HDL-C females compared with CON females, but was decreased in L_HDL-C males compared with CON males.

Research conclusions

This study provides evidence of the associations between GM and serum lipid profiles based on sex differences, suggesting a complex interaction between GM and distinct lipid metabolisms, and providing new insights into the pathogenesis of dyslipidemia.

Research perspectives

Future studies are needed to determine which specific taxa have the potential to ameliorate dyslipidemia, to investigate the underlying biological functions of the key GM in dyslipidemia, and to explore the differences in diet and other factors between females and males as possible causes for the observed differences in GM and the lipid profiles.

FOOTNOTES

Author contributions: All the authors solely contributed to this article; Guo L and Lv J searched and reviewed published articles, interpreted data, constructed tables, drafted the article, and made substantial contributions to the conception and design of this study; Wang YY, Wang JH and Yan YZ conducted the experiments, performed sequencing analysis and constructed the figures; Wang YY, Wang JH and Wang GD performed statistical analysis; Zhao HP, Yu Y and Dai K constructed the figures and tables; Yang YJ contributed to the conception of the study; and all authors critically reviewed the manuscript, and approved the final version to be published.

Supported by Youth Program of Xi'an Municipal Health Commission of China, No. 2022qn07; General Program of Xi'an Municipal Health Commission of China, No. 2020ms14; and National Natural Science Foundation of China, No. 81702067.

Institutional review board statement: This study was reviewed and approved by the Ethics Committee of Honghui Hospital, Xi'an Jiaotong University, No. 201801022.

Informed consent statement: All study participants provided informed consent prior to study enrollment.

Conflict-of-interest statement: All the authors report no relevant conflicts of interest for this article.

Data sharing statement: The raw data supporting the conclusions of this article available from the corresponding author at lvjing-1219@163.com.

Country/Territory of origin: China

ORCID number: Lei Guo 0000-0002-5166-5374; Yang-Yang Wang 0000-0002-4259-2804; Ji-Han Wang 0000-0003-1925-330X; He-Ping Zhao 0000-0002-7896-6636; Yan Yu 0000-0003-1587-7748; Guo-Dong Wang 0000-0002-1346-8396; Kun Dai 0000-0001-5091-7800; Yu-Zhu Yan 0000-0003-1355-0266; Yan-Jie Yang 0000-0002-7259-2995; Jing Lv 0000-0003-2801-743X.

S-Editor: Fan JR
L-Editor: A
P-Editor: Qi WW

REFERENCES

1 **World Health Organization**. Obesity and overweight Fact Sheet. 2021. [cited 10 January 2022]. Available from: https://www.who.int/news-room/fact-sheets/detail/obesity-and-overweight
2 **Sun B**, Karin M. Obesity, inflammation, and liver cancer. *J Hepatol* 2012; **56**: 704-713 [PMID: 22120206 DOI: 10.1016/j.jhep.2011.09.020]
3 **Bloor ID**, Symonds ME. Sexual dimorphism in white and brown adipose tissue with obesity and inflammation. *Horm Behav* 2014; **66**: 95-103 [PMID: 24589990 DOI: 10.1016/j.yhbeh.2014.02.007]
4 **Gao N**, Yu Y, Zhang B, Yuan Z, Zhang H, Song Y, Zhao M, Ji J, Liu L, Xu C, Zhao J. Dyslipidemia in rural areas of North China: prevalence, characteristics, and predictive value. *Lipids Health Dis* 2016; **15**: 154 [PMID: 27619340 DOI: 10.1186/s12944-016-0328-y]
5 **Tóth PP**, Potter D, Ming EE. Prevalence of lipid abnormalities in the United States: the National Health and Nutrition Examination Survey 2003-2006. *J Clin Lipidol* 2012; **6**: 325-330 [PMID: 22836069 DOI: 10.1016/j.jacl.2012.05.002]
6 **García-Giustiniani D**, Stein R. Genetics of Dyslipidemia. *Arq Bras Cardiol* 2016; **106**: 434-438 [PMID: 27305287 DOI: 10.5935/abc.20160074]
7 **Kokkinos PF**, Fernhall B. Physical activity and high density lipoprotein cholesterol levels: what is the relationship? *Sports Med* 1999; **28**: 307-314 [PMID: 10593643 DOI: 10.2165/00007256-199928050-00002]
8 **O'Doherty AF**, Jones HS, Sathyapalan T, Ingle L, Carroll S. The Effects of Acute Interval Exercise and Strawberry Intake on Postprandial Lipemia. *Med Sci Sports Exerc* 2017; **49**: 2315-2323 [PMID: 29045326 DOI: 10.1249/MSS.0000000000001341]
9 **Matey-Hernandez ML**, Williams FMK, Potter T, Valdes AM, Spector TD, Menni C. Genetic and microbiome influence on lipid metabolism and dyslipidemia. *Physiol Genomics* 2018; **50**: 117-126 [PMID: 29341867 DOI: 10.1152/physiolgenomics.00053.2017]
10 **Tremaroli V**, Bäckhed F. Functional interactions between the gut microbiota and host metabolism. *Nature* 2012; **489**: 242-249 [PMID: 22972297 DOI: 10.1038/nature11552]
11 **Cani PD**. Metabolism in 2013: The gut microbiota manages host metabolism. *Nat Rev Endocrinol* 2014; **10**: 74-76 [PMID: 24322652 DOI: 10.1038/nrendo.2013.240]
12 **Plaza-Diaz J**. Nutrition, Microbiota and Noncommunicable Diseases. *Nutrients* 2020; **12** [PMID: 32630712 DOI: 10.3390/nu12071971]
13 **Turnbaugh PJ**, Ley RE, Hamady M, Fraser-Liggett CM, Knight R, Gordon JI. The human microbiome project. *Nature* 2007; **449**: 804-810 [PMID: 17943116 DOI: 10.1038/nature06244]
14 **Yatsunenko T**, Rey FE, Manary MJ, Trehan I, Dominguez-Bello MG, Contreras M, Magris M, Hidalgo G, Baldassano RN, Anokhin AP, Heath AC, Warner B, Reeder J, Kuczynski J, Caporaso JG, Lozupone CA, Lauber C, Clemente JC, Knights D, Knight R, Gordon JI. Human gut microbiome viewed across age and geography. *Nature* 2012; **486**: 222-227 [PMID: 22699611 DOI: 10.1038/nature11053]
15 **Schloissnig S**, Arumugam M, Sunagawa S, Mitreva M, Tap J, Zhu A, Waller A, Mende DR, Kultima JR, Martin J, Kota K, Sunyaev SR, Weinstock GM, Bork P. Genomic variation landscape of the human gut microbiome. *Nature* 2013; **493**: 45-50 [PMID: 23222524 DOI: 10.1038/nature11711]
16 **Dominguez-Bello MG**, Blaser MJ, Ley RE, Knight R. Development of the human gastrointestinal microbiota and insights

from high-throughput sequencing. *Gastroenterology* 2011; **140**: 1713-1719 [PMID: 21530737 DOI: 10.1053/j.gastro.2011.02.011]

17 **Jernberg C**, Löfmark S, Edlund C, Jansson JK. Long-term impacts of antibiotic exposure on the human intestinal microbiota. *Microbiology (Reading)* 2010; **156**: 3216-3223 [PMID: 20705661 DOI: 10.1099/mic.0.040618-0]

18 **Wu GD**, Chen J, Hoffmann C, Bittinger K, Chen YY, Keilbaugh SA, Bewtra M, Knights D, Walters WA, Knight R, Sinha R, Gilroy E, Gupta K, Baldassano R, Nessel L, Li H, Bushman FD, Lewis JD. Linking long-term dietary patterns with gut microbial enterotypes. *Science* 2011; **334**: 105-108 [PMID: 21885731 DOI: 10.1126/science.1208344]

19 **Sommer F**, Bäckhed F. The gut microbiota--masters of host development and physiology. *Nat Rev Microbiol* 2013; **11**: 227-238 [PMID: 23435359 DOI: 10.1038/nrmicro2974]

20 **Rinninella E**, Raoul P, Cintoni M, Franceschi F, Miggiano GAD, Gasbarrini A, Mele MC. What is the Healthy Gut Microbiota Composition? *Microorganisms* 2019; **7** [PMID: 30634578 DOI: 10.3390/microorganisms7010014]

21 **Oliphant K**, Allen-Vercoe E. Macronutrient metabolism by the human gut microbiome: major fermentation by-products and their impact on host health. *Microbiome* 2019; **7**: 91 [PMID: 31196177 DOI: 10.1186/s40168-019-0704-8]

22 **Evans JM**, Morris LS, Marchesi JR. The gut microbiome: the role of a virtual organ in the endocrinology of the host. *J Endocrinol* 2013; **218**: R37-R47 [PMID: 23833275 DOI: 10.1530/JOE-13-0131]

23 **Dieterich W**, Schink M, Zopf Y. Microbiota in the Gastrointestinal Tract. *Med Sci (Basel)* 2018; **6** [PMID: 30558253 DOI: 10.3390/medsci6040116]

24 **Blander JM**, Longman RS, Iliev ID, Sonnenberg GF, Artis D. Regulation of inflammation by microbiota interactions with the host. *Nat Immunol* 2017; **18**: 851-860 [PMID: 28722709 DOI: 10.1038/ni.3780]

25 **Nicholson JK**, Holmes E, Kinross J, Burcelin R, Gibson G, Jia W, Pettersson S. Host-gut microbiota metabolic interactions. *Science* 2012; **336**: 1262-1267 [PMID: 22674330 DOI: 10.1126/science.1223813]

26 **Fu J**, Bonder MJ, Cenit MC, Tigchelaar EF, Maatman A, Dekens JA, Brandsma E, Marczynska J, Imhann F, Weersma RK, Franke L, Poon TW, Xavier RJ, Gevers D, Hofker MH, Wijmenga C, Zhernakova A. The Gut Microbiome Contributes to a Substantial Proportion of the Variation in Blood Lipids. *Circ Res* 2015; **117**: 817-824 [PMID: 26358192 DOI: 10.1161/CIRCRESAHA.115.306807]

27 **Ghazalpour A**, Cespedes I, Bennett BJ, Allayee H. Expanding role of gut microbiota in lipid metabolism. *Curr Opin Lipidol* 2016; **27**: 141-147 [PMID: 26855231 DOI: 10.1097/MOL.0000000000000278]

28 **Schoeler M**, Caesar R. Dietary lipids, gut microbiota and lipid metabolism. *Rev Endocr Metab Disord* 2019; **20**: 461-472 [PMID: 31707624 DOI: 10.1007/s11154-019-09512-0]

29 **Magkos F**, Mittendorfer B. Gender differences in lipid metabolism and the effect of obesity. *Obstet Gynecol Clin North Am* 2009; **36**: 245-265, vii [PMID: 19501312 DOI: 10.1016/j.ogc.2009.03.001]

30 **Palmisano BT**, Zhu L, Eckel RH, Stafford JM. Sex differences in lipid and lipoprotein metabolism. *Mol Metab* 2018; **15**: 45-55 [PMID: 29858147 DOI: 10.1016/j.molmet.2018.05.008]

31 **Imamura F**, Micha R, Khatibzadeh S, Fahimi S, Shi P, Powles J, Mozaffarian D; Global Burden of Diseases Nutrition and Chronic Diseases Expert Group (NutriCoDE). Dietary quality among men and women in 187 countries in 1990 and 2010: a systematic assessment. *Lancet Glob Health* 2015; **3**: e132-e142 [PMID: 25701991 DOI: 10.1016/S2214-109X(14)70381-X]

32 **Kim YS**, Unno T, Kim BY, Park MS. Sex Differences in Gut Microbiota. *World J Mens Health* 2020; **38**: 48-60 [PMID: 30929328 DOI: 10.5534/wjmh.190009]

33 **Zheng W**, Ma Y, Zhao A, He T, Lyu N, Pan Z, Mao G, Liu Y, Li J, Wang P, Wang J, Zhu B, Zhang Y. Compositional and functional differences in human gut microbiome with respect to equol production and its association with blood lipid level: a cross-sectional study. *Gut Pathog* 2019; **11**: 20 [PMID: 31168326 DOI: 10.1186/s13099-019-0297-6]

34 **Xia MF**, Chen Y, Lin HD, Ma H, Li XM, Aleteng Q, Li Q, Wang D, Hu Y, Pan BS, Li XJ, Li XY, Gao X. A indicator of visceral adipose dysfunction to evaluate metabolic health in adult Chinese. *Sci Rep* 2016; **6**: 38214 [PMID: 27905531 DOI: 10.1038/srep38214]

35 **Joint Committee on Revision of guidelines for prevention and treatment of dyslipidemia in Chinese adults**. Guidelines for Prevention and Treatment of Dyslipidemia in Chinese Adults (Revised Edition 2016). *Zhongguo Xunhuan Zazhi* 2016; **31**: 937-953 [DOI: 10.3969/j.issn.1000-3614.2016.10.001]

36 **Zhu X**, Li Y, Jiang Y, Zhang J, Duan R, Liu L, Liu C, Xu X, Yu L, Wang Q, Xiong F, Ni C, Xu L, He Q. Prediction of Gut Microbial Community Structure and Function in Polycystic Ovary Syndrome With High Low-Density Lipoprotein Cholesterol. *Front Cell Infect Microbiol* 2021; **11**: 665406 [PMID: 34350129 DOI: 10.3389/fcimb.2021.665406]

37 **Franzosa EA**, Morgan XC, Segata N, Waldron L, Reyes J, Earl AM, Giannoukos G, Boylan MR, Ciulla D, Gevers D, Izard J, Garrett WS, Chan AT, Huttenhower C. Relating the metatranscriptome and metagenome of the human gut. *Proc Natl Acad Sci U S A* 2014; **111**: E2329-E2338 [PMID: 24843156 DOI: 10.1073/pnas.1319284111]

38 **Louca S**, Parfrey LW, Doebeli M. Decoupling function and taxonomy in the global ocean microbiome. *Science* 2016; **353**: 1272-1277 [PMID: 27634532 DOI: 10.1126/science.aaf4507]

39 **Razavi AC**, Potts KS, Kelly TN, Bazzano LA. Sex, gut microbiome, and cardiovascular disease risk. *Biol Sex Differ* 2019; **10**: 29 [PMID: 31182162 DOI: 10.1186/s13293-019-0240-z]

40 **Markle JG**, Frank DN, Mortin-Toth S, Robertson CE, Feazel LM, Rolle-Kampczyk U, von Bergen M, McCoy KD, Macpherson AJ, Danska JS. Sex differences in the gut microbiome drive hormone-dependent regulation of autoimmunity. *Science* 2013; **339**: 1084-1088 [PMID: 23328391 DOI: 10.1126/science.1233521]

41 **Castaner O**, Goday A, Park YM, Lee SH, Magkos F, Shiow STE, Schröder H. The Gut Microbiome Profile in Obesity: A Systematic Review. *Int J Endocrinol* 2018; **2018**: 4095789 [PMID: 29849617 DOI: 10.1155/2018/4095789]

42 **Cotillard A**, Kennedy SP, Kong LC, Prifti E, Pons N, Le Chatelier E, Almeida M, Quinquis B, Levenez F, Galleron N, Gougis S, Rizkalla S, Batto JM, Renault P; ANR MicroObes consortium, Doré J, Zucker JD, Clément K, Ehrlich SD. Dietary intervention impact on gut microbial gene richness. *Nature* 2013; **500**: 585-588 [PMID: 23985875 DOI: 10.1038/nature12480]

43 **Le Chatelier E**, Nielsen T, Qin J, Prifti E, Hildebrand F, Falony G, Almeida M, Arumugam M, Batto JM, Kennedy S, Leonard P, Li J, Burgdorf K, Grarup N, Jørgensen T, Brandslund I, Nielsen HB, Juncker AS, Bertalan M, Levenez F, Pons

N, Rasmussen S, Sunagawa S, Tap J, Tims S, Zoetendal EG, Brunak S, Clément K, Doré J, Kleerebezem M, Kristiansen K, Renault P, Sicheritz-Ponten T, de Vos WM, Zucker JD, Raes J, Hansen T; MetaHIT consortium, Bork P, Wang J, Ehrlich SD, Pedersen O. Richness of human gut microbiome correlates with metabolic markers. *Nature* 2013; **500**: 541-546 [PMID: 23985870 DOI: 10.1038/nature12506]

44 **Karlsson FH**, Tremaroli V, Nookaew I, Bergström G, Behre CJ, Fagerberg B, Nielsen J, Bäckhed F. Gut metagenome in European women with normal, impaired and diabetic glucose control. *Nature* 2013; **498**: 99-103 [PMID: 23719380 DOI: 10.1038/nature12198]

45 **Amato MC**, Giordano C, Galia M, Criscimanna A, Vitabile S, Midiri M, Galluzzo A; AlkaMeSy Study Group. Visceral Adiposity Index: a reliable indicator of visceral fat function associated with cardiometabolic risk. *Diabetes Care* 2010; **33**: 920-922 [PMID: 20067971 DOI: 10.2337/dc09-1825]

46 **Gao Z**, Yin J, Zhang J, Ward RE, Martin RJ, Lefevre M, Cefalu WT, Ye J. Butyrate improves insulin sensitivity and increases energy expenditure in mice. *Diabetes* 2009; **58**: 1509-1517 [PMID: 19366864 DOI: 10.2337/db08-1637]

47 **Hatayama H**, Iwashita J, Kuwajima A, Abe T. The short chain fatty acid, butyrate, stimulates MUC2 mucin production in the human colon cancer cell line, LS174T. *Biochem Biophys Res Commun* 2007; **356**: 599-603 [PMID: 17374366 DOI: 10.1016/j.bbrc.2007.03.025]

48 **Louis P**, Flint HJ. Diversity, metabolism and microbial ecology of butyrate-producing bacteria from the human large intestine. *FEMS Microbiol Lett* 2009; **294**: 1-8 [PMID: 19222573 DOI: 10.1111/j.1574-6968.2009.01514.x]

49 **Karlsson FH**, Fåk F, Nookaew I, Tremaroli V, Fagerberg B, Petranovic D, Bäckhed F, Nielsen J. Symptomatic atherosclerosis is associated with an altered gut metagenome. *Nat Commun* 2012; **3**: 1245 [PMID: 23212374 DOI: 10.1038/ncomms2266]

50 **Suharja AAS**, Henriksson A, Liu SQ. Impact of Saccharomyces cerevisiae on viability of probiotic Lactobacillus rhamnosus in fermented milk under ambient conditions. *J Food Process Preserv* 2014; **38**: 326-337 [DOI: 10.1111/j.1745-4549.2012.00780.x]

51 **An HM**, Park SY, Lee DK, Kim JR, Cha MK, Lee SW, Lim HT, Kim KJ, Ha NJ. Antiobesity and lipid-lowering effects of Bifidobacterium spp. in high fat diet-induced obese rats. *Lipids Health Dis* 2011; **10**: 116 [PMID: 21745411 DOI: 10.1186/1476-511X-10-116]

52 **Huang ZR**, Chen M, Guo WL, Li TT, Liu B, Bai WD, Ai LZ, Rao PF, Ni L, Lv XC. Monascus purpureus-fermented common buckwheat protects against dyslipidemia and non-alcoholic fatty liver disease through the regulation of liver metabolome and intestinal microbiome. *Food Res Int* 2020; **136**: 109511 [PMID: 32846589 DOI: 10.1016/j.foodres.2020.109511]

53 **Yoo SR**, Kim YJ, Park DY, Jung UJ, Jeon SM, Ahn YT, Huh CS, McGregor R, Choi MS. Probiotics L. plantarum and L. curvatus in combination alter hepatic lipid metabolism and suppress diet-induced obesity. *Obesity (Silver Spring)* 2013; **21**: 2571-2578 [PMID: 23512789 DOI: 10.1002/oby.20428]

54 **Zhu Y**, Zhang JY, Wei YL, Hao JY, Lei YQ, Zhao WB, Xiao YH, Sun AD. The polyphenol-rich extract from chokeberry (*Aronia melanocarpa* L.) modulates gut microbiota and improves lipid metabolism in diet-induced obese rats. *Nutr Metab (Lond)* 2020; **17**: 54 [PMID: 32655675 DOI: 10.1186/s12986-020-00473-9]

55 **Cui C**, Shen CJ, Jia G, Wang KN. Effect of dietary Bacillus subtilis on proportion of Bacteroidetes and Firmicutes in swine intestine and lipid metabolism. *Genet Mol Res* 2013; **12**: 1766-1776 [PMID: 23765983 DOI: 10.4238/2013.May.23.1]

56 **Emoto T**, Yamashita T, Sasaki N, Hirota Y, Hayashi T, So A, Kasahara K, Yodoi K, Matsumoto T, Mizoguchi T, Ogawa W, Hirata K. Analysis of Gut Microbiota in Coronary Artery Disease Patients: a Possible Link between Gut Microbiota and Coronary Artery Disease. *J Atheroscler Thromb* 2016; **23**: 908-921 [PMID: 26947598 DOI: 10.5551/jat.32672]

57 **Yoshida N**, Emoto T, Yamashita T, Watanabe H, Hayashi T, Tabata T, Hoshi N, Hatano N, Ozawa G, Sasaki N, Mizoguchi T, Amin HZ, Hirota Y, Ogawa W, Yamada T, Hirata KI. Bacteroides vulgatus and Bacteroides dorei Reduce Gut Microbial Lipopolysaccharide Production and Inhibit Atherosclerosis. *Circulation* 2018; **138**: 2486-2498 [PMID: 30571343 DOI: 10.1161/CIRCULATIONAHA.118.033714]

58 **Kelly TN**, Bazzano LA, Ajami NJ, He H, Zhao J, Petrosino JF, Correa A, He J. Gut Microbiome Associates With Lifetime Cardiovascular Disease Risk Profile Among Bogalusa Heart Study Participants. *Circ Res* 2016; **119**: 956-964 [PMID: 27507222 DOI: 10.1161/CIRCRESAHA.116.309219]

59 **Hendijani F**, Akbari V. Probiotic supplementation for management of cardiovascular risk factors in adults with type II diabetes: A systematic review and meta-analysis. *Clin Nutr* 2018; **37**: 532-541 [PMID: 28318686 DOI: 10.1016/j.clnu.2017.02.015]

60 **Chapman CM**, Gibson GR, Rowland I. Health benefits of probiotics: are mixtures more effective than single strains? *Eur J Nutr* 2011; **50**: 1-17 [PMID: 21229254 DOI: 10.1007/s00394-010-0166-z]

61 **Makki K**, Deehan EC, Walter J, Bäckhed F. The Impact of Dietary Fiber on Gut Microbiota in Host Health and Disease. *Cell Host Microbe* 2018; **23**: 705-715 [PMID: 29902436 DOI: 10.1016/j.chom.2018.05.012]

World Journal of Gastroenterology

Submit a Manuscript: https://www.f6publishing.com

World J Gastroenterol 2022 July 21; 28(27): 3476-3487

DOI: 10.3748/wjg.v28.i27.3476

ISSN 1007-9327 (print) ISSN 2219-2840 (online)

ORIGINAL ARTICLE

Retrospective Cohort Study

Prognostic significance of hemoglobin, albumin, lymphocyte, platelet in gastrointestinal stromal tumors: A propensity matched retrospective cohort study

Zhou Zhao, Xiao-Nan Yin, Jian Wang, Xin Chen, Zhao-Lun Cai, Bo Zhang

Specialty type: Gastroenterology and hepatology

Provenance and peer review: Unsolicited article; Externally peer reviewed.

Peer-review model: Single blind

Peer-review report's scientific quality classification

Grade A (Excellent): A
Grade B (Very good): B
Grade C (Good): 0
Grade D (Fair): 0
Grade E (Poor): 0

P-Reviewer: Elpek GO, Turkey; Fusaroli P, Italy

Received: February 11, 2022
Peer-review started: February 11, 2022
First decision: April 10, 2022
Revised: April 19, 2022
Accepted: June 19, 2022
Article in press: June 19, 2022
Published online: July 21, 2022

Zhou Zhao, Xiao-Nan Yin, Jian Wang, Xin Chen, Zhao-Lun Cai, Bo Zhang, Department of Gastrointestinal Surgery, Sichuan University West China Hospital, Chengdu 610041, Sichuan Province, China

Corresponding author: Bo Zhang, MD, PhD, Professor, Department of Gastrointestinal Surgery, Sichuan University West China Hospital, No. 37 Guoxue Alley, Wuhou District, Chengdu 610041, Sichuan Province, China. hxwcwk@126.com

Abstract

BACKGROUND

The combined index of hemoglobin, albumin, lymphocyte, and platelet (HALP) can reflect systemic inflammation and nutritional status simultaneously, with some evidence revealing its prognostic value for some tumors. However, the effect of HALP on recurrence-free survival (RFS) in patients with gastrointestinal stromal tumors (GISTs) has not been reported.

AIM

To investigate the prognostic value of HALP in GIST patients.

METHODS

Data from 591 untreated patients who underwent R0 resection for primary and localized GISTs at West China Hospital between December 2008 and December 2016 were included. Clinicopathological data, preoperative albumin, blood routine information, postoperative treatment, and recurrence status were recorded. To eliminate baseline inequivalence, the propensity scores matching (PSM) method was introduced. Ultimately, the relationship between RFS and preoperative HALP was investigated.

RESULTS

The optimal cutoff value for HALP was determined to be 31.5 by X-tile analysis. HALP was significantly associated with tumor site, tumor size, mitosis, Ki67, National Institutes of Health (NIH) risk category, and adjuvant therapy (all $P < 0.001$). Before PSM, GIST patients with an increased HALP had a significantly poor RFS ($P < 0.001$), and low HALP was an independent risk factor for poor RFS [hazard ratio (HR): 0.506, 95% confidence interval (95%CI): 0.291-0.879, $P = 0.016$]. In NIH high-risk GIST patients, GIST patients with low HALP had a worse RFS

than patients with high HALP ($P < 0.05$). After PSM, 458 GIST patients were identified; those with an increased HALP still had significantly poor RFS after PSM ($P < 0.001$) and low HALP was still an independent risk factor for poor RFS (HR: 0.558, 95%CI: 0.319-0.976, $P = 0.041$).

CONCLUSION

HALP was significantly correlated with postoperative pathology and postoperative treatment. Furthermore, HALP showed a strong ability to predict RFS in GIST patients who underwent radical resection.

Key Words: Gastrointestinal stromal tumors; Nutrition assessment; Immuno-inflammatory-based prognostic scores; Prognosis; Propensity score

Core Tip: The combined index of hemoglobin, albumin, lymphocyte, and platelet (HALP) can reflect systemic inflammation and nutritional status simultaneously. We demonstrated that HALP has a statistically significant correlation with postoperative pathology and postoperative treatment in patients with gastrointestinal stromal tumors (GISTs). Furthermore, we revealed that a low level of HALP was an independent risk factor for poor recurrence-free survival in GIST patients following radical resection before and after propensity scores matching.

Citation: Zhao Z, Yin XN, Wang J, Chen X, Cai ZL, Zhang B. Prognostic significance of hemoglobin, albumin, lymphocyte, platelet in gastrointestinal stromal tumors: A propensity matched retrospective cohort study. *World J Gastroenterol* 2022; 28(27): 3476-3487

URL: https://www.wjgnet.com/1007-9327/full/v28/i27/3476.htm

DOI: https://dx.doi.org/10.3748/wjg.v28.i27.3476

INTRODUCTION

Gastrointestinal stromal tumors (GISTs), a rare type of tumor, are the most frequent mesenchymal tumors arising from the gastrointestinal tract[1]. GISTs may occur anywhere in the digestive tract and even occasionally outside the gastrointestinal tract, with the stomach accounting for 60% and the small intestine 30% of all GISTs[2]. The morphology, immunohistochemistry, and molecular markers are helpful to the diagnosis of GISTs. Surgical resection is the standard treatment for resectable GISTs[3]. Nowadays, novel small molecular tyrosine kinase inhibitors, such as imatinib and sunitinib, have revolutionized the integrated treatment of GISTs and greatly improved the long-term prognosis of patients[4].

Some GIST-specific parameters based on postoperative pathologies, such as tumor size, primary tumor location, mitotic index, and tumor rupture, have been used to stratify the risk of recurrence for GISTs[2,5-7]. Meanwhile, a recent effort has shed light on the role of preoperative cancer-related inflammation and nutrition status in progression of various cancers, such as those of gastric[8], colorectal[9], non-small lung[10], and GIST[11-15]. Several preoperative immuno-inflammatory-based prognostic scores, such as the preoperative neutrophil-to-lymphocyte ratio (NLR), the lymphocyte-to-monocyte ratio (LMR), and the platelet-to-lymphocyte ratio (PLR), reflect the systematic inflammatory response, with some evidence supporting their prognostic ability for GISTs[13-17]. Furthermore, nutritional status, such as measured by the prognostic nutritional index (PNI), has also been shown to play an important role in GIST progression[10,11].

Recent studies have proposed a new combined index of hemoglobin, albumin, lymphocyte, and platelet (HALP) which can reflect systemic inflammation and nutritional status simultaneously[18]. It has already been reported as related to the prognosis of patients with pancreatic cancer[19], renal cancer [20], gastric cancer[18], prostate cancer[21], bladder cancer[22], esophageal cancer[23], and small cell lung cancer[24]. However, there are no studies on the relationship between HALP and recurrence in GIST patients who undergo radical resection. Therefore, this study aimed to investigate the prognostic value of preoperative HALP in resected GIST patients.

MATERIALS AND METHODS

Patient population

A flow diagram of the patient selection process is shown in Figure 1. Data from consecutive, previously untreated patients who underwent R0 resection for primary, localized GISTs at West China Hospital between December 2008 and December 2016 were included in this study. Patients who were younger than 18 years in age, without complete preoperative blood routine information or medical history, or with infectious diseases, blood counts with white blood cells (WBCs) > 10×10^9/L, neutrophils > 8×10^9/L, or lymphocytes > 5×10^9/L, other tumors, severe liver, kidney or heart diseases, emergency surgery, or follow-up less than 6 mo were excluded. In total, 591 GIST patients were enrolled for the current analysis.

This study was reviewed and approved by the Ethics Committee of the West China Hospital of Sichuan University, No. 1135(2019) and adhered to the tenets of the Declaration of Helsinki. All patients provided written informed consent.

Definition

Recurrence-free survival (RFS) was defined as the time interval between the time of surgery and the time of the first documented appearance of tumor after complete resection. The HALP, PNI, NLR, PLR, and LMR were calculated using the following formulas: HALP = hemoglobin level (g/L) × albumin level (g/L) × lymphocyte count (/L)/platelet count (/L)[19]; PNI = albumin level (g/L) + 5 × lymphocyte count (n/mm^3)[25]; NLR = neutrophil count (n/mm^3)/lymphocyte count (n/mm^3)[15,16]; PLR = platelet count (n/mm^3)/lymphocyte count (n/mm^3)[14]; LMR = lymphocyte count (n/mm^3)/monocyte count (n/mm^3)[26].

Data collection

Clinicopathological data, postoperative treatment, and recurrence status were recorded. The following data of each patient were retrieved from the self-built GISTs database: Demographic characteristics, tumor sites, tumor size, mitotic index [mitosis/50 high-power field (HPF) or mitosis/50 mm^2], morphology, immunohistochemistry, molecular markers, preoperative hemoglobin, albumin, WBC count, absolute neutrophil count, monocyte count, platelet count, and lymphocyte count. Tumor risk stratification was determined based on the modified National Institutes of Health (NIH) classification [27].

Perioperative evaluation and postoperative histopathological diagnosis

For all patients, the laboratory tests were evaluated within 1 wk before operation. Preoperative blood routine and blood biochemical examination were performed by the Laboratory Department of Sichuan University West China Hospital. The parameters included complete blood cell count and serum albumin. Histopathological diagnosis was performed by the Department of Pathology of Sichuan University West China Hospital; the postoperative pathological findings included data on gross appearance, tumor size, tumor site, resection margin status, tumor cell morphology, lymph node metastasis status, and immunohistochemical staining, *etc*.

Follow-up

Abdominal/pelvic computed tomography was performed every 3-6 mo in the first 3 years after operation, and then every 6-12 mo, until 5 years after the operation, and then once a year until recurrence. Recurrence status was ascertained up to December 2020.

Statistical analysis

The optimal cutoff values for the HALP, PNI, NLR, PLR, and LMR were determined to be 31.5, 48.6, 2.60, 134.8, and 4.0, respectively, by X-tile analysis[28]. Propensity scores matching (PSM) was performed as 1:1 matching and a 0.02 caliper based on the patient's age, tumor size, tumor site, mitosis, and adjuvant targeted therapy using nearest neighbor matching with the MatchIt R package (https://cran.r-project.org/web/packages/MatchIt/MatchIt.pdf). The categorical variables are reported as n (%) and quantitative variables are reported as mean ± SD or median (range). Statistical significance of group comparisons was analyzed *via* parametric and nonparametric tests for continuous variables and *via* chi-square analysis or Fisher's test for categorical variables. Survival curves of the RFS were calculated by the Kaplan-Meier methods and compared by log-rank tests. Hazard ratio (HR) for recurrence was calculated by Cox regression analysis. Sensitivity and specificity of HALP, PNI, NLR, LMR, and PLR were defined using time-dependent receiver operating characteristic (ROC) curves, and areas under the curve (AUCs) were detected utilizing survival ROC R package[29]. All statistical analyses were performed using SPSS Statistics version 21 (SPSS 21.0; IBM Corp., Armonk, NY, United States) and GraphPad Prism version 7.0 (GraphPad Software, La Jolla, CA, United States). Statistical significance was set at $P < 0.05$ as two-sided.

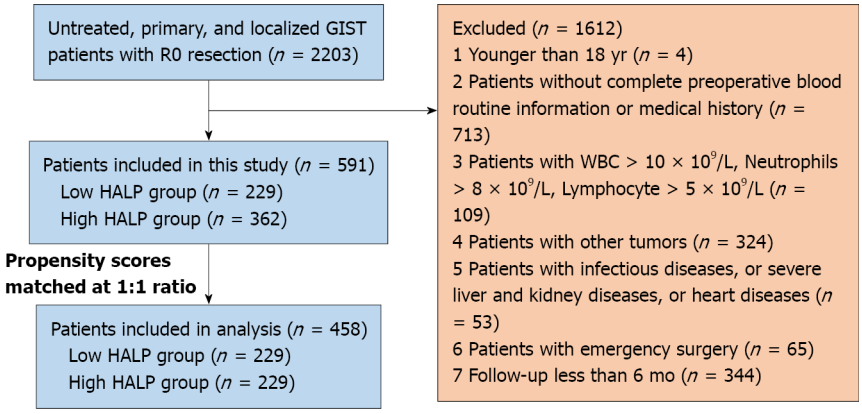

DOI: 10.3748/wjg.v28.i27.3476

Figure 1 Flow diagram of the patient selection process. GIST: Gastrointestinal stromal tumor; HALP: Combination index of hemoglobin, albumin, lymphocyte, and platelet; WBC: White blood cell.

RESULTS

Baseline characteristics

The demographic and clinicopathological characteristics of the 591 GIST patients are listed in Table 1 and Supplementary Table 1. The study population consisted of 280 (46.8%) male and 311 (53.2%) female patients. The median age was 57 (range: 21-86) years. The median follow-up time was 56 (range: 4-138) mo. The mean ± SD findings for the HALP, PNI, NLR, PLR, and LMR values were 45.81 ± 33.73, 49.04 ± 5.43, 2.64 ± 1.74, 152.8 ± 84.6 and 5.13 ± 3.00, respectively. The mean ± SD of tumor size was 6.16 ± 4.87 cm. One hundred ninety-one tumors (32.3%) had a mitotic index of > 5/50 HPF. A total of 34.0% (201/691) of the GIST patients received adjuvant therapy with imatinib or sunitinib. According to NIH risk classification, 72 (12.2%) patients were classified as very low risk, 178 (30.1%) patients as low risk, 114 (19.3%) patients as intermediate risk, and 227 (38.4%) patients as high risk. Recurrence occurred in 62 GIST patients.

Association of HALP and clinicopathological factors

The clinicopathological characteristics between the high and low groups of HALP were categorized and analyzed as shown in Table 1 and Supplementary Table 1. Together, 229 patients were assigned to the low HALP group and 362 patients to the high HALP group. The results demonstrated that tumor site, tumor size, mitotic index, Ki67, NIH risk category, and adjuvant therapy were significantly associated with HALP (all $P < 0.05$).

PSM analysis was further carried out to avoid confounding variables that might interfere with the association between RFS and HALP level. After 1:1 matching, PSM analysis identified 229 pairs of GIST patients. After PSM, HALP was still associated with sex, Ki67, and recurrence but not with any other clinicopathological characteristics (Table 1 and Supplementary Table 1).

Association of clinicopathological factors and RFS

Before PSM, tumor site, tumor size, mitotic index, Ki67, NIH risk category, NLR, PLR, PNI, and HALP were associated with RFS (all $P < 0.05$) (Table 2). RFS in GIST patients with low HALP was significantly worse than in those with high HALP (Figure 2). Cox multiple regression analysis showed that HALP was an independent prognostic factor for RFS in GIST patients before PSM [HR: 0.506, 95% confidence interval (CI): 0.291-0.879, $P = 0.016$].

After PSM, tumor site, tumor size, mitotic index, Ki67, NIH risk category, PNI, NLR, PLR, and HALP were still related to RFS (all $P < 0.05$) (Table 2). RFS was also significantly worse in GIST patients with low HALP than in those with high HALP (Figure 2). Furthermore, Cox multiple regression analysis showed that HALP was an independent prognostic factor for RFS in GIST patients (HR: 0.558, 95%CI: 0.319-0.976, $P = 0.041$).

Subgroup analysis

The clinicopathological characteristics of high-risk GIST patients between the high and low groups of HALP were categorized in Supplementary Table 1. Together, 125 patients were assigned to the low HALP group and 102 patients to the high HALP group. The results demonstrated that sex and Ki67 were associated with HALP (both $P < 0.05$). Not surprisingly, patients in the low HALP group had significantly worse survival than patients in the high HALP group (Figure 2). Furthermore, Cox multiple regression analysis indicated that HALP was an independent prognostic factor for RFS in GIST patients (HR: 0.469, 95%CI: 0.245-0.896, $P = 0.022$) (Supplementary Table 2).

Table 1 Baseline characteristics in patients with high or low combination index of hemoglobin, albumin, lymphocyte, and platelet before and after propensity scores matching (mean ± SD)

Characteristics	Before PSM[1]				After PSM			
	All	Low HALP, < 31.5	High HALP, ≥ 31.5	*P* value	All	Low HALP, < 31.5	High HALP, ≥ 31.5	*P* value
n (%)	591	229 (38.7)	362 (61.3)	-	458	229 (50)	229 (50)	-
Age in yr	56.3 ± 12.0	56.7 ± 12.2	56.1 ± 11.8		56.8 ± 12.1	56.7 ± 12.2	57.0 ± 12.1	
< 60	337 (57.0)	129	208		256 (55.9)	129	127	
≥ 60	254 (43.0)	100	154	0.788	202 (44.1)	100	102	0.851
Sex								
Male	280 (47.4)	98	182		233 (50.9)	131	102	
Female	311 (52.6)	131	180	0.076	225 (49.1)	98	127	0.007[a]
Tumor site								
Stomach	424 (71.7)	143	281		299 (65.3)	143	156	
Non-stomach	167 (28.3)	86	81	< 0.001[a]	159 (34.7)	86	73	0.202
Tumor size in cm	6.16 ± 4.87	7.69 ± 5.65	5.18 ± 4.02		7.13 ± 5.08	7.69 ± 5.65	6.57 ± 4.38	
≤ 2	86 (14.6)	10	76		27 (5.9)	10	17	
2.1-5.0	251 (42.5)	87	164		177 (38.6)	87	90	
5.1-10.0	184 (31.1)	95	89		184 (40.2)	95	89	
> 10.0	70 (11.8)	37	33	< 0.001[a]	70 (15.3)	37	33	0.514
Mitotic index/50 HPF								
≤ 5	332 (56.2)	107	225		220 (48.0)	107	113	
6-10	100 (16.9)	45	55		91 (19.9)	45	46	
> 10	91 (15.4)	49	42		89 (19.4)	49	40	
Unknown	68 (11.5)	28	40	0.001[a]	58 (12.7)	28	30	0.764
Ki67								
≤ 10	417 (70.6)	140	277		308 (67.3)	140	168	
> 10	98 (16.6)	61	37		94 (20.5)	61	33	
Unknown	76 (12.9)	28	48	< 0.001[a]	26 (12.2)	28	28	0.004[a]
NIH risk category								
Very low risk	72 (12.2)	9	63		21 (4.6)	9	12	
Low risk	178 (30.1)	52	126		113 (24.7)	52	61	
Intermediate risk	114 (19.3)	43	71		100 (21.8)	43	57	
High risk	227 (38.4)	125	102	< 0.001[a]	224 (48.9)	125	99	0.106
Adjuvant therapy								
Yes	201 (34.0)	99	102		193 (42.1)	99	94	
No	390 (66.0)	130	260	< 0.001[a]	265 (57.9)	130	135	0.636
Recurrence								
Yes	62 (10.5)	42	20		61 (13.3)	42	19	
No	529 (89.5)	187	342	< 0.001[a]	397 (86.7)	187	210	0.002[a]

[1]Method = nearest; Cliper value = 0.02.

[a]$P < 0.05$ was considered statistically significant.

HALP: Combination index of hemoglobin, albumin, lymphocyte, and platelet; HPF: High-power field; NIH: National Institutes of Health; PSM: Propensity scores matching; SD: Standard deviation.

Sensitivity analysis

Time-dependent ROCs were generated for HALP, PNI, NLR, LMR, and PLR to predict 5-year RFS. According to the results, the 5-year AUC reached 0.661 in the HALP group, while PNI, NLR, LMR, and PLR reached 0.622, 0.591, 0.505, and 0.627, respectively (Figure 3).

DISCUSSION

There is growing evidence that preoperative nutritional status and inflammatory response may be a potentially powerful predictor of the prognosis of cancer patients. Consistent with previous research, the present study found that preoperative inflammation scores, such as NLR and PLR, were associated with the prognosis of GIST patients, both before and after PSM[14,16,30,31] (Supplementary Figure 1). However, LMR seemed to have no effect on the RFS of GIST patients (Supplementary Figure 1), which differs from findings of previous studies[14]. In addition, the PNI, a nutritional score based on albumin levels and lymphocytes, was also related to RFS of GIST patients, both before and after PSM in the present study[11,12] (Supplementary Figure 1).

In this study, we also found that preoperative HALP was significantly correlated with tumor site, tumor size, mitosis, Ki67, NIH risk category, and adjuvant therapy (Table 1). To balance the patient characteristics and standard prognostic factors between groups, we utilized the PSM method to balance patient's age, tumor size, tumor site, mitosis, and adjuvant targeted therapy. After PSM, sex, Ki67, PNI, NLR, LMR, and PLR were still associated with HALP (Supplementary Table 1). Notably, there was no difference in standard prognostic factors (*i.e.* tumor site, tumor size, mitosis, NIH risk category, and adjuvant therapy) between the low and high HALP groups (Table 1). Given that HALP shared several parameters with PNI, NLR, LMR, and PLR, their statistically significant correlation is unsurprising. The correlation between HALP and sex may be due to the fact that the male and female patients had significantly different hemoglobin levels (123.22 ± 2.08 g/L for males and 105.46 ± 1.84 g/L for females, $P < 0.001$). Remarkably, recurrence was not associated with either sex or histologic subtype (Supplementary Table 1). Subgroup analysis by sex revealed that a low level of HALP was associated with recurrence in both male and female patients ($P = 0.048$ and $P = 0.018$, respectively) (Supplementary Figure 2).

Finally, consistent with previous research on HALP in other tumors[18,19], our findings revealed prognostic value of HALP in GIST[20-24]. HALP was an independent risk factor for GIST patients before PSM, after PSM, and in high-risk subgroups (Table 2 and Supplementary Table 3). Thus, HALP can be used to not only evaluate GIST patients' postoperative risk prior to surgery but also to assess their prognosis. Notably, the HALP index can be utilized to predict the prognosis of patients in a convenient and cost-effective manner.

Although the underlying mechanism of systemic inflammation in tumorigenesis, progression and metastasis remains obscure, some theories suggest that it stimulates angiogenesis, immunosuppression, and formation of the supporting microenvironment. Lymphocytes are well known to play a critical role in tumor growth inhibition[32-34]. A higher lymphocyte signature is associated with improved prognosis in a variety of tumors[34], whereas platelets can infiltrate the tumor microenvironment and interact directly with cancer cells[35,36], assisting circulating tumor cells in adhering to endothelial cells and establishing a niche environment prior to metastasis[37-41].

Anemia is one of the most common symptoms of GIST, which can be caused by both gastrointestinal bleeding and intratumoral bleeding[42]. Yang *et al*[43] identified GIST with gastrointestinal bleeding as an independent prognostic predictor of poor RFS. Several studies have demonstrated that low hemoglobin levels can result in tumor hypoxia, which is associated with an increased risk of local failure and distant metastasis[31,44]. Furthermore, a hypoxic tumor environment may result in limited drug accumulation and hinder drug efficacy[45]. Most importantly, anemia is a common adverse effect of imatinib[46], which may require the prescribing physician to stop the drug or reduce the dose. High levels of preoperative hemoglobin may help to prevent this adverse effect.

Low levels of serum albumin are also associated with poor long-term survival in GIST patients[44,45], which is consistent with our findings. Serum albumin is generally considered as associated with nutritional status and liver or renal function, both of which may affect the prescribing physician's decision-making, similar to hemoglobin. Additionally, tumor tissues have abnormal vascular endothelial gaps and lack effective lymphatic drainage, allowing macromolecules, such as albumin, to accumulate more readily in tumor tissue than in normal tissue[47,48]. Consequently, serum albumin is suspected of being a possible nutritional source for tumor growth, due to its elevated accumulation in tumors[49-51]. This effect is referred to as the 'enhanced permeability and retention effect'. Moreover, about 95% of imatinib is bound to serum proteins, mainly albumin and 1-acid glycoprotein, which may facilitate drug accumulation in tumors and improve therapeutic effect[52,53]. Subsequently, serum albumin levels have been shown to be an independent prognostic factor of survival in a variety of cancers, including those of colorectal[54], gastric[55], pancreatic[56], and breast[57]. As a result, it is unsurprising that HALP, which reflects systemic inflammation and nutritional status simultaneously, is associated with the risk and prognosis of GIST.

Table 2 Univariate and multivariate regression analysis of prognostic factors in patients before and after propensity scores matching

Risk factors	Before PSM				After PSM			
	Univariate analysis, HR (95%CI)	Univariate analysis, *P* value	Multivariate analysis, HR (95%CI)	Multivariate analysis, *P* value	Univariate analysis, HR (95%CI)	Univariate analysis, *P* value	Multivariate analysis, HR (95%CI)	Multivariate analysis, *P* value
Age	1.009 (0.987-1.030)	0.431		NS	1.006 (0.984-1.027)	0.607		NS
Sex: Male *vs* female	0.639 (0.386-1.056)	0.081		NS	0.711 (0.429-1.179)	0.186		NS
Tumor site: Stomach *vs* non-stomach	2.273 (1.377-3.752)	0.001[a]	2.979 (1.716-5.171)	< 0.001[a]	1.702 (1.028-2.818)	0.039[a]	2.865 (1.631-5.032)	< 0.001[a]
Tumor size in cm: ≤ 2/2.1-5.0/5.1-10.0/> 10.0	2.629 (1.948-3.548)	< 0.001[a]	1.070 (1.032-1.109)	0.001[a]	1.086 (1.056-1.116)	< 0.001[a]	1.068 (1.029-1.107)	< 0.001[a]
Mitotic index as/50 HPF: ≤ 5/6-10/> 10/unknown	2.071 (1.686-2.545)	< 0.001[a]		< 0.001[a]		< 0.001[a]		0.001[a]
≤ 5 *vs* 6-10			5.659 (2.151-14.887)	0.002[a]	5.442 (2.067-14.323)	0.001[a]	5.444 (1.955-15.162)	0.001[a]
≤ 5 *vs* > 10			8.259 (3.140-21.720)	< 0.001[a]	14.722 (6.037-35.904)	< 0.001[a]	7.675 (2.759-21.348)	< 0.001[a]
≤ 5 *vs* unknown			5.299 (2.041-13.757)	< 0.001[a]	9.851 (3.843-25.251)	< 0.001[a]	5.107 (1.873-13.923)	0.001[a]
CD117: +/-	1.231 (0.300-5.059)	0.773		NA	1.291 (0.314-5.313)	0.723	-	NA
DOG1: +/-/unknown	1.464 (0.773-2.774)	0.242		NA	1.626 (0.853-3.102)	0.140	-	NA
Ki67: ≤ 10/> 10/unknown	1.919 (1.453-2.533)	< 0.001[a]		0.001[a]		< 0.001[a]		0.001[a]
< 10 *vs* ≤ 10			3.579 (1.771-7.233)	< 0.001[a]	8.625 (4.750-15.660)	< 0.001[a]	3.710 (1.811-7.599)	< 0.001[a]
Unknown *vs* ≤ 10			2.844 (1.290-6.270)	0.024[a]	3.310 (1.528-7.169)	0.002[a]	3.050 (1.365-6.816)	0.007
Histologic subtypes: Spindle/epithelioid/mixed	1.361 (0.981-1.889)	0.065		NS	1.236 (0.891-1.715)	0.204	-	NA
NIH risk category: Very low/low/intermediate/high	3.218 (2.180-4.751)	< 0.001[a]		NS	2.892 (1.865-4.484)	< 0.001[a]	-	NS
Adjuvant therapy: Yes/no	1.289 (0.768-2.162)	0.336	0.445 (0.257-0.769)	0.004[a]	0.923 (0.549-1.551)	0.761		0.003[a]
NLR: < 2.60/≥ 2.60	2.025 (1.229-3.337)	0.006[a]		NS	1.746 (1.055-2.890)	0.030[a]		NS
PLR: < 134.8/≥ 134.8	2.925 (1.673-5.112)	< 0.001[a]		NS	1.991 (1.137-3.486)	0.016[a]		NS
LMR: < 4.0/≥ 4.0	1.296 (0.777-2.163)	0.321		NA	1.088 (0.650-1.821)	0.749	-	NA
PNI: < 48.6/≥ 48.6	0.291 (0.171-0.496)	< 0.001[a]		NS	1.991 (1.137-3.486)	0.016[a]		NS
HALP: < 31.5/≥ 31.5	0.341 (0.197-0.590)	< 0.001[a]	0.506 (0.291-0.879)	0.016[a]	0.457 (0.265-0.785)	0.005[a]	0.558 (0.319-0.976)	0.041[a]

[a]*P* < 0.05 was considered statistically significant.

CI: Confidence interval; HALP: Combination index of hemoglobin, albumin, lymphocyte, and platelet; HPF: High-power field; HR: Hazard ratio; NA: Not adopted; LMR: Lymphocyte-to-monocyte ratio; NIH: National Institutes of Health; NLR: Neutrophil-to-lymphocyte ratio; NS: Not significant; PLR: Platelet-to-lymphocyte ratio; PNI: Prognostic nutritional index; PSM: Propensity scores matching.

There are some limitations to this study. First, because this is a retrospective study, biases in the data collection process are possible. Second, our cases were collected between 2008 and 2016, the period during which imatinib was used for adjuvant treatment of GIST in China. Despite the adverse reaction

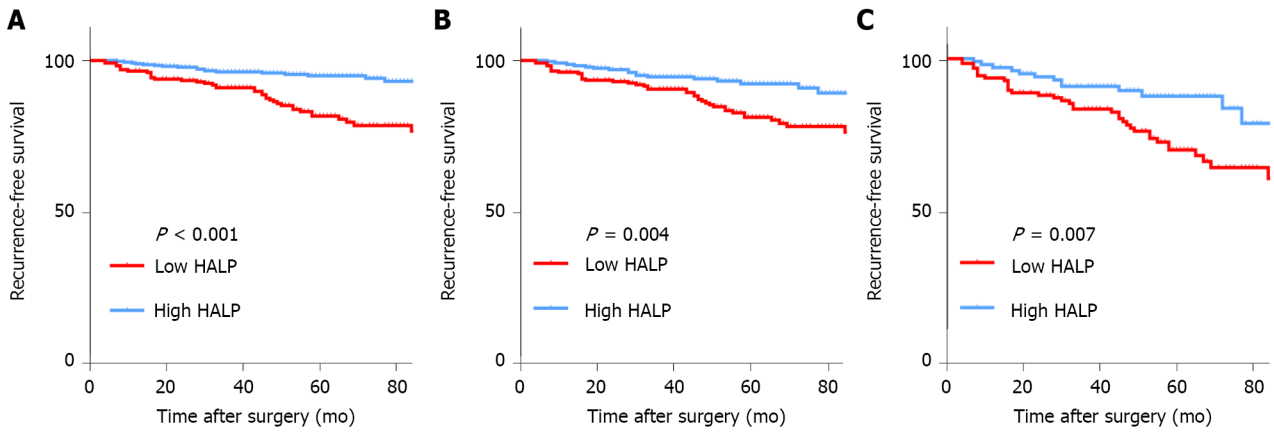

DOI: 10.3748/wjg.v28.i27.3476

Figure 2 Kaplan-Meier curves of recurrence-free survival. A: Stratified by low/high levels of the combination index of hemoglobin, albumin, lymphocyte, and platelet (HALP) in gastrointestinal stromal tumors (GISTs) patients before propensity scores matching (PSM); B: Stratified by low/high levels of HALP in GIST patients after PSM; C: Stratified by low/high levels of HALP in high-risk GIST patients. GIST: Gastrointestinal stromal tumors; PSM: Propensity scores matching; HALP: Hemoglobin, albumin, lymphocyte, and platelet.

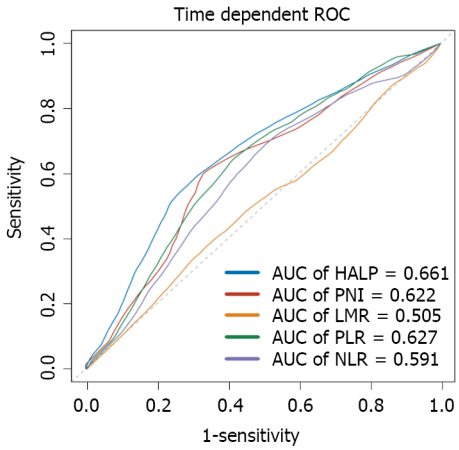

DOI: 10.3748/wjg.v28.i27.3476

Figure 3 Comparison of hemoglobin, albumin, lymphocyte, and platelet and other parameters in prediction ability of 5-year recurrence-free survival by receiver operating characteristic curve analysis before propensity scores matching. AUC: Area under the curve; HALP: Hemoglobin, albumin, lymphocyte, and platelet; LMR: Lymphocyte-to-monocyte ratio; NLR: Neutrophil-to-lymphocyte ratio; PLR: Platelet-to-lymphocyte ratio; PNI: Prognostic nutritional index; PSM: Propensity scores matching; ROC: Receiver operating characteristic.

and high costs, 201/591 (34.0%) of GIST patients still received adjuvant imatinib therapy. As an important treatment after GIST, adjuvant imatinib therapy can significantly improve the prognosis of GIST patients[58], and its benefits are also shown in the present study (Supplementary Figure 3). However, there was no adequate collection and analysis of the time, dose, and adverse reactions of patients with imatinib or sunitinib therapy, which may also be related to HALP. Moreover, this study did not evaluate other clinicopathological factors related to prognosis, especially gene mutation status. Furthermore, the effect of preoperative or postoperative improvement of nutritional status or inflammation response on the prognosis of GIST remains obscure, and will require further confirmation in clinical studies.

CONCLUSION

HALP was associated with postoperative pathological data (*i.e.* tumor site, tumor size, mitosis, Ki67, NIH risk category) and adjuvant therapy. Furthermore, HALP was an independent risk factor for RFS in GIST patients who underwent radical resection.

ARTICLE HIGHLIGHTS

Research background

The combination index of hemoglobin, albumin, lymphocyte, and platelet (HALP) has been reported as associated with prognosis in many cancers but not yet in gastrointestinal stromal tumors (GISTs). Therefore, this study aimed to investigate the prognostic value of preoperative HALP in resected GIST patients.

Research motivation

At present, the risk of GIST is mainly based on postoperative pathological indicators. The motivation for this article involved the need to find a convenient, non-invasive, preoperative indicator that will assist in prognostic prediction of GIST.

Research objectives

To investigate the prognostic value of HALP in GIST patients.

Research methods

This retrospective cohort study enrolled patients with GIST using propensity scores matching to explore the relationship between HALP, postoperative clinicopathological data, and the prognostic significance of HALP.

Research results

HALP can be conveniently used preoperatively to assess risk and prognosis of GIST patients. However, the effect of improving nutritional status or immune-inflammatory status on the prognosis of GIST is still unclear and requires further confirmation through clinical studies.

Research conclusions

HALP was associated with postoperative pathological data (*i.e.* tumor site, tumor size, mitosis, Ki67, National Institutes of Health risk category) and adjuvant therapy. Furthermore, HALP was an independent risk factor for recurrence-free survival in GIST patients who underwent radical resection. This study is the first to report the prognostic significance of HALP in GIST. In this study, HALP was found to be an independent risk factor for GIST patients with R0 resection. Consistent with reports of HALP in other tumors, HALP is also associated with prognosis in GIST. HALP was also found to be an independent risk factor for GIST patients with R0 resection. In clinical practice, convenient and non-invasive preoperative HALP may be used to assist in the prediction of risk and prognosis for GIST patients.

Research perspectives

Through this retrospective cohort study, we found the prognostic significance of HALP in GIST. This study did not evaluate other clinicopathological factors related to prognosis, especially gene mutation status. Subsequent studies should employ a prospective cohort method and incorporate additional factors to further explore the prognostic significance of HALP in GIST patients.

FOOTNOTES

Author contributions: All authors made a significant contribution to the work reported, whether that is in the conception, study design, execution, acquisition of data, analysis and interpretation, or in all these areas; and all authors took part in drafting, revising or critically reviewing the article, gave final approval of the version to be published, agreed on the journal to which the article has been submitted and agreed to be accountable for all aspects of the work.

Supported by National Natural Science Foundation of China, No. 81572931; and The 1.3.5 Project for Disciplines of Excellence, West China Hospital, Sichuan University, No. ZYJC18034.

Institutional review board statement: The Institutional Review Board of the West China Hospital of Sichuan University provided approval for this study, No. 1135(2019).

Informed consent statement: This study examined only patients' electronic health records. Each patient had been asked to sign an informed consent form authorizing the use of their electronic health record for scientific research. If the patient had not consented, we were unable to access his/her information in the hospital's information system.

Conflict-of-interest statement: All the authors report no relevant conflicts of interest for this article.

Data sharing statement: The data that supporting the findings of this study are available from the corresponding author (e-mail: hxwcwk@126.com) upon reasonable request.

STROBE statement: The authors have read the STROBE Statement – checklist of items, and the manuscript was prepared and revised according to the STROBE Statement – checklist of items.

Country/Territory of origin: China

ORCID number: Zhou Zhao 0000-0001-7349-7159; Xiao-Nan Yin 0000-0003-4525-1877; Jian Wang 0000-0002-7407-2504; Xin Chen 0000-0001-7025-0337; Zhao-Lun Cai 0000-0002-3706-6703; Bo Zhang 0000-0002-0254-5843.

S-Editor: Fan JR
L-Editor: A
P-Editor: Fan JR

REFERENCES

1 **Ma GL**, Murphy JD, Martinez ME, Sicklick JK. Epidemiology of gastrointestinal stromal tumors in the era of histology codes: results of a population-based study. *Cancer Epidemiol Biomarkers Prev* 2015; **24**: 298-302 [PMID: 25277795 DOI: 10.1158/1055-9965.EPI-14-1002]
2 **Nishida T**, Blay JY, Hirota S, Kitagawa Y, Kang YK. The standard diagnosis, treatment, and follow-up of gastrointestinal stromal tumors based on guidelines. *Gastric Cancer* 2016; **19**: 3-14 [PMID: 26276366 DOI: 10.1007/s10120-015-0526-8]
3 **Barrios CH**, Blackstein ME, Blay JY, Casali PG, Chacon M, Gu J, Kang YK, Nishida T, Purkayastha D, Woodman RC, Reichardt P. The GOLD ReGISTry: a Global, Prospective, Observational Registry Collecting Longitudinal Data on Patients with Advanced and Localised Gastrointestinal Stromal Tumours. *Eur J Cancer* 2015; **51**: 2423-2433 [PMID: 26248685 DOI: 10.1016/j.ejca.2015.07.010]
4 **DeMatteo RP**, Ballman KV, Antonescu CR, Corless C, Kolesnikova V, von Mehren M, McCarter MD, Norton J, Maki RG, Pisters PW, Demetri GD, Brennan MF, Owzar K; American College of Surgeons Oncology Group (ACOSOG) Intergroup Adjuvant GIST Study Team for the Alliance for Clinical Trials in Oncology. Long-term results of adjuvant imatinib mesylate in localized, high-risk, primary gastrointestinal stromal tumor: ACOSOG Z9000 (Alliance) intergroup phase 2 trial. *Ann Surg* 2013; **258**: 422-429 [PMID: 23860199 DOI: 10.1097/SLA.0b013e3182a15eb7]
5 **Demetri GD**, von Mehren M, Antonescu CR, DeMatteo RP, Ganjoo KN, Maki RG, Pisters PW, Raut CP, Riedel RF, Schuetze S, Sundar HM, Trent JC, Wayne JD. NCCN Task Force report: update on the management of patients with gastrointestinal stromal tumors. *J Natl Compr Canc Netw* 2010; **8** Suppl 2: S1-41; quiz S42 [PMID: 20457867 DOI: 10.6004/jnccn.2010.0116]
6 **Casali PG**, Abecassis N, Aro HT, Bauer S, Biagini R, Bielack S, Bonvalot S, Boukovinas I, Bovee JVMG, Brodowicz T, Broto JM, Buonadonna A, De Álava E, Dei Tos AP, Del Muro XG, Dileo P, Eriksson M, Fedenko A, Ferraresi V, Ferrari A, Ferrari S, Frezza AM, Gasperoni S, Gelderblom H, Gil T, Grignani G, Gronchi A, Haas RL, Hassan B, Hohenberger P, Issels R, Joensuu H, Jones RL, Judson I, Jutte P, Kaal S, Kasper B, Kopeckova K, Krákorová DA, Le Cesne A, Lugowska I, Merimsky O, Montemurro M, Pantaleo MA, Piana R, Picci P, Piperno-Neumann S, Pousa AL, Reichardt P, Robinson MH, Rutkowski P, Safwat AA, Schöffski P, Sleijfer S, Stacchiotti S, Sundby Hall K, Unk M, Van Coevorden F, van der Graaf WTA, Whelan J, Wardelmann E, Zaikova O, Blay JY; ESMO Guidelines Committee and EURACAN. Gastrointestinal stromal tumours: ESMO-EURACAN Clinical Practice Guidelines for diagnosis, treatment and follow-up. *Ann Oncol* 2018; **29**: iv68-iv78 [PMID: 29846513 DOI: 10.1093/annonc/mdy095]
7 **Koo DH**, Ryu MH, Kim KM, Yang HK, Sawaki A, Hirota S, Zheng J, Zhang B, Tzen CY, Yeh CN, Nishida T, Shen L, Chen LT, Kang YK. Asian Consensus Guidelines for the Diagnosis and Management of Gastrointestinal Stromal Tumor. *Cancer Res Treat* 2016; **48**: 1155-1166 [PMID: 27384163 DOI: 10.4143/crt.2016.187]
8 **Ubukata H**, Motohashi G, Tabuchi T, Nagata H, Konishi S. Evaluations of interferon-γ/interleukin-4 ratio and neutrophil/lymphocyte ratio as prognostic indicators in gastric cancer patients. *J Surg Oncol* 2010; **102**: 742-747 [PMID: 20872813 DOI: 10.1002/jso.21725]
9 **Malietzis G**, Giacometti M, Askari A, Nachiappan S, Kennedy RH, Faiz OD, Aziz O, Jenkins JT. A preoperative neutrophil to lymphocyte ratio of 3 predicts disease-free survival after curative elective colorectal cancer surgery. *Ann Surg* 2014; **260**: 287-292 [PMID: 24096764 DOI: 10.1097/SLA.0000000000000216]
10 **Pinato DJ**, Shiner RJ, Seckl MJ, Stebbing J, Sharma R, Mauri FA. Prognostic performance of inflammation-based prognostic indices in primary operable non-small cell lung cancer. *Br J Cancer* 2014; **110**: 1930-1935 [PMID: 24667648 DOI: 10.1038/bjc.2014.145]
11 **Sun J**, Mei Y, Zhu Q, Shou C, Tjhoi WEH, Yang W, Yu H, Zhang Q, Liu X, Yu J. Relationship of prognostic nutritional index with prognosis of gastrointestinal stromal tumors. *J Cancer* 2019; **10**: 2679-2686 [PMID: 31258776 DOI: 10.7150/jca.32299]

12 **Shi WK**, Zhang XH, Zhang J, Yu M, Yuan YJ, Xiong W, Zhang CH, He YL, Wei ZW. Predictive ability of prognostic nutritional index in surgically resected gastrointestinal stromal tumors: a propensity score matching analysis. *Jpn J Clin Oncol* 2019; **49**: 823-831 [PMID: 31162583 DOI: 10.1093/jjco/hyz078]

13 **Yin XN**, Tang SM, Yin Y, Shen CY, Zhang B, Chen ZX. [Associations of Preoperative Platelet-to-lymphocyte Ratio and Derived Neutrophil-to-lymphocyte Ratio with thePrognosis of Gastrointestinal Stromal Tumor]. *Sichuan Da Xue Xue Bao Yi Xue Ban* 2017; **48**: 239-243 [PMID: 28612534]

14 **Feng F**, Tian Y, Liu S, Zheng G, Liu Z, Xu G, Guo M, Lian X, Fan D, Zhang H. Combination of PLR, MLR, MWR, and Tumor Size Could Significantly Increase the Prognostic Value for Gastrointestinal Stromal Tumors. *Medicine (Baltimore)* 2016; **95**: e3248 [PMID: 27057867 DOI: 10.1097/MD.0000000000003248]

15 **Yin Z**, Gao J, Liu W, Huang C, Shuai X, Wang G, Tao K, Zhang P. Clinicopathological and Prognostic Analysis of Primary Gastrointestinal Stromal Tumor Presenting with Gastrointestinal Bleeding: a 10-Year Retrospective Study. *J Gastrointest Surg* 2017; **21**: 792-800 [PMID: 28275959 DOI: 10.1007/s11605-017-3385-2]

16 **Racz JM**, Cleghorn MC, Jimenez MC, Atenafu EG, Jackson TD, Okrainec A, Venkat Raghavan L, Quereshy FA. Predictive Ability of Blood Neutrophil-to-Lymphocyte and Platelet-to-Lymphocyte Ratios in Gastrointestinal Stromal Tumors. *Ann Surg Oncol* 2015; **22**: 2343-2350 [PMID: 25472648 DOI: 10.1245/s10434-014-4265-6]

17 **Luo XF**, Zhou LH. Prognostic significance of neutrophil to lymphocyte ratio in patients with gastrointestinal stromal tumors: A meta-analysis. *Clin Chim Acta* 2018; **477**: 7-12 [PMID: 29175648 DOI: 10.1016/j.cca.2017.11.029]

18 **Chen XL**, Xue L, Wang W, Chen HN, Zhang WH, Liu K, Chen XZ, Yang K, Zhang B, Chen ZX, Chen JP, Zhou ZG, Hu JK. Prognostic significance of the combination of preoperative hemoglobin, albumin, lymphocyte and platelet in patients with gastric carcinoma: a retrospective cohort study. *Oncotarget* 2015; **6**: 41370-41382 [PMID: 26497995 DOI: 10.18632/oncotarget.5629]

19 **Xu SS**, Li S, Xu HX, Li H, Wu CT, Wang WQ, Gao HL, Jiang W, Zhang WH, Li TJ, Ni QX, Liu L, Yu XJ. Haemoglobin, albumin, lymphocyte and platelet predicts postoperative survival in pancreatic cancer. *World J Gastroenterol* 2020; **26**: 828-838 [PMID: 32148380 DOI: 10.3748/wjg.v26.i8.828]

20 **Peng D**, Zhang CJ, Tang Q, Zhang L, Yang KW, Yu XT, Gong Y, Li XS, He ZS, Zhou LQ. Prognostic significance of the combination of preoperative hemoglobin and albumin levels and lymphocyte and platelet counts (HALP) in patients with renal cell carcinoma after nephrectomy. *BMC Urol* 2018; **18**: 20 [PMID: 29544476 DOI: 10.1186/s12894-018-0333-8]

21 **Guo Y**, Shi D, Zhang J, Mao S, Wang L, Zhang W, Zhang Z, Jin L, Yang B, Ye L, Yao X. The Hemoglobin, Albumin, Lymphocyte, and Platelet (HALP) Score is a Novel Significant Prognostic Factor for Patients with Metastatic Prostate Cancer Undergoing Cytoreductive Radical Prostatectomy. *J Cancer* 2019; **10**: 81-91 [PMID: 30662528 DOI: 10.7150/jca.27210]

22 **Peng D**, Zhang CJ, Gong YQ, Hao H, Guan B, Li XS, Zhou LQ. Prognostic significance of HALP (hemoglobin, albumin, lymphocyte and platelet) in patients with bladder cancer after radical cystectomy. *Sci Rep* 2018; **8**: 794 [PMID: 29335609 DOI: 10.1038/s41598-018-19146-y]

23 **Cong L**, Hu L. The value of the combination of hemoglobin, albumin, lymphocyte and platelet in predicting platinum-based chemoradiotherapy response in male patients with esophageal squamous cell carcinoma. *Int Immunopharmacol* 2017; **46**: 75-79 [PMID: 28268208 DOI: 10.1016/j.intimp.2017.02.027]

24 **Shen XB**, Zhang YX, Wang W, Pan YY. The Hemoglobin, Albumin, Lymphocyte, and Platelet (HALP) Score in Patients with Small Cell Lung Cancer Before First-Line Treatment with Etoposide and Progression-Free Survival. *Med Sci Monit* 2019; **25**: 5630-5639 [PMID: 31356586 DOI: 10.12659/MSM.917968]

25 **Ichikawa K**, Mizuno S, Hayasaki A, Kishiwada M, Fujii T, Iizawa Y, Kato H, Tanemura A, Murata Y, Azumi Y, Kuriyama N, Usui M, Sakurai H, Isaji S. Prognostic Nutritional Index After Chemoradiotherapy Was the Strongest Prognostic Predictor Among Biological and Conditional Factors in Localized Pancreatic Ductal Adenocarcinoma Patients. *Cancers (Basel)* 2019; **11** [PMID: 30974894 DOI: 10.3390/cancers11040514]

26 **Hsu JT**, Wang CC, Le PH, Chen TH, Kuo CJ, Lin CJ, Chou WC, Yeh TS. Lymphocyte-to-monocyte ratios predict gastric cancer surgical outcomes. *J Surg Res* 2016; **202**: 284-290 [PMID: 27229102 DOI: 10.1016/j.jss.2016.01.005]

27 **Joensuu H**. Risk stratification of patients diagnosed with gastrointestinal stromal tumor. *Hum Pathol* 2008; **39**: 1411-1419 [PMID: 18774375 DOI: 10.1016/j.humpath.2008.06.025]

28 **Camp RL**, Dolled-Filhart M, Rimm DL. X-tile: a new bio-informatics tool for biomarker assessment and outcome-based cut-point optimization. *Clin Cancer Res* 2004; **10**: 7252-7259 [PMID: 15534099 DOI: 10.1158/1078-0432.Ccr-04-0713]

29 **Heagerty PJ**, Lumley T, Pepe MS. Time-dependent ROC curves for censored survival data and a diagnostic marker. *Biometrics* 2000; **56**: 337-344 [PMID: 10877287 DOI: 10.1111/j.0006-341x.2000.00337.x]

30 **Goh BK**, Chok AY, Allen JC Jr, Quek R, Teo MC, Chow PK, Chung AY, Ong HS, Wong WK. Blood neutrophil-to-lymphocyte and platelet-to-lymphocyte ratios are independent prognostic factors for surgically resected gastrointestinal stromal tumors. *Surgery* 2016; **159**: 1146-1156 [PMID: 26688506 DOI: 10.1016/j.surg.2015.10.021]

31 **Rutkowski P**, Teterycz P, Klimczak A, Bylina E, Szamotulska K, Lugowska I. Blood neutrophil-to-lymphocyte ratio is associated with prognosis in advanced gastrointestinal stromal tumors treated with imatinib. *Tumori* 2018; **104**: 415-422 [PMID: 29714669 DOI: 10.1177/0300891618765543]

32 **Ostroumov D**, Fekete-Drimusz N, Saborowski M, Kühnel F, Woller N. CD4 and CD8 T lymphocyte interplay in controlling tumor growth. *Cell Mol Life Sci* 2018; **75**: 689-713 [PMID: 29032503 DOI: 10.1007/s00018-017-2686-7]

33 **Shankaran V**, Ikeda H, Bruce AT, White JM, Swanson PE, Old LJ, Schreiber RD. IFNgamma and lymphocytes prevent primary tumour development and shape tumour immunogenicity. *Nature* 2001; **410**: 1107-1111 [PMID: 11323675 DOI: 10.1038/35074122]

34 **Thorsson V**, Gibbs DL, Brown SD, Wolf D, Bortone DS, Ou Yang TH, Porta-Pardo E, Gao GF, Plaisier CL, Eddy JA, Ziv E, Culhane AC, Paull EO, Sivakumar IKA, Gentles AJ, Malhotra R, Farshidfar F, Colaprico A, Parker JS, Mose LE, Vo NS, Liu J, Liu Y, Rader J, Dhankani V, Reynolds SM, Bowlby R, Califano A, Cherniack AD, Anastassiou D, Bedognetti D, Mokrab Y, Newman AM, Rao A, Chen K, Krasnitz A, Hu H, Malta TM, Noushmehr H, Pedamallu CS, Bullman S, Ojesina AI, Lamb A, Zhou W, Shen H, Choueiri TK, Weinstein JN, Guinney J, Saltz J, Holt RA, Rabkin CS; Cancer Genome Atlas Research Network, Lazar AJ, Serody JS, Demicco EG, Disis ML, Vincent BG, Shmulevich I. The Immune

Landscape of Cancer. *Immunity* 2018; **48**: 812-830.e14 [PMID: 29628290 DOI: 10.1016/j.immuni.2018.03.023]
35 **Nash GF**, Turner LF, Scully MF, Kakkar AK. Platelets and cancer. *Lancet Oncol* 2002; **3**: 425-430 [PMID: 12142172 DOI: 10.1016/s1470-2045(02)00789-1]
36 **Haemmerle M**, Stone RL, Menter DG, Afshar-Kharghan V, Sood AK. The Platelet Lifeline to Cancer: Challenges and Opportunities. *Cancer Cell* 2018; **33**: 965-983 [PMID: 29657130 DOI: 10.1016/j.ccell.2018.03.002]
37 **Davì G**, Patrono C. Platelet activation and atherothrombosis. *N Engl J Med* 2007; **357**: 2482-2494 [PMID: 18077812 DOI: 10.1056/NEJMra071014]
38 **Abdol Razak NB**, Jones G, Bhandari M, Berndt MC, Metharom P. Cancer-Associated Thrombosis: An Overview of Mechanisms, Risk Factors, and Treatment. *Cancers (Basel)* 2018; **10** [PMID: 30314362 DOI: 10.3390/cancers10100380]
39 **Olsson AK**, Cedervall J. The pro-inflammatory role of platelets in cancer. *Platelets* 2018; **29**: 569-573 [PMID: 29584534 DOI: 10.1080/09537104.2018.1453059]
40 **Schlesinger M**. Role of platelets and platelet receptors in cancer metastasis. *J Hematol Oncol* 2018; **11**: 125 [PMID: 30305116 DOI: 10.1186/s13045-018-0669-2]
41 **Wojtukiewicz MZ**, Sierko E, Hempel D, Tucker SC, Honn KV. Platelets and cancer angiogenesis nexus. *Cancer Metastasis Rev* 2017; **36**: 249-262 [PMID: 28681240 DOI: 10.1007/s10555-017-9673-1]
42 **Sorour MA**, Kassem MI, Ghazal Ael-H, El-Riwini MT, Abu Nasr A. Gastrointestinal stromal tumors (GIST) related emergencies. *Int J Surg* 2014; **12**: 269-280 [PMID: 24530605 DOI: 10.1016/j.ijsu.2014.02.004]
43 **Yang Z**, Wang F, Liu S, Guan W. Comparative clinical features and short-term outcomes of gastric and small intestinal gastrointestinal stromal tumours: a retrospective study. *Sci Rep* 2019; **9**: 10033 [PMID: 31296939 DOI: 10.1038/s41598-019-46520-1]
44 **Italiano A**, Cioffi A, Coco P, Maki RG, Schöffski P, Rutkowski P, Le Cesne A, Duffaud F, Adenis A, Isambert N, Bompas E, Blay JY, Casali P, Keohan ML, Toulmonde M, Antonescu CR, Debiec-Rychter M, Coindre JM, Bui B. Patterns of care, prognosis, and survival in patients with metastatic gastrointestinal stromal tumors (GIST) refractory to first-line imatinib and second-line sunitinib. *Ann Surg Oncol* 2012; **19**: 1551-1559 [PMID: 22065192 DOI: 10.1245/s10434-011-2120-6]
45 **Hompland I**, Bruland ØS, Hølmebakk T, Poulsen JP, Stoldt S, Hall KS, Boye K. Prediction of long-term survival in patients with metastatic gastrointestinal stromal tumor: analysis of a large, single-institution cohort. *Acta Oncol* 2017; **56**: 1317-1323 [PMID: 28557540 DOI: 10.1080/0284186X.2017.1330555]
46 **Xia Y**, Chen S, Luo M, Wu J, Cai S, He Y, Chen X, Zhang X. Correlations between imatinib plasma trough concentration and adverse reactions in Chinese patients with gastrointestinal stromal tumors. *Cancer* 2020; **126** Suppl 9: 2054-2061 [PMID: 32293723 DOI: 10.1002/cncr.32751]
47 **Allen TM**, Cullis PR. Drug delivery systems: entering the mainstream. *Science* 2004; **303**: 1818-1822 [PMID: 15031496 DOI: 10.1126/science.1095833]
48 **Kalyane D**, Raval N, Maheshwari R, Tambe V, Kalia K, Tekade RK. Employment of enhanced permeability and retention effect (EPR): Nanoparticle-based precision tools for targeting of therapeutic and diagnostic agent in cancer. *Mater Sci Eng C Mater Biol Appl* 2019; **98**: 1252-1276 [PMID: 30813007 DOI: 10.1016/j.msec.2019.01.066]
49 **Babson AL**, Winnick T. Protein transfer in tumor-bearing rats. *Cancer Res* 1954; **14**: 606-611 [PMID: 13199806]
50 **Kratz F**. Albumin as a drug carrier: design of prodrugs, drug conjugates and nanoparticles. *J Control Release* 2008; **132**: 171-183 [PMID: 18582981 DOI: 10.1016/j.jconrel.2008.05.010]
51 **Kratz F**, Beyer U. Serum proteins as drug carriers of anticancer agents: a review. *Drug Deliv* 1998; **5**: 281-299 [PMID: 19569996 DOI: 10.3109/10717549809065759]
52 **Peng B**, Lloyd P, Schran H. Clinical pharmacokinetics of imatinib. *Clin Pharmacokinet* 2005; **44**: 879-894 [PMID: 16122278 DOI: 10.2165/00003088-200544090-00001]
53 **Kim B**, Seo B, Park S, Lee C, Kim JO, Oh KT, Lee ES, Choi HG, Youn YS. Albumin nanoparticles with synergistic antitumor efficacy against metastatic lung cancers. *Colloids Surf B Biointerfaces* 2017; **158**: 157-166 [PMID: 28688365 DOI: 10.1016/j.colsurfb.2017.06.039]
54 **Boonpipattanapong T**, Chewatanakornkul S. Preoperative carcinoembryonic antigen and albumin in predicting survival in patients with colon and rectal carcinomas. *J Clin Gastroenterol* 2006; **40**: 592-595 [PMID: 16917399 DOI: 10.1097/00004836-200608000-00006]
55 **Oñate-Ocaña LF**, Aiello-Crocifoglio V, Gallardo-Rincón D, Herrera-Goepfert R, Brom-Valladares R, Carrillo JF, Cervera E, Mohar-Betancourt A. Serum albumin as a significant prognostic factor for patients with gastric carcinoma. *Ann Surg Oncol* 2007; **14**: 381-389 [PMID: 17160496 DOI: 10.1245/s10434-006-9093-x]
56 **Siddiqui A**, Heinzerling J, Livingston EH, Huerta S. Predictors of early mortality in veteran patients with pancreatic cancer. *Am J Surg* 2007; **194**: 362-366 [PMID: 17693283 DOI: 10.1016/j.amjsurg.2007.02.007]
57 **Lis CG**, Grutsch JF, Vashi PG, Lammersfeld CA. Is serum albumin an independent predictor of survival in patients with breast cancer? *JPEN J Parenter Enteral Nutr* 2003; **27**: 10-15 [PMID: 12549592 DOI: 10.1177/014860710302700110]
58 **Cohen MH**, Cortazar P, Justice R, Pazdur R. Approval summary: imatinib mesylate in the adjuvant treatment of malignant gastrointestinal stromal tumors. *Oncologist* 2010; **15**: 300-307 [PMID: 20200041 DOI: 10.1634/theoncologist.2009-0120]

World Journal of Gastroenterology

Submit a Manuscript: https://www.f6publishing.com

World J Gastroenterol 2022 July 21; 28(27): 3488-3502

DOI: 10.3748/wjg.v28.i27.3488

ISSN 1007-9327 (print) ISSN 2219-2840 (online)

ORIGINAL ARTICLE

Retrospective Study

Contrast-enhanced ultrasound Liver Imaging Reporting and Data System: Lights and shadows in hepatocellular carcinoma and cholangiocellular carcinoma diagnosis

Gianpaolo Vidili, Marco Arru, Giuliana Solinas, Diego Francesco Calvisi, Pierluigi Meloni, Assunta Sauchella, Davide Turilli, Claudio Fabio, Antonio Cossu, Giordano Madeddu, Sergio Babudieri, Maria Assunta Zocco, Giovanni Iannetti, Enza Di Lembo, Alessandro Palmerio Delitala, Roberto Manetti

Specialty type: Medicine, research and experimental

Provenance and peer review: Invited article; Externally peer reviewed.

Peer-review model: Single blind

Peer-review report's scientific quality classification

Grade A (Excellent): 0
Grade B (Very good): B
Grade C (Good): C
Grade D (Fair): D, D
Grade E (Poor): 0

P-Reviewer: Cao X, China; Kamimura H, Japan; Lu Q, China; Zhou JH, China

A-Editor: Chen Z, China

Received: December 17, 2021
Peer-review started: December 17, 2021
First decision: January 27, 2022
Revised: February 10, 2022
Accepted: June 16, 2022
Article in press: June 16, 2022
Published online: July 21, 2022

Gianpaolo Vidili, Marco Arru, Diego Francesco Calvisi, Pierluigi Meloni, Assunta Sauchella, Davide Turilli, Claudio Fabio, Antonio Cossu, Giordano Madeddu, Sergio Babudieri, Alessandro Palmerio Delitala, Roberto Manetti, Department of Medical, Surgical and Experimental Sciences, University of Sassari, Sassari 07100, Italy

Giuliana Solinas, Department of Biomedical Sciences, Public Health-Laboratory of Biostatistics, University of Sassari, Sassari 07100, Italy

Maria Assunta Zocco, Department of Internal Medicine and Gastroenterology, Fondazione Policlinico Universitario A. Gemelli IRCCS, Catholic University, Rome 00168, Italy

Giovanni Iannetti, Enza Di Lembo, Ultrasound Unit, Ospedale S. Spirito, Pescara 65123, Italy

Corresponding author: Gianpaolo Vidili, MD, Assistant Professor, Department of Medical, Surgical and Experimental Sciences, University of Sassari, 8 Viale San Pietro, Sassari 07100, Italy. gianpaolovidili@uniss.it

Abstract

BACKGROUND

Contrast-enhanced ultrasound (CEUS) is considered a secondary examination compared to computed tomography (CT) and magnetic resonance imaging (MRI) in the diagnosis of hepatocellular carcinoma (HCC), due to the risk of misdiagnosing intrahepatic cholangiocarcinoma (ICC). The introduction of CEUS Liver Imaging Reporting and Data System (CEUS LI-RADS) might overcome this limitation. Even though data from the literature seems promising, its reliability in real-life context has not been well-established yet.

AIM

To test the accuracy of CEUS LI-RADS for correctly diagnosing HCC and ICC in cirrhosis.

METHODS

CEUS LI-RADS class was retrospectively assigned to 511 nodules identified in 269 patients suffering from liver cirrhosis. The diagnostic standard for all nodules was

either biopsy (102 nodules) or CT/MRI (409 nodules). Common diagnostic accuracy indexes such as sensitivity, specificity, positive predictive value (PPV), and negative predictive value (NPV) were assessed for the following associations: CEUS LR-5 and HCC; CEUS LR-4 and 5 merged class and HCC; CEUS LR-M and ICC; and CEUS LR-3 and malignancy. The frequency of malignant lesions in CEUS LR-3 subgroups with different CEUS patterns was also determined. Inter-rater agreement for CEUS LI-RADS class assignment and for major CEUS pattern identification was evaluated.

RESULTS

CEUS LR-5 predicted HCC with a 67.6% sensitivity, 97.7% specificity, and 99.3% PPV ($P < 0.001$). The merging of LR-4 and 5 offered an improved 93.9% sensitivity in HCC diagnosis with a 94.3% specificity and 98.8% PPV ($P < 0.001$). CEUS LR-M predicted ICC with a 91.3% sensitivity, 96.7% specificity, and 99.6% NPV ($P < 0.001$). CEUS LR-3 predominantly included benign lesions (only 28.8% of malignancies). In this class, the hypo-hypo pattern showed a much higher rate of malignant lesions (73.3%) than the iso-iso pattern (2.6%). Inter-rater agreement between internal raters for CEUS-LR class assignment was almost perfect ($n = 511$, $k = 0.94$, $P < 0.001$), while the agreement among raters from separate centres was substantial ($n = 50$, $k = 0.67$, $P < 0.001$). Agreement was stronger for arterial phase hyperenhancement (internal $k = 0.86$, $P < 2.7 \times 10^{-214}$; external $k = 0.8$, $P < 0.001$) than washout (internal $k = 0.79$, $P < 1.6 \times 10^{-202}$; external $k = 0.71$, $P < 0.001$).

CONCLUSION

CEUS LI-RADS is effective but can be improved by merging LR-4 and 5 to diagnose HCC and by splitting LR-3 into two subgroups to differentiate iso-iso nodules from other patterns.

Key Words: Contrast-enhanced ultrasound Liver Imaging Reporting and Data System; Hepatocellular carcinoma; Intrahepatic cholangiocarcinoma; Cirrhosis; Contrast-enhanced ultrasound; Liver

Core Tip: This is a retrospective study to evaluate the accuracy of contrast-enhanced ultrasound Liver Imaging Reporting and Data System (CEUS LI-RADS) in correctly diagnosing hepatocellular carcinoma (HCC) and intrahepatic cholangiocarcinoma (ICC) in patients with cirrhosis. CEUS LR-5 showed a 97.7% specificity for HCC with a low sensitivity (67.6%), while the CEUS LR-4 and 5 merged class showed a 93.9% sensitivity and 94.3% specificity for HCC. CEUS LR-M predicted ICC with a 91.3% sensitivity and 96.7% specificity. CEUS LR-3 predominantly included benign lesions (28.8% of malignancies) but was heterogeneous as the hypo-hypo pattern showed a higher rate of malignant lesions (73.3%) than the iso-iso pattern (2.6%).

Citation: Vidili G, Arru M, Solinas G, Calvisi DF, Meloni P, Sauchella A, Turilli D, Fabio C, Cossu A, Madeddu G, Babudieri S, Zocco MA, Iannetti G, Di Lembo E, Delitala AP, Manetti R. Contrast-enhanced ultrasound Liver Imaging Reporting and Data System: Lights and shadows in hepatocellular carcinoma and cholangiocellular carcinoma diagnosis. *World J Gastroenterol* 2022; 28(27): 3488-3502
URL: https://www.wjgnet.com/1007-9327/full/v28/i27/3488.htm
DOI: https://dx.doi.org/10.3748/wjg.v28.i27.3488

INTRODUCTION

Liver cirrhosis is a strong risk factor for primitive liver cancer, the seventh most commonly diagnosed malignancy worldwide and the third most common cause of cancer-related death[1]. In this scenario, the most prevalent malignant lesion is hepatocellular carcinoma (HCC), followed by intrahepatic cholangiocarcinoma (ICC); however, other types of cancer are rare. The development of a malignant lesion represents a critical point in the clinical history of chronic liver diseases since it significantly reduces life expectancy, especially in case of late diagnosis. Therefore, regular follow-up is essential for these patients with mandatory ultrasonography every 6 mo for detecting solid focal liver lesions[2-5].

Contrast-enhanced ultrasound (CEUS) is an effective, well-recognized, and safe imaging technique for visualising the onset of new nodules in liver cirrhosis, that adheres to national and international guidelines[2,6,7]. One of the initial limitations of CEUS, reported in 2010, was the possibility of missing ICC cases, since a significant proportion of the ICC nodules that develop in a cirrhotic liver show the

same enhancement pattern as HCC[8]. Since then, subsequent studies have demonstrated that the timing and intensity of washout are different in HCC and ICC. In particular, for the vast majority of ICC nodules (50%-85%), washout starts earlier than 60 *s*, while this is rarely observed in HCC. Furthermore, washout intensity during late phase is clearer in ICC than in HCC[9-14]. These findings led the American College of Radiology to release the CEUS Liver Imaging Reporting and Data System (CEUS LI-RADS), similar to previous releases for computed tomography (CT) and magnetic resonance imaging (MRI). The algorithm was officially approved in June 2016, and the latest update was published in 2017 [15].

CEUS LI-RADS is a standardized system for technique, interpretation, reporting, and data collection on focal liver lesions in patients at high risk for HCC. It encompasses features such as size, conventional ultrasound morphology, contrast enhancement behaviours, and dimensional variations in order to stratify the risk of HCC and to avoid ICC misdiagnosis[16-20]. In particular, CEUS LR-5 is a class specifically designed to include HCC. It encompasses nodules > 1 cm that show arterial phase hyperenhancement (APHE) that is neither rim nor globular, followed by a late (> 60 *s*) mild-degree washout. Other CEUS LI-RADS categories (*e.g.*, CEUS LR-4 and 3) express a very probable and intermediate risk of HCC, while CEUS LR-M has an intermediate/high risk of malignancy without a typical HCC pattern. CEUS LR-M includes lesions of any size that show arterial phase rim enhancement pattern and/or early (before 60 *s*) washout and/or marked washout.

So far, only a few studies have presented actual data from the application of CEUS LI-RADS diagnostic algorithm in cirrhotic patients with suspicious nodules[21-27]. The aim of this study was to test the capability of CEUS LI-RADS in accurately diagnosing focal liver lesions in patients affected by cirrhosis. In particular, we tested the accuracy of CEUS LR-5 and LR-M in correctly diagnosing HCC and ICC, respectively. In addition, we merged classes LR-4 and LR-5 and tested their accuracy in correctly diagnosing HCC as a joint class. Finally, we assessed the rate of malignancy for specific LR-3 class patterns.

MATERIALS AND METHODS

Study design and data collection

The present retrospective study involved patients with cirrhosis associated nodules that were visible using conventional ultrasound, for which it was possible to review the basal appearance and dynamic pattern of the ultrasound contrast agent. Cirrhosis was diagnosed on the basis of clinical data, biochemical parameters, imaging criteria, and elastosonography.

We reviewed all the liver CEUS performed at our centre (Medical Ultrasound Unit, University Hospital, Sassari, Italy) between December 2008 and January 2020. All examinations aimed to characterize a new nodule developed in the context of surveillance programmes for liver cirrhosis. Nodules located in different liver segments were analysed separately with individual boluses of contrast. Within the same segment, only one target nodule was included for analysis based on best visualization criteria.

CT and/or MRI, when typical for HCC or definitely benign (haemangioma, hepatic fat deposition/sparing, and hypertrophic pseudomass), were used as the gold standard imaging modalities. For all other cases, histology obtained by a percutaneous biopsy or surgical resection was considered the reference standard (Supplementary Figures 1 and 2).

Specifically, nodules showing a CT/MRI dynamic pattern with hyperenhancement during the arterial phase followed by washout in the portal or late phase (Supplementary Figures 3 and 4), were diagnosed as HCC in accordance with both the American Association for the Study of Liver Diseases (AASLD) and the Italian Association for the Study of the Liver (AISF) guidelines[2,28]. Benign lesions received a further 2-year follow-up; in case of any increase in size and/or CEUS enhancement variations, a biopsy was performed.

All cases where it was not possible to review the timing and the degree of washout on CEUS (23 cases), or a validated diagnostic reference standard, either CT/MRI scan or histology, was not available (35 cases), were excluded. The algorithm of the study is shown in Figure 1.

CEUS examination and CEUS LI-RADS classification

All CEUS examinations were performed by a physician with 15 years of experience (G.V.) using a second-generation ultrasound contrast agent (SonoVue, Bracco, Milan, Italy).

The signal coming from the bubbles was detected through the following ultrasound scanners: (1) Acuson Sequoia 512 with a 4C1 convex probe and cadence contrast pulse sequencing (CPS, Acuson Siemens, Mountain View, CA, United States) until 2014; and (2) Aixplorer (SuperSonic Imaging, S.A., Aix en Provence, France) with a convex broadband probe (SC6-1) and dedicated software also known as Power Modulated Pulse Inversion (PMPI) from January 2015 until the end of the study.

The CEUS examination was performed continuously for 120 s starting from the injection of contrast. Subsequently, short clips lasting 15-30 *s* were recorded until 5 min after injection.

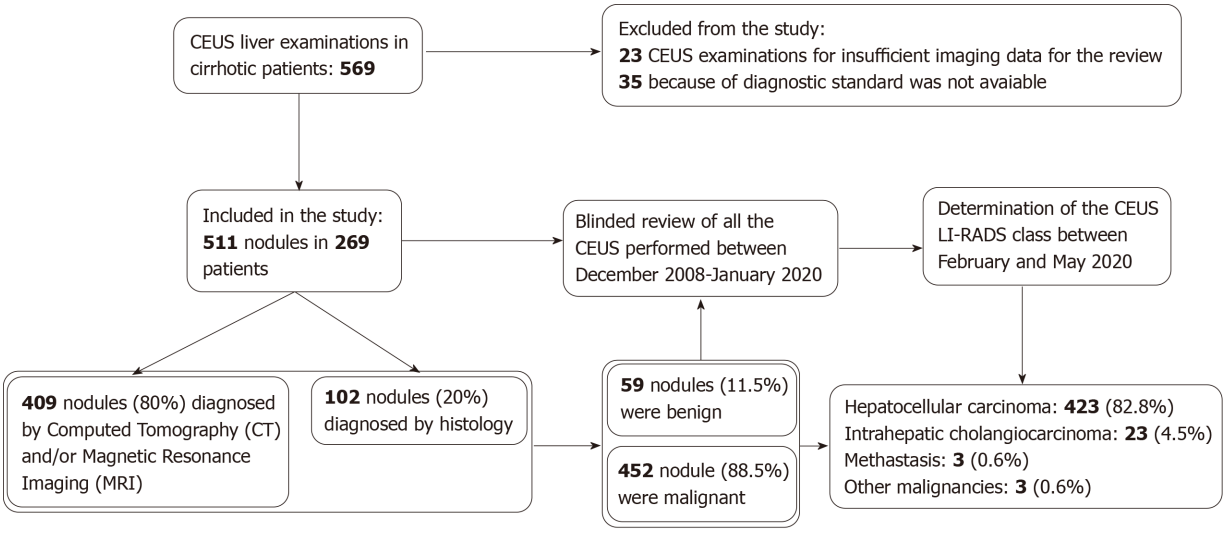

DOI: 10.3748/wjg.v28.i27.3488

Figure 1 Flow chart of the study.

The CEUS LI-RADS patterns were established after evaluation of all clips and images, with particular attention to the behaviour of intranodular contrast enhancement in dynamic phases.

The review process was independently performed by two operators (G.V. and M.A.) with 15 and 2 years of experience, respectively. In case of disagreement, the class indicated by the more experienced operator was assigned.

The reviewers were blinded to patient identity and final diagnosis. The specific targets of the review process were: (1) Nodule size; (2) the presence of APHE and the type of filling (global, rim, or peripheral discontinuous globular enhancement); and (3) the presence of washout during portal and parenchymal phases, focusing on its timing (before or after 60 *s*) and intensity (mild or marked); washout before 60 *s* was considered early, while washout happening after 60 *s* was considered late.

Inter-rater reliability of CEUS LI-RADS class assignment and of CEUS major features between the two raters (internal agreement) was evaluated for all the nodules (n = 511). Inter-rater reliability among our centre and two other operators from external centres (M.A.Z and G.I., both with more than 20 years of experience in CEUS) was also evaluated for a subgroup of 50 nodules (external agreement). To avoid an excess of typical HCCs, a total of 26 HCCs, 11 ICCs, 11 benign lesions, and 2 other malignancies were randomly selected for the external agreement analysis.

The entire process, including folder preparation, CEUS LI-RADS class assignment, and dataset preparation for analysis, was completed over a period of 5 mo. A systematic review of all CT and MRI scans was not performed.

Statistical analysis

Descriptive statistics (median, interquartile range, range, and percentage) were calculated for patients' demographic and clinical characteristics (age, sex, aetiology of cirrhosis, number, and size of nodules). The normal distribution of continuous variables was evaluated through Shapiro-Wilk test. Discrete and qualitative variables are expressed as frequencies and percentages.

Sensitivity, specificity, positive predictive value (PPV), negative predictive value (NPV), diagnostic accuracy, Youden's index, relative risk, odds ratio, positive likelihood ratio, and negative likelihood ratio were calculated to assess the accuracy of different CEUS-LR classes and subclasses in diagnosing HCC (LR-5, LR-4, and LR-4 and 5 merging class), ICC (LR-M), and malignancies (LR-3). The associations between different CEUS LI-RADS classes and definite diagnosis were evaluated by Pearson's chi-square test or Fisher's exact test. To determine the uncertainty of the estimates on sensitivity, specificity, PPV, NPV, and diagnostic accuracy, 95% confidence intervals (CIs) were calculated.

Cohen's k and Fleiss' k statistics were used to evaluate the interobserver agreement among different examiners in the assignment of the CEUS LI-RADS classes and identification of APHE (absent, homogeneous, or rim-like), and washout (absent, late and mild, or early and/or marked). Additionally, a visual graphical representation of the agreement was created, based on the agreement chart proposed by Bangdiwala[29]. All statistical tests were considered significant for a P value < 0.05. Data were analysed using Stata/MP version 17.0 (Statacorp LP, TX, United States) and R version 4.1.1 (The R Foundation for Statistical Computing, Vienna, Austria).

RESULTS

A total of 511 nodules identified in 269 patients were considered in this study. The complete dataset concerning patients and nodule characteristics is shown in Table 1.

Four-hundred and fifty-two out of 511 nodules (88.5%) turned out to be malignant, consisting of 423 HCCs (82.8%), 23 ICCs (4.5%), 3 metastases (0.6%), and 3 other malignancies (0.6%). Non-invasive diagnosis was obtained for 409 nodules (80%), while histology was followed for 102 nodules (20%). Complete data concerning each definite diagnosis rate for every CEUS LI-RADS class are reported in Table 2. Table 3 shows the rates of HCC and ICC in different CEUS LI-RADS classes. The pathological findings for hepatic nodules are shown in Supplementary Table 1.

The most prevalent pattern in the arterial phase was homogeneous APHE (79.1% of all nodules), followed by isoenhancement (12.7%). In the portal and late phases, the majority of nodules showed a late and mild washout (60.7%) while the second most frequent pattern was isoenhancement (30.7%). See Table 4 and Table 5 for complete data on CEUS pattern in the arterial and venous phases, respectively.

LR-M nodules

Thirty-seven lesions (7.2%) were assigned to the CEUS LR-M class (Figure 2A). Twenty-one of these nodules turned out to be ICCs, eleven were HCCs, three were metastases, one was a lymphoepithelioma, and one was benign. CEUS LR-M predicted ICC with a 91.3% sensitivity, 96.7% specificity, 56.8% PPV, 99.6% NPV, and 96.5% diagnostic accuracy ($P < 0.001$) (Table 6). Examining the CEUS behaviour of ICC, it was observed that 16 out of 21 nodules (76%) showed a rim APHE, while 11 out of 21 nodules (52%) showed an early washout (Supplementary Table 2). HCC nodules reported as LR-M showed a rim APHE in 6 out of 11 cases (54.5%) and an early washout in 7 out of 11 cases (63.6%; Supplementary Table 3).

LR-5 nodules

A total of 288 nodules (56.4%) were categorized as CEUS LR-5 (Figure 2B), of which 286 turned out to be HCC, and 2 were benign lesions. The median diameter of these nodules was 25 mm. The conclusive diagnosis was achieved by CT/MRI for 248 nodules and by histology for 40. CEUS LR-5 class predicted HCC with a 67.6% sensitivity, 97.7% specificity, 99.3% PPV, 38.6% NPV, and 72.8% diagnostic accuracy ($P < 0.001$) (Table 6).

LR-4 nodules

One-hundred and fourteen nodules (22.3%) were reported as CEUS LR-4 (Figure 2C), of which 111 were HCC and 3 were regenerative nodules, as confirmed by histology. The median diameter of these nodules was 21.5 mm. In 95 cases, the diagnosis was given by CT/MRI and in 19 cases by biopsy. CEUS LR-4 predicted HCC with a 26.2% sensitivity, 96.6% specificity, 97.4% PPV, 21.4% NPV, and 38.4% diagnostic accuracy ($P < 0.001$) (Table 6). Table 7 show data relative to different LR-4 patterns.

LR 4-5 merged class

The merging of CEUS LR-4 and CEUS LR-5 classes predicted HCC with a 93.9% sensitivity, 94.3% specificity, 98.8% PPV, 76.1% NPV, and 93.9% diagnostic accuracy ($P < 0.001$) (Table 6).

LR-3 nodules

Sixty-six lesions (12.9%) were assigned to the CEUS LR-3 class (Figure 2D and E). Specifically, 15 of these nodules were HCCs, 2 were ICCs, 2 were other malignancies, and 47 were benign lesions. The median diameter of these nodules was 16 mm. Fifty-three lesions were diagnosed non-invasively by CT/MRI, while 13 by biopsy. CEUS LR-3 predicted benign lesions with a 79.7% sensitivity, 95.8% specificity, 71.2% PPV, 97.3% NPV, and 93.9% diagnostic accuracy ($P < 0.001$) (Table 6). Lesions belonging to the CEUS LR-3 class showed great heterogeneity. In fact, iso-iso nodules (Figure 2D) were most likely benign (only 1 malignancy out of 39 nodules), while other patterns showed a higher risk of cancer (18 malignancies out of 27). The second most frequent CEUS LR-3 pattern was the hypo-hypo pattern assigned to 15 nodules (Figure 2E), of which 11 were malignant (7 HCCs, 2 ICCs, 1 lymphoma, and 1 carcinosarcoma). The rate of malignancy for the CEUS LR-3 class and its subclasses are shown in Figure 3. We also calculated the correlation between specific CEUS LR-3 subgroups and malignancy, with analysis limited to CEUS LR-3 nodules ($n = 66$). It was observed that CEUS LR-3 iso-iso pattern predicted malignancy with a 5.3% sensitivity, 19.1% specificity, 2.6% PPV, 33.3% NPV, and 15.2% diagnostic accuracy ($P < 0.001$). Conversely, CEUS LR-3 hypo-hypo pattern predicted malignancy with a 57.9% sensitivity, 91.5% specificity, 73.3% PPV, 84.3% NPV, and 81.8% diagnostic accuracy ($P < 0.001$) (Table 6). Data concerning different LR-3 patterns are reported in Table 7.

LR 1-2 nodules

Only one nodule (0.2%) was categorized as CEUS LR-1, and five nodules (1%) as CEUS LR-2. All these nodules were found to be benign.

Table 1 Characteristics of patients and hepatic nodules

Item	Number or range
Nodules, *n*	511
Patients, *n*	269
Males, *n* (%)	219 (81.4)
Females, *n* (%)	50 (18.6)
Median age at first nodule (IQR; range)	69 years (61-75; 43-88)
Males (IQR; range)	67 years (59-74; 43-88)
Females (IQR; range)	74.5 years (71-78; 59-85)
Hepatic cirrhosis aetiology (n)	
Chronic HCV infection, *n* (%)	129 (48)
Alcohol abuse, *n* (%)	45 (16.7)
Chronic HBV infection, *n* (%)	24 (8.9)
Chronic HCV infection + alcohol abuse, *n* (%)	21 (7.8)
Chronic HBV + HCV infection, *n* (%)	8 (3)
NASH, *n* (%)	6 (2.2)
ChronicHBV infection + alcohol abuse, *n* (%)	5 (1.9)
Other aetiologies, *n* (%)	6 (2.2)
Unknown aetiology, *n* (%)	25 (9.3)
Median diameter of nodules (IQR; range)	24 mm (16-36; 5-200)

IQR: Inter quartile range; HCV: Hepatitis C virus; HBV: Hepatitis B virus; NASH: Non-alcoholic steatohepatitis.

Table 2 Rates of different conclusive diagnoses for each Contrast-enhanced ultrasound Liver Imaging Reporting and Data System class

		Conclusive diagnosis						%
		HCC	ICC	Metastasis	Other malignancy	Benign lesion	Total	
CEUS LI-RADS class	CEUS LR-M	11	21	3	1	1	37	7.2
	CEUS LR-5	286	0	0	0	2	288	56.4
	CEUS LR-4	111	0	0	0	3	114	22.3
	CEUS LR-3	15	2	0	2	47	66	12.9
	CEUS LR-2	0	0	0	0	5	5	1.0
	CEUS LR-1	0	0	0	0	1	1	0.2
	Total	423	23	3	3	59	511	100.0
%		82.8	4.5	0.6	0.6	11.5	100.0	

CEUS LI-RADS: Contrast-enhanced ultrasound Liver Imaging Reporting and Data System; HCC: Hepatocellular carcinoma; ICC: Intrahepatic cholangiocarcinoma.

Interobserver agreement

The observed agreement between the two internal raters (1 and 2) for the assignment of CEUS LI-RADS class was 95.7%, with Cohen's $k = 0.94$ (95%CI: 0.92-0.97, $P < 0.0001$), which represents an almost perfect agreement, according to Landis and Koch[30] classification. The agreement is clearly visualized in Figure 4A. Supplementary Table 4 shows the assignments of the two raters.

The observed agreement among the three raters from different centres (2, 3, and 4) for the assignment of CEUS LI-RADS class was 68% and Fleiss's k coefficient showed a value of 0.67 ($P < 0.0001$), which represents a substantial agreement. In particular, the agreement was almost perfect between raters 2 and

Table 3 Rates of hepatocellular carcinoma and intrahepatic cholangiocarcinoma in different Contrast-enhanced ultrasound Liver Imaging Reporting and Data System classes

CEUS LI-RADS class	HCC	ICC
LR-3	15/66 (22.7%)	2/66 (3%)
LR-4	111/114 (97.4%)	0/114 (0%)
LR-5	286/288 (99.3%)	0/288 (0%)
LR-M	11/37 (29.7%)	21/37 (56.8%)

CEUS LI-RADS: Contrast-enhanced ultrasound Liver Imaging Reporting and Data System; HCC: Hepatocellular carcinoma; ICC: Intrahepatic cholangiocarcinoma.

Table 4 Rates of different contrast-enhanced ultrasound patterns in arterial phase

Arterial phase CEUS pattern	Nodules, *n* (%)
Homogeneous hyperenhancement	404 (79.1)
Rim hyperenhancement	23 (4.5)
Globular hyperenhancement	1 (0.2)
Isoenhancement	65 (12.7)
Hypoenhancement	18 (3.5)

CEUS: Contrast-enhanced ultrasound.

Table 5 Rate of different portal and late phase contrast-enhanced ultrasound patterns

Portal and late phase CEUS pattern	Nodules, *n* (%)
Late and mild washout	310 (60.7%)
Early/marked washout	27 (5.3%)
Isoenhancement	157 (30.7%)
Hypoenhancement	15 (2.9%)
Hyperenhancement	2 (0.4%)

CEUS: Contrast-enhanced ultrasound.

3 (k = 0.88, $P < 1.7 \times 10^{-68}$), substantial between raters 2 and 4 (k = 0.66, $P < 1.5 \times 10^{-14}$), and substantial between raters 3 and 4 (k = 0.61, $P < 8.5 \times 10^{-10}$). The agreement is visualized in Figure 4B-D.

With regards to specific CEUS patterns, we found a higher degree of agreement for APHE (internal k = 0.86, $P < 2.7 \times 10^{-214}$; external k = 0.8, $P < 0.001$) than for washout (internal k = 0.79, $P < 1.6 \times 10^{-202}$; external k = 0.71, $P < 0.001$).

DISCUSSION

CEUS LI-RADS is a valuable diagnostic tool for non-invasive differential diagnosis of focal liver lesions in patients with cirrhosis. Based on our experience, employing this approach improves the performance of CEUS in the characterization of nodules, especially to discriminate between HCC and ICC.

In the current study, CEUS LR-5 was extremely specific for HCC with a very high PPV (99.3%). Only two false-positive results were observed, which were not ICC. We can therefore maintain that CEUS LR-5 is an appropriate tool for non-invasive diagnosis of HCC with virtually no risk of ICC misdiagnosis. Our data agree with recent publications on the subject[22]. However, CEUS LR-5 lacked sensitivity (67.6%) due to the large number of CEUS LR-4 nodules with a final diagnosis of HCC (97.4%). The high specificity of CEUS LR-5 for HCC combined with a low sensitivity was confirmed by a recent prospective multicentric study that compared the accuracy of different CEUS algorithms for the non-

Table 6 Diagnostic statistics of different contrast-enhanced ultrasound Liver Imaging Reporting and Data System classes for different diagnosis

Tested association	Sensitivity (%)	Specificity (%)	PPV (%)	NPV (%)	Diagnostic accuracy (%)	Youden's index	Odds Ratio	*P* value
CEUS LR M-ICC	91.3 (72.0-98.9)	96.7 (94.7-98.1)	56.8 (39.5-72.9)	99.6 (98.5-99.9)	96.5 (94.5-97.9)	0.880	309.75	< 0.001
CEUS LR 5-HCC	67.6 (62.9-72.1)	97.7 (92.0-99.7)	99.3 (97.5-99.9)	38.6 (32.1-45.3)	72.8 (68.7-76.6)	0.653	89.80	< 0.001
CEUS LR 4-HCC	26.2 (22.1-30.7)	96.6 (90.4-99.3)	97.4 (92.5-99.5)	21.4 (17.5-25.8)	38.4 (34.1-42.7)	0.228	10.10	< 0.001
CEUS LR 4/5-HCC	93.9 (91.1-95.9)	94.3 (87.2-98.1)	98.8 (97.1-99.6)	76.1 (67.0-83.8)	93.9 (91.5-95.8)	0.882	253.50	< 0.001
CEUS LR 3-benign lesion	79.7 (67.2-89.0)	95.8 (93.5-97.5)	71.2 (58.7-81.7)	97.3 (95.3-98.6)	93.9 (91.5-95.8)	0.755	89.26	< 0.001
CEUS LR-3-malignancy	4.2 (2.5-6.5)	20.3 (11.0-32.8)	28.8 (18.3-41.3)	2.7 (1.4-4.7)	6.0 (4.2-8.5)	-0.755	0.01	< 0.001
CEUS LR-3-iso-iso-malignancy	5.3 (0.1-26.0)	19.1 (9.1-33.3)	2.6 (0.1-13.5)	33.3 (16.5-54.0)	15.2 (7.5-26.1)	-0.756	0.01	< 0.001
CEUS LR-3-hypo-hypo-malignancy	57.9 (33.5-79.7)	91.5 (79.6-97.6)	73.3 (44.9-92.2)	84.3 (71.4-93.0)	81.8 (70.4-90.2)	0.494	14.78	< 0.001

CEUS: Contrast-enhanced ultrasound; HCC: Hepatocellular carcinoma; ICC: Intrahepatic cholangiocarcinoma; PPV: Positive predictive value; NPV: Negative predictive value.

Table 7 Classification of nodules for LR-3, LR-4, and LR-5 classes, reported in yellow, orange, and red, respectively

Nodule size	No APHE[1]		APHE[1]		Total
	< 20 mm	≥ 20 mm	< 10 mm	≥ 10 mm	
No washout of any type	37 (4)	21 (5)	1 (1)	106 (104)	165
Late and mild washout	7 (5)	8 (7)	0	288 (286)	303
Total	44	29	1	394	468

[1]With the exclusion of nodules with rim and peripheral discontinuous globular arterial phase hyper-enhancement belonging to contrast-enhanced ultrasound LR-M and contrast-enhanced ultrasound LR-1 classes, respectively.
Number of hepatocellular carcinomas in brackets. APHE: Arterial phase hyperenhancement.

invasive diagnosis of HCC[31] and a recent meta-analysis[32].

Considering the high risk of HCC for the LR-4 class (97.4% PPV), the possibility of merging LR-4 and 5 classes was tested. By doing so, sensitivity in identifying HCC rose from 67.6% to 93.9%. The loss in specificity was low (from 97.7% to 94.3%), and was entirely attributed to two nodules > 10 mm classified as CEUS LR-4, which turned out to be benign. Data from the literature supports such an approach, showing that around 50% of HCCs do not display any washout in the portal and late venous phases on CEUS. In particular, Giorgio *et al*[33] demonstrated in their series that 55.4% of the biopsied HCC nodules < 20 mm showed this pattern after APHE. These findings were further corroborated by Leoni *et al*[34], who found that the hyper-iso pattern shows a high PPV (94%) for HCC and identifies nodules that are HCC or with a strong tendency to malignant progression. This pattern was detected in 36.2% (46 out 127) of HCCs[34].

Therefore, it should be considered that the introduction of the washout criteria in CEUS is based on findings from studies exploring the role of contrast-enhanced CT in the non-invasive diagnosis of HCC [35-37]. These findings were then extended to CEUS and MRI with little consideration for the differences in the pharmacokinetics of contrast agents among these techniques and the importance of the nodule visibility at baseline. Indeed, the requirement for washout as a diagnostic criterion is less stringent for CEUS and MRI, since these techniques have an improved capability to evaluate and determine whether APHE reflects the presence of a distinct nodule or merely abnormalities of intrahepatic vessels. CEUS, in particular, is performed for improved characterization of a nodule that has already been detected through conventional ultrasound.

Unfortunately, the introduction of washout in CEUS has significantly lowered the sensitivity of non-invasive diagnostic criteria for HCC. The inclusion of hyper-iso pattern among criteria for non-invasive HCC diagnosis might be a solution to increase CEUS sensitivity. Using this strategy, it can be concluded that there is no significant risk of overestimating the diagnosis of HCC, as in our series 98% of the

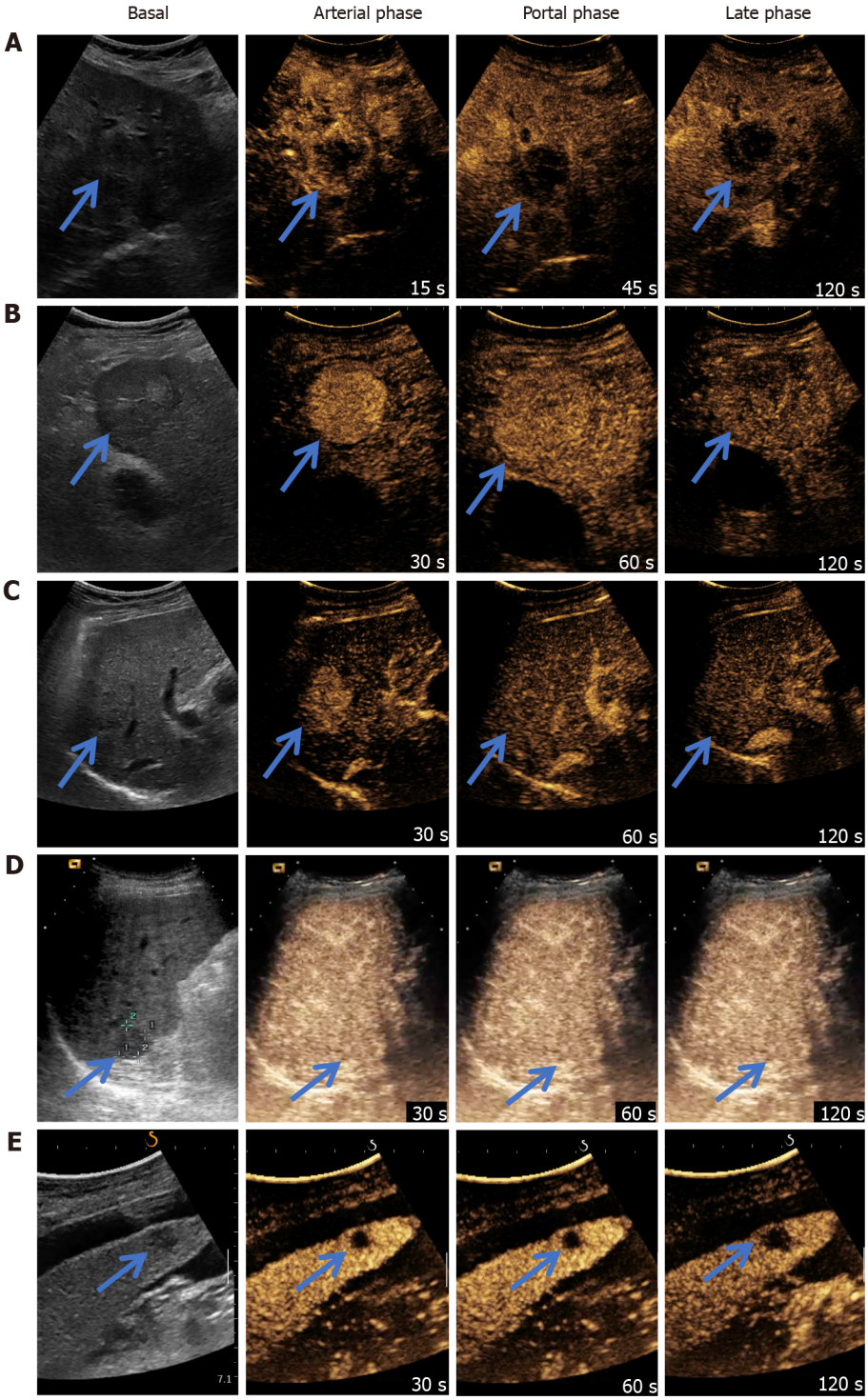

DOI: 10.3748/wjg.v28.i27.3488

Figure 2 Examples of different contrast-enhanced ultrasound Liver Imaging Reporting and Data System classes. A: Contrast-enhanced ultrasound (CEUS) LR-M. Notice rim arterial phase hyperenhancement and early washout, before 60 *s*; B: CEUS LR-5. Notice homogeneous arterial phase hyperenhancement, isoenhancement in portal phase, and mild washout in the late phase; C: CEUS LR-4. Notice homogeneous arterial phase hyperenhancement and isoenhancement in both portal and late phases; D: CEUS LR-3 iso-iso. Notice isoenhancement in all phases; E: CEUS LR-3 hypo-hypo. Notice hypoenhancement in all phases. The arrows show the target lesion.

nodules with the hyper-iso pattern were HCCs and only 2% were benign nodules. These considerations and results agree with another study on the combination of CEUS LR-4 and LR-5 criteria[38]. Furthermore, different studies demonstrated that the identification of washout has higher inter-rater variability than APHE identification[39,40]. These findings are also confirmed by the present study.

Regarding ICC, we observed that the majority of the nodules (21/23, 91.3%) were correctly diagnosed using the LR-M class of risk. Only two ICC cases were not assigned to this class due to a hypovascular aspect in all phases. The high sensitivity and specificity of the CEUS LR-M class for ICC (91.3% and

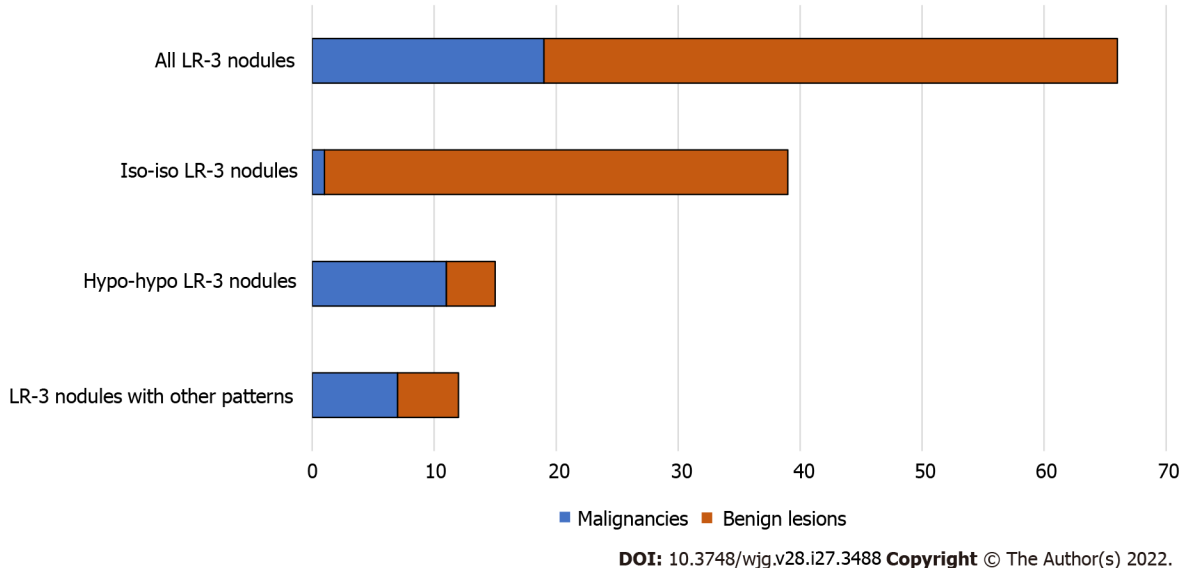

DOI: 10.3748/wjg.v28.i27.3488

Figure 3 Absolute frequency (*n*) of malignancies and benign lesions in LR-3 nodules and LR-3 subgroups with different contrast-enhanced ultrasound patterns.

96.7%, respectively) in our series of patients demonstrate that this class is a valuable diagnostic tool for this type of cancer. Still, this class is not entirely specific for ICC as other types of malignancy can be found, such as HCC, metastatic lesions, and rarer malignancies[41]. We found that 11 out of 37 nodules (30%) classified as LR–M turned out to be HCC. This was due to the presence of an early washout (63.6% of nodules) and/or a rim enhancement pattern (54.5% of nodules). These observations are in agreement with the previously published literature. In particular, a multicentre retrospective study published by Terzi *et al*[22] reported that about 40% of LR-M lesions were HCCs. Another study by Wilson *et al*[16] identified that 35% of HCCs were reported to be LR-M. Several other authors have attempted to decrease the risk of HCC misdiagnosis by proposing a modified LR-M class of risk with the introduction of new criteria, such as the shortening of washout timing to < 45 *s* or the possibility to detect a significant washout to < 3 min[42-44]. Interestingly, Chen *et al*[45] were able to reduce the ICC misdiagnosis rate with CEUS LR-M from 38 to 12 cases by considering other criteria such as the presence of an intratumoral vein or an unclear boundary of the intratumoral non-enhanced area. However, we did not test these new criteria that require validation in multicentric and prospective studies. Another recent study by Huang *et al*[46] suggested that the integration of CEUS with the dosage of serum tumour markers (AFP and CA 19.9) improves the differentiation of LR-M nodules. Even though there are some limitations related to LR-M in this scenario, the adoption of this class of risk allows the improvement of diagnostic performance of CEUS for ICC, overcoming the drawbacks that resulted in the elimination of CEUS from the diagnostic flow charts of the most important hepatological international guidelines[3,8].

At present, CEUS LR-3 lesions are considered to hold an intermediate risk of malignancy, which is around 50% according to a recent study published by Terzi *et al*[22]. This rate was much lower in our case series (28.8%), which might be attributable to the lower figures of our study. Still, looking at the data from single centres in the multicentric study by Terzi *et al*[22], the rate of HCC in the CEUS LR-3 class ranged between 28.3% and 74.3%. One possible explanation for these results could be the high intrinsic heterogeneity of this class. Indeed, the algorithm only considers either the presence or absence of APHE, without any distinction between isoenhancement and hypoenhancement in all phases. However, in our clinical experience, hypo-hypo lesions are more likely to be malignant than iso-iso lesions. The present study confirmed this observation: Within the CEUS LR-3 class, the PPV for malignancy moved from 28.8% for CEUS LR-3 overall class to 2.6% for CEUS LR-3 iso-iso nodules, and 73.3% for CEUS LR-3 hypo-hypo nodules (Table 5). These considerations are in concordance with studies published before the advent of CEUS LI-RADS, when the problem of hypovascular nodules, which represent around 10% of HCC, was highlighted[47-49]. Likewise, we should be aware of the possibility of detecting ICC nodules in this class when a nodule shows hypoenhancement in all the phases; as observed in two out of 15 (13%) hypo-hypo nodules in our study. In light of these observations, we believe that it might be advantageous to split the CEUS LR-3 class into two subgroups (*e.g.*, CEUS LR-3a and CEUS LR-3b) in order to separate iso-iso lesions from other patterns. To the best of our knowledge, this is the first study suggesting a CEUS LR-3 refinement based on real-life results. We believe that more attention should be directed towards the behaviour of nodule enhancement, rather than focusing on the size of the lesion alone.

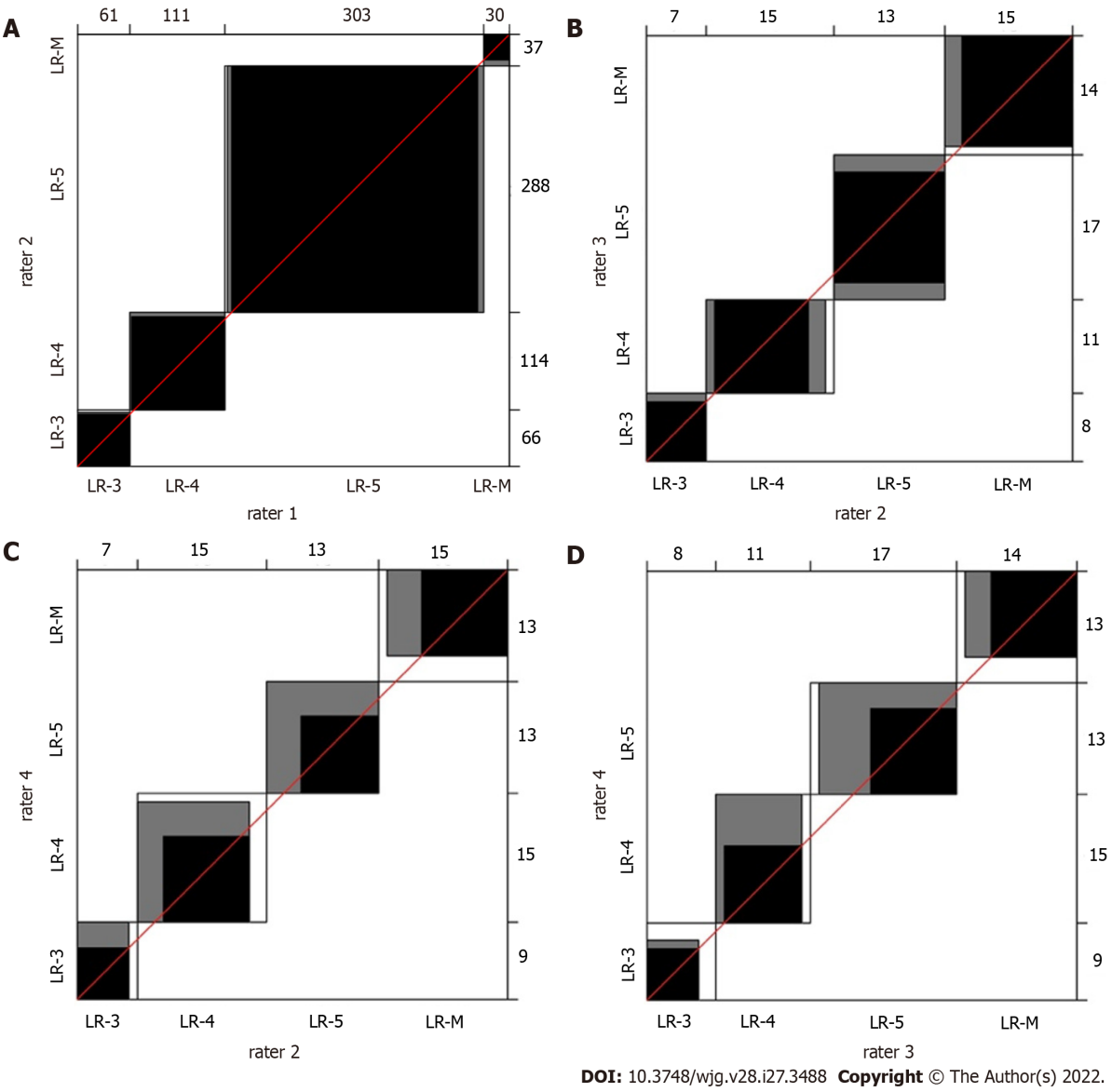

DOI: 10.3748/wjg.v28.i27.3488

Figure 4 Bangdiwala's agreement charts of the Contrast-enhanced ultrasound Liver Imaging Reporting and Data System class assignments between different raters. In the case of perfect agreement, the *k* rectangles are represented by perfect squares and the shaded squares determined by the diagonal cell entries are exactly equal to the rectangles; lesser agreement is visualized by comparing the area of the blackened squares to the area of the rectangles. A: Agreement chart between the two internal raters (1 and 2), with the exclusion of LR-1 and LR-2 classes due to their rarity (n = 505); B-D: Agreement charts among the three raters from different centres (2, 3, and 4) for the subgroup of 50 nodules. We list the agreement charts between raters 2 and 3 (B), between raters 2 and 4 (C), and between raters 3 and 4 (D).

Finally, this study demonstrated excellent inter-rater reliability of this classification system. Therefore, the use of CEUS LI-RADS in clinical practice could improve the reproducibility of CEUS and partially reduce the gap due to the difference in experience, as suggested by a recent study[50].

Our study also has some critical shortcomings, namely, its retrospective nature and the limited number of nodules analysed. These drawbacks are primarily due to the fact that data were collected from a single centre. Another debatable aspect of our investigation is the limited number of biopsies. However, we would like to highlight that current guidelines do not routinely recommend biopsy for nodules with typical HCC pattern on CT or MRI, allowing a non-invasive diagnosis[4,28].

Further prospective multicentric studies are warranted to confirm our findings and to investigate whether our considerations could be applied to the general population of patients with cirrhosis.

CONCLUSION

The present study supports the use of CEUS LI-RADS for the characterization of focal liver lesions in liver cirrhosis and the usefulness of LR-5 and LR-M classes to diagnose HCC and ICC, respectively. Additionally, our findings suggest that the merging of LR-4 and LR-5 classes provides innovative

benefits in terms of diagnostic accuracy for HCC. Furthermore, it seems reasonable to split the CEUS LR-3 class into two subgroups to differentiate the risk of malignancy between iso-iso nodules, which are more likely to be benign, and other patterns, namely, hypo-hypo nodules, which are more likely to be malignant and not specific for HCC.

ARTICLE HIGHLIGHTS

Research background

Patients affected by liver cirrhosis are at high risk of developing hepatocellular carcinoma (HCC) and other malignancies such us intrahepatic cholangiocellular carcinoma (ICC). Diagnostic tools to characterize new-onset nodules in cirrhosis include contrast-enhanced ultrasound (CEUS), but this technique has been challenged for the possibility of misdiagnosing HCC and ICC.

Research motivation

The CEUS Liver Imaging Reporting and Data System (CEUS LI-RADS) aims to refine CEUS interpretation in order to improve the differentiation of HCC from other malignancies. Nevertheless, its effectiveness in real-life context has not yet been well established.

Research objectives

To test the accuracy of CEUS LI-RADS in correctly diagnosing HCC and ICC in cirrhosis with LR-5 and LR-M class, respectively, to evaluate the performance of LR-4 and 5 merging class in the diagnosis of HCC, and to investigate the rate of malignancies in different LR-3 patterns.

Research methods

This study consecutively collected 511 nodules in 269 cirrhotic patients from December 2008 to January 2020. A CEUS LI-RADS class was retrospectively attributed to each nodule based on review of CEUS examination. Common diagnostic accuracy indexes were assessed for the following associations: CEUS LR-5 and HCC; CEUS LR-4 and 5 merged class and HCC; CEUS LR-M and ICC; CEUS LR-3 and malignancy. The diagnostic standard was either biopsy or computed tomography/magnetic resonance imaging. The frequency of malignant lesions in CEUS LR-3 subgroups with different CEUS patterns was also determined.

Research results

CEUS LR-5 showed a 97.7% specificity for HCC with a low sensitivity (67.6%), while the CEUS LR-4 and 5 merged class showed a 93.9% sensitivity and 94.3% specificity for HCC. CEUS LR-M predicted ICC with a 91.3% sensitivity and 96.7% specificity. CEUS LR-3 predominantly included benign lesions (28.8% of malignancies) but was heterogeneous as the hypo-hypo pattern showed a higher rate of malignant lesions (73.3%) than the iso-iso pattern (2.6%).

Research conclusions

HCC diagnosis could benefit from the merging of CEUS LI-RADS classes 4 and 5. In addition, splitting LR-3 class could be advantageous to differentiate iso-iso nodules from other patterns with a higher risk of malignancy.

Research perspectives

Further prospective multicentric studies are necessary to confirm and extend our findings to the general population.

ACKNOWLEDGEMENTS

The authors thank Cabigiosu F for his help in data entry, and Fois SS for contributing to English language revision of the manuscript.

FOOTNOTES

Author contributions: Vidili G designed the study, performed contrast-enhanced ultrasound examinations, biopsies, and the blinded review of cases, and wrote and revised the manuscript; Arru M performed the blinded review of the cases, collected and analysed the data, and participated in paper writing and review; Solinas G performed the statistical analysis and participated in the final draft; Calvisi DF collected and analysed the data, and participated in writing, review, and editing of the manuscript; Meloni P, Sauchella A, and Di Lembo E participated in collecting and

preparing the data for the analysis; Turilli D and Fabio C performed computed tomography and magnetic resonance imaging scans and participated in data collection; Cossu A reviewed the pathology material; Madeddu G participated in data collection and writing the paper; Zocco MA and Iannetti G performed the external blinded review of the cases; Delitala AP and Babudieri S participated in data analysis and writing of the manuscript; Manetti R participated in writing and reviewing the final draft; all authors have read and agreed to the final version of the manuscript.

Supported by the Fondazione di Sardegna, No. FDS2019VIDILI; and the University of Sassari, No. FAR2019.

Institutional review board statement: This study was reviewed and approved by the Ethics Committee of Azienda Ospedaliero Universitaria di Sassari and the Ethics Committee of Azienda Ospedaliero Universitaria di Cagliari (No. PG/2020/16814).

Informed consent statement: All study participants, or their legal guardian, provided informed written consent prior to study enrollment.

Conflict-of-interest statement: There are no conflicts of interest to report.

Data sharing statement: Data presented in this study is available on request from the corresponding author.

Country/Territory of origin: Italy

ORCID number: Gianpaolo Vidili 0000-0003-0003-1272; Marco Arru 0000-0002-7112-5025; Giuliana Solinas 0000-0003-2174-0983; Diego Francesco Calvisi 0000-0002-6038-8567; Pierluigi Meloni 0000-0003-3313-0445; Assunta Sauchella 0000-0003-1116-7458; Davide Turilli 0000-0002-2063-994X; Claudio Fabio 0000-0002-5372-1552; Antonio Cossu 0000-0002-2390-2205; Giordano Madeddu 0000-0001-6099-2273; Sergio Babudieri 0000-0001-7291-8687; Maria Assunta Zocco 0000-0002-0814-9542; Giovanni Iannetti 0000-0002-1880-0829; Enza Di Lembo 0000-0003-1652-600X; Alessandro Palmerio Delitala 0000-0003-1729-8969; Roberto Manetti 0000-0001-7376-2303.

S-Editor: Chen YL
L-Editor: Wang TQ
P-Editor: Wu RR

REFERENCES

1 **Sung H**, Ferlay J, Siegel RL, Laversanne M, Soerjomataram I, Jemal A, Bray F. Global Cancer Statistics 2020: GLOBOCAN Estimates of Incidence and Mortality Worldwide for 36 Cancers in 185 Countries. *CA Cancer J Clin* 2021; **71**: 209-249 [PMID: 33538338 DOI: 10.3322/caac.21660]

2 **Italian Association for the Study of the Liver (AISF)**, AISF Expert Panel; AISF Coordinating Committee, Bolondi L, Cillo U, Colombo M, Craxì A, Farinati F, Giannini EG, Golfieri R, Levrero M, Pinna AD, Piscaglia F, Raimondo G, Trevisani F, Bruno R, Caraceni P, Ciancio A, Coco B, Fraquelli M, Rendina M, Squadrito G, Toniutto P. Position paper of the Italian Association for the Study of the Liver (AISF): the multidisciplinary clinical approach to hepatocellular carcinoma. *Dig Liver Dis* 2013; **45**: 712-723 [PMID: 23769756 DOI: 10.1016/j.dld.2013.01.012]

3 **European Association For The Study Of The Liver**. EASL-EORTC clinical practice guidelines: management of hepatocellular carcinoma. *J Hepatol* 2012; **56**: 908-943 [DOI: 10.1016/j.jhep.2012.03.006]

4 **European Association for the Study of the Liver**. EASL Clinical Practice Guidelines: Management of hepatocellular carcinoma. *J Hepatol* 2018; **69**: 182-236 [DOI: 10.1016/j.jhep.2018.03.019]

5 **Bolondi L**, Sofia S, Siringo S, Gaiani S, Casali A, Zironi G, Piscaglia F, Gramantieri L, Zanetti M, Sherman M. Surveillance programme of cirrhotic patients for early diagnosis and treatment of hepatocellular carcinoma: a cost effectiveness analysis. *Gut* 2001; **48**: 251-259 [PMID: 11156649 DOI: 10.1136/gut.48.2.251]

6 **Vidili G**, De Sio I, D'Onofrio M, Mirk P, Bertolotto M, Schiavone C; SIUMB experts committee. SIUMB guidelines and recommendations for the correct use of ultrasound in the management of patients with focal liver disease. *J Ultrasound* 2019; **22**: 41-51 [PMID: 30580390 DOI: 10.1007/s40477-018-0343-0]

7 **Claudon M**, Dietrich CF, Choi BI, Cosgrove DO, Kudo M, Nolsøe CP, Piscaglia F, Wilson SR, Barr RG, Chammas MC, Chaubal NG, Chen MH, Clevert DA, Correas JM, Ding H, Forsberg F, Fowlkes JB, Gibson RN, Goldberg BB, Lassau N, Leen EL, Mattrey RF, Moriyasu F, Solbiati L, Weskott HP, Xu HX; World Federation for Ultrasound in Medicine; European Federation of Societies for Ultrasound. Guidelines and good clinical practice recommendations for Contrast Enhanced Ultrasound (CEUS) in the liver - update 2012: A WFUMB-EFSUMB initiative in cooperation with representatives of AFSUMB, AIUM, ASUM, FLAUS and ICUS. *Ultrasound Med Biol* 2013; **39**: 187-210 [PMID: 23137926 DOI: 10.1016/j.ultrasmedbio.2012.09.002]

8 **Vilana R**, Forner A, Bianchi L, García-Criado A, Rimola J, de Lope CR, Reig M, Ayuso C, Brú C, Bruix J. Intrahepatic

peripheral cholangiocarcinoma in cirrhosis patients may display a vascular pattern similar to hepatocellular carcinoma on contrast-enhanced ultrasound. *Hepatology* 2010; **51**: 2020-2029 [PMID: 20512990 DOI: 10.1002/hep.23600]

9 **de Sio I**, Iadevaia MD, Vitale LM, Niosi M, Del Prete A, de Sio C, Romano L, Funaro A, Meucci R, Federico A, Loguercio C, Romano M. Optimized contrast-enhanced ultrasonography for characterization of focal liver lesions in cirrhosis: A single-center retrospective study. *United European Gastroenterol J* 2014; **2**: 279-287 [PMID: 25083285 DOI: 10.1177/2050640614538964]

10 **Forner A**, Vidili G, Rengo M, Bujanda L, Ponz-Sarvisé M, Lamarca A. Clinical presentation, diagnosis and staging of cholangiocarcinoma. *Liver Int* 2019; **39** Suppl 1: 98-107 [PMID: 30831002 DOI: 10.1111/liv.14086]

11 **Wildner D**, Schellhaas B, Strack D, Goertz RS, Pfeifer L, Fiessler C, Neurath MF, Strobel D. Differentiation of malignant liver tumors by software-based perfusion quantification with dynamic contrast-enhanced ultrasound (DCEUS). *Clin Hemorheol Microcirc* 2019; **71**: 39-51 [PMID: 29865043 DOI: 10.3233/CH-180378]

12 **Liu GJ**, Wang W, Lu MD, Xie XY, Xu HX, Xu ZF, Chen LD, Wang Z, Liang JY, Huang Y, Li W, Liu JY. Contrast-Enhanced Ultrasound for the Characterization of Hepatocellular Carcinoma and Intrahepatic Cholangiocarcinoma. *Liver Cancer* 2015; **4**: 241-252 [PMID: 26779444 DOI: 10.1159/000367738]

13 **Galassi M**, Iavarone M, Rossi S, Bota S, Vavassori S, Rosa L, Leoni S, Venerandi L, Marinelli S, Sangiovanni A, Veronese L, Fraquelli M, Granito A, Golfieri R, Colombo M, Bolondi L, Piscaglia F. Patterns of appearance and risk of misdiagnosis of intrahepatic cholangiocarcinoma in cirrhosis at contrast enhanced ultrasound. *Liver Int* 2013; **33**: 771-779 [PMID: 23445369 DOI: 10.1111/liv.12124]

14 **Chen LD**, Ruan SM, Liang JY, Yang Z, Shen SL, Huang Y, Li W, Wang Z, Xie XY, Lu MD, Kuang M, Wang W. Differentiation of intrahepatic cholangiocarcinoma from hepatocellular carcinoma in high-risk patients: A predictive model using contrast-enhanced ultrasound. *World J Gastroenterol* 2018; **24**: 3786-3798 [PMID: 30197484 DOI: 10.3748/wjg.v24.i33.3786]

15 **American College of Radiology**. CEUS LI RADS v2017 CORE. 2017. Avaiable from: https://www.acr.org/Quality-Safety/Resources/LIRADS

16 **Wilson SR**, Lyshchik A, Piscaglia F, Cosgrove D, Jang HJ, Sirlin C, Dietrich CF, Kim TK, Willmann JK, Kono Y. CEUS LI-RADS: algorithm, implementation, and key differences from CT/MRI. *Abdom Radiol (NY)* 2018; **43**: 127-142 [PMID: 28819825 DOI: 10.1007/s00261-017-1250-0]

17 **Lyshchik A**, Kono Y, Dietrich CF, Jang HJ, Kim TK, Piscaglia F, Vezeridis A, Willmann JK, Wilson SR. Contrast-enhanced ultrasound of the liver: technical and lexicon recommendations from the ACR CEUS LI-RADS working group. *Abdom Radiol (NY)* 2018; **43**: 861-879 [PMID: 29151131 DOI: 10.1007/s00261-017-1392-0]

18 **Kim TK**, Noh SY, Wilson SR, Kono Y, Piscaglia F, Jang HJ, Lyshchik A, Dietrich CF, Willmann JK, Vezeridis A, Sirlin CB. Contrast-enhanced ultrasound (CEUS) liver imaging reporting and data system (LI-RADS) 2017 - a review of important differences compared to the CT/MRI system. *Clin Mol Hepatol* 2017; **23**: 280-289 [PMID: 28911220 DOI: 10.3350/cmh.2017.0037]

19 **Rimola J**, Forner A, Tremosini S, Reig M, Vilana R, Bianchi L, Rodríguez-Lope C, Solé M, Ayuso C, Bruix J. Non-invasive diagnosis of hepatocellular carcinoma ≤ 2 cm in cirrhosis. Diagnostic accuracy assessing fat, capsule and signal intensity at dynamic MRI. *J Hepatol* 2012; **56**: 1317-1323 [PMID: 22314420 DOI: 10.1016/j.jhep.2012.01.004]

20 **Barreiros AP**, Piscaglia F, Dietrich CF. Contrast enhanced ultrasound for the diagnosis of hepatocellular carcinoma (HCC): comments on AASLD guidelines. *J Hepatol* 2012; **57**: 930-932 [PMID: 22739095 DOI: 10.1016/j.jhep.2012.04.018]

21 **Huang JY**, Li JW, Lu Q, Luo Y, Lin L, Shi YJ, Li T, Liu JB, Lyshchik A. Diagnostic Accuracy of CEUS LI-RADS for the Characterization of Liver Nodules 20 mm or Smaller in Patients at Risk for Hepatocellular Carcinoma. *Radiology* 2020; **294**: 329-339 [PMID: 31793849 DOI: 10.1148/radiol.2019191086]

22 **Terzi E**, Iavarone M, Pompili M, Veronese L, Cabibbo G, Fraquelli M, Riccardi L, De Bonis L, Sangiovanni A, Leoni S, Zocco MA, Rossi S, Alessi N, Wilson SR, Piscaglia F; CEUS LI-RADS Italy study group collaborators:. Contrast ultrasound LI-RADS LR-5 identifies hepatocellular carcinoma in cirrhosis in a multicenter restropective study of 1,006 nodules. *J Hepatol* 2018; **68**: 485-492 [PMID: 29133247 DOI: 10.1016/j.jhep.2017.11.007]

23 **Huang Z**, Zhou P, Li S, Li K. MR versus CEUS LI-RADS for Distinguishing Hepatocellular Carcinoma from other Hepatic Malignancies in High-Risk Patients. Ultrasound Med Biol 2021; 47: 1244-1252 [PMID: 33610338 DOI: 10.1016/j.ultrasmedbio.2021.01.020]

24 **Li S**, Zhou L, Chen R, Chen Y, Niu Z, Qian L, Fang Y, Xu L, Xu H, Zhang L. Diagnostic efficacy of contrast-enhanced ultrasound versus MRI Liver Imaging Reporting and Data System (LI-RADS) for categorising hepatic observations in patients at risk of hepatocellular carcinoma. Clin Radiol 2021; 76: 161.e1-161.e10 [PMID: 33198943 DOI: 10.1016/j.crad.2020.10.009]

25 **Makoyeva A**, Kim TK, Jang HJ, Medellin A, Wilson SR. Use of CEUS LI-RADS for the Accurate Diagnosis of Nodules in Patients at Risk for Hepatocellular Carcinoma: A Validation Study. *Radiol Imaging Cancer* 2020; **2**: e190014 [PMID: 33778701 DOI: 10.1148/rycan.2020190014]

26 **Pan JM**, Chen W, Zheng YL, Cheng MQ, Zeng D, Huang H, Huang Y, Xie XY, Lu MD, Kuang M, Hu HT, Chen LD, Wang W. Tumor size-based validation of contrast-enhanced ultrasound liver imaging reporting and data system (CEUS LI-RADS) 2017 for hepatocellular carcinoma characterizing. *Br J Radiol* 2021; **94**: 20201359 [PMID: 34545763 DOI: 10.1259/bjr.20201359]

27 **Lv K**, Cao X, Dong Y, Geng D, Zhang J. CT/MRI LI-RADS version 2018 versus CEUS LI-RADS version 2017 in the diagnosis of primary hepatic nodules in patients with high-risk hepatocellular carcinoma. Ann Transl Med 2021; 9: 1076 [PMID: 34422988 DOI: 10.21037/atm-21-1035]

28 **Bruix J**, Sherman M; American Association for the Study of Liver Diseases. Management of hepatocellular carcinoma: an update. *Hepatology* 2011; **53**: 1020-1022 [PMID: 21374666 DOI: 10.1002/hep.24199]

29 **Bangdiwala SI**, Shankar V. The agreement chart. *BMC Med Res Methodol* 2013; **13**: 97 [PMID: 23890315 DOI: 10.1186/1471-2288-13-97]

30 **Landis JR**, Koch GG. The measurement of observer agreement for categorical data. *Biometrics* 1977; **33**: 159-174 [PMID:

843571]
31 **Schellhaas B**, Bernatik T, Bohle W, Borowitzka F, Chang J, Dietrich CF, Dirks K, Donoval R, Drube K, Friedrich-Rust M, Gall C, Gittinger F, Gutermann M, Haenle MM, von Herbay A, Ho CH, Hochdoerffer R, Hoffmann T, Hüttig M, Janson C, Jung EM, Jung N, Karlas T, Klinger C, Kornmehl A, Kratzer W, Krug S, Kunze G, Leitlein J, Link A, Lottspeich C, Marano A, Mauch M, Moleda L, Neesse A, Petzold G, Potthoff A, Praktiknjo M, Rösner KD, Schanz S, Schultheiß M, Sivanathan V, Stock J, Thomsen T, Vogelpohl J, Vogt C, Wagner S, Wiegard C, Wiesinger I, Will U, Ziesch M, Zimmermann P, Strobel D. Contrast-Enhanced Ultrasound Algorithms (CEUS-LIRADS/ESCULAP) for the Noninvasive Diagnosis of Hepatocellular Carcinoma - A Prospective Multicenter DEGUM Study. *Ultraschall Med* 2021; **42**: e20 [PMID: 32717752 DOI: 10.1055/a-1220-8561]
32 **Peng J**, Zhang T, Wang H, Ma X. The Value of Contrast-Enhanced Ultrasound Liver Imaging Reporting and Data System in the Diagnosis of Hepatocellular Carcinoma: A Meta-Analysis. *J Ultrasound Med* 2022; **41**: 1537-1547 [PMID: 34617296 DOI: 10.1002/jum.15837]
33 **Giorgio A**, Montesarchio L, Gatti P, Amendola F, Matteucci P, Santoro B, Merola MG, Merola F, Coppola C, Giorgio V. Contrast-Enhanced Ultrasound: a Simple and Effective Tool in Defining a Rapid Diagnostic Work-up for Small Nodules Detected in Cirrhotic Patients during Surveillance. *J Gastrointestin Liver Dis* 2016; **25**: 205-211 [PMID: 27308652 DOI: 10.15403/jgld.2014.1121.252.chu]
34 **Leoni S**, Piscaglia F, Granito A, Borghi A, Galassi M, Marinelli S, Terzi E, Bolondi L. Characterization of primary and recurrent nodules in liver cirrhosis using contrast-enhanced ultrasound: which vascular criteria should be adopted? *Ultraschall Med* 2013; **34**: 280-287 [PMID: 23616066 DOI: 10.1055/s-0033-1335024]
35 **Baron RL**, Oliver JH 3rd, Dodd GD 3rd, Nalesnik M, Holbert BL, Carr B. Hepatocellular carcinoma: evaluation with biphasic, contrast-enhanced, helical CT. *Radiology* 1996; **199**: 505-511 [PMID: 8668803 DOI: 10.1148/radiology.199.2.8668803]
36 **Oliver JH 3rd**, Baron RL, Federle MP, Rockette HE Jr. Detecting hepatocellular carcinoma: value of unenhanced or arterial phase CT imaging or both used in conjunction with conventional portal venous phase contrast-enhanced CT imaging. *AJR Am J Roentgenol* 1996; **167**: 71-77 [PMID: 8659425 DOI: 10.2214/ajr.167.1.8659425]
37 **Hwang GJ**, Kim MJ, Yoo HS, Lee JT. Nodular hepatocellular carcinomas: detection with arterial-, portal-, and delayed-phase images at spiral CT. *Radiology* 1997; **202**: 383-388 [PMID: 9015062 DOI: 10.1148/radiology.202.2.9015062]
38 **Schellhaas B**, Görtz RS, Pfeifer L, Kielisch C, Neurath MF, Strobel D. Diagnostic accuracy of contrast-enhanced ultrasound for the differential diagnosis of hepatocellular carcinoma: ESCULAP versus CEUS-LI-RADS. *Eur J Gastroenterol Hepatol* 2017; **29**: 1036-1044 [PMID: 28562394 DOI: 10.1097/MEG.0000000000000916]
39 **Li J**, Ling W, Chen S, Ma L, Yang L, Lu Q, Luo Y. The interreader agreement and validation of contrast-enhanced ultrasound liver imaging reporting and data system. *Eur J Radiol* 2019; **120**: 108685 [PMID: 31606712 DOI: 10.1016/j.ejrad.2019.108685]
40 **Schellhaas B**, Pfeifer L, Kielisch C, Goertz RS, Neurath MF, Strobel D. Interobserver Agreement for Contrast-Enhanced Ultrasound (CEUS)-Based Standardized Algorithms for the Diagnosis of Hepatocellular Carcinoma in High-Risk Patients. *Ultraschall Med* 2018; **39**: 667-674 [PMID: 29879746 DOI: 10.1055/a-0612-7887]
41 **Yang J**, Zhang YH, Li JW, Shi YY, Huang JY, Luo Y, Liu JB, Lu Q. Contrast-enhanced ultrasound in association with serum biomarkers for differentiating combined hepatocellular-cholangiocarcinoma from hepatocellular carcinoma and intrahepatic cholangiocarcinoma. *World J Gastroenterol* 2020; **26**: 7325-7337 [PMID: 33362387 DOI: 10.3748/wjg.v26.i46.7325]
42 **Li F**, Li Q, Liu Y, Han J, Zheng W, Huang Y, Zheng X, Cao L, Zhou JH. Distinguishing intrahepatic cholangiocarcinoma from hepatocellular carcinoma in patients with and without risks: the evaluation of the LR-M criteria of contrast-enhanced ultrasound liver imaging reporting and data system version 2017. *Eur Radiol* 2020; **30**: 461-470 [PMID: 31297632 DOI: 10.1007/s00330-019-06317-2]
43 **Ding J**, Qin Z, Zhou Y, Zhou H, Zhang Q, Wang Y, Jing X, Wang F. Impact of Revision of the LR-M Criteria on the Diagnostic Performance of Contrast-Enhanced Ultrasound LI-RADS. *Ultrasound Med Biol* 2021; **47**: 3403-3410 [PMID: 34598799 DOI: 10.1016/j.ultrasmedbio.2021.08.007]
44 **Zeng D**, Xu M, Liang JY, Cheng MQ, Huang H, Pan JM, Huang Y, Tong WJ, Xie XY, Lu MD, Kuang M, Chen LD, Hu HT, Wang W. Using new criteria to improve the differentiation between HCC and non-HCC malignancies: clinical practice and discussion in CEUS LI-RADS 2017. *Radiol Med* 2022; **127**: 1-10 [PMID: 34665430 DOI: 10.1007/s11547-021-01417-w]
45 **Chen LD**, Ruan SM, Lin Y, Liang JY, Shen SL, Hu HT, Huang Y, Li W, Wang Z, Xie XY, Lu MD, Kuang M, Wang W. Comparison between M-score and LR-M in the reporting system of contrast-enhanced ultrasound LI-RADS. *Eur Radiol* 2019; **29**: 4249-4257 [PMID: 30569182 DOI: 10.1007/s00330-018-5927-8]
46 **Huang JY**, Li JW, Ling WW, Li T, Luo Y, Liu JB, Lu Q. Can contrast enhanced ultrasound differentiate intrahepatic cholangiocarcinoma from hepatocellular carcinoma? *World J Gastroenterol* 2020; **26**: 3938-3951 [PMID: 32774068 DOI: 10.3748/wjg.v26.i27.3938]
47 **Boozari B**, Soudah B, Rifai K, Schneidewind S, Vogel A, Hecker H, Hahn A, Schlue J, Dietrich CF, Bahr MJ, Kubicka S, Manns MP, Gebel M. Grading of hypervascular hepatocellular carcinoma using late phase of contrast enhanced sonography - a prospective study. *Dig Liver Dis* 2011; **43**: 484-490 [PMID: 21377941 DOI: 10.1016/j.dld.2011.01.001]
48 **Choi BI**, Lee JM, Kim TK, Dioguardi Burgio M, Vilgrain V. Diagnosing Borderline Hepatic Nodules in Hepatocarcinogenesis: Imaging Performance. *AJR Am J Roentgenol* 2015; **205**: 10-21 [PMID: 26102378 DOI: 10.2214/AJR.14.12655]
49 **Bolondi L**, Gaiani S, Celli N, Golfieri R, Grigioni WF, Leoni S, Venturi AM, Piscaglia F. Characterization of small nodules in cirrhosis by assessment of vascularity: the problem of hypovascular hepatocellular carcinoma. *Hepatology* 2005; **42**: 27-34 [PMID: 15954118 DOI: 10.1002/hep.20728]
50 **Li W**, Li L, Zhuang BW, Ruan SM, Hu HT, Huang Y, Lin MX, Xie XY, Kuang M, Lu MD, Chen LD, Wang W. Inter-reader agreement of CEUS LI-RADS among radiologists with different levels of experience. *Eur Radiol* 2021; **31**: 6758-6767 [PMID: 33675388 DOI: 10.1007/s00330-021-07777-1]

World Journal of Gastroenterology

Submit a Manuscript: https://www.f6publishing.com

World J Gastroenterol 2022 July 21; 28(27): 3503-3513

DOI: 10.3748/wjg.v28.i27.3503

ISSN 1007-9327 (print) ISSN 2219-2840 (online)

ORIGINAL ARTICLE

Retrospective Study

Novel index for the prediction of significant liver fibrosis and cirrhosis in chronic hepatitis B patients in China

Min-Jun Liao, Jun Li, Wei Dang, Dong-Bo Chen, Wan-Ying Qin, Pu Chen, Bi-Geng Zhao, Li-Ying Ren, Ting-Feng Xu, Hong-Song Chen, Wei-Jia Liao

Specialty type: Gastroenterology and hepatology

Provenance and peer review: Unsolicited article; Externally peer reviewed.

Peer-review model: Single blind

Peer-review report's scientific quality classification
Grade A (Excellent): 0
Grade B (Very good): B
Grade C (Good): C
Grade D (Fair): 0
Grade E (Poor): 0

P-Reviewer: Jiang KP, China; Leowattana W, Thailand

Received: February 14, 2022
Peer-review started: February 14, 2022
First decision: March 9, 2022
Revised: March 23, 2022
Accepted: June 18, 2022
Article in press: June 18, 2022
Published online: July 21, 2022

Min-Jun Liao, Jun Li, Wei Dang, Wan-Ying Qin, Bi-Geng Zhao, Li-Ying Ren, Ting-Feng Xu, Wei-Jia Liao, Laboratory of Hepatobiliary and Pancreatic Surgery, The Affiliated Hospital of Guilin Medical University, Guilin 541001, Guangxi Zhuang Autonomous Region, China

Min-Jun Liao, Guangdong Provincial Key Laboratory of Gastroenterology, Department of Gastroenterology and Hepatology Unit, Nanfang Hospital, Southern Medical University, Guangzhou 510515, Guangdong Province, China

Jun Li, Genetics and Precision Medicine Laboratory, The Affiliated Hospital of Guilin Medical University, Guilin 541001, Guangxi Zhuang Autonomous Region, China

Dong-Bo Chen, Pu Chen, Hong-Song Chen, Beijing Key Laboratory of Hepatitis C and Immunotherapy for Liver Disease, Peking University People's Hospital, Beijing 100044, China

Corresponding author: Wei-Jia Liao, MD, Chief Doctor, Professor, Laboratory of Hepatobiliary and Pancreatic Surgery, The Affiliated Hospital of Guilin Medical University, No. 15 Lequn Road, Xiufeng District, Guilin 541001, Guangxi Zhuang Autonomous Region, China. liaoweijia288@163.com

Abstract

BACKGROUND

Noninvasive, practical, and convenient means of detection for the prediction of liver fibrosis and cirrhosis in China are greatly needed.

AIM

To develop a precise noninvasive test to stage liver fibrosis and cirrhosis.

METHODS

With liver biopsy as the gold standard, we established a new index, [alkaline phosphatase (U/L) + gamma-glutamyl transpeptidase (U/L)/platelet (10^9/L) (AGPR)], to predict liver fibrosis and cirrhosis. In addition, we compared the area under the receiver operating characteristic curve (AUROC) of AGPR, gamma-glutamyl transpeptidase to platelet ratio, aspartate transaminase to platelet ratio index, and FIB-4 and evaluated the accuracy of these routine laboratory indices in predicting liver fibrosis and cirrhosis.

RESULTS

Correlation analysis revealed a significant positive correlation between AGPR and liver fibrosis stage ($P < 0.001$). In the training cohort, the AUROC of AGPR was 0.83 (95%CI: 0.78-0.87) for predicting fibrosis (≥ F2), 0.84 (95%CI: 0.79-0.88) for predicting extensive fibrosis (≥ F3), and 0.87 (95%CI: 0.83-0.91) for predicting cirrhosis (F4). In the validation cohort, the AUROCs of AGPR to predict ≥ F2, ≥ F3 and F4 were 0.83 (95%CI: 0.77-0.88), 0.83 (95%CI: 0.77-0.89), and 0.84 (95%CI: 0.78-0.89), respectively.

CONCLUSION

The AGPR index should become a new, simple, accurate, and noninvasive marker to predict liver fibrosis and cirrhosis in chronic hepatitis B patients.

Key Words: Liver; Fibrosis; Cirrhosis; Prediction; Novel noninvasive marker; Chronic hepatitis B

Core Tip: Chronic hepatitis B virus (HBV) infection is highly endemic in China, and routine assessment of chronic hepatitis B patients is greatly needed to guide management and indicate the need for treatment. In this study, we established a new index to stage liver fibrosis and cirrhosis in patients with chronic HBV infection in China. In addition, the study compared the predictive performance between the new index and other noninvasive indices. The new index is suitable for regular monitoring and is crucial for the management of patients with liver fibrosis/cirrhosis.

Citation: Liao MJ, Li J, Dang W, Chen DB, Qin WY, Chen P, Zhao BG, Ren LY, Xu TF, Chen HS, Liao WJ. Novel index for the prediction of significant liver fibrosis and cirrhosis in chronic hepatitis B patients in China. *World J Gastroenterol* 2022; 28(27): 3503-3513
URL: https://www.wjgnet.com/1007-9327/full/v28/i27/3503.htm
DOI: https://dx.doi.org/10.3748/wjg.v28.i27.3503

INTRODUCTION

Chronic hepatitis B virus (HBV) infection is a public issue that affects human health. Patients who are chronically infected with HBV have a tendency to develop liver fibrosis, liver cirrhosis and even more serious conditions, such as hepatocellular carcinoma (HCC). It has been reported that liver fibrosis can be reversed in patients with varying degrees of fibrosis by removing pathogenic factors, including HBV infection and alcohol[1,2]. It would benefit patients to obtain early diagnosis and effective treatment of liver fibrosis before the disease worsens. Hence, measures should be taken to achieve early diagnosis of liver fibrosis to avoid disease progression caused by HBV infection.

Liver biopsy has always been regarded as the gold standard to evaluate liver histology and assess the degree of fibrosis[3]. However, liver biopsy has shortcomings. Like any surgery, liver biopsy carries some risks, such as puncture of the lung or gallbladder, infection, bleeding, and pain, although these complications are rare[4]. In addition, a major problem is the sampling error and significant variability of fibrosis assessment by liver biopsy[5]. Transient elastography performed with FibroScan is a new technique to measure liver stiffness, and it has the advantages of noninvasiveness, good reproducibility and higher objectivity[6-8]. However, the FibroScan device and its maintenance are expensive, limiting the use of transient elastography in low- and middle-income countries and making it unsuitable for routine monitoring of liver fibrosis/cirrhosis in patients with chronic liver disease in economically poor areas. In recent years, researchers have been interested in finding a potential marker of liver fibrosis/cirrhosis or developing a multifactorial model from peripheral blood[9]. Noninvasive fibrosis tests based on routine laboratory indices have become available and are increasingly used to both assess and stage liver fibrosis; these include the aspartate transaminase (AST)-to-platelet (PLT) ratio index (APRI)[10], FIB-4[11] and the gamma-glutamyl transpeptidase (γ-GT) to PLT ratio (GPR)[12]. These indices are inexpensive, available and noninvasive for assessment of the stages of fibrosis/cirrhosis and can be easily performed in outpatient settings with limited conditions. Among these, the APRI was recommended by the World Health Organization as the most useful noninvasive tool to assess cirrhosis in resource-limited settings; however, FIB-4 was not recommended because it is not used for the detection of cirrhosis[13]. However, the levels of sensitivity and positive predictive value were low for APRI[14]. Therefore, there is an urgent need to find a more reliable method that is noninvasive, inexpensive, convenient and feasible for assessing liver disease stage and identifying patients who need treatment.

Table 1 Clinical and biochemical data of examined patients

Parameter	Training cohort (*n* = 296)[1]	Validation cohort (*n* = 211)[1]	*P* value
Age (yr)	42.47 ± 11.98	41.21 ± 11.36	0.167
Gender: Female/male (*n*)	75/221	40/171	0.091
Drinking: Yes/no (*n*)	127/169	101/110	0.268
Smoking: Yes/no (*n*)	92/204	68/143	0.784
HbeAg: Negative/positive	16/280	15/196	0.430
Fibrosis stage: F0/F1/F2/F3/F4	55/58/75/64/44	47/47/37/54/26	0.194
Activity grade: A0/A1/A2/A3/A4	16/92/113/69/6	15/72/69/52/3	0.446
WBC (× 10^9/L)	5.89 ± 2.55	6.34 ± 4.32	0.150
NEUT × 10^9/L)	3.55 ± 2.44	3.66 ± 2.61	0.611
LYMPH (× 10^9/L)	1.72 ± 0.62	1.80 ± 0.63	0.063
PLT (× 10^9/L)	171.61 ± 66.87	174.48 ± 61.62	0.636
Albumin (g/L)	41.12 ± 19.09	39.94 ± 6.07	0.380
Globulin (g/L)	29.67 ± 5.45	29.14 ± 5.80	0.298
TBIL (μmol/L)	16.51 ± 8.44	16.73 ± 7.63	0.768
DBIL (μmol/L)	6.91 ± 5.03	7.07 ± 4.33	0.699
ALT (U/L)	73.31 ± 65.41	96.85 ± 83.62	0.002
AST (U/L)	72.59 ± 63.29	77.44 ± 67.34	0.411
ALP (U/L)	97.70 ± 41.98	104.32 ± 49.25	0.104
γ-GT (U/L)	85.64 ± 69.68	97.98 ± 75.36	0.058
AGPR	1.26 ± 0.84	1.32 ± 0.89	0.431

[1]Data presented as the mean ± SD or proportions.

HbeAg: Hepatitis B e-antigen; WBC: White blood cell; NEUT: Neutrophil count; LYMPH: Lymphocyte count; PLT: Platelet; TBIL: Total bilirubin; DBIL: Direct bilirubin; ALT: Alanine aminotransferase; AST: Aspartate aminotransferase; ALP: Alkaline phosphatase; γ-GT: Gamma-glutamyl transpeptidase; AGPR: [Alkaline phosphatase (U/L) + gamma-glutamyl transpeptidase (U/L)]/platelet (10^9/L).

In this study, we tested a novel noninvasive index, the alkaline phosphatase (ALP) and γ-GT to PLT ratio (AGPR), for the assessment of liver fibrosis and cirrhosis through statistical analysis of clinical data. Moreover, we compared the diagnostic values of the AGPR, GPR, APRI and FIB-4 indices.

MATERIALS AND METHODS

Patients

The patients who participated in this study were divided into a training set and a validation set. Patients in the training set received treatment at the Affiliated Hospital of Guilin Medical University (Guilin, People's Republic of China). Patients in the validation set received treatments at the Peking University People's Hospital (Beijing, Guangxi Zhuang Autonomous Region, China). All patients were under treatment from May 2005 to October 2016, and all underwent systematic examinations, including abdominal ultrasound, routine laboratory tests and liver histological examination tests. The clinicopathologic characteristics of all patients, including age, gender, alcohol consumption, smoking status, hepatitis B e-antigen (HbeAg) status, fibrosis and cirrhosis stage, activity grade, white blood cell (WBC) count, neutrophil count (NEUT), lymphocyte count (LYMPH), PLT count, albumin, globulin, total bilirubin (TBIL), direct bilirubin (DBIL), alanine aminotransferase (ALT), AST, ALP, γ-GT and AGPR were collected and are detailed in Table 1. All patients in the study were chronically infected with HBV and were positive for hepatitis B surface antigen.

Liver histological examination

Some basic clinical examinations that ensure that patients are relatively safe when performing liver puncture surgery should be performed. In addition, physicians should obtain informed consent from

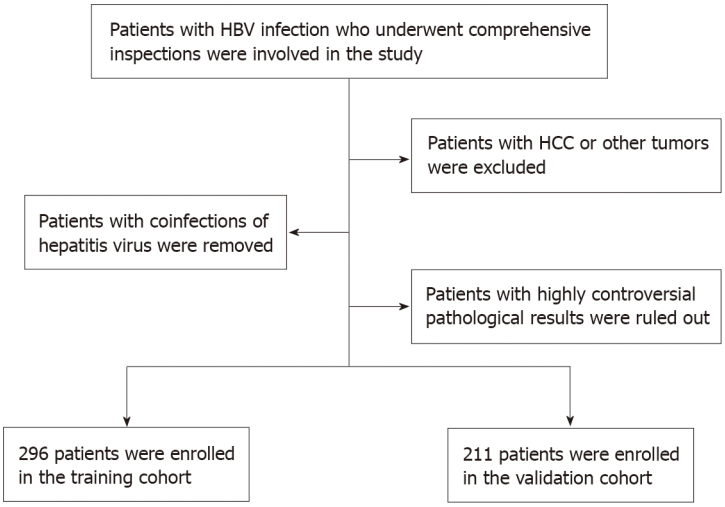

DOI: 10.3748/wjg.v28.i27.3503

Figure 1 Selection principles of study population. HBV: Hepatitis B virus; HCC: Hepatocellular carcinoma.

the patients prior to surgery. Ultrasound localization was performed on consenting and suitable patients for liver biopsy procedures. Qualified liver tissue samples were formalin-fixed and paraffin-embedded for pathological analysis. Liver fibrosis and cirrhosis were graded as follows according to the METAVIR system: F0, no fibrosis; F1, fibrosis in the portal vein zone but no fibrous septa; F2, a small amount of fibrous septa; F3, many fibrous septa but no cirrhosis; F4, cirrhosis[15]. All biopsy samples were assessed separately by two liver pathologists who were blinded to the clinical information. If the results of their evaluation were discordant, a third highly experienced hepatopathologist blinded to patient information reviewed the contested samples. Samples were excluded from the study population if the pathologists failed to reach consensus.

Computational formula

AGPR was calculated as [ALP (U/L) + γ-GT (U/L)]/PLT count (10^9/L). APRI was calculated as (AST/ULN)/PLT count (10^9/L) × 100[10]. FIB-4 was calculated by the formula: Age (years) × AST (U/L)/[PLT (10^9/L) × ALT (U/L)$^{1/2}$][11]. The formula for GPR was γ-GT/ULN of γ-GT/PLT count (10^9/L) × 100[12].

Statistical analysis

Student's *t* test was used for continuous variables, and Pearson's χ^2 test or Fisher's exact test was used for categorical variables to compare baseline characteristics. Data are presented as the mean ± SD or proportions. Univariable logistic regression was used for the variables of age, gender, WBC, NEUT, LYMPH, PLT, albumin, globulin, TBIL, DBIL, ALT, AST, ALP, γ-GT and AGPR. The receiver operating characteristic (ROC) curves were drawn to evaluate the accuracy rate of diagnosis for the AGPR, GPR, APRI, and FIB-4. The sensitivity, specificity, positive and negative predictive values, positive and negative likelihood ratio, hazard ratio and the area under the ROC curve (AUROC) of the four non-invasive markers for fibrosis and cirrhosis staging were obtained through comparison and analysis of F0-1 *vs* F2-4, F0-2 *vs* F3-4, and F0-3 *vs* F4, respectively. Data analysis was performed using SPSS software (version 24.0). A P value < 0.05 was regarded as statistically significant.

RESULTS

Study populations of the training and validation cohorts

Patients involved in this study needed to meet certain criteria. Those criteria were as follows: (1) Study patients were infected with HBV and underwent systematic examinations, including abdominal ultrasound, routine laboratory tests and liver biopsies; (2) Patients with HCC or other tumors were excluded; (3) Patients with coinfection of HCV, HIV or HDV were excluded; and (4) Patients with highly controversial results on liver fibrosis pathological grading were excluded. Figure 1 displays the selection principles.

Clinical data related to this study are summarized in Table 1. There were no statistically significant differences between the training and validation cohorts in terms of age, gender, drinking status, smoking status, HbeAg, fibrosis stage, activity grade, WBC, NEUT, LYMPH, PLT, albumin, globulin, TBIL, DBIL, ALT, AST, ALP, γ-GT or AGPR (P > 0.05). Nonsignificant differences between the two

Table 2 Univariate analysis in the training cohort

Parameter	Fibrosis (F0-1) (*n* = 113)[1]	Fibrosis (F2-4) (*n* = 183)[1]	*P* value
Age (yr)	45.15 ± 14.97	43.63 ± 13.32	0.363
Gender: Female/male (*n*)	37/76	38/145	0.021
WBC (× 10^9/L)	6.45 ± 3.02	5.55 ± 2.14	0.003
NEUT (× 10^9/L)	4.14 ± 3.0	3.18 ± 1.95	0.001
LYMPH (× 10^9/L)	1.67 ± 0.60	1.68 ± 0.63	0.828
PLT (× 10^9/L)	206.0 ± 68.39	150.55 ± 56.49	< 0.001
Albumin (g/L)	41.26 ± 5.93	39.29 ± 5.66	0.005
Globulin (g/L)	27.46 ± 4.46	31.04 ± 5.56	< 0.001
TBIL (μmol/L)	13.82 ± 7.06	17.12 ± 8.8	< 0.001
DBIL (μmol/L)	6.43 ± 3.72	7.81 ± 4.49	< 0.001
ALT (U/L)	65.01 ± 70.72	78.42 ± 66.62	0.101
AST (U/L)	56.61 ± 55.11	82.45 ± 66.09	0.001
ALP (U/L)	79.06 ± 34.16	109.2 ± 42.31	< 0.001
γ-GT (U/L)	51.84 ± 47.06	106.5 ± 73.21	< 0.001
AGPR	0.72 ± 0.49	1.61 ± 0.83	< 0.001

[1]Data presented as the mean ± SD or proportions.
WBC: White blood cell; NEUT: Neutrophil count; LYMPH: Lymphocyte count; PLT: Platelet; TBIL: Total bilirubin; DBIL: Direct bilirubin; ALT: Alanine aminotransferase; AST: Aspartate aminotransferase; ALP: Alkaline phosphatase; γ-GT: Gamma-glutamyl transpeptidase; AGPR: [Alkaline phosphatase (U/L) + gamma-glutamyl transpeptidase (U/L)]/platelet (10^9/L).

study groups revealed that the selection of training and validation cohorts was reasonable.

AGPR predicts significant hepatic fibrosis and cirrhosis

Univariable analyses showed that the presence of significant liver fibrosis (≥ F2) was related to gender, WBC, NEUT, PLT, albumin, globulin, TBIL, DBIL, AST, ALP, γ-GT and AGPR (Table 2). In the training cohort, correlation analysis revealed a significant positive correlation between AGPR and liver fibrosis stage (r = 0.567, P < 0.001) (Figure 2A). In the validation cohort, there was also a positive correlation between AGPR and liver fibrosis stage (r = 0.524, P < 0.001), as shown in Supplementary Table 1 and Supplementary Figure 1A. Box plots showed that liver fibrosis stage positively correlated with ALP + γ-GT (r = 0.352, P < 0.001), GPR (r = 0.509, P < 0.001), APRI (r = 0.428, P < 0.001) and FIB-4 (r = 0.416, P < 0.001) in the training cohort (Figure 2B and D-F). The severity of liver fibrosis stage correlated significantly with a gradual increase in the levels of these indicators. There was a negative correlation between PLT count and liver fibrosis stage (r = -0.362, P < 0.001) in the training cohort (Figure 2C). The severity of liver fibrosis decreased with increasing PLT count. Similar results were obtained in the validation cohort, and the specific data related to these results are shown in Supplementary Figure 1B-F and Supplementary Table 2.

Comparisons of AUROC between AGPR and other noninvasive indices

The summary AUROC, sensitivity, specificity, positive and negative predictive values, positive and negative likelihood ratios, and hazard ratios for the detection of fibrosis and cirrhosis for AGPR, GPR, APRI and FIB-4 are displayed in Table 3. In the training cohort, the AUROC of AGPR (0.83, 95%CI: 0.78-0.87) was higher than that of GPR (0.77, 95%CI: 0.72-0.82; P = 0.008), APRI (0.72, 95%CI: 0.67-0.77; P < 0.0001) and FIB-4 (0.74, 95%CI: 0.69-0.79; P = 0.0004) for the prediction of significant fibrosis (≥ F2). For the assessment of extensive fibrosis (≥ F3), the AUROC of AGPR (0.84, 95%CI: 0.79-0.88) was also higher than that of GPR (0.81, 95%CI: 0.76-0.85; P < 0.0001), APRI (0.70, 95%CI: 0.64-0.75; P < 0.0001) and FIB-4 (0.75, 95%CI: 0.69-0.80; P = 0.0005). For the diagnosis of cirrhosis (F4), the AUROC of AGPR was 0.87 (95%CI: 0.83-0.91), which was higher than that of GPR (0.80, 95%CI: 0.75-0.84; P = 0.0001), APRI (0.76, 95%CI: 0.70-0.8; P = 0.0002) and FIB-4 (0.80, 95%CI: 0.75-0.84; P = 0.022) (Figure 3A and Table 3). For identifying patients with significant fibrosis and cirrhosis, the summary sensitivities of AGPR were 83.1% and 88.6%, respectively, while the summary specificities of AGPR were 73.4% and 75.4%, respectively. The sensitivity, specificity, positive and negative predictive values, positive and negative likelihood ratios, and hazard ratios of the other noninvasive indices are detailed in Table 3. Our results

Table 3 Comparisons of the receiver operating characteristic curve between different non-invasive indices

	Training cohort (*n* = 296)			Validation cohort (*n* = 211)		
	F0-1 *vs* F2-4	F0-2 *vs* F3-4	F0-3 *vs* F4	F0-1 *vs* F2-4	F0-2 *vs* F3-4	F0-3 *vs* F4
AGPR						
AUROC (95%CI)	0.83 (0.78-0.87)	0.84 (0.79-0.88)	0.87 (0.83-0.91)	0.83 (0.77-0.88)	0.83 (0.77-0.89)	0.84 (0.78-0.89)
Cut-off values	0.87	1.20	1.40	0.87	1.20	1.40
Se/Sp (%)	83.1/73.4	72.22/80.3	88.6/75.4	85.5/68.1	78.7/70.2	92.3/67.0
PPV/NPV (%)	83.5/72.8	67.8/83.4	38.6/97.4	76.9/79.0	61.8/84.4	28.2/98.4
Positive/negative LR	3.13/0.23	3.67/0.35	3.60/0.15	2.68/0.21	2.65/0.30	2.80/0.11
HR (95%CI)	8.48 (5.22-14.33)	7.56 (4.76-9.83)	8.10 (5.11-11.63)	8.02 (4.95-15.62)	7.06 (4.51-12.35)	5.06 (3.89-7.72)
GPR						
AUROC (95%CI)	0.77 (0.72-0.82)	0.81 (0.76-0.85)	0.80 (0.75-0.84)	0.80 (0.74-0.85)	0.81 (0.74-0.87)	0.78 (0.71-0.83)
Cut-off values	0.32	0.32	0.56	0.32	0.32	0.56
Se/Sp (%)	73.7/70.8	76.8/54.8	79.5/65.9	86.3/67.0	91.2/56.5	75.0/62.3
PPV/NPV (%)	80.4/62.5	49.4/80.5	28.9/94.9	76.5/79.7	56.2/91.4	26.5/86.9
Positive/negative LR	2.53/0.37	1.70/0.42	2.33/0.31	2.62/0.20	2.10/0.15	1.95/0.41
HR (95%CI)	6.53 (4.81-9.62)	6.72 (3.96-9.63)	6.47 (4.08-9.83)	6.45 (3.58-11.61)	7.30 (3.87-14.62)	4.84 (3.28-7.95)
APRI						
AUROC (95%CI)	0.72 (0.67-0.77)	0.70 (0.64-0.75)	0.76 (0.70-0.81)	0.76 (0.70-0.82)	0.74 (0.67-0.82)	0.77 (0.70-0.83)
Cut-off values	0.5 1.5	-	1.0 2.0	0.5 1.5	- 1.0	2.0
Se/Sp (%)	80.9/58.4 36.1/79.7	-	77.3/64.7 43.2/83.3	83.8/54.3 34.1/76.6	- 70.1/68.6	50.1/78.3
PPV/NPV (%)	75.9/65.3 74.2/43.5	-	27.6/94.2 31.1/89.4	69.5/72.9 64.5/48.3	- 26.3/92.7	30.8/91.9
Positive/negative LR	1.94/0.33 1.77/0.80	-	2.19/0.35 2.59/0.68	1.83/0.30 1.46/0.86	- 2.12/0.44	3.16/0.63
HR (95%CI)	2.61 (1.85-3.67)	1.85 (1.41-2.42)	2.09 (1.63-2.55)	1.59 (1.23-2.07)	2.64 (1.76-4.32)	2.13 (1.71-2.58)
FIB-4						
AUROC (95%CI)	0.74 (0.69-0.79)	0.75 (0.69-0.80)	0.80 (0.75-0.84)	0.74 (0.67-0.80)	0.79 (0.73-0.84)	0.77 (0.71-0.83)
Cut-off values	-	1.45 3.25	-	-	1.45 3.25	-
Se/Sp (%)	-	87.9/47.3 42.6/87.2	-	-	77.5/58.1 37.5/93.1	-
PPV/NPV (%)	-	49.0/87.3 65.7/72.6	-	-	53.0/80.9 76.9/70.9	-
Positive/negative LR	-	1.67/0.25 3.34/0.66	-	-	1.85/0.39 5.46/0.67	-
HR (95%CI)	1.86 (1.52-2.53)	1.94 (1.55-2.42)	2.17 (1.77-2.56)	1.98 (1.50-2.62)	2.11 (1.63-2.74)	1.87 (1.68-2.36)
Comparison of AUROC						
AGPR and GPR	$P = 0.008$	$P < 0.0001$	$P = 0.0001$	$P = 0.028$	$P = 0.005$	$P = 0.0008$
AGPR and APRI	$P < 0.0001$	$P < 0.0001$	$P = 0.0002$	$P = 0.0001$	$P = 0.0001$	$P = 0.134$
AGPR and FIB-4	$P = 0.0004$	$P = 0.0005$	$P = 0.022$	$P = 0.007$	$P = 0.174$	$P = 0.100$
GPR and APRI	$P = 0.0007$	$P = 0.0028$	$P = 0.284$	$P = 0.003$	$P = 0.016$	$P = 0.831$

GPR and FIB-4	$P = 0.026$	$P = 0.331$	$P = 0.922$	$P = 0.093$	$P = 0.929$	$P = 0.591$
APRI and FIB-4	$P = 0.455$	$P = 0.028$	$P = 0.061$	$P = 0.248$	$P = 0.008$	$P = 0.795$

AGPR: [Alkaline phosphatase (U/L) + gamma-glutamyl transpeptidase (U/L)]/platelet count (10^9/L); AUROC: Area under the receiver operating characteristic curve; Se: Sensitivity; Sp: Specificity; PPV: Positive predictive value; NPV: Negative predictive value; LR: Likelihood ratio; HR: Hazard ratio; CI: Confidence interval; GPR: Gamma-glutamyl transpeptidase to platelet ratio; APRI: Aspartate aminotransferase-to-platelet ratio index; FIB-4: Age (years) × aspartate aminotransferase (U/L)/[platelet (10^9/L) × alanine aminotransferase (U/L)$^{1/2}$].

revealed that AGPR had the best overall performance among these noninvasive indices.

We further evaluated the diagnostic accuracy and performance of these noninvasive indices in the validation cohort. Similar to the results from the training cohort, the AUROC of AGPR was better than that of GPR (0.78, 95%CI: 0.71-0.83), APRI (0.77, 95%CI: 0.70-0.83), and FIB-4 (0.77, 95%CI: 0.71-0.83) (Figure 3B and Table 3).

DISCUSSION

Cirrhosis is one of the top 20 causes of disability-adjusted life years and life lost years, accounting for 1.6% and 2.1% of the global burden, respectively[16]. Cirrhosis is also the 11th most common cause of death worldwide[16]. Recently, Xu *et al*[17] provided updated guidelines for the management of liver cirrhosis in China. However, better screening for early fibrosis or cirrhosis remains a challenge. Finding an inexpensive, noninvasive, convenient, feasible and precise parameter to stage liver fibrosis is the expectation of all medical staff in China. Although liver biopsy is a good measure for the assessment of liver fibrosis grade, many patients do not accept it, or they are not suitable for the test[18,19]. FibroScan is a noninvasive diagnostic technique and its diagnostic accuracy is high. However, its application is limited because of its high cost[20]. Consequently, the development of noninvasive assessment methods for liver fibrosis in patients with chronic HBV infection appears especially important in clinical practice.

In the present study, we developed a new simple, convenient and noninvasive index (AGPR) to predict significant liver fibrosis in chronic HBV-infected patients in China. The correlation coefficients between liver fibrosis stage and AGPR suggest that AGPR is a good test for the assessment of significant liver fibrosis and cirrhosis.

The AGPR index was established on the basis of ALP, γ-GT and PLT. These three indicators are clinical evaluations of features of fibrosis/cirrhosis and evidence of decompensation. Hepatitis is related to ALP[21,22] and γ-GT[23,24]. ALP is useful in the diagnosis of chronic liver diseases[25]. A study showed that serum ALP level was significantly different in patients with or without liver cirrhosis[26]. In a report, γ-GT was demonstrated to be an independent predictor of hepatic fibrosis[27]. The circulating PLT count has been recommended as a biomarker of hepatic fibrosis and cirrhosis[28]. Based on these findings, each of the three variables is related to the degree of liver fibrosis. The antiviral treatment, anti-inflammatory and hepatoprotective treatment have a greater impact on serum levels of aminotransferases, such as AST and ALT. However, according to clinical observation, ALP and γ-GT are regarded as less specific for liver injury than AST and ALT. The effects of antiviral therapy, anti-inflammatory therapy and hepatoprotective therapy on ALP and γ-GT are not as obvious as on AST and ALT. As a matter of fact, elevated serum γ-GT levels are strongly associated with alcohol consumption. However, the researchers have reported that the high-risk liver disease mortality due to elevated γ-GT was not affected by alcohol consumption[29].

A routine assessment of liver fibrosis stage for patients with chronic HBV infection is needed to guide management and to indicate the need for treatment. However, the diagnosis of liver fibrosis and compensated cirrhosis cannot be based on clinically obvious features. Noninvasive fibrosis tests are now increasingly used for evaluating liver fibrosis, reducing the need for liver biopsy. AGPR may be a new promising noninvasive fibrosis test to assist in the selection of optimal candidates for antiviral therapy. The AGPR test is inexpensive, routinely available at health-care facilities, and can be performed by untrained staff. It is suitable for conventional monitoring of hepatic fibrosis and cirrhosis. The Guidelines Development Group prioritized urgent initiation of antiviral therapy for patients with cirrhosis based on APRI score > 2 in adults, regardless of ALT or HBV DNA levels[13]. However, when applying an APRI score > 2 in this study, the sensitivity for the diagnosis of cirrhosis was only 43.2% and 50.1% in the training and validation cohorts, respectively. This suggested that more than 50% of patients with cirrhosis would be incorrectly classified as not having cirrhosis, which may lead to delayed initiation of treatment. In contrast, the sensitivity of AGPR for the diagnosis of cirrhosis was high at 88.6% and 92.3% in the training and validation cohorts, respectively. Therefore, our data suggested that AGPR may be a preferred noninvasive test to detect the presence of significant fibrosis and cirrhosis. It may serve as a simple index to make treatment decisions in patients without evidence of cirrhosis in China and other resource-limited settings where HBV infection is endemic.

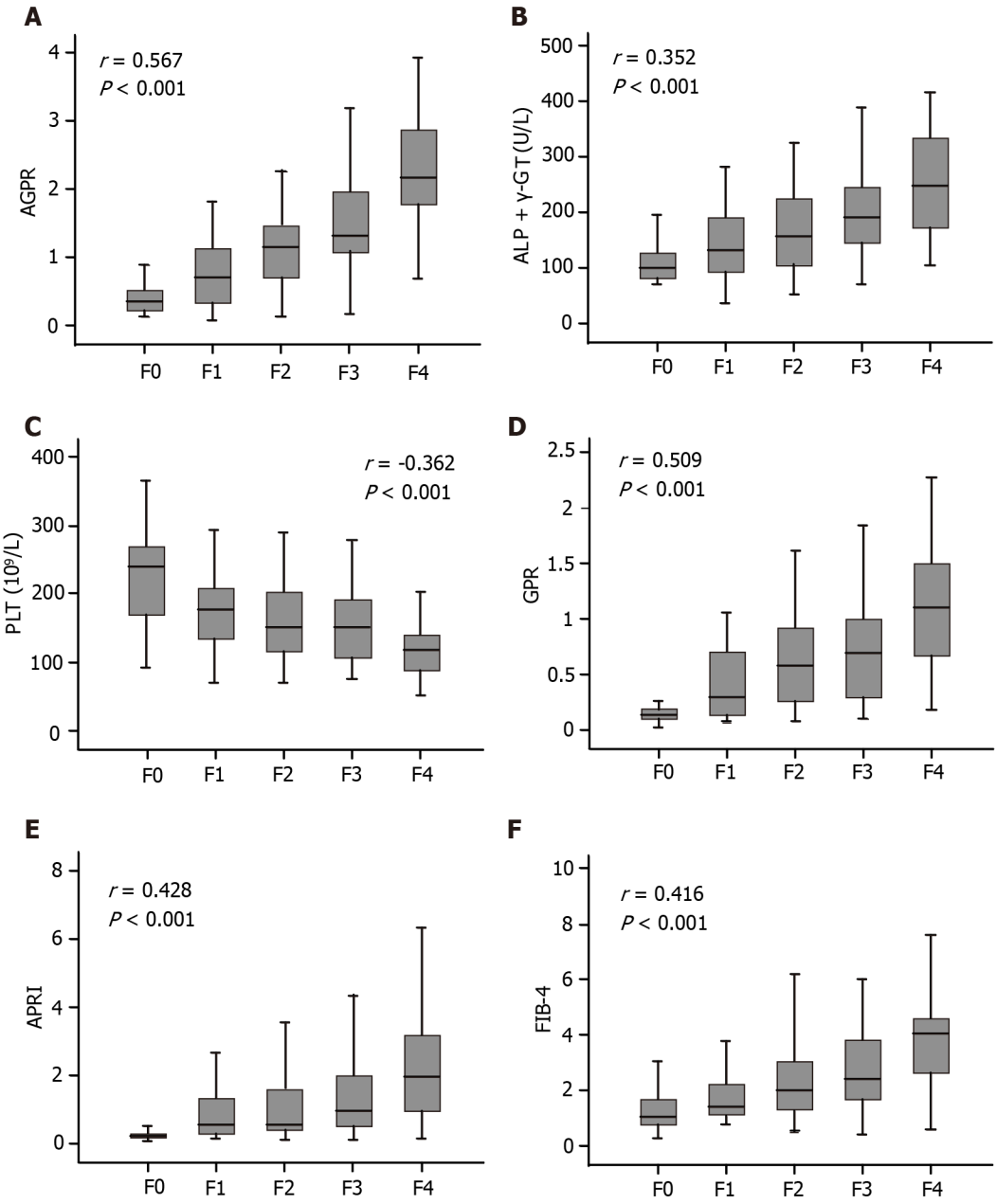

DOI: 10.3748/wjg.v28.i27.3503

Figure 2 Box plots of [alkaline phosphatase (U/L) + gamma-glutamyl transpeptidase (U/L)]/platelet (10^9/L) (A), alkaline phosphatase + gamma-glutamyl transpeptidase (B), platelet (C), gamma-glutamyl transpeptidase to platelet ratio (D), aspartate aminotransferase-to-platelet ratio index (E), and age × aspartate transaminase/platelet × alanine aminotransferase (F) according to the METAVIR fibrosis stage in the training cohort. AGPR: [Alkaline phosphatase (U/L) + gamma-glutamyl transpeptidase (U/L)]/platelet (10^9/L); ALP + γ-GT: Alkaline phosphatase + gamma-glutamyl transpeptidase; PLT: Platelet; GPR: Gamma-glutamyl transpeptidase to platelet ratio; APRI: Aspartate aminotransferase-to-platelet ratio index; FIB-4: Age × aspartate transaminase/platelet × alanine aminotransferase.

Our study has some limitations. First, the selection of samples was limited to a population with chronic HBV infection in China. Whether AGPR can be generalized to different geographical areas (the infection of hepatitis C virus is endemic) remains to be determined. Second, the time span of over 10 years for our selected samples was too long (from May 2005 to October 2016). Over this time period, substantial changes have taken place in terms of medical equipment and physical examination technologies, which may reduce the accuracy of our study results. Finally, there are many factors involved in liver fibrosis. The impact of various interference factors on the diagnostic accuracy of the AGPR index has not been fully evaluated. Some interference may affect the precision of our index.

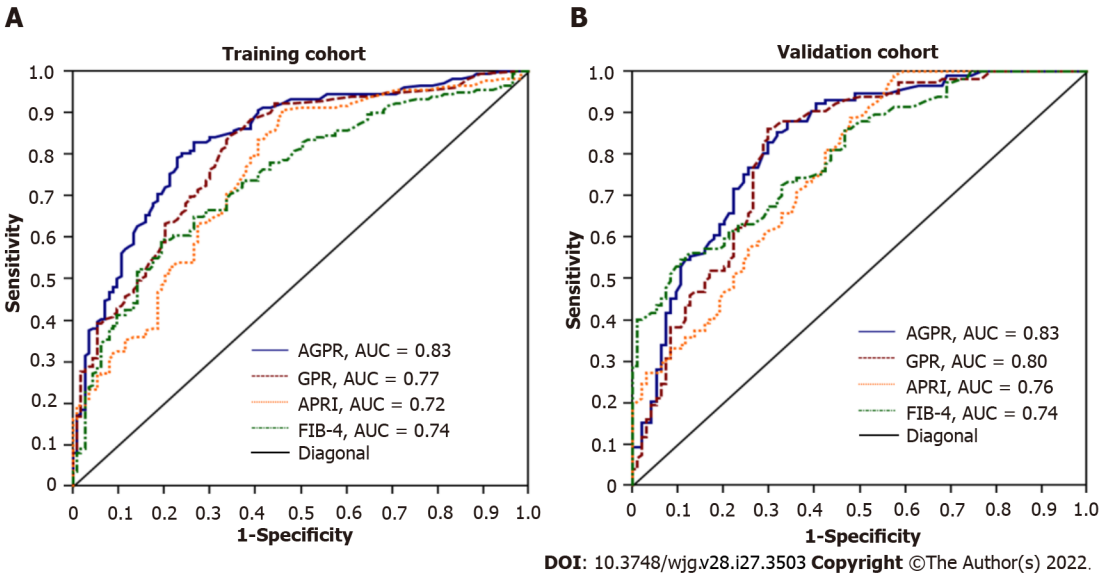

DOI: 10.3748/wjg.v28.i27.3503 **Copyright** ©The Author(s) 2022.

Figure 3 The receiver operating characteristic analysis of [alkaline phosphatase (U/L) + gamma-glutamyl transpeptidase (U/L)]/platelet (10^9/L), amma-glutamyl transpeptidase to platelet ratio, aspartate aminotransferase-to-platelet ratio index and age × aspartate transaminase/platelet × alanine aminotransferase in the training (A) and validation cohorts (B). AGPR: [Alkaline phosphatase (U/L) + gamma-glutamyl transpeptidase (U/L)]/platelet (10^9/L); GPR: Gamma-glutamyl transpeptidase to platelet ratio; APRI: Aspartate aminotransferase-to-platelet ratio index; FIB-4: Age × aspartate transaminase/platelet × alanine aminotransferase; AUC: Area under the curve.

CONCLUSION

In summary, the AGPR index may be an accurate noninvasive test for predicting significant liver fibrosis and cirrhosis in patients with chronic HBV infection in China. In addition, it is suitable for conventional monitoring. Therefore, for the prediction of liver fibrosis and cirrhosis, the AGPR index is a promising noninvasive marker that is worthy of further attention and research.

ARTICLE HIGHLIGHTS

Research background

Patients infected with hepatitis B virus (HBV) tend to develop liver fibrosis and liver cirrhosis. Those with cirrhosis have a high risk of hepatic decompensation and hepatitis B- related hepatocellular carcinoma.

Research motivation

Liver biopsy was used to ascertain the degree of fibrosis/cirrhosis. However, as an invasive procedure, liver biopsy has many disadvantages. The Guidelines Development Group recommended the use of noninvasive tests to assist in the assessment of liver disease stage and the diagnosis of fibrosis/cirrhosis. The use of a noninvasive test can reduce the need for liver biopsy.

Research objectives

The present study aimed to develop a precise noninvasive test to stage liver fibrosis/cirrhosis and compare the diagnostic values between different noninvasive methods.

Research methods

Univariable logistic regression was used to identify significant predictive factors. Correlation analysis was performed to reveal the correlation between clinical parameters and liver stage. Receiver operating characteristic (ROC) curves were drawn to evaluate the diagnostic accuracy of different noninvasive methods.

Research results

The presence of liver fibrosis was significantly related to alkaline phosphatase and the gamma-glutamyl transpeptidase to platelet ratio (AGPR). There was a significant positive correlation between AGPR and liver fibrosis stage. The area under the ROC curve values of AGPR were 0.83, 0.84, and 0.87 for the prediction of significant fibrosis, extensive fibrosis, and cirrhosis, respectively. The AGPR index had a

better overall performance than other noninvasive indices.

Research conclusions

AGPR can be used to detect the presence of significant fibrosis, extensive fibrosis, and cirrhosis with high diagnostic accuracy, sensitivity, and specificity in patients with chronic HBV infection.

Research perspectives

The AGPR index is a promising noninvasive marker for assessing liver disease stage. The use of AGPR can help with the routine monitoring of hepatic fibrosis and cirrhosis.

FOOTNOTES

Author contributions: Liao MJ, Li J, and Dang W contributed equally to this work; Liao WJ was the guarantor and designed the study; Liao MJ, Li J, Chen DB, Qin WY, Chen P, Zhao BG, Ren LY, Xu TF, and Liao WJ participated in the acquisition, analysis, and interpretation of the data; Li J and Dang W drafted the initial manuscript; Chen HS and Liao WJ revised the article critically for important intellectual content.

Supported by the National Natural Science Foundation of China, No. 81372163; the Natural Science Foundation of Guangxi, No. 2018GXNSFDA138001; the Science and Technology Planning Project of Guilin, No. 20190218-1; the Opening Project of Key laboratory of High-Incidence-Tumor Prevention & Treatment (Guangxi Medical University), Ministry of Education, No. GKE-KF202101; and the Program of Guangxi Zhuang Autonomous Region Health and Family Planning Commission, No. Z20210706 and No. Z20190665.

Institutional review board statement: The study was reviewed and approved by the research ethics committee of Affiliated Hospital of Guilin Medical University.

Informed consent statement: Informed consent was obtained from all patients.

Conflict-of-interest statement: There are no conflicts of interest to report.

Data sharing statement: No additional data are available.

Country/Territory of origin: China

ORCID number: Min-Jun Liao 0000-0002-2328-8209; Jun Li 0000-0002-6210-4062; Wei Dang 0000-0002-9263-5841; Dong-Bo Chen 0000-0001-5173-6999; Wan-Ying Qin 0000-0001-6040-9340; Pu Chen 0000-0003-1437-2617; Bi-Geng Zhao 0000-0001-6203-4159; Li-Ying Ren 0000-0003-3624-5483; Ting-Feng Xu 0000-0003-0303-5471; Hong-Song Chen 0000-0001-6858-8398; Wei-Jia Liao 0000-0002-8906-8612.

S-Editor: Yan JP
L-Editor: A
P-Editor: Yan JP

REFERENCES

1 **Sun M**, Kisseleva T. Reversibility of liver fibrosis. *Clin Res Hepatol Gastroenterol* 2015; **39** Suppl 1: S60-S63 [PMID: 26206574 DOI: 10.1016/j.clinre.2015.06.015]
2 **Rockey DC**. Liver Fibrosis Reversion After Suppression of Hepatitis B Virus. *Clin Liver Dis* 2016; **20**: 667-679 [PMID: 27742006 DOI: 10.1016/j.cld.2016.06.003]
3 **Park YE**, Kim BK, Park JY, Kim DY, Ahn SH, Han KH, Han S, Jeon MY, Heo JY, Song K, Kim SU. Gamma-glutamyl transpeptidase-to-platelet ratio is an independent predictor of hepatitis B virus-related liver cancer. *J Gastroenterol Hepatol* 2017; **32**: 1221-1229 [PMID: 27859587 DOI: 10.1111/jgh.13653]
4 **Li Y**, Chen Y, Zhao Y. The diagnostic value of the FIB-4 index for staging hepatitis B-related fibrosis: a meta-analysis. *PLoS One* 2014; **9**: e105728 [PMID: 25165830 DOI: 10.1371/journal.pone.0105728]
5 **Friedman LS**. Controversies in liver biopsy: who, where, when, how, why? *Curr Gastroenterol Rep* 2004; **6**: 30-36 [PMID: 14720451 DOI: 10.1007/s11894-004-0023-4]
6 **Meng F**, Zheng Y, Zhang Q, Mu X, Xu X, Zhang H, Ding L. Noninvasive evaluation of liver fibrosis using real-time tissue elastography and transient elastography (FibroScan). *J Ultrasound Med* 2015; **34**: 403-410 [PMID: 25715361 DOI:

10.7863/ultra.34.3.403]
7 **Dong DR**, Hao MN, Li C, Peng Z, Liu X, Wang GP, Ma AL. Acoustic radiation force impulse elastography, FibroScan®, Forns' index and their combination in the assessment of liver fibrosis in patients with chronic hepatitis B, and the impact of inflammatory activity and steatosis on these diagnostic methods. *Mol Med Rep* 2015; **11**: 4174-4182 [PMID: 25651500 DOI: 10.3892/mmr.2015.3299]
8 **Jia J**, Hou J, Ding H, Chen G, Xie Q, Wang Y, Zeng M, Zhao J, Wang T, Hu X, Schuppan D. Transient elastography compared to serum markers to predict liver fibrosis in a cohort of Chinese patients with chronic hepatitis B. *J Gastroenterol Hepatol* 2015; **30**: 756-762 [PMID: 25353058 DOI: 10.1111/jgh.12840]
9 **Liao Y**, Wei R, Yao R, Qin L, Li J, Yu J, Liao W. AGLR is a novel index for the prognosis of hepatocellular carcinoma patients: a retrospective study. *BMC Surg* 2021; **21**: 72 [PMID: 33536005 DOI: 10.1186/s12893-020-01037-7]
10 **Wai CT**, Greenson JK, Fontana RJ, Kalbfleisch JD, Marrero JA, Conjeevaram HS, Lok AS. A simple noninvasive index can predict both significant fibrosis and cirrhosis in patients with chronic hepatitis C. *Hepatology* 2003; **38**: 518-526 [PMID: 12883497 DOI: 10.1053/jhep.2003.50346]
11 **Sterling RK**, Lissen E, Clumeck N, Sola R, Correa MC, Montaner J, S Sulkowski M, Torriani FJ, Dieterich DT, Thomas DL, Messinger D, Nelson M; APRICOT Clinical Investigators. Development of a simple noninvasive index to predict significant fibrosis in patients with HIV/HCV coinfection. *Hepatology* 2006; **43**: 1317-1325 [PMID: 16729309 DOI: 10.1002/hep.21178]
12 **Lemoine M**, Shimakawa Y, Nayagam S, Khalil M, Suso P, Lloyd J, Goldin R, Njai HF, Ndow G, Taal M, Cooke G, D'Alessandro U, Vray M, Mbaye PS, Njie R, Mallet V, Thursz M. The gamma-glutamyl transpeptidase to platelet ratio (GPR) predicts significant liver fibrosis and cirrhosis in patients with chronic HBV infection in West Africa. *Gut* 2016; **65**: 1369-1376 [PMID: 26109530 DOI: 10.1136/gutjnl-2015-309260]
13 **World Health Organization**. Guidelines for the Prevention, Care and Treatment of Persons with chronic Hepatitis B infection. 2015. [Cited 13 Mar 2018]. Available from: http://whoint/hiv/pub/hepatitis/hepatitis-b-guidelines/en/
14 **Li Q**, Song J, Huang Y, Li X, Zhuo Q, Li W, Chen C, Lu C, Qi X, Chen L. The Gamma-Glutamyl-Transpeptidase to Platelet Ratio Does not Show Advantages than APRI and Fib-4 in Diagnosing Significant Fibrosis and Cirrhosis in Patients With Chronic Hepatitis B: A Retrospective Cohort Study in China. *Medicine (Baltimore)* 2016; **95**: e3372 [PMID: 27100421 DOI: 10.1097/MD.0000000000003372]
15 **Bedossa P**, Poynard T. An algorithm for the grading of activity in chronic hepatitis C. The METAVIR Cooperative Study Group. *Hepatology* 1996; **24**: 289-293 [PMID: 8690394 DOI: 10.1002/hep.510240201]
16 **Asrani SK**, Devarbhavi H, Eaton J, Kamath PS. Burden of liver diseases in the world. *J Hepatol* 2019; **70**: 151-171 [PMID: 30266282 DOI: 10.1016/j.jhep.2018.09.014]
17 **Xu XY**, Ding HG, Li WG, Xu JH, Han Y, Jia JD, Wei L, Duan ZP, Ling-Hu EQ, Zhuang H. Chinese guidelines on the management of liver cirrhosis (abbreviated version). *World J Gastroenterol* 2020; **26**: 7088-7103 [PMID: 33362370 DOI: 10.3748/wjg.v26.i45.7088]
18 **McGill DB**, Rakela J, Zinsmeister AR, Ott BJ. A 21-year experience with major hemorrhage after percutaneous liver biopsy. *Gastroenterology* 1990; **99**: 1396-1400 [PMID: 2101588 DOI: 10.1016/0016-5085(90)91167-5]
19 **Nalbantoglu IL**, Brunt EM. Role of liver biopsy in nonalcoholic fatty liver disease. *World J Gastroenterol* 2014; **20**: 9026-9037 [PMID: 25083076 DOI: 10.3748/wjg.v20.i27.9026]
20 **Sun W**, Cui H, Li N, Wei Y, Lai S, Yang Y, Yin X, Chen DF. Comparison of FIB-4 index, NAFLD fibrosis score and BARD score for prediction of advanced fibrosis in adult patients with non-alcoholic fatty liver disease: A meta-analysis study. *Hepatol Res* 2016; **46**: 862-870 [PMID: 26763834 DOI: 10.1111/hepr.12647]
21 **Aggarwal SK**, Radhakrishnan S. Syphilitic hepatitis: Look for raised alkaline phosphatase level. *Med J Armed Forces India* 2016; **72**: 192-193 [PMID: 27257335 DOI: 10.1016/j.mjafi.2015.11.011]
22 **Kasztelan-Szczerbinska B**, Slomka M, Celinski K, Szczerbinski M. Alkaline phosphatase: the next independent predictor of the poor 90-day outcome in alcoholic hepatitis. *Biomed Res Int* 2013; **2013**: 614081 [PMID: 24151614 DOI: 10.1155/2013/614081]
23 **Huang CF**, Chuang WL, Yu ML. Interference of diabetes on the association of γ-glutamyl transpeptidase to platelet ratio with liver fibrosis in chronic hepatitis C. *Kaohsiung J Med Sci* 2016; **32**: 334-335 [PMID: 27377848 DOI: 10.1016/j.kjms.2016.04.004]
24 **Benini F**, Pigozzi MG, Baisini O, Romanini L, Ahmed H, Pozzi A, Ricci C, Lanzini A. Increased serum gamma-glutamyl-transpeptidase concentration is associated with nonalcoholic steatosis and not with cholestasis in patients with chronic hepatitis C. *J Gastroenterol Hepatol* 2007; **22**: 1621-1626 [PMID: 17845689 DOI: 10.1111/j.1440-1746.2006.04733.x]
25 **Barreto AV**, Alecrim VM, Medeiros TB, Domingues AL, Lopes EP, Martins JR, Nader HB, Diniz GT, Montenegro SM, Morais CN. New index for the diagnosis of liver fibrosis in Schistosomiasis mansoni. *Arq Gastroenterol* 2017; **54**: 51-56 [PMID: 28079240 DOI: 10.1590/S0004-2803.2017v54n1-10]
26 **Cho HJ**, Kim SS, Ahn SJ, Park JH, Kim DJ, Kim YB, Cho SW, Cheong JY. Serum transferrin as a liver fibrosis biomarker in patients with chronic hepatitis B. *Clin Mol Hepatol* 2014; **20**: 347-354 [PMID: 25548740 DOI: 10.3350/cmh.2014.20.4.347]
27 **Nishikawa H**, Hasegawa K, Ishii A, Takata R, Enomoto H, Yoh K, Kishino K, Shimono Y, Iwata Y, Nakano C, Nishimura T, Aizawa N, Sakai Y, Ikeda N, Takashima T, Iijima H, Nishiguchi S. A proposed predictive model for advanced fibrosis in patients with chronic hepatitis B and its validation. *Medicine (Baltimore)* 2016; **95**: e4679 [PMID: 27583895 DOI: 10.1097/MD.0000000000004679]
28 **Pradella P**, Bonetto S, Turchetto S, Uxa L, Comar C, Zorat F, De Angelis V, Pozzato G. Platelet production and destruction in liver cirrhosis. *J Hepatol* 2011; **54**: 894-900 [PMID: 21145808 DOI: 10.1016/j.jhep.2010.08.018]
29 **Ruhl CE**, Everhart JE. Elevated serum alanine aminotransferase and gamma-glutamyltransferase and mortality in the United States population. *Gastroenterology* 2009; **136**: 477-85.e11 [PMID: 19100265 DOI: 10.1053/j.gastro.2008.10.052]

World Journal of Gastroenterology

Submit a Manuscript: https://www.f6publishing.com

World J Gastroenterol 2022 July 21; 28(27): 3514-3523

DOI: 10.3748/wjg.v28.i27.3514

ISSN 1007-9327 (print) ISSN 2219-2840 (online)

SYSTEMATIC REVIEWS

Percutaneous transhepatic cholangiography *vs* endoscopic ultrasound-guided biliary drainage: A systematic review

Zeinab Hassan, Eyad Gadour

Specialty type: Gastroenterology and hepatology

Provenance and peer review: Unsolicited article; Externally peer reviewed

Peer-review model: Single blind

Peer-review report's scientific quality classification

Grade A (Excellent): A
Grade B (Very good): 0
Grade C (Good): C
Grade D (Fair): 0
Grade E (Poor): 0

P-Reviewer: Jin G, China; Villa E, United States

Received: November 22, 2021
Peer-review started: November 23, 2021
First decision: January 9, 2022
Revised: January 21, 2022
Accepted: June 23, 2022
Article in press: June 23, 2022
Published online: July 21, 2022

Zeinab Hassan, Internal Medicine, Stockport Hospitals NHS Foundation Trust, Manchester SK2 7JE, United Kingdom

Eyad Gadour, Department of Gastroenterology, University Hospitals of Morecambe Bay NHS Foundation Trust, Lancaster LA1 4RP, United Kingdom

Corresponding author: Eyad Gadour, CCST, FRCP, MBBS, MRCP, Consultant Physician-Scientist, Department of Gastroenterology, University Hospitals of Morecambe Bay NHS Foundation Trust, Royal Lancaster Infirmary, Lancaster LA1 4RP, United Kingdom.
eyadgadour@doctors.org.uk

Abstract

BACKGROUND

Percutaneous transhepatic cholangiography is a diagnostic and therapeutic procedure that involves inserting a needle into the biliary tree, followed by the immediate insertion of a catheter. Endoscopic ultrasound-guided biliary drainage (EUS-BD) is a novel technique that allows BD by echoendoscopy and fluoroscopy using a stent from the biliary tree to the gastrointestinal tract.

AIM

To compare the technical aspects and outcomes of percutaneous transhepatic BD (PTBD) and EUS-BD.

METHODS

Different databases, including PubMed, Embase, clinicaltrials.gov, the Cochrane library, Scopus, and Google Scholar, were searched according to the guidelines for Preferred Reporting Items for Systematic reviews and Meta-Analyses to obtain studies comparing PTBD and EUS-BD.

RESULTS

Among the six studies that fulfilled the inclusion criteria, PTBD patients underwent significantly more reinterventions (4.9 *vs* 1.3), experienced more postprocedural pain (4.1 *vs* 1.9), and experienced more late adverse events (53.8% *vs* 6.6%) than EUS-BD patients. There was a significant reduction in the total bilirubin levels in both the groups (16.4-3.3 μmol/L and 17.2-3.8 μmol/L for EUS-BD and PTBD, respectively; P = 0.002) at the 7-d follow-up. There were no significant differences observed in the complication rates between PTBD and EUS-BD (3.3 *vs* 3.8). PTBD was associated with a higher adverse event rate than EUS-BD in all the procedures, including reinterventions (80.4% *vs* 15.7%, respectively)

and a higher index procedure (39.2% *vs* 18.2%, respectively).

CONCLUSION
The findings of this systematic review revealed that EUS-BD is linked with a higher rate of effective BD and a more manageable procedure-related adverse event profile than PTBD. These findings highlight the evidence for successful EUS-BD implementation.

Key Words: Percutaneous transhepatic cholangiography; Endoscopic ultrasound; Biliary drainage; Obstructive cholangiopathy

Core Tip: Endoscopic transpapillary biliary drainage (BD) is the preferred approach for biliary decompression in patients with unresectable pancreatic cancer and obstructive jaundice. We conducted a systematic review of studies comparing the technical aspects and outcomes of two distinct approaches for BD: Endoscopic ultrasound-guided BD (EUS-BD) and percutaneous transhepatic BD (PTBD). The evaluation of six studies that fulfilled the inclusion criteria revealed that PTBD was associated with more reinterventions, postprocedural pain, and late adverse events compared with EUS-BD. Both procedures were associated with a significant reduction in the total bilirubin levels at the 7-d follow-up, and there were no significant differences in the complication rates between the two procedures. In summary, EUS-BD was associated with a higher rate of effective BD and manageable procedure-related adverse events compared with PTBD, highlighting its utility in successful BD.

Citation: Hassan Z, Gadour E. Percutaneous transhepatic cholangiography *vs* endoscopic ultrasound-guided biliary drainage: A systematic review. *World J Gastroenterol* 2022; 28(27): 3514-3523
URL: https://www.wjgnet.com/1007-9327/full/v28/i27/3514.htm
DOI: https://dx.doi.org/10.3748/wjg.v28.i27.3514

INTRODUCTION

Endoscopic transpapillary biliary drainage (BD) is the preferred approach for biliary decompression in patients with unresectable pancreatic cancer and obstructive jaundice[1]. Percutaneous transhepatic cholangiography (PTC) is a diagnostic and therapeutic procedure that involves inserting a needle into the biliary tree, followed by immediately inserting a catheter to achieve percutaneous BD. During the procedure, contrast is injected into one or more bile ducts (cholangiography) and sometimes into the duodenum. PTC can be performed using fluoroscopic guidance alone or using both fluoroscopic and ultrasound guidance[2,3].

In cases of suspected malignant biliary stricture, imaging alone may not be sufficient to provide a precise diagnosis. PTC was first introduced several decades ago to visualize biliary obstructions, treat malignant obstructive jaundice palliatively, and access BD[4]. Fine needle aspiration (FNA), brush cytology, and forceps biopsy have been performed using percutaneous biliary catheterization during PTC since the 1980s[5]. For biliary stenosis, endoscopic retrograde cholangiopancreatography (ERCP) has recently been recognized as a reliable diagnostic and therapeutic procedure.

Endoscopic retrograde BD (ERBD) is the most commonly used method of biliary decompression in patients with blockage of the distal central bile duct. This technique has a success rate of 90%-95% in the United States[6]. Altered anatomy, presenting pathology (tumor infiltration, impacted stone, and duodenal compression by a pancreatic pseudocyst), previous surgery, or variations in normal anatomy (periampullary diverticula and tortuous ducts) can contribute to the failure of ERBD. The failure rate of ERBD is 6%-7% in cases with obstructive jaundice caused by a blockage or altered anatomy[7]. Percutaneous transhepatic BD (PTBD) has a lower risk of complications than surgical decompression, but it is associated with complications such as fistula formation, repeat intervention, recurrent infection, and the requirement for long-term external catheter drainage, which contribute to a low quality of life [8]. Although PTBD is associated with severe morbidity and mortality, the only relative contraindication of PTBD is perihepatic ascites[6-9]. Furthermore, PTBD usually requires separate surgery after the failure of ERCP BD, thereby increasing the morbidity associated with biliary stasis.

Endoscopic ultrasound-guided BD (EUS-BD) has become more widely used as an alternative to PTBD in patients with anatomical abnormalities, which make endoscopic transpapillary insertion of a biliary stent difficult[10]. It offers advantages of being compatible with anatomic internal drainage, being more comfortable, and resulting in a recovery associated with fewer complications and reduced expenditure [11].

EUS is an extremely useful imaging method for examining the gastrointestinal luminal wall and surrounding tissues. The proximity of the EUS probe to the area of interest enables high-resolution imaging and EUS-guided FNA tissue collection in real time. EUS has become a crucial diagnostic technique due to its high-quality imaging and FNA capacity and is also used as a treatment tool. However, until recently, its use was limited to the introduction of various drugs[12,13]. The therapeutic uses of EUS have been expanded due to larger channel echoendoscopes, which combine the benefits of real-time ultrasound and fluoroscopy imaging with the use of ERCP-based devices and procedures, such as EUS-BD. In 1996, Wiersema *et al*[14] first reported EUS-guided diagnostic cholangiography and in 2001, Giovannini *et al*[10] first reported EUS-BD in a patient with pancreatic cancer, establishing a choledochoduodenal fistula with a needle knife followed by transduodenal stenting.

These early reports were followed by modified techniques and expanded indications, such as EUS-guided hepatic gastrostomy with stent placement[15], transduodenal EUS-rendezvous (EUS-RV) biliary access[16], and EUS-guided choledocholithiasis therapy with the creation of a neo papilla[17]. Since then, several studies have reported modifications to these techniques, including the use of a covered metal stent as a conduit for interventional endoscopic procedures in the bile duct[18,19]. Few studies have compared EUS-BD and PTBD in failed ERCP cases in terms of success rate and adverse event profile[20]; therefore, we performed a systematic review of the relevant literature to investigate the combined efficacy and adverse effects of EUS-BD and PTBD.

MATERIALS AND METHODS

Literature search

This systematic review was conducted using an electronic search of different databases, including PubMed, Embase, clinicaltrials.gov, the Cochrane library, Scopus, and Google Scholar using the guidelines for Preferred Reporting Items for Systematic reviews and Meta-Analyses[21]. Two investigators independently searched for the following key terms: all field "failed EUS", all field "Percutaneous biliary drainage", and all field "EUS-guided biliary drainage". All the three search headings were connected using the Boolean operator "AND". Studies published in English comparing PTBD with EUS-BD were chronologically limited to those published from their inception to October 2021. After completing the literature search, the references were imported to Endnote citation manager (Endnote X9) for removing any duplicates, following which the abstracts were screened for potential relevance by two independent investigators. This study included intervention studies, retrospective or prospective observational studies, case reports, randomized controlled trials, and published abstracts that reported at least some adverse events. And this study also cited high-quality articles in Reference Citation Analysis (https://www.referencecitationanalysis.com).

Letters, comments, seminar proceedings, and animal studies were excluded from our analysis. Moreover, only human studies were included and limited to the English language. Publications judged to be potentially relevant underwent a full text assessment by two independent investigators to determine their inclusion. Disagreements regarding study eligibility were resolved by consensus or adjudication between the investigators.

Data extraction

The baseline study details, including study identifiers, such as first author, publication year, title, and country, and study-specific methodological data, such as sample size, study design, single-center *vs* multicenter study types, and healthcare setting, are presented in Table 1. Technical and clinical success rates, including the total number of patients enrolled, number of patients in each arm, mean age, sex ratio, comorbidity index, mean preprocedural bilirubin, mean diameter of the bile duct, etiology of biliary obstruction, and reasons for EUS failure are shown in Table 2.

Risk of bias evaluation

The GRADE checklist was used to evaluate the risk of bias in the included studies[22]. Table 3 shows a summary of the methodological qualities of studies reporting the prevalence data. Questions were answered as "yes", "no", "unclear", or "not applicable".

RESULTS

Our literature search yielded 315 manuscripts, of which 132 studies remained after excluding duplicate studies. After reviewing the title and abstract, only nine articles were left for the thorough screening of data by reviewing the full text. Further, two studies were eliminated after reading the manuscripts because they included primary EUS-BD cases wherein EUS was not attempted as the primary procedure. The third study was excluded, as it did not contain full text. A total of six studies met the abovementioned inclusion criteria of the study[23-28] (Figure 1).

Table 1 Baseline characteristics of the studies

Ref.	Artifon *et al*[23]	Bapaye *et al*[24]	Khashab *et al*[25]	Giovannini[26]	Jung *et al*[27]	Sharaiha *et al*[28]
Type of study (country)	Single-center, prospective, randomized, controlled trial(Brazil)	Single-center, retrospective, comparative study (India)	Single-center, retrospective, comparative, cohort study (United States)	Multicenter, randomized, phase II trial (France)	Multicenter, prospective, randomized, controlled trial (South Korea)	Single-center, retrospective, cohort review (United States)
Age [mean (SD)/median ± SD], yr	63.4 (11.1) *vs* 71.0 (11.9)	59.9 ± 13.3 *vs* 62.4 ± 10.2	64.9 ± 12.5 *vs* 66.9 ± 12.5	N/A	66.5 *vs* 68.4	68.7 ± 13.9 *vs* 58.8 ± 13.6
Males/females	2.25 *vs* 2.0	1.08 *vs* 1.6	1.2 *vs* 1.31	0.91 *vs* 9	3.25 *vs* 3	12 *vs* 1.47
Comorbidity/quality index (mean)	58.3 *vs* 57.8 (QoL sF 36)	N/A	N/A	N/A	40.7 *vs* 40.5 (global health status/QoL)	5.9 *vs* 6.4 (Charleston comorbidity index)
Total bilirubin (mean), mg/dL	16.4 *vs* 17.2	7.11 ± 7.6 *vs* 9.41 ± 12.4	15.8 ± 11.3 *vs* 14.5 ± 8.8	N/A	10.4 *vs* 11.8	N/A
Mean diameter of bile duct	13.7 *vs* 11.9	N/A	N/A	N/A	11.22 *vs* 12.6	N/A
Etiology of obstruction						
Adenocarcinoma of the pancreatic	10 *vs* 6	15 *vs* 18	43	N/A	12 *vs* 12	22
Advanced lymphoma/liposarcoma	0 *vs* 1	0	1	N/A	0	0
Cholangiocarcinoma	1 *vs* 1	2 *vs* 2	12	N/A	7 *vs* 14	9
Duodenal carcinoma	0	0	1	N/A	3 *vs* 0	5
Gall bladder cancer	0	0	0	N/A	5 *vs* 5	0
Gastric carcinoma	0 *vs* 1	0	1	N/A	3 *vs* 2	4
Metastasis	0 *vs* 3	0	12	N/A	3 *vs* 1	7
Plasmacytoma	1 *vs* 0	0	0	N/A	0	0
Total malignancy		0	37	N/A		
Reason for ERCP failure						
Altered anatomy	1	9	0	N/A	12 *vs* 10	N/A
Duodenal/stomach invasion	8	32	0	N/A	22 *vs* 22	N/A
Indwelling duodenal stent	0	16	0	N/A	0	N/A
Unable to cannulate	16	42	0	N/A	0	N/A

N/A: Not applicable; QoL sF: Quality of life Short Form Survey (SF-36); ERCP: Endoscopic retrograde cholangiopancreatography.

DISCUSSION

The most common method for gaining access to the biliary tree is ERCP. In patients with unmodified upper gastrointestinal anatomy, the success rate of bile duct cannulation using ERCP is > 90%[25]. Affected or variant anatomy, ampullary pathology (stones, stenosis, and tumor infiltration), periampullary diverticulum, gastric outlet obstruction, indwelling duodenal stent, and previous gastric bypass surgery are the prevalent causes of failed cannulation[29]. The rate of adverse outcomes associated with PTBD and surgery is extremely high, although these approaches are traditionally used to treat these clinical conditions[30]. The most prevalent issues related to long-term PTBD therapy are drain blockage, dislocation, and cholangitis, which require multiple interventions and longer hospital stays[31]. Moreover, patients are left with a permanent external drain, resulting in poor quality of life[32]. EUS-BD has emerged as a viable, extremely safe, effective, and minimally invasive approach[33]. Using echoendoscopy and fluoroscopy, the biliary tree is accessed from the gastrointestinal lumen, a fistulous tract is created, and a stent is deployed in a single step, eliminating the need for an external drain[34]. However, the rates of success and adverse events associated with EUS-BD remain unclear. The use of EUS-BD was first reported by Giovannini *et al*[10] in 2001. Subsequently, several studies reported the

Table 2 Rates of clinical and technical success in the included studies

Ref.	Technical success		Clinical success	
	EUS-guided Choledochoduodenostomy	Percutaneous transhepatic biliarydrainage	EUS-guided Choledochoduodenostomy	Percutaneous transhepatic biliarydrainage
Artifon *et al* [23]	13/13	12/12	13/13	12/12
Bapaye *et al* [24]	23/25	26/26	23/25	26/26
Khashab *et al* [25]	19/22	51/51	19/19	47/51
Giovannini [26]	19/20	17/17	18/19	17/17
Jung *et al*[27]	32/34	31/32	28/32	27/31
Sharaiha *et al* [28]	43/47	12/13	27/43	3/12

Table 3 Quality of identified studies

Ref.	Criteria									Overall appraisal
	C1	C2	C3	C4	C5	C6	C7	C8	C9	
Artifon *et al*[23]	Yes	Yes	Yes	Yes	Yes	Yes	Yes	Unclear	Yes	Included
Bapaye *et al*[24]	Yes	Yes	Yes	Yes	Yes	Yes	Yes	Yes	Yes	Included
Khashab *et al*[25]	Yes	Yes	Yes	Yes	Yes	Yes	Yes	Yes	Yes	Included
Giovannini[26]	Unclear	Yes	Yes	Yes	Yes	Yes	Yes	Yes	Yes	Included
Jung *et al*[27]	Yes	Yes	Yes	Yes	Yes	Yes	Yes	Unclear	Yes	Included
Sharaiha *et al*[28]	Yes	Yes	Yes	Yes	Yes	Unclear	Yes	Yes	Yes	Included

C1: Did the study sample represent the target population? C2: Were participants in the study appropriately recruited? C3: Was the sample size adequate? C4: Were the study subjects and study setting described in detail? C5: Did the data analysis cover a sufficient portion of the identified population? C6: Were objective and standard criteria used to measure the condition of interest? C7: Was the condition reliably measured? C8: Was the statistical analysis appropriate? C9: Were all important confounding factors/subgroups/differences identified and taken into account?

efficacy of EUS-BD as an alternative BD method after a failed ERCP. The EUS-BD procedures are divided into three techniques: (1) EUS-RV; (2) EUS-guided antegrade (EUS-AG); and (3) EUS-guided transluminal BD, including EUS-guided choledochoduodenostomy (EUS-CDS) and EUS-guided hepaticogastrostomy (EUS-HGS)[6]. In EUS-RV, the biliary duct is accessed using fluoroscopy and EUS, forming a temporary fistula, followed by guidewire placement into the duodenum *via* the biliary duct and ampulla. After guidewire placement, ERCP is performed using the EUS-placed guidewire, which is removed once biliary cannulation is obtained. Thus, EUS-RV should be performed in patients with an endoscopically accessible ampulla after unsuccessful biliary cannulation using conventional ERCP.

In EUS-AG, the intrahepatic biliary duct is accessed by creating a temporary fistula between the intestine and intrahepatic biliary duct from the upper intestine. Stent placement or balloon dilation is performed after the dilation of the fistula to achieve biliary obstruction through the fistula without reaching the ampulla using the endoscope. This technique is appropriate when reaching the biliary orifice using endoscopy is impossible or unmanageable, such as in biliary obstruction in patients with surgically altered anatomy or upper intestinal obstruction.

In EUS-guided transluminal BD, including EUS-CDS and EUS-HGS, the biliary duct is accessed followed by guidewire placement and fistula dilation under EUS guidance. For BD, a permanent fistula is created by inserting the stent between the biliary duct and the intestine. This procedure can be performed in cases where reaching the biliary orifice using endoscopy is possible or accessible; however, in patients with unresectable malignant biliary obstruction, its indication should be limited given the features of permanent fistula creation.

Recent studies have demonstrated that EUS-BD could be an alternative to PTBD in patients with inoperable malignant biliary blockage and failed ERCP. However, individual study outcomes show inconsistent results. We performed a systemic analysis to aggregate information from individual trials

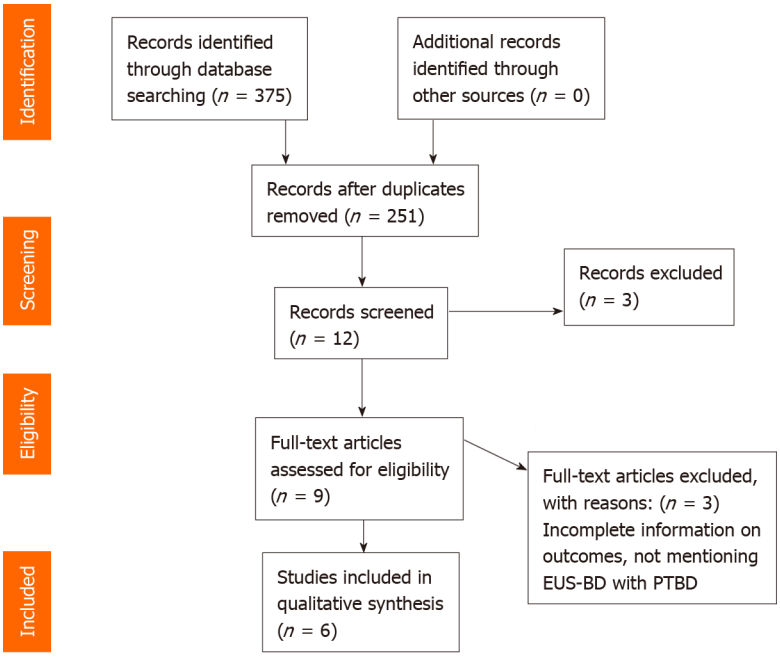

DOI: 10.3748/wjg.v28.i27.3514

Figure 1 PRISMA Flow Diagram. EUS-BD: Endoscopic ultrasound-guided biliary drainage; PTBD: Percutaneous transhepatic biliary drainage.

and examine the overall outcomes of EUS-BD compared with PTBD. EUS-BD was associated with a lower rate of adverse events compared with PTBD. The healthcare cost of PTBD was twice that of EUS-BD due to the high reintervention rate in the PTBD group. A retrospective study by Sharaiha *et al*[28] reported that the technical success rate was comparable between PTBD and EUS-BD in patients with inoperable malignant biliary obstruction and inaccessible papilla. In a retrospective study examining patients with incurable malignant biliary obstruction with failed ERCP due to an inaccessible papilla, Bapaye *et al*[24] found that the EUS-BD group had a higher success rate of BD (92% *vs* 46%, respectively, $P > 0.05$) and a lower rate of adverse events than the PTBD group (20% *vs* 46%, respectively, $P = 0.05$) [24]. These results were partially due to the use of EUS-BD in high-volume centers by experienced endoscopists. The rates of success and the complications of EUS-BD are expected to improve with technical advances.

In the present systematic review, the only randomized controlled study comparing EUS-BD and PTBD in patients with inoperable malignant biliary blockage was conducted by Artifon *et al*[8]. The study, which included 13 patients in the EUS-BD group and 12 patients in the PTBD group, reported that EUS-BD and PTBD were comparable in terms of cost, adverse events, and clinically meaningful improvements in bilirubin levels. The bilirubin levels in the EUS-BD group declined from 16.4 μmol/L to 3.3 μmol/L, whereas the bilirubin levels in the PTBD group declined from 17.2 μmol/L to 3.3 μmol/L [8]. The postprocedural follow-up period was 7 d in both the groups. Choi *et al*[32] reported a higher technical success rate in the PTBD group than in the EUS-BD group, although the functional success rate was comparable between the two groups[35].

In most facilities, PTBD is used as an alternative technique in cases of failed ERCP. In high-volume clinics, endoscopic ultrasound-guided gallbladder drainage has begun replacing PTBD, which was developed only a decade ago as the fourth approach for biliary decompression after surgical drainage, percutaneous transhepatic drainage, and endoscopic transpapillary drainage[36]. Although the type of BD approach used in cases of failed ERCP is currently determined by local competence, EUS-BD is a less intrusive and more physiologic technique. This approach improves nutrition absorption, prevents electrolyte loss, reduces reinterventions, and eliminates the stress of external drainage[37]. EUS-BD can also be performed in a single setting before ERCP if the patient agrees.

However, EUS-BD is associated with several specific issues. Only a small number of centers have the operational skills to perform EUS-BD, whereas most centers have extensive experience and skills to perform PTBD, and interventional radiologists are well-trained and equipped to perform PTBD[25]. The inherent risk of advanced endoscopy necessitates specialized training. Therefore, EUS-BD can only be performed in high-volume treatment institutions with adequate interventional radiology and surgical backup to prevent complications such as bile leak, pneumoperitoneum, hemorrhage, and stent migration[38,39].

The invasion of the sterile biliary tree by transmural puncture from the luminal side of the gastrointestinal tract poses a modest theoretical risk of infection in EUS-BD[40]. However, such negative events should improve with the further evolution of this technique. Despite its classification as a rescue

treatment for failed ERCP, primary EUS-BD is currently compared with ERCP, and a recent study indicated similar short-term outcomes between EUS-BD and ERCP[41]. In addition, unlike ERCP, there is no risk of pancreatitis following EUS-BD. Furthermore, the clinical success rates and complications do not differ between EUS-BD and ERCP if performed by skilled endoscopists. The current systematic review revealed that EUS-BD was safe and effective when performed by skilled individuals, with a lower risk of adverse events and similar technical and clinical success rates.

Our analyses also indicated that: In patients with inoperable biliary blockage after a failed ERCP, EUS-BD was associated with a higher chance of successful BD and a lower risk of procedure-related adverse effects and infectious complications compared with PTBD. Furthermore, the number of patients with bile leaks was lower in the EUS-BD group than in the PTBD group.

CONCLUSION

Several case reports, series, and retrospective investigations regarding EUS-BD have been published to date. However, no prospective studies or comparisons of the various BD systems have been published; therefore, the technical success, functional success, adverse events, and stent patency of EUS-BD with long-term follow-up remain unknown. Prospective, randomized controlled studies are required to clarify these issues. However, it is clear that EUS-BD is clinically useful as a BD option. EUS-BD could become a first-line BD treatment instead of ERCP if the outcomes of clinical studies are positive and technologies are simplified.

ARTICLE HIGHLIGHTS

Research background

Percutaneous transhepatic cholangiography is a diagnostic and therapeutic procedure. Endoscopic ultrasound-guided biliary drainage (EUS-BD) is a novel technique that allows BD whose technicality, success rate, and outcomes are not negligible.

Research motivation

We aimed to compare the technical details and outcomes of 132 studies concerning interventional BD procedures in patients with obstructive cholangiopathy. We conducted a systematic review of six studies that met the inclusion criteria.

Research objectives

To assess the suitability and appropriability of different clinical biliary interventions in achieving optimal BD for obstructive cholangiopathy.

Research methods

An extensive systematic review was independently conducted by two investigators using an electronic search of different databases, including PubMed, Embase, clinicaltrials.gov, the Cochrane library, Scopus, and Google Scholar, using the guidelines for Preferred Reporting Items for Systematic reviews and Meta-Analyses to identify studies comparing percutaneous transhepatic BD (PTBD) and EUS-BD.

Research results

PTBD patients underwent significantly more reinterventions (4.9 *vs* 1.3), experienced more postprocedural pain (4.1 *vs* 1.9), and experienced more late adverse events (53.8% *vs* 6.6%) than EUS-BD patients. There was a significant reduction in the total bilirubin levels in both the groups (16.4-3.3 μmol/L and 17.2-3.8 μmol/L in the EUS-BD and PTBD groups, respectively; $P = 0.002$) at the postprocedural 7-d follow-up. There were no significant differences in the complication rates between the PTBD and EUS-BD groups (3.3 *vs* 3.8). PTBD was associated with a higher adverse event rate than EUS-BD in all the procedures, including reinterventions (80.4% *vs* 15.7%, respectively) and a higher rate of index procedure (39.2% *vs* 18.2%, respectively).

Research conclusions

EUS-BD might be considered as a first-line BD treatment instead of PTBD if the outcomes of clinical studies are favorable and the technical approach is simplified.

Research perspectives

EUS-BD following failed ERCP was superior to PTBD in patients with obstructive cholangiopathy.

FOOTNOTES

Author contributions: Hassan Z contributed in study selection, data analysis, and writing of the manuscript; Gadour E contributed in study conception, analysis and interpretation of the data, and drafting of the manuscript; and all authors have approved the final manuscript.

Conflict-of-interest statement: All the authors report no relevant conflicts of interest for this article.

PRISMA 2009 Checklist statement: The authors have read the PRISMA 2009 Checklist, and the manuscript was prepared and revised according to the PRISMA 2009 Checklist.

Country/Territory of origin: United Kingdom

ORCID number: Zeinab Hassan 0000-0003-0703-6500; Eyad Gadour 0000-0001-5087-1611.

Corresponding Author's Membership in Professional Societies: British Society of Gastroenterology, BSG64346.

S-Editor: Wang JJ
L-Editor: A
P-Editor: Wang JJ

REFERENCES

1 **Ang TL**, Teo EK, Fock KM. EUS-guided transduodenal biliary drainage in unresectable pancreatic cancer with obstructive jaundice. *JOP* 2007; **8**: 438-443 [PMID: 17625296]
2 **Mastier C**, Valette PJ, Adham M, Mabrut JY, Glehen O, Ponchon T, Rousset P, Rode A. Complex Biliary Leaks: Effectiveness of Percutaneous Radiological Treatment Compared to Simple Leaks in 101 Patients. *Cardiovasc Intervent Radiol* 2018; **41**: 1566-1572 [PMID: 29872897 DOI: 10.1007/s00270-018-2005-1]
3 **Azeemuddin M**, Turab N Al Qamari, Chaudhry MBH, Hamid S, Hasan M, Sayani R. Percutaneous Management of Biliary Enteric Anastomotic Strictures: An Institutional Review. *Cureus* 2018; **10**: e2228 [PMID: 29713573 DOI: 10.7759/cureus.2228]
4 **DeMasi CJ**, Akdamar K, Hunter FM, Sparks RD. Percutaneous transhepatic cholangiography in the diagnosis of jaundice. *Am J Med Sci* 1967; **254**: 316-321 [PMID: 6054533 DOI: 10.1097/00000441-196709000-00006]
5 **Voegeli DR**, Crummy AB, Weese JL. Percutaneous transhepatic cholangiography, drainage, and biopsy in patients with malignant biliary obstruction. An alternative to surgery. *Am J Surg* 1985; **150**: 243-247 [DOI: 10.1016/0002-9610(85)90129-1]
6 **Komaki T**, Kitano M, Sakamoto H, Kudo M. Endoscopic ultrasonography-guided biliary drainage: evaluation of a choledochoduodenostomy technique. *Pancreatology* 2011; **11** Suppl 2: 47-51 [PMID: 21464587 DOI: 10.1159/000323508]
7 **Enochsson L**, Swahn F, Arnelo U, Nilsson M, Löhr M, Persson G. Nationwide, population-based data from 11,074 ERCP procedures from the Swedish Registry for Gallstone Surgery and ERCP. *Gastrointest Endosc* 2010; **72**: 1175-1184, 1184.e1 [PMID: 20970787 DOI: 10.1016/j.gie.2010.07.047]
8 **Artifon EL**, Sakai P, Cunha JE, Dupont A, Filho FM, Hondo FY, Ishioka S, Raju GS. Surgery or endoscopy for palliation of biliary obstruction due to metastatic pancreatic cancer. *Am J Gastroenterol* 2006; **101**: 2031-2037 [PMID: 16968509 DOI: 10.1111/j.1572-0241.2006.00764.x]
9 **Weber A**, Gaa J, Rosca B, Born P, Neu B, Schmid RM, Prinz C. Complications of percutaneous transhepatic biliary drainage in patients with dilated and nondilated intrahepatic bile ducts. *Eur J Radiol* 2009; **72**: 412-417 [PMID: 18926655 DOI: 10.1016/j.ejrad.2008.08.012]
10 **Giovannini M**, Moutardier V, Pesenti C, Bories E, Lelong B, Delpero JR. Endoscopic ultrasound-guided bilioduodenal anastomosis: a new technique for biliary drainage. *Endoscopy* 2001; **33**: 898-900 [PMID: 11571690 DOI: 10.1055/s-2001-17324]
11 **Lesmana CRA**, Gani RA, Hasan I, Sulaiman AS, Ho KY, Dhir V, Lesmana LA. Palliative Endoscopic Ultrasound Biliary Drainage for Advanced Malignant Biliary Obstruction: Should It Replace the Percutaneous Approach? *Case Rep Gastroenterol* 2019; **13**: 385-397 [PMID: 31616233 DOI: 10.1159/000502835]
12 **Kozarek RA**. Malignant jaundice. *Eur J Cancer Suppl* 2005; **3**: 183-190 [DOI: 10.1016/S1359-6349(05)80275-7]
13 **Collins D**, Penman I, Mishra G, Draganov P. EUS-guided celiac block and neurolysis. *Endoscopy* 2006; **38**: 935-939 [PMID: 16981114 DOI: 10.1055/s-2006-944734]
14 **Wiersema MJ**, Sandusky D, Carr R, Wiersema LM, Erdel WC, Frederick PK. Endosonography-guided cholangiopancreatography. *Gastrointest Endosc* 1996; **43**: 102-106 [PMID: 8635700 DOI: 10.1016/s0016-5107(06)80108-2]
15 **Giovannini M**, Dotti M, Bories E, Moutardier V, Pesenti C, Danisi C, Delpero JR. Hepaticogastrostomy by echo-endoscopy as a palliative treatment in a patient with metastatic biliary obstruction. *Endoscopy* 2003; **35**: 1076-1078 [PMID:

14648424 DOI: 10.1055/s-2003-44596]
16 **Mallery S**, Matlock J, Freeman ML. EUS-guided rendezvous drainage of obstructed biliary and pancreatic ducts: Report of 6 cases. *Gastrointest Endosc* 2004; **59**: 100-107 [PMID: 14722561 DOI: 10.1016/s0016-5107(03)02300-9]
17 **Itoi T**, Itokawa F, Sofuni A, Kurihara T, Tsuchiya T, Ishii K, Tsuji S, Ikeuchi N, Moriyasu F. Endoscopic ultrasound-guided choledochoduodenostomy in patients with failed endoscopic retrograde cholangiopancreatography. *World J Gastroenterol* 2008; **14**: 6078-6082 [PMID: 18932289 DOI: 10.3748/wjg.14.6078]
18 **Kahaleh M**, Yoshida C, Kane L, Yeaton P. Interventional EUS cholangiography: A report of five cases. *Gastrointest Endosc* 2004; **60**: 138-142 [PMID: 15229448 DOI: 10.1016/s0016-5107(04)01528-7]
19 **Chavalitdhamrong D**, Draganov PV. Endoscopic ultrasound-guided biliary drainage. *World J Gastroenterol* 2012; **18**: 491-497 [PMID: 22363114 DOI: 10.3748/wjg.v18.i6.491]
20 **Lee TH**, Choi JH, Park do H, Song TJ, Kim DU, Paik WH, Hwangbo Y, Lee SS, Seo DW, Lee SK, Kim MH. Similar Efficacies of Endoscopic Ultrasound-guided Transmural and Percutaneous Drainage for Malignant Distal Biliary Obstruction. *Clin Gastroenterol Hepatol* 2016; **14**: 1011-1019.e3 [PMID: 26748220 DOI: 10.1016/j.cgh.2015.12.032]
21 **Beller EM**, Glasziou PP, Altman DG, Hopewell S, Bastian H, Chalmers I, Gøtzsche PC, Lasserson T, Tovey D; PRISMA for Abstracts Group. PRISMA for Abstracts: reporting systematic reviews in journal and conference abstracts. *PLoS Med* 2013; **10**: e1001419 [PMID: 23585737 DOI: 10.1371/journal.pmed.1001419]
22 **Guyatt GH**, Oxman AD, Schünemann HJ, Tugwell P, Knottnerus A. GRADE guidelines: a new series of articles in the Journal of Clinical Epidemiology. *J Clin Epidemiol* 2011; **64**: 380-382 [PMID: 21185693 DOI: 10.1016/j.jclinepi.2010.09.011]
23 **Artifon EL**, Aparicio D, Paione JB, Lo SK, Bordini A, Rabello C, Otoch JP, Gupta K. Biliary drainage in patients with unresectable, malignant obstruction where ERCP fails: endoscopic ultrasonography-guided choledochoduodenostomy versus percutaneous drainage. *J Clin Gastroenterol* 2012; **46**: 768-774 [PMID: 22810111 DOI: 10.1097/MCG.0b013e31825f264c]
24 **Bapaye A**, Dubale N, Aher A. Comparison of endosonography-guided vs. percutaneous biliary stenting when papilla is inaccessible for ERCP. *United European Gastroenterol J* 2013; **1**: 285-293 [PMID: 24917973 DOI: 10.1177/2050640613490928]
25 **Khashab MA**, Valeshabad AK, Afghani E, Singh VK, Kumbhari V, Messallam A, Saxena P, El Zein M, Lennon AM, Canto MI, Kalloo AN. A comparative evaluation of EUS-guided biliary drainage and percutaneous drainage in patients with distal malignant biliary obstruction and failed ERCP. *Dig Dis Sci* 2015; **60**: 557-565 [PMID: 25081224 DOI: 10.1007/s10620-014-3300-6]
26 **Giovannini M**. Learning in therapeutic EUS. *Endosc Ultrasound* 2021; **10**: 317-318 [PMID: 34677158 DOI: 10.4103/EUS-D-21-00205]
27 **Jung Y**, Lee J, Cho JY, Kim YD, Park CG, Kim MW, Kim KJ, Kim SW. Comparison of efficacy and safety between endoscopic submucosal dissection and transanal endoscopic microsurgery for the treatment of rectal tumor. *Saudi J Gastroenterol* 2018; **24**: 115-121 [PMID: 29637919 DOI: 10.4103/sjg.SJG_440_17]
28 **Sharaiha RZ**, Kumta NA, Desai AP, DeFilippis EM, Gabr M, Sarkisian AM, Salgado S, Millman J, Benvenuto A, Cohen M, Tyberg A, Gaidhane M, Kahaleh M. Endoscopic ultrasound-guided biliary drainage versus percutaneous transhepatic biliary drainage: predictors of successful outcome in patients who fail endoscopic retrograde cholangiopancreatography. *Surg Endosc* 2016; **30**: 5500-5505 [PMID: 27129552 DOI: 10.1007/s00464-016-4913-y]
29 **Laméris JS**, Stoker J, Nijs HG, Zonderland HM, Terpstra OT, van Blankenstein M, Schütte HE. Malignant biliary obstruction: percutaneous use of self-expandable stents. *Radiology* 1991; **179**: 703-707 [PMID: 2027978 DOI: 10.1148/radiology.179.3.2027978]
30 **Smith AC**, Dowsett JF, Russell RC, Hatfield AR, Cotton PB. Randomised trial of endoscopic stenting versus surgical bypass in malignant low bileduct obstruction. *Lancet* 1994; **344**: 1655-1660 [PMID: 7996958 DOI: 10.1016/S0140-6736(94)90455-3]
31 **Nennstiel S**, Weber A, Frick G, Haller B, Meining A, Schmid RM, Neu B. Drainage-related Complications in Percutaneous Transhepatic Biliary Drainage: An Analysis Over 10 Years. *J Clin Gastroenterol* 2015; **49**: 764-770 [PMID: 25518004 DOI: 10.1097/MCG.0000000000000275]
32 **Choi JH**, Kim HW, Lee JC, Paik KH, Seong NJ, Yoon CJ, Hwang JH, Kim J. Percutaneous transhepatic versus EUS-guided gallbladder drainage for malignant cystic duct obstruction. *Gastrointest Endosc* 2017; **85**: 357-364 [PMID: 27566055 DOI: 10.1016/j.gie.2016.07.067]
33 **Irani S**, Baron TH, Grimm IS, Khashab MA. EUS-guided gallbladder drainage with a lumen-apposing metal stent (with video). *Gastrointest Endosc* 2015; **82**: 1110-1115 [PMID: 26142558 DOI: 10.1016/j.gie.2015.05.045]
34 **Teoh AY**, Binmoeller KF, Lau JY. Single-step EUS-guided puncture and delivery of a lumen-apposing stent for gallbladder drainage using a novel cautery-tipped stent delivery system. *Gastrointest Endosc* 2014; **80**: 1171 [PMID: 24830582 DOI: 10.1016/j.gie.2014.03.038]
35 **Caglar E**, Atasoy D, Tozlu M, Altınkaya E, Dogan S, Senturk H. Experience of the Endoscopists Matters in Endoscopic Retrograde Cholangiopancreatography in Billroth II Gastrectomy Patients. *Clin Endosc* 2020; **53**: 82-89 [PMID: 31476843 DOI: 10.5946/ce.2019.073]
36 **Baniya R**, Upadhaya S, Madala S, Subedi SC, Shaik Mohammed T, Bachuwa G. Endoscopic ultrasound-guided biliary drainage versus percutaneous transhepatic biliary drainage after failed endoscopic retrograde cholangiopancreatography: a meta-analysis. *Clin Exp Gastroenterol* 2017; **10**: 67-74 [PMID: 28408850 DOI: 10.2147/CEG.S132004]
37 **Holt BA**, Hawes R, Hasan M, Canipe A, Tharian B, Navaneethan U, Varadarajulu S. Biliary drainage: role of EUS guidance. *Gastrointest Endosc* 2016; **83**: 160-165 [PMID: 26215648 DOI: 10.1016/j.gie.2015.06.019]
38 **Kahaleh M**, Artifon EL, Perez-Miranda M, Gupta K, Itoi T, Binmoeller KF, Giovannini M. Endoscopic ultrasonography guided biliary drainage: summary of consortium meeting, May 7th, 2011, Chicago. *World J Gastroenterol* 2013; **19**: 1372-1379 [PMID: 23538784 DOI: 10.3748/wjg.v19.i9.1372]
39 **Kawakubo K**, Isayama H, Kato H, Itoi T, Kawakami H, Hanada K, Ishiwatari H, Yasuda I, Kawamoto H, Itokawa F, Kuwatani M, Iiboshi T, Hayashi T, Doi S, Nakai Y. Multicenter retrospective study of endoscopic ultrasound-guided biliary

drainage for malignant biliary obstruction in Japan. *J Hepatobiliary Pancreat Sci* 2014; **21**: 328-334 [PMID: 24026963 DOI: 10.1002/jhbp.27]

40 **Lakhtakia S**. Complications of diagnostic and therapeutic Endoscopic Ultrasound. *Best Pract Res Clin Gastroenterol* 2016; **30**: 807-823 [PMID: 27931638 DOI: 10.1016/j.bpg.2016.10.008]

41 **Dhir V**, Itoi T, Khashab MA, Park DH, Yuen Bun Teoh A, Attam R, Messallam A, Varadarajulu S, Maydeo A. Multicenter comparative evaluation of endoscopic placement of expandable metal stents for malignant distal common bile duct obstruction by ERCP or EUS-guided approach. *Gastrointest Endosc* 2015; **81**: 913-923 [PMID: 25484326 DOI: 10.1016/j.gie.2014.09.054]

World Journal of Gastroenterology

Submit a Manuscript: https://www.f6publishing.com

World J Gastroenterol 2022 July 21; 28(27): 3524-3531

DOI: 10.3748/wjg.v28.i27.3524

ISSN 1007-9327 (print) ISSN 2219-2840 (online)

CASE REPORT

Isolated gastric variceal bleeding related to non-cirrhotic portal hypertension following oxaliplatin-based chemotherapy: A case report

Xu Zhang, Yan-Ying Gao, De-Zhao Song, Bao-Xin Qian

Specialty type: Medicine, general and internal

Provenance and peer review: Unsolicited article; Externally peer reviewed.

Peer-review model: Single blind

Peer-review report's scientific quality classification

Grade A (Excellent): 0
Grade B (Very good): B, B
Grade C (Good): C
Grade D (Fair): D
Grade E (Poor): 0

P-Reviewer: Dambrauskas Z, Lithuania; Fiorentini G, Italy; Yeoh SW, Australia; Yoshida H, Japan

Received: December 26, 2021
Peer-review started: December 26, 2021
First decision: April 16, 2022
Revised: April 27, 2022
Accepted: June 26, 2022
Article in press: June 26, 2022
Published online: July 21, 2022

Xu Zhang, Yan-Ying Gao, Department of Gastroenterology and Hepatology, The Third Central Hospital of Tianjin; Tianjin Key Laboratory of Extra-corporeal Life Support for Critical Diseases; Artificial Cell Engineering Technology Research Center; Tianjin Institute of Hepatobiliary Disease, Tianjin 300000, China

De-Zhao Song, Department of Interventional Radiology, The Third Central Hospital of Tianjin; Tianjin Key Laboratory of Extracorporeal Life Support for Critical Diseases; Artificial Cell Engineering Technology Research Center; Tianjin Institute of Hepatobiliary Disease, Tianjin 300000, China

Bao-Xin Qian, Department of Gastroenterology and Hepatology, The Third Central Hospital of Tianjin; Tianjin Key Laboratory of Extracorporeal Life Support for Critical Diseases; Artificial Cell Engineering Technology Research Center; Tianjin Institute of Hepatobiliary Disease, Tianjin 300000, China

Corresponding author: Bao-Xin Qian, MD, Attending Doctor, Department of Gastroenterology and Hepatology, The Third Central Hospital of Tianjin; Tianjin Key Laboratory of Extracorporeal Life Support for Critical Diseases; Artificial Cell Engineering Technology Research Center; Tianjin Institute of Hepatobiliary Disease, No. 83 Jintang Road, Hedong District, Tianjin 300000, China. baoxinqian@126.com

Abstract

BACKGROUND

Sinusoidal obstruction syndrome has been reported after oxaliplatin-based chemotherapy, but liver fibrosis and non-cirrhotic portal hypertension (NCPH) are rarely reported.

CASE SUMMARY

Here, we describe the case of a 64-year-old woman who developed isolated gastric variceal bleeding 16 mo after completing eight cycles of oxaliplatin combined with capecitabine chemotherapy after colon cancer resection. Surprisingly, splenomegaly and thrombocytopenia were not accompanied by variceal bleeding, which has been reported to have predictive value for gastric variceal formation. However, a liver biopsy showed fibrosis in the portal area, suggesting NCPH. The patient underwent endoscopic treatment and experienced no further symptoms.

CONCLUSION
It is necessary to guard against long-term complications after oxaliplatin-based chemotherapy. Sometimes splenic size and platelet level may not always accurately predict the occurrence of portal hypertension.

Key Words: Non-cirrhotic portal hypertension; Sinusoidal obstruction syndrome; Isolated gastric varices; Oxaliplatin chemotherapy; Colon cancer; Case report

Core Tip: The occurrence of portal hypertension after oxaliplatin chemotherapy is mostly considered to be related to sinusoidal obstruction syndrome, and few studies clearly support non-cirrhotic portal hypertension (NCPH). We present a case of isolated gastric variceal bleeding after oxaliplatin chemotherapy. The pathological results support NCPH.

Citation: Zhang X, Gao YY, Song DZ, Qian BX. Isolated gastric variceal bleeding related to non-cirrhotic portal hypertension following oxaliplatin-based chemotherapy: A case report. *World J Gastroenterol* 2022; 28(27): 3524-3531
URL: https://www.wjgnet.com/1007-9327/full/v28/i27/3524.htm
DOI: https://dx.doi.org/10.3748/wjg.v28.i27.3524

INTRODUCTION

The third-generation platinum anticancer drug, oxaliplatin, is often used in combination with 5-fluorouracil or capecitabine as one of the main chemotherapy strategies for neoadjuvant/adjuvant treatment of stage III and metastatic colon cancer[1]. Oxaliplatin can induce different degrees of liver injury, from mild to acute liver failure, and sinusoidal obstruction syndrome (SOS) is a characteristic manifestation. In addition, chronic injury from endothelial cell damage and architectural distortion may develop nodular regenerative hyperplasia (NRH) and non-cirrhotic portal hypertension (NCPH) years after chemotherapy[2]. As a result, there are manifestations of portal hypertension, such as splenomegaly, thrombocytopenia, ascites, and esophagogastric varices. Since these complications occur long after chemotherapy completion, clinicians may not attribute these findings to oxaliplatin. Here, we report the case of a 64-year-old woman who was treated with eight cycles of oxaliplatin combined with capecitabine after radical resection of the right colon for ascending colon cancer. Isolated gastric variceal bleeding was diagnosed and treated endoscopically, but there was no obvious accompanying splenomegaly, thrombocytopenia, or broadened portal vein. The liver biopsy was indicative of NCPH.

CASE PRESENTATION

Chief complaints

A 64-year-old woman was transferred to our hospital on account of hematemesis and melena.

History of present illness

The patient complained of hematemesis and melena 2 d prior to presentation. She underwent hemostasis and rehydration at the previous hospital. Colonoscopy and gastroscopy were successively performed, and severe gastric varices were found before administration.

History of past illness

Laparoscopic radical resection of right colon cancer had been performed 16 mo earlier due to ascending colon cancer (pT4N2Mx). Preoperative gastroscopy did not show any abnormalities (Figure 1). She received eight cycles of oxaliplatin combined with capecitabine for 6 mo postoperatively. No tumor recurrence was found after intermittent re-examination.

Personal and family history

The patient had no known history of liver disease. She had no history of habitual use of alcohol and no significant history of exposure to liver injury-inducing drugs other than chemotherapy.

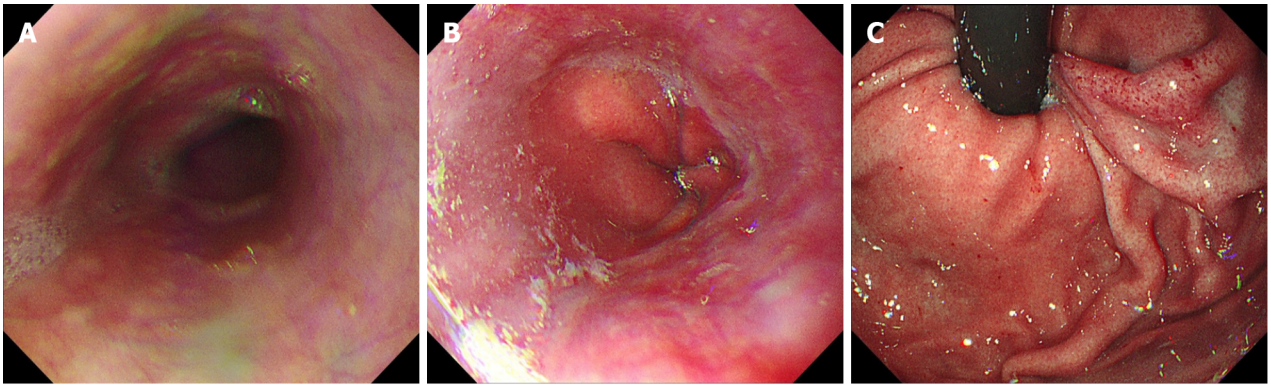

DOI: 10.3748/wjg.v28.i27.3524

Figure 1 Gastroscopic images taken before colon cancer surgery. A: Upper esophageal segment; B: Lower esophageal segment; C: The gastric fundus. No varices were found.

Physical examination

The patient's temperature was 36.6°C, heart rate was 93 bpm, respiratory rate was 16 breaths per minute, blood pressure was 125/65 mmHg, and oxygen saturation in room air was 98%. The patient had an anemic appearance and pale palpebral conjunctiva. No signs of chronic liver disease, such as palmar erythema and spider nevus, were found. No significant enlargement of the liver or spleen was detected on palpation.

Laboratory examinations

Blood examination indicated severe anemia with normal levels of leukocytes and platelets. Prothrombin time was normal with a slight increase in plasma D-dimer level. Liver function test indicated mild hypoproteinemia with normal transaminase and bilirubin levels; renal function was normal. Liver tests were negative for hepatitis viruses; autoimmune liver diseases; and metabolic liver diseases, such as hepatolenticular degeneration and hemochromatosis (Table 1).

Imaging examinations

An enhanced computed tomography (CT) scan of the abdomen and pelvis showed postoperative changes of the colon, an irregular liver contour, slightly enlarged spleen, low-grade fatty liver, and varices in the gastric fundus with gastro-renal shunting (Figure 2). Contrast-enhanced ultrasonography showed that the size of the spleen was 4.2 cm × 11.2 cm. The diameter of the retropancreatic splenic vein was 0.67 cm with a mean blood flow velocity of 33.0 cm/s and volume flow of 528.7 mL/min.

Pathological examination

A transjugular liver biopsy was performed, and the hepatic venous pressure gradient (HVPG, wedged hepatic venous pressure – free hepatic venous pressure) was measured as 15 mmHg. Liver biopsy showed that the hepatic lobule was essentially complete with sinusoidal dilatation, and no pseudolobular formation was observed. Hepatocyte nuclear size slightly varied. Focal perisinusoidal fibrosis could be observed in the hepatic central vein area, which showed a diffuse distribution of necrotic hepatocytes engulfed by phagocytes. There were slight inflammatory reactions in hepatic portal areas, with slight fibrosis in the interstitium and around the bile duct. The vascular wall of the portal vein was thickened, indicating portal hypertension, and the final pathological diagnosis considered NCPH (Figure 3).

FINAL DIAGNOSIS

The final diagnosis of the presented case was NCPH due to oxaliplatin.

TREATMENT

After admission, the patient was immediately administered with octreotide (50 μg/h, iv, for 72 h), proton pump inhibitor, omeprazole (8 mg/h, iv, for 72 h), and hemocoagulase. An erythrocyte suspension of volume, 400 mL, was transfused. Gastroscopy after cessation of active gastrointestinal bleeding revealed severe isolated gastric varices in the fundus of the stomach, Lg-f, F3, Cb, and RC2

Table 1 Clinical indicators

Routine examination		Biochemical examination		Immune examination	
White blood count	11.95 x 10^9/L	Alaninetransaminase	1831 U/L	Hepatitis B surface antigen	(-)
Red blood count	1.9 x 10^{12}/L	Aspartate transaminase	31 U/L	Hepatitis C antibody	(-)
Hemoglobin	60 g/L	Alkaline phosphatase	103 U/L	Antinuclear antibody	(-)
Platelet	171 x 10^9/L	Gamma glutamyl transpeptidase	29 U/L	Antimitochondrial antibody	(-)
Prothrombin time	14.3 s	Total bilirubin	12.0 mmol/L	Immunoglobulin G	(-)
International standard ratio	1.12	Direct bilirubin	1.2 mmol/L	Immunoglobulin M	(-)
D-dimer	4.38 mg/L	Albumin	33.7 g/L	Immunoglobulin G4	(-)
		Globulose	29.3 g/L		
		Serum creatinine	82 mmol/L		
		Potassium	3.58 mmol/L		
		Ferritin	(-)		
		Ceruloplasmin	(-)		

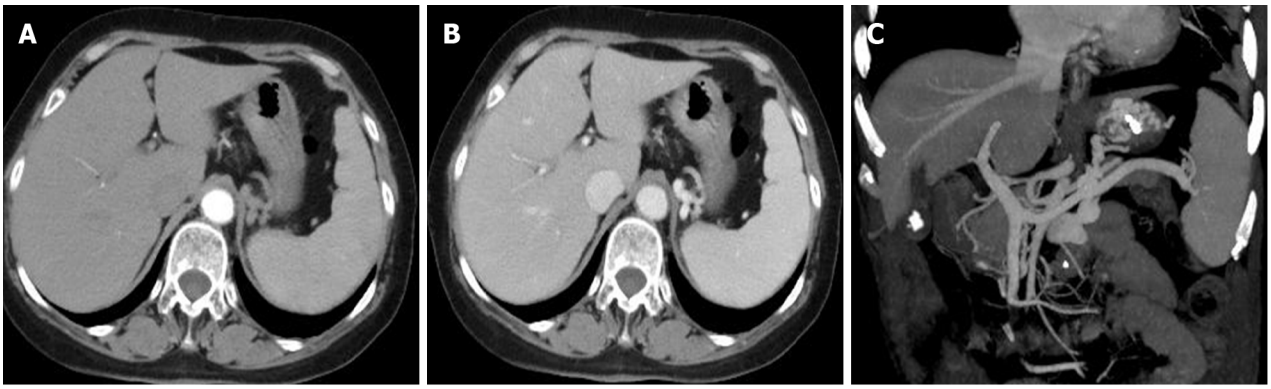

DOI: 10.3748/wjg.v28.i27.3524

Figure 2 Abdominal enhanced computed tomography images. A: Arterial phase; B: Portal vein phase. There was no atrophy or cirrhotic features, and the liver parenchyma density was uniform; C: 3D vascular reconstruction of portal vein system. The blood flows of the portal and retropancreatic splenic veins were unobstructed without obvious widening of the inner diameters. Severe gastric fundal varices were clearly visible.

(Figure 4). Cyanoacrylate glue was injected.

OUTCOME AND FOLLOW-UP

The patient had an uneventful postoperative clinical course. Therefore, she was discharged 7 d after operation. Beta blockers were not administered because the patient' s mean heart rate was 58 ± 6 bpm. During a follow-up visit 2 mo after the operation, signs of anemia was absent and a new gastroscopy showed varices in fundus of stomach relieved obviously.

DISCUSSION

As one of the main chemotherapeutic agents for stage III and metastatic colon cancer, oxaliplatin is widely used in chemotherapy. Common side effects of oxaliplatin are neurotoxicity, gastrointestinal reactions, and hematological toxicity. In recent years, SOS has received more attention as a long-term complication of oxaliplatin use, and its reported incidence rate ranges from 19% to 52%[3,4]. SOS is an obliterative venulitis of the terminal hepatic venules, which is characterized by jaundice, right upper quadrant pain, tender hepatomegaly, ascites, and unexplained weight gain. SOS usually occurs as a result of cytoreductive therapy prior to hematopoietic stem cell transplantation. In China, it is often associated with the oral intake of plants that contain pyrrolidine alkaloids. This patient did not have any

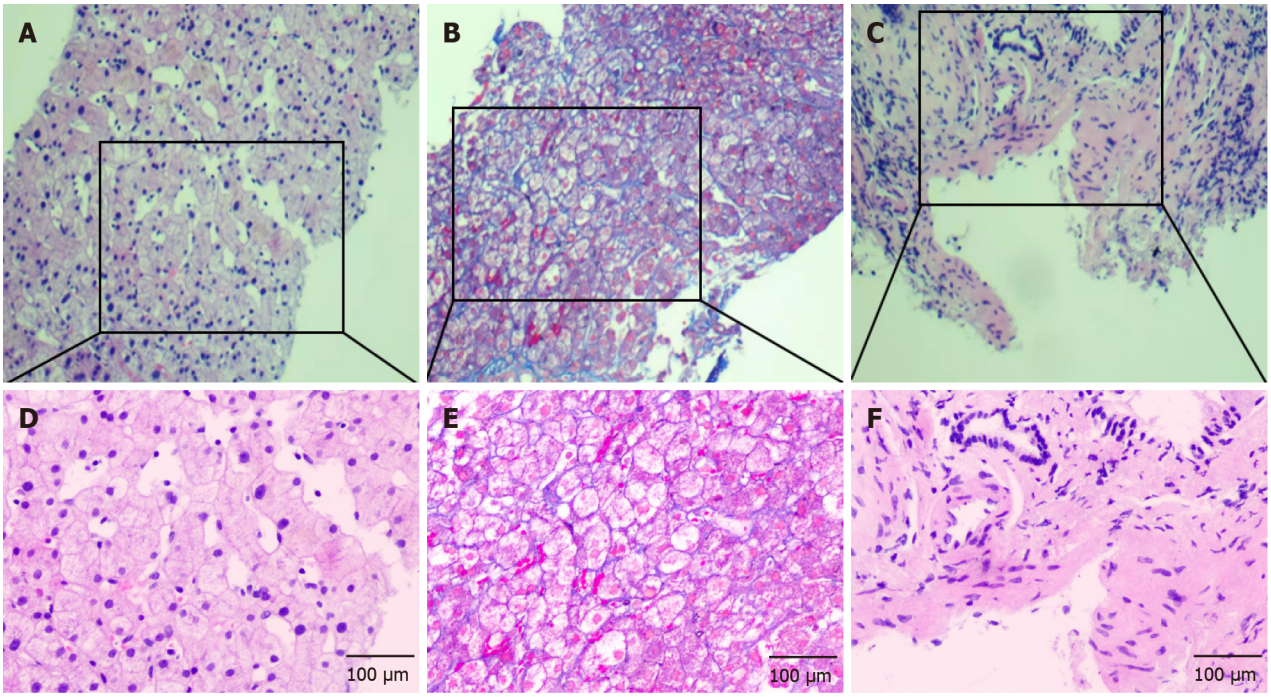

DOI: 10.3748/wjg.v28.i27.3524

Figure 3 Pathological examination images. A, D: Hematoxylin and eosin (HE) staining showed obvious sinusoidal dilatation (A: 100 ×; D: 200 ×); B, E: Masson staining showed mild peri-sinusoidal fibrosis (B: 100 ×; E: 200 ×); C, F: HE staining showed obvious portal vein wall thickening and mild fibrosis in the portal area (C: 100 ×; F: 200 ×).

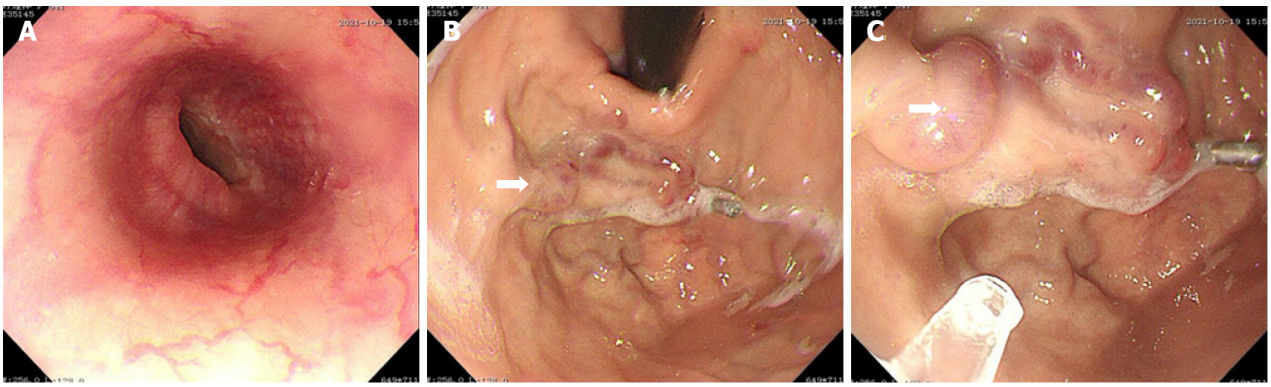

DOI: 10.3748/wjg.v28.i27.3524

Figure 4 Gastroscopic examination and treatment images in our hospital. A: Image showing smooth esophageal mucosa without varices; B: Isolated gastric fundus varices (white arrow); C: Cyanoacrylate glue injection (white arrow) was administered for varices after blocking blood flow with a titanium clip to prevent ectopic embolism.

significant history of exposure to liver injury-inducing drugs other than chemotherapy. Therefore, the liver damage was considered to be directly related to oxaliplatin-containing chemotherapy.

The mechanism by which oxaliplatin causes hepatic sinusoidal injury is relatively clear. The inflammation caused by oxaliplatin can increase the expression of many cytokines and chemokines[5], leading to atrophy and apoptosis of hepatocytes around the hepatic sinusoids, which decreases the supporting capacity. Oxidative stress[6] and glutathione depletion[7] caused by oxaliplatin metabolism could destroy the integrity and permeability of liver sinusoidal endothelial cells (LSECs). Necrotic LSECs and red blood cells can then form emboli with platelets, which causes obstruction and expansion of the hepatic sinusoids, leading to SOS. LSECs produce cytokines and inflammatory factors, such as interleukin-6, platelet-derived growth factor, tissue inhibitor of metalloproteinase, matrix metalloproteinases, and vascular endothelial growth factor. These activate hepatic stellate cells to increase collagen levels in the extracellular matrix, ultimately leading to hepatic fibrosis[8] that can progress to NRH, NCPH, and portal sclerosis in subsequent years.

In the pathological examination of our patient, there was an obvious expansion of the hepatic sinusoids with fibrosis in the hepatic sinusoids and portal areas. The lack of typical SOS manifestations, such as intrasinusoidal hemorrhage, thrombosis, and obstruction, suggested NCPH. This pathological manifestation was similar to that described by Ryuta *et al*[9]. In that case, esophageal and gastric varices were found 3.5 years after the termination of oxaliplatin-based chemotherapy, compared to 16 mo in this report. Both patients developed long-term portal complications after chemotherapy completion. Vigano *et al*[10] analyzed liver injury reversibility after the interruption of chemotherapy and reported that SOS may resolve within 9 mo. Therefore, we suspected that the sinusoidal injury in this patient was not enough to cause typical clinical presentations of SOS, which had gradually recovered after chemotherapy termination. However, fibrosis persisted in the hepatic sinusoids and portal areas, resulting in portal hypertension and severe gastric variceal bleeding.

NCPH etiology can be divided into five groups: infection, immune disorders, thrombophilia, genetic defect, and exposure history of drugs or poisons[11]. Currently, drugs that can reportedly induce NCPH include difenoxin, azathioprine, mercaptopurine, and allopurinol[12,13]. A recent study proposed that oxaliplatin is related to NCPH[2]. The main clinical manifestations of NCPH are esophagogastric varices, splenomegaly, thrombocytopenia, and ascites, with the first being the most common[14]. Park *et al*[15] investigated the predictors of portal hypertension formation related to oxaliplatin use and found that noninvasive fibrosis prediction models including, the age-platelet index, aspartate aminotransferase-to-platelet ratio index, platelet-to-spleen ratio, and fibrosis-4 score, have good predictive values. Satta *et al*[16] reported that platelet count and spleen index under CT correlated with esophagogastric variceal formation. These indicators are often used to screen whether patients need gastroscopy because they are easily obtained. However, in this case, the patient had severe isolated gastric varices accompanied by gastro-renal shunting. No obvious increase in splenic volume or thrombocytopenia during or after chemotherapy was observed, and no widening of the portal vein was observed on enhanced CT, which was different from common esophagogastric varices related to oxaliplatin. These findings exemplify why diagnoses may be missed. Apparently, gastroscopy was not performed during follow-up after surgery and chemotherapy, which is why the varices were not discovered until bleeding occurred.

Notably, NCPH is considered as pre-sinusoidal portal hypertension. Therefore, HVPG in patients with NCPH may not exactly reflect portal hypertension with measurements lower than those in patients with liver cirrhosis. A retrospective study reported that the average HVPG of patients with NCPH was 8.3 ± 4.5 mmHg, 60% of patients had normal or slightly elevated HVPG (≤ 10 mmHg), and 40% of patients had HVPG > 11 mmHg[14]. The HVPG level in our patient was 15 mmHg, which was significantly higher than normal, possibly due to hepatic sinusoidal injury and peri-sinusoidal fibrosis.

Ligation and cyanoacrylate glue injection under gastroscopy are the first-line treatment options for esophageal and gastric variceal bleeding in liver cirrhosis[17], but whether they are appropriate for esophageal and gastric variceal bleeding related to NCPH remains controversial. A previous study reported that the effect of endoscopic therapy in preventing variceal rebleeding in patients with NCPH is not ideal, compared to its effect in preventing hepatitis B cirrhosis-related portal hypertension[18]. Due to good functional liver reserve in patients with NCPH, transjugular intrahepatic portosystemic shunt (TIPS) treatment has a lower rebleeding rate, and the incidence and mortality of postoperative hepatic encephalopathy are lower[19]. For these reasons, TIPS may be used as the first-line treatment for esophageal and gastric variceal bleeding due to NCPH.

However, this report describes a patient with NCPH who underwent colon cancer resection. Therefore, it is necessary to guard against the possibility of malignant tumor recurrence and maintain good liver function, in case reoperation and additional chemotherapy rounds are required. Liver compensation ability may decrease after TIPS treatment. Instead, gastroscopic therapy was performed with successful cyanoacrylate glue injection, and the patient was discharged.

CONCLUSION

Oxaliplatin can cause hepatic sinusoidal injury and SOS, which could lead to portal hypertension years later. Splenomegaly and thrombocytopenia have a certain predictive value for SOS occurrence in patients who previously received chemotherapy, but few unique cases remain in the clinic. The formation of esophageal and gastric varices is the only manifestation of portal hypertension; therefore, these patients are likely to be misdiagnosed. Therefore, gastroscopy should be considered as part of follow-up after oxaliplatin-based chemotherapy.

FOOTNOTES

Author contributions: Zhang X and Gao YY contributed equally to this article; Zhang X and Gao YY contributed to writing-original draft preparation; Song DZ contributed to performing transjugular liver biopsy; and Qian BX contributed to writing-reviewing and editing.

Supported by Tianjin Science and Technology Plan Project, No. 19ZXDBSY00030.

Informed consent statement: The legal guardian of the study participant provided informed written consent prior to study enrollment.

Conflict-of-interest statement: All authors report no relevant conflicts of interest for this article.

CARE Checklist (2016) statement: The authors have read the CARE Checklist (2016), and the manuscript was prepared and revised according to the CARE Checklist (2016).

Country/Territory of origin: China

ORCID number: Xu Zhang 0000-0001-7399-0509; Yan-Ying Gao 0000-0001-6102-9681; De-Zhao Song 0000-0003-3405-531X; Bao-Xin Qian 0000-0001-7462-8034.

S-Editor: Ma YJ
L-Editor: A
P-Editor: Ma YJ

REFERENCES

1 **André T**, Boni C, Mounedji-Boudiaf L, Navarro M, Tabernero J, Hickish T, Topham C, Zaninelli M, Clingan P, Bridgewater J, Tabah-Fisch I, de Gramont A; Multicenter International Study of Oxaliplatin/5-Fluorouracil/Leucovorin in the Adjuvant Treatment of Colon Cancer (MOSAIC) Investigators. Oxaliplatin, fluorouracil, and leucovorin as adjuvant treatment for colon cancer. *N Engl J Med* 2004; **350**: 2343-2351 [PMID: 15175436 DOI: 10.1056/NEJMoa032709]

2 **Tavernier E**, Chalayer E, Cornillon J, Pouvaret A, Martignoles JA, Casteillo F, Terreaux J, Daguenet E, Guyotat D. Fulminant hepatitis due to very severe sinusoidal obstruction syndrome (SOS/VOD) after autologous peripheral stem cell transplantation: a case report. *BMC Res Notes* 2018; **11**: 436 [PMID: 29970140 DOI: 10.1186/s13104-018-3533-0]

3 **Rubbia-Brandt L**, Audard V, Sartoretti P, Roth AD, Brezault C, Le Charpentier M, Dousset B, Morel P, Soubrane O, Chaussade S, Mentha G, Terris B. Severe hepatic sinusoidal obstruction associated with oxaliplatin-based chemotherapy in patients with metastatic colorectal cancer. *Ann Oncol* 2004; **15**: 460-466 [PMID: 14998849 DOI: 10.1093/annonc/mdh095]

4 **Rubbia-Brandt L**, Lauwers GY, Wang H, Majno PE, Tanabe K, Zhu AX, Brezault C, Soubrane O, Abdalla EK, Vauthey JN, Mentha G, Terris B. Sinusoidal obstruction syndrome and nodular regenerative hyperplasia are frequent oxaliplatin-associated liver lesions and partially prevented by bevacizumab in patients with hepatic colorectal metastasis. *Histopathology* 2010; **56**: 430-439 [PMID: 20459550 DOI: 10.1111/j.1365-2559.2010.03511.x]

5 **Robinson SM**, Mann J, Vasilaki A, Mathers J, Burt AD, Oakley F, White SA, Mann DA. Pathogenesis of FOLFOX induced sinusoidal obstruction syndrome in a murine chemotherapy model. *J Hepatol* 2013; **59**: 318-326 [PMID: 23624001 DOI: 10.1016/j.jhep.2013.04.014]

6 **Takada S**, Miyashita T, Yamamoto Y, Kanou S, Munesue S, Ohbatake Y, Nakanuma S, Okamoto K, Sakai S, Kinoshita J, Makino I, Nakamura K, Tajima H, Takamura H, Ninomiya I, Fushida S, Ohta T. Soluble Thrombomodulin Attenuates Endothelial Cell Damage in Hepatic Sinusoidal Obstruction Syndrome. *In Vivo* 2018; **32**: 1409-1417 [PMID: 30348695 DOI: 10.21873/invivo.11393]

7 **Vreuls CP**, Olde Damink SW, Koek GH, Winstanley A, Wisse E, Cloots RH, van den Broek MA, Dejong CH, Bosman FT, Driessen A. Glutathione S-transferase M1-null genotype as risk factor for SOS in oxaliplatin-treated patients with metastatic colorectal cancer. *Br J Cancer* 2013; **108**: 676-680 [PMID: 23287989 DOI: 10.1038/bjc.2012.590]

8 **Rubbia-Brandt L**, Tauzin S, Brezault C, Delucinge-Vivier C, Descombes P, Dousset B, Majno PE, Mentha G, Terris B. Gene expression profiling provides insights into pathways of oxaliplatin-related sinusoidal obstruction syndrome in humans. *Mol Cancer Ther* 2011; **10**: 687-696 [PMID: 21330458 DOI: 10.1158/1535-7163.MCT-10-1072]

9 **Shigefuku R**, Watanabe T, Mizukami T, Matsunaga K, Hattori N, Ehira T, Suzuki T, Nakano H, Sato Y, Matsuo Y, Nakahara K, Ikeda H, Matsumoto N, Tsuda T, Katayama M, Koizumi S, Okuse C, Suzuki M, Otsubo T, Nakajima TE, Yasuda H, Itoh F. Esophagogastric varices were diagnosed in a non-cirrhotic liver case during long-term follow-up after oxaliplatin-based chemotherapy. *Clin J Gastroenterol* 2018; **11**: 487-492 [PMID: 29948819 DOI: 10.1007/s12328-018-0873-1]

10 **Vigano L**, De Rosa G, Toso C, Andres A, Ferrero A, Roth A, Sperti E, Majno P, Rubbia-Brandt L. Reversibility of chemotherapy-related liver injury. *J Hepatol* 2017; **67**: 84-91 [PMID: 28284915 DOI: 10.1016/j.jhep.2017.02.031]

11 **Schouten JN**, Garcia-Pagan JC, Valla DC, Janssen HL. Idiopathic noncirrhotic portal hypertension. *Hepatology* 2011; **54**: 1071-1081 [PMID: 21574171 DOI: 10.1002/hep.24422]

12 **Cachay ER**, Peterson MR, Goicoechea M, Mathews WC. Didanosine Exposure and Noncirrhotic Portal Hypertension in a HIV Clinic in North America: a Follow-up Study. *Br J Med Med Res* 2011; **1**: 346-355 [PMID: 22268001 DOI: 10.9734/bjmmr/2011/554]

13 **Seinen ML**, van Asseldonk DP, de Boer NK, Bouma G, van Nieuwkerk CM, Mulder CJ, Bloemena E, van Bodegraven AA. Nodular Regenerative Hyperplasia of the Liver in Patients with IBD Treated with Allopurinol-Thiopurine Combination Therapy. *Inflamm Bowel Dis* 2017; **23**: 448-452 [PMID: 28151736 DOI: 10.1097/MIB.0000000000001036]

14 **Siramolpiwat S**, Seijo S, Miquel R, Berzigotti A, Garcia-Criado A, Darnell A, Turon F, Hernandez-Gea V, Bosch J, Garcia-Pagán JC. Idiopathic portal hypertension: natural history and long-term outcome. *Hepatology* 2014; **59**: 2276-2285 [PMID: 24155091 DOI: 10.1002/hep.26904]

15 **Park S**, Kim HY, Kim H, Park JH, Kim JH, Kim KH, Kim W, Choi IS, Jung YJ, Kim JS. Changes in Noninvasive Liver Fibrosis Indices and Spleen Size During Chemotherapy: Potential Markers for Oxaliplatin-Induced Sinusoidal Obstruction Syndrome. *Medicine (Baltimore)* 2016; **95**: e2454 [PMID: 26765438 DOI: 10.1097/MD.0000000000002454]

16 **Satta Y**, Shigefuku R, Watanabe T, Mizukami T, Tsuda T, Suzuki T, Ehira T, Hattori N, Kiyokawa H, Nakahara K, Ikeda H, Matsunaga K, Takahashi H, Matsumoto N, Okuse C, Suzuki M, Sunakawa Y, Yasuda H, Itoh F. Prediction of esophagogastric varices associated with oxaliplatin administration. *JGH Open* 2021; **5**: 1289-1297 [PMID: 34816015 DOI: 10.1002/jgh3.12668]

17 **He FL**, Qi RZ, Zhang YN, Zhang K, Zhu-Ge YZ, Wang M, Wang Y, Jia JD, Liu FQ. Transjugular intrahepatic portosystemic shunt and splenectomy are more effective than endoscopic therapy for recurrent variceal bleeding in patients with idiopathic noncirrhotic portal hypertension. *World J Clin Cases* 2020; **8**: 1871-1877 [PMID: 32518776 DOI: 10.12998/wjcc.v8.i10.1871]

18 **Huang X**, Li F, Wang L, Xiao M, Ni L, Jiang S, Ji Y, Zhang C, Zhang W, Wang J, Chen S. Endoscopic treatment of gastroesophageal variceal bleeding after oxaliplatin-based chemotherapy in patients with colorectal cancer. *Endoscopy* 2020; **52**: 727-735 [PMID: 32380558 DOI: 10.1055/a-1157-8611]

19 **Lv Y**, Li K, He C, Luo B, Zhang B, Liu H, Wang Z, Guo W, Wang Q, Chen H, Bai W, Yuan X, Yu T, Li X, Yuan J, Han N, Zhu Y, Niu J, Xie H, Wang J, Chen L, Yin Z, Fan D, Li Z, Han G. TIPSS for variceal bleeding in patients with idiopathic non-cirrhotic portal hypertension: comparison with patients who have cirrhosis. *Aliment Pharmacol Ther* 2019; **49**: 926-939 [PMID: 30820990 DOI: 10.1111/apt.15186]

World Journal of Gastroenterology

Submit a Manuscript: https://www.f6publishing.com

World J Gastroenterol 2022 July 21; 28(27): 3532-3534

DOI: 10.3748/wjg.v28.i27.3532

ISSN 1007-9327 (print) ISSN 2219-2840 (online)

LETTER TO THE EDITOR

Hepatitis B core-related antigen: Are we near a treatment endpoint?

Tarana Gupta

Specialty type: Gastroenterology and hepatology

Provenance and peer review: Unsolicited article; Externally peer reviewed

Peer-review model: Single blind

Peer-review report's scientific quality classification

Grade A (Excellent): 0
Grade B (Very good): B
Grade C (Good): C, C, C, C
Grade D (Fair): D
Grade E (Poor): 0

P-Reviewer: Caviglia GP, Italy; Feng B, China; Tong GD, China; Yin GQ, China

Received: November 7, 2021
Peer-review started: November 7, 2021
First decision: December 12, 2021
Revised: December 25, 2021
Accepted: June 24, 2022
Article in press: June 24, 2022
Published online: July 21, 2022

Tarana Gupta, Medicine, Pandit Bhagwat Dayal Sharma Post Graduate Institute of Medical Sciences, Rohtak 124001, Haryana, India

Corresponding author: Tarana Gupta, Doctor, MBBS, MD, Professor, Medicine, Pandit Bhagwat Dayal Sharma Post Graduate Institute of Medical Sciences, House No. 1065 A Sector 1, Rohtak 124001, Haryana, India. taranagupta@gmail.com

Abstract

Different serological and virological markers in chronic hepatitis B patients guide staging of viral infection, and initiation and response to therapy. Due to the persistence of intrahepatic covalently closed circular DNA (cccDNA) in the hepatocyte nucleus, hepatitis B is not curable. Even after undetectable hepatitis B virus DNA levels, the persistence of hepatitis B surface antigen and novel markers such as hepatitis B core-related antigen (HBcrAg) indicate the persistence of intrahepatic cccDNA. In this study, HBcrAg levels at baseline and after 24 and 48 wk of antiviral therapy predicted hepatitis B e antigen seroconversion. Due to the poor sensitivity of assays and detectable levels in HBsAg-negative patients, the long-term utility of HBcrAg needs future research.

Key Words: Hepatitis B core-related antigen; Chronic hepatitis B; Covalently closed circular DNA; Hepatitis B e antigen seroconversion; Hepatitis B virus DNA; Pregenomic RNA

Core Tip: This study highlights the predictive role of hepatitis B core-related antigen (HBcrAg) levels at baseline, and after 24 and 48 wk of antiviral therapy for hepatitis B e antigen seroconversion in chronic hepatitis B patients. The issues related to poor sensitivity of assays and detectable levels in hepatitis B surface antigen-negative patients are major concerns. Future research on the utility of HBcrAg in hepatitis B virus (HBV) flare after nucleotide cessation, occult HBV reactivation, and risk of developing hepatocellular carcinoma is also needed.

Citation: Gupta T. Hepatitis B core-related antigen: Are we near a treatment endpoint? *World J Gastroenterol* 2022; 28(27): 3532-3534
URL: https://www.wjgnet.com/1007-9327/full/v28/i27/3532.htm
DOI: https://dx.doi.org/10.3748/wjg.v28.i27.3532

TO THE EDITOR

We read with interest the study titled, "Serum hepatitis B core-related antigen as a surrogate marker of hepatitis B e antigen seroconversion in chronic hepatitis B" by Chi *et al*[1] in the World Journal of Gastroenterology. Hepatitis B core-related antigen (HBcrAg) and hepatitis B virus (HBV) RNA are potential serological markers of chronic hepatitis B infection and activity. In the HBV life cycle, intrahepatic covalently closed circular DNA (cccDNA) is transcribed into five RNAs of which pregenomic RNA is a precursor to synthesis of the viral genome by reverse transcription and precore mRNA is precursor to proteins hepatitis B core antigen. Hepatitis B e antigen (HBeAg) and p22cr are collectively called HBcrAg due to their identical 149 amino acid sequences. In addition, viral sequences also integrate in the host genome and can express hepatitis B surface antigen (HBsAg). Therefore, HBsAg quantification may not be exactly reflective of intrahepatic cccDNA levels. On the other hand, only cccDNA can express the viral genome. In real world settings, liver biopsy is not feasible for cccDNA quantification and a surrogate marker is needed in serum for intrahepatic cccDNA quantification. HBcrAg-related proteins can be detected in Dane particles, HBV DNA-negative Dane particles, and possibly in HBV RNA-containing virions[2]. Interestingly, nucleotide analogues (NAs) inhibit DNA polymerase and viral replication; they do not affect production of viral intermediate proteins such as HBcrAg. Therefore, even on antiviral treatment, HBcrAg can reflect cccDNA quantity and activity in hepatocytes.

This study determined the predictive role of HBcrAg for HBeAg seroconversion in chronic hepatitis B (CHB) patients. All patients were analyzed for HBcrAg, HBV RNA, and HBV DNA levels in blood and cccDNA quantification in liver biopsy specimen. Although there is treatment heterogeneity with two different cohorts of entecavir (n = 109) and pegylated-interferon (PEG-IFN) (n = 30) therapy, the authors found baseline HBcrAg levels correlating with cccDNA levels in patients with and without HBeAg seroconversion. However, the PEG-IFN group only had 30 patients, and as IFNs are immunomodulators that increase innate immune response in controlling HBV infection with higher HBeAg seroconversion rates compared to NA therapy, it may be premature to conclude that it only affects viral replication and not the production of other viral proteins. Therefore, some bias may be related to treatment heterogeneity.

This study also highlights that serum qHBcrAg levels at 24 and 48 wk of treatment better predict HBeAg seroconversion than qHBcrAg levels at baseline. Song *et al*[3] showed baseline HBcrAg levels < 4.9 log U/mL, > 2 log reduction of HBcrAg at week 28 having a positive predictive value 74% and 76%, and negative predictive value of 96% and 94%, respectively, for the prediction of spontaneous HBeAg seroconversion. In HBeAg-positive CHB patients, HBcrAg is high in the immune tolerant phase compared to the immune clearance phase. And in HBeAg-negative patients, lower HBcrAg levels are present in the inactive carrier state than in HBeAg-negative CHB. Recently Ghany *et al*[4] demonstrated a correlation of HBV RNA and HBcrAg levels with HBV DNA in different phases of CHB infection.

Wong *et al*[5] demonstrated that correlation coefficients of serum HBV DNA and HBcrAg with intrahepatic cccDNA are 0.7 and 0.64-0.7, respectively, which are similar; however, in patients on antiviral therapy with undetectable serum HBV DNA, HBcrAg is the preferred marker for estimating intrahepatic cccDNA levels. Tseng *et al*[6] recently showed risk stratification of development of cirrhosis, and its complications and liver-related mortality in CHB patients over a period of 15.9 years by baseline HBcrAg levels. Carey *et al*[7] showed that HBcrAg and HBV RNA predict clinical flares in HBeAg-negative CHB patients with suppressed HBV DNA levels on nucleotide analogue therapy. Together, HBcrAg is a promising novel serum marker but with many limitations. First, with current available assays, the lower limit of detection is 2 log U/mL, so more sensitive assays are needed. Second, one study found detectable serum HBcrAg in 40% patients with HBsAg seroclearance[8]. Finally, large-scale studies in different ethnic groups are needed to determine the predictive value of HBcrAg with certain cut-off values in clinical practice especially occult HBV reactivation, HBV flare after nucleotide analogue cessation, and risk of hepatocellular carcinoma development.

FOOTNOTES

Author contributions: Gupta T wrote and critically revised the manuscript.

Conflict-of-interest statement: The author has no conflicts of interest to declare.

Country/Territory of origin: India

ORCID number: Tarana Gupta 0000-0003-3453-2040.

S-Editor: Wang JJ
L-Editor: Filipodia
P-Editor: Wang JJ

REFERENCES

1 **Chi XM**, Wang XM, Wang ZF, Wu RH, Gao XZ, Xu HQ, Ding YH, Niu JQ. Serum hepatitis B core-related antigen as a surrogate marker of hepatitis B e antigen seroconversion in chronic hepatitis B. *World J Gastroenterol* 2021; **27**: 6927-6938 [PMID: 34790015 DOI: 10.3748/wjg.v27.i40.6927]
2 **Park Y**, Hong DJ, Shin S, Cho Y, Kim HS. Performance evaluation of new automated hepatitis B viral markers in the clinical laboratory: two quantitative hepatitis B surface antigen assays and an HBV core-related antigen assay. *Am J Clin Pathol* 2012; **137**: 770-777 [PMID: 22523216 DOI: 10.1309/AJCP8QDN7NAUXJFJ]
3 **Song G**, Yang R, Rao H, Feng B, Ma H, Jin Q, Wei L. Serum HBV core-related antigen is a good predictor for spontaneous HBeAg seroconversion in chronic hepatitis B patients. *J Med Virol* 2017; **89**: 463-468 [PMID: 27505145 DOI: 10.1002/jmv.24657]
4 **Ghany MG**, King WC, Lisker-Melman M, Lok ASF, Terrault N, Janssen HLA, Khalili M, Chung RT, Lee WM, Lau DTY, Cloherty GA, Sterling RK. Comparison of HBV RNA and Hepatitis B Core Related Antigen With Conventional HBV Markers Among Untreated Adults With Chronic Hepatitis B in North America. *Hepatology* 2021; **74**: 2395-2409 [PMID: 34133774 DOI: 10.1002/hep.32018]
5 **Wong DK**, Seto WK, Cheung KS, Chong CK, Huang FY, Fung J, Lai CL, Yuen MF. Hepatitis B virus core-related antigen as a surrogate marker for covalently closed circular DNA. *Liver Int* 2017; **37**: 995-1001 [PMID: 27992681 DOI: 10.1111/liv.13346]
6 **Tseng TC**, Liu CJ, Yang WT, Hsu CY, Hong CM, Su TH, Tsai CH, Chen CL, Yang HC, Liu CH, Chen HH, Chen PJ, Kao JH. Serum hepatitis B core-related antigen level stratifies risk of disease progression in chronic hepatitis B patients with intermediate viral load. *Aliment Pharmacol Ther* 2021; **53**: 908-918 [PMID: 33465271 DOI: 10.1111/apt.16266]
7 **Carey I**, Gersch J, Wang B, Moigboi C, Kuhns M, Cloherty G, Dusheiko G, Agarwal K. Pregenomic HBV RNA and Hepatitis B Core-Related Antigen Predict Outcomes in Hepatitis B e Antigen-Negative Chronic Hepatitis B Patients Suppressed on Nucleos(T)ide Analogue Therapy. *Hepatology* 2020; **72**: 42-57 [PMID: 31701544 DOI: 10.1002/hep.31026]
8 **Seto WK**, Wong DK, Fung J, Huang FY, Liu KS, Lai CL, Yuen MF. Linearized hepatitis B surface antigen and hepatitis B core-related antigen in the natural history of chronic hepatitis B. *Clin Microbiol Infect* 2014; **20**: 1173-1180 [PMID: 24975365 DOI: 10.1111/1469-0691.12739]

Published by **Baishideng Publishing Group Inc**
7041 Koll Center Parkway, Suite 160, Pleasanton, CA 94566, USA
Telephone: +1-925-3991568
E-mail: bpgoffice@wjgnet.com
Help Desk: https://www.f6publishing.com/helpdesk
https://www.wjgnet.com